



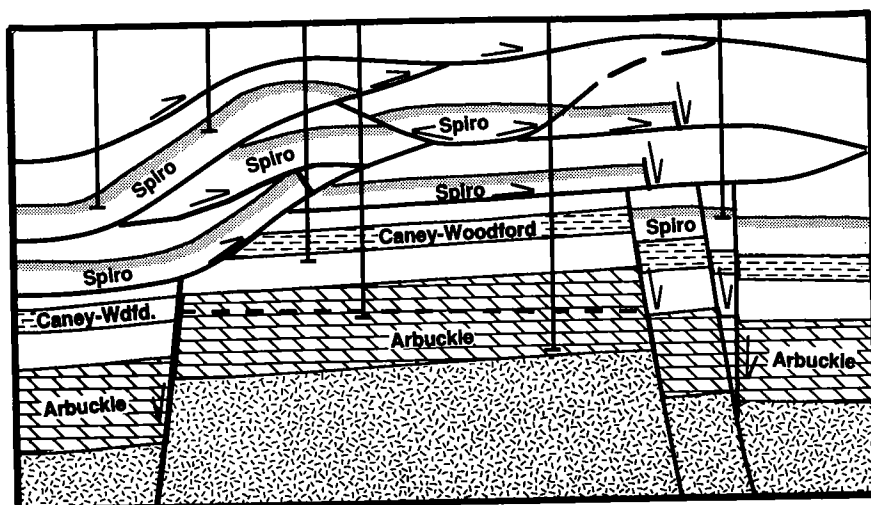
OKLAHOMA GEOLOGICAL SURVEY
Charles J. Mankin, *Director*

CIRCULAR 95

ISSN 0078-4397

PETROLEUM-RESERVOIR GEOLOGY IN THE SOUTHERN MIDCONTINENT, 1991 SYMPOSIUM

KENNETH S. JOHNSON AND JOCK A. CAMPBELL
Editors



Proceedings of a symposium held March 26–27, 1991, in Norman, Oklahoma.

Co-sponsored by:
Oklahoma Geological Survey
and
Bartlesville Project Office,
U.S. Department of Energy



**The University of Oklahoma
Norman
1993**

OKLAHOMA GEOLOGICAL SURVEY

CHARLES J. MANKIN, *Director*
KENNETH S. JOHNSON, *Associate Director*

SURVEY STAFF

JAMES H. ANDERSON, <i>Cartographic Draftsperson II</i>	JAMES E. LAWSON, JR., <i>Chief Geophysicist</i>
ROBERT H. ARNDT, <i>Economic Geologist IV</i>	DONALD G. LEITNER, <i>Log Library Assistant</i>
BETTY D. BELLIS, <i>Word-Processing Operator II/Technical Typist</i>	CHARLOTTE C. LLOYD, <i>Cartographic Draftsperson II</i>
TOM L. BINGHAM, <i>Geologist II</i>	KENNETH V. LUZA, <i>Engineering Geologist IV</i>
MITZI G. BLACKMON, <i>Clerk-Typist I</i>	TODD McCORMICK, <i>Electronic Technician</i>
JOCK A. CAMPBELL, <i>Petroleum Geologist IV</i>	MIKE MERCER, <i>Core and Sample Library Assistant</i>
BRIAN J. CARDOTT, <i>Geologist III</i>	RICHARD G. MURRAY, <i>Copy Center Operator</i>
JAMES R. CHAPLIN, <i>Geologist IV</i>	LINDA NERO, <i>Senior Receptionist-Clerk</i>
JANISE COLEMAN, <i>Chief Clerk, Publication Sales</i>	DAVID O. PENNINGTON, <i>Operations Assistant</i>
CHRISTIE L. COOPER, <i>Editor</i>	JO LYNN PIERCE, <i>Publications Assistant</i>
TAMMIE K. CREEL, <i>Secretary I</i>	JUDY A. SCHMIDT, <i>Office Manager</i>
CHARLES DYER III, <i>Drilling Technician</i>	CONNIE G. SMITH, <i>Promotion and Information Specialist</i>
WALTER C. ESRY, <i>Manager, Core and Sample Library</i>	PAUL E. SMITH, <i>Supervisor, Offset Press Copy Center</i>
ROBERT O. FAY, <i>Geologist IV</i>	JANICE S. SPURLOCK, <i>Office Assistant II</i>
SAMUEL A. FRIEDMAN, <i>Senior Coal Geologist IV</i>	MICHELLE J. SUMMERS, <i>Coordinator, Geological Computer Systems</i>
T. WAYNE FURR, <i>Manager of Cartography</i>	NEIL H. SUNESON, <i>Stratigrapher/Geologist IV</i>
L. JOY HAMPTON, <i>Petroleum Geologist III</i>	DANNY L. SWINK, <i>Drilling Technician</i>
PATRONALIA HANLEY, <i>Chemist</i>	JANE L. WEBER, <i>Organic Chemist</i>
LEROY A. HEMISH, <i>Coal Geologist III</i>	STEPHEN J. WEBER, <i>Chief Chemist</i>
SHIRLEY A. JACKSON, <i>Research Specialist I</i>	GWEN C. WILLIAMSON, <i>Assistant to the Director</i>
PRISCILLA A. JOHNSON, <i>Office Assistant III</i>	
RUTH KING, <i>Research Specialist I</i>	

Title-Page Illustration

North-south structure section through the Wilburton gas field in the Arkoma basin (from p. 242 of this volume).



printed on recycled paper

This publication, printed by the Oklahoma Geological Survey, is issued by the Oklahoma Geological Survey as authorized by Title 70, Oklahoma Statutes, 1981, Sections 231-238. 1,050 copies have been prepared for distribution at a cost of \$8,037 to the taxpayers of the State of Oklahoma. Copies have been deposited with the Publications Clearinghouse of the Oklahoma Department of Libraries.

PREFACE

This is the fourth symposium in as many years dealing with topics of major interest to geologists and others involved in petroleum-resource development in Oklahoma and adjacent states. These symposia are intended to foster the exchange of information that will improve our ability to find and recover our nation's oil and gas resources. Proceedings of the first symposium (the Anadarko basin) were published as OGS Circular 90, proceedings of the second symposium (Late Cambrian–Ordovician geology of the southern Midcontinent) were published as OGS Circular 92, and proceedings of the third symposium (Source rocks in the southern Midcontinent) were published as OGS Circular 93.

To facilitate the exchange of information on petroleum occurrence, reservoir characterization, and petroleum recovery, the Oklahoma Geological Survey (OGS) and the Bartlesville Project Office of the U.S. Department of Energy (BPO-DOE) co-sponsored this symposium dealing with reservoir characterization and petroleum geology in the southern Midcontinent. The symposium was held on March 26–27, 1991, at the Oklahoma Center for Continuing Education, The University of Oklahoma, in Norman. This volume contains the proceedings of that symposium.

Research reported upon at the symposium focused on the geology and characterization of petroleum reservoirs in the southern Midcontinent. These reservoirs can be divided into three major categories: clastic, carbonate, and fractured reservoirs. The distribution and character of these reservoirs can be influenced by their depositional environment, sedimentation, diagenesis, karstification (in carbonates), and subsequent tectonic history. All these factors can affect reservoir heterogeneity and our ability to efficiently recover the hydrocarbons they contain. We hope that the symposium and these proceedings will bring such research to the attention of the geoscience and energy-research community, and will help foster exchange of information and increased research interest by industry, university, and government workers.

Nineteen papers were presented orally at the symposium, and they are presented here as full papers or abstracts. An additional 14 reports were given as posters, and they are presented here as short reports or abstracts. About 250 persons attended the symposium. Stratigraphic nomenclature and age determinations used by the various authors in this volume do not necessarily agree with those of the OGS.

Persons involved in the organization and planning of this symposium include Kenneth Johnson, Jock Campbell, and Charles Mankin of the OGS, and Tom Wesson, Michael Ray, and Chandra Nautiyal, of BPO-DOE. Other personnel who contributed include: Michelle Summers and Tammie Creel, Registration Co-Chairs; Brian Cardott, Poster Session Chair; Connie Smith, Publicity Chair; and Helen Brown and Gwen Williamson, Exhibits Coordinators. Appreciation is expressed to each of them and to the many authors who worked toward a highly successful symposium.

KENNETH S. JOHNSON
and JOCK A. CAMPBELL
General Chairmen

CONTENTS

iii Preface

PART I—Papers Presented Orally at the Symposium

- 3 **Role of Reservoir Characterization in Improved Petroleum Exploration**
James M. Forgotson, Jr.
- 10 **The Vanoss Conglomerate—A Record of Late Pennsylvanian Basin Inversion on the Northern Flank of the Arbuckle Mountains, Southern Oklahoma**
R. Nowell Donovan and Todd Butaud
- 25 **Petrology and Sedimentology of Morrow/Springer Rocks and Their Relationship to Reservoir Quality, Anadarko Basin, Oklahoma**
C. William Keighin and Romeo M. Flores
- 26 **The Upper Morrowan Fan-Delta Chert Conglomerate in Cheyenne and Reydon Fields: Completely Sealed Gas-Bearing Pressure Compartments**
Zuhair Al-Shaieb, James Puckette, Patrick Ely, and Azhari Abdalla
- 40 **Depositional Variations and Reservoir Characterization in the Red Fork Sandstone, Northwest Tecumseh Field, Pottawatomie County, Oklahoma**
Fletcher S. Lewis
- 52 **Characterization and Simulation of the Fractured Sycamore Limestone Reservoir within the Springer Field, Carter County, Oklahoma**
Dan J. Garvey, Mark C. Potts, J. M. Forgotson, Jr., and R. M. Knapp
- 60 **Reservoir Characteristics of the McFarland and Magutex (Queen) Reservoirs, Permian Basin, Texas**
Mark H. Holtz
- 66 **Application of Horizontal Drilling in Fractured Carbonates of Oklahoma**
Richard D. Fritz, Christopher L. Johnson, and Patrick L. Medlock
- 69 **Secondary Recovery of Oil Through Mine Workings in the Keystone Field, Northeastern Oklahoma**
Maynard F. Ayler and Tom L. Bingham
- 74 **Regional Geology of the Woodford Shale, Anadarko Basin, Oklahoma—An Overview of Relevance to Horizontal Drilling**
Timothy C. Hester and James W. Schmoker
- 82 **Depositionally and Diagenetically Controlled Reservoir Heterogeneity at Jordan Field**
R. P. Major and Mark H. Holtz
- 91 **Diagenesis, Continuity, and Reservoir Character of Grainstone Lenses: Lansing–Kansas City “I” and “J” Zones, Pen Field, Graham County, Kansas**
Roderick A. Phares and Anthony W. Walton
- 104 **Unusual Occurrence of Oil in the Viola Limestone, Pratt Anticline, Kansas**
Harold A. Brown and Alan D. Banta
- 113 **Geology and Reservoir Characteristics of the Arbuckle Brown Zone in the Cottonwood Creek Field, Carter County, Oklahoma**
David L. Read and Grant L. Richmond
- 126 **Geologic Study of the Upper Arbuckle Group in the Healdton Field, Carter County, Oklahoma**
R. Todd Waddell, James M. Forgotson, Jr., and Huaibo Liu
- 140 **Paleokarstic Features and Reservoir Characteristics of the Hunton Group in Central and Western Oklahoma**
Felicia D. Matthews and Zuhair Al-Shaieb
- 163 **Feasibility Study of Heavy-Oil Recovery in the Midcontinent Region (Oklahoma, Kansas, Missouri)**
David K. Olsen and William I. Johnson

- 173 **Potential of Microbial Enhanced Oil Recovery (MEOR) in the Petroleum Reservoirs of the Midcontinent Region**
E. O. Edegbunam, R. M. Knapp, M. J. McInerney, and R. S. Tanner
- 182 **Three-Dimensional Reservoir Description Using Conditional Simulation**
Godofredo Perez and Mohan Kelkar

PART II—Abstracts and Short Reports Related to Poster Presentations

- 195 **Upper Strawn (Desmoinesian) Carbonate and Clastic Depositional Environments, Southeast King County, Texas**
Todd H. Boring
- 199 **Petroleum Production from Potentially Fractured Pre-Pennsylvanian Reservoirs in Oklahoma**
Jock A. Campbell, David P. Brown, Brian J. Cardott, and Anne Mycek-Memoli
- 206 **Distribution and Orientation of Arbuckle Group Fracture Patterns in the Slick Hills and Arbuckle Mountains, Southern Oklahoma: An Analogy for Fractured Arbuckle Reservoirs**
R. Nowell Donovan, Scott W. White, Ken M. Morgan, and Michael D. Stephenson
- 208 **Geologic and Production Characteristics of Deep Oil and Gas Wells and Reservoirs in the Conterminous U.S.**
T. S. Dyman, D. D. Rice, D. T. Nielsen, R. C. Obuch, and J. K. Baird
- 216 **Lower Atoka Group (Spiro Sand) Stratigraphic Relationships, Depositional Environments, and Sand Distribution, Frontal Ouachita Mountains, Oklahoma**
Robert C. Grayson, Jr., and Lawrence K. Hinde
- 225 **Trends of Sandstone Porosity in the Anadarko Basin—A Preliminary Evaluation**
Timothy C. Hester
- 230 **Midcontinent Fluvial-Dominated Deltaic Depositional Environments and Their Influence on Enhanced Oil Recovery**
William I. Johnson and David K. Olsen
- 236 **Application of a Transpressive Tectonic Model to Fractured Hunton and Sycamore Development, Eola Field, Garvin County, Southern Oklahoma**
Jerome J. Kendall
- 240 **Lithology and Reservoir Development of the Arbuckle Dolomite, Wilburton Field, Latimer County, Oklahoma**
Paul K. Mescher, Douglas J. Schultz, Steven J. Hendrick, Mark A. Ward, and Jeffrey A. Schwarz
- 246 **Kinta Field—Characterization and Geology of a Multi-Reservoir Giant Arkoma Basin Gas Field**
Robert A. Northcutt and David P. Brown
- 254 **Outcrop Characteristics of Asphaltic Lewis Sandstone, Black Warrior Basin, Alabama: Application to Subsurface Studies of Reservoir Heterogeneity**
Jack C. Pashin and Ralph L. Kugler
- 259 **Microseismic Monitoring as a Tool for Mapping Fractures in the San Andres Dolomite**
James T. Rutledge, Thomas D. Fairbanks, Leigh S. House, and Mark B. Murphy
- 262 **Interpretation of Depositional Facies and Porosity Evolution in the Arbuckle Brown Zone Reservoir, Healdton Field, Carter County, Oklahoma**
Huaibo Liu, James M. Forgotson, Jr., and R. Todd Waddell
- 265 **Stratigraphic Controls on Natural-Gas Accumulation in Morrowan Reservoirs, Batson Field Area, Arkoma Basin, Arkansas**
Doy L. Zachry, Roy VanArsdale, and Patrick Harris

PART I

**PAPERS PRESENTED ORALLY
AT THE SYMPOSIUM**

Role of Reservoir Characterization in Improved Petroleum Recovery

James M. Forgotson, Jr.

University of Oklahoma
Norman, Oklahoma

ABSTRACT.—Reservoir characterization is the description of the physical and chemical properties of a porous medium and its pore fluids over the broad range of dimensions from pore throat through reservoir sizes. The purpose of such descriptions is to provide an accurate quantitative physical model of the reservoir that can be translated for use with a numerical reservoir simulation model to predict oil and gas recoveries under various production scenarios. Mineralogy, texture, grain size, bedding and flow structures, depositional sequences and the geometry of genetically related depositional units are a few attributes covering a range of scales commonly identified and described by geologists. Petrophysicists measure porosity, permeability, fluid saturations, electrical and acoustical properties of samples taken from cores, or interpret these properties from well-bore measurements. Petroleum engineers analyze drill-stem test, pressure test, and tracer data to infer permeability of the reservoir. The reservoir engineer seeks to use these data and production history to build a numerical model that accurately represents the flow of fluids through the reservoir under a variety of conditions.

Porosity, permeability, relative permeability, fluid composition, fluid saturations, and pressure control fluid flow within the reservoir; therefore, reservoir characterization must focus on these parameters. Reservoir characterization studies must accurately define flow units within the reservoir and predict their size, shape, internal variations, and continuity. Recognizing reservoir heterogeneities that are no-flow boundaries or barriers to flow and the presence of exceptionally high transmissivity units are the first-order requirements. Improved oil and gas recovery from compartmentalized reservoirs requires accurate prediction of the location and extent of such features within a reservoir. Data used to make such predictions are limited by: the sample examined by cores and logs, small compared to total reservoir volume; the lack of resolution inherent in the measuring processes; ambiguities related to interpretation methods used; and uncertainty at the required levels of detail within the geological models constructed. There is also the fundamental question whether a selected geological model is an appropriate analog for a particular reservoir. Comprehensive reservoir characterization using complex, interrelated data requires interdisciplinary study to properly integrate the information acquired and interpreted by geological or geophysical methods, petrophysical analysis, and engineering technology. The interdisciplinary approach should begin with problem definition and data acquisition planning and continue through final interpretation.

Reservoir characterization has evolved during the last 40 years. Only during the last five years, however, has it been recognized that integrated interdisciplinary studies are required for optimum improved oil and gas reservoir management. The significant increase in emphasis on interdisciplinary studies during the past five years has been driven by major technological developments and by economics related to lower oil prices. Applications have been focused primarily on relatively new giant fields in such high-cost areas as Prudhoe Bay and the North Sea, and on the recovery of additional mobile oil from producing fields in the lower 48 states. The latter has been stimulated by studies and concepts of the Texas Bureau of Economic Geology that identified the large potential for increased recovery from compartmentalized reservoirs, and the relationships between such reservoirs and their depositional environments. U.S. Department of Energy data suggest that previously discovered Oklahoma reservoirs contain ~6 billion bbl of mobile oil that will not be recovered by current production practices. A high percentage of this resource is believed to be in reservoirs deposited in various fluvial-deltaic environments.

INTRODUCTION

Reservoir characterization is the quantitative description of the physical and chemical properties of a porous medium and its contained fluids.

The purpose of such a description is to develop a geological model of the reservoir that combined with reservoir fluid properties and with production and pressure data can be used to increase the recovery of petroleum from the reservoir while

Forgotson, J. M., Jr., 1993, Role of reservoir characterization in improved petroleum recovery, *in* Johnson, K. S.; and Campbell, J. A. (eds.), Petroleum-reservoir geology in the southern Midcontinent, 1991 symposium: Oklahoma Geological Survey Circular 95, p. 3–9.

maintaining favorable economics. The design of appropriate reservoir management schemes is assisted by reservoir simulation based on a sufficiently detailed and accurate model.

State-of-the-art geological modeling and reservoir simulation has evolved during the last 40 years. However, the present emphasis on interdisciplinary studies integrating geological, geophysical, and engineering data began during the mid-1980s. This increased emphasis is primarily the result of three factors: (1) the need to recover additional oil from older fields approaching their economic limit, (2) the desire for better economics in the development and reservoir management of new fields in areas with high drilling and operating costs, and (3) the development of computer hardware and software that are cost effective for numerical simulation of reservoir models based on detailed data obtained from comprehensive reservoir characterization.

Reservoir characterization spans the range from microscopic (microns) through field (kilometers) scale. Different tools and scientific disciplines are used to obtain and interpret data throughout this wide range of scales. A comprehensive study may include data from well cores; well logs; cross-well, vertical seismic profiling (VSP), and surface seismic; drill-stem tests; tracer and injection tests; bottom-hole pressures; production records; analogies based on genetically similar reservoirs; and studies of outcrops or modern sediments that are genetically similar to the reservoir.

The objective of an integrated study is to define the external and internal reservoir geometry with particular emphasis on delineating flow units that have similar transmissivity properties throughout the unit and different transmissivity from other units. Recognition of features that control extreme permeability differences, such as barriers, baffles, and high transmissivity conduits, are most important. Accurately mapping these features at interwell scale is the major challenge in detailed reservoir description.

SIGNIFICANCE OF IMPROVED RECOVERY TECHNOLOGY

Proper application of improved recovery technology is critical to maintaining the economic viability of exploration for, and production from, most Midcontinent reservoirs. Demonstrated improved recovery from producing reservoirs can be used to support higher reserve figures for similar exploration targets.

U.S. production of 9 million bbl/day from the lower 48 states in 1973 declined to only 5.4 million bbl/day in 1992. Approximately half of this decline in the lower 48 states has occurred since 1986, and all of the decline from ~2 to ~1.8 million bbl/day in

Alaska has occurred since then. Thus, the requirements for imports continue to rise to supply the U.S. petroleum product demand of 17 million bbl/day.

According to data published by the Texas Bureau of Economic Geology, the total U.S. endowment of oil is estimated to be 698 billion bbl. Proved reserves are 25 billion bbl; ~90 billion bbl of mobile oil and 240 billion bbl of immobile oil remain in previously discovered fields, and 95 billion bbl of mobile oil and 90 billion bbl of immobile oil remain to be discovered. The U.S. endowment of natural gas is 2,180 trillion cubic feet (Tcf), of which 18% is attributed to reserve growth and only 9% to proved reserves.

The target for reserve growth attributable to improved recovery from existing oil and gas fields is very large. Unfortunately, many large fields containing significant volumes of unrecovered mobile oil have been abandoned and others are fast approaching their economic limit. In 1985, ~70% of the remaining resource of oil in the lower 48 states was contained in active reservoirs. The estimate for the year 2015 is that only 25% of this resource will be contained in active reservoirs. This situation is extremely critical in the southern Midcontinent where, based on an average oil price of \$22 per barrel, it is estimated that all of the remaining resource in Kansas and 90% in Oklahoma will be abandoned by the year 2000. Favorable economics for improved recovery generally require access to the reservoir through existing well bores prior to field abandonment.

Reservoir management using simulation studies based on accurate models obtained from detailed reservoir characterization data should, on the average, improve recovery by 10% for most Midcontinent fields. This additional production may extend the life of fields and, thus, provide access to reservoirs suitable for the application of advanced recovery technologies that may be developed within the next decade. Extension of the productive life of existing fields is necessary if a significant part of the mobile and immobile oil that will not be recovered by current production operations is to be obtained.

CLASSIFICATION OF RESERVOIRS

During the mid-1980s, the Texas Bureau of Economic Geology published generalized data that related recovery factors to depositional environment. These data showed, as would be expected, that reservoir genesis had a strong influence on recovery factors; common types of reservoirs, such as sandstones deposited in a fluvial-deltaic environment and carbonates deposited on a platform margin, typically have recovery efficiencies that range from 20 to 40% and, thus, are good targets for improved recovery applications.

The Geoscience Institute for Oil and Gas Recovery Research, supported by U.S. Department of Energy funds, published classifications for siliciclastic and carbonate reservoirs based on reservoir genesis, diagenesis, and structure. If a reservoir's classification according to this system is known, it is reasonable to assume that its production characteristics and recovery factor would be similar to those of other reservoirs within this class. Thus, reservoirs with good geological data and production histories can be used as models for those that are not fully developed or do not have adequate data for a detailed characterization study.

In the absence of significant diagenetic alteration, specific depositional environments typically produce predictable permeability patterns. Channel sands have high permeability in their lower part, and the permeability becomes less as the sand becomes finer in an upward direction; bar sands have lower permeability near their base, and the permeability increases upward as the sand becomes coarser and cleaner. The lateral continuity of shales within a sandstone reservoir is also a function of depositional environment. For example, shales interbedded within a marine sandstone usually extend for several thousands of feet parallel and normal to the depositional strike. Shales interbedded with distributary channel sandstones usually are laterally continuous for only a few hundred feet. The distribution of shales and clay laminae strongly influences the vertical permeability within a reservoir and may effectively separate permeability zones within a heterogeneous reservoir. The distribution of permeability within a reservoir has a stronger influence on displacement processes than on primary recovery. Hence, for successful implementation, improved recovery projects require detailed reservoir description.

SCALES OF RESERVOIR HETEROGENEITY

The very wide range of scales at which various types of reservoir heterogeneities occur can be classified into four levels: microscopic → mesoscopic → macroscopic → and megascopic.

Comprehensive reservoir characterization requires the use of data from all scales. Sophisticated averaging methods that consider the volume of reservoir measured or sampled by various tools or tests and scaling up methods that estimate the properties of a flow unit from data measured at a smaller scale are used to translate the geological model into a numerical model for reservoir simulation. Considering the unit volume of a core plug to be 1, the reservoir volume measured by several common tools and tests is:

<u>Tool or test</u>	<u>Reservoir volume measured</u>
Core plug	1
Average porosity from 200 core plugs	2×10^2
Microlaterolog	1.6×10^4
Deep Induction Log	4×10^7
Chemical Tracer test	1×10^9
Pressure buildup test	2×10^{12}

Microscopic Heterogeneity

Variability at the pore and pore-throat scale produces microscopic scale heterogeneity which is the scale of variability that governs the nature of gas and oil saturation in a reservoir. Oil globules and gas are trapped in pores by capillary forces, and fluid flow characteristics are controlled by the size and distribution of pore space at the microscopic scale.

Mesoscopic Heterogeneity

Variability at the lamination to bed scale within distinctive lithofacies deposited during a relatively short period of accumulation produces mesoscopic scale heterogeneity. Barriers to flow (such as shale layers in sandstone reservoirs, laterally and vertically discontinuous beds in carbonate reservoirs, high-permeability zones including vugs and fractures in carbonates, and sandstones that act as thief zones and cycle injected fluids) segment a reservoir and prevent oil or gas zones from being contacted during a displacement process. Correlation between core and well log properties is made at this scale.

Macroscopic Heterogeneity

Lateral changes in lithofacies and lithologic changes across depositional sequence boundaries commonly produce marked changes in fluid transmissibility at the macroscopic scale. At this scale of interwell spacing, flow properties are inferred from well tests or log correlations. The current emphasis on acquisition and interpretation of high-resolution seismic data is to obtain better reservoir characterization at the interwell scale.

Megascopic Heterogeneity

Lithologic variability across depositional systems and geometry of structural features are the major controls on the distribution of reservoirs within a trend or play. This megascopic, field-wide scale used to depict the external architecture of reservoirs is the domain of conventional subsurface mapping and the structural and stratigraphic interpretation of seismic data.

DATA SOURCES FOR RESERVOIR CHARACTERIZATION

The sources of data used for reservoir characterization are different for each scale and scientific discipline. Several major subdisciplines of geology, geophysics, and petroleum engineering contribute to the science of reservoir characterization. Geostatistics is important in data analysis and interpretation. The sources of data for geological and petrophysical study include samples from analogous outcrops, drill cuttings, cores, open-hole logs, and geological descriptions. Geophysical data are primarily based on acoustic wave methods and include surface seismic, VSP, and cross-well seismic surveys. The engineering data include cased-hole logs, drill-stem tests, bottom-hole pressure tests, tracer studies, injection tests, production history, and reservoir fluid properties.

Outcrop Studies

During the last decade, studies of the three-dimensional distribution and the internal architecture of potential reservoir rocks have contributed to reservoir characterization. Subsurface studies to determine the nature of unit boundaries that control the internal structure of reservoirs are limited by well spacing and core availability. Outcrops deemed analogous to subsurface reservoirs permit detailed two-dimensional examination of bounding surfaces and sedimentary features that produce reservoir heterogeneity. Data from core holes adjacent to the outcrop can provide a three-dimensional perspective to the reservoir geometry and architectural elements that determine reservoir flow units. Scales of heterogeneity from microscopic through large macroscopic features can be observed on many outcrops and continuously sampled. Several outcrops within an area can provide the megascopic-scale reservoir outline. Porosity and permeability measured from outcrop samples can provide a template for the range and scale of variations to be expected within an analogous reservoir. Diagenesis and the effects of overburden must be considered in such comparisons. Subsurface studies are limited to lower-order boundary surfaces such as unconformities and marine flooding surfaces observed at well locations. Geostatistical modeling techniques are used to infer interwell variations within the reservoir based on detailed outcrop studies.

Cores

Information obtained from cores provides the only verification of reservoir properties derived from log analysis and other indirect methods. Laboratory measurements and tests made on cores obtained and handled properly for the analyses performed provide the following types of

data: (1) porosity and formation resistivity factor; (2) absolute permeability, compressibility, and rock mechanics measurements; (3) relative permeability, wettability, and residual saturations; (4) dispersivity, adsorption properties, fraction of dead-end pores, and diffusivity; (5) mineralogy, clay content and type, cation exchange capacity; (6) capillary pressure/saturation relationships, drainage and imbibition properties; (7) tortuosity, specific surface area, pore-size distribution, grain-size distribution; (8) water flood and enhanced-oil recovery (EOR) displacement tests; and (9) parameter sensitivity to pressure, temperature, stress conditions, and fluids.

Cores are necessary to develop statistical relationships between porosity and permeability that can be applied to log-derived data from lithologies similar to intervals that were cored. Continuous cores through the reservoir interval can aid in the interpretation of the depositional environment and the recognition of boundary surfaces that determine reservoir flow units.

Open-hole Logs

Open-hole logs are the most widely available sources of data for reservoir characterization and are often the only source for gross and net reservoir thickness, lithology, porosity, position of possible flow barriers, fluid saturation, and permeability. Geological models and the rock and fluid properties used in numerical reservoir simulation are based largely on log-derived information. Many of the core-derived properties listed above can be measured reliably by logs calibrated with core data.

Open-hole logs measure reservoir properties from the mesoscopic through the megascopic scale. Formation microscanner and bore-hole televiwer logs have vertical resolution in the 1- to 2-in. range and can detect many types of mesoscopic features at the surface of the well bore. Other open-hole logs have vertical resolution typically in the 1- to 3-ft range and a depth of investigation beyond the borehole ranging from several inches to several feet.

Open-hole well logs are particularly useful in determining external reservoir geometry, major flow barriers, porosity, and fluid saturation. Because these logs sample only a very small fraction of the reservoir, reliability of the interpretations of lateral extent and continuity of these properties in the interwell area depends on (1) the depositional environment in which the reservoir unit was deposited, (2) the complexity of local structure, (3) diagenetic alteration, and (4) well spacing.

Seismic Surveys

Conventional seismic surveys are usually interpreted to map the structural attitude of the reser-

voir and detect faults that provide traps or segment the reservoir. Properly designed three-dimensional surveys can provide an image of a field with higher resolution and greater accuracy. The increased cost of this more accurate picture is justified by detection of additional reserves and proper placement of wells for optimum development economics. Two types of seismic analysis can be performed on three-dimensional data and some two-dimensional surveys: (1) mapping of geometric framework to represent detailed attitude of reservoir beds and (2) interwell interpolations of reservoir properties. Imaging of three-dimensional data has revealed meandering stream channels and other detailed sedimentary and structural features that are not apparent on two-dimensional data. Amplitudes, phase changes, interval times, and other attributes of the seismic data can be correlated with lithology, porosity, and fluid type. Comparison of reflection amplitudes with porosity/thickness measured in wells can be used to transform seismic amplitude values into porosity/thickness values at points between wells; the accuracy of reserve estimates is increased and the risk of drilling development wells for fluid injection or production is reduced. Comparison of three-dimensional surveys performed at different times with a base survey has been successful in monitoring the temperature and pressure changes occurring in relatively shallow thermal-recovery projects.

Vertical seismic profiling (VSP), in which the receivers are placed in the well bore, provides accurate depths to reflectors seen in surface seismic and provides high resolution structural and stratigraphic information within a few hundred feet of the well. Reverse VSP, in which the energy source is in the well bore and receivers are on the surface, can provide 3-D areal coverage of $\sim 1 \text{ mi}^2$. This method provides less extensive coverage than surface 3-D, but, in a short time, produces a large amount of data with a resolution of $\sim 10 \text{ ft}$. Well-to-well seismic (often referred to as cross-well seismic) uses a downhole energy source in one well and multi-geophone receiver tools in one or more offset wells. This method, which uses a higher frequency source (100–5000 Hz) than surface seismic (20–100 Hz), has a 1-ft resolution and can provide data between wells spaced up to 40 acres. This developing technology, designed to investigate an interval between wells, shows promise of filling the data gap between log-scale and reservoir-scale properties. Interpretations of reservoir properties in the interwell area are based on tomographic and reflection methods. The short-term practical use of this technology may be determination of the continuity of reservoirs and boundary surfaces between wells rather than the quantitative determination of interwell rock and fluid properties.

Wells Tests

Production tests, tracer tests, and pressure-transient tests are used to obtain megascopic properties of the reservoir. Production tests are helpful for determining thief zones, fractures, coning, and limits of producing zones. Interwell tracer tests are used to determine the direction and rate of fluid movement, volumetric sweep efficiency, permeability distribution, and fluid dispersivity. Single-well tracer tests are used to measure residual oil saturation and dispersion coefficients. Pressure-transient tests are used to measure horizontal and vertical permeability, porosity, productivity index, reservoir volume, distance to fault or reservoir boundary, vertical zonation and directional permeability, fracture length, length of shale barriers, and average reservoir pressure.

RESERVOIR DESCRIPTION AND SIMULATION

Reservoir simulation is the process of modeling the flow of fluids through a porous medium. It can be used to predict the performance of reservoirs of all sizes and degrees of complexity. Generally, it is used to predict the flow of multiple phases of fluids in a heterogeneous reservoir. The simulation process represents the hydrodynamics of flow within the reservoir using a flow model consisting of partial differential equations that describe the unsteady-state flow of all fluid phases in the reservoir medium. Because these equations generally cannot be solved analytically, they are solved numerically by replacing the differential equations with difference equations. This requires describing the reservoir as if it were composed of discrete volume elements referred to as grid blocks.

All properties of the fluids and rock matrix within a grid block are assumed to be constant. Thus, a block has only a single value for each property, such as phase saturation, relative permeability, and pressure. However, these properties vary from block to block, and the change in the value of a property between adjacent blocks depends on the grid-block size. The accuracy with which the flow of fluids within the reservoir can be calculated usually improves as the number of grid blocks becomes larger. The computer time required to obtain a solution also increases with the number of grid blocks. Thus, a simulation model should contain the minimum number of grid blocks necessary to adequately represent the reservoir behavior for the purpose of the study. Whether reservoir simulation is performed using a one-dimensional, two-dimensional, radial, or three-dimensional model depends on the type of problem to be solved. Grid blocks within the model do not have to be the same size. Smaller

grid blocks are commonly used for those parts of the reservoir in which pressure and fluid saturations change more rapidly, i.e., near well bores and fluid-front boundaries.

Properties within a grid block are constant only for a specified time interval referred to as a time step. The changes of properties within a block between time steps are directly related to the time interval selected. Time steps do not have to be constant throughout the time period covered by the simulation study. Time steps must be small enough to determine saturations, pressures, and production at specific locations and times required by the study and to model fluid mechanics properly.

An accurate geological description of a reservoir is necessary to provide guidelines for grid-block orientation and size. The increased speed of computers using state-of-the-art software permits the economical use of a large enough number of grid blocks to adequately represent fairly complex geology in a reservoir model. Typically, 3-D models contain three to 10 vertical layers and 20–100 grid blocks in each direction. Grid-block design should consider the presence of internal barriers to fluid flow, such as shale layers, low permeability zones, faults, and other vertical and horizontal reservoir heterogeneities. Geostatistical methods are used to determine the “best” average values of porosity, permeability, and other properties for a grid block, based on measurements of these properties from cores or well logs (which examine only a very small fraction of the reservoir volume compared to the volume of a typical grid block). Geostatistical methods to estimate properties of the geological model in the interwell regions and scaling-up algorithms are critical steps in a comprehensive reservoir simulation.

The following outline indicates the sequence of major steps required in a reservoir simulation study:

- Reservoir description
 - Geological model
 - Recovery mechanism
 - Fluid properties
- Mathematical model
- Numerical model
- Computer model—Grid blocks
- History match to validate model
- Performance prediction
 - Pressure and fluid saturations within reservoir—Design plan for improved recovery using infill wells (vertical or horizontal), water flood, or other improved-recovery process

A simulation study should be an iterative process involving feedback between the results of a history match or performance prediction and the reservoir description.

SUMMARY

Existing fields within the lower 48 states are estimated to contain ~90 billion bbl of mobile oil that will not be recovered by current production operations. Six billion of these barrels are in Oklahoma and 2.4 billion are in Kansas. This resource provides an important target in the southern Mid-continent for major reserve growth through improved recovery. Proper application of available data and technology should provide favorable economics for the recovery of a significant part of this resource.

Technological advancements in reservoir description and numerical reservoir simulation during the last decade will assist operators in the design and operation of improved recovery projects. Important among these advances are the recognition of relationships between depositional environment and recovery, advances in well logging, development of cost effective 3-D high-resolution seismic acquisition and processing, improvements in acquisition and interpretation of cross-well seismic data, and computer hardware and software that can economically process complex reservoir models and provide interactive capability for visualization of three-dimensional data. Advances in the technology of drilling and completing horizontal wells provide the ability to solve economically some of the problems that reduce mobile oil recovery, such as reservoir compartmentalization, coning of gas or water, and low production rates from thin, low-permeability reservoirs.

Successful results will require the integration of interdisciplinary studies, such as geology, geophysics, and reservoir engineering, with field development operations and production technology.

SELECTED REFERENCES

- Becker, A. B.; Brashear, J. P.; and Biglarbigi, K., 1990, Evaluation of unrecovered mobile oil in Texas, Oklahoma, and New Mexico: Society of Petroleum Engineers/U.S. Department of Energy, paper no. 20255, p. 791–800.
- Fisher, W. L.; and Galloway, W. E., 1983, Potential for additional oil recovery in Texas: University of Texas at Austin, Bureau of Economic Geology Geological Circular 83-2, 20 p.
- Geoscience Institute for Oil and Gas Recovery Research, 1989, Major program elements for an advanced geoscience oil and gas recovery research initiative: Program Study Summary Report, The University of Texas at Austin; prepared on behalf of the Office of Fossil Energy, Bartlesville Project Office, U.S. Department of Energy, DOE/BC-89/9/SP, 50 p.
- Honorpour, M. M.; and others, 1990, Integrated methodology for constructing a quantified hydrodynamic model for application to clastic petroleum reservoirs: Prepared for U.S. Department of Energy,

- Bartlesville Project Office, NIPER-439 (DE 90 000211), 156 p.
- Krohn, Christine, 1992, Cross-well continuity logging using guided seismic waves: *The Leading Edge*, v. 11, no. 7, p. 34–37.
- Lou, Min; and Crampin, Stuart, 1992, Guided-wave propagation between boreholes: *The Leading Edge*, v. 11, no. 7, p. 39–45.
- Mattax, C. C.; and Dalton, R. L., 1990, Reservoir simulation: Society of Petroleum Engineers Monograph, v. 13.
- Paulsson, B. N. P.; Smith, M. E.; Tucker, K. E.; and Fairborn, J. W., 1992, Characterization of a steamed oil reservoir using cross-well seismology: *The Leading Edge*, v. 11, no. 7, p. 24–32.
- Reservoir Classification Task Force, 1990, Reservoir heterogeneity classification system for characterization and analysis of oil resource base in known reservoirs: Geoscience Institute for Oil and Gas Recovery Research, The University of Texas at Austin; prepared on behalf of the Office of Fossil Energy, Bartlesville Project Office, U.S. Department of Energy, 27 p.
- Schlumberger–Doll Research, 1992a, Trends in reservoir management: *Oilfield Review*, v. 4, no. 1, p. 8–24.
- _____, 1992b, Reservoir characterization using expert knowledge, data, and statistics: *Oilfield Review*, v. 4, no. 1, p. 25–39.
- Tyler, Noel; and Gholston, J. C., 1988, Heterogeneous deep-sea fan reservoirs, Shackelford and Preston waterflood units, Spraberry trend, West Texas: The University of Texas at Austin, Bureau of Economic Geology Report of Investigations No. 171, 37 p.
- Tyler, Noel; Galloway, W. E.; Garrett, C. M., Jr.; and Ewing, T. E., 1984, Oil accumulation, production characteristics, and targets for additional recovery in major oil reservoirs of Texas: The University of Texas at Austin, Bureau of Economic Geology Geological Circular 84-2, 31 p.

The Vanoss Conglomerate—A Record of Late Pennsylvanian Basin Inversion on the Northern Flank of the Arbuckle Mountains, Southern Oklahoma

R. Nowell Donovan

Texas Christian University
Fort Worth, Texas

Todd Butaud

Union Pacific Resources
Fort Worth, Texas

INTRODUCTION

The dominant tectonic control in Phanerozoic southern Oklahoma has been a N. 60° W.-trending zone of crustal weakness extending from the neighborhood of Durant, Oklahoma, into the Texas Panhandle. The principal role played by this zone has been to guide the Paleozoic evolution of the southern Oklahoma aulacogen (Shatski, 1946). Four distinct stages in this evolution can be recognized. The earliest (Cambrian) stage involved the intrusion and extrusion of a bimodal suite of igneous rocks within an extensional rift setting. The northern boundary of this rift is a complex granitic and gneissic terrain, ~1.4 billion years old. To the south, the boundary, which is by no means clearly understood, appears to be a horizontally layered Proterozoic basin of uncertain character. Xenoliths in the oldest intrusions within the aulacogen suggest that at least part of this basin consists of metasediments.

The second stage in the evolution of the aulacogen was a long (Cambrian–Mississippian) period of cratonic sedimentation. Volumetrically, most of the rocks deposited during this period were carbonates. At this time, the aulacogen was a linear depocenter in which sediment-entrapment rates within the aulacogen were approximately 2–4 times those on the adjacent craton. In geometric terms, each of the lithostratigraphic divisions recognized can be traced laterally for great distances, from the craton into the aulacogen.

Stratigraphic continuity was interrupted during the late Paleozoic when, under a generally compressive-stress regime, the integrity of the aulacogen was broken and the area was differentiated into a series of linear basins and uplifts. As a result

of this partial inversion of the aulacogen, erosion of the entire lower Paleozoic sedimentary sequence, as well as substantial parts of the igneous basement, took place in such areas as the Wichita, Criner, and Arbuckle uplifts. Sediment shed from these uplifts was deposited in adjacent basins, such as the Ardmore, Anadarko, and Marietta basins.

Subsequently, in the fourth stage of its existence, the aulacogen terrane has functioned, by and large, as an undefined and inert component of the North American craton.

In a broader context, the late Paleozoic dismemberment of the aulacogen coincided with the completion of the formation of Pangaea, due to the final closure of the ocean complex that had existed off the eastern seaboard of the North American craton. This closure is marked by the Appalachian–Ouachita–Marathon orogene. Although the timing of individual events is variable, the deformation of southern Oklahoma can be viewed as one of a number of similar inversional events occurring within the North American craton that are collectively referred to as the Ancestral Rockies deformation. In each case, inversion of linear fault-bounded uplifts exposed a sequence of lower Paleozoic sedimentary rocks and underlying igneous and metamorphic basement to erosion, while considerable quantities of clastics were shed into adjacent syntectonic basins. On a gross scale, each basin can be regarded as a syntectonic half graben, characterized by markedly asymmetric facies distributions. Each complex of basins and uplifts had a “life” of no more than 50 million years. Following initiation, basin subsidence appears to have been controlled by a combination of isostatic response and structural overloading. In

Donovan, R. N.; and Butaud, Todd, 1993, The Vanoss conglomerate—a record of Late Pennsylvanian basin inversion on the northern flank of the Arbuckle Mountains, southern Oklahoma, *in* Johnson, K. S.; and Campbell, J. A. (eds.), *Petroleum-reservoir geology in the southern Midcontinent*, 1991 symposium: Oklahoma Geological Survey Circular 95, p. 10–24.

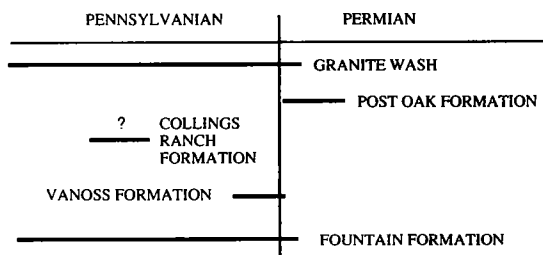


Figure 1. General age of sedimentary deposits discussed in the text. The granite wash and Post Oak Formation were deposited adjacent to the Wichita uplift (by definition the term “granite wash” is restricted to the subsurface, whereas “Post Oak” refers to outcrop). The Collings Ranch is found within a small linear transtensional basin in the Arbuckle Mountains, the Vanoss on the northern flank of the Arbuckles, and the Fountain on the eastern flank of the present-day Rockies in Colorado.

some cases, including the southern Oklahoma aulacogen, it is clear that preexisting structures were reactivated. Typically the basins are no larger than 75 × 200 mi, and may be considerably smaller (as, for example, in the case of the probable Late Pennsylvanian Collings Ranch basin in the Arbuckle Mountains of Oklahoma).

In this paper we describe one example of a proximal facies deposited in this setting (the Upper Pennsylvanian Vanoss Formation), and develop a general discussion of the defining parameters of such facies (Fig. 1).

Structural Styles Associated with Inversion

Within the area of the southern Oklahoma aulacogen, the Pennsylvanian dismemberment appears to have involved compressive stresses that were oriented approximately (but not exactly) normal to the existing N. 60° W. aulacogen trend. As a result, shortening across the aulacogen is the principal feature of the dismemberment. Uplifts (i.e., inversions) and downwarps (i.e., basins) in the area can be viewed as giant folds that accommodated this shortening within the area of weakened basement that characterizes the aulacogen. Second-order structures include large folds, generated at several levels within the aulacogen section, including the layered basement (Donovan, 1991) and large basement-cutting faults. The geometries of most large faults are consistent with substantial components of reverse motion.

The tectonic fabric encountered within the dismembered area also is consistent with a component of left-lateral strike slip during deformation. The amount of horizontal slip has not been satisfactorily quantified; the strongest evidence suggests that it is not much greater than the vertical component (e.g., McConnell, 1989). Stephenson

and Donovan (1991) suggest that both large- and small-scale structures in the eastern Slick Hills of southwestern Oklahoma are consistent with a compressive stress oriented approximately N. 50° E. (i.e., slightly clockwise of normal to the original aulacogen boundaries).

Provenance of the Upper Paleozoic Rocks

The lower Paleozoic stratigraphy of much of the Midcontinent is remarkably consistent in that a carbonate-dominated sequence lies atop an igneous metamorphic basement. Hence, there is a general similarity in the fill of the late Paleozoic basins; the “inverted stratigraphy” of clasts derived from adjacent uplifts consists of a sequence of dominantly carbonate-derived detritus overlain by siliciclastic detritus derived from the basement (Fig. 2). Although provenance generally reflects depth of erosion (Fig. 3), this generality may be masked both by structural complexity and by the considerable variations in thickness of the carbonate cover that exist.

Facies and provenance patterns in the coarse-grained rocks deposited adjacent to uplifts can be extraordinarily complex and particularly difficult to correlate in the subsurface. This is particularly so in the case of the earlier (Pennsylvanian) deposits, which generally were laid down in a more active tectonic setting than later (Permian) deposits. Furthermore, in southern Oklahoma, especially the Anadarko basin, most of the Pennsylvanian rocks (the “granite wash”) are below the present level of erosion.

An example of this complexity is provided by a short section of the Fountain Formation in Priest Canyon, near Cañon City, Colorado, where variations in clast content suggest that fan overlap has taken place (Fig. 4). In this example, some of the

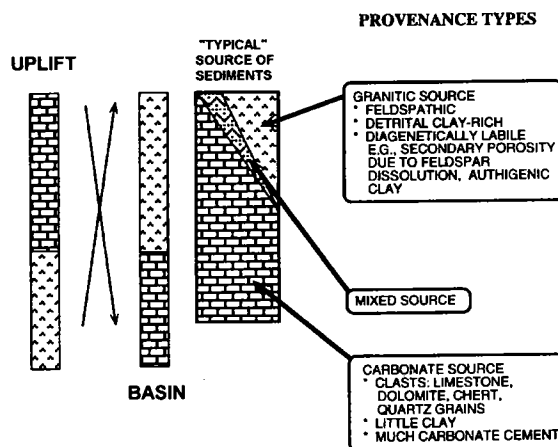


Figure 2. Generalized provenance model of proximal sediments associated with inversion in which clasts record an “inverted stratigraphy.”

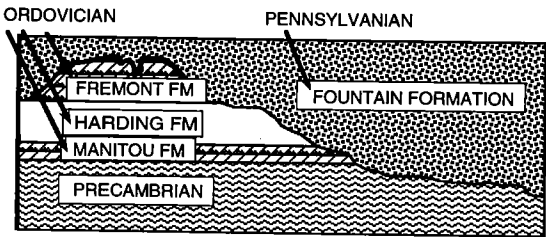


Figure 3. Generalized stratigraphic relationships developed between the Fountain Formation and older rocks in the Cañon City area of Colorado. This section displays several features that are common to the settings under discussion: (1) an unconformity with pronounced relief, (2) karst where the unconformity is developed in carbonate rocks, and (3) a distinctive coupling of lower Paleozoic carbonates atop an igneous and/or high grade metamorphic basement.

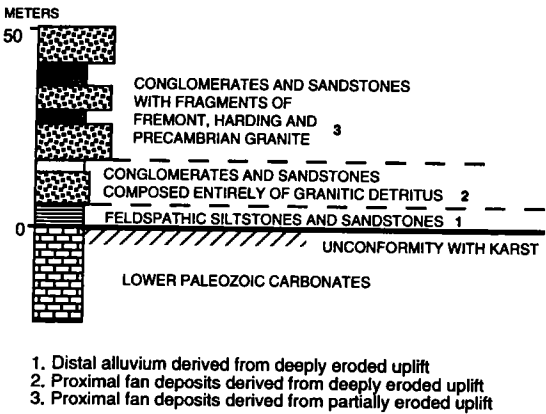


Figure 4. Section of the Fountain Formation measured in Priest Canyon, Cañon City, Colorado, in which provenance of the clasts in the fans contradicts the expected "inverted stratigraphy" (see Fig. 3).

clasts in the upper fan are from stratigraphically younger rocks than those in the lower fan.

Generally, in such cases, it is difficult to decide whether such variations have a direct tectonic cause, or whether they reflect avulsion, scarp recession, or overlap of fans sourced by different areas. On occasion the cause may be clear. Thus, in a well-exposed example of overlap, documented from the Early Permian Post Oak Conglomerate deposited in Blue Creek Canyon in the Slick Hills of southwestern Oklahoma, it is clear that clast variation reflects sources from two sides of a fault that juxtaposes very different rock types (Donovan, 1982).

Facies Patterns

In general terms, the early histories of the larger and more sharply pronounced (i.e., deeper) sedimentary basins are characterized by the deposi-

tion of a greater proportion of marine facies. In their later history these basins display an increasing component of continental facies. This general facies pattern appears to be related to a gradual slowing of tectonic activity. In terms of proximal deposits, this means that many Permian conglomerates are simply the result of the reduction of available relief, whereas Pennsylvanian conglomerates may also reflect a more dynamic tectonic setting.

Given the fault-bounded geometry of the basins, it is scarcely surprising that both marine and nonmarine facies patterns may be highly asymmetric within individual basins. For example, in the earlier Pennsylvanian history of the Anadarko basin, small fan-delta conglomeratic deposits mark the juxtaposition of the basin and adjacent Wichita uplift, whereas the gentle northern edge of the basin is characterized by fine-grained deltaic deposits. A similar grain-size pattern is found in the succeeding Late Pennsylvanian and Early Permian alluvial deposits (reviewed in Johnson and others, 1988).

Climatic Imprint

During the late Paleozoic, the Oklahoma area gradually drifted from an equatorial setting into the northern low-latitude desert zone. Indications of this are manifest in the sedimentary record as:

- 1) "Fossilization" of the existing topography, including karst, during the Early Permian, due to a slowdown in the effectiveness of weathering processes in the relative absence of water.
- 2) A change in pedogenic profiles, from leached underclays supporting coal swamps in Pennsylvanian deposits to calcrete in Late Pennsylvanian and Early Permian rocks (Fig. 5).
- 3) The appearance of evaporites in Early and Middle Permian rocks.
- 4) The upward replacement of kaolinite by illite as a detrital clay (Donovan, 1991).

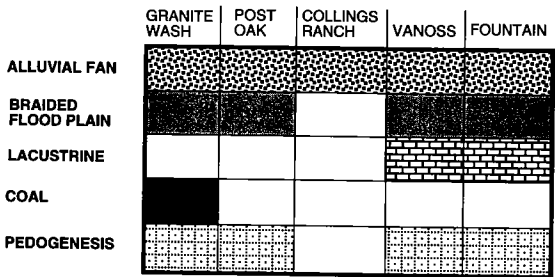


Figure 5. Generalized comparative depositional environments developed in proximal (nonmarine) settings in selected deposits. Sources: granite wash (Al-Shaieb and others, 1977; our own work); Post Oak (Donovan, 1982, 1988); Collings Ranch (Ham, 1954; Donovan and Heinlen, 1988); Vanoss (Al-Shaieb and others, 1977; Donovan and Heinlen, 1988); Fountain (our own work).

Diagenetic Patterns

Early diagenetic patterns are, to some extent, controlled by the provenance of the detritus involved. Typically, patterns in siliciclastic-dominated deposits are characterized by the growth of clay, usually kaolinite and/or illite (Al-Shaieb and others, 1980), whereas calcite cements (often with a variety of textures) are in a preponderance in carbonate-dominated deposits (Donovan, 1986). In younger beds, hematite is commonly observed as a grain coating. In conglomerates composed of dolomite clasts, dolosparite cement is seen, as for example in the Post Oak Conglomerate that mantles the Maukeen dolomite in the Saddle Mountain area of the western Slick Hills. An additional example occurs in a Fremont dolomite facies of the Fountain Formation. Another unusual cement is barite, generally in the form of euhedral crystals.

The extraordinary depth of some of the basins resulted in the maturation of source rocks in the Paleozoic section (particularly the Upper Devonian Woodford Formation). Activation coincided with the deposition of some of the beds under discussion, and as a result bitumen partially impregnates some deposits, e.g., the granite wash (Al-Shaieb and others, 1977) and the Post Oak Conglomerate (Donovan and others, 1992). In addition to hydrocarbon migration, structural overpressuring of basin brines led to the precipitation of a number of other cements, such as pyrite, illite, dolomite, calcite, and barite (Younger and others, 1986; Donovan, 1991).

THE VANOSS FORMATION

Introduction

The Vanoss Formation, first recognized by Morgan (1924), is a Late Pennsylvanian deposit that crops out over an area of ~900 km² north of the Arbuckle Mountains in southern Oklahoma. Subsequent workers have recognized upper shale and lower conglomeratic members with a combined thickness variously estimated at 365–475 m (Ham and McKinley, 1954; Tanner, 1956; Thomas, 1973). The current study, which was undertaken to try to elucidate factors that controlled the architecture of proximal detritus in dismemberment-related basins, is restricted to conglomerate-dominated facies adjacent to the Arbuckle Mountains, some part of which has been examined previously by Al-Shaieb and others (1977) and by Donovan and Heinlen (1988).

Exposure in this area is generally scrappy, with the exception of three outstanding sites: (1) natural cliffs on the southern bank of Travertine Creek in the Chickasaw National Refuge (formerly Platt National Park); (2) an abandoned gravel pit ~2 km east-northeast of Sulphur; and (3) an abandoned asphalt quarry in the Buckhorn asphalt district, ~7 km south of Sulphur.



Figure 6. Exposure of the unconformity between the Vanoss Formation and the Ordovician Oil Creek Formation in a quarry of the Buckhorn asphalt district. The Oil Creek is a tar sand, clasts of which can be found in the overlying conglomerate. However the conglomerate is also bitumen-impregnated, indicating that oil migration took place before and after deposition of the Vanoss.

The last-named exposure is of considerable interest in that it displays the unconformity between the Vanoss and the underlying lower Paleozoic, in this case the Lower Ordovician Oil Creek Sandstone. The surface of unconformity has been tilted to the west at ~5°, and the underlying Oil Creek dips to the northeast at ~12° (Fig. 6).

Sedimentology of the Vanoss

General Characteristics

In the area examined, the dominant lithology of the Vanoss is conglomerate, with subordinate sandstone and shale and minor nodular limestones. Two thin, laminated limestones were found, one of which is the “Carla member” of Donovan and Heinlen (1988). Sequences display a crude organization into upward-fining cycles, in which thick conglomerates pass upwards into interbedded sandstones and conglomerates. In turn, these pass upwards into sandstones and siltstones, some of which contain carbonate nodules.

Conglomerates

Conglomerates are composed primarily of well-rounded to subangular limestone and dolomite pebbles and boulders, with lesser amounts of sandstone and siltstone clasts (some of intraformational origin). At the asphalt quarry, angular clasts of bitumen-impregnated sandstone are clearly derived from the underlying Oil Creek Sandstone (Fig. 6). The conglomerates are mostly clast-supported orthoconglomerates with a sandy matrix composed of quartz grains, although a mud matrix is present in some places.

The bases of the thicker conglomerate units mentioned above are markedly erosive, with as much as 3 m of downcutting observed in as little as 10 m of exposure width (Fig. 7). In addition, some impressive undercut channel margins are present (Fig. 8). In general, units are multistoried deposits in which individual beds (from 3 cm to 3 m thick) are characterized by lenticular geometry. The beds are separated by subtle surfaces of erosion that can be distinguished by changes in grain size and, more rarely, by clay drapes. At some locations the conglomerate units show a general fining up-

wards; however most individual beds have a consistent grain size. Large-scale cross-bedding, in sets as much as 1.5 m thick (in one case overturned), was observed at a few locations.

In the Sulphur gravel pit, parallel linear grooves are present on the base of a multistoried conglomerate unit (Fig. 9). These grooves are erosional and may have resulted from the rolling or sliding of large boulders on a muddy substrate (Conybeare and Crook, 1963; Greensmith, 1989). The lineation of these grooves, the orientation of cut banks, and the direction of cross-bed dip and overturn are all consistent with a northward direction of sediment transport (i.e., away from the Arbuckle Mountains).

Sandstones

Most sandstones in the Vanoss are fine grained and quartzose; they form beds from 1 cm to 1 m thick. These sandstones commonly are found above conglomerate beds but also form lenticular beds within conglomerate units. At the western end of Bromide Hill, sandstones are interbedded with siltstones and shales. While most of the sandstones are parallel-laminated, trough cross-bedding, in sets as much as 5 cm thick, is common in the Sulphur gravel pit. Some sandstones contain nodules of limestone.

A second type of sandstone unit is found in the Carla member on Bromide Hill (Donovan and Heinlen, 1988). It comprises thinly bedded fine-grained sandstones and siltstones that are interbedded with thin limestones (Fig. 10). Features of these sandstones include small-scale trough cross-bedding, symmetrical ripple marks, and slightly erosive bases where they overlie limestone layers.

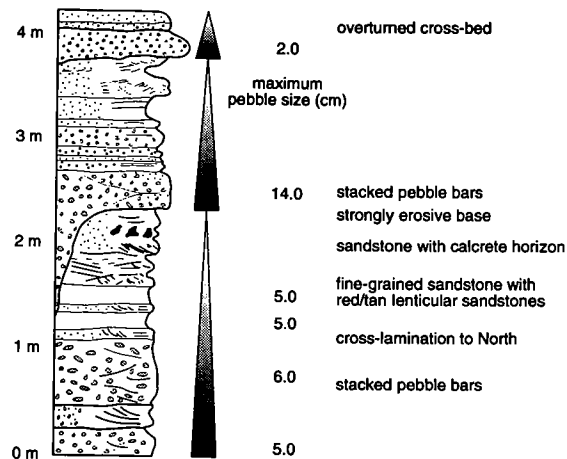


Figure 7. Sketch section of the Vanoss in the north wall of the Sulphur gravel pit. Parts of three upward-fining units are exposed. A calcareous soil profile (calcrete), which marks the top of the lower cycle, is truncated by the highly erosive base of the middle cycle.

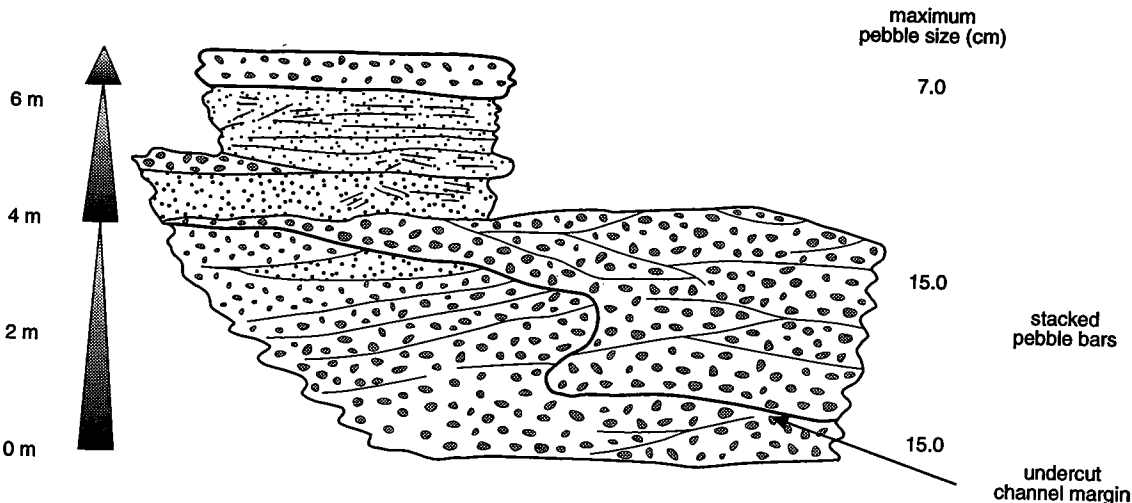


Figure 8. Sketch section of the Vanoss on the east wall of the Sulphur gravel pit, showing part of three upward-fining cycles. The base of the middle cycle displays an undercut channel margin, suggesting that the lower unit was lithified (i.e., cemented by calcite) prior to the deposition of the middle cycle.



Figure 9. Contact between a conglomerate bed and a siltstone on the south wall of the Sulphur gravel pit. The contact is erosional and five basal grooves are oriented north/south.

Shales

Two varieties of shale are found in the Vanoss. The first consists of red fissile shales, forming beds as much as 1.5 m thick, interbedded with horizontally laminated sandstones on Bromide Hill. The second type occurs as lenticular deposits atop conglomerates.

Interpretation of Depositional Environments in the Vanoss

We suggest that deposition of the conglomeratic facies of the Vanoss Formation occurred in a high-energy environment as the proximal facies of an alluvial-fan system. This interpretation, which is in accord with those of Ham (1973), Al-Shaeib and others (1977), and Donovan and Heinlen

(1988), is supported by studies of modern and ancient analogues of alluvial fans (Bull, 1964,1972, 1977; Hooke, 1967; Steel and Wilson, 1975; Steel and Thompson, 1983; Mack and Rasmussen, 1984; Nemec and Steel, 1984). In detail, the massive-appearing conglomerates that commonly occur at or near the base of multistoried units are interpreted as coalesced bars, which were deposited by streams powerful enough to move all but the coarsest of the alluvium. In those cases where lenticular conglomerate beds can be distinguished, either by variations in pebble size and/or sediment drapes, it is suggested that stream power was less effective in totally removing finer material; as a result, individual gravel bars were preserved. Typically, these bar deposits are from 30 cm to 1 m thick and 3–12 m in apparent width. The common occurrence of erosive channel margins and undercut channel edges in these deposits supports the suggestions offered above and implies that avulsion occurred frequently. A small number of thin (as much as 30 cm thick), relatively fine-grained conglomerates show considerable lateral persistence (i.e., throughout the width of available outcrop). These may well record sheet floods similar to those noted by Davis (1938), Bull (1964), Mack and Rasmussen (1984), and Nemec and Steel (1984).

In general, the sandstones offer fewer diagnostic clues as to their depositional environment than do the conglomerates. Within the general alluvial-fan model applied to this sequence, the cross-bedded lenticular sandstones are interpreted as either a record of the migration of small sand bars or as the finer portion of pebble bars. Those sandstones (seen only on Bromide Hill) that are more persistent laterally (i.e., are exposed throughout the width of available outcrop) and are characterized

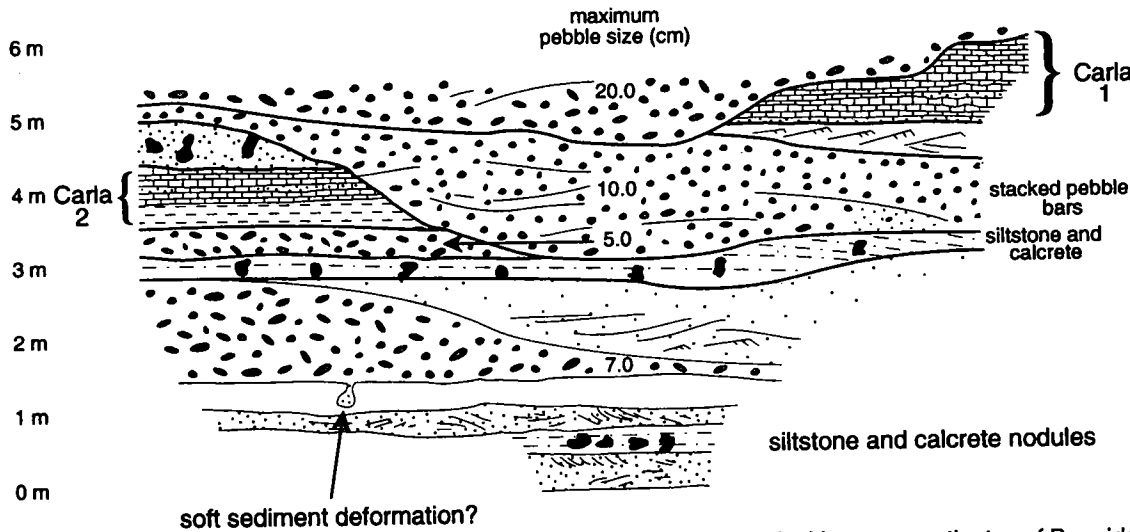


Figure 10. Diagrammatic sketch section of the relationships displayed by the Vanoss near the top of Bromide Hill. Vertical scale exaggerated approximately three times. The section shows a complex interplay between a variety of facies and erosional surfaces. The Carla members are interpreted as lacustrine interludes.

by parallel lamination are similar to those noted by Bull (1972,1977) and DeFeyter and Molenaar (1984). These authors interpret such sandstones as a record of sheet floods on the more distal parts of an alluvial fan.

The preservation of laterally persistent shale and mudstone interbeds in the red-bed sequence at Bromide Hill further suggests a more distal, lower energy setting (Mack and Rasmussen, 1984; Nemec and Steel, 1984; Collinson, 1986). Those lenticular shale deposits that are intimately associated with conglomerates are interpreted as the fillings of abandoned channels on the fan surface (i.e., "clay plugs").

The two thinly bedded sandstone and limestone sequences on Bromide Hill are interpreted as the deposits of a low-energy lacustrine environment, as suggested by Donovan and Heinlen (1988). Within this environment, the clastics are thought to be lake-margin sediments, molded by the wind into sheets of ripple-marked sand, whereas the limestones record higher stands of the lake when algal photosynthesis led indirectly to carbonate precipitation. If this is so, then lamination in the limestones records fluctuations in the algal biomass, and, hence, the carbonate budget of the lake. Such fluctuations have been recorded from several modern lakes (Kelts and Hsu, 1978; Dean and Fouch, 1983). In these instances, it can be shown that the laminae are varves (i.e., they record annual cycles). If the laminae seen in the thinly bedded limestones record annual fluctuations, then a count of the number of "varves" in the Carla member, as defined by Donovan and Heinlen (1988), suggests that the lake system existed for ~1,000 years.

Fenestrae which cut the primary micrite fabric probably record the escape of gas from the partially lithified sediment as the algae decayed. Lake dessication is recorded by the mud cracks that formed during particularly dry seasons; the intraformational clasts within sandstones are a record of stormy conditions.

A lacustrine interpretation for these limestones is supported by carbon- and oxygen-isotope data. The analyzed samples plot near the field for freshwater limestones (Fig. 11).

On textural evidence, the nodular limestones have been interpreted as fossil soils or calcretes by Al-Shaeib and others (1977) and Donovan and Heinlen (1988). In detail, these densely micrite limestones show the sparry calcite-filled circumgranular cracks that are commonly shown by calcretes (Steel, 1974; Leeder, 1975). This interpretation also is supported by carbon- and oxygen-isotope data which indicate a freshwater origin for the carbonate (Fig. 11).

Many modern calcretes form as a result of the accumulation of calcite in soil horizons in evaporative, semi-arid conditions. These deposits begin

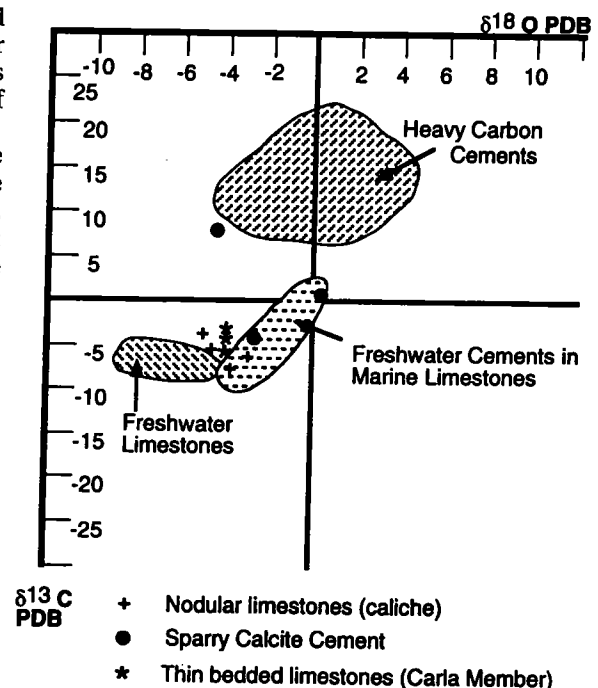


Figure 11. The isotope data presented here were obtained from three separate limestone layers in the Carla member, four calcrete (caliche) horizons, and three sparry cements. With the exception of the values for two cements, all the data "cluster" around a value of approximately $-4 \delta^{18}\text{O PDB}$ and $-7 \delta^{13}\text{C PDB}$. As all the clustering values were obtained from samples that were identified as early precipitates in the Vanoss system, it is suggested that the isotope cluster average can be regarded as a general value for contemporary ground water. The other two cement values were obtained from cements that, on textural grounds, were suspected to be later precipitates. Field boundaries from Hudson (1977).

as a chalky, porous horizon, and progressively lose porosity and permeability as calcium carbonate precipitation continues within the soil profile. The resulting rock can range from a thick, dense, massive limestone to an irregular, nodular horizon (Estaban and Klappa, 1983).

The formation of calcretes in continental deposits of the Vanoss type normally requires semi-arid conditions and long periods of geomorphic stability (Leeder, 1975). Hence, the recognition of calcretes in the Vanoss has important paleogeographic and paleoclimatic implications. The Vanoss calcretes presumably record the beginning of the increasing aridity that characterized the Permian of the Midcontinent. Calcretes observed in the Vanoss can all be classified as immature (i.e., small, irregular-shaped nodules composing <10% of the host rock; Stage One of Steel, 1974). Accord-

ing to the data accumulated by Leeder (1975), such deposits may have taken 1,000–4,500 years to form.

Within a regional context, it is pertinent to note that calcretes also are found commonly in Lower Permian conglomeratic sequences (the Post Oak Conglomerate), which mantle the Wichita Mountains and Slick Hills in southwestern Oklahoma (Donovan, 1982, 1986). In this area, calcretes are more mature than those in the Vanoss Formation. This change probably records a decrease in sedimentation rates, which in turn may be linked to decreased tectonic activity in the aulacogen.

Cycles in the Vanoss

As noted previously, the Vanoss Formation, which is characterized by coarse-grained alluvial-fan conglomerates, fine-grained floodplain sandstones, lake limestones, and fossil soil horizons, displays a contrasting variety of facies. The juxtapositions of these facies suggests that the Vanoss records a time when considerable environmental fluctuation occurred. Frequent avulsion is indicated by preserved channel margins and clay plugs, whereas flashy discharge is suggested by preserved bar forms, sediment drapes, and sheet flood deposits.

The architecture of the Vanoss provides evidence for contemporary erosion in the form of cut banks, oversized intraformational clasts, and erosive bases that may cut deeply into underlying beds. Thus, it is clear that the Vanoss preserves only a fraction of the sediment that was transported into the area of deposition.

Somewhat crudely defined cycles can be recognized in the Vanoss. Each cycle begins with an erosive base, overlain by conglomerates. The cycle may then fine upward, first into sandstones and then shales; it may be capped by a calcrete horizon. More rarely, cycles may be capped by a sequence of lacustrine origin. Cycles may be partially or fully preserved, depending on the degree of erosion at the base of the overlying cycle. Few cycles appear to persist laterally, largely because of erosion before deposition of the overlying cycle.

Fining-upwards cycles in alluvium have been described frequently (Hooke, 1967; Mack and Rasmussen, 1984; Nemec and Steel, 1984; Walker and Cant, 1984; Collinson, 1986). They fall into two broad categories; autochthonous (i.e., the product of the depositional system itself) or allochthonous (i.e., a response to an outside control, such as tectonism or climatic fluctuation). Two varieties of autochthonous cycles have been recognized: those attributable to meandering streams and those produced by braided systems. The Vanoss cycles resemble the latter, as described in the works of Hooke (1967), DeFeyter and Molenaar (1984), Mack and Rasmussen (1984), and Nemec and Steel (1984).

It is possible that all of the features of the Vanoss Formation could be explained by autocyclic controls. However, the sequence contains some features that can be used to indicate a degree of allocyclic influence. For example, the joint occurrence of calcretes and lake beds can be used to support the argument that long-term climatic fluctuations were taking place during Vanoss deposition. The calcretes may record extended semiarid periods when little sediment movement took place on the fan surface; during ensuing extended wet periods, incision and transport could have been accelerated.

The weakness of this argument is that the case for extended wet climatic periods is based primarily on the suggestion that the laminae in the limestones of the Carla member are varves. This may not be the case; it is possible that the lake systems may have existed for a much shorter period of time as flood-plain ponds. If the latter is the case, then calcrete formation and the existence of short-period lakes are not necessarily exclusive phenomena. At present, no firm conclusions can be drawn to resolve the argument, although it may be significant that the Carla member limestones contain no evidence of evaporite precipitation.

Evidence of Contemporary Tectonic Activity

It is also possible that tectonism provided an allocyclic control during deposition of the Vanoss by rejuvenating fan systems. The most striking evidence for contemporaneous tectonic activity in the Vanoss occurs on Bromide Hill. Here, a small fault, trending approximately north-south and exposed in a cliff face, appears to have formed before lithification of the conglomerate (Fig. 12). The fault can only be detected where it cuts thin sandstones; it cannot be traced into adjacent conglomerate horizons. It is suggested that pebbles in the unlithified conglomerate layers reacted to fault-related stresses by rolling instead of breaking.

In order to test this idea, the inclination from horizontal of the long axis of elongate pebbles (with a length-width ratio of at least 2:1) within a single stratigraphic level was compared for areas on either side of, and within, the presumed fault zone. A significant change was noted in the fabric of the conglomerate near the fault trace. This change in pebble orientation supports the suggestion that the pebbles were reorganized as a result of fault movement, before lithification of the conglomerate.

A second indication of seismic/tectonic activity in the Vanoss is the occurrence of sand dikes at the Sulphur gravel pit (Fig. 13). The dikes are restricted to a single horizon and, in at least one case, have an eroded top. Numerous authors (e.g., Friend and Williams, 1978) associate clastic dikes (injected from below) with earthquake disturbances.

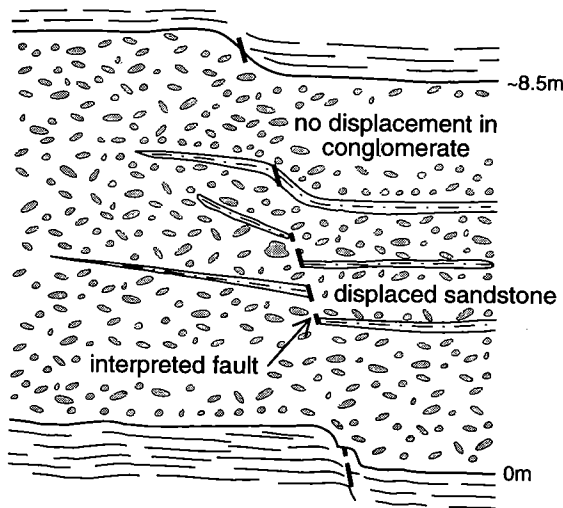


Figure 12. Diagrammatic field sketch of the lower part of the cliff on Bromide Hill. The cliff trends approximately east-west and the view is to the south; i.e., east is to the left of the view. The sketch illustrates a small north-south-trending normal fault that clearly cuts sandstone layers but does not have a discrete zone of severance where it crosses conglomerates. However, pebbles have been rotated within the projected trend of the fault, suggesting that it is an early prelithification structure.

The presence of faults and sand dikes suggests that, although Pennsylvanian tectonic activity had waned, the Arbuckle area had not stabilized completely. It should be noted in this regard that Donovan and others (1989) have found evidence that tectonic activity in the Wichita uplift area continued into the Early Permian.

Detrital Mineralogy of the Vanoss

As noted previously, most of the pebbles in the Vanoss are varieties of carbonate; subordinate chert, quartzose sandstone, granite, and intraformational clasts are also found. In the sandstones and the sandy matrix of the conglomerates, the majority of the framework grains are quartz and limestone fragments. Smaller amounts of dolomite, feldspar, chert, sandstone, granite, and other grains are also present.

Quartz

Two distinct populations of quartz-sand grains can be distinguished on the basis of size and roundness. The most common type is well-rounded, well-sorted, medium- to fine-grained quartz, which is found throughout the area examined. The majority of this population is monocrystalline and nonundulose; there are lesser amounts of mono-

crystalline undulose quartz and only a trace of polycrystalline quartz.

The second quartz type consists primarily of coarse, angular or subangular, poorly sorted grains, found primarily in the area of the Sulphur gravel pit. This population contains roughly equal amounts of monocrystalline nonundulose and monocrystalline undulose quartz grains; there is a substantial percentage of polycrystalline quartz.

Feldspars

Microcline is much the most common K-feldspar present. Plagioclase feldspars are rare. As in the case of quartz, two distinct populations of feldspars can be separated on the basis of size and roundness. The less common type of feldspar consists of fine, well-rounded microcline grains. Members of this population are found throughout the study area, are mostly unaltered, and are commonly coated by a rim of hematite.

The more common type of microcline consists of coarse, angular grains of variable size and is found primarily at the Sulphur gravel pit. A majority of this population exhibits some degree of chemical alteration, mostly to calcite and kaolinite; the degree of alteration varies greatly, which suggests that the clasts have been subject to variable rates of weathering, erosion, and deposition. These clasts are commonly associated with the coarse, angular quartz grains that make up the second population of quartz grains described above.

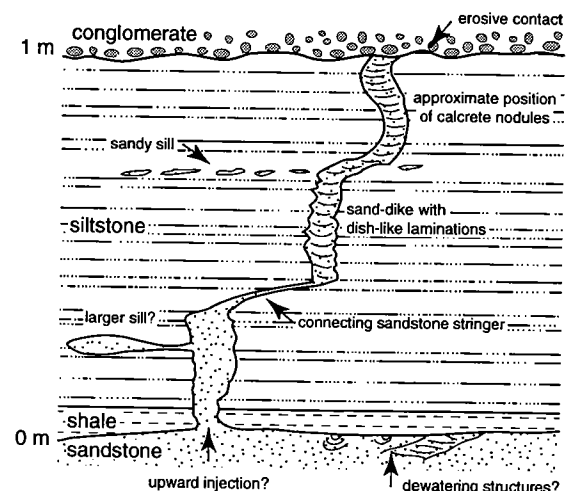


Figure 13. Field sketch of a clastic-dike horizon exposed in the south wall of the Sulphur gravel pit. The dish-like laminations possibly are due to the escape of water during repacking of the sand within the dike. The overlying conglomerate is at least 4 m thick and has a markedly erosive base.

Rock Fragments

As noted previously, several types of rock fragments are found throughout the Vanoss study area. These include limestone, dolomite, quartzose sandstone, siltstone, chert, granite, and gneiss. Limestone fragments are ubiquitous, and they contain a wide variety of fossils. Staining indicates that some of the limestones are Fe-rich, whereas others are Fe-poor.

Various amounts and proportions of quartzose sandstone and chert fragments also are ubiquitous. The relative proportions of the sandstone and chert fragments show no apparent pattern with regard to stratigraphic position or geographic location.

In contrast, granite, gneiss and dolomite fragments are restricted mostly to the Sulphur gravel pit. All granitic clasts show some degree of feldspar alteration, including both replacement by calcite and alteration to kaolinite. The majority of granitic fragments contain very large microcline phenocrysts; these usually are heavily altered to kaolinite.

Miscellaneous Detrital Grains

Miscellaneous detrital grains, found only in trace amounts, include glauconite, detrital zoned dolomite, and biotite. Some of the biotite is relatively fresh, but some is largely pseudomorphed by chlorite.

Provenance of the Vanoss

All of the clasts found within the Vanoss Formation appear to be derived from local sources (i.e., they can be related to the local stratigraphic section). This section is composed of a thick sequence of carbonates, quartzose sandstones, and shales deposited during the early Paleozoic subsiding stage of the southern Oklahoma aulacogen. These sedimentary rocks overlie either Precambrian granites or Cambrian rhyolite (Denison, 1973).

Limestone clasts, the most common detrital grains, have several possible sources: these include limestones in the Arbuckle, Simpson, Viola, and Hunton Groups (Fig. 14). All of these rocks are currently exposed in the Arbuckle Mountains, south of the area examined. As noted previously, paleocurrent data also suggest that the source area lay to the south.

Chert fragments in the Vanoss also are thought to have been derived locally. Possible sources include the Hunton, Arbuckle, and Viola Groups, all of which crop out south of the study area and contain significant amounts of chert.

As noted previously, most quartz grains are fine grained, well rounded, monocrystalline, and non-undulose. It is suggested that these grains are at least second cycle, with several possible sources. At the asphalt quarry, a major source is undoubtedly the Oil Creek Formation of the underlying Simpson Group (Denison and Ham, 1973). Other pos-

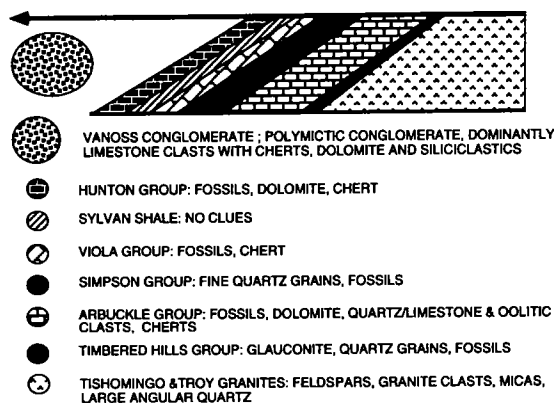


Figure 14. Diagrammatic representation of the potential sources of detritus available during deposition of the Vanoss, showing the various "clues" that can be used to determine provenance.

sible sources for this population of quartz include other sandstones within the Simpson Group, the Reagan Formation, and possibly the Arbuckle Group, where quartz-rich horizons are known (Ragland and Donovan, 1985). The latter two units may well have been the source of the fine, well-rounded and well-sorted microcline population.

The second population of quartz is composed of large, angular, poorly sorted undulose and non-undulose quartz grains. These grains are found mostly in the area of the Sulphur gravel pit and commonly are associated with granitic fragments and large feldspar fragments. We suggest that these grains are first cycle, derived from local outcrops of the Tishomingo Granite and associated intrusions. A similar source is suggested for the second population of feldspars, which consists of coarse, angular, K-feldspar grains. Likewise, granitic fragments are found mostly in the Sulphur gravel pit area. The Tishomingo Granite and related intrusives crop out southeast of the Sulphur area. A northward transport direction, as indicated by the paleocurrent data, would provide a direct pathway for granite clasts to be transported from the Tishomingo outcrops to the Sulphur pit, while passing east of the other areas studied.

Miscellaneous grains, such as glauconite and zoned dolomite, also can be used to define the source of clasts in the Vanoss. The source for glauconite in the Vanoss is thought to be the Reagan and Honeycreek Formations, but could include the lower part of the Arbuckle Group, the Hunton Group, or the Mississippian Sycamore Formation (Donovan, 1986). Zoned dolomite commonly is found in both the Simpson and Arbuckle Groups. The rare gneiss encountered was probably derived from the Blue River Gneiss, a sequence that is intruded by the Tishomingo Granite and is the oldest rock exposed in Oklahoma.

Diagenesis of the Vanoss

Post-depositional modifications within the Vanoss Formation are mostly simple and straightforward. The rocks are variably lithified, depending on the degree of cementation to which they have been subjected. Cements consist of drusy calcite primarily and of smaller amounts of kaolinite, quartz, dolomite, bitumen, pyrite; minor chlorite is present.

In some conglomerate exposures, large, clear, and void-filling sparry calcite can be seen readily. Calcite of this type commonly occurs as a poikiloplastic cement with respect to the smaller detrital grains. Most of this cement is Fe-poor, but small amounts of Fe-rich calcite are present. In addition, calcite also replaces detrital feldspar grains. The degree of this replacement varies from minor to complete.

Kaolinite occurs both as pore-filling vermiform booklets and as an alteration product of microcline. Minor amounts of quartz cement, seen as euhedral syntaxial overgrowths on detrital quartz grains, are found in sandstones and less commonly in the conglomerates.

Dolomite occurs both as syntaxial overgrowth on detrital dolomite grains and as pore-filling cement. Stained sections indicate that the overgrowths are ferroan, whereas most of the detrital clasts are non-ferroan. Dolomite cement is most common in the Sulphur gravel pit.

Pyrite is common in the sandstones at the asphalt quarry and is associated with caliche horizons throughout the area. Pyrite cement generally shows a displacive texture and forms small, irregularly shaped nodules.

Sequence of Diagenetic Events

The sequence of events in the diagenetic history of the Vanoss Formation varies with location (Fig. 15). At the asphalt quarry, the first diagenetic event recorded was the migration of hydrocarbons into the sandstones and conglomerates, as evidenced by thin coatings of bitumen on most grains. Migration early in the diagenesis of the rock resulted in some of the channel sands becoming completely impregnated with bitumen. In such rocks, bitumen is the only cement present. In other areas, the bitumen is present only as a thin and incomplete coating around detrital grains; other minerals, dominantly calcite and pyrite, cement the rock. Trace amounts of syntaxial quartz overgrowths, followed by pore-filling kaolinite, also formed at this location.

Elsewhere, cementation patterns are more complex. In some areas, an early generation of calcite was precipitated, either as sparite between pebbles (as evidenced by preserved cut banks in conglomerates) or in the form of caliche horizons. The latter are discontinuous, cementing only cer-

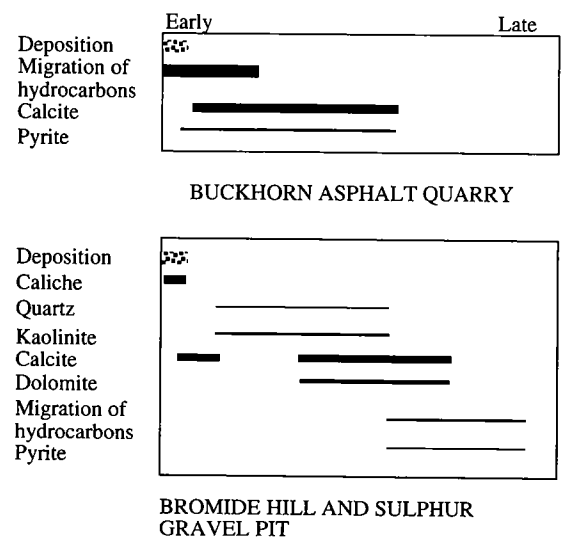


Figure 15. The early migration of hydrocarbons into the Vanoss led to a considerable restriction in the variety and amount of cements in the Buckhorn area. Where hydrocarbon infiltration was delayed, as at Bromide Hill and the Sulphur gravel pit, a more complex diagenetic history developed.

tain stratigraphic levels. Because caliche formation took place in an active alluvial-fan setting, some caliche was reworked into overlying sediments.

Where present, quartz and kaolinite appear to predate other cements, excluding the aforementioned calcite. For example, intergrown syntaxial quartz overgrowths and kaolinite booklets line the walls of pores which have been filled subsequently by calcite and ferroan dolomite.

The mineralogy of the later carbonate cements varies with location. At Bromide Hill, the predominant cement type is calcite, whereas at the Sulphur gravel pit, dolomite cements are present in significant amounts. Thus, the general cementation sequence is early calcite (including caliche), followed by silica and kaolinite, and a final precipitation of carbonate.

Only minor amounts of hydrocarbon are present on Bromide Hill and at the Sulphur gravel pit. Here the hydrocarbons appear to postdate much of the cementation and are commonly associated with pyrite.

Hydrocarbons

The Vanoss Formation is somewhat unusual in that it overlies an unconformity that records erosion of an oil-saturated formation. At the asphalt quarry, the Vanoss rests unconformably on the Ordovician Oil Creek Sandstone. The Oil Creek in this area is a mineralogically and texturally super-mature sandstone, characterized by very high pri-

mary porosity and permeability (Denison and Ham, 1973). The only impediment to oil migration into this rock was provided by impersistent pressure-solution seams and minor amounts of poikilitic calcite cement. As a result, the Oil Creek is saturated with bitumen and forms a commercial tar-sand deposit. The source rock for hydrocarbons in this area is thought to be the Woodford Shale (Cardott and Lambert, 1985). Basin-subsidence curves for the Sulphur area indicate the Woodford was at depths great enough for source-rock maturation ~25 million years before deposition of the Vanoss (Fig. 16).

At the asphalt quarry, the Vanoss contains clasts of bitumen-impregnated Oil Creek Sandstone in a sandy matrix that is not impregnated with bitumen. This indicates that hydrocarbons were present in the Oil Creek during deposition of the Vanoss. On the other hand, several of the channel sands in the Vanoss are impregnated with bitumen, suggesting that hydrocarbon migration continued during and after Vanoss deposition.

The early presence of oil in the asphalt quarry affected the diagenesis of the Vanoss in that it plugged most of the available pore space and effectively inhibited cement precipitation, except for minor amounts of calcite and pyrite. In the latter context, migrating hydrocarbons in the form of hydrogen sulphide gas may have provided a source of sulfur for the pyrite.

Isopach maps produced by Johnson and others (1988) indicate a maximum burial depth of only about 300 m for the Vanoss in the area of study. This shallow depth suggests that pressure and temperature conditions have not varied significantly since early in the history of the formation.

Source of Cements in the Vanoss

Carbonate minerals, particularly calcite, are the most common cement type in the Vanoss. The absence of grain-to-grain contacts and pressure dissolution of carbonate grains suggests that most of the carbonate making up the cement was derived from sources other than dissolution of detrital grains in the formation. This is in marked contrast to the nearby Collings Ranch Conglomerate, where tectonically controlled pressure solution has greatly modified many clast shapes and is probably responsible for much of the patchy calcite cement in that formation (Donovan and Heinen, 1988).

We suggest that most cements in the Vanoss were precipitated from waters that had flowed across or through the lower Paleozoic section, and that variations in the type of cement reflect local variations in this section. For example, south and east of the Sulphur gravel pit, where the Vanoss contains much dolomite cement, the Arbuckle Group outcrops contain more dolomite than in other areas.

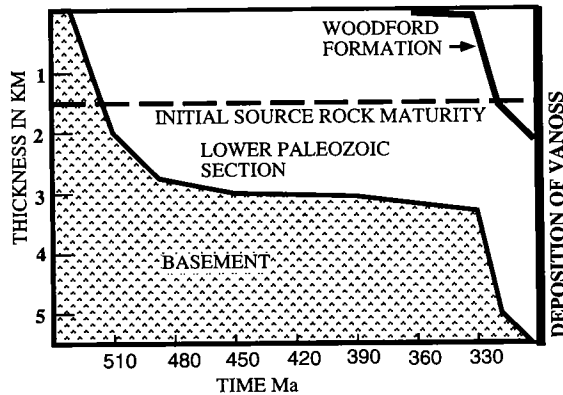


Figure 16. The history of the southern Oklahoma aulacogen in the Arbuckle Mountain area, showing how the Woodford was activated as a hydrocarbon source rock prior to Vanoss deposition.

In addition, it is clear that fluids from deeper sources were moving through parts of the Vanoss almost from the moment of deposition. The most obvious evidence for this is the occurrence of hydrocarbons in the Buckhorn asphalt quarry. Supporting evidence is provided by syntaxial overgrowths of ferroan dolomite around nonferroan dolomite clasts. Additionally, while carbon- and oxygen-isotope data suggest that the calcite cements in most areas were deposited from meteoric waters, one sample from Bromide Hill showed relatively heavy carbon values that might be related to oil-field brines migrating upwards from the subsurface (Fig. 11). Such brines characteristically show a heavy carbon-isotope signature (Scoffin, 1987). It is pertinent that the numerous flowing natural springs around Bromide Hill, which have high ionic concentrations and presumably are waters derived from some depth, indicate that such migration paths exist to this day; it may be significant also that a number of small oil seeps were found on Bromide Hill in the course of this study.

As in the case of calcite and dolomite, the source of silica for the quartz overgrowths may be from outside the Vanoss. The lack of grain-to-grain contacts and corrosion surfaces implies that no silica dissolution has taken place within the Vanoss. Likely external sources of silica include the Simpson Group (much of which is quartzose) and the Arbuckle Group (which contains quartz sandstones as well as numerous cherty layers). Alternatively, it is possible that the alteration of detrital feldspars in the Vanoss supplied at least some of the silica.

In summary, we think that the flow of ground water through the Vanoss was controlled both by a topographically controlled hydraulic gradient related to the adjacent Arbuckle uplift (in the case of near-surface ground waters) and by structural

overpressuring related to the dismemberment of the aulacogen (in the case of deeper, reducing and hydrocarbon-related brines, Fig. 17). Thus, cementation patterns in the Vanoss mostly reflect the interplay of two aqueous systems, both of which were allochthonous to the formation.

GENERAL CONCLUSIONS OF THE VANOSS STUDY

The detrital mineralogy of the Vanoss Formation is dominated by well-rounded limestone and dolomite clasts, with a sandy matrix composed primarily of well-rounded, well-sorted, fine-grained quartz. Lesser amounts of feldspar, sandstone and siltstone fragments, granitic fragments, chert, glauconite, and biotite are also present.

In response to tectonism associated with dismemberment of the southern Oklahoma aulacogen, the conglomeratic portion of the Vanoss was deposited late in the Pennsylvanian (Virgilian) in an alluvial-fan environment fringing the Arbuckle Mountains. The environment was dominated by erosive braided streams with flashy discharges. The resulting deposits include interbedded conglomerates, sandstones, shales, caliche horizons, and lake beds. The association of these widely varied facies attests to the environmental instability characteristic of an active alluvial-fan tract. The climatic imprint on the sequence is problematical. Abundant calcrete horizons attest to semi-arid conditions. On the other hand, two lacustrine deposits indicate that higher water tables may have developed from time to time. The duration of these presumably wetter periods is uncertain.

All of the detritus in the Vanoss appears to have been derived from local sources; it is clear that the entire lower Paleozoic section and the underlying basement granites in the Tishomingo area were exposed in Vanoss time. Variations in clast composition permit some discrimination of source area. A relatively small number of paleocurrent readings suggest that the dominant direction of transport was to the north.

Factors influencing the diagenesis of the Vanoss include a semi-arid climate (under which caliche formed), the early presence of hydrocarbons (migrating contemporaneously with deposition at one location), and a generally shallow burial depth. The most commonly seen sequence of cements is caliche and early sparite, followed by silica and kaolinite, and subsequently carbonate of meteoric origin. However, this paragenesis is not always fully developed, and was inhibited by hydrocarbon migration in some areas.

The Vanoss is characterized by crudely developed cyclicity. In general, such cycles average 3–4 m thick. Characteristically they have markedly erosive bases overlain by pebble conglomerates. The conglomerates fine upwards into sandstones

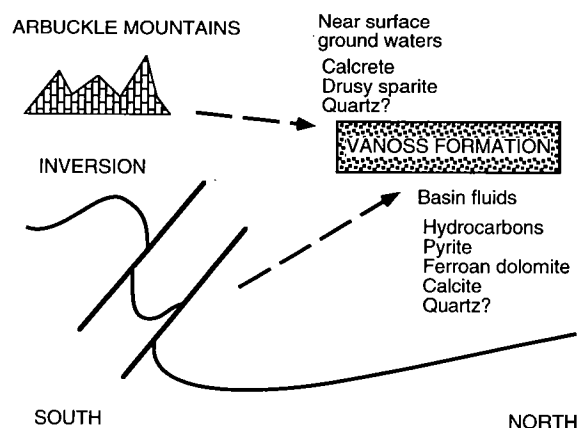


Figure 17. A schematic model illustrating the suggestion that, as a result of partial tectonic inversion of the southern Oklahoma aulacogen, early diagenesis of the Vanoss was controlled by the interplay of near-surface and deeper basinal fluids.

and siltstones. The latter may contain fossil soil horizons (calcrete); in two cases, thin lacustrine limestones are developed at the top of the cycles. Throughout the study area, the average size of pebbles within the conglomerate does not change significantly. The consistent grain size has two possible explanations: either the areas examined are on the same stratigraphic level, or tectonic activity resulted in a rate of uplift of the source area equal to the rate of erosion.

The Vanoss preserves some evidence of contemporary tectonism. This is seen as a single horizon of clastic dikes and a fault that appears to be syndepositional. The origin of the Vanoss cycles is not completely clear, but evidence found in this study suggests that they may reflect a combination of allocyclic (tectonic and climatic) and autocyclic (depositional) controls.

Our general conclusion is that the Vanoss may represent a fruitful model against which to measure the depositional architecture and diagenetic histories of other inversion-related proximal deposits in southern Oklahoma.

ACKNOWLEDGMENTS

We gratefully acknowledge the financial support of the Adkins Fund and Moncrief Chair of Geology at Texas Christian University. We are indebted to Randy Hosey for his help with drafting.

REFERENCES CITED

- Al-Shaieb, Z.; Shelton, J. W.; Donovan, R. N.; Hanson, R. E.; May, R.; Hansen, C.; Morrison, C.; White, S.; and Adams, S., 1977, Evaluation of uranium potential in selected Pennsylvanian and Permian units and igneous rocks in southwestern and southern

- Oklahoma: Report for the U.S. Department of Energy, contracts 76-024-E and EY-76-13-1664, 248 p.
- Al-Shaieb, Z.; Hanson, R. E.; Donovan, R. N.; and Shelton, J. W., 1980, Petrology and diagenesis of sandstones in the Post Oak Formation (Permian), southwestern Oklahoma: *Journal of Sedimentary Petrology*, v. 50, p. 43–50.
- Bull, W. B., 1964, Alluvial fans and near-surface subsidence in western Fresno County, California: U.S. Geological Survey Professional Paper 437-A.
- 1972, Recognition of alluvial fan deposits in the stratigraphic record, in Rigby, J. K.; and Hamblin, W. K. (eds.), *Recognition of ancient sedimentary environments: Society of Economic Paleontologists and Mineralogists Special Publication 16*, p. 63–83.
- 1977, The alluvial-fan environment: Progress in physical geography, v. 1, p. 222–270.
- Cardott, B. J.; and Lambert, M. W., 1985, Thermal maturation by vitrinite reflectance of Woodford Shale, Anadarko Basin, Oklahoma: *American Association of Petroleum Geologists*, v. 69, p. 1982–1998.
- Collinson, J. D., 1986, Alluvial sediments, in Reading, H. G. (ed.), *Sedimentary environments and facies: Blackwell Scientific Publications*, Oxford, p. 20–54.
- Conybeare, C. E. B.; and Crook, K. A. W., 1963, Manual of sedimentary structures: Bulletin No. 102, Department of National Development, Bureau of Mineral Resources, Geology and Geophysics, 327 p.
- Davis, W. M., 1938, Sheetfloods and streamfloods: *Geological Society of America Bulletin*, v. 49, p. 1337–1416.
- Dean, W. E.; and Fouch, T. D., 1983, Lacustrine environments, in Scholle, P. A.; Bebout, D. G.; and Moore, C. H. (eds.), *Carbonate depositional environments: American Association of Petroleum Geologists Memoir 33*, p. 97–130.
- DeFeyter, A. J.; and Molenaar, N., 1984, Messinian fanglomerates: the Colambacci Formation in the Dietrarubbia Basin, Italy: *Journal of Sedimentary Petrology*, v. 54, p. 746–758.
- Denison, R. E., 1973, Basement rocks in the Arbuckle Mountains, in Ham, W. E. (ed.), *Regional geology of the Arbuckle Mountains, Oklahoma: Oklahoma Geological Survey Special Publication 73-3*, p. 43–45.
- Denison, R. E.; and Ham, W. E., 1973, Oil Creek (Middle Ordovician) in quarry of Pennsylvania Glass Sand Corp., in Ham, W. E. (ed.), *Regional geology of the Arbuckle Mountains, Oklahoma: Oklahoma Geological Survey Special Publication 73-3*, p. 49–51.
- Donovan, R. N., 1982, Blue Creek Canyon, in Gilbert, M. C.; and Donovan, R. N. (eds.), *Geology of the eastern Wichita Mountains, southwestern Oklahoma: Oklahoma Geological Survey Guidebook 21*, p. 148–153.
- 1986, Geology of the Slick Hills, in Donovan, R. N. (ed.), *The Slick Hills of southwestern Oklahoma—fragments of an aulacogen?: Oklahoma Geological Survey Guidebook 24*, p. 1–12.
- 1991, The Arbuckle Group—an aide de memoir, in Johnson, K. S. (ed.), *Arbuckle Group core workshop and field trip: Oklahoma Geological Survey Special Publication 91-3*, p. 199–208.
- Donovan, R. N.; and Heilen, W. D., 1988, Pennsylvanian conglomerates in the Arbuckle Mountains, southern Oklahoma, in Hayward, O. T. (ed.), *South-Central Section: Geological Society of America Centennial Field Trip Guide*, v. 4, p. 159–164.
- Donovan, R. N.; Marchini, W. R. D.; McConnell, D. A.; Beauchamp, W.; and Sanderson, D. J., 1989, Structural imprint on the Slick Hills, southern Oklahoma: *Oklahoma Geological Survey Circular 90*, p. 78–84.
- Donovan, R. N.; Busbey, A. B.; Elmore, R. D.; and Engel, M. H., 1992, Oil in Permian karst in the Slick Hills of southwestern Oklahoma, in Johnson, K. S.; and Cardott, B. J. (eds.), *Source rocks in the southern Midcontinent, 1990 symposium: Oklahoma Geological Circular 93*, p. 198–209.
- Friend, P. F.; and Williams, B. P. J. (eds.), 1978, A field guide to selected outcrop areas of the Devonian of Scotland, the Welsh Borderland and South Wales: *The Paleontological Association, London*, 106 p.
- Greensmith, J. T., 1989, *Petrology of sedimentary rocks [7th edition]: University Printing House, Oxford*, 262 p.
- Ham, W. E., 1973, *Regional geology of the Arbuckle Mountains, Oklahoma: Oklahoma Geological Survey Special Publication 73-3*, 63 p.
- Ham, W. E.; and McKinley, M. E., 1954, Geologic map and sections of the Arbuckle Mountains, Oklahoma: *Oklahoma Geological Survey Map A-2*.
- Hooke, R. Le B., 1967, Processes on arid region alluvial fans: *Journal of Geology*, v. 75, p. 438–460.
- Hudson, J. D., 1977, Stable isotopes and limestone cement: *Geology*, v. 3, p. 19–22.
- Johnson, K. S.; Amsden, T. W.; Denison, R. E.; Dutton, S. P.; Goldstein, A. G.; Rascoe, Bailey, Jr.; Sutherland, P. K.; and Thompson, D. M., 1988, Southern Midcontinent region, in Sloss, L. L. (ed.), *Sedimentary cover—North American craton; U.S.: Geology of North America: Geological Society of America, Decade of North American Geology*, v. D-2, p. 307–359. [Reprinted as *Geology of the southern Midcontinent: Oklahoma Geological Survey Special Publication 89-2*, 1989, 53 p.]
- Kelts, K.; and Hsu, K. J., 1978, Freshwater carbonate sedimentation, in Lerman, A. (ed.), *Lakes: chemistry, geology, physics: Springer-Verlag, Berlin*, p. 297–323.
- Leeder, M. R., 1975, Pedogenic carbonates and flood sediment accretion rates: a quantitative model for alluvial and arid-zone lithofacies: *Geological Magazine*, v. 112, p. 257–270.
- Mack, G. H.; and Rasmussen, K. A., 1984, Alluvial fan sedimentation of the Cutler Formation (Permian-Pennsylvanian) near Gateway, Colorado: *Geological Society of America Bulletin*, v. 95, p. 109–116.
- McConnell, D. A., 1989, Constraints on magnitude and sense of slip across the northern margin of the Wichita uplift, southwest Oklahoma, in Johnson, K. S. (ed.), *Anadarko basin symposium, 1988: Oklahoma Geological Survey Circular 90*, p. 85–96.
- Morgan, G. D., 1924, *Geology of the Stonewall Quadrangle, Oklahoma: Oklahoma Bureau of Geology Bulletin 2*, 248 p.
- Nemec, W.; and Steel, R. J., 1984, Alluvial and coastal conglomerates: their significant features and some

- comments on gravel mass-flow deposits, *in* Koster, E. H.; and Steel, R. J. (eds.), *Sedimentology of gravels and conglomerates*: Canadian Society of Petroleum Geologists Memoir 10, p. 1–31.
- Ragland, D. A.; and Donovan, R. N., 1985, The Thatcher Creek Member: basal unit of the Cool Creek Formation in southern Oklahoma: *Oklahoma Geology Notes*, v. 45, p. 84–91.
- Scoffin, T. P., 1987, *An introduction to carbonate sediments and rocks* (first edition): Blackie and Sons, Ltd., Glasgow and London, 274 p.
- Shatski, N. S., 1946, The Great Donetz basin and Wichita System, comparative tectonics of ancient platforms: *Akademiya Nauk SSSR Izvestiya, Seriya Geologicheskaya*, no. 6, p. 57–90.
- Steel, R. J., 1974, Cornstone (fossil caliche)—its origin, stratigraphic and sedimentological importance in the New Red Sandstone, Western Scotland: *Journal of Geology*, v. 82, p. 351–369.
- Steel, R. J.; and Thompson, D. B., 1983, Structures and textures in Triassic braided stream conglomerates (Bunter Pebble Beds) in the Sherwood Sandstone Group, North Staffordshire, England: *Sedimentology*, v. 30 p. 341–367.
- Steel, R. J.; and Wilson, A. C., 1975, Sedimentation and tectonism on the margin of the North Minch basin, Lewis: *Journal of the Geological Society of London*, v. 131, p. 183–202.
- Stephenson, M. D.; and Donovan, R. N., 1991, Pennsylvanian deformation in the eastern Slick Hills, southwestern Oklahoma: *Geological Society of America Abstracts with Programs*, v. 23, no. 4, p. 97.
- Tanner, W. F., 1956, *Geology of Seminole County, Oklahoma*: Oklahoma Geological Survey Bulletin 74, 170 p.
- Thomas, J., 1973, Mineralogic dispersal patterns of the Vanoss Formation, south-central Oklahoma: University of Oklahoma unpublished Ph.D. thesis, 162 p.
- Walker, R. G.; and Cant, D. J., 1984, Sandy fluvial systems, *in* Walker, R. G. (ed.), *Facies models: Geosciences*, Canada, p. 71–89.
- Younger, Paul; Donovan, R. N.; and Hounslow, A. W., 1986, Barite travertine at Zodletone Mountain in the Slick Hills, southwestern Oklahoma, *in* Donovan, R. N. (ed.), *The Slick Hills of southwestern Oklahoma—fragments of an aulacogen?*: Oklahoma Geological Survey Guidebook 24, p. 75–81.

Petrology and Sedimentology of Morrow/Springer Rocks and Their Relationship to Reservoir Quality, Anadarko Basin, Oklahoma

C. William Keighin and Romeo M. Flores

U.S. Geological Survey
Denver, Colorado

ABSTRACT.—Petrographic examination of 100 samples of sandstone from Springer and Morrow rocks (Mississippian and Pennsylvanian age) from 30 core holes in the Anadarko basin, ranging in depth from 4,000 to 18,000 ft, reveals pervasive diagenetic alterations that enhance or diminish reservoir quality. Facies analysis of cores collected from drill holes ranging from Texas County, in the Oklahoma Panhandle, to Grady County, in the southwestern portion of the Anadarko basin, indicates three types of depositional facies: (1) fluvial-influenced coastal; (2) tidal-influenced nearshore; and (3) mixed, a combination of tidal and nontidal marine influence. All facies types appear to have been affected equally by diagenetic alterations. Sandstones with some reservoir potential are channel sandstones mainly of facies types 1 and 2; these sandstones rarely attain thicknesses greater than 10 ft.

Thin-section examination of sandstones reveals compositions of quartzarenite, subarkose, and sublitharenite. Calcite fragments of brachiopods and crinoids are common locally. X-ray diffraction of whole-rock samples and thin sections indicates absence of potassium feldspar and irregular lateral and vertical distribution of calcite and dolomite. Effects of diagenetic alteration, visible in all samples, include mechanical compaction, dissolution, precipitation of silica or carbonate cements (calcite and/or ankerite), and formation of clay minerals (including chlorite, kaolinite, and illite). Porosity, typically <10%, has been reduced by mechanical deformation of labile sedimentary-rock fragments and glauconite grains. Porosity has been reduced also by formation of carbonate cement (distribution of which varies widely) and, less commonly, by formation of silica cement. Porosity has been enhanced by dissolution of polycrystalline quartz, feldspars, fragments of chert and other rocks, glauconite, and clays or clay matrix. Many pores, however, have been partially to completely filled with clay, primarily kaolinite, leaving only micropores. Most of the porosity identified in the sandstones is secondary. Thus, from the standpoint of reservoir quality, the generation of secondary porosity is the most important diagenetic reaction.

Keighin, C. W.; and Flores, R. M., 1993, Petrology and sedimentology of Morrow/Springer rocks and their relationship to reservoir quality, Anadarko basin, Oklahoma, *in* Johnson, K. S.; and Campbell, J. A. (eds.), Petroleum-reservoir geology in the southern Midcontinent, 1991 symposium: Oklahoma Geological Survey Circular 95, p. 25.

The Upper Morrowan Fan-Delta Chert Conglomerate in Cheyenne and Reydon Fields: Completely Sealed Gas-Bearing Pressure Compartments

Zuhair Al-Shaieb, James Puckette,
Patrick Ely, and Azhari Abdalla

Oklahoma State University
Stillwater, Oklahoma

ABSTRACT.—Gas volumes exceeding 1.0 tcf have been produced from upper Morrowan chert-conglomerate reservoirs in the Reydon and Cheyenne field areas in Roger Mills County, Oklahoma, and Wheeler County, Texas. These extremely overpressured reservoirs exhibit pressure gradients that approach 0.98 psi/ft, and potentiometric heads >20,000 ft. Chert-conglomerate reservoirs in these fields represent individual compartments with distinct pressure regimes. Thick shales in the upper Morrowan interval seal and isolate the individual productive chert members. These shales act as lateral seals along the western, northern, and eastern boundaries of the chert-clastic wedge. The chert-conglomerate reservoirs exhibit low porosity and permeability in the vicinity of the frontal fault zone of the Wichita Mountain uplift. Extensive cementation in this area has completely occluded porosity along the frontal fault zone forming the southern lateral seal for the chert wedge. Silica liberated by pressure-solution processes during compaction was the main source for quartz overgrowths around chert pebbles and quartz grains.

Within the chert-conglomerate clastic wedge, lithofacies variations and cementation patterns have played an important role in isolating various compartments with distinct high-pressure regimes. Pressure-gradient and potentiometric-surface maps were used to delineate individual compartments.

INTRODUCTION

The upper Morrowan chert-conglomerate reservoirs located in Roger Mills County, Oklahoma, and Wheeler and Hemphill Counties, Texas, exhibit some of the highest pressure gradients in the Anadarko basin. These extremely overpressured reservoirs have gradients approaching 0.98 psi/ft, and potentiometric values >20,000 ft. Pressure and sedimentological data from the Cheyenne and Reydon fields (CRF) area (Fig. 1) indicate that the chert-conglomerate clastic wedge is a completely sealed compartment within the overpressured interval of the Anadarko basin called the Mega-Compartment Complex (Al-Shaieb and others, 1990). Furthermore, this chert-conglomerate clastic wedge is subdivided into individual, completely sealed "nested compartments" that correspond to different reservoirs within the upper Morrowan interval. Pressure-gradient and potentiometric-surface maps were used to delineate

these individual chert compartments and to demonstrate their unique pressure regimes.

STRATIGRAPHY

In the CRF study area (Fig. 1), the upper Morrowan Series is defined as all strata between the base of the Atokan Thirteen Finger limestone and the top of the underlying Squaw Belly limestone (Fig. 2). Within the northern part of the study area, the upper Morrowan is a shale-dominated sequence that contains thinner chert-conglomerate and chert-sandstone reservoirs. The conglomerate-to-shale ratio increases southward, and the upper Morrowan becomes a conglomerate-dominated sequence in the vicinity of the Wichita Mountain frontal fault zone.

The upper Morrowan reservoirs contain an abundance of detrital chert that ranges from sand-sized to cobble-sized fragments (Hawthorne, 1984; Al-Shaieb and others, 1990). The source of these

Al-Shaieb, Zuhair; Puckette, James; Ely, Patrick; and Abdalla, Azhari, 1993, The upper Morrowan fan-delta chert conglomerate in Cheyenne and Reydon fields: completely sealed gas-bearing pressure compartments, *in* Johnson, K. S.; and Campbell, J. A. (eds.), *Petroleum-reservoir geology in the southern Midcontinent*, 1991 symposium: Oklahoma Geological Survey Circular 95, p. 26–39.

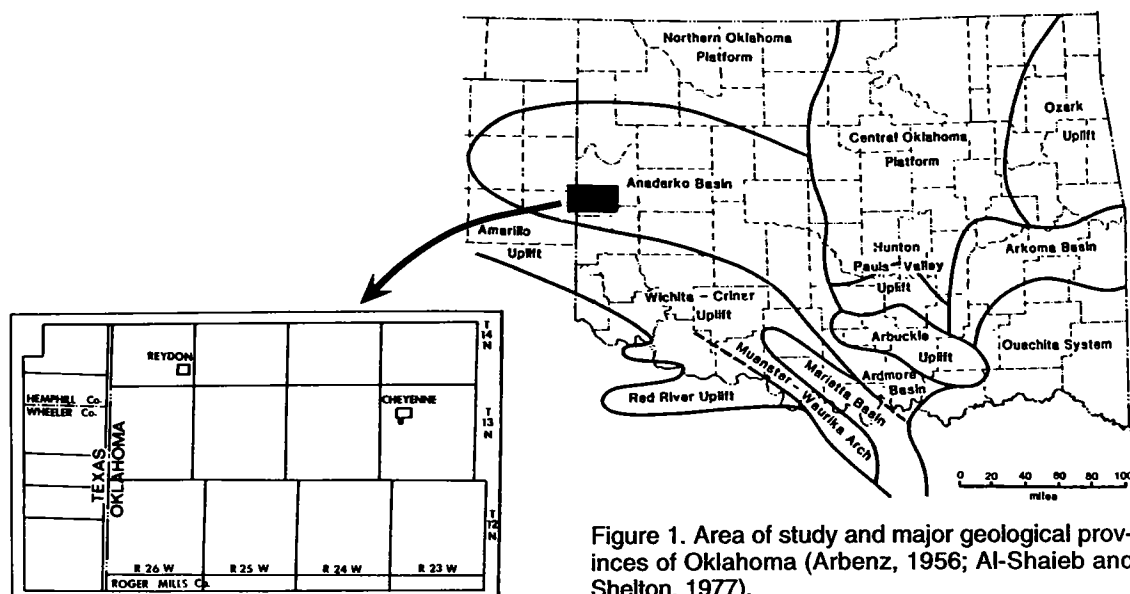


Figure 1. Area of study and major geological provinces of Oklahoma (Arbenz, 1956; Al-Shaieb and Shelton, 1977).

fragments was the chert-rich Mississippian rocks exposed on the rising Wichita Mountains to the south. During the initial stages of the Wichita orogeny, chert fragments were eroded from the uplift and deposited in a northward-prograding clastic wedge. The variability in areal extent and thickness of the individual chert-conglomerate members within this wedge reflects fluctuation in the uplift rate, among other factors.

The individual chert reservoirs are named locally and include, in descending order, the Coffey, Purvis (also known as Allison and Key in Texas), Puryear, Hollis, Pierce, Bradstreet, and Armstrong (Dwight's, 1989; Petroleum Information, 1990). The more commonly recognized terms are shown in Figure 2.

DEPOSITIONAL ENVIRONMENT AND FACIES

The upper Morrowan chert-conglomerate sequences have been interpreted as fan-delta complexes (Alberta, 1987) and coastal alluvial fans (Johnson, 1989). Al-Shaieb and others (1989) conducted an integrated study that examined the sedimentary features, geometry, and wire-line log characteristics of the upper Morrowan chert interval. They examined cores from both the Purvis and Puryear intervals. These cores contain stacked, fining-upward, braided-stream deposits indicative of the mid- to distal-fan facies present in the fan-delta models of McGowen and Groat (1971) and Dutton (1982) (Fig. 3).

These braided-stream, multi-storied channel deposits are characterized by beds with sharp basal contacts with underlying fossiliferous shal-

low-marine and prodelta shales. The basal sequences of the conglomerate/sandstone deposits consist of light-gray imbricated pebbly conglomerates that fine upward to coarse-grained then medium- and fine-grained cherty sandstone. Individual sequences vary from a few inches to several feet thick. However, the upper sequences are generally thicker than the lower ones.

Marsh/swamp, abandoned-channel, and fan-delta-plain deposits were also recognized in Purvis and Puryear cores (Al-Shaieb and others, 1989). A Pierce conglomerate core, described in Johnson (1989), is interpreted as a braided-stream deposit. Wire-line logs were calibrated to all cores to facilitate interpretation of depositional facies from log signatures.

CHERT CONGLOMERATE DEPOSITIONAL FACIES

The depositional facies of the chert conglomerates were identified using specific wire-line log signatures (Alberta, 1987). The various facies recognized include main and minor distributary channels, crevasse splays, overbank deposits, delta plain, lignites, swamp, delta front, and shallow marine/prodelta (Fig. 4). Reservoir distribution and geometries suggest most chert-conglomerate deposition occurred in a northward-prograding fan-delta system composed of main distributary channels, minor distributary channels, splays, marshes, and overbank deposits. However, some elongate chert reservoirs encased in deltaic or shallow-marine shales have large thickness-to-width ratios which suggest that some fill in the fan-delta system occurred within deeply incised

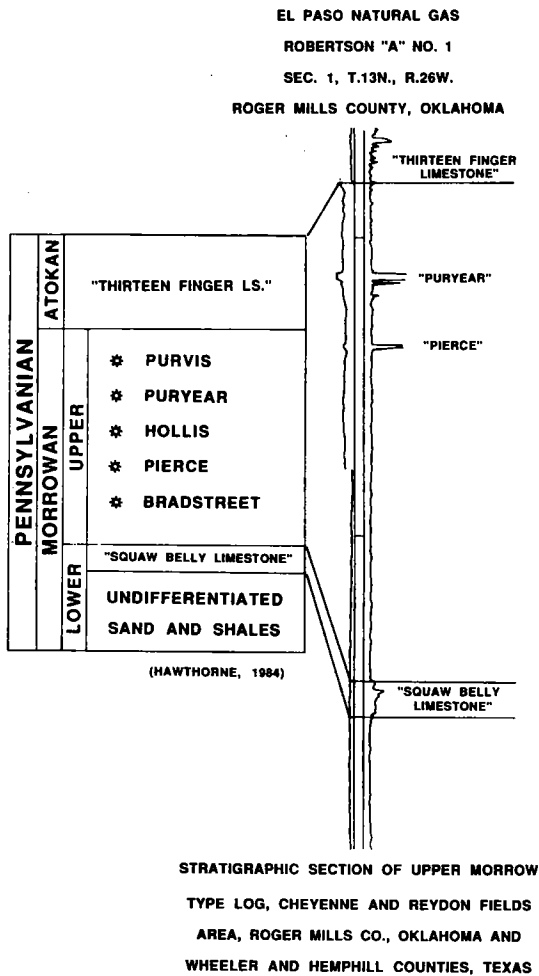


Figure 2. Upper Morrowan stratigraphic section and representative log of Cheyenne and Reydon fields study area.

channels. These channels are present in the lower mid- to distal-fan areas. Tectonically induced sea-level fluctuations may have been the primary agent causing the stream incision and subsequent channel fill.

The facies most pertinent to this study are the distributary channels, crevasse splays, and overbank deposits. These facies represent the most productive reservoirs found in the chert-conglomerate fan-delta system.

THICKNESS AND
POTENTIOMETRIC MAPS

Thickness maps for the chert-conglomerate reservoirs were constructed using wire-line logs. A dichotomic pattern of reservoir distribution supports the interpretation of these deposits as a northward prograding fan-delta complex. The mapped facies all exhibit clean gamma-ray log signatures

characteristic of conglomerate and sandstone lithologies.

Channel-fill facies were recognized by blocky-to bell-shaped gamma-ray log signatures (Fig. 4). Bell-shaped signatures reflect upward fining or upward increase in clay content, which are characteristic of sandstones deposited from waning flow. The geometry of some channel-fill reservoirs suggests that the streams were rather confined and formed lower mid- to distal-fan distributary channel systems. The thick nature of some reservoirs (>100 ft) indicates that channelization or incision of older deltaic sediments occurred during sea-level lowstands.

Overbank sandstone deposits are characterized by a thin (<10-ft-thick) gamma-ray log signature that is spike-like in appearance (Fig. 4). These deposits are located in interchannel areas between the more prominent fan-delta lobes.

Along the southern boundary of the study area, the chert-conglomerate sequence is dominated by stacked upper mid- to proximal-fan braided-stream deposits.

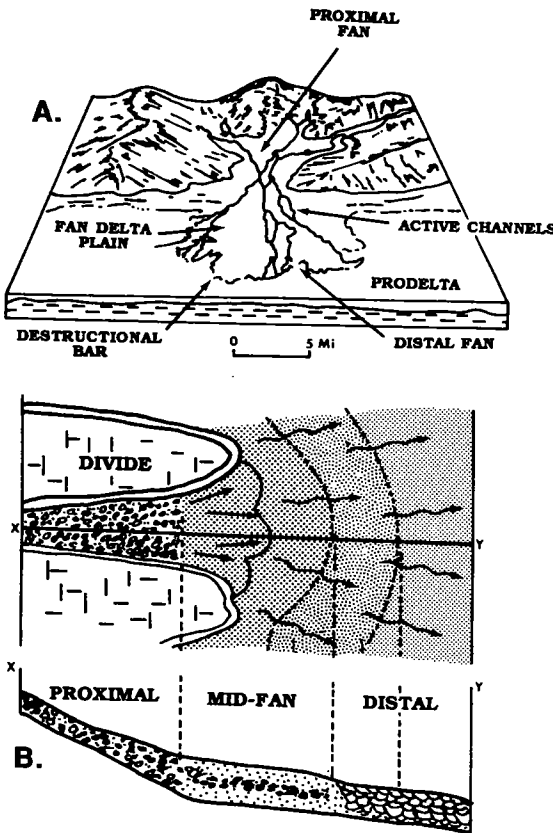


Figure 3. A—Schematic diagram of a fan-delta system (modified from Dutton, 1982; after Alberta, 1987). B—Plan view and cross section of the fan-delta system model (after McGowen and Groat, 1971; and Alberta, 1987).

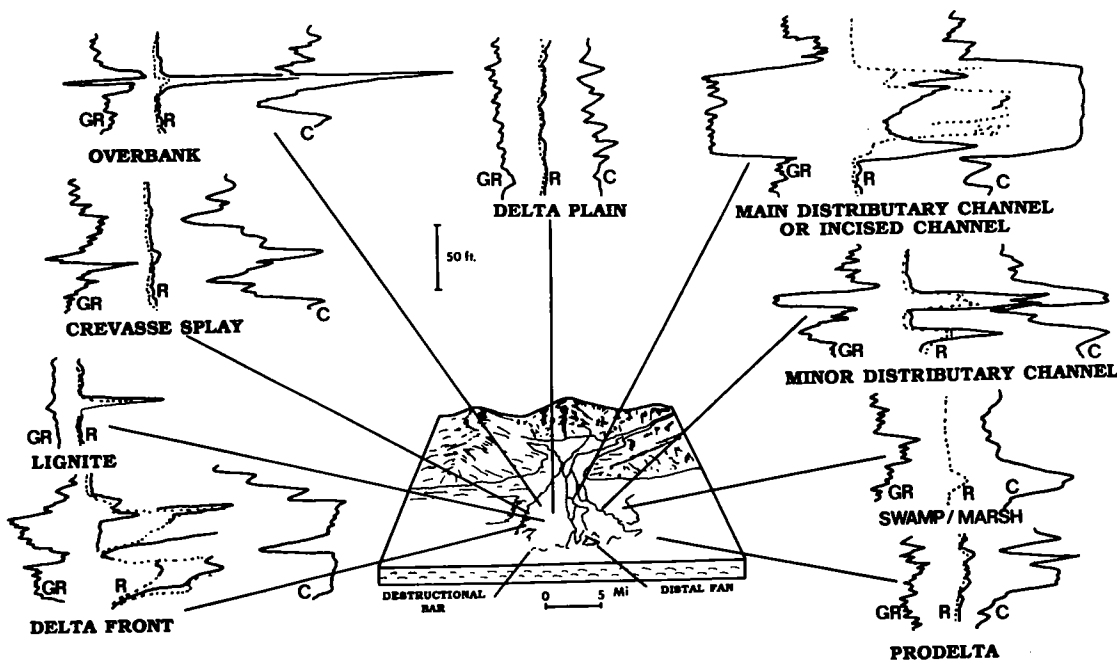


Figure 4. Characteristic log signatures of various depositional facies within the study area (after Alberta, 1987). GR = gamma ray, R = resistivity, C = conductivity.

Potentiometric and pressure-gradient maps were constructed from available reservoir-pressure data. Static bottom-hole (reservoir) pressures were calculated from reported initial well-head shut-in pressures, using software developed by Echometer (1986). Pressure gradients were calculated by dividing reservoir pressure by the perforation depth. Only single-zone completions were utilized in the study.

Potentiometric-surface values were calculated using Dahlberg's formula (1982). A constant fluid gradient of 0.465 psi/ft was used in the conversion of bottom-hole (reservoir) pressure to potentiometric-head values. All head values are standardized to sea level.

The thickness and potentiometric maps of four chert-conglomerate reservoirs are included to demonstrate pressure isolation and compartmentalization within the chert-conglomerate interval. These conglomerate sequences represent stratigraphic intervals where the most pressure data were available. In ascending order, the reservoirs are the Pierce, Hollis, Puryear, and Purvis chert conglomerates.

Pierce Chert Conglomerate

Thickness Map

The thickness map of the Pierce (Fig. 5) indicates two northeast-trending fan-delta lobes. The western lobe is larger and trends northeast from

the area of stacked upper-mid-fan sequences in the southwest corner of the mapped area. Within T. 13 N., R. 25 W., and T. 13 N., R. 26 W., areally widespread deposition probably resulted from avulsion and channel migration.

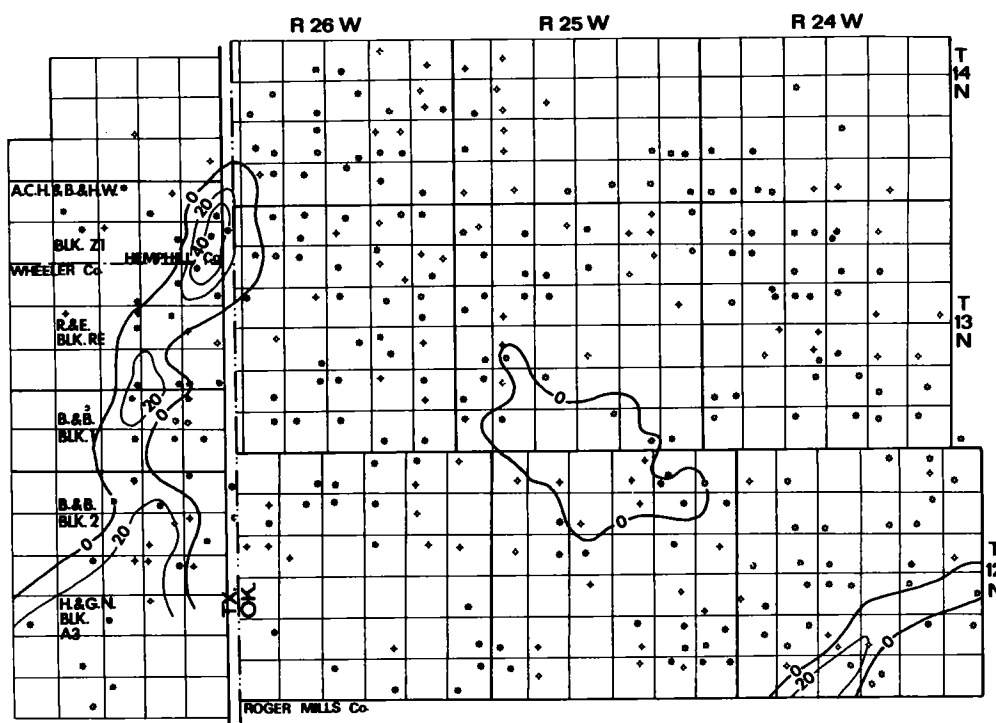
The eastern Pierce lobe has a dominant northeast trend. In this area, thickening within the Pierce interval indicates that mid- or distal-fan braided streams incised the delta-plain/shallow-marine silts and muds in response to a sea-level drop.

A small isolated chert deposit in secs. 1 and 2, T. 12 N., R. 25 W., and secs. 35 and 36, T. 13 N., R. 25 W., is located between the two prominent Pierce fan-delta lobes and is therefore believed to be an overbank deposit.

Pressure Regimes

Reservoir pressure measurements for the Pierce (Fig. 6) indicate that the different Pierce facies display significantly different pressure domains. The eastern fan-delta lobe has pressure gradients that range from 0.91 to 0.93 psi/ft and potentiometric-surface values >19,600 ft. The western lobe has a maximum pressure gradient of 0.82 psi/ft and a potentiometric-surface value of ~14,200 ft. The small Pierce reservoir has a pressure gradient of 0.98 psi/ft and a potentiometric-surface value >20,600 ft.

The substantial difference in pressure regimes for these three separate Pierce reservoirs indicates



complete isolation of the reservoirs through compartmentalization of the Pierce stratigraphic interval. The extremely high pressure of the areally small overbank reservoir may have resulted from early auto-isolation, a process by which pockets of porosity can be isolated from their hydraulic environments via mechano-chemical processes such as pressure solution and differential compaction due to textural heterogeneity (Ortoleva and Al-Shaieb, 1991).

Hollis Chert Conglomerate

The Hollis chert conglomerate (Fig. 7) is not as extensive as the underlying Pierce; however, it has a similar distribution pattern which suggests a southerly source area.

The thickness map indicates that the Hollis consists of two northerly trending fan-delta channels. The lens between the two channels is interpreted to be an interlying flood-plain deposit. The sinuous geometry and thickness of the northern distal portion of the western fan-delta lobe suggests channel incision into the underlying delta-plain and prodelta muds and silts. Braided-stream deposits filled these channels to form the Hollis chert-conglomerate reservoirs. The western Hollis fan-delta channel system is highly productive, but commingling of the Hollis production with that of other chert reservoirs makes Hollis pressure analysis impossible.

Puryear Chert Conglomerate

Thickness Map

The Puryear is the most extensive chert conglomerate. This is clearly shown on the thickness map (Fig. 8). It is possible the abundant chert detritus may have been triggered by a significant pulse of tectonism in the Wichita Mountain area. These extensive deposits are an amalgamation of several north-trending lobes of the fan-delta system.

Two dominant Puryear lobes are mapped in the study area. The western lobe trends north approximately along a pathway similar to the underlying (Pierce and Hollis) lobes. The channel within this western area bifurcates in northwesterly and northeasterly directions. The eastern trend extends northwestward and also exhibits bifurcation and merging. Thick channel-fill reservoirs (local areas, >100 ft thick, not shown on Fig. 8) suggest deep incision of the underlying deltaic muds and silts by Puryear channels.

Pressure Regimes

Pressure data for the Puryear reservoirs (Fig. 9) suggest that the two primary lobes are not in communication. Pressure gradients in the eastern lobe range from 0.88 to 0.92 psi/ft, whereas gradients in the western lobe have a maximum value of 0.83 psi/ft. Potentiometric-surface values for the east-

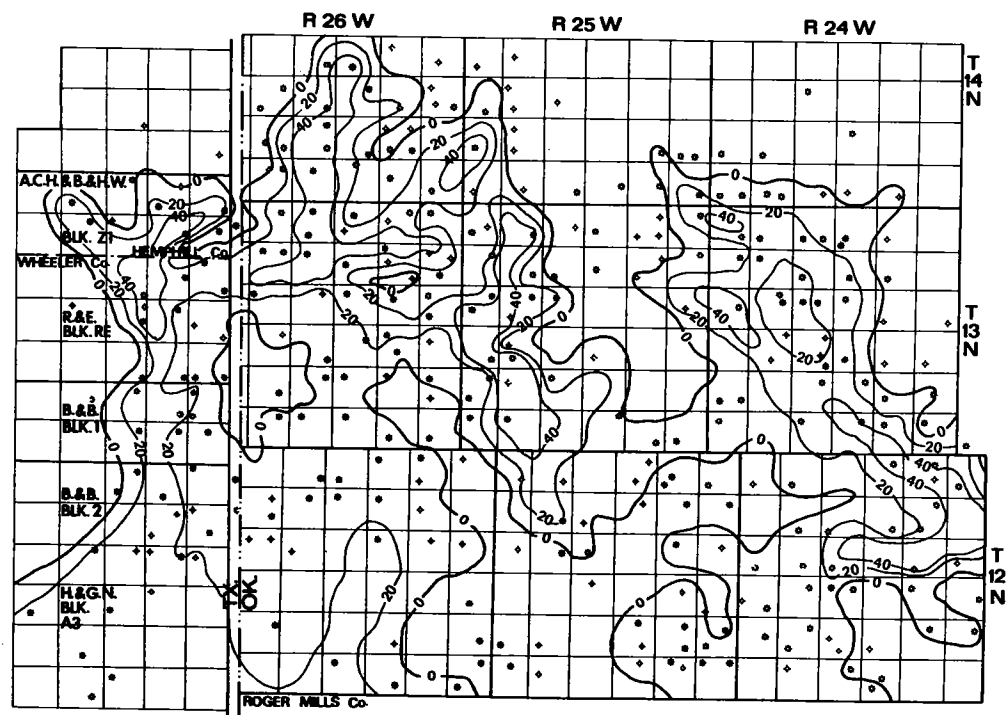


Figure 8. Thickness map of the Puryear chert conglomerate; thickness in feet.

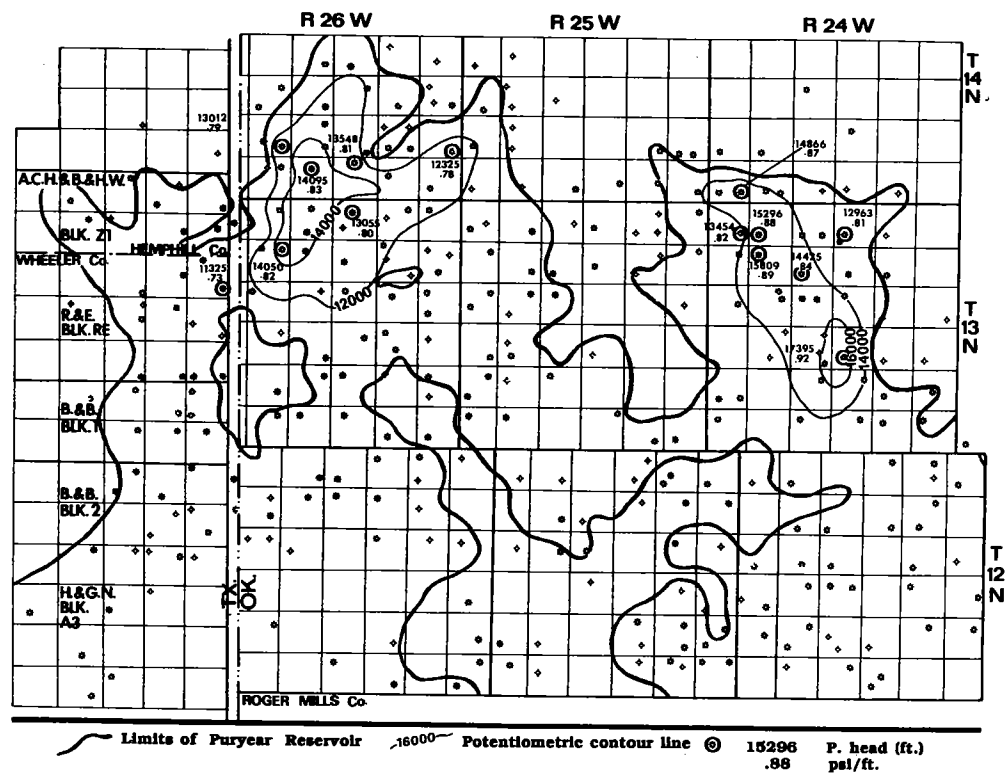


Figure 9. Potentiometric map of the Puryear chert conglomerate. Corresponding pressure-gradient values are also shown.

ern lobe exceed 17,300 ft, whereas the maximum potentiometric-surface values of the western lobe are ~14,000 ft. The difference in reservoir pressures between the two lobes suggests isolation and compartmentalization of the Purvis interval. Therefore, reservoirs in the western and eastern Purvis lobes comprise separate compartments. It is also important to note that pressure and lithologic data suggest complete isolation of the Pierce from the overlying Purvis reservoir.

Purvis Chert Conglomerate

Thickness Map

The Purvis is the uppermost chert conglomerate. It has a distribution pattern (Fig. 10) that is similar to those of the older chert, and apparently was also derived from the south. The dominant site of Purvis deposition is a north-trending braided-stream channel-fill along the Texas/Oklahoma border. The primary channel bifurcates to form northerly and east-northeasterly trends. The sedimentary structures (crude stratification, imbrication, and grading) observed in a core located in sec. 35, T. 13 N., R. 26 W. (Fig. 11), support the braided-stream interpretation. A relatively small, isolated deposit in T. 12 N., R. 25 W., may be a splay or overbank deposit.

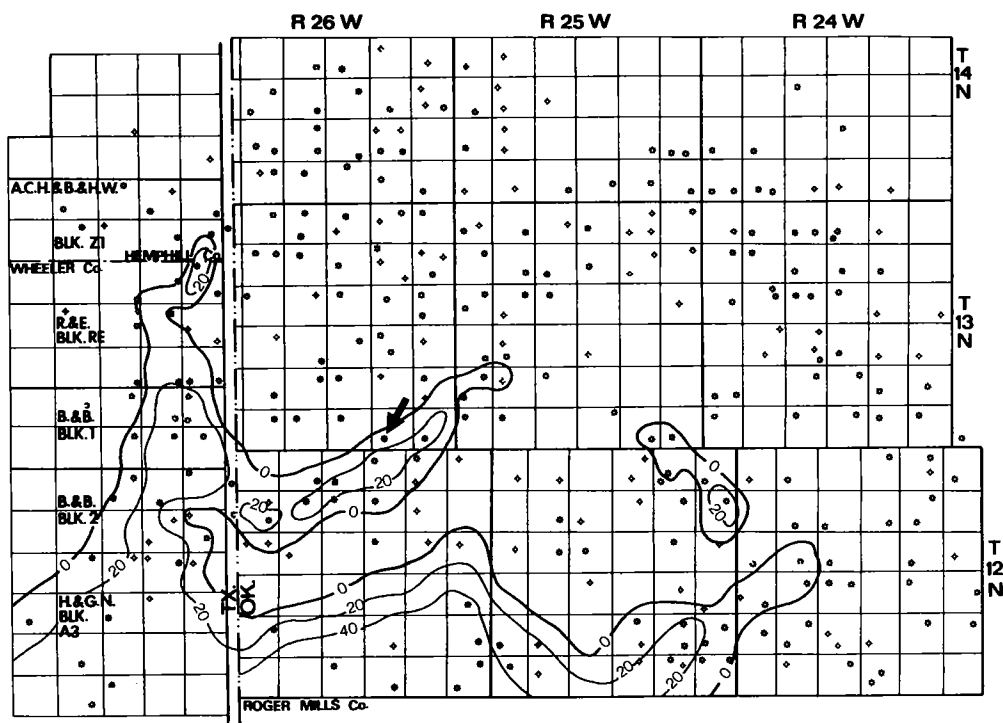
In the southernmost part of the study area, the Purvis is more widespread and sheet-like. It is interpreted to be stacked and amalgamated braided channels, which are typical of alluvial-fan settings.

Pressure Regimes

The Purvis interval contains completely isolated reservoirs with their own distinct pressure values (Fig. 12). Pressure gradients for the larger Purvis accumulation range from 0.79 to 0.86 psi/ft. The maximum potentiometric-surface value is ~16,600 ft above sea level. However, the small accumulation in the northeast part of T. 12 N., R. 25 W., has a pressure gradient of 0.98 psi/ft and a potentiometric-surface value of 20,645 ft. The marked differences in pressure gradients and potentiometric surfaces between the small accumulation and the rest of the Purvis is evidence of compartmentalization of the Purvis chert interval.

COMPARTMENTALIZATION, SEALS, AND IMPLICATIONS

Compartmentalization of the chert-interval reservoirs is detectable on potentiometric and pressure-gradient maps. In Figure 13, a three-dimensional diagram of potentiometric values in the Morrowan interval, the chert conglomerate is repre-



sented by the "castle-like" complex of peaks in the southwestern part of the basin that has a distinct pressure regime from other Morrowan reservoirs in the basin. Each individual peak represents a compartment within the chert-conglomerate interval.

The entire interval is sealed laterally by a change in lithology from conglomerate and sandstone to black shale along the northern (distal) boundary of the chert-clastic wedge. However, stacked conglomerate sequences in the proximal southern part of the complex are sealed in the vicinity of the frontal fault zone of the Wichita Mountain uplift. Figure 14 is a cross section extending from the frontal fault zone in Texas to the Reynon field that depicts this relationship. A wide band silica-cemented conglomerate along the fault zone serves as the southern, lateral seal for the entire chert interval. A cored interval in the

Hunt no. 1-57 Bryant well, Wheeler County, Texas (Fig. 15), represents a silica-cemented lateral seal in a stacked conglomerate sequence that is believed to correlate to the Puryear/Pierce intervals. It is composed primarily of poorly sorted, interstratified pebble-conglomerate and coarse-sandstone sequences that show crude stratification and upward fining (Fig. 15). Sutured and penetrating grain contacts are indicative of pressure solution (Figs. 15,16). Stylolites, with their characteristic fine saw-tooth appearance, are also common (Fig. 17). Extensive silica cementation obliterates the porosity in these rocks. Coarse, equant quartz and radial-fibrous chalcedonic quartz are present as pore fillings (Fig. 18). The matrix between the larger chert fragments (Fig. 19) is commonly composed of detrital quartz grains, cemented by micro-quartz.

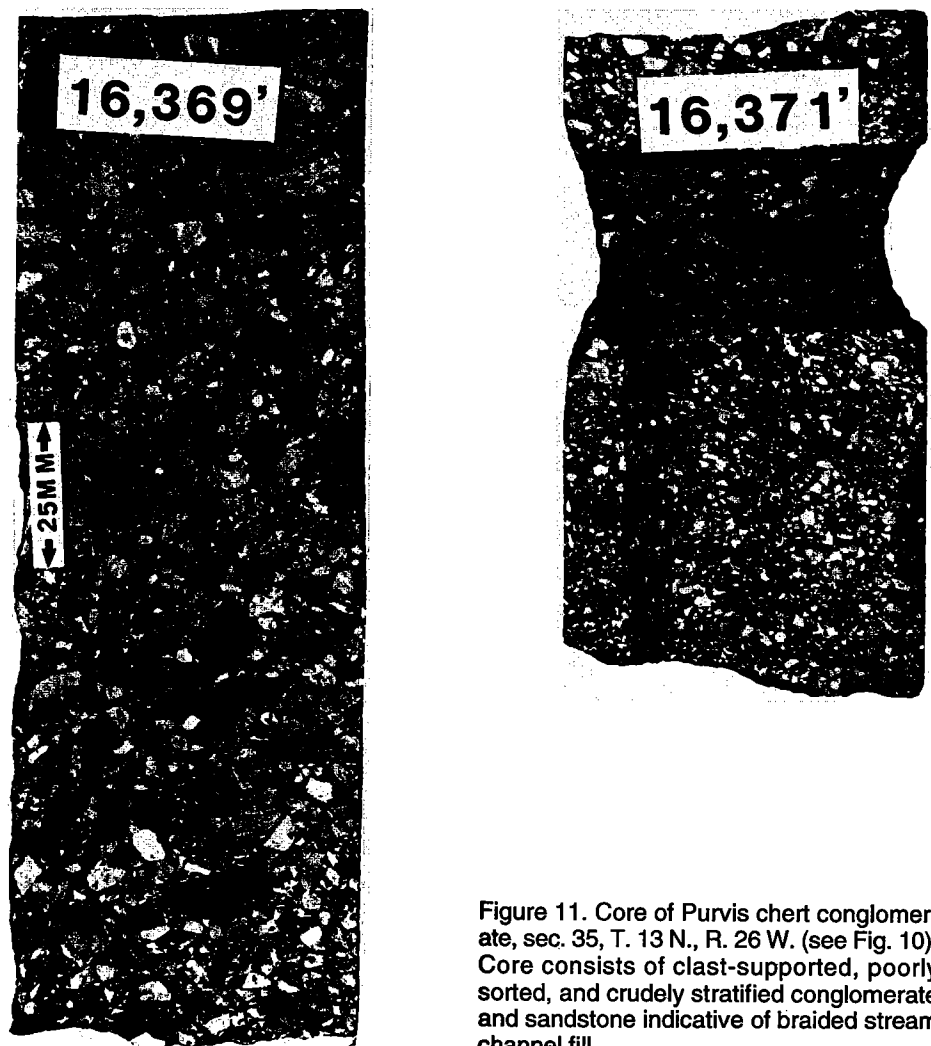


Figure 11. Core of Purvis chert conglomerate, sec. 35, T. 13 N., R. 26 W. (see Fig. 10). Core consists of clast-supported, poorly sorted, and crudely stratified conglomerate and sandstone indicative of braided stream channel fill.

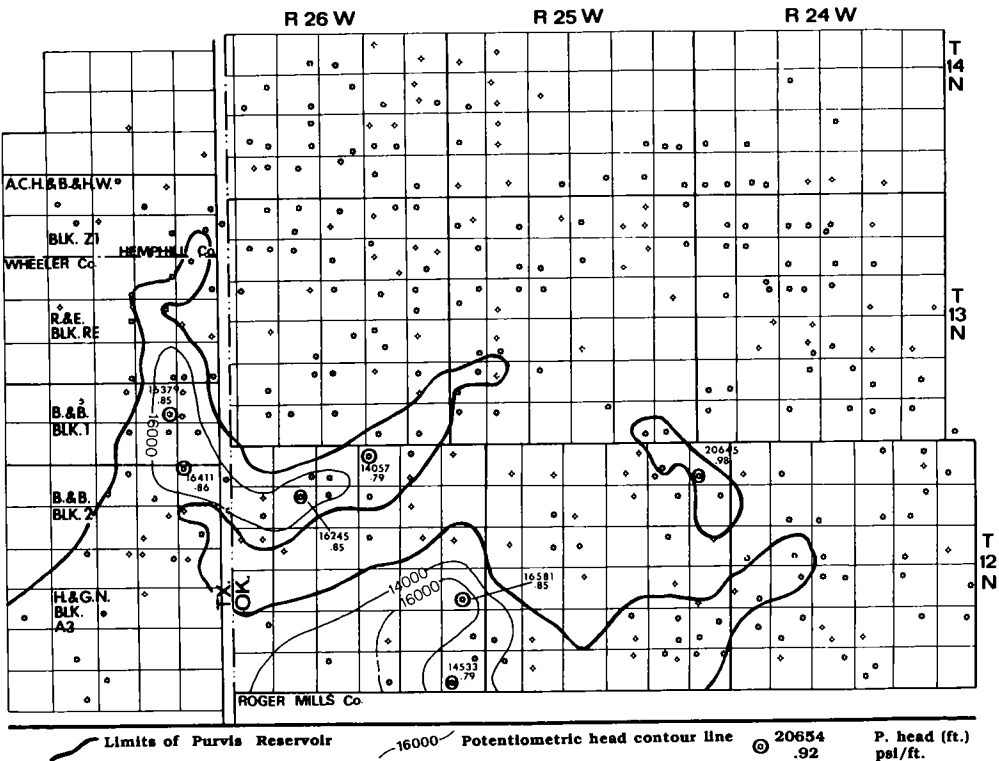


Figure 12. Potentiometric map of the Purvis chert conglomerate. Corresponding pressure-gradient values are also shown.

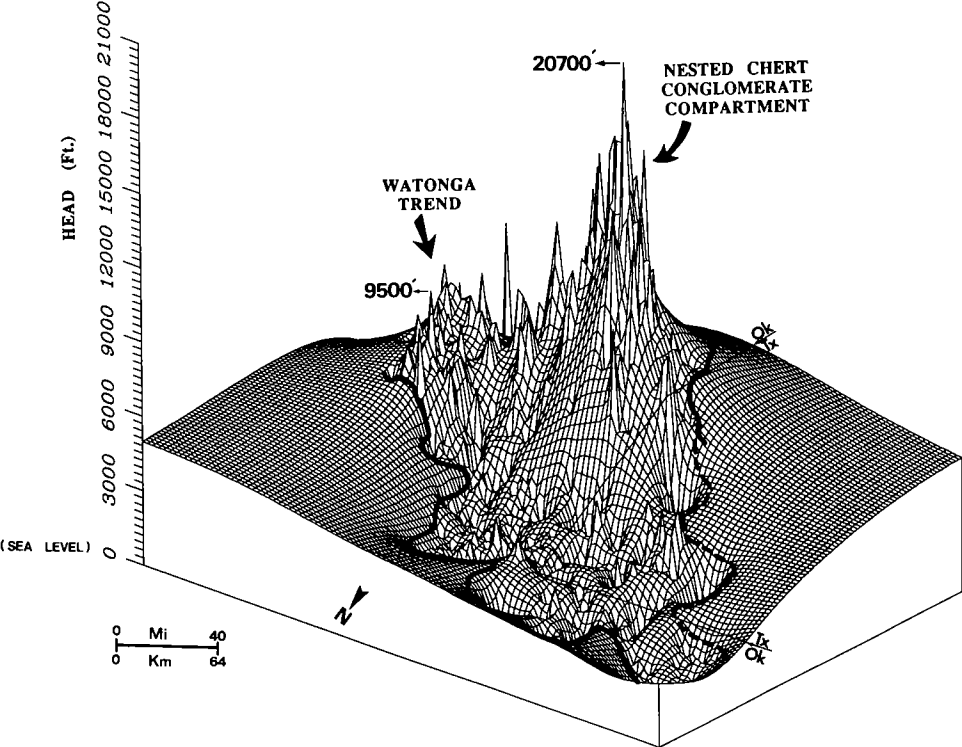


Figure 13. Three-dimensional diagram of the potentiometric values of the upper Morrowan chert conglomerate in the study area.

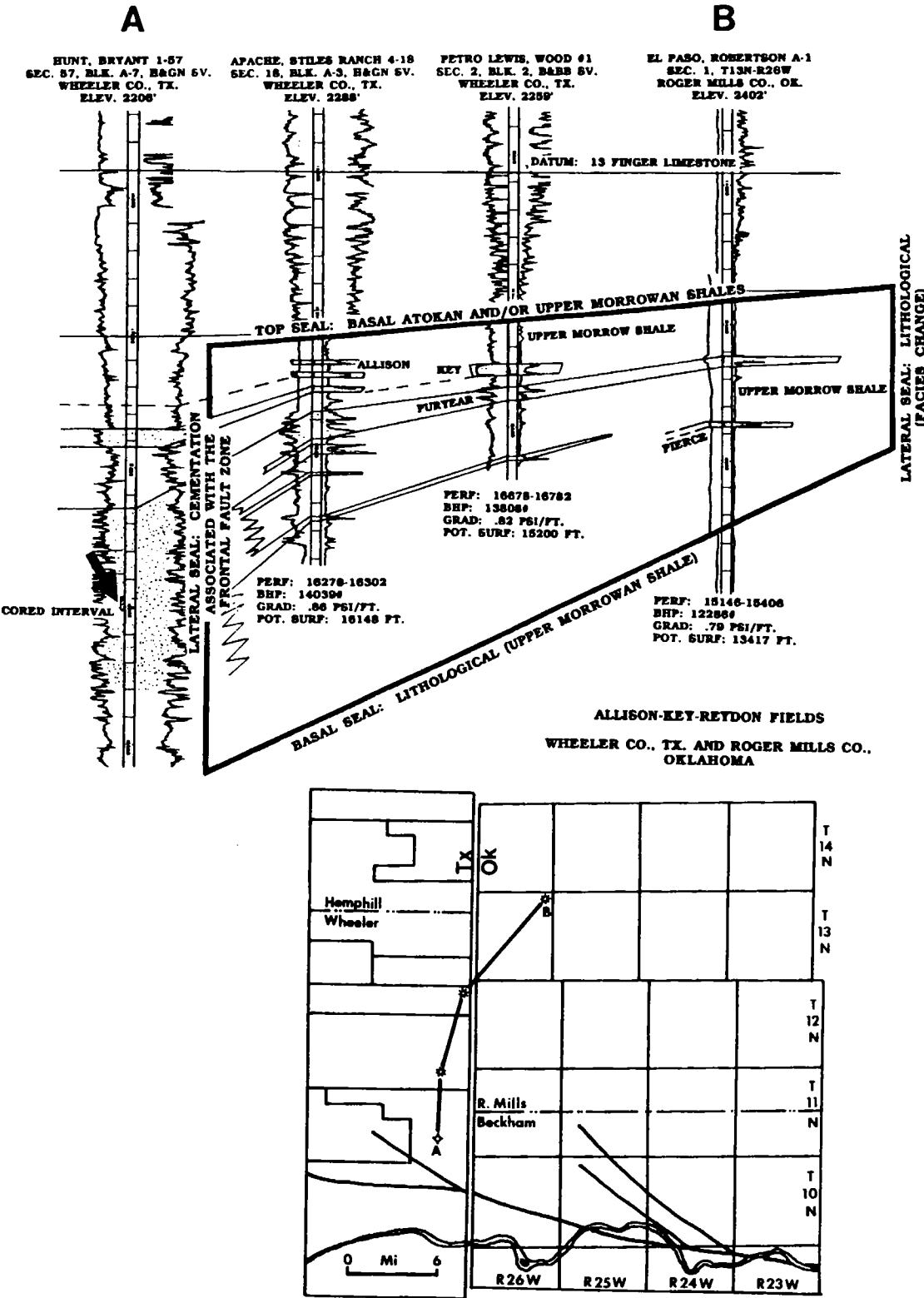


Figure 14. Cross section extending from the Wichita Mountain frontal fault zone through the Allison, Key, and Reydon fields, depicting the location of pressure seals and the isolated nature of the reservoirs. Cored interval in the Hunt no. 1-57 Bryant well indicated by arrow.

Reservoir quality and productivity show significant improvement away from the highly cemented fault zone to the south. Highly productive lower mid- to distal-fan channel-fill and overbank reservoirs occur in the Cheyenne and Reydon fields, which are located along the northern margin of the chert-clastic wedge. These reservoirs are completely sealed by shale (Fig. 14). Therefore, each reservoir is a sealed compartment with its own distinct pressure regime. Within field boundaries, nonpro-

ducing compartments may exist in close proximity to producing ones. These undrilled compartments offer additional targets for deep, overpressured-gas exploration.

ACKNOWLEDGMENTS

The authors gratefully acknowledge the Gas Research Institute for funding this research through Contract No. 5089-26-1805.

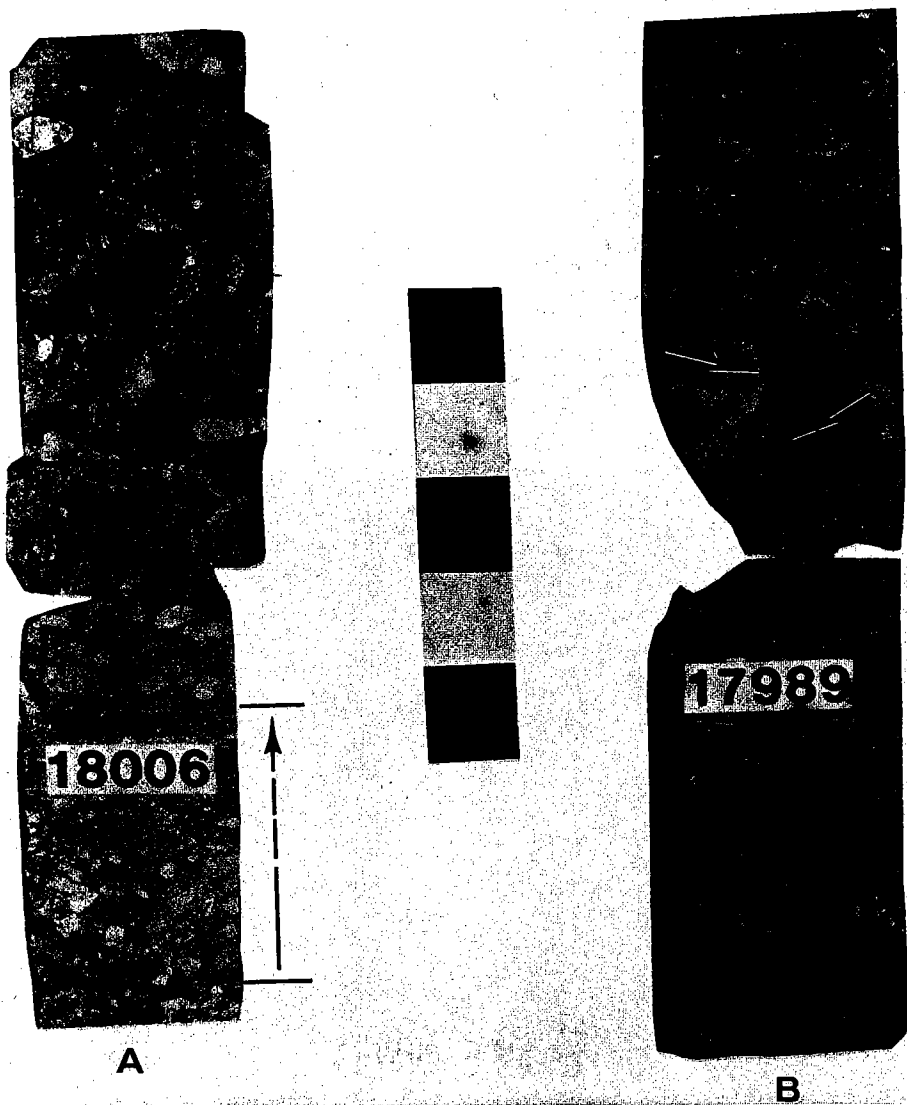


Figure 15. Cores from the Hunt no. 1-57 Bryant well, Wheeler County, Texas; bar scale is 5 in. long. *A*—Poorly sorted, interstratified conglomerate and coarse sandstone. Vertical arrow identifies fining-upward sequence. *B*—Contact between coarser and finer pebble conglomerates. Note sutured grain contact (arrows) between large pebbles.

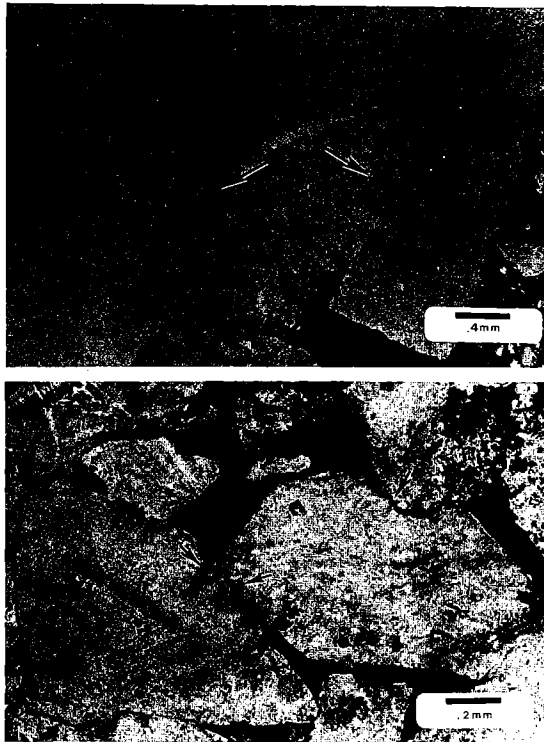


Figure 16. Sutured pressure solution contacts (arrows) between chert grains. Sample from Hunt no. 1-57 Bryant well.

REFERENCES CITED

- Alberta, P. L., 1987, Depositional facies analysis and porosity development of the (Pennsylvanian) upper Morrow chert conglomerate Puryear member, Roger Mills and Beckham Counties, Oklahoma: Oklahoma State University unpublished M.S. thesis, 135 p.
- Al-Shaieb, Z.; and Shelton, J. W., 1977, Evaluation of uranium potential in selected Pennsylvanian and Permian units and igneous rocks in southwestern and southern Oklahoma: U.S. Department of Energy, Open File Report GJBX-35 (78) 248 p.
- Al-Shaieb, Z.; Alberta, P. L.; and Gaskins, M., 1989, Depositional environment, petrology, diagenesis, and porosity of the upper Morrow chert conglomerate in Oklahoma [abstract]: American Association of Petroleum Geologists Bulletin, v. 73, p. 1043.
- Al-Shaieb, Z.; Ely, P.; Puckette, J.; and Abdalla, A., 1990, Unpublished annual report prepared for the Gas Research Institute, Chicago, Illinois, 340 p.
- Arbenz, J. K., 1956, Tectonic map of Oklahoma: Oklahoma Geological Survey Map GM-3, scale 1:750,000.
- Dahlberg, E. C., 1982, Applied hydrodynamics in petroleum exploration: Springer-Verlag, New York, 161 p.
- Dutton, S. P., 1982, Pennsylvanian fan-delta and carbonate deposition, Mobeetie field, Texas Panhandle: American Association of Petroleum Geologists Bulletin, v. 66, p. 389-407.
- Dwight's Energy Data Inc., 1989, Natural gas well production histories: Richardson, Texas.

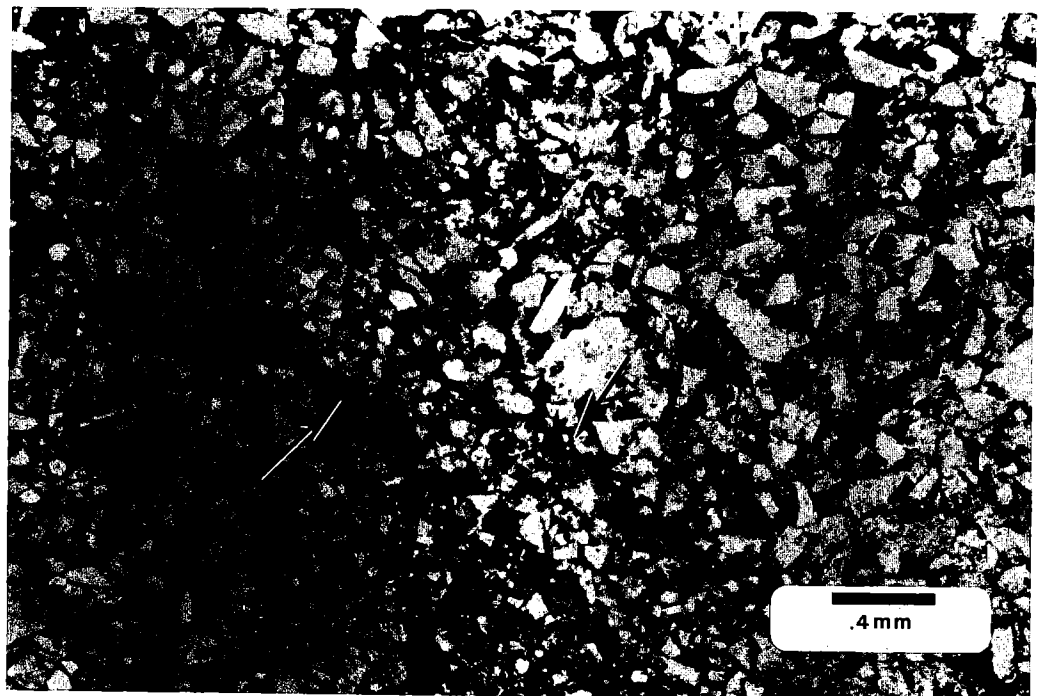


Figure 17. Two stylolites (arrows) with characteristic fine saw-tooth appearance. Sample from Hunt no. 1-57 Bryant well.

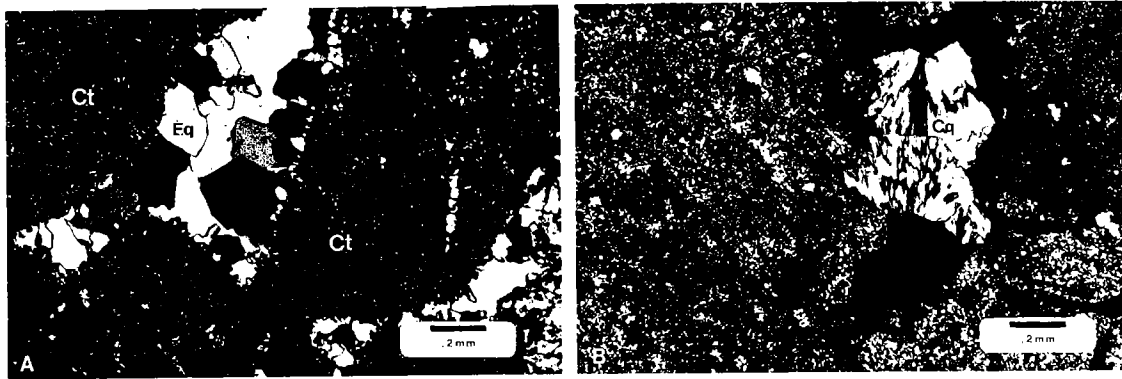


Figure 18. Cements occluding intergranular porosity between chert grains (Ct). Samples from Hunt no. 1-57 Bryant well. Cross-polarized light. *A*—Coarse, equant quartz cement (Eq). *B*—Radial-fibrous chalcedonic-quartz cement (Cq).

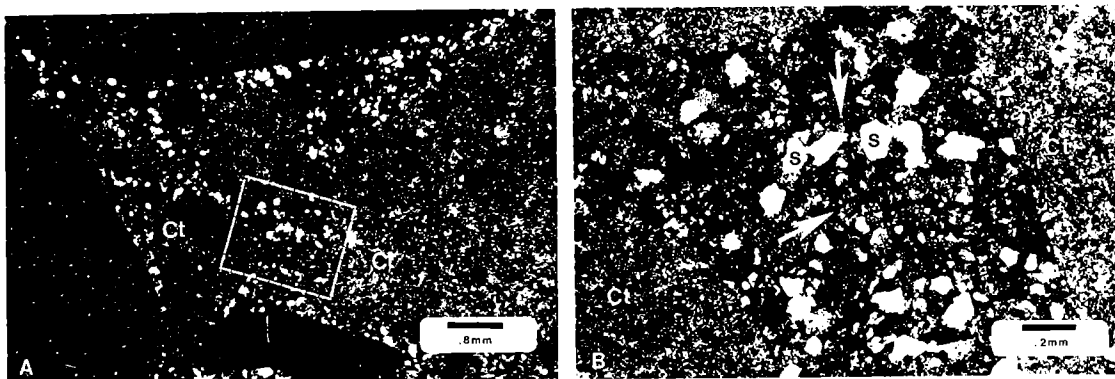


Figure 19. Thin sections of samples from Hunt no. 1-57 Bryant well. *A*—Large chert grains (Ct) with sandy matrix. *B*—Enlarged view of outlined area in *A*. Sandy matrix that surrounds large chert grains (Ct) contains quartz sand(s) cemented with microcrystalline quartz (arrow) which appears dark and speckled in the photomicrograph. Cross-polarized light.

Echometer Company, 1986, Analyzing well performance: Wichita Falls, Texas.

Hawthorne, H. W., 1984, Upper Morrow (Pennsylvanian) chert conglomerates and sandstones of the Reydon and Cheyenne fields, Roger Mills County, Oklahoma: Baylor University unpublished M.S. thesis, 117 p.

Johnson, B., 1989, Regional geology of the Pierce member of the upper Morrow Formation in the Anadarko basin, with a detailed look at South Dempsey field in Roger Mills County, Oklahoma [abstract]: American Association of Petroleum Geologists Bulletin, v. 73, p. 1047.

McGowen, J. H.; and Groat, C. G., 1971, Van Horn Sandstone, West Texas, an alluvial fan model for mineral exploration: Texas University Bureau of Economic Geology Report of Investigations 69, 91 p.

Ortoleva, P.; and Al-Shaieb, Z., 1991, Unpublished supplemental report prepared for the Gas Research Institute, Chicago, Illinois, 57 p.

Petroleum Information Corporation, 1990, Oklahoma City, Oklahoma.

Shelby, J. M., 1980, Geologic and economic significance of the upper Morrow chert conglomerate reservoir of the Anadarko basin: Journal of Petroleum Technology, v. 32, p. 489–495.

Depositional Variations and Reservoir Characterization in the Red Fork Sandstone, Northwest Tecumseh Field, Pottawatomie County, Oklahoma

Fletcher S. Lewis

Fletcher Lewis Engineering, Inc.
Oklahoma City, Oklahoma

ABSTRACT.—The Northwest Tecumseh field, primarily a stratigraphic trap producing from a NNE-trending Red Fork sandstone, is ~1 mi wide and 6 mi long; it is located in nine sections of T. 10 N., R. 3 E., in Pottawatomie County, Oklahoma. Since discovery of the field in 1979, 56 wells completed in the Red Fork have produced a cumulative of 7,134,000 bbl of oil and 26,423 million cubic feet of gas, as of January 1, 1991. Because the potential for secondary recovery from this field was recognized early in its development, 28 wells were cored, predominantly in the northern part of the field, and all wells have Dual-Induction and Compensated Neutron-Density logs. The field was unitized in March 1990, and a waterflood-recovery program was initiated early in 1991.

The lowest Red Fork interval consists of a dark marine shale which overlies the Inola Limestone. Two major Red Fork sandstone units are distinguished: (1) a fine-grained, lower sandstone unit which truncates the underlying marine shale and commonly has a deposit of pebbles at the base, and (2) an upper very fine-grained sandstone unit characterized by ripples and cross bedding. The Red Fork sandstones are overlain by interlaminated sandstone and shale or gray nonmarine shale, which in turn are overlain locally by the Skinner sandstone. The Pink lime, which typically occurs at the top of the Red Fork interval and below the Skinner sandstone, is absent throughout this area. The entire Red Fork sequence is interpreted to have been deposited in a river-dominated estuarine deltaic system.

The lower Red Fork sandstone unit varies in thickness from 10 to 66 ft, has few sedimentary structures, and is fairly homogeneous, with an average porosity of 17.5% and average permeability of 70 millidarcies (md). Most of this unit is water saturated, and only 13 of the field wells were completed in this unit above the water contact.

The upper Red Fork sandstone consists of one to five sand lobes, with a maximum net-sand thickness of 82 ft. It is interpreted as a series of meandering stacked crosscutting channels. The upper unit is dominated by silty to very fine-grained sandstones, with an average porosity of 17% and average permeability of 60 md. The upper unit shows more cross bedding and ripples than the lower unit, and it has greater vertical variation in both porosity and permeability.

The crosscutting and removal of portions of previously deposited channel fills of the upper Red Fork sandstone, and deposition of shale laminae and sandstones associated with the meandering channels, resulted in a series of elongate sand lenses of various sizes with boundaries of varying permeability. This reservoir has permeabilities that are greater in the horizontal direction than in the vertical direction, because of the shale laminae and cross bedding; and this is further complicated by communication with the water-saturated lower Red Fork unit where it has been truncated by the overlying upper Red Fork unit. To determine the size and extent of the productive-sand hydraulic-flow units, and the influence of heterogeneities within the system, a reservoir-simulation study of this field is being conducted.

INTRODUCTION

The Northwest Tecumseh field is a NNE-trending oil and gas field that produces from the Red Fork sandstone in T. 10 N., R. 3 E., Pottawatomie County, Oklahoma (Fig. 1). The field, located with-

in a nine section area, is ~1 mi wide and 6 mi long.

The field was discovered in 1979 by drilling of the Washburn no. 1-32. Prior to unitization in 1990, 56 wells were completed in the Red Fork with 40-acre well spacing. Cumulative production as of January 1, 1991, was 7,134,000 bbl of oil and 26,423

Lewis, F. S., 1993, Depositional variations and reservoir characterization in the Red Fork Sandstone, Northwest Tecumseh field, Pottawatomie County, Oklahoma, in Johnson, K. S.; and Campbell, J. A. (eds.), Petroleum-reservoir geology in the southern Midcontinent, 1991 symposium: Oklahoma Geological Survey Circular 95, p. 40-51.

million cubic feet of gas. The field was unitized in March 1990, and a waterflood-recovery program was initiated in early 1991.

The secondary recovery potential of the Northwest Tecumseh field was recognized early in its development, with the result that 28 wells (half the wells in the field) were cored. Only a few wells were cored in the southern end of the field, whereas almost every well was cored in the northern end; therefore, reservoir characteristics of the northern portion of the field could be measured at 40-acre intervals. This high-density core availability allows an excellent opportunity to evaluate the depositional variations and reservoir characteristics of a producing oil field.

REGIONAL TECTONIC SETTING AND STRATIGRAPHY

The Northwest Tecumseh field is located in the southern part of the central Oklahoma platform, which is bound by the Seminole–Cushing uplift (east), the Nemaha uplift (west), and the Pauls Valley uplift (south). This area is between two major sedimentary basins, the Anadarko basin to the west and the Arkoma basin to the southeast.

The NNE-trending Wilzetta fault marks the western edge of the Seminole–Cushing uplift, which plunges northward from the Pauls Valley uplift (Pulling, 1979). The fault was active as early as Middle Devonian time; however, the greatest movement occurred in late Morrowan time, during the Wichita orogeny. Raising of the Seminole–Cushing uplift resulted in erosion of Mississippian strata over the uplift and thinning of the Cherokee Group, including both the Red Fork and Skinner intervals (Cole, 1969). This indicates that the uplift was a topographic feature throughout Cherokee deposition.

The Nemaha uplift formed in late Morrowan time, during the Wichita orogeny, and was subaerially exposed during the Early Pennsylvanian. The ridge was again submerged by the end of the Cherokee deposition. The McClain County fault zone, an extension of the Nemaha uplift that extends through Cleveland and McClain Counties, has a maximum displacement of 2,300 ft where it meets the Pauls Valley uplift. This fault was the major shearing zone between the central Oklahoma platform and the Anadarko basin (Jacobsen, 1949). The Pauls Valley uplift had its major movement during the Wichita orogeny, when it was uplifted and tilted toward the east; this resulted in erosion and truncation of the Mississippian Caney Shale and Mayes limestone. This area was relatively stable during later Pennsylvanian times, and Pennsylvanian strata overlying the unconformity consist of repeated sequences of shale and sandstone and thin shelf limestones. Correlation of the Pennsylvanian limestones shows that younger

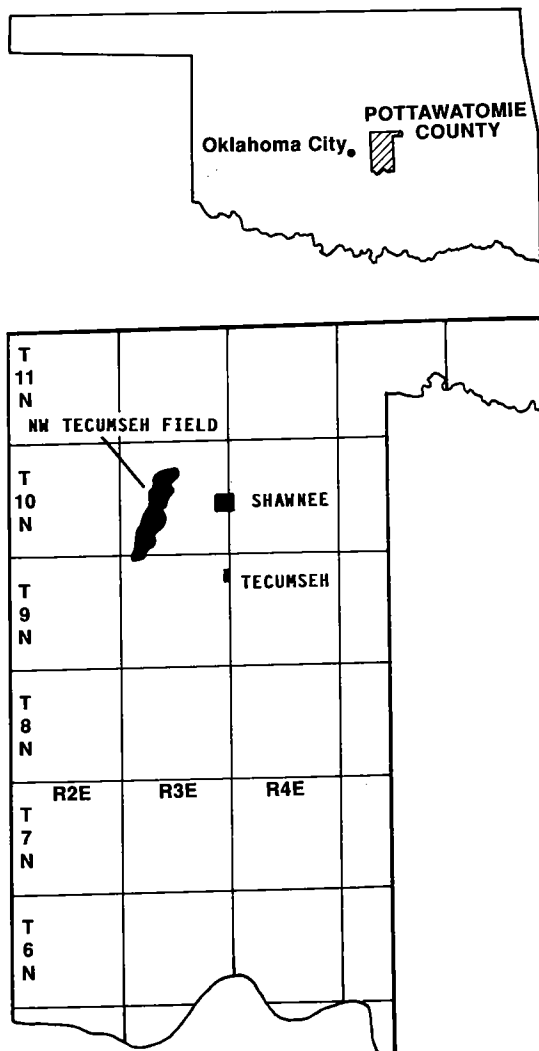


Figure 1. General location of the Northwest Tecumseh field in Pottawatomie County, Oklahoma.

time-stratigraphic units extend farther north onto the platform, indicating an overall Pennsylvanian transgression interrupted by progradational episodes (Visher and others, 1971). Westward tilting in post-Permian to pre-Cretaceous time caused the present-day W dip.

A well log and subsurface nomenclature are shown in Figure 2. The oldest Pennsylvanian sedimentary unit in the study area is the Booch sandstone zone or unconformity zone, which lies unconformably on top of the Mississippian and is, in turn, overlain by the Brown limestone. The Bartlesville sandstone overlies the Brown limestone and produces oil in this area along a NESW trend that is ~0.5 mi wide and 8 mi long that crosses the Northwest Tecumseh field. The Bar-

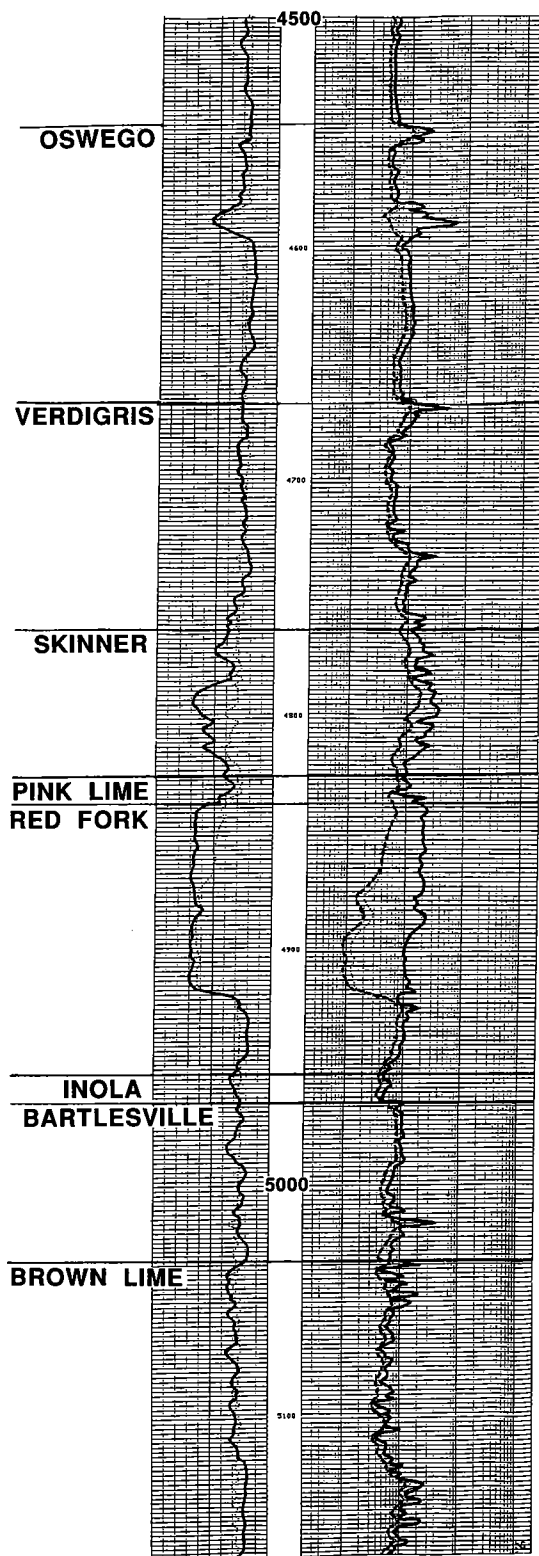


Figure 2. Well log and stratigraphic column in the Parson no. 1-16, sec. 16, T. 10 N., R. 3 E., Pottawatomie County, Oklahoma.

tlesville zone is overlain by the Inola Limestone which in turn is overlain by the Red Fork zone. The Pink lime separates the Red Fork zone from the overlying Skinner zone (Fig. 2) but is absent over the Northwest Tecumseh field. The Skinner is productive 2 mi east of this field.

DEPOSITIONAL FACIES

All 28 cores were examined for lithology, texture, fabric, and sedimentary structures. The information derived from individual cores was then compared to the well logs. Compensated Neutron-Density logs and Dual-Induction Laterologs were run on each well in this field. Logs from cored intervals were then correlated to logs of uncored intervals.

The Red Fork zone has five major facies: lower shale, lower Red Fork sandstone, intermediate shale, upper Red Fork sandstone, and upper shale. Approximately half of the wells in this field contain all five facies; the remaining wells have one or more facies missing due to erosion by cross-cutting channels or nondeposition.

The Red Fork sandstone is underlain by a dark marine prodelta shale. In turn, this shale is underlain by the Inola Limestone. Analyses of the seven cores in the study area which have penetrated this shale indicate that it is a very thinly laminated, gray-black shale to shaley siltstone. The laminae are predominantly flat, but some wavy to convolute zones, which commonly are fossiliferous, are also present. The fossiliferous zones contain brachiopod shell fragments and spines, echinoderm fragments, other shell fragments, and foraminifera (Dale, 1985). Some of the cores contain maroon-to reddish-colored bands, 2-8 in. thick. The bands have no known lithologic control. In one core, three such maroon bands are present, but there are not enough cores of this shale to enable correlation of the maroon zones between wells.

Regional mapping of the area, utilizing electric logs, indicates that this lower shale interval thickens from southwest to northeast. The shale thins beneath the Red Fork sandstone due to downcutting and incising of the Red Fork channel. In the southern part of the field, where the lower Red Fork is thickest, the entire lower shale and the underlying Inola Limestone have been eroded, and the lower Red Fork sandstone is in contact with shale of the Bartlesville zone (no actual Red Fork/Bartlesville sandstone contact was evident).

The lower Red Fork sandstone unit, exhibiting a sharp scour-surface contact and commonly containing a deposit of pebbles at the base, lies on the truncated underlying marine shale. Some clay clasts consisting of rounded and subrounded ironstone masses as much as 1 in. long were incorporated in the sandstone. These are mostly in thin layers, predominantly in the lower third of the unit.

This sandstone appears to be a massive, structureless sandstone, although in some cores it contains a few thick cross beds. The aggregate thickness of sand zones that have a low shale content and a porosity >6% is 10–66 ft.

Most of the lower Red Fork sandstone is water saturated. Only 13 of the wells in the field are completed in the lower Red Fork, and most of these were completed because the upper Red Fork sandstone was of poor quality or absent. Analysis of the well logs and the cores through the lower sandstone shows a fairly consistent porosity, averaging 17.5%, and a fairly consistent permeability averaging 70 md.

Except where overlain by the upper Red Fork sandstone, the lower Red Fork sandstone is overlain by a gray-black, thinly laminated shale (intermediate shale). This shale, separating the upper and lower sandstones, is as much as 40 ft thick along the edges of the field.

The upper Red Fork sandstone lies on top of the lower Red Fork sandstone or the intermediate shale. Contact between the upper and lower sandstone (cored in 11 wells) is conformable and is difficult to distinguish, except for the more laminated nature of the upper sandstone unit. The upper sandstone/intermediate shale contacts are gradational or sharp with small-scale load structures.

The upper Red Fork sandstone consists of a series of interbedded shales and silty to very fine-grained sandstones. Locally, a few thin beds of subrounded, ironstone-clay clasts are present near the base of this unit. The upper sandstone is finer grained than the lower sandstone, and it consists of several sequences of shale laminae interbedded with very fine-grained sandstones. Ripples exist within the sandstone laminae and some minor amounts of cross bedding are present. The aggregate thickness of sands that have a low shale content and porosity >6% is 10–82 ft.

Locally, erosional surfaces within sandstone beds are clean sandstone-to-sandstone contacts, between depositional sequences. But more often these depositional sequences are separated by thin layers of shale 0.5–1 in. thick. These depositional-sequence boundaries are easily recognizable in the well logs and can be correlated to define individual sand lobes. The various cores and well logs analyzed contain one to five depositional sequences. As would be expected, wells with only one or two depositional sequences are at the edge of the field; wells in the center of the field contain more depositional sequences.

Porosities and permeabilities of the upper sandstone are much more variable than those of the lower sandstone, although the greatest variability is near boundaries of the depositional sequences. Within depositional sequences, the porosity averaged 17% and the permeability averaged 60 md.

Shale overlying the upper Red Fork sandstone is

immediately overlain by the lower Skinner shale. The Pink lime that is present both east and west of the field is absent. Analysis of well logs and cores that lack an overlying Skinner sandstone indicate that the limestone was never deposited and that the absence of the Pink lime is not caused by Skinner erosion. The electric logs throughout this field do, however, exhibit a consistent resistivity spike that correlates with the stratigraphic position of the Pink lime in wells to the east and west.

The Skinner has locally cut into the upper Red Fork shale. However, none of the well logs or cores show any direct contact of the Skinner and Red Fork sandstones. Strata between these sandstones are at least 1.5 ft thick and consist of thinly laminated shale and silt, often containing a coal bed or organic content shale at the base.

FIELD GEOLOGY AND INTERPRETATION

Structural interpretation is based on maps prepared for both the top of the Inola Limestone (Fig. 3) and the top of the Verdigris Limestone (Fig. 4). These units were chosen because they occur below and above the Red Fork zone, and may be considered isochronal surfaces.

Both structure maps show a general dip of 80–90 ft/mi toward the WNW and the presence of two minor faults. Both faults trend WNW with displacements of 10–30 ft. These faults, which would not have been evident except for the high density of wells provided by the 40-acre spacing in this area, may restrict the drainage of hydrocarbons, but they do not have sufficient throw to isolate portions of the field. The faulting probably occurred after Cherokee deposition; however, the thickest portions of the Red Fork sandstone correspond with the location of the faults, suggesting that some movement might have been contemporaneous with Red Fork deposition.

The lower Red Fork was deposited as a relatively straight, narrow sandbody (Fig. 5). Cores indicate that the lower Red Fork is a structureless sheet sand. The upper Red Fork sandstone channel is wider and slightly more sinuous than the lower unit (Fig. 6). The aggregate thickness of the lower and upper Red Fork sands is shown in Figure 7. In contrast to the lower Red Fork, upper Red Fork cores contain a larger number of crosscutting channels. This suggests that although it was constrained to the same linear trend as the lower Red Fork sandstone, its channel meandered more and therefore had greater sinuosity.

Red Fork sandstones in the Northwest Tecumseh field are interpreted to be valley-fill deposits located at or near the marine shoreline of a river-dominated estuarine delta. The maroon bands in the lower marine or prodelta shale are interpreted as evidence of subaerial exposure during one or more episodes of lower sea level. The marine shelf,

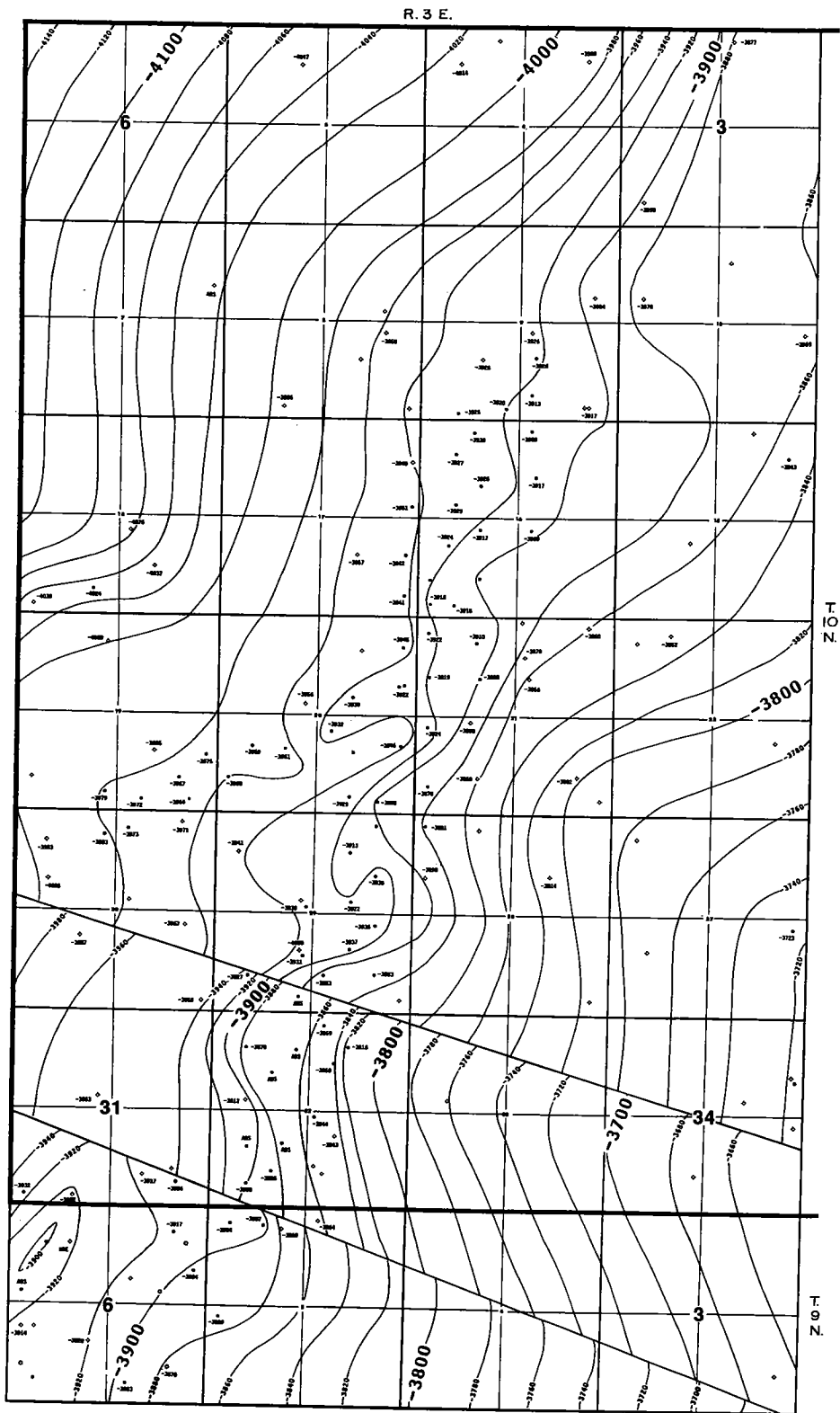


Figure 3. Structure map of the Northwest Tecumseh field on the top of the Inola Limestone; contour interval, 20 ft.

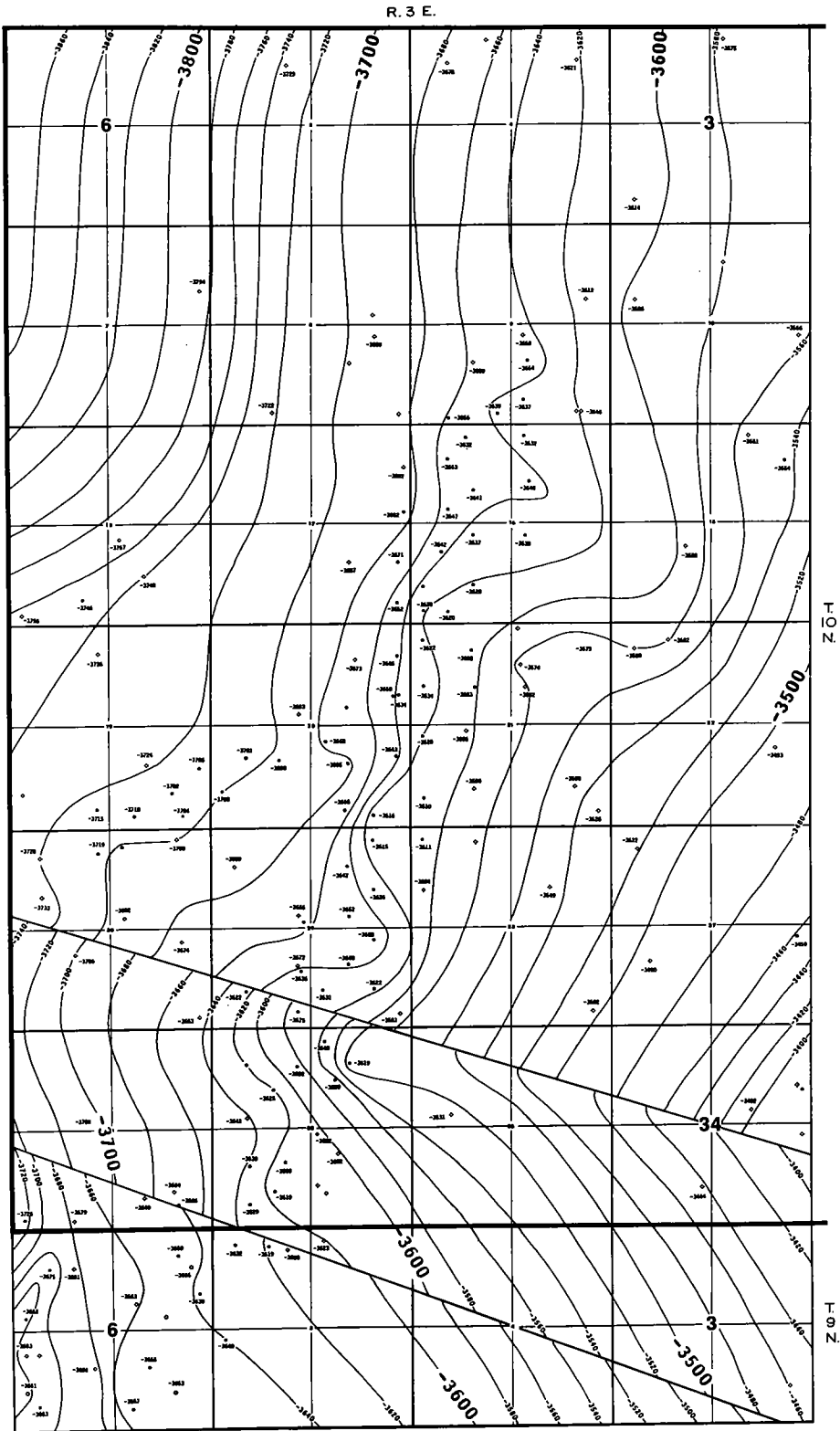


Figure 4. Structure map of the Northwest Tecumseh field on the top of the Verdigris Limestone; contour interval, 20 ft.

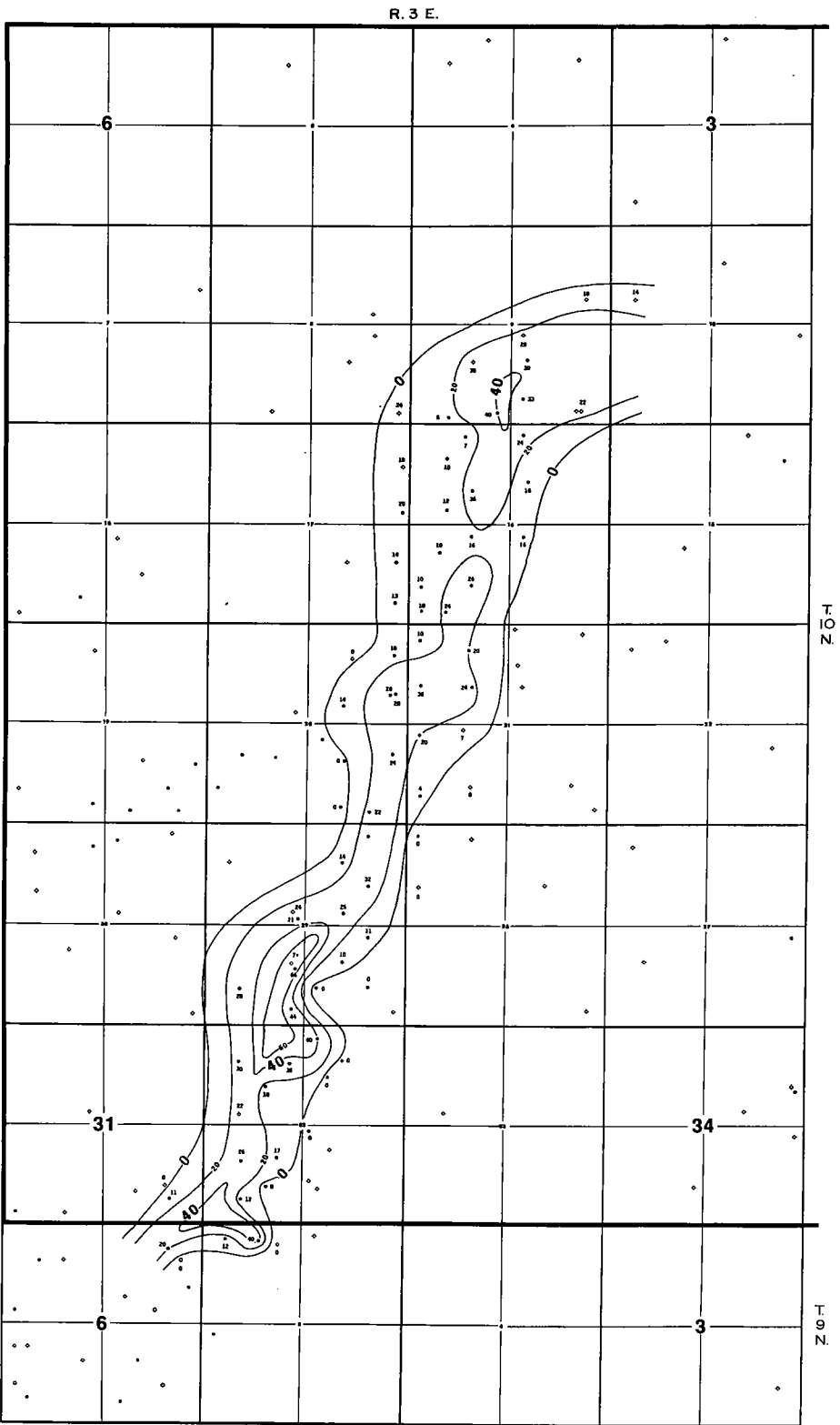


Figure 5. Aggregate thickness of lower Red Fork sands that have a low shale content and a porosity >6%; Northwest Tecumseh field. Contour interval is 20 ft.

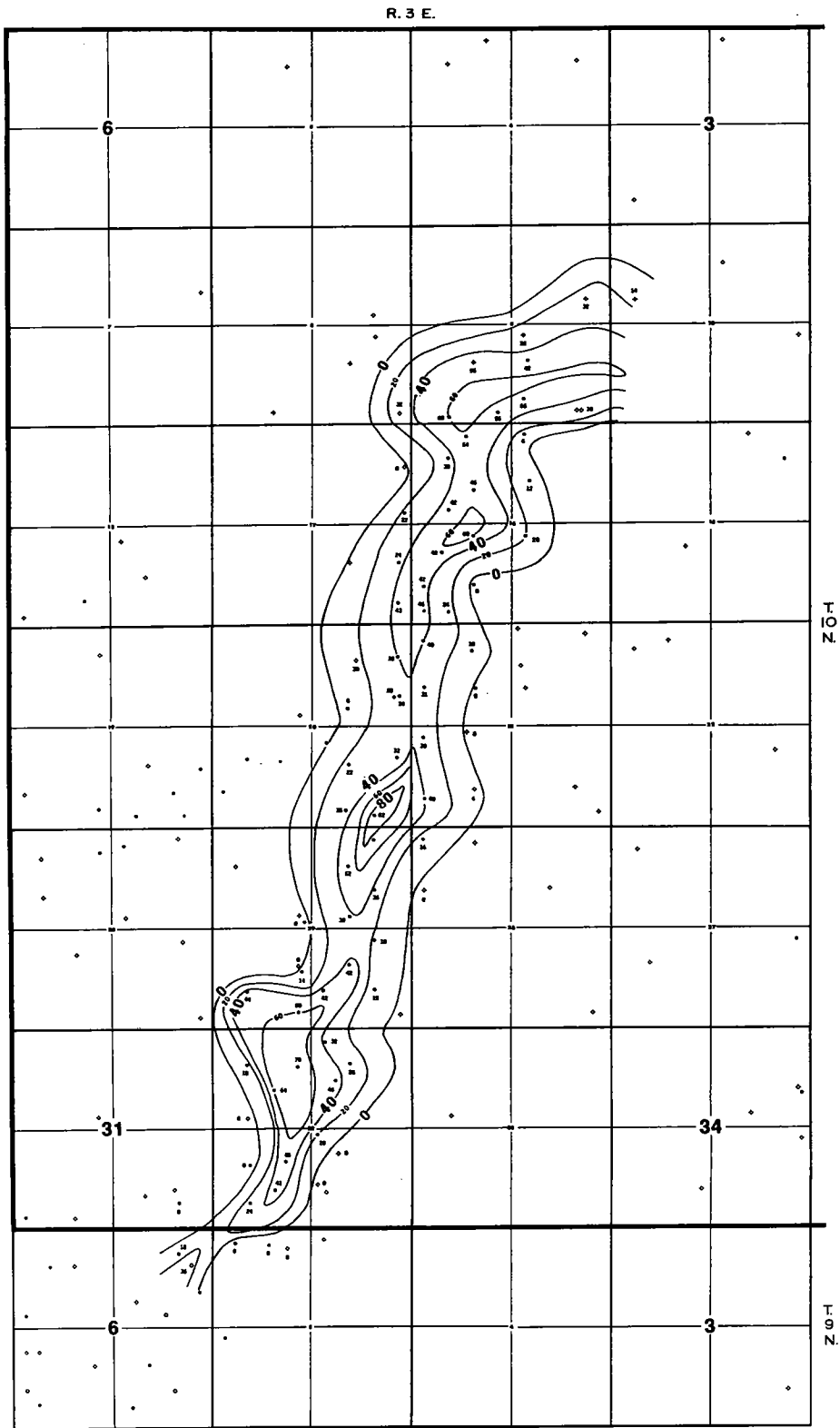


Figure 6. Aggregate thickness of upper Red Fork sands that have a low shale content and a porosity >6%; Northwest Tecumseh field. Contour interval is 20 ft.

during deposition of the Red Fork, was shallow, and the overall sea-level change necessary to cause exposure of the marine shales could have been as small as 160 ft. The Northwest Tecumseh field is one of the southernmost Red Fork producing fields in eastern Oklahoma.

During a low stand of sea level, a channel was incised into the exposed prodelta shale and, in the southern part of the field, into the underlying Inola Limestone; this incision probably was done by the same fluvial system that supplied the sediment for the underlying prodelta facies. The thick, fine-grained, lower Red Fork sandstone was then deposited in the incised valley. Although this typical valley-fill sequence was deposited close to the marine shoreline, it does not have characteristics of tide- or wave-dominated deposits. However, it may be that such features are not apparent because of the lack of sufficient shale laminae within this thick, massive sand. A subsequent sea level rise allowed another period of shale deposition (the intermediate shale).

An additional period of progradation allowed another episode of channel cutting, followed by deposition of a series of shales and very fine-grained sandstones. These were deposited as a series of meandering cut-and-fill channels, typical of fluvial or upper delta-plain deposits. The area of deposition would have been larger except for the topographic control exerted by the original incised valley.

MINERALOGY AND POROSITY

Thin sections of cores from both the upper and lower Red Fork sandstone in various wells show both units to be sublitharenites (Folk, 1968) with similar compositions. Generally, the lower Red Fork is fine-grained sandstone and the upper unit is very fine-grained sandstone. The sandstones of each unit are composed of 90% quartz, 3% feldspar, and 5% rock fragments. Of the total rock, 2–10% is clay matrix consisting predominantly of kaolinite, with some chlorite and illite (Dale, 1985). Mica, predominantly muscovite, with some biotite and chlorite, constitute ~1% of the lower sandstone and as much as 4% of the upper sandstone.

Porosity in these sandstones was caused by the partial dissolution of carbonate cement that was predominantly deposited after compaction and loss of primary porosity; this is seen in the irregular fabric and sutured grain-to-grain quartz contacts. The secondary porosity appears to correspond closely to the original intergranular pore network, with the result that the pore-distribution patterns of these two sandstones may closely track the original depositional patterns. This hypothesis needs to be tested because significant anisotropies may have been introduced by the secondary porosity.

The two sandstones contain both mica and

shale laminae. They do not prevent vertical fluid flow, but they probably significantly reduce the vertical-to-horizontal permeability ratios. If dissolution has also been affected by the shale laminae and mica, the vertical-to-horizontal permeability ratio might be reduced even further.

RESERVOIR-MODELING CONSIDERATIONS

The Northwest Tecumseh field is complicated by the W dip of the formation, along with higher water saturations in the western wells and higher gas/oil ratios in the eastern wells. The waterflood is scheduled to have 21 water-injection wells, predominantly along the western edge of the field, and two gas-injection wells along the eastern edge (Fig. 8).

The lower Red Fork sandstone appears to have fairly consistent porosity and permeability values (at least, it shows no extremes) that can be fit easily into a three-dimensional grid system for the reservoir simulation. However, the upper Red Fork sandstone consists of a series of elongate sand lenses of different sizes, with boundaries of various permeabilities; this results from the cross-cutting channels, the removal of portions of previously deposited channel fills, and the deposition of shale laminae associated with meandering channels.

The upper Red Fork sandstone unit appears to have a fairly consistent permeability and porosity within lenses, and fluid flow within each of the lenses (with the same water saturations and pressures) should be the same. The ability of a lens, or a productive hydraulic-flow unit, to communicate with its neighboring hydraulic-flow unit is a function of the unit/unit boundary. A sandstone/sandstone lens boundary may not be a boundary to flow, but a sufficiently thick layer of shale may prevent communication.

Many of the individual depositional sequences identified in cores and well logs may be correlated between wells as individual channels, but with 40-acre spacing this cannot be proven. It is not known if sequences at the same stratigraphic level are actually continuous and connected, or are separated by a cross-cutting channel. A large number of the sequences either cannot be correlated, or offer many potential correlations, all of equal probability. These sequences or hydraulic-flow units appear to range in size from 10 to 80 acres drainage; this means that additional hydraulic-flow units should exist between the current wells, with no evidence of their existence in either the cores or well logs.

To complete a proper reservoir simulation of this field, it will be necessary to determine the probable number of hydraulic-flow units between each producing well, the size distribution of those hydraulic-flow units, and the unit/unit boundary

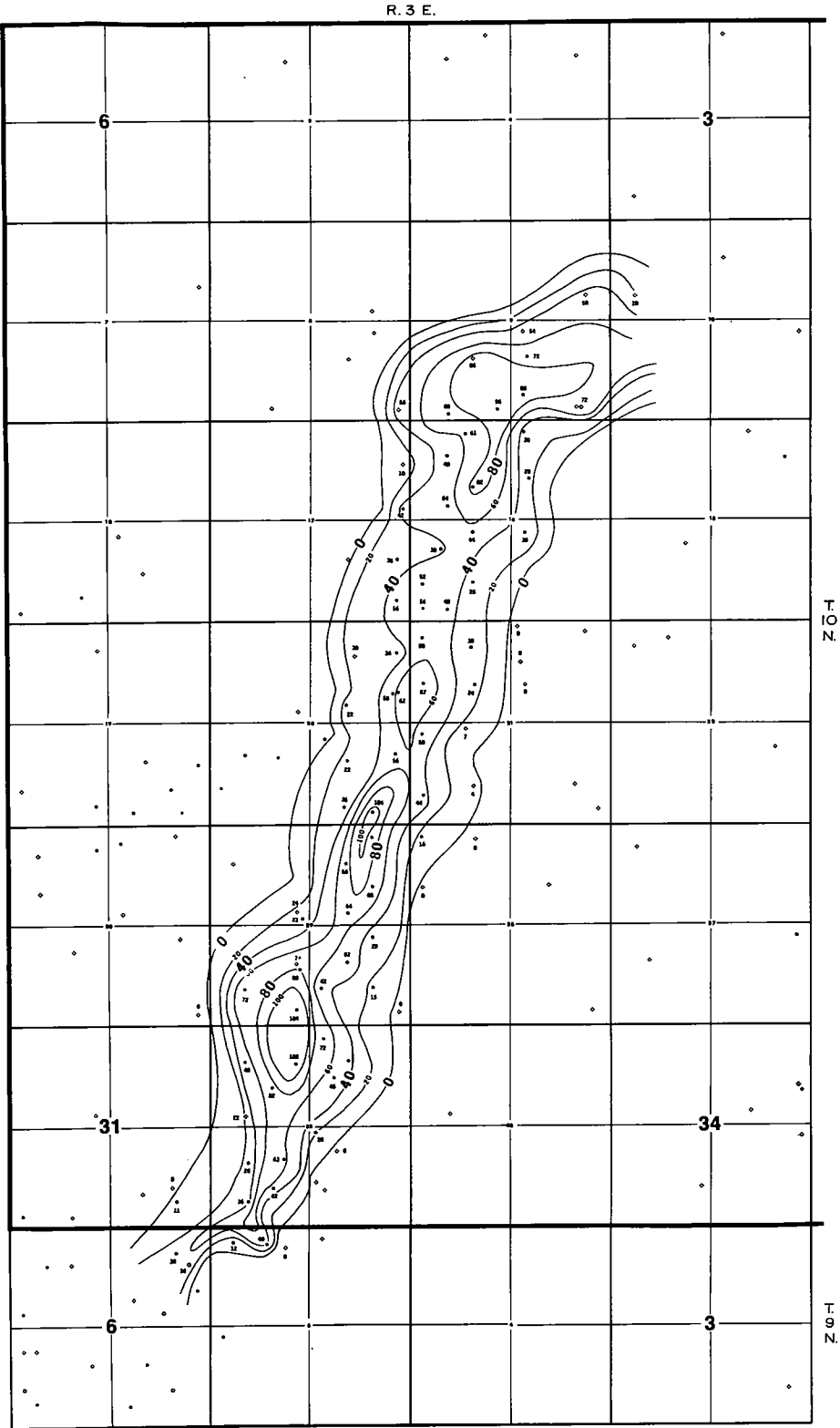
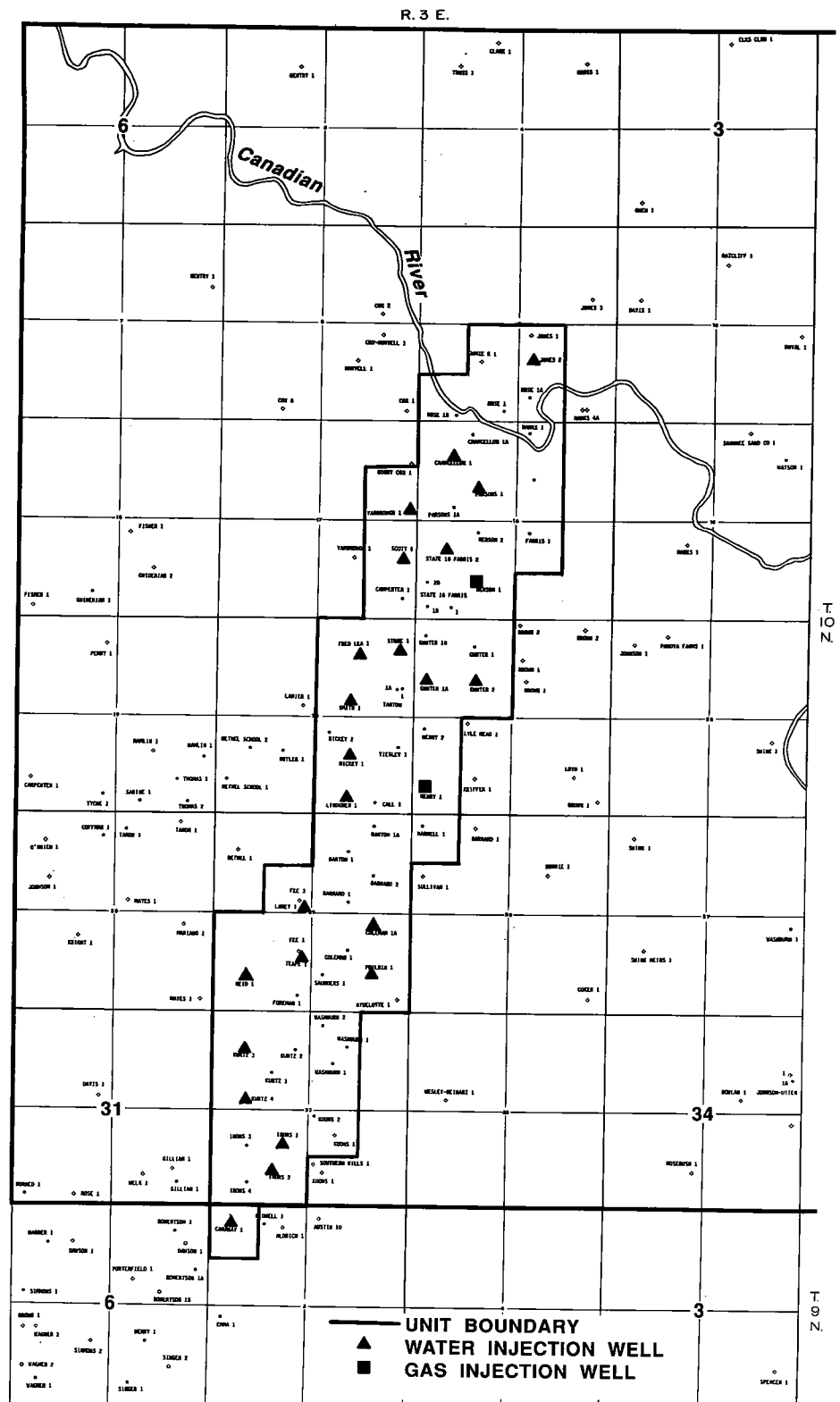


Figure 7. Aggregate thickness of lower and upper Red Fork sands that have a low shale content and a porosity >6%; Northwest Tecumseh field. Contour interval is 20 ft.



conditions. The determination of these parameters may never be accurately known, but they might be statistically determined in order to assign an average or weighted permeability for each reservoir-simulation grid block.

Once the values of porosity, permeability (vertical and the two horizontal directions), and other conditions are determined for each grid block, the field may be modeled. A reservoir simulation may then be performed to determine how closely the actual and modeled productions match.

REFERENCES CITED

- Cole, J. G., 1969, Stratigraphic study of the Cherokee and Marmaton sequences, Pennsylvanian (Desmoinesian), east flank of the Nemaha ridge, north-central Oklahoma: Oklahoma City Geological Society Shale Shaker, v. 21, p. 52-67.
- Dale, T. B., 1985, The Red Fork and lower Skinner sandstones in the Northwest Tecumseh field, T. 10 N., R. 3 E., north-central Pottawatomie County, Oklahoma: University of Tulsa unpublished M.S. thesis, 91 p.
- Folk, R. L., 1968, Petrology of sedimentary rocks: Hemphill Book Store, Austin, Texas, 170 p.
- Jacobsen, L., 1949, Structural relationships on the east flank of the Anadarko basin, in Cleveland and McClain Counties, Oklahoma: American Association of Petroleum Geologists Bulletin, v. 33, p. 695-719.
- Pulling, D. M., 1979, Subsurface stratigraphic and structural analysis, Cherokee Group, Pottawatomie County, Oklahoma: Oklahoma City Geological Society Shale Shaker, v. 29, p. 124-127, 148-158.
- Visher, G. S.; Saitta, S.; and Phares, R. S., 1971, Pennsylvanian delta patterns and petroleum occurrences in eastern Oklahoma: American Association of Petroleum Geologists Bulletin, v. 55, p. 1206-1230.

Characterization and Simulation of the Fractured Sycamore Limestone Reservoir within the Springer Field, Carter County, Oklahoma

Dan J. Garvey, Mark C. Potts,
J. M. Forgotson, Jr., and R. M. Knapp

University of Oklahoma
Norman, Oklahoma

ABSTRACT.—The Springer field, an anticlinal structure located south of the Arbuckle Mountains and north of the Caddo anticline in Carter County, Oklahoma, has produced oil and gas from several different horizons. The Sycamore Limestone (Early Mississippian) is the main producing horizon in the field and is the subject of this study.

Within the study area, the Sycamore averages 400 ft thick and is composed of three silty carbonate intervals separated by shaly carbonate sequences. Porosity of the silty carbonates ranges from 9 to 2%. Extensive fracturing of the resistive, silty beds of the Sycamore in the Springer field, evident in both outcrops and the subsurface, is the result of regional and local tectonic forces.

Characterizing the Sycamore reservoir to obtain an accurate model for simulation presented special challenges. The Sycamore was not cored in the field area, although a fairly extensive suite of logs was run on most of the wells. Samples were taken from Sycamore outcrops to obtain analogous core-plug, thin-section, and fracture data to assist in the field modeling. Uncertainties of subsurface fracture spacing and matrix storage capacities, in addition to a short primary production history for the field, made modeling difficult.

The performance of the Sycamore reservoir was simulated using the Eclipse 100 simulator. The geologic model consisted of six layers of alternating silty lime and calcareous shale beds. The geologic model was simplified into a four-layer simulation model. Each layer was characterized by structural position, thickness, porosity, and permeability in the X, Y, and Z directions. In addition, a dual porosity feature allowed for modeling a fracture system for each layer.

The reservoir fluid was characterized as a gas with vaporized oil (condensate). Because reservoir pressure was above the dew point, and no water contact had been defined, only one phase was used to model the reservoir. Gas-production rate was the control variable. Average reservoir pressure and individual well bottom-hole pressures served as match variables.

Objectives of the study were to obtain an accurate history match for the production to date, to determine reservoir capacity and the extent of fracturing within the reservoir, and ultimately to better understand the Sycamore reservoir within the Springer field. The results of this study may be useful for infield development planning and the possible application of horizontal drilling technology.

INTRODUCTION

The Springer field is in southern Oklahoma and is positioned along the northern boundary of the Ardmore basin in Carter County, Oklahoma (Fig. 1). It produces from an anticlinal structure located between the southwest flank of the Arbuckle Mountains and the northeast limb of the Caddo anticline. The crest of the structure is located in sec. 6, T. 3 S., R. 2 E. (Fig. 2), near the town of Springer. The field has produced oil and gas from several horizons, including the Goddard, Sycamore, Woodford, Hunton, Viola, and Arbuckle.

The Sycamore Limestone, one of the main objectives during initial field development, produces natural gas and associated liquid hydrocarbons.

The Sycamore Limestone (Lower Mississippian) reservoir in the Springer field was geologically characterized and then modeled with the Eclipse 100 3-D black-oil simulator. The reservoir characteristics of the Sycamore are discussed first. The simplified geologic model and grid system used to model the reservoir are then discussed, followed by the initial conditions and controls used in the simulation. The modifications required to achieve a history match are then out-

Garvey, D. J.; Potts, M. C.; Forgotson, J. M., Jr.; and Knapp, R. M., 1993, Characterization and simulation of the fractured Sycamore Limestone reservoir within the Springer field, Carter County, Oklahoma, in Johnson, K. S.; and Campbell, J. A. (eds.), *Petroleum-reservoir geology in the southern Midcontinent*, 1991 symposium: Oklahoma Geological Survey Circular 95, p. 52–59.

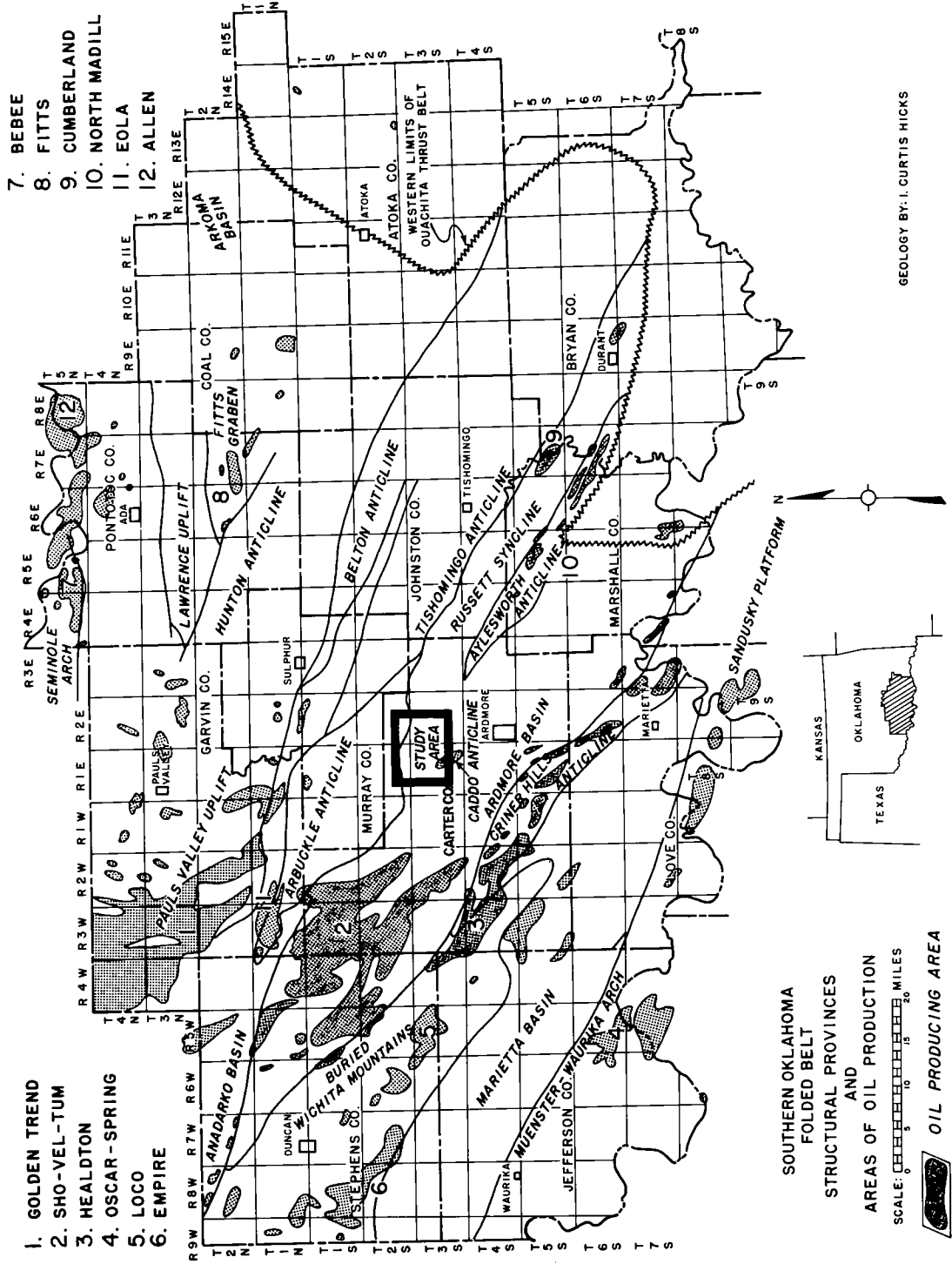


Figure 1. Regional geologic setting of the study area in southern Oklahoma (adapted from Hicks, 1971).

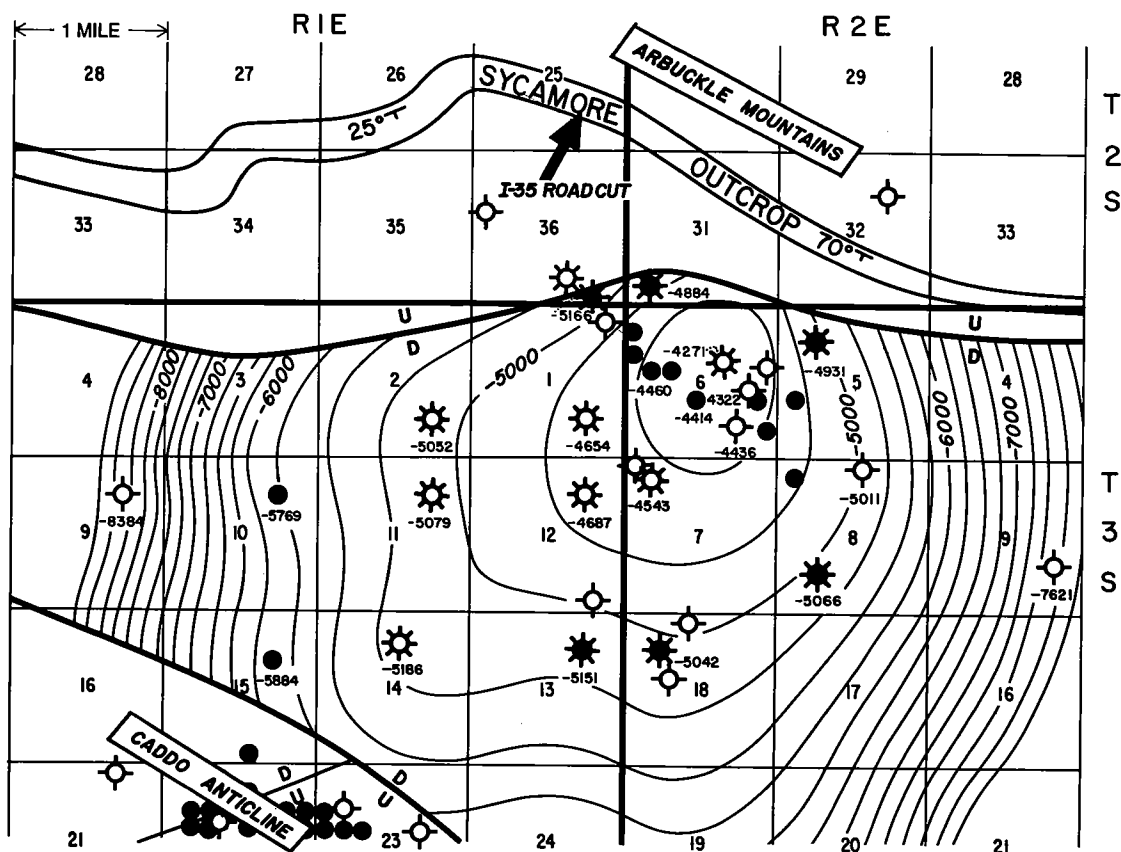


Figure 2. Local geologic setting of the study area. Structure contours on the Sycamore Limestone; contour interval: 250 ft.

lined, and, finally, conclusions and directions for future work obtained from the simulation are presented.

RESERVOIR CHARACTERIZATION

Stratigraphically, the Sycamore overlies the Woodford Shale and underlies the Caney Shale (Fig. 3). In the study area the Sycamore averages 400 ft thick and consists of slate-blue, hard, silty to fine sandy limestone intervals, separated by intervals of predominantly calcareous shale. It is generally characterized by three main silty carbonate intervals with high log resistivities separated by lower resistivity shaly intervals. The three resistive silty intervals have porosities, determined from density/neutron-log analysis and core plugs from outcrops, ranging from 9% in the uppermost interval, down to 2% in the lower two intervals. Because of its brittle nature and tectonic setting, the Sycamore is extensively fractured. This is apparent in outcrops along the southern flank of the Arbuckle uplift and in wellbores within the Springer field.

Reservoir characteristics of the Sycamore in the Springer field presented special challenges to cre-

ating an accurate simulation model. The Sycamore was not cored in the Springer field, but a fairly complete log suite (including fracture-identification logs) was run on most of the wells. In those wells in which a Frac-ID log was run and open fractures were interpreted, a majority of the fractures were oriented NESW (Fig. 4).

Fortunately, the Sycamore crops out ~1 mi north of the Springer field, and it is exposed in the Interstate-35 road cut along the south flank of the Arbuckle Mountain uplift (Fig. 2). The outcrop was studied and samples were taken to obtain analog core-plug, thin-section, and fracture data to assist in the field modeling. Tests run on the outcrop core plugs yielded porosity values similar to those determined from neutron/density logs of the three silty carbonate intervals in the field. Attempts to obtain good permeability data from the outcrop core plugs were not successful. The effects of weathering, deformation involved in the Arbuckle uplift, and excavation during construction of the highway probably had a significant impact on the Sycamore outcrop. As a result, outcrop characteristics may not be reflective of the Sycamore in the subsurface in the Springer field.

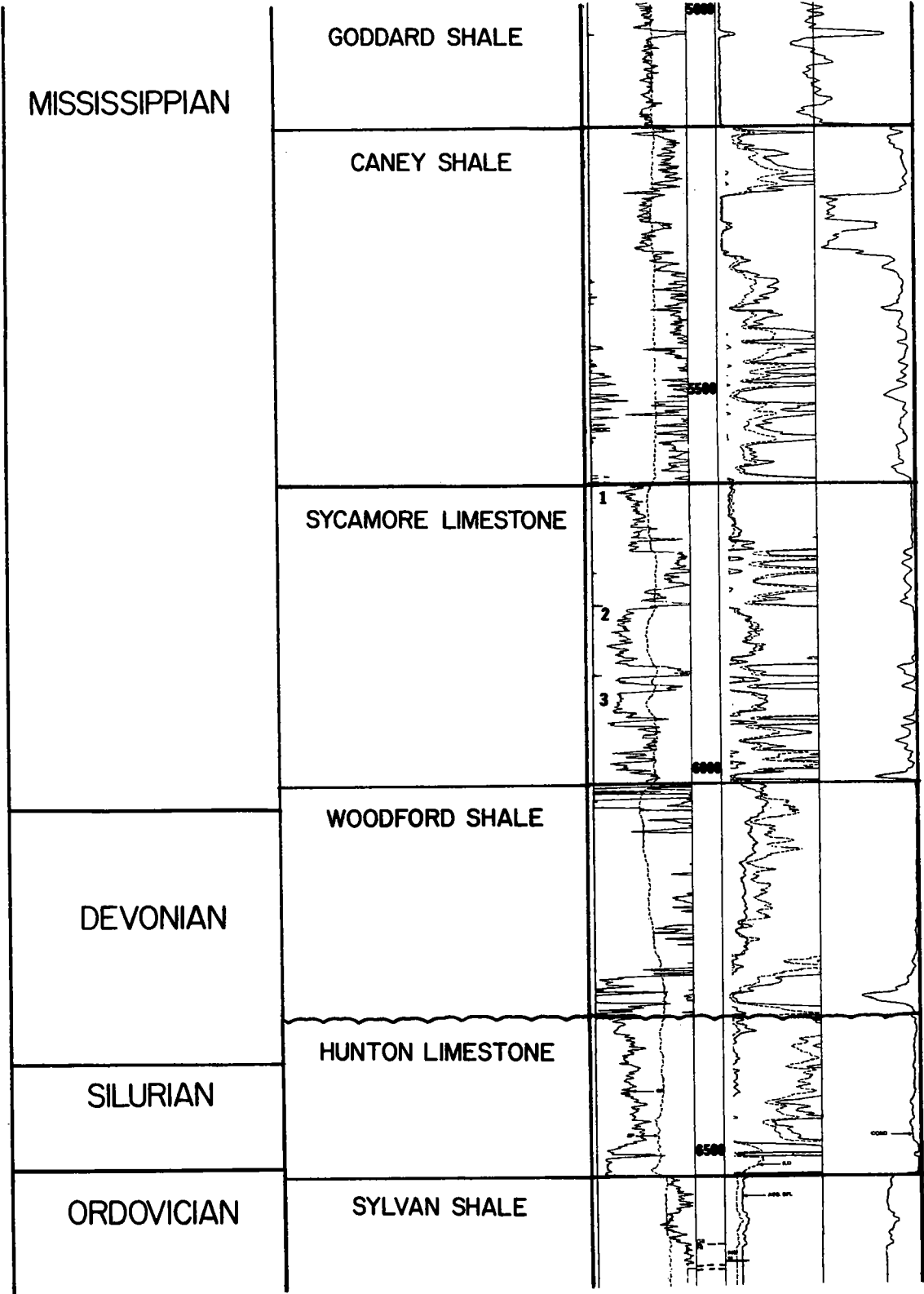


Figure 3. Stratigraphic column and representative log illustrating the three main silty intervals (numbered 1, 2, and 3) of the Sycamore Limestone.

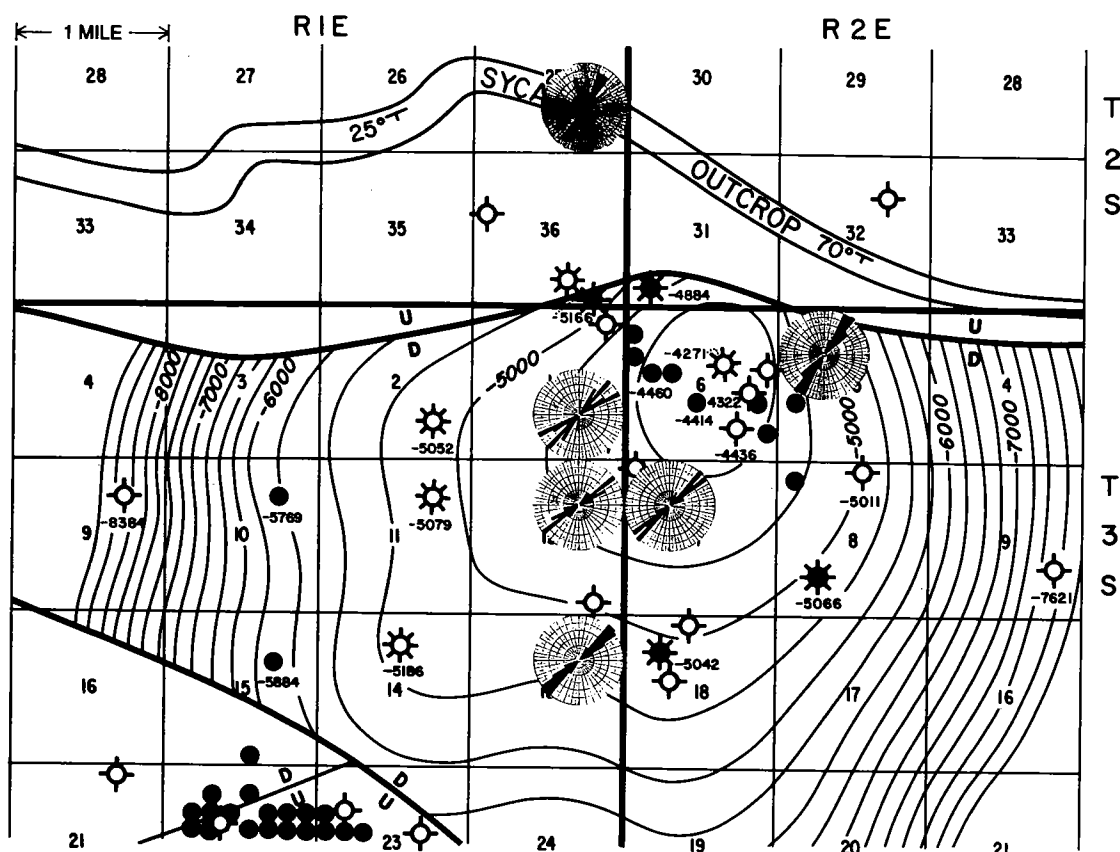


Figure 4. Fracture-orientation map using rose diagrams generated from the Frac-ID logs and outcrop data. Structure contours on the Sycamore Limestone; contour interval: 250 ft.

GEOLOGIC MODEL AND GRID SYSTEM

The geologic model of the Sycamore Limestone within the Springer field was simplified for reservoir simulation. A $20 \times 10 \times 4$ grid system was used to model the reservoir (Fig. 5). The X dimension used for each block was 1,155 ft, and the Y dimension was 1,515 ft. The four layers used to model the reservoir in the near-vertical dimension represent: (1) the silty carbonate matrix, (2) the interbedded shaly carbonate, (3) fractures within the silty carbonate, and (4) the fractures within the shaly carbonate interbeds (Fig. 6).

Although the thickness of individual strata within the Sycamore differs from well to well, the total thickness is fairly constant throughout the study area. Accordingly, layer one of the model was 225 ft thick, which is the average total thickness of the more resistive silty carbonate intervals, with 3% average porosity and 1 md average permeability.

Layer two of the model is 460 ft thick, and it represents a combination of both the interbedded Sycamore shales and the underlying Woodford

Shale. The average total thickness of the interbedded Sycamore shales is 175 ft, and the Woodford Shale is 285 ft. The porosity and permeability assigned to this layer were 15% and 0.1 md, respectively.

Layer three of the model represented the porosity and permeability attributable to fractures in the silty carbonate. Layer three was 225 ft thick, with 1% porosity and 50 D permeability. Constraints on the model included the restriction that reservoir fluids from layer one could flow only into layer three (i.e., the fluids in the silty carbonate matrix could flow only into fractures in the silty carbonates.). Since perforations in the reservoir only receive fluids from the fractures, layer three was the only layer open to the wellbores.

Layer four of the model which represented the fractures in the interbedded shaly intervals was 460 ft thick with 1% porosity and 50 D of permeability. Constraints on the model included the restriction that reservoir fluids from layer four could flow only into layer three (i.e., the fluids in the fractures within the interbedded shale could flow only into fractures in the silty carbonates.).

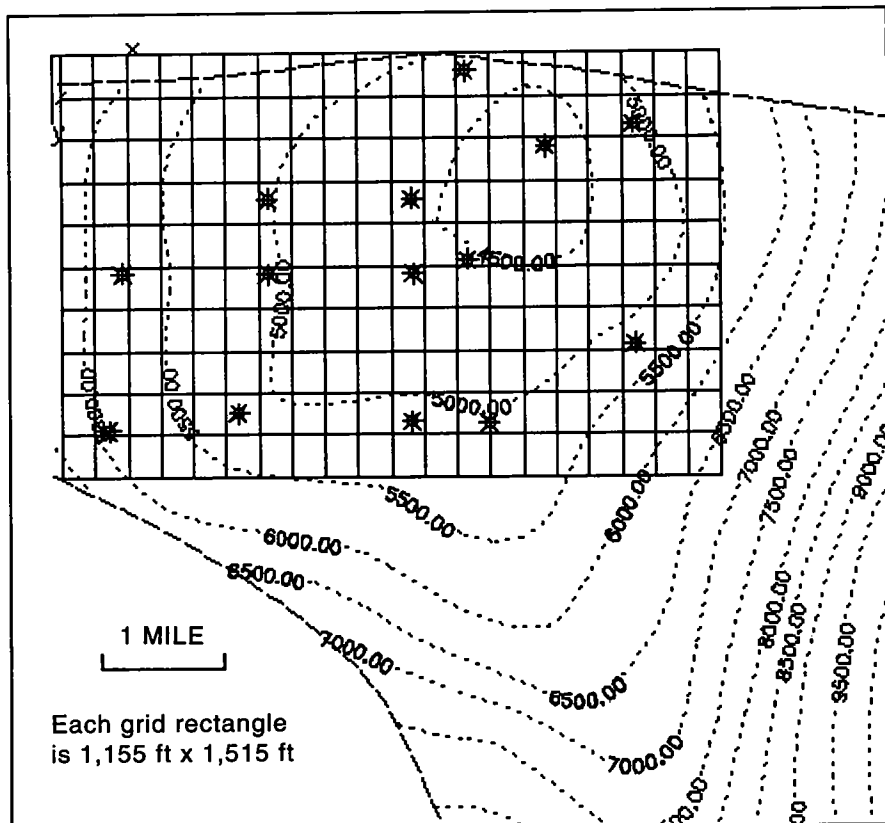


Figure 5. Map view of the grid system used to model the reservoir. Structure contours (feet below sea level) on the Sycamore Limestone; contour interval: 500 ft.

It should be noted here that layers one and three taken together describe the limestones, layer one being a description of the matrix and layer three being a description of the fractures. Similarly, layers two and four taken together describe the shales. Consequently, the thickness of the geologic model is 685 ft, the sum of layers one and two.

Factors which made accurate modeling of the field difficult were uncertainties of fracture spacing and orientation, unknown matrix storage capacities, and only a brief primary production history.

INITIAL CONDITIONS AND SIMULATION CONTROLS

The initial reservoir pressure used was 2,040 psia with a connate water saturation of 30%. A volumetric calculation of original gas in place (OGIP) indicated that ~3.9 trillion cubic feet (Tcf) of gas was present in the silty limestone, shale, and fractures. For each well within the field, the gas production rate versus time was preset in the simulation, and fieldwide average reservoir pressure and individual well tubing-head pressures (THPs) were the history-matching targets.

HISTORY MATCH

The initial simulation of the 4 Bcf production history did not reduce the simulated average reservoir pressure to that observed in bottom-hole pressure (BHP) tests in the field, nor did it cause simulated THPs to drop to observed THPs. Two possible causes were: (1) less than 3.9 Tcf of gas was actually present, and/or (2) observed BHP data did not accurately reflect average reservoir pressure.

Over the period from February 1987 through August 1988, four BHP tests in the Strader no. 1-8 indicated average reservoir pressures of 890, 1,085, 1,125, and 1,235 psia, respectively. It appeared that the low permeability of the matrix rock was not allowing the BHP tests to equilibrate average reservoir pressure. Shut-in periods of six months or more might be required of wells in the field for BHPs to reach the average reservoir pressure.

In order to match the actual flowing THPs, matrix permeability values were lowered from 1 to 0.5 md for the Sycamore matrix (layer 1) and from 0.1 to 0.005 md for the shale (layer 2). Porosity values

of the shale were lowered to 7.5%. Also, in the limbs of the anticline, fracture-permeability values were reduced from 50 D to 50 md and shale porosity values were lowered to 4.5%.
As a result of these changes, a good history match of flowing THPs was achieved for each well

(Fig. 7). However, simulated average reservoir pressure did not agree with observed average reservoir pressure. A possible reason why the observed BHPs did not accurately reflect simulated average reservoir pressure is that the simulated average reservoir pressure includes unsteady-state shale-matrix grid blocks that are unlikely to be observed in the BHP tests.

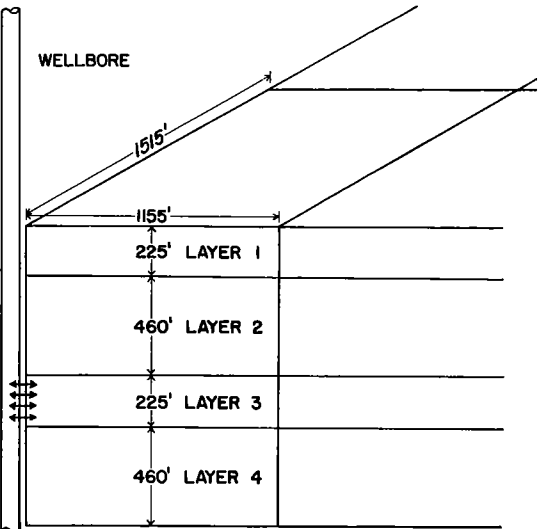


Figure 6. Block diagram showing the layers used in the simulation model.

CONCLUSIONS AND DIRECTIONS FOR FUTURE WORK

The results of the reservoir simulation indicate that OGIP is ~340 Bcf in the Sycamore matrix, 1 Tcf in the interbedded shale, and 38 Bcf in the fracture system. Since total produced gas represents <1% of the estimated OGIP, these results should be considered gross approximations and raise new questions. Is the fracture system less extensive or less connected than the model represents? Due to the tight nature of the reservoir, how much of the OGIP is actually recoverable?
The low permeability in the shale probably precludes drainage, even into a shale fracture system. The expected behavior of this low-permeability reservoir may require large fracture-stimulation treatments as well as periodic shut-in of wells to rebuild pressure for pipeline sales. Additional wells may be required, possibly horizontal, to adequately drain recoverable reserves.

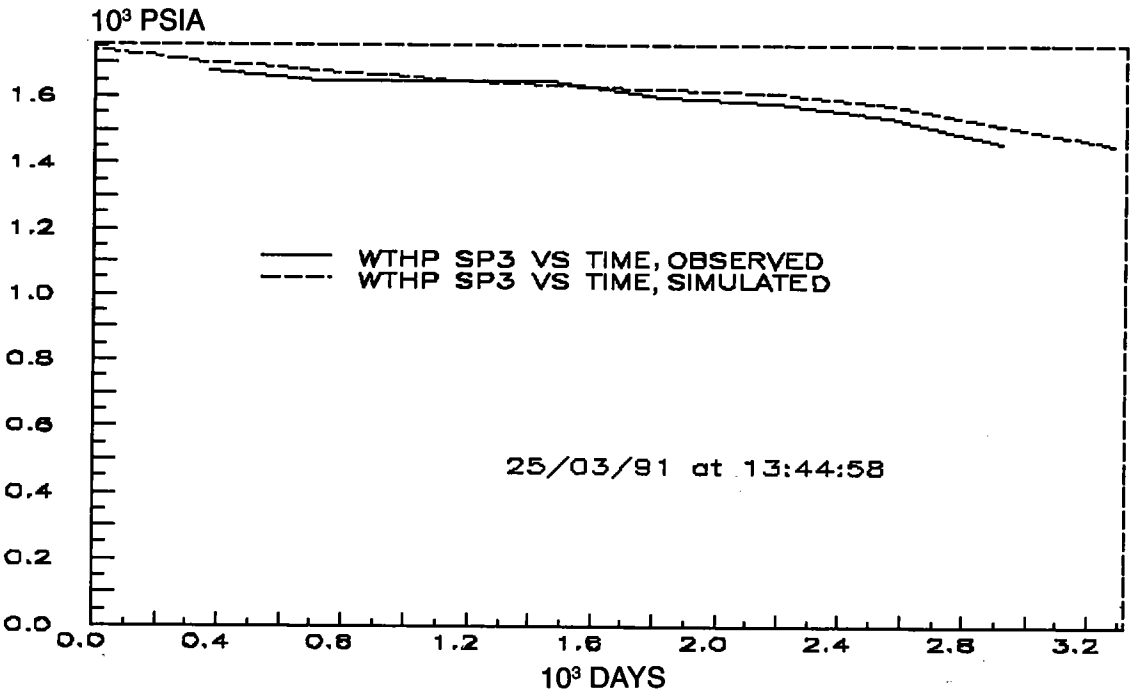


Figure 7. Graph of typical history match for observed vs. simulated well THPs in the Springer field.

Future work might investigate increasing well density to 160-acre spacing, the possible closure of the natural fractures as reservoir pressure declines, and the determination of the nature and orientation of the open natural fractures within the reservoir so the potential performance of horizontal wells could be simulated.

SELECTED REFERENCES

- Cole, Tony, 1988, A surface to subsurface study of the Sycamore Limestone (Mississippian) along the north flank of the Arbuckle anticline: University of Oklahoma unpublished M.S. thesis, 140 p.
- Fletcher, T. E., 1986, The structural geology of the Caddo anticline, Carter County, Oklahoma: Baylor University unpublished M.S. thesis, 83 p.
- Hicks, I. C., 1971, Southern Oklahoma folded belt, *in* Future petroleum provinces of the United States—their geology and potential: American Association of Petroleum Geologists Memoir 15, v. 2, p. 1070–1077.
- Johnson, K. S.; and others, 1989, Geology of the southern Midcontinent: Oklahoma Geological Survey Special Publication 89-2, 53 p.
- Nelson, R. A., 1985, Geologic analysis of naturally fractured reservoirs: Gulf Publishing Co., Houston, 320 p.
- Prestridge, J. D., 1957, A subsurface stratigraphic study of the Sycamore Formation in the Ardmore basin: University of Oklahoma unpublished M.S. thesis, 62 p.

Reservoir Characteristics of the McFarland and Magutex (Queen) Reservoirs, Permian Basin, Texas*

Mark H. Holtz

Bureau of Economic Geology
The University of Texas at Austin
Austin, Texas

INTRODUCTION

The Queen Formation (upper Guadalupian, Permian) is a sandstone reservoir that produces oil from the McFarland and Magutex fields in Andrews County of West Texas (Fig. 1). The McFarland Queen reservoir was discovered May 8, 1955, and the McFarland East Queen reservoir is an extension of McFarland field. Discovery of Magutex Queen field, 2 mi to the east, followed three years later. By 1963 the fields had been developed to 40-acre well spacing. This complex accounts for 73%, or 175 million stock-tank barrels (MMSTB), of the oil within the Queen tidal-flat sandstone play. Typical wells initially flowed ~100 bbl of oil per day; they decreased to ~10 bbl, on pump, within two to three years. In the early 1960s, waterflood programs in many of the units began to increase production rates and to improve recovery. The McFarland/Magutex reservoir complex currently has 311 producing, 100 injection, and 106 shut-in wells.

The Queen reservoir study was undertaken at two scales of investigation. A subregional-scale geological investigation provided the framework for a detailed engineering study that concentrated on State University Consolidated Units Nos. 1 and 2, a smaller, information-rich area located in the south-central portion of the McFarland Queen reservoir (Fig. 2). This study focused on core analyses from 38 wells (cores from all but one had been discarded), well-test data on file with the Railroad Commission of Texas for 1956–62, and antiquated gamma-ray/neutron logs that could be used for qualitative analysis only. The geologic study area includes University Block 4, which contains the portion of the McFarland Queen reservoir on University Lands, and the area of Block 5 containing the Magutex Queen reservoir. Cores were available from seven wells, two of which have suites of mod-

ern logs. Also available were >500 pre-1960 gamma-ray and neutron logs.

GEOLOGIC SETTING

Most of the Queen reservoirs are located along the west side of the central basin platform. The McFarland/Magutex Queen reservoir complex, however, is one of a smaller group of Queen reservoirs located on the east and south sides of the central basin platform. Within the Queen Formation, the reservoir complex produces oil from two sandstone zones, the upper denoted the A sandstone and the lower called the B sandstone. These two sandstone zones are separated by a supratidal-facies flow barrier consisting of dolomudstone and massive anhydrite.

Structure

Structure maps on the top of the A (top of the Queen Formation, Fig. 2) and B sandstones in University Blocks 4 and 5 indicate dip to the east

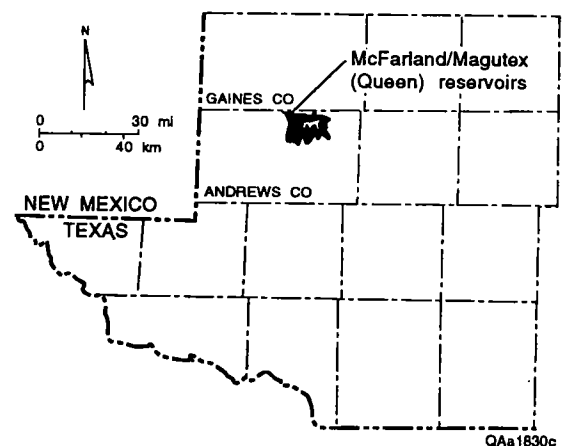


Figure 1. Location of McFarland/ Magutex reservoirs in Andrews County, Texas.

*Condensed from Tyler and others (1991).

Holtz, M. H., 1993, Reservoir characteristics of the McFarland and Magutex (Queen) reservoirs, Permian basin, Texas, in Johnson, K. S.; and Campbell, J. A. (eds.), Petroleum-reservoir geology in the southern Midcontinent, 1991 symposium: Oklahoma Geological Survey Circular 95, p. 60–65.

and south, with local highs. The eastern dip forms a nose that extends halfway into Block 4. A high with 50 ft of closure is centered in sec. 15, Block 4; a trough extends from the northeastern area of Block 4 to the south to separate the McFarland Queen and Magutex Queen reservoirs.

The structure appears to be the result of compaction deformation (drape) of the Queen Formation over preexisting paleotopography. Queen structural highs are coincident with, and are underlain by, similar Strawn, Devonian, and Ellenburger structures, which are also productive. The Queen thickens where there are structural lows in the underlying formations, and it thins where

there are structural highs. This relationship between thickness of the Queen and underlying structure suggests differential compaction over a preexisting paleostructure.

Development drilling of the reservoir complex was influenced by this structure. Nearly all of the developed area is on structural highs. This pattern implies that initial development proceeded on the premise that oil was trapped by structure. There are producing wells downdip of undeveloped areas, however, indicating a highly complex oil/water contact that has stratigraphic as well as structural control. This points to the potential for drilling additional infill and extension wells.

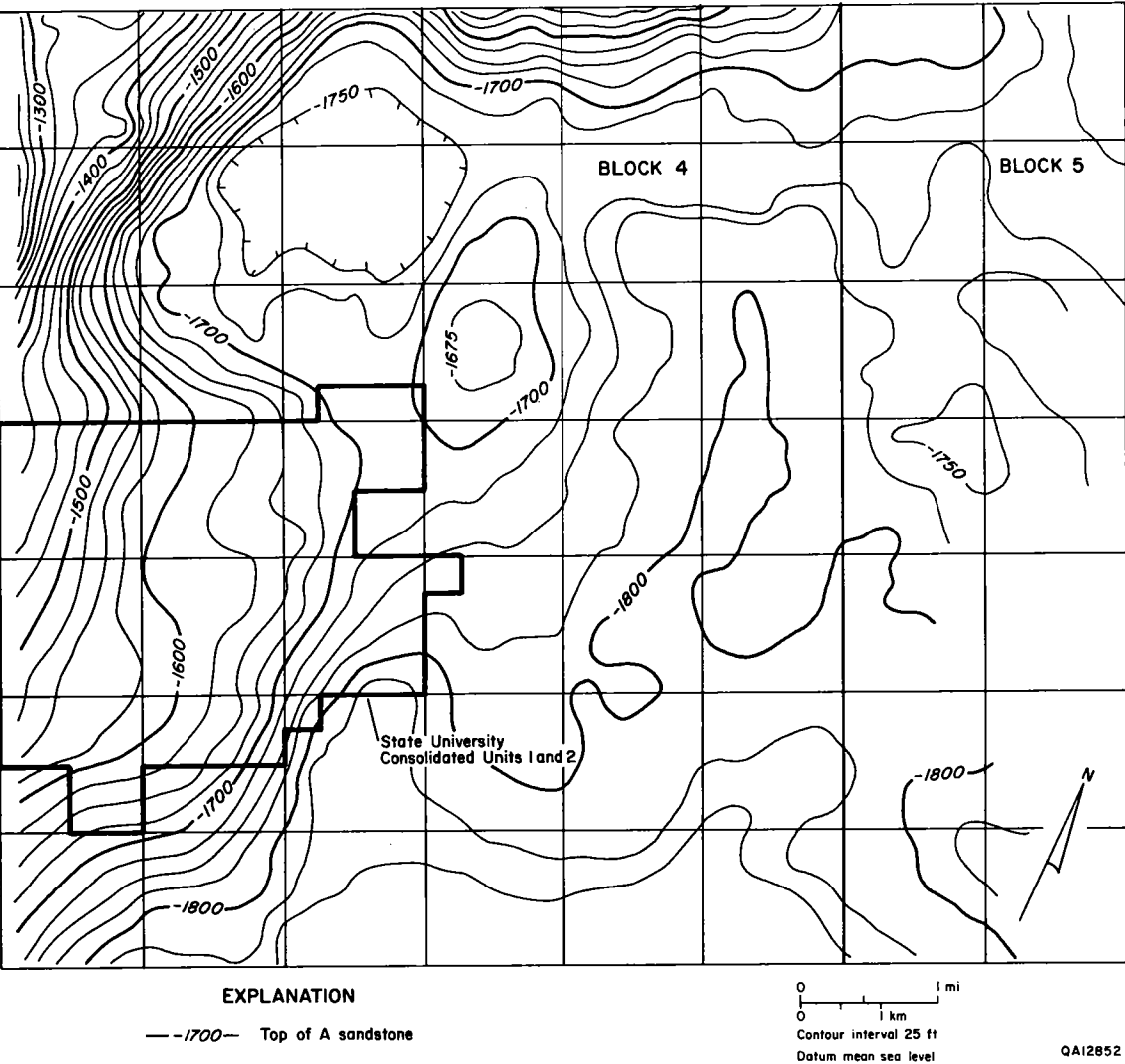


Figure 2. Structure map contoured on the top of the Queen Formation (top of A sandstone), University Block 4 and west half of Block 5. State University Consolidated Units No. 1 and 2 are outlined.

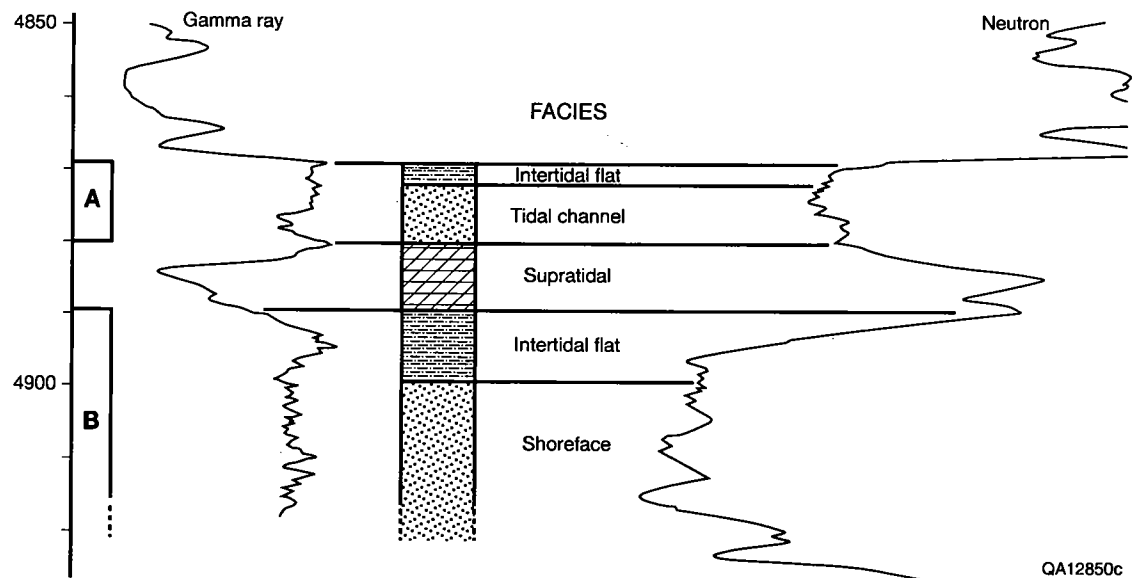


Figure 3. Type log of the McFarland/Magutex Queen reservoir complex. Intervals labeled A and B denote the two reservoir sandstone units; depths are in feet.

Stratigraphy and Facies

The reservoir consists of two sandstone zones (A and B) that lie within two progradational depositional cycles (Fig. 3). Each cycle grades upward from tan to brown, very fine to silty sandstones at the bottom, into massive red to gray-blue anhydrite at the top. Each depositional cycle has a sharp contact at the base and is overlain by a combination of intertidal-flat, tidal-channel, and shoreface sandstone facies. These sandstones grade into dolomudstones, which in turn grade into massive anhydrite, representing a sabkha facies. The cycles thicken toward the east and south, and a local thickening of the cycle is present in the northwestern part of Block 4, coincident with a local structural low.

Both the A and B sandstones extend throughout the reservoir complex and both are of uniform thickness on the western edge of Block 4. To the east, off structure, both sandstones thicken, and have local thick channels subparallel and subperpendicular to present structural strike. The highest production in the McFarland/Magutex Queen Units is coincident with those areas where either the A or B sandstone channels are thicker.

Four main depositional facies are recognized within Queen reservoirs: supratidal, intertidal-flat, tidal-channel, and shoreface. The supratidal facies consists of massive anhydrite and dolomudstone. An isopach map of the lower supratidal facies shows a regional thinning to the northwest and localized thick areas present in structural lows. This thinning is the result of reduction of the massive anhydrite component in the supratidal facies,

and also is coincident with present structural highs. The anhydrite contains various structures, including 0.5- to 1-in.-thick layers, nodular mosaics, and vertical gypsum pseudomorphs. Dolomudstone is light gray to cream colored and very finely crystalline. The mudstone contains nodular anhydrite and algal laminates, but it is barren of other fossils. The structures and rock types suggest that this supratidal facies was deposited in hypersaline ponds on a tidal flat, and that it was affected by only minor subaerial exposure. The intertidal-flat facies is characterized by root traces, algal laminations, and flaser bedding. These sandstones also display a mottled texture that is interpreted to have been produced by bioturbation. Tidal-channel facies are inferred from sandstone isopach maps, cross sections, and sedimentary structures. Basal channel-lag deposits in this area, described by Holley and Mazzullo (1988), have channel-floor erosion at the base, planar laminations, crossbeds, climbing ripples in the middle, and small ripples grading into planar-to-massive bedding at the top. The shoreface facies is characterized by parallel and massive bedding. The massive sandstone is commonly poorly consolidated and friable. Where observed in core, this facies is heavily oil stained and contains well-developed porosity and permeability, which make it a relatively highly productive facies.

Lithology and Porosity

The A and B sandstones are arkosic, with anhydrite and dolomite cement. They average 40% detrital quartz, 15% feldspar, and 25% anhydrite and

dolomite cement. Minor (up to 5%) clay and lithic fragments are also present. Both detrital and authigenic feldspar occur in the A and B sandstones. The detrital feldspar consists of partly leached plagioclase and orthoclase feldspar. Authigenic potassium feldspar is present as 5- μ m euhedral crystals, which preferentially nucleated on detrital feldspar. Clay types include illite and layers of chlorite mixed with smectite. The clay coats both quartz and feldspar detrital grains. Electron backscatter imagery indicates a high potassium content within the sandstones and a lack of uranium or thorium. Thus, the high gamma-ray response on well logs indicates relative amounts of potassium; because there is much more feldspar than clay, the gamma-ray log actually shows the relatively high amount of potassium feldspar.

Porosity and permeability in the reservoirs are directly related to the amount of anhydrite and dolomite cement present. Anhydrite occurs as poikilotopic cement and small, 0.5-in.-diameter, nodules. Dolomite cements the detrital grains and also occurs as authigenic, multifaceted, pore-filling dolomite. Dolomite cementation commonly follows small fractures and sedimentary struc-

tures, filling in between cross laminae. Porosity is of three types: interparticle porosity, separate-vug porosity, and microporosity. Interparticle porosity constitutes 50–85% of the total and occurs between detrital quartz and feldspar grains. Separate-vug porosity resulted from partial or total feldspar dissolution; this porosity type constitutes 10–40% of the total. Microporosity occurs along feldspar cleavage planes, enlarged by dissolution, and between clay blades.

PETROPHYSICS AND VOLUMETRICS

The engineering portion of the field study concentrated on State University Consolidated Units Nos. 1 and 2 because of the large number of core-porosity and permeability analyses available from this area. Log data for the area consist of 93 gamma-ray/neutron logs, most of which are pre-1960 vintage. Core analyses are available from 38 of these wells. Semilog crossplots of core porosity versus neutron counts for individual wells give excellent correlations, with correlation coefficients of approximately 0.9. However, extrapolation of these correlations to wells without cores yielded poor

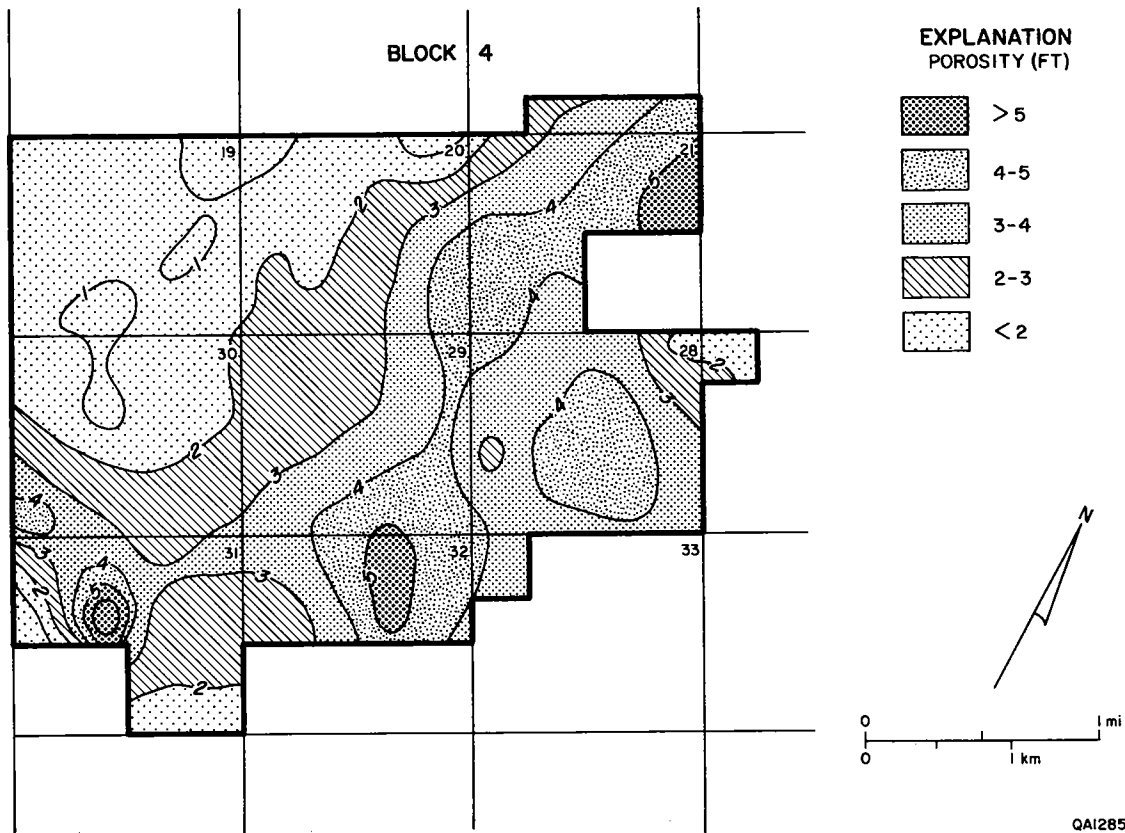


Figure 4. Map showing net pore volume in both A and B sandstones, State University Consolidated Units No. 1 and 2.

results; the logs were the products of more than 10 different logging companies, each using different radiation sources, sonde spacing, and radiation-counting scales. Tool response to porosity, therefore, varied greatly. Attempts to normalize the logs, using the sealing massive anhydrite as one baseline and neutron peaks at various horizons as another baseline, proved unsatisfactory. Thus, core analysis was considered the only useful measure of porosity and permeability.

Net pay for the cored wells was determined using a cutoff of 4% porosity and 0.1 md permeability. A map (Fig. 4) was constructed that shows the distribution and amount of net pore volume of both the A and B sandstones. Assuming an initial water saturation of 0.34, formation volume factor of 1.16, and a residual oil saturation of 0.25, there were originally 10.3 MMSTB of mobile oil and 6.2 MMSTB of residual oil in the A sandstone and 22.3 MMSTB of mobile oil and 10.3 MMSTB of residual oil in the B sandstone. As of December 1987, these two units collectively had produced 9 MMSTB, leaving 23.6 MMSTB of mobile oil remaining in these units.

Relating oil-in-place to production patterns was complicated by the lack of individual-well production data. Well-test and lease-production data for the period between 1956 and 1963 were available at the Railroad Commission of Texas; however, well data were not available after 1963, when water injection began. Production by lease in the early years was apportioned to individual wells according to the ratio of an individual well's test to the sum of the well tests on the lease (Fig. 5). Anomalous high values for wells that had produced for only one year were discarded because they had not begun the steep production decline that affects the value of other data points. Comparison of the production map (Fig. 5) with the pore-volume map (Fig. 4) shows some similarities. An area of low values on both maps, extending from the north-central area to the southwest, is the most obvious similarity. This area contains the more tightly cemented intertidal-flat sandstones, which have porosity of <10% and permeability below the detection limit of the measuring devices. Both maps also have an area of high values that trends from the east edge of sec. 32 toward the

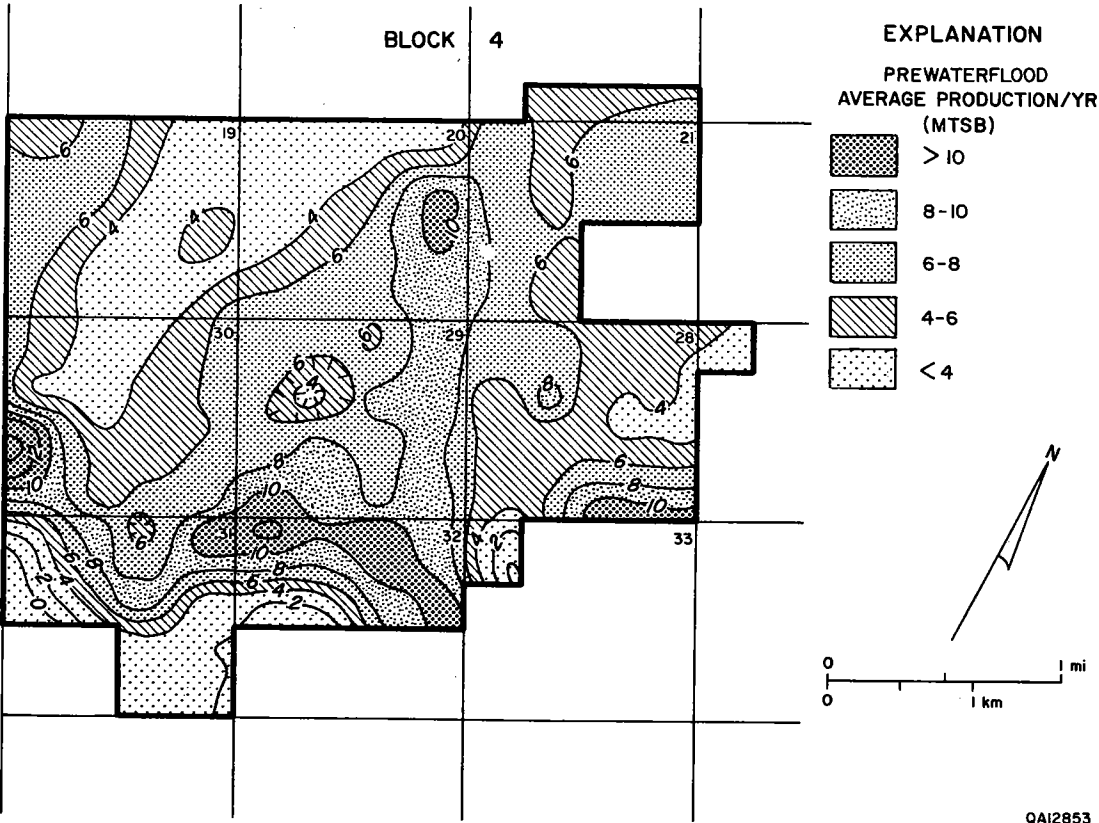


Figure 5. Map of prewaterflood average annual production from wells in State University Consolidated Units No. 1 and 2.

west edge of the study area. The reservoir storage-capacity map (Fig. 4) in this area is heavily influenced by the B sandstone, which is interpreted to be a thick tidal-channel deposit with high porosity and permeability. The most obvious dissimilarity is in sec. 28, on the southeast edge of the study area; the reservoir storage-capacity map shows a high capacity, whereas production is low. In this southeastern area many wells are perforated in only one of the two sandstones.

STRATEGIES FOR RECOVERY OF REMAINING MOBILE OIL

There are 23.6 MMSTB of mobile oil remaining in the study area, much of which is concentrated in thick, tidal-channel sandstones. The reservoir is currently drilled to 40-acre well spacing, but evidence suggests that a targeted infill-drilling program could increase production and recovery efficiency. In 1988, two wells drilled ~0.5 mi south of the study area had high initial-potential tests: 110 bbl of oil was pumped from one well, and 203 bbl of oil flowed from the other. This area previously was the site of abandoned and stripper wells. Thicker tidal-channel sandstones should be isolated as the primary target for an infill-drilling program. Existing completions should also be reviewed to locate oil that remains behind casing pipe. As discussed earlier, many wells have been opened to only one production interval. Recom-

pletions in the untapped sandstones should result in an immediate boost to production.

ACKNOWLEDGMENTS

Funding for this research was provided by The University of Texas System; the paper is condensed from an earlier report by Tyler and others (1991). The manuscript was reviewed by Ray Levey, Seay Nance, Jeff Grigsby, and Shirley Dutton of the Bureau of Economic Geology. Tucker F. Hentz was the technical editor.

REFERENCES CITED

- Holley, Carolayne; and Mazzullo, Jim, 1988, The lithology, depositional environments, and reservoir properties of sandstones in the Queen Formation, Magutex North, McFarland North, and McFarland fields, Andrews County, Texas, *in* Permian and Pennsylvanian stratigraphy, Midland basin, West Texas: study to aid hydrocarbon exploration: Permian Basin Section, Society of Economic Paleontologists and Mineralogists, Special Publication 88-28, p. 55-63.
- Tyler, Noel; Bebout, D. G.; Garrett, C. M., Jr.; Hocott, C. R.; Holtz, M. H.; Hovorka, S. D.; Kerans, Charles; Lucia, F. J.; Major, R. P.; Ruppel, S. C.; and Vander Stoep, G. W., 1991, Opportunities for additional recovery in University Lands reservoirs: Final project report prepared for The University of Texas System, 255 p.

Application of Horizontal Drilling in Fractured Carbonates of Oklahoma

Richard D. Fritz, Christopher L. Johnson,
and Patrick L. Medlock

MASERA Corporation
Tulsa, Oklahoma

If the cost of drilling a horizontal well were equal to that of drilling a vertical well, most reservoirs would be candidates for horizontal drilling. In fact, most explorers would prefer to see as much pay zone in the hole as possible. Although this is not practical, there are some reservoirs that have certain characteristics that lend themselves to horizontal-drilling potential. Geological and/or engineering considerations define each potential reservoir, and it is difficult to arrive at a universal definition. For the purpose of this brief report, a general definition of a horizontal-drilling reservoir (HD reservoir) is one in which horizontal drilling can improve production significantly and economically in comparison to a vertical well.

Geological applications for horizontal drilling have proven most effective in tight fractured reservoirs, heterogeneous paleokarst reservoirs, and porous and permeable reservoirs with coning problems. A modified version of standard fracture classification can be used to sort most potential horizontal-drilling targets in the Midcontinent into four types (Fig. 1). Potential carbonate HD reservoirs can be further categorized by facies-related reservoir characteristics.

Tight, fractured carbonate reservoirs, with features similar to the Bakken Shale, are commonly developed in low-energy basinal settings. These reservoirs are characterized by little or no matrix porosity; porosity and permeability are provided only by fractures. The Sycamore Limestone, which currently produces from vertical wells in southern Oklahoma, is an example of this first type of potential HD reservoir (type A); it is a primary horizontal-drilling target in the Midcontinent.

The Austin Chalk is a basinal pelagic carbonate that typifies the second type of HD reservoir (type B); it has fair-to-good matrix porosity and very low permeability. The only producing chalk reservoirs near the Midcontinent region are in the northern and northwestern parts of the Denver basin, as

exemplified by the Upper Cretaceous Niobrara Formation.

The Viola and Mississippian limestones (also type-B reservoirs) were deposited in relatively low-energy subtidal conditions on shallow marine ramps, and they can have porosity and permeability profiles similar to chinks. Both these limestones require fracturing for good production and are being pursued actively as horizontal-drilling candidates.

Limestones and dolomites of the Hunton Group are similar to the Viola and Mississippian limestones in that they were deposited on a carbonate ramp. Except for the Frisco and Sallisaw Formations, reservoirs in the Hunton Group often are composed of interfingering upper-subtidal, intertidal, and supratidal facies. These carbonates commonly are highly heterogeneous and represent the third type of HD reservoir (type C), which has good porosity and fair permeability, often complemented by fractures. Reservoir heterogeneity is further complicated by a long and varied diagenetic overprint.

Platform-margin carbonates, in particular reefs, may also represent good horizontal-drilling targets; however, there are few significant reef build-ups in the southern Midcontinent. Mud mounds, such as those found in the Frisco Formation, are a type of reef and can be heterogeneous; but most commonly these mounds have good reservoir parameters similar to the fourth type of HD reservoir (type D), which is a zone with good porosity and permeability. It is usually homogeneous and has either gas- or water-coning problems. This fourth type of HD reservoir may or may not be fractured; in fact, an abundance of fractures may actually increase coning problems.

Some carbonates, such as the platform carbonates of the Arbuckle Group, may contain examples of all four types of HD reservoirs. Arbuckle production typically is from rather heterogeneous

Fritz, R. D.; Johnson, C. L.; and Medlock, P. L., 1993, Application of horizontal drilling in fractured carbonates of Oklahoma, *in* Johnson, K. S.; and Campbell, J. A. (eds.), Petroleum-reservoir geology in the southern Midcontinent, 1991 symposium: Oklahoma Geological Survey Circular 95, p. 66-68.

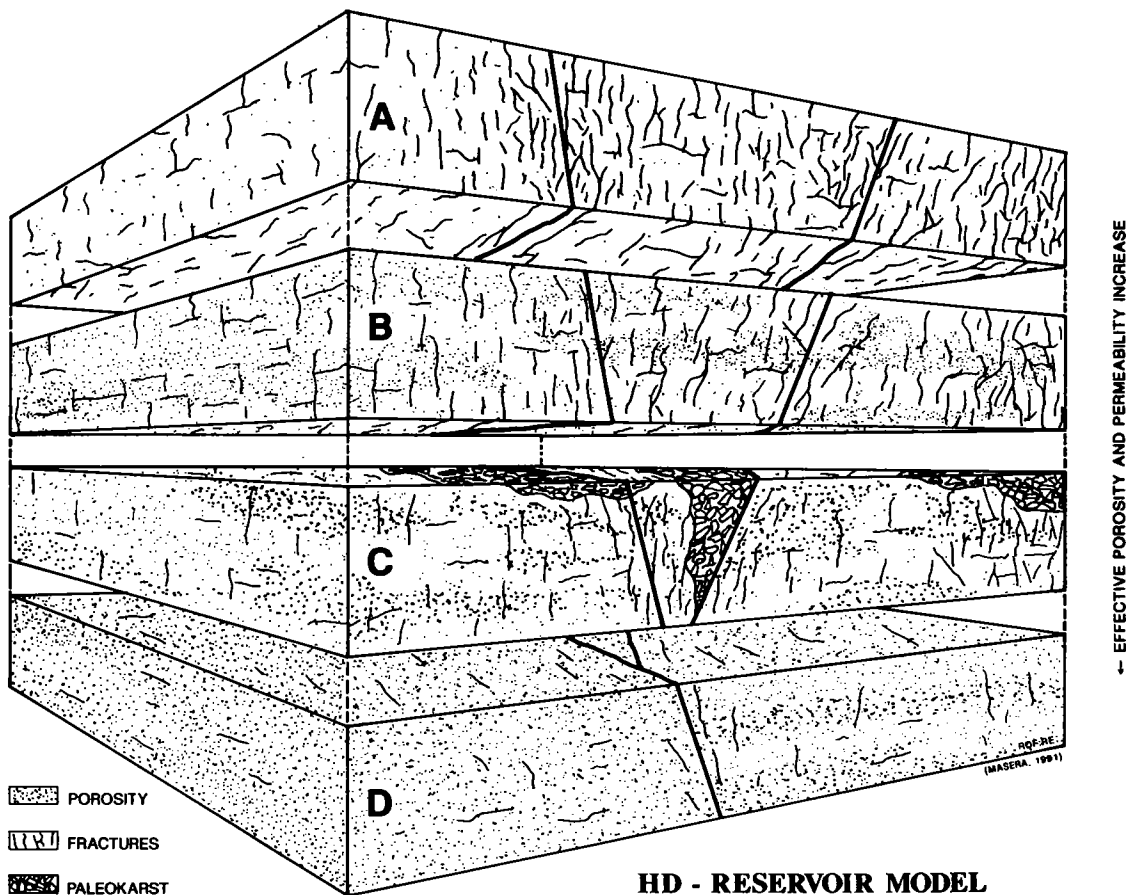


Figure 1. Geological classification for HD reservoirs: type A reservoirs (top) have little or no matrix porosity, can be homogeneous or heterogeneous, and fractures provide basic porosity and permeability; type B reservoirs have low permeability with effective matrix porosity, can be homogeneous or heterogeneous, and fractures provide permeability; type C reservoirs are usually heterogeneous, with complex porosity and permeability profiles, and fractures complement permeability; type D reservoirs have good porosity and permeability, are usually homogeneous with coning problems, but can be heterogeneous with fractures that complement permeability. Fractures may also cause reservoir anisotropy, which contributes to coning.

fractured and karstic dolomites which, under certain conditions, can be exploited using horizontal-drilling methods.

Fracturing is the most important factor in developing a good HD reservoir. In the United States there are nearly 700 fields which are categorized as containing fractured reservoirs. Few have been examined for horizontal-drilling potential. Any exploration or production venture involving horizontal drilling should take into account the fracture history of a potential HD reservoir.

Most reservoirs have some degree of heterogeneity; this is especially true of HD-type reservoirs. Permeability problems caused by heterogeneity

can be overcome by fracturing. Heterogeneity commonly is caused by secondary processes, such as karstification, which is pervasive in many carbonates due to the presence of numerous unconformities in the Midcontinent. One of the most mature karstic formations is the Sallisaw (or Penters) karst breccia of the Arkoma basin. The Penters is a mature karst regolith, and production is usually found only in fractured units.

The Midcontinent has an abundance of potential HD reservoirs (Fig. 2), due in part to its complex structural history. Fractured and karstic carbonates provide excellent targets for future horizontal drilling.

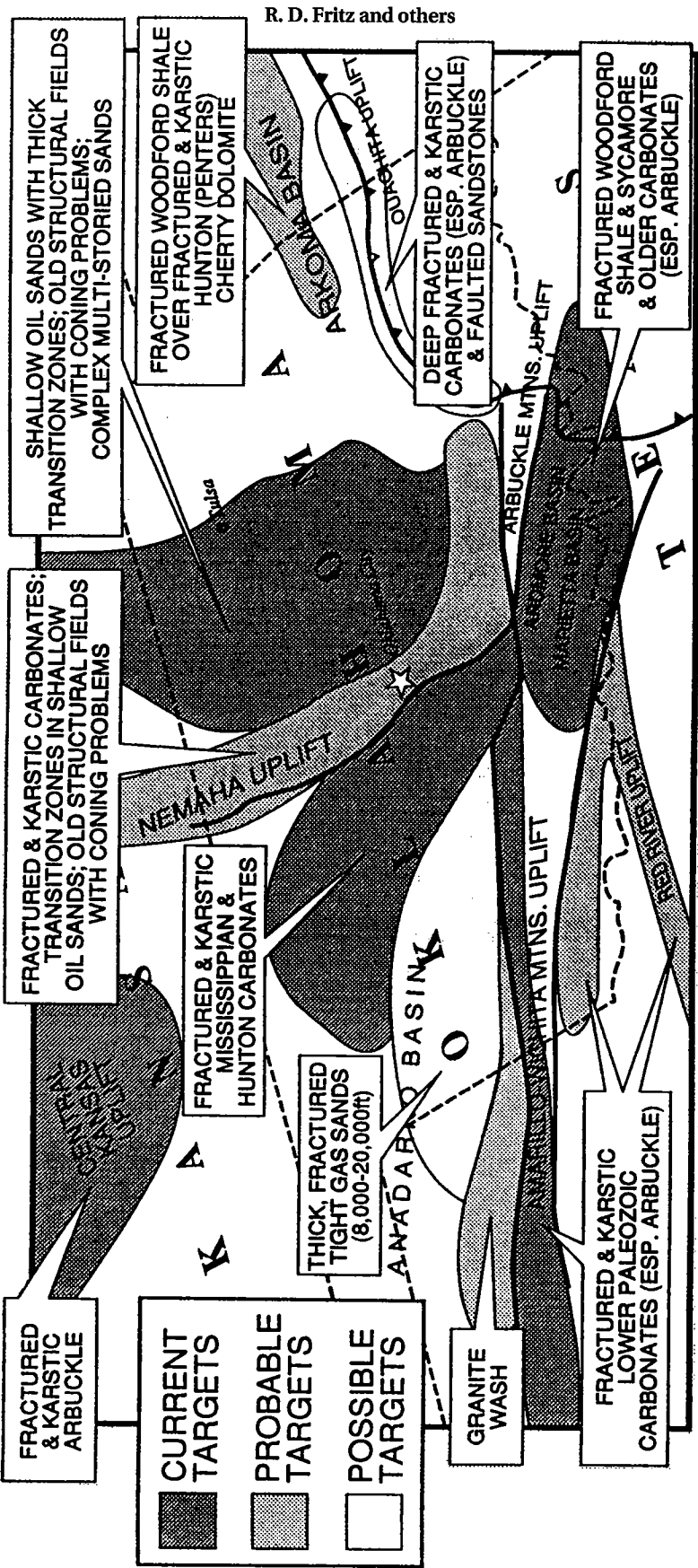


Figure 2. Index map of the Midcontinent showing reservoirs with horizontal-drilling potential.

Secondary Recovery of Oil Through Mine Workings in the Keystone Field, Northeastern Oklahoma

Maynard F. Ayler

Hydrocarbon Mining Co.
Golden, Colorado

Tom L. Bingham

Oklahoma Geological Survey
Norman, Oklahoma

INTRODUCTION

Many of the oil fields in the United States were discovered before 1936; a considerable number of those fields are in northeastern Oklahoma. At that time, the science of petroleum engineering was in its infancy, and the importance of a gas drive to efficient recovery was not understood. Consequently, many reservoirs developed before 1936 were allowed to produce with no thought of retaining the gas drive. As a result, the first day's production for a well may have been quite good, but production the second day was often much less. Eventually, production was essentially gravity drainage of reservoirs to wells; the result was low daily production in wells over an extended period of time. It is now thought that a substantial portion of the original oil in place is still contained in these reservoirs. The Cleveland sand of the Keystone field is one example.

Historically, the most effective way of increasing the recovery from any oil field has been through infill drilling. In the past, this always has been done by decreasing the surface well spacing. The cost of the well and of the potential oil recoverable through that well has always been a limiting factor for infill drilling. In recent years, environmental considerations also have become major limiting factors.

With advances in technology and equipment for shaft sinking and tunnel driving, it now is possible to consider infill drilling from mine access below the producing reservoir. A main shaft and a secondary shaft could serve a system of tunnels and develop an area of ~5,000 acres. From tunnels ≥ 100 ft below the producing horizon, fans of holes drilled upward through the reservoir could provide infill drains on 1-acre or closer spacing. Produced oil would flow through collection pipelines

in the mine workings back to the shaft for pumping to the surface.

The first well in the Keystone field, the Pomeroy and Hamilton G.W. Besser no. 1 well in the SW corner SE $\frac{1}{4}$ SE $\frac{1}{4}$ sec. 24, T. 20 N., R. 9 E., drilled during March 1919, was credited as the discovery well. The Cleveland sand, from 1,145 to 1,205 ft below the surface, initially produced 75 bbl of oil per day (BOPD). The reservoir was drilled extensively between 1919 and 1923. Drillers' logs indicate that the sand ranged from 24 to 49 ft thick. One log indicated that production the first 24 hours was 178 bbl of 35.4° oil; the second day, the well produced 135 bbl of 34.4° oil. Records from other wells indicate that shooting was needed. In one such case, the well produced 10 BOPD initially but produced 57 bbl of oil the first day after shooting.

The Cleveland reservoir proved to be more or less restricted to parts of secs. 24 and 25, T. 20 N., R. 9 E. Later drilling proved, however, that 10 or 11 other stratigraphic units, both above and below the Cleveland, contained gas and/or oil reserves within a 2,500-ft depth range in what is now known as the Keystone oil field.

During the mid-1960s, the Keystone dam was built. The resulting reservoir (the water supply for Tulsa) covered portions of the Cleveland part of the Keystone oil field as it is now known. Additional drilling of the Cleveland sand was further complicated by construction of the Appalachian Bay Recreation Area and nearby housing development. Records indicate that wells within the reservoir and construction area were producing 6–8 BOPD when they were shut in and abandoned.

Surface developments such as a lake, recreation facilities, or housing need not restrict closely spaced wells drilled up through the Cleveland sand from mine tunnels located below the producing horizon. Since, in this case, the workings

Ayler, M. F.; and Bingham, T. L., 1993, Secondary recovery of oil through mine workings in the Keystone field, northeastern Oklahoma, *in* Johnson, K. S.; and Campbell, J. A. (eds.), *Petroleum-reservoir geology in the southern Midcontinent*, 1991 symposium: Oklahoma Geological Survey Circular 95, p. 69–73.

would be about 1,250–1,300 ft below the surface, with a thick shale interval above the Cleveland sand, there would be no reason to expect any communication between the mine and the overlying surface.

DATA SOURCE FOR THIS STUDY

The data available for evaluating the Cleveland sand reservoir are the drillers' logs. Since ground or derrick floor elevations were rarely given, stated well locations were used to estimate ground elevations on topographic maps. Some wells penetrated to shales below the Cleveland sand and provided an estimate of the full sand thickness. Many of the wells, however, were completed within the sand, and those wells could not be used to develop an isopach map of the sand. In some cases, there is reason to question whether the producing zone was the Cleveland sand or another sand just above or below the Cleveland.

THE CLEVELAND SAND RESERVOIR

As indicated above, available data leaves many questions concerning the Cleveland sand reservoir. First, what is the trapping mechanism for this reservoir? Initially, the structure was interpreted as a minor fold, but later attempts to prepare a detailed structure map have been very inconclusive. Structure may or may not control oil accumulation.

The authors postulate that a stratigraphic pinch-out was the control. Work done to this date seems to indicate a thickening of the Cleveland sand toward the east side of secs. 24 and 25, yet there seems to be an abrupt edge of the reservoir along the east side of those two sections. Those wells reporting gas in the Cleveland sand are also located near this edge of the field. Is it possible that a north-south fault, not a stratigraphic pinch-out updip, is the main trapping mechanism for this sand?

A number of the drillers' logs for wells show a 1- to 4-ft-thick coal bed 10–25 ft above the top of the Cleveland sand. A number of the logs report a limestone zone or a shell-shale and sand zone between the coal and the top of Cleveland sand. Preparation of good cross-section control through this field, using these logs, should permit a much better understanding of limits of the Cleveland sand and, thus, permit preparation of good isopach maps and probably a structure map as well.

Logs examined so far have not given an indication of initial reservoir pressures or pressures after a period of production. A few of the wells reported flowing initial production and a marked drop the second day of production. This suggests a gas drive that dissipated rapidly. Some wells were shot and had considerable improvement in production, which suggests that either the sand had poor

permeability or drilling mud had sealed the well walls. If mud sealing was a factor, it implies that the weight of the mud column exceeded the reservoir pressure.

The base of the oil column, and the top of the water, in one well seems to be at –415 ft elevation. There is no record of how active a water drive was present.

OTHER PRODUCING HORIZONS

Several wells within the Keystone field in T. 20 N., R. 9 E. have reported gas or oil shows in strata other than the Cleveland sand reservoir. Examples are given in Table 1.

The logs pertinent to the data presented in Table 1 illustrate that there are a number of horizons (some identified, some not) both above and below the Cleveland sand that contain either gas or oil. The two wells reporting Bartlesville production indicate sand thickness to be 39–41 ft. Since the wells reporting Burgess and Hominy production bottomed within these formations, it is not possible to estimate from them how thick those units may be in that area. The well reporting 8.75 MMcf (million cubic feet) of gas in the Skinner sand was drilled 25 ft into the formation and bottomed within it. We do not know how thick the Skinner is there. More than that, however, why wasn't gas or oil reported in the Skinner in the other wells of sec. 25?

KEYSTONE FIELD PRODUCTION

Dwight's Energy Data Inc., Petroleum Data System (PDS) Total Records for the Keystone field indicate that cumulative production through 1992 was 13,255,836 BO and 1,020,161 Mcf (thousand cubic feet) nonassociated gas. Most recent yearly totals from PDS data are for 1992 and indicate 53,084 BO, 23,927 Mcf nonassociated gas, and 68,938 Mcf dissolved gas.

During the period 1983–90, the main producing intervals within the Keystone field were the Wilcox, Red Fork, and Bartlesville. During this period, 59,424 BO were produced from the Cleveland sand interval. The Petroleum Information tabulation "Oklahoma Abandoned Leases," updated through December 1987, indicates Cleveland production in secs. 7 and 17, T. 19 N., R. 10 E. and secs. 24–26 and 29, T. 20 N., R. 9 E. It does not indicate how many wells were producing or whether or not any active leases exist, and it does not include pre-1935 production data.

With such limited data, it is hard to make a valid estimate of the reserve that may remain in the Cleveland reservoir. We know the initial field discovery was in the Cleveland sand and that this reservoir was extensively drilled between 1919 and 1923. The logs indicate that many of the wells had

TABLE 1. — OIL AND GAS RECOVERY INFORMATION
FOR RESERVOIRS OTHER THAN THE CLEVELAND SAND*

Location	Formation	Initial Production	Reported Shows	Depth In Feet
NW/NE/NW Sec 24	Limestone Sand Broken Sand Broken Sand Burgess Sand	164 BO in 15 hrs	Little gas Little gas Little gas Little gas	487-503 1326-1361 1728-1786 1803-1895 2319-2324TD
NE/SE/NE Sec 25	Sand		Small gas	755-782
Lot 20, Blk 72, Sec 25	Limestone Limestone Bartlesville	178 BO 1st 24 hrs 135 BO 2nd 24 hrs	Oil show Oil show	290-310 960-980 1957-1998TD
NW/NW/SE Sec 25	Sand Sand Bartlesville Wilcox	70 BO in 24 hrs	Puff of gas Show oil Oil	720-750 1578-1592 1956-1995 2422-2427TD
NE/NW/SE Sec 25	Sand Sand Sand Sand Hominy	65 BO in 24 hrs	Show gas & oil Gas Oil Oil	360-370 1000-1020 2225-2230 2330-2342 2496-2501TD
NW/SW/SE Sec 25	Skinner	8.75 MM gas		1693-1718TD

*Data from drillers' logs of early wells drilled in the Keystone field, secs. 24 and 25, T. 20 N., R. 9. E.

initial productions from 25 to as much as 330 BOPD. There are no data indicating what any of the wells may have been producing a month after completion. By 1955, a number of wells had been completed in the Red Fork in other parts of the Keystone field, and they too had good initial production. Some of the Red Fork wells were drilled as early as 1920, but most seem to have been drilled after 1950. Attempts to waterflood parts of the field have been made by small operators on localized five-well patterns, but no systematic waterflood has ever been undertaken. From data found so far, it is not possible to estimate how much oil was produced from the Cleveland sand in secs. 24 and 25, T. 20 N., R. 9 E.

RECOMMENDED EVALUATION
PROCEDURE

Since mine-assisted oil recovery as suggested here is technically and environmentally feasible, the limiting factor will be economics. It is very likely that any oil produced will have a market, but the future price for that oil is unknown. That, of course, is a problem for any economic evaluation.

At present, there does not seem to be any good way to estimate what percentage of mobile re-

sidual oil can be recovered by closely spaced wells drilled upward through the reservoir. Estimates from various sources range from none to as much as 90%. About 50% seems to be reasonable, and that estimate has been used by engineers of at least one company.

Since many of the other factors, such as environmental problems, royalties, taxes, financial agreements, etc., will depend upon target location, they need to be evaluated after a target reservoir is identified. The problem, then, is to identify the target.

Since mine-assisted oil recovery is not an exploration tool, only fields with a production history should be considered. All fields meeting certain basic criteria should be considered.

1. The remaining oil saturation and the percentage of that oil that is mobile must be known in order to calculate economics. A minimum of 20,000 bbl/acre has been assumed somewhat arbitrarily for desirable profitability.

2. The reservoir temperature cannot be >120°F; preferably, it should be <90°F since men will be working in the mine.

3. There should be a competent, reasonably impermeable stratigraphic unit ~100 ft below the reservoir. The mine workings would be in that unit.

4. Permeability of the reservoir should be such that production by gravity drainage would be possible.

5. Target areas should have minimal faulting since faulting could cause mine-design problems.

6. Target reservoirs should be larger than 640 acres.

How does the Cleveland sand of the Keystone field measure up to these criteria? With respect to items 2, 3, 4, and 5, it seems to be satisfactory. Items 1 and 6 may be problems.

A reasonable estimate of the location of the central portion of the field can be made from well data. Since the reservoir is relatively shallow in this case, it should be possible to drill a test hole, coring through the Cleveland sand and through ~100 ft of the strata just below it. Analysis of the core through the Cleveland sand could help determine how much mobile residual oil may remain in this reservoir as well as provide other data about reservoir characteristics. If these first data are favorable, rock mechanics tests should be performed on the core from strata below the reservoir to determine if that stratigraphic unit is favorable for mining.

If a decision is made to proceed, all available data should be used to compile, so far as possible, detailed structure and isopach maps for each of the producing reservoirs in this central part of the Keystone field. Since production in secs. 24 and 25 is reported from wells to the Bartlesville at 1,957–1,998 ft, the Burgess at 2,319–2,324 ft, and the Hominy at 2,496–2,501 ft, as well as the Red Fork, structure and isopach maps should be prepared for each of these units.

It is possible that mine-assisted recovery of oil from the Cleveland zone alone may not be feasible. However, it might be feasible to plan a shaft with workings to extend under the Cleveland as well as a lower level in order to develop one or more of the deeper horizons. It should be remembered that the most costly part of the shaft is the surface hoisting equipment. The equipment for operating a deeper shaft is not much more expensive proportionally. Mine development and further oil production could be simultaneous. It would not be necessary to complete the mine first.

Before the mine plan is finalized, one or more cores from each potentially productive unit and from below the potentially productive zone should be obtained in order to provide the additional oil-reserve-potential and rock-mechanics data necessary for mine design. This procedure will take time and cost money, but it will be part of an exploration budget well spent.

ADVANTAGES OF MINE-ASSISTED OIL RECOVERY

There are several major advantages of mine-assisted oil recovery:

1) The advantages of close-well spacing can be realized in areas where it would otherwise be unacceptable environmentally, such as under the Keystone reservoir or residential area.

2) It should be possible to determine the size, shape, and reserve potential of a target reservoir for no greater expenditure than is now needed to find a drilling prospect.

3) There should be no dry holes since development would be within a known field.

4) Since movement of oil from the reservoir to the production flow line would be by gravity, no pumping unit for each well would be needed. As few as one pumping unit for the entire operation would be needed to lift the oil through the mine shaft.

5) Flow from each well could be controlled to utilize any pressure drive within the reservoir.

6) Recovery of mobile residual oil would be a major form of conservation and one that is usually forgotten. Oil not recovered from a reservoir is just as wasted as oil burned in inefficient cars.

7) Perhaps the greatest advantage is that the opportunity for mine-assisted oil recovery is great because there is a potentially large volume of oil in known fields that may be profitably recovered by this technique.

POTENTIAL FOR THE KEYSTONE FIELD

The Keystone field is one of more than 300 Oklahoma oil fields with reservoirs 3,000 ft or shallower in depth. As indicated above, there are multiple productive zones in this field. The Cleveland reservoir was the main one considered in this study. As work progressed, it became apparent that the Cleveland reservoir is of limited areal extent and thickness and that one or more of the deeper reservoirs should be considered in addition if mine-assisted development is contemplated.

Mine-assisted development as suggested here could easily permit tunnels under several reservoirs at different depths. If reservoirs of interest are one above the other, development of these reservoirs from the same tunnel system should be considered.

Any study of this field to evaluate the mine-assisted development potential should include identification of the main producing horizons. Structure and isopach maps then should be prepared for each horizon. That would permit a preliminary estimate of the reserve potential and development cost. If this work suggested a favorable economic potential, cores would be needed for rock mechanics tests and to help quantify the reserve potential. These data would be used for mine design.

The 1919 field discovery date, the rapid development of the Cleveland reservoir over the suc-

ceeding four years, the wasting of gas drives during those early years, the quality of the oil, the relatively shallow reservoir depth, all combine to suggest that further study of this reservoir and those deeper in the section is desirable. It should be remembered, however, that the Keystone is only one of many fields in northern Oklahoma; it may, or may not, be the best for mine-assisted oil recovery.

SELECTED REFERENCES

Dwight's Energy Data Inc., 1992, Petroleum Data System (PDS): Available from Dwight's Energy Data Inc., Oklahoma City.

Natural Resources Information System (NRIS), 1993, Oil and Gas Production data base: Available from Geological Information Systems, University of Oklahoma, Norman.

Petroleum Information Corp., 1988, Oklahoma abandoned leases (updated through December 1987): Petroleum Information Corp., Tulsa, 804 p.

Regional Geology of the Woodford Shale, Anadarko Basin, Oklahoma— An Overview of Relevance to Horizontal Drilling

Timothy C. Hester and James W. Schmoker

U.S. Geological Survey
Denver, Colorado

ABSTRACT.—The Woodford Shale (Upper Devonian and Lower Mississippian) is a major hydrocarbon source rock in the Anadarko basin. With the advent of horizontal drilling, the Woodford may also prove to be an economically significant reservoir rock. Three regional geologic characteristics of the Woodford Shale discussed here are likely to be important in planning horizontal-drilling programs.

First, a paleotopographic high that was rising before and during Woodford deposition divided the Woodford Shale into northeast and southwest depocenters. This high is interpreted as a basin-margin forebulge that developed as the direct result of loading and subsidence along the central trough of the southern Oklahoma aulacogen.

Second, the Woodford Shale is not vertically uniform but can be subdivided into upper, middle, and lower informal members based on log character. The middle shale has higher kerogen content (average total organic carbon [TOC] = 5.5 wt%) than the upper and lower members (average TOC = 2.7 and 3.2 wt%, respectively).

Third, Woodford depositional patterns are overprinted by thermal-maturity trends shaped primarily by differential burial of the Woodford during Mississippian through Permian time. On the present-day shelf of the Anadarko basin northeast of the forebulge, the Woodford Shale is generally immature to marginally mature with respect to oil generation. Southwest of the forebulge, thermal maturity of the Woodford ranges from mature to postmature with respect to oil generation. As a rule of thumb, a formation resistivity of 35 ohm-m indicates the mature-immature boundary, and by inference, marks the probable updip limit of oil-saturated Woodford Shale.

INTRODUCTION

The Woodford Shale is one of several organic-rich “black” shales of Late Devonian and Early Mississippian age present in basins of the North American craton. Examples of similar shales include the Antrim Shale of the Michigan basin, the New Albany Shale of the Illinois basin, the lower and upper members of the Bakken Formation of the Williston basin, the Exshaw Formation of the Alberta basin, and the “Devonian” shales of the Appalachian basin.

Where thermally mature, these black shales are economically important as hydrocarbon source rocks. With the rapid development and increasingly widespread application of horizontal drilling, such shales may also prove to be economically important as reservoir rocks. The Bakken Formation, for example, is well established as an oil-satu-

rated reservoir amenable to horizontal drilling (Hester and Schmoker, 1985; Montgomery, 1989).

The Woodford Shale also warrants consideration as a target for horizontal drilling. In this report, three regional geologic aspects of the Woodford Shale that may prove relevant to horizontal-drilling programs are reviewed: (1) the presence of northeast and southwest Woodford depocenters, (2) the presence of lithologically distinct upper, middle, and lower members, and (3) the nature of Woodford thermal-maturity trends. The present report is a review and synthesis of material drawn largely from Hester and others (1990,1992) and Schmoker and Hester (1990). However, the question of how these regional geologic aspects should be incorporated into an exploration program is not addressed, and direct implications for drilling strategy must await empirical data from horizontal tests.

Hester, T. C.; and Schmoker, J. W., 1993, Regional geology of the Woodford Shale, Anadarko basin, Oklahoma—an overview of relevance to horizontal drilling, *in* Johnson, K. S.; and Campbell, J. A. (eds.), *Petroleum-reservoir geology in the southern Midcontinent, 1991 symposium: Oklahoma Geological Survey Circular 95*, p. 74–81.

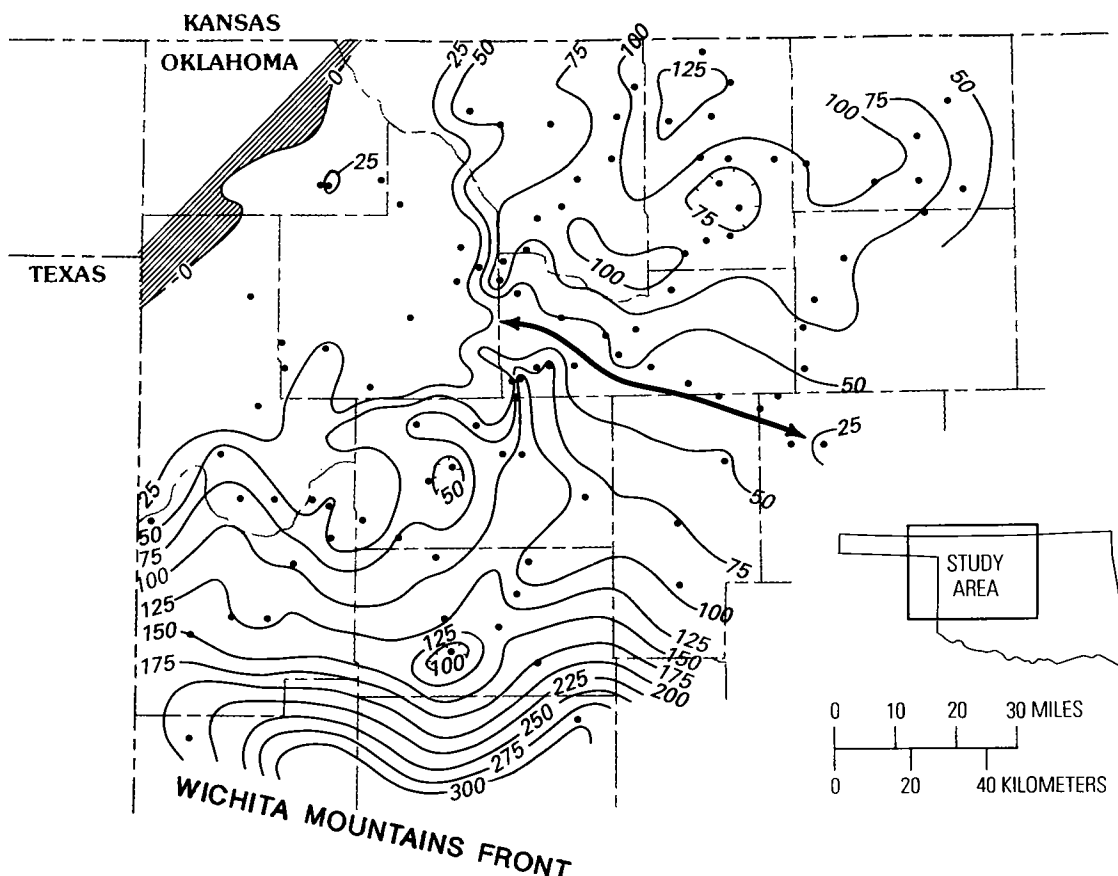


Figure 1. Thickness (ft) of Woodford Shale. Heavy line with arrows marks axis of paleotopographic high that separates Woodford into northeast and southwest depocenters (from Hester and others, 1990). Dots show locations of wells from which data are obtained. Area where Woodford Shale is absent is hachured. Contour interval: 25 ft.

DEPOSITIONAL PATTERNS

Figure 1, which also serves as an index map of the study area, shows the axis of a positive paleotopographic feature that influenced deposition throughout Woodford time. The paleotopographic high is parallel to and ~75 mi north of the Wichita Mountains front. As shown by the isopachs of Figure 1, the high divides the Woodford into southwest and northeast depocenters. The positive paleotopographic feature and southwest and northeast depocenters are also apparent in the regional cross sections of Figure 2.

The Anadarko basin formed in two stages (Perry, 1989). The first stage was characterized by formation of the southern Oklahoma aulacogen. During the second stage, the Anadarko basin evolved as a foreland-style basin. The Woodford Shale was deposited on a regional unconformity developed in the Late Devonian upon sediments deposited during subsidence of the southern Oklahoma evolution (Amsden, 1975; Feinstein, 1981). Erosional

channels on the unconformity surface were mapped on the assumption that the lower member of the Woodford is thicker where it fills channels (Fig. 3). The paleotopographic high separated the area into two distinct drainage areas. To the southwest, the channels trend generally southward. To the northeast, the channels are deflected roughly 90° by the paleotopographic high to parallel its northeast flank. Erosional channels do not cross the axis of the paleotopographic high (Fig. 3), suggesting that the paleotopographic high was rising during the pre-Woodford episode of regional erosion.

The Late Devonian Misener sandstone, a basal facies of the Woodford, was deposited in topographic lows during the early stages of the marine transgression which also deposited the Woodford Shale (Amsden and Klapper, 1972). The Misener is discontinuous across the paleotopographic high of the study area and is not present on its southwest slope (Fig. 3). The absence of the Misener suggests positive paleotopography and continued

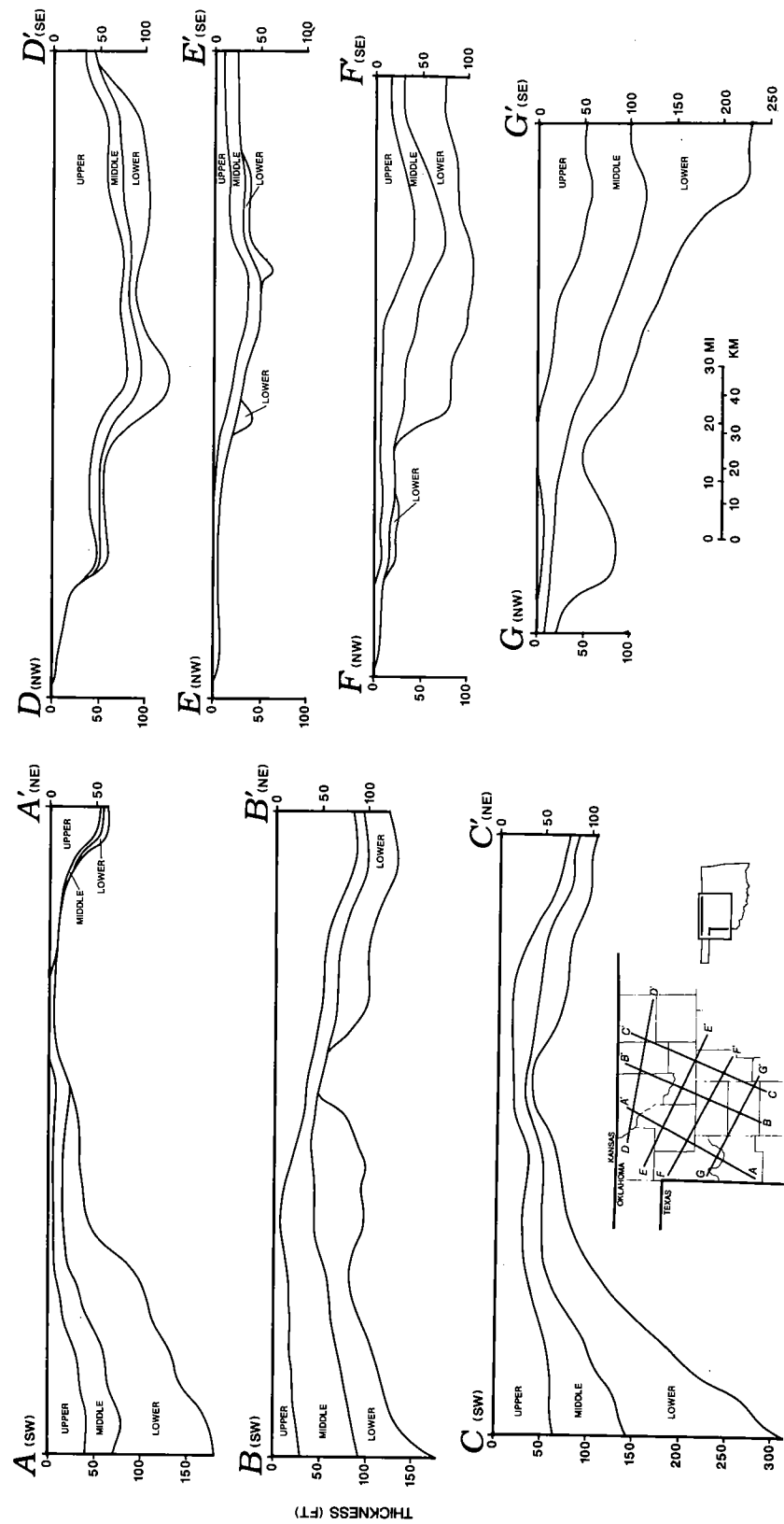


Figure 2. Regional cross sections of Woodford Shale (modified from Hester and others, 1990). Datum is top of upper member.

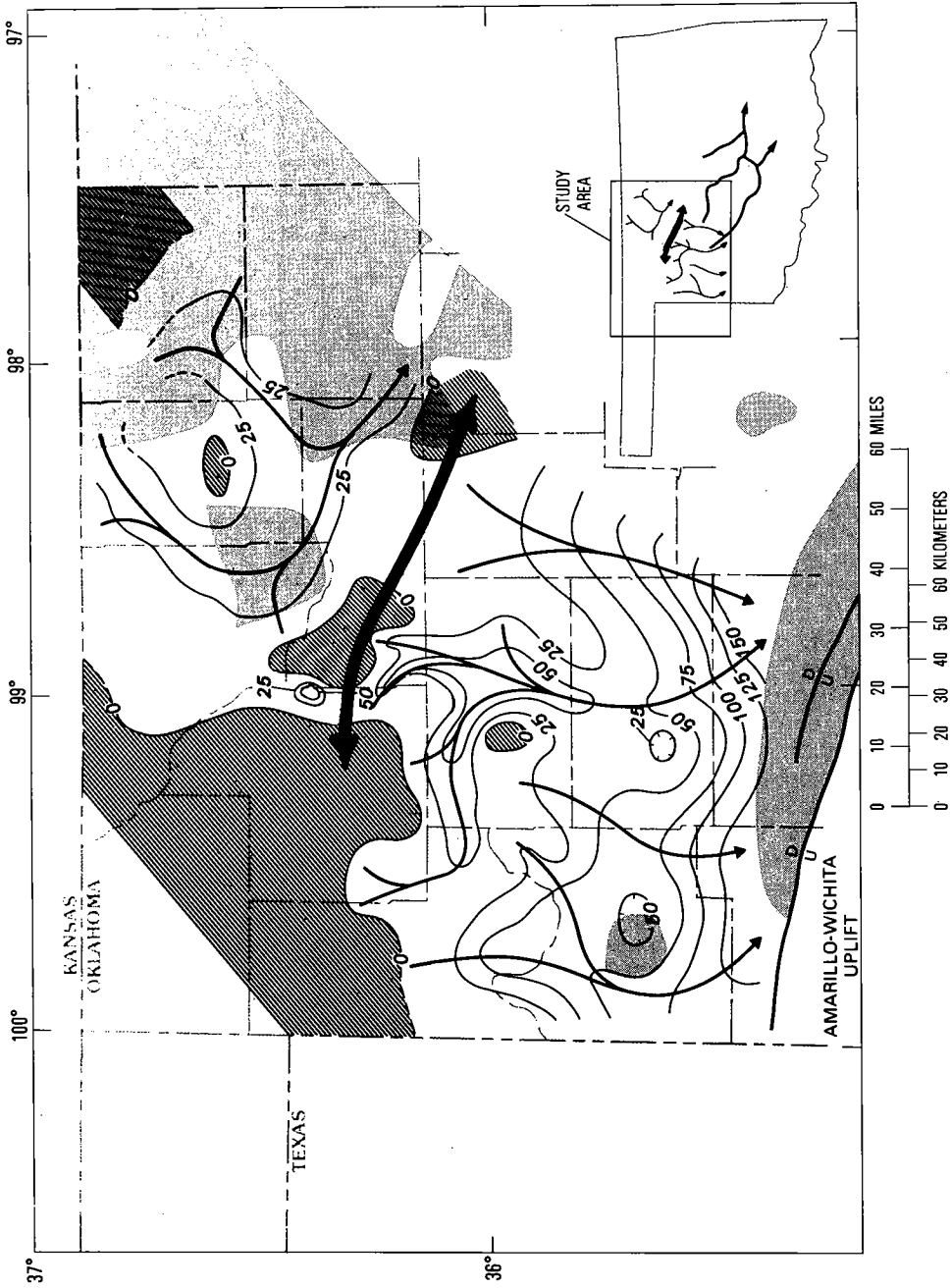


Figure 3. Thickness (ft) of lower member of Woodford Shale. Major erosional channels on the pre-Woodford surface (thin lines with arrows) are inferred from thickness of lower member. Areas where the lower member is absent are hachured. The distribution of Misener sandstone (shaded) as depicted by Amsden (1975) (from Hester and others, 1992). Heavy line with arrows marks axis of paleotopographic high. Contour interval: 25 ft. Inset map shows study area.

uplift of the paleotopographic high during lower Woodford deposition.

The paleotopographic high also affected depositional patterns of the lower, middle, and upper members of the Woodford (Fig. 2). Cross section C-C' (Fig. 2), in particular, indicates that the paleotopographic high was rising with respect to the southwest and northeast depocenters throughout the period of Woodford deposition.

These three points of evidence indicate that the paleotopographic high was rising prior to and throughout Woodford deposition. During the same time period, the central trough of the southern Oklahoma aulacogen was subsiding, as shown by the thickening of each member of the Woodford (Fig. 2), toward the aulacogen axis. These opposing tectonic movements can be genetically linked if the paleotopographic high is explained as a forebulge resulting from loading and subsidence along the central trough of the southern Oklahoma aulacogen.

On a geologic time scale, the behavior of the lithosphere is analogous to that of an elastic plate floating on a viscous fluid. Downward deflection of the plate in response to a linear load creates an upwarp or forebulge adjacent and parallel to the trough caused by the applied load (Turcotte and Schubert, 1982; Peterman and Sims, 1988). The height and position of the forebulge depend on the magnitude of downward deflection and the thickness and strength of the lithosphere. As a rule of thumb, the ratio of subsidence along the load axis to uplift of the forebulge is about 15:1 (Turcotte and Schubert, 1982).

Formation of a forebulge in response to loading is an integral part of basin development, but clear examples are not common in the literature. One well-documented example that is somewhat analogous to the present case is the Goodman swell in northern Wisconsin, which was recognized by Peterman and Sims (1988) as a forebulge of the failed Precambrian Midcontinent rift system. The distance between the Goodman swell and the nearest load axis of the Midcontinent rift system is about the same as that between the paleotopographic high of this report and the axis of the southern Oklahoma aulacogen.

Measuring flexural uplift of the paleotopographic high and concurrent subsidence along the load axis of the southern Oklahoma aulacogen is not a straightforward exercise. The decompacted thickness of the middle member of the Woodford Shale, which is minimally affected by erosional relief on the sub-Woodford unconformity and by subsidence of the northeast part of the study area during deposition of the upper Woodford, is used for estimating the ratio of basin subsidence to forebulge uplift (Hester and others, 1992). The paleotopographic high is estimated to have risen ~30 ft during deposition of the middle member of

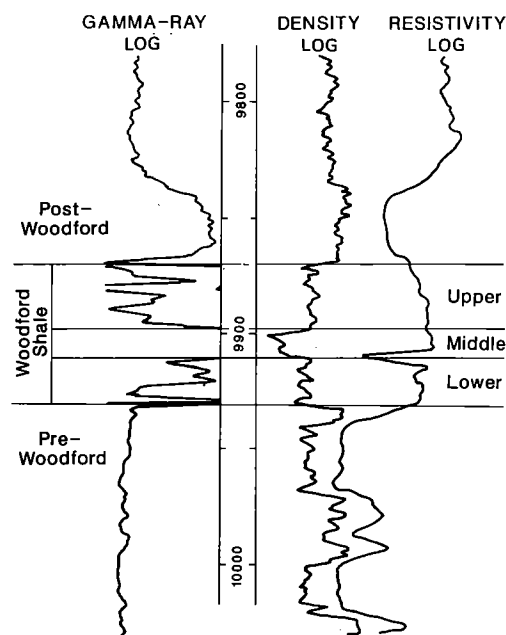


Figure 4. Characteristic log signatures of lower, middle, and upper members of Woodford Shale in study area (from Texas Oil and Gas no. 1-B Jellison, sec. 1, T. 20 N., R. 16 W.; modified from Hester and others, 1988).

the Woodford; the trough of the southern Oklahoma aulacogen is estimated to have subsided at least 320 ft during the same time span. The ratio of subsidence to uplift is thus approximately 11:1, demonstrating that interpretation of the paleotopographic high as a forebulge is reasonable.

VERTICAL HETEROGENEITY

The Woodford Shale at a given location should not be considered as a formation with uniform physical properties. Vertical variations have been documented by Adkison (1960), Urban (1960), Sullivan (1985), and Hester and others (1988). Distinctive variations in the signatures of gamma-ray, formation-density, and resistivity logs reflect variations in physical properties of the Woodford. Locally, the Woodford Shale can be divided into numerous minor subunits on the basis of log signatures, but the three major subdivisions proposed by Hester and others (1988) and shown in the cross sections of Figure 2 can be correlated throughout the study area.

Criteria for defining the informally named log identification of the upper, middle, and lower members of the Woodford Shale are illustrated in Figure 4. The Woodford Shale of the study area can be generally described as having upper and lower sections with similar log characteristics separated by a middle shale that is less dense, more radio-

active, and commonly more resistive (Fig. 4). Higher kerogen content of the middle member accounts for the distinctive log characteristics and is the physical basis for subdividing the Woodford Shale into three units. Total organic carbon (TOC) of the middle shale averages 5.5 wt%, whereas TOC of the upper and lower shales average 2.7 and 3.2 wt%, respectively (Hester and others, 1990).

As shown by Figure 2, the thickness of one member relative to another varies laterally. In synthesizing scattered Woodford data, care must be taken to avoid confusing lateral geochemical variations with those attributable to stratigraphic position of the samples analyzed.

Northeast of the forebulge, the maximum thickness of the lower Woodford is only ~25 ft. Southwest of the forebulge (Fig. 2), toward the axis of the southern Oklahoma aulacogen, the lower Woodford thickens to >150 ft. The thickness of the lower section varies locally, on a scale not shown by the regional cross sections of Figure 2, due to filling of topographic depressions on the sub-

Woodford unconformity.

The thickness of the middle member is locally more uniform than that of the lower member because sediments of the lower member covered surface irregularities on the sub-Woodford unconformity. Northeast of the forebulge, the maximum thickness of the middle member is ~25 ft. Southwest of the forebulge, the thickness of the middle member increases to >75 ft.

In contrast to the lower and middle members, the upper member of the Woodford thickens significantly to the northeast and only slightly toward the axis of the southern Oklahoma aulacogen (Fig. 2). This thickness pattern records slowing subsidence of the southern Oklahoma aulacogen and concurrent downwarping of the northeastern shelf during upper-Woodford deposition.

THERMAL MATURITY TRENDS

The depositional patterns of the Woodford Shale discussed in the two previous sections result

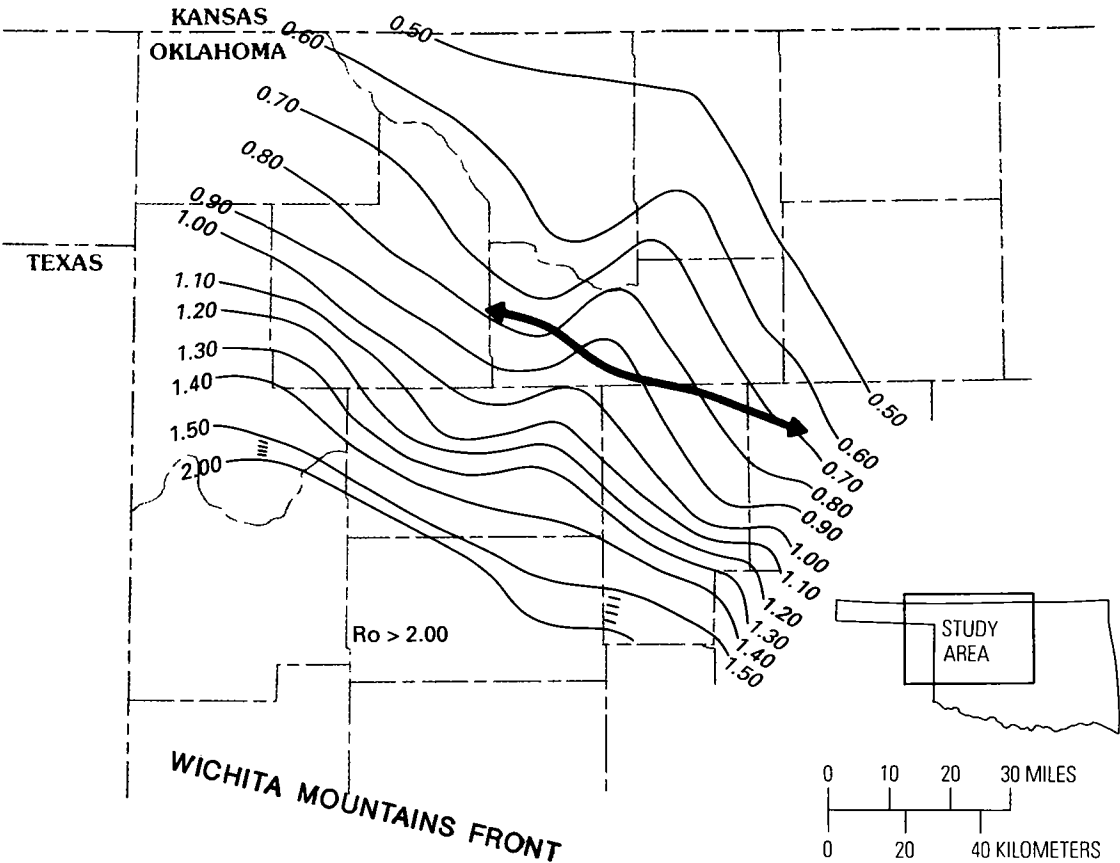


Figure 5. Vitrinite reflectance (% R_o) of Woodford Shale, contoured from data of Cardott and Lambert (1985) and Cardott (personal communication, 1987) (from Hester and others, 1990). Inferred updip limit of oil-saturated Woodford Shale at 0.56–0.57% R_o . Heavy line with arrows marks axis of paleotopographic high. Contour interval: 0.1% R_o .

directly or indirectly from evolution of the southern Oklahoma aulacogen, which was the first stage in the formation of the Anadarko basin. The present-day configuration of the Anadarko basin, however, is largely attributable to the development of a second-stage foreland-style basin during Late Mississippian through Permian time. Thermal maturity trends of the Woodford Shale are primarily related to differential burial of the formation during this second stage of basin development.

Burial depths of the Woodford Shale in the study area differ by more than 20,000 ft. The large range of burial depths has produced a correspondingly broad range of thermal maturities (Cardott and Lambert, 1985). Vitrinite reflectance (R_o) of the Woodford ranges from slightly less than 0.5% on the northeastern shelf to well over 2.0% in the deep basin (Fig. 5).

Much of the Woodford in the area northeast of the forebulge, where thickness is dominated by the upper member, is immature to marginally mature with respect to oil generation (Fig. 5). Thermal maturity southwest of the forebulge, where thickness is dominated by the lower and middle members, ranges from mature to post-mature with respect to oil generation (Fig. 5). Most hydrocarbons sourced by the Woodford Shale have therefore been generated by the lower and middle members southwest of the forebulge.

With the onset of oil generation in an organic-rich, low-porosity shale such as the Woodford, nonconductive petroleum begins to replace conductive pore water. As the process continues, formation resistivity increases from the low levels typical of water-saturated shales and can reach hundreds of ohm-m if sufficient oil is generated.

The volatile-hydrocarbon component (S_1) present in a rock sample is one of the properties measured by Rock-Eval thermal analysis (Tissot and Welte, 1984). In a low-permeability shale such as the Woodford, initiation of oil generation is indicated by a marked increase in S_1 , which reflects the internal transformation of kerogen into petroleum. Crossplots of S_1 versus formation resistivity indicate that the transition from low to high values of S_1 for the Woodford Shale occurs at a resistivity between 15 and 35 ohm-m (Schmoker and Hester, 1990). A resistivity ≥ 35 ohm-m is therefore good evidence that oil generation has occurred in the Woodford Shale. The 35 ohm-m resistivity contour marks the updip limit of the region where the Woodford Shale is thermally mature and oil saturated.

Vitrinite reflectance of the Woodford Shale is plotted against formation resistivity in Figure 6. In accordance with the preceding discussion, data points in the upper-left rectangle, which are characterized by lower resistivity and lower thermal maturity, are interpreted to represent thermally immature shales. Data points in the lower-right

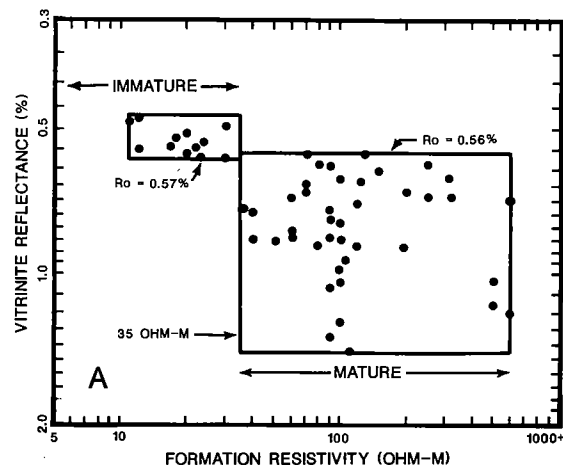


Figure 6. Vitrinite reflectance versus formation resistivity for Woodford Shale (from Schmoker and Hester, 1990).

rectangle, which are characterized by higher resistivity and higher thermal maturity, are interpreted to represent shales that are thermally mature and have generated volumes of oil sufficient to replace much of the pore water.

The horizontal boundary that separates the rectangles of Figure 6 corresponds to the level of thermal maturity at which resistivity increases sharply as a result of oil generation. Oil generation sufficient to increase resistivity to ≥ 35 ohm-m occurs at $R_o = 0.56$ – 0.57% in the Woodford Shale of the study area (Fig. 6). The updip limit of significant internal oil generation in the Woodford, which is a factor in planning horizontal drilling programs, can thus be mapped (Fig. 5).

SUMMARY

The Woodford Shale is thought to be a major source of hydrocarbons in the Anadarko basin. With the advent of horizontal drilling in low-permeability, self-sourced formations, the Woodford could prove to be important as a reservoir rock as well.

The Woodford Shale is often treated as a single depositional unit. However, the review and synthesis presented here emphasizes the point that the Woodford Shale of the central and western Anadarko basin was deposited in two depocenters separated by a forebulge that was rising during Woodford time. Furthermore, the Woodford Shale of both depocenters is not vertically uniform but can be subdivided into three members. Woodford thermal-maturity trends are shaped by Mississippian through Permian subsidence and are superimposed upon depositional patterns controlled by evolution of the southern Oklahoma aulacogen.

REFERENCES CITED

- Adkison, W. L., 1960, Subsurface cross section of Paleozoic rocks from Barber County, Kansas, to Caddo County, Oklahoma: U.S. Geological Survey Oil and Gas Investigations Chart OC-61.
- Amsden, T. W., 1975, Hunton Group (Late Ordovician, Silurian, and Early Devonian) in the Anadarko basin of Oklahoma: Oklahoma Geological Survey Bulletin 121, 214 p.
- Amsden, T. W.; and Klapper, Gilbert, 1972, Misener Sandstone (Middle–Upper Devonian), north-central Oklahoma: American Association of Petroleum Geologists Bulletin, v. 56, p. 2323–2334.
- Cardott, B. J.; and Lambert, M. W., 1985, Thermal maturation by vitrinite reflectance of Woodford Shale, Anadarko basin, Oklahoma: American Association of Petroleum Geologists Bulletin, v. 69, p. 1982–1998.
- Feinstein, S., 1981, Subsidence and thermal history of southern Oklahoma aulacogen: implications for petroleum exploration: American Association of Petroleum Geologists Bulletin, v. 65, p. 2521–2533.
- Hester, T. C.; and Schmoker, J. W., 1985, Selected physical properties of the Bakken Formation, North Dakota and Montana part of the Williston basin: U.S. Geological Survey Oil and Gas Investigations Chart OC-126, 1 plate.
- Hester, T. C.; Sahl, H. L.; and Schmoker, J. W., 1988, Cross sections based on gamma-ray, density, and resistivity logs showing stratigraphic units of the Woodford Shale, Anadarko basin, Oklahoma: U.S. Geological Survey Miscellaneous Field Studies Map MF-2054, 2 plates.
- Hester, T. C.; Schmoker, J. W.; and Sahl, H. L., 1990, Log-derived regional source-rock characteristics of the Woodford Shale, Anadarko basin, Oklahoma: U.S. Geological Survey Bulletin 1866-D, 38 p.
- , 1992, Tectonic controls on deposition and source-rock properties of the Woodford Shale, Anadarko basin, Oklahoma—loading, subsidence, and forebulge development, *in* Thorman, C. H. (ed.), Application of structural geology to mineral and energy resources of the central and western United States: U.S. Geological Survey Bulletin 2012-B, 11 p.
- Montgomery, S. L., 1989, Williston basin Bakken Shale: learning curve on the horizontal: Petroleum Frontiers, v. 6, no. 4, 52 p.
- Perry, W. J., 1989, Tectonic evolution of the Anadarko basin region, Oklahoma: U.S. Geological Survey Bulletin 1866-A, 19 p.
- Peterman, Z. E.; and Sims, P. K., 1988, The Goodman swell: a lithospheric flexure caused by crustal loading along the Midcontinent rift system: Tectonics, v. 7, p. 1077–1090.
- Schmoker, J. W.; and Hester, T. C., 1990, Formation resistivity as an indicator of oil generation—Bakken Formation of North Dakota and Woodford Shale of Oklahoma: The Log Analyst, v. 31, p. 1–9.
- Sullivan, K. L., 1985, Organic facies variation of the Woodford Shale in western Oklahoma: Oklahoma City Geological Society Shale Shaker, v. 35, p. 76–89.
- Tissot, B. P.; and Welte, D. H., 1984, Petroleum formation and occurrence [2nd edition]: Springer-Verlag, New York, 699 p.
- Turcotte, D. L.; and Schubert, Gerald, 1982, Geodynamics, applications of continuum physics to geological problems: John Wiley, New York, 450 p.
- Urban, J. B., 1960, Microfossils of the Woodford Shale (Devonian) of Oklahoma: University of Oklahoma unpublished M.S. thesis, 77 p.

Depositionally and Diagenetically Controlled Reservoir Heterogeneity at Jordan Field¹

R. P. Major and Mark H. Holtz

Bureau of Economic Geology
The University of Texas at Austin
Austin, Texas

ABSTRACT.—The University Lands Jordan San Andres reservoir has produced 68 million stock-tank bbl (MMSTB) of the 182 MMSTB of original oil in place; an estimated 44 MMSTB of mobile oil remain in this reservoir. The reservoir is divided into four flow units on the basis of depositional textures and subsequent diagenetic overprint. The locus of highest production corresponds to a trend of high reservoir-storage capacity in zone C, which has been affected by a permeability-increasing, carbonate-leaching diagenetic alteration. This locus crosscuts structure. An area of low production corresponds to an area of highest reservoir-storage capacity in zone B, which has not been affected by this diagenetic alteration. This low-production area is in an updip position but has been inefficiently swept by the waterflood.

INTRODUCTION

Jordan field is located on the eastern margin of the central basin platform in the Permian basin of West Texas (Fig. 1), on the Ector/Crane county line. The field is part of a five-field complex that produces oil from a combined structural and stratigraphic trap on the eastern flank of a broad, asymmetric anticline (Major and others, 1988). Discovered in 1937, Jordan field produces oil from a Permian (Guadalupian) San Andres Formation reservoir at a depth of ~3,500 ft. Following peripheral waterflooding in 1968, a program of infill drilling, well deepening, and conversion of producing wells to water-injection wells began in 1969. By 1971 the University Lands part of the field was on a modified five-spot waterflood with a producing-well spacing of ~20 acres per well (Fig. 2).

The two Jordan field units on University Lands have produced 68 MMSTB of the 182 MMSTB of original oil in place, and an estimated 44 MMSTB of mobile oil remain in the University Lands part of the reservoir (Tyler and others, 1990). This high remaining-mobile-oil resource prompted a combined geological and engineering study of the Jor-

dan San Andres reservoir on University Lands to develop strategies for recovering the oil.

RESERVOIR DESCRIPTION

Lithologic description of the San Andres reservoir at Jordan field is based on examination of seven cores from within two University Lands

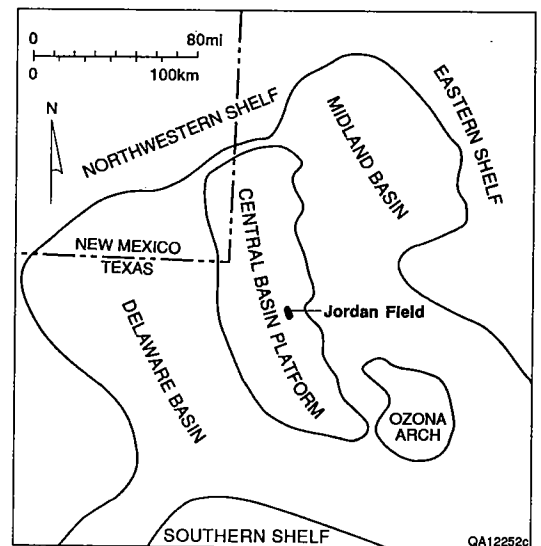


Figure 1. Permian basin paleogeography and location of Jordan field.

¹This paper was invited for presentation at the Society of Petroleum Engineers Annual Technical Conference and Exhibition as a "Best of AAPG for SPE" paper and was published in the *Journal of Petroleum Technology* (1990, v. 2, no. 10, p. 1304–1309). It is copyrighted by SPE and reprinted here with permission.

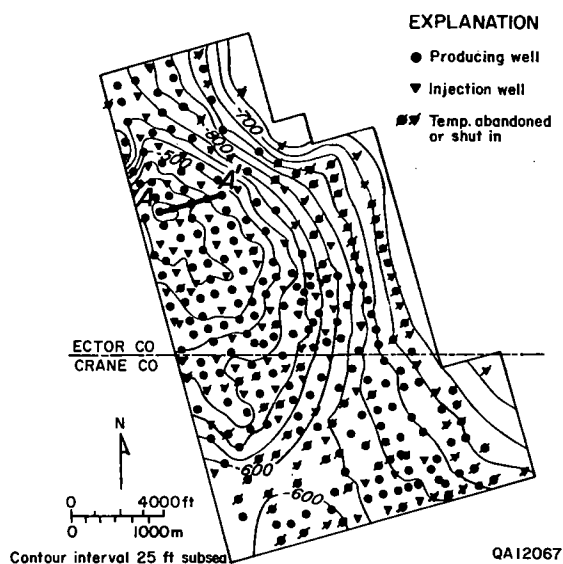


Figure 2. San Andres structure map, University Lands Jordan field. Cross section A-A' shown in Figure 7.

units, and is augmented by the study of two Jordan field cores immediately west of the University Lands boundary and 14 cores in the East Penwell San Andres unit, which offsets Jordan field to the north (Major and others, 1988, 1990). The reservoir is composed of thoroughly dolomitized carbonate rocks cemented by sulfates.

Depositional Facies

The San Andres Formation at Jordan field is composed of an approximately 400-ft-thick upward-shoaling sequence of rocks deposited as shallow-water ramp sediments (Major and others, 1988). For this discussion, the description of depositional facies is divided into two parts: rocks deposited as tidal-flat sediments, and rocks deposited as open-marine sediments.

Tidal-Flat Depositional Facies

Tidal-flat facies are pisolite packstone and mudstone. Pisolite packstone is composed of symmetrical and asymmetrical pisolites generally 0.2–4 mm in diameter with fine-grained muddy matrix. Pisolites commonly have a fitted fabric. This facies is characterized by abundant caliche, fenestrae, and desiccation and sheet cracks. Locally the pisolite packstone facies contains karst collapse breccias generally <3 ft thick. This facies is generally nonporous, but locally is both porous and permeable. The presence of caliche, collapse breccia, and desiccation features indicates periodic subaerial exposure, and the pisolite packstone facies is interpreted as having been deposited in an intertidal or supratidal environment.

Mudstone is composed of cream-colored, generally massive dolomite, although some mudstone is faintly laminated. Stromatolitic laminae are present but rare. Mudstone is composed of dolomite crystals generally smaller than 0.02 mm but lacks fossils, suggesting it was deposited in a hypersaline environment in which stromatolites could survive but marine invertebrates were excluded. The absence of fossils and the close association with the pisolite packstone facies suggest deposition in hypersaline ponds on a tidal flat isolated from, and probably landward of, the open-marine depositional environment.

Tidal-flat facies are interbedded with three intervals of siliciclastic silt that may be correlated regionally with gamma-ray logs. Tidal-flat facies are separated from subjacent open-marine facies by an interval of greenish-gray organic-rich shale that may be correlated throughout Jordan field using gamma-ray logs.

Open-Marine Depositional Facies

Subtidal facies are pellet packstone/grainstone and bioherms composed of bryozoans, algae, and corals, with flanking skeletal grainstone. The pellet packstone/grainstone facies is composed of variable amounts of muddy matrix and spherical to ovoid fecal pellets, approximately 0.2–0.5 mm in diameter. Fossils of open-marine invertebrates, especially fusulinids, are common. Burrow structures are rare, and few laminations exist because of bioturbation. Fecal pellets were deposited as soft carbonate mud and vary greatly in degree of preservation. The thorough bioturbation and presence of abundant fossils of open-marine invertebrates indicate that this sediment was deposited in a shallow subtidal setting as pelleted mud, in an environment similar to Holocene carbonate shelf and ramp settings.

Bryozoan, algal, and coral bioherms occur locally and discontinuously in the lower part of the open-marine section. Crinoid fragments are a common accessory grain in this facies. Bioherms, which are generally nonporous, contain abundant internal muddy sediment, and geopetal structures are common. Skeletal grainstone, composed principally of bryozoan and crinoid fragments, and (less abundantly) fusulinid and mollusk fragments, is closely associated with bioherms. The presence of abundant fossils of open-marine organisms, lack of desiccation features, and stratigraphic proximity to pellet packstone/grainstone indicate that bioherms and skeletal grainstone were deposited in a subtidal environment.

Diagenetic Effects

Tidal-flat pisolite packstone is generally nonporous because fenestrae and sheet cracks are cemented with sulfates. Locally, sulfate cementation

was either incomplete or did not occur; more likely, sulfate cements were leached. Where little or no cement occurs in pisolite packstone, this facies is porous and permeable, in some locations with porosities as high as 15% and permeabilities as high as 1,000 md. The volumetrically dominant pore type is fenestral. This diagenetically controlled porous texture is important because, where porous, the pisolite packstone facies is part of the reservoir, and, where nonporous, it is part of the reservoir seal (Fig. 3A).

Open-marine facies have been partly to completely altered by a postburial leaching. The "diagenetically altered" dolomite can be identified on

slabbed core surfaces as tan- to brown-colored dolomite that contrasts with the dark-gray color of unaltered dolomite. Altered dolomite in some cases mimics the geometry of burrows, whereas in other cases it forms aureoles around stylolites, suggesting that the fluids causing this alteration preferentially flowed along stylolites and that diagenetic alteration was a postburial, postcompaction event.

The diagenetically altered dolomite is more permeable than the unaltered dolomite, as indicated by the mini-permeameter (Eijpe and Weber, 1971; Chandler and others, 1988) data plotted in Figure 4. Large parts of the reservoir contain both

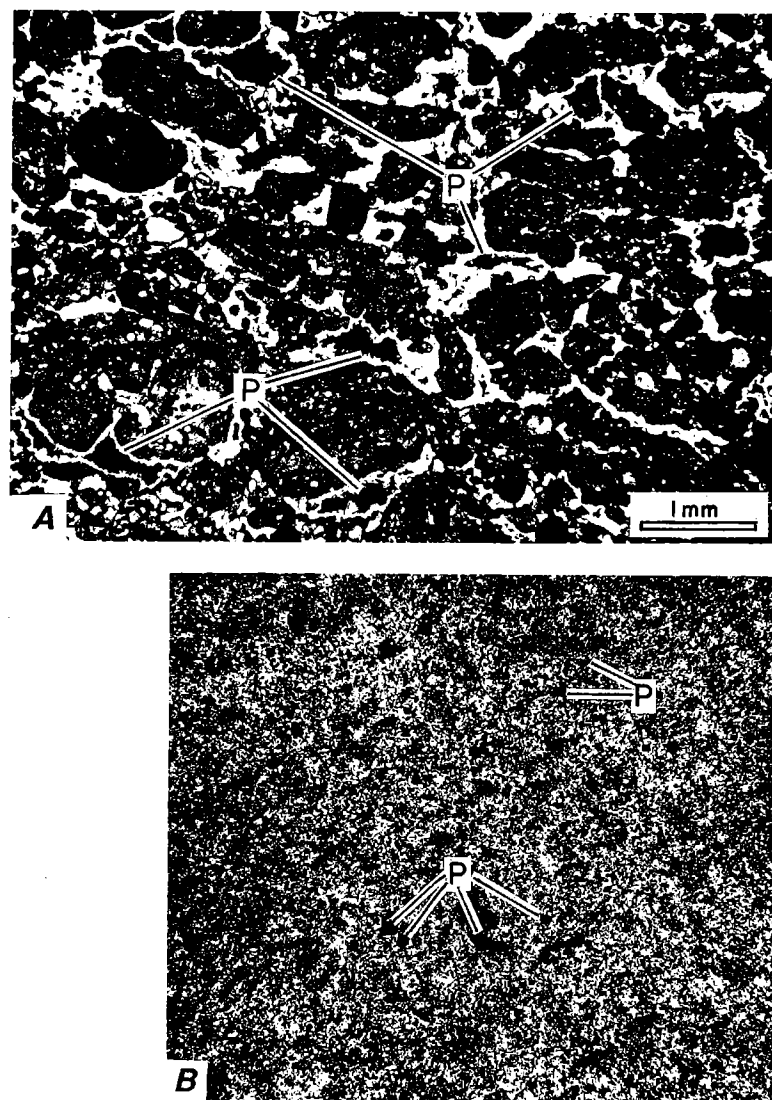


Figure 3. Photomicrographs illustrating the two major pore types in the San Andres Reservoir at Jordan field. A—Fenestral (vugular) porosity (P) in the tidal-flat facies. Locally these pores are plugged with sulfate cement, but where cementation is incomplete this facies is part of the reservoir. B—Interparticle porosity in the open-marine facies.

altered and unaltered dolomite textures so closely associated that sampling for conventional whole-core or core-plug permeability analysis is difficult. Sampling for permeability measurements made by the operator prior to our study did not separate these two rock types. Thus, the order-of-magnitude difference in permeability between the two rock types (Fig. 4) is commonly below the resolution of conventional permeability analyses.

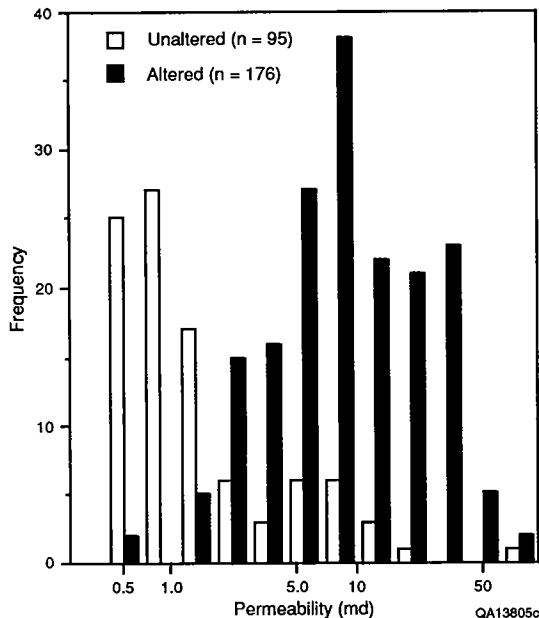


Figure 4. Permeability histograms for diagenetically unaltered and diagenetically altered pellet packstone/grainstone. Data from East Penwell San Andres unit wells 207 and 1914.

Diagenetically altered dolomite of higher permeability is characterized by hollow and corroded dolomite rhombs, indicating that the alteration was a carbonate-leaching process. Diagenetically altered dolomite is commonly closely associated with anhydrite nodules rimmed by gypsum; thin-section point-count data confirm the association of diagenetically altered (leached) dolomite and gypsum. Some samples of diagenetically altered rock contain as much as 20% gypsum. One can infer from this relationship that the fluids causing the leaching of dolomite also altered some of the anhydrite nodules and cements to gypsum.

Calibration of Logs and Cores

Acoustic-, neutron-, and density-porosity logs are available for Jordan field. The presence of abundant gypsum in the reservoir, however, precludes the use of neutron and density logs for porosity measurements. The bound water of hydration within gypsum crystals is recorded as porosity by neutron logs, and the relatively low density of gypsum (2.35, compared with 2.87 for dolomite and 2.95 for anhydrite) causes density logs to record erroneously high porosities (Tilly and others, 1982; Bebout and others, 1987). Simultaneous equations solved with data from all three porosity logs yielded a poor correlation between bulk volume mineralogy and mineralogy determined from point-count analysis. Alternatively, acoustic transit time was calibrated to core porosity, which provides a relationship that was used to measure porosity with acoustic logs in wells that were not cored. Critical considerations when using core porosity in gypsum-bearing formations are: (1) the methods of cleaning the cores before porosity

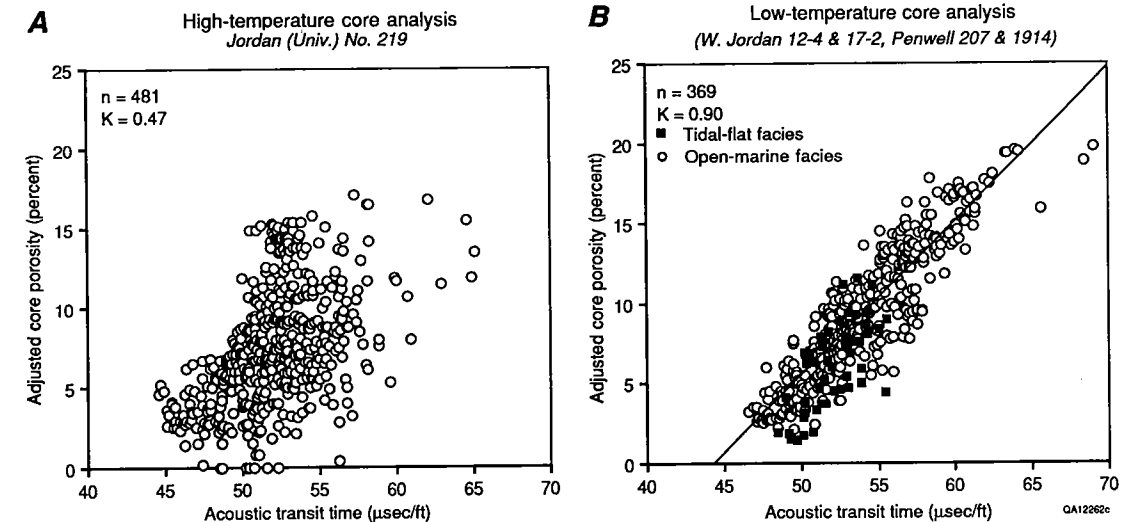


Figure 5. Cross plots of acoustic transit time versus core porosity (3-ft running averages) for (A) high-temperature core analyses and (B) low-temperature core analyses.

analysis, and (2) the method of porosity measurement. Specifically, high-temperature cleaning processes will dehydrate gypsum crystals and create porosity, and measurements made by the summation-of-fluids method will calculate the water of hydration in gypsum crystals as porosity. All available cores from Jordan field units were subjected to high-temperature core analysis processes and, as illustrated by the example in Figure 5A, cross plots of high-temperature core porosity and acoustic transit time do not yield a statistically significant linear relationship. (Core porosity values used in Figure 5 are 3-ft running averages, so that these data represent approximately the same volume of rock as the data measured by acoustic logs.) Four cores from wells that offset Jordan field were analyzed using low-temperature, nondestructive techniques. The cross plot of these porosity data with acoustic transit time yields a linear relationship with a correlation coefficient (K) of 0.90 (Fig. 5B). Similar comparisons of core porosity with neutron- and density-log porosities and multiple-log cross-plot porosities did not yield as good a relationship. Thus, the most reliable porosity tool is the acoustic log, and porosity was calculated from acoustic transit time using the formula:

$$\phi = -41.159 + 1.006 \Delta t \quad (1)$$

(For explanation of symbols, see Nomenclature section below.)

Some of the data illustrated in Figure 5B are from the pisolite packstone facies. The pores in this facies are large fenestrae and sheet cracks; i.e., this facies is characterized by vuggy porosity, in contrast to the dominantly interparticle porosity in open-marine facies (Fig. 3). The relationship of acoustic transit time to true rock porosity commonly varies greatly between rocks containing vuggy porosity and rocks containing interparticle porosity (Lucia, 1983; Lucia and Conti, 1987). Thus, an *a priori* reason exists to suppose that the acoustic transit time of pisolite packstone is different from that of open-marine facies. This is not true, however, and the relationship between low-temperature core porosity and acoustic transit time is valid for both tidal-flat and open-marine facies rocks (Fig. 5B). This suggests that when fenestral porosity is sufficiently interconnected, the rock has high permeability, and the acoustic-log response to this porosity type is similar to the response to interparticle porosity.

Because responses of neutron and acoustic logs to gypsum-bearing rocks differ, these two logs can be used to identify these diagenetically altered rock textures in wells that are not cored. As indicated previously, the high-permeability diagenetically altered rock is associated with higher gypsum content than is unaltered rock. Thus, altered reservoir rock containing abundant gypsum may be

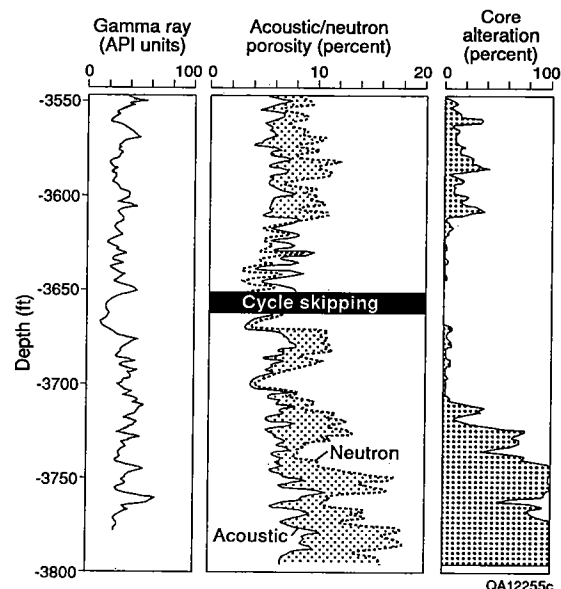


Figure 6. Calibration of acoustic-log porosity, neutron-log porosity, and percentage of diagenetically altered facies observed in core. Zones in which neutron porosity exceeds acoustic porosity are stippled (note that porosity is scaled with higher values toward the right).

identified on wire-line logs where dolomitic neutron-log porosity exceeds acoustic porosity normalized to a dolomite matrix. The relationship of acoustic-log porosity, neutron-log porosity, and percentage of altered texture observed in slabbed core (Fig. 6) demonstrates the use of wire-line logs to identify the diagenetically altered facies.

FLOW UNITS

We divided the Jordan field San Andres reservoir into four flow units (*sensu* Ebanks, 1987) on the basis of both depositional facies and diagenetic effects. Open-marine rocks are divided into three flow units defined by the stratigraphic patterns of diagenetically altered facies as identified using wire-line logs (Fig. 7). Zone A is 100%, or nearly 100%, altered-texture rock, and is identified on logs by a neutron-log/acoustic-log porosity curve separation. Zone B is composed of diagenetically unaltered rock identified by a normalized neutron log that is in good agreement with a normalized acoustic log. Zone C is composed of a mottled mixture of diagenetically altered and unaltered rock, and is characterized by a normalized neutron-log/normalized acoustic-log separation.

Zone D is composed of tidal-flat rocks that occur above the organic-rich shale identified with a gamma-ray marker (labeled ORS on Fig. 7). This marker can be correlated across the field. Porosity in the section occurs in pisolite packstone in

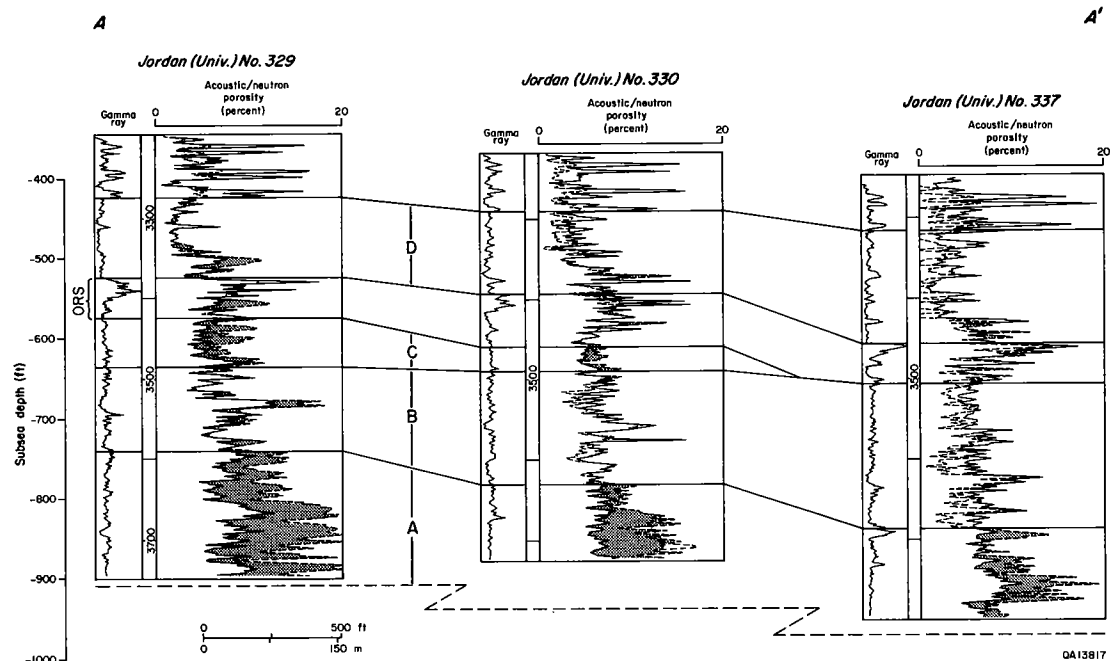


Figure 7. Log cross section illustrating the four flow units. Location of cross section shown in Figure 2.

which fenestrae and sheet cracks are not plugged with sulfate cements. Porous pisolite packstone of the tidal-flat section constitutes zone D, the fourth flow unit.

Reservoir storage capacity (ϕh) maps were constructed for three flow units (Figs. 8–10) using the acoustic transit time/porosity relationship developed for low-temperature core data (Fig. 5B). A porosity cutoff of 5% was used to construct these maps. A reservoir storage-capacity map was not constructed for zone A, because no wellbores penetrate the base of this zone and because few wells reached the depth of this zone before well deepening and infill drilling in the early 1970s, immediately before waterflood began. Before waterflooding, most wells were open-hole completions.

Zone B ϕh map (Fig. 8) indicates relatively low reservoir-storage capacity in this zone in the downdip northern and eastern parts of the field, and relatively high storage capacity in the southwestern updip part of the field. The updip central-western boundary and the downdip southeastern corner of the field are areas where zone B is absent and zones A and C cannot be differentiated.

Zone C ϕh map (Fig. 9) illustrates a trend of relatively high reservoir-storage capacity extending from the updip central-western boundary of the field to the downdip southeastern corner. A zero ϕh contour separates this trend from the downdip northeastern corner and the updip southwestern corner of the field.

The area of highest storage capacity in zone D (Fig. 10) occurs in the downdip eastern part of the field.

PRODUCTION PATTERNS

The patterns of reservoir storage capacity illustrated by the ϕh maps can be compared with maps

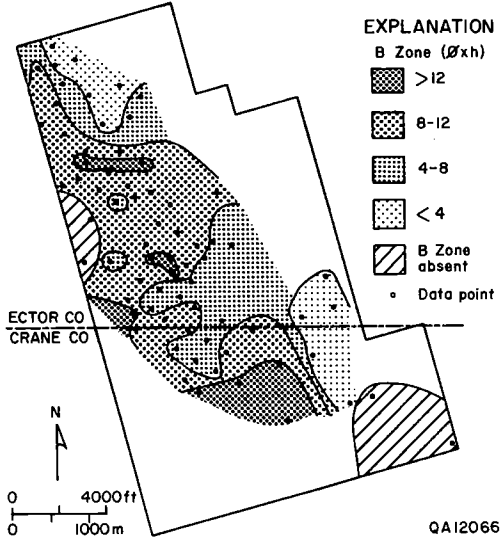


Figure 8. Zone B ϕh map.

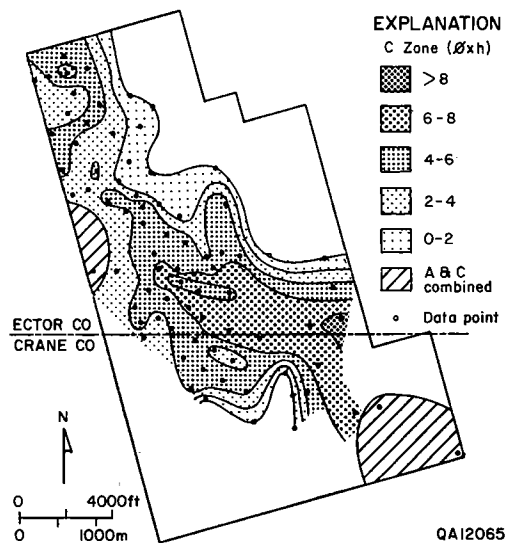


Figure 9. Zone C ϕh map.

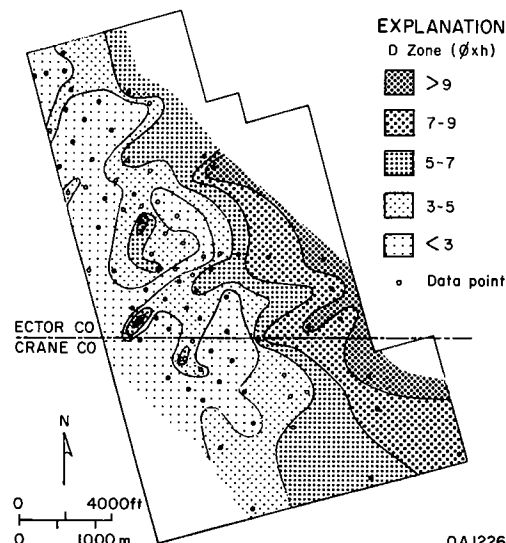


Figure 10. Zone D ϕh map.

of production at various times during the reservoir's life. Per-well production data are available only for the postwaterflood time period (1969 to the present). Production data before 1969 are available on a per-lease basis (the two Jordan field units on University Lands were composed of several separate leases during different time periods). Individual wells within each lease were periodically flow-tested, and these test data were used to apportion lease production to each well within the lease according to the relationship:

$$N_{pw} = \frac{q_w \times N_{pl}}{\sum q_t} \tag{2}$$

These data were added to the postwaterflood data to reconstruct the per-well production history for the reservoir.

The University Lands Jordan field contains wells that have produced oil for more than 40 years and wells that have been on production for less than five years, and the spacing of these wells is irregular. To minimize this "cultural effect," production values were averaged over time and normalized to a 40-acre grid. The cumulative production (or production for a specified time period) for each well was divided by the number of years that the well has been on production, yielding an average cumulative production expressed as stock-tank barrels per year. The drainage area of each well was approximated within arbitrarily defined 40-acre square cells. The fraction of well drainage areas within each cell was used to apportion the time-averaged production. Thus, a single data point for each 40-acre cell expresses production in units of stock-tank barrels per year per acre.

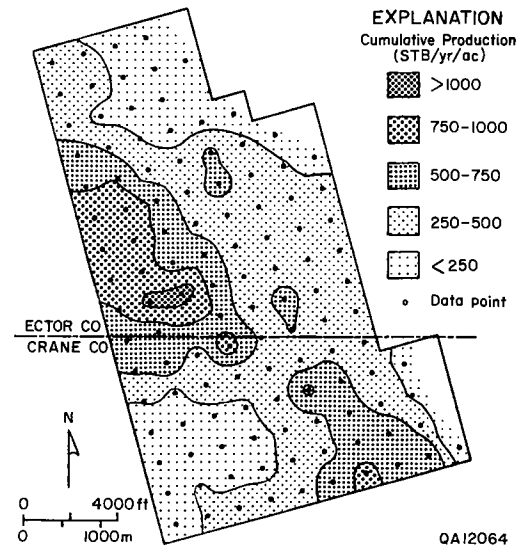


Figure 11. Map of average cumulative production through 1988 in stock tank barrels per year per acre (STB/yr/ac).

The map of averaged cumulative production through 1988 (Fig. 11) exhibits a trend of high production extending from the updip central-western margin of the University Lands Jordan field to the downdip southeastern corner. The updip southwestern corner of the field is an area of low production. Postwaterflood production (1969–88, Fig. 12) has a similar pattern. Prewaterflood production (Fig. 13) has this pattern, and in addition contains an area of high production in the downdip eastern part of the field.

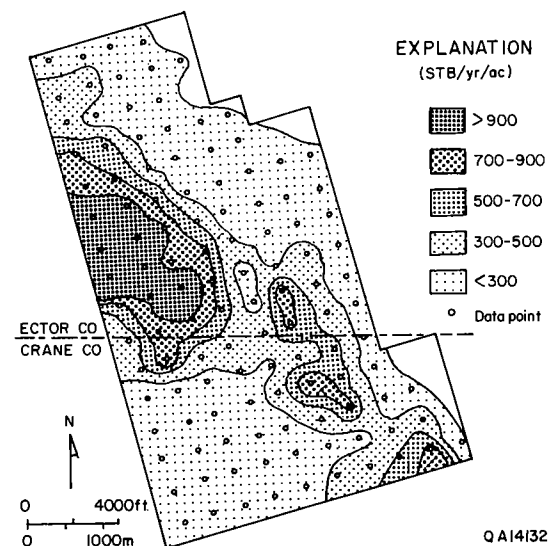


Figure 12. Map of postwaterflood (1969–88) average production.

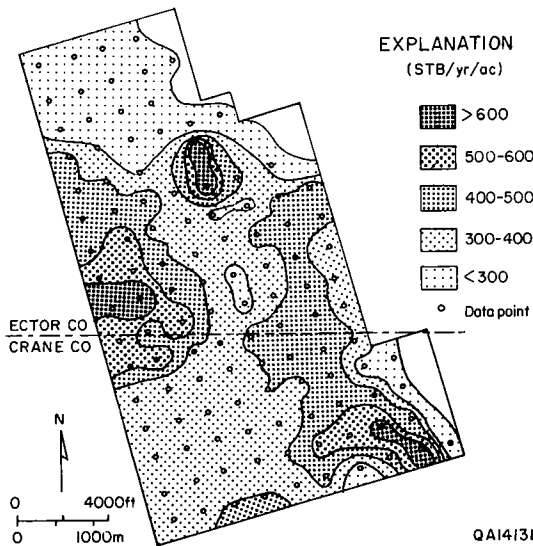


Figure 13. Map of prewaterflood (pre-1969) production.

DISCUSSION

Comparisons of the ϕh maps (Figs. 8–10) with the cumulative-production maps (Figs. 11–13) indicate some correlations. Note when comparing these maps that the ϕh data points are limited to those wells for which acoustic logs are available. In contrast, the cumulative-production map data points are averaged production normalized on a 40-acre grid. Thus, the data control for these two types of illustrations is different. Note also that the similarities of the patterns in the cumulative production, postwaterflood production, and prewaterflood production maps indicate that the waterflood did not greatly alter the loci of high and low production in the field.

The northwest/southeast trend of high reservoir-storage capacity in zone C (Fig. 9) crosscuts structure and correlates well with the high production trend (Figs. 11–13), indicating that this diagenetically altered, high-permeability zone is the main source of oil for both prewaterflood and postwaterflood production. The updip southwestern area of high reservoir-storage capacity in zone B (Fig. 8) corresponds to an area of low cumulative production (Figs. 11–13), indicating that this diagenetically unaltered, relatively low-permeability zone was not a large contributor to prewaterflood production and has been inefficiently swept by the waterflood. The downdip eastern area of high reservoir storage capacity in zone D (Fig. 10) correlates with an area of high prewaterflood production (Fig. 13), indicating that zone D was most productive early in the history of this reservoir.

CONCLUSIONS

1. The University Lands Jordan field San Andres reservoir is composed of a 400-ft-thick sequence of upward-shoaling, shallow-water carbonate facies now thoroughly dolomitized and cemented with sulfates.
2. A postcompaction, postburial diagenetic alteration has leached carbonate and partly altered anhydrite to gypsum in the reservoir. This diagenetic alteration, which affected only some parts of the reservoir, increased permeability.
3. The locus of highest oil production is from a zone affected by this permeability-increasing diagenetic alteration.
4. A zone that was not diagenetically altered is a zone of relatively low oil production that has been inefficiently swept by the waterflood. Selective wellbore plugging and perforation squeezing may focus injection water into zone B, thus contacting bypassed oil that would otherwise remain in the reservoir.

NOMENCLATURE

- n = Number of data points
- t = Acoustic transit time in $\mu\text{sec}/\text{ft}$
- ϕ = Porosity
- h = Thickness
- N_{pl} = Cumulative production of lease in bbl
- Σ = The summation of
- K = Correlation coefficient
- N_{pw} = Cumulative production of well in bbl

- q_t = Rate of production on well test for all wells in the lease in bbl/d
 q_w = Rate of production on well test in bbl/d

ACKNOWLEDGMENTS

Funding for this study was provided by the University of Texas System as part of a larger study of reservoirs on University Lands. Shell Oil Co., Hondo Oil Co., the University of Texas Lands Office, and the Railroad Commission of Texas provided access to data. We thank M. G. Kittridge, who collected the mini-permeameter data in the laboratories of the Department of Petroleum Engineering, the University of Texas at Austin. We have benefited from discussion with several colleagues, notably D. G. Bebout, F. J. Lucia, Charles Kerans, S. C. Ruppel, Noel Tyler, and G. W. Vander Stoep. J. M. Coleman, J. E. Nicol, and J. A. Tenison provided technical support. Publication of this report was authorized by the Director of the Bureau of Economic Geology, the University of Texas at Austin.

REFERENCES CITED

- Bebout, D. G.; Lucia, F. J.; Hocott, C. R.; Fogg, G. E.; and Vander Stoep, G. W., 1987, Characterization of the Grayburg reservoir, University Lands Dune field, Crane County, Texas: The University of Texas at Austin, Bureau of Economic Geology Report of Investigations No. 168, 104 p.
- Chandler, M. A.; Goggin, D. J.; and Lake, L. W., 1988, A mechanical permeameter for making rapid, non-destructive, permeability measurements: *Journal of Sedimentary Petrology*, v. 59, p. 613–615.
- Ebanks, W. J., Jr., 1987, Flow unit concept—integrated approach to reservoir description for engineering projects [abstract]: *American Association of Petroleum Geologists Bulletin*, v. 71, p. 551–552.
- Eijpe, R.; and Weber, K. J., 1971, Mini-permeameters for consolidated rock and unconsolidated sand: *American Association of Petroleum Geologists Bulletin*, v. 55, p. 307–309.
- Lucia, F. J., 1983, Petrophysical parameters estimated from visual descriptions of carbonate rocks: a field classification of carbonate pore space: *Journal of Petroleum Technology*, v. 35, p. 629–637.
- Lucia, F. J.; and Conti, R. D., 1987, Rock fabric, permeability, and log relationships in an upward-shoaling, vuggy carbonate sequence: The University of Texas at Austin, Bureau of Economic Geology Geological Circular 87-5, 22 p.
- Major, R. P.; Bebout, D. G.; and Lucia, F. J., 1988, Depositional facies and porosity distribution, Permian (Guadalupian) San Andres and Grayburg Formations, P.J.W.D.M. field complex, central basin platform, West Texas, *in* Giant oil and gas fields: Society of Economic Paleontologists and Mineralogists Core Workshop No. 12, p. 615–648.
- Major, R. P.; Vander Stoep, G. W.; and Holtz, M. H., 1990, Delineation of unrecovered mobile oil in a mature dolomite reservoir: East Penwell San Andres unit, University Lands, West Texas: The University of Texas at Austin, Bureau of Economic Geology Report of Investigations No. 194, 52 p.
- Tilly, H. P.; Gallagher, B. J.; and Taylor, T. D., 1982, Methods for correcting porosity data in a gypsum-bearing carbonate reservoir: *Journal of Petroleum Technology*, v. 34, p. 2449–2454.
- Tyler, Noel; Bebout, D. G.; Garrett, C. M., Jr.; Hocott, C. R.; Holtz, M. H.; Hovorka, S. D.; Kerans, Charles; Lucia, F. J.; Major, R. P.; Ruppel, S. C.; and Vander Stoep, G. W., 1990, Opportunities for additional recovery in University Lands reservoirs—characterization of University Lands reservoirs: The University of Texas at Austin, Bureau of Economic Geology Final Project Report, prepared for The University of Texas System, 255 p.

Diagenesis, Continuity, and Reservoir Character of Grainstone Lenses: Lansing–Kansas City “I” and “J” Zones, Pen Field, Graham County, Kansas¹

Roderick A. Phares and Anthony W. Walton

University of Kansas
Lawrence, Kansas

ABSTRACT.—The Pen field produces from five zones in the Lansing–Kansas City interval, chiefly the Alpha grainstone of the “J” zone and grainstones of the “I” zone. The “J” zone Alpha grainstone forms a lens as much as 6 ft thick that is nearly coextensive with productive wells in the field. Pressure data show that most of the wells completed in the Alpha grainstone are in close pressure communication and intersect the same reservoir compartment. Only the southernmost two wells are rendered noncommercial by a pervasive early marine cement that reduced permeability; molds of allochems are the only pores.

Grainstones of the “I” zone form three smaller, thinner lenses within the field, two of which are productive. Diagenesis has divided one of them into two separate compartments. Other production is from other grainstone lenses and mud-rich carbonates with moldic porosity.

Eleven cores provide extensive data on lithology, diagenesis, porosity, and permeability. Neutron and density logs give porosity measurements for rocks that contain varying proportions of limestone and dolomite. Induction logs indicate water saturation. Well-by-well monthly production data form a basis for history matching and modeling of production. In the geological description, porosity determined from well-log measurements was interpolated between wells and modified using geological insight. Values of permeability and water saturation were calculated for each grid block from their empirical relationships to porosity.

INTRODUCTION

The Pen field was discovered in May 1985, with completion of the PanCanadian Petroleum Co.’s Pennington no. 1 well in SW¼NE¼ sec. 17, T. 6 S., R. 22 W., in Graham County, Kansas (Fig. 1). During the next three years, 17 productive wells and eight dry holes delineated the field and proved out ~680 productive acres (Fig. 2). Most of the oil (75%) comes from grainstones in the “I” and “J” zones of the Lansing–Kansas City interval, as defined by Morgan (1952), but the “D”, “K”, and “L” zones, and non-grainstone intervals in the “J”

zone also contribute. The field produced 530,000 bbl of oil through June 1990.

Eleven cores, good-quality logs, numerous drill-stem tests, and well-by-well monthly production records provide a better data base for understanding this oil field than is available for most Lansing–Kansas City oil fields in Kansas. The Tertiary Oil Recovery Project (TORP) of the University of Kansas undertook study of the Pen field as an example of reservoir management in a Lansing–Kansas City oil field. This paper reports on the first phase of that project, a geological reservoir characterization.

It is hoped that the second phase will produce models that reproduce production history of the field quantitatively and predict its performance under waterflood. Successful completion of the project will provide a well-described example of a

¹This manuscript was also published in the Proceedings of the Ninth Tertiary Oil Recovery Conference, Tertiary Oil Recovery Project, University of Kansas, 1991, Contribution 11, p. 57–69.

Phares, R. A.; and Walton, A. W., 1993, Diagenesis, continuity, and reservoir character of grainstone lenses: Lansing–Kansas City “I” and “J” zones, Pen field, Graham County, Kansas, *in* Johnson, K. S.; and Campbell, J. A. (eds.), Petroleum-reservoir geology in the southern Midcontinent, 1991 symposium: Oklahoma Geological Survey Circular 95, p. 91–103.

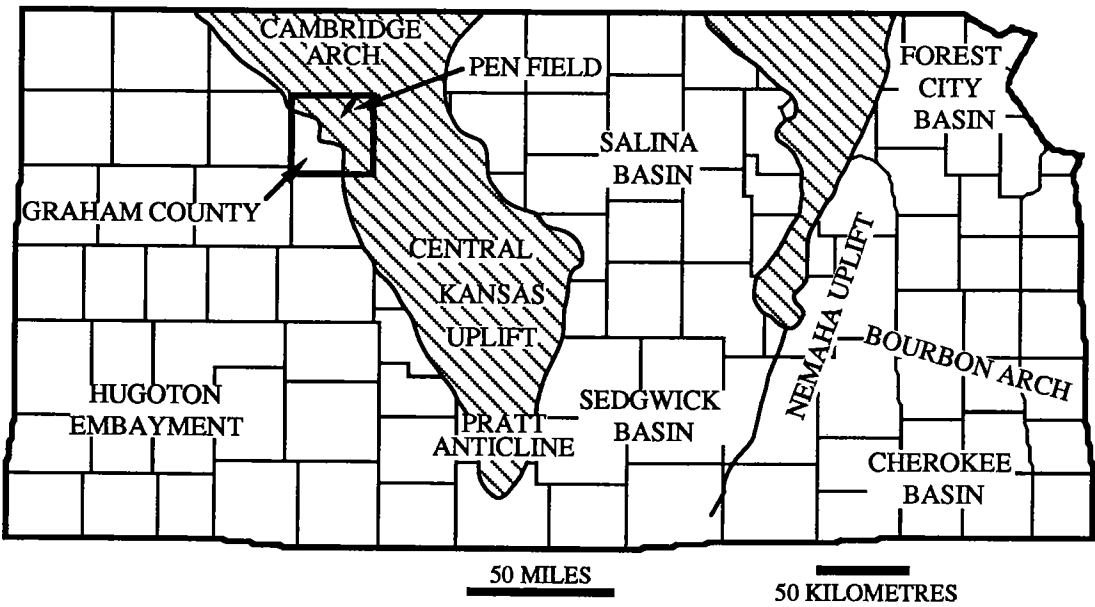


Figure 1. Location of the Pen field in Graham County, Kansas, in the saddle area between the Central Kansas uplift and the Cambridge arch.

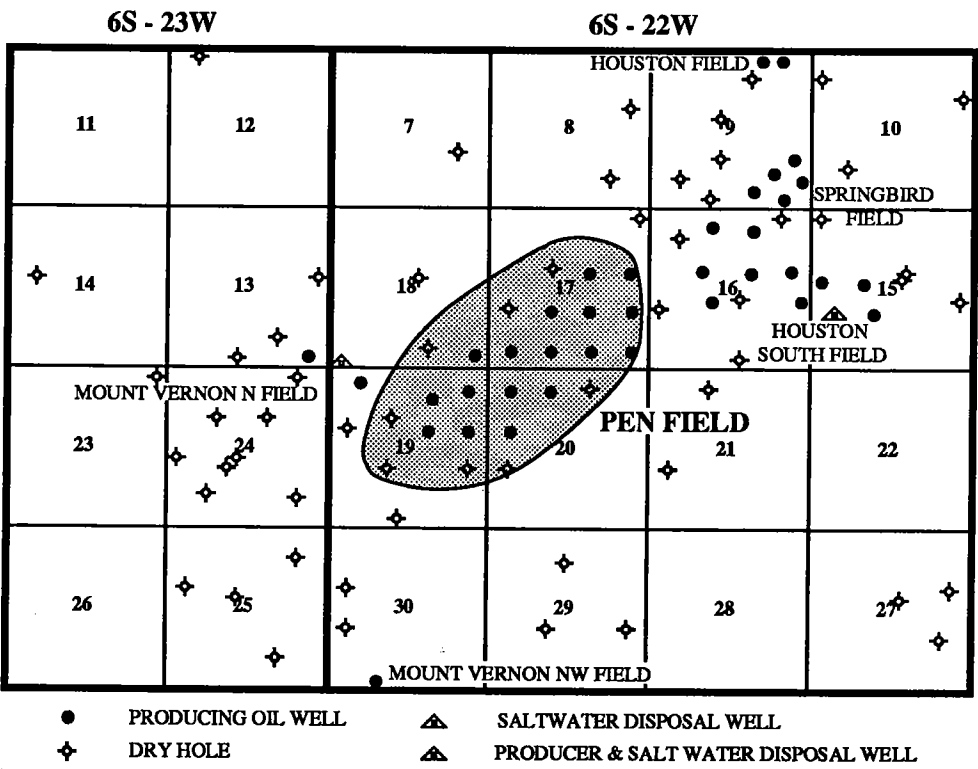


Figure 2. The Pen field and surrounding oil fields. The 17 producing wells and eight dry holes in the shaded area were drilled as part of the Pen field development.

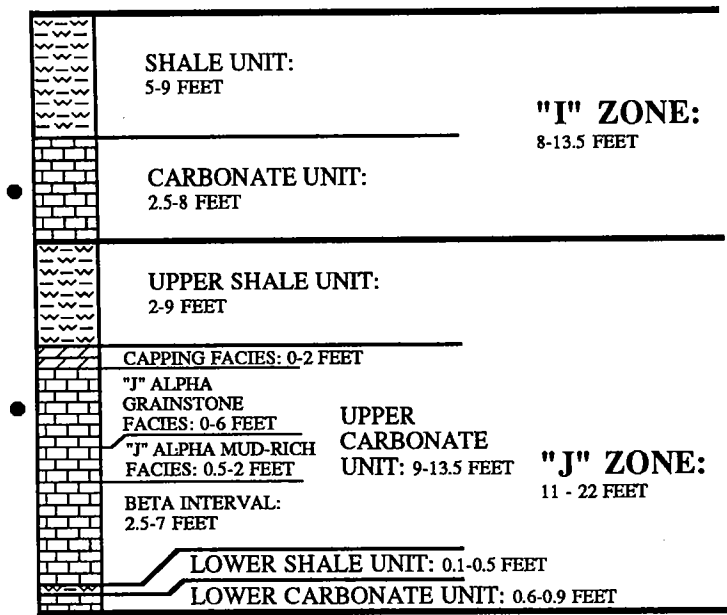


Figure 3. "I" and "J" zones of the Lansing-Kansas City interval of the Pen field. About 75% of the original oil in place in the Pen field was in these two units.

Lansing-Kansas City oil field and an indication of the kind of results that can be obtained with abundant high-quality data.

LANSING-KANSAS CITY
OF THE PEN FIELD

The Pen field lies in the saddle between the Central Kansas uplift and the Cambridge arch of Nebraska and northern Kansas (Fig. 1). On the flanks and crest of these post-Mississippian structural features, Morrowan, Atokan, Desmoinesian, and Missourian rocks successively onlap an unconformity cut into Mississippian, lower Paleozoic, and Precambrian rocks.

The Lansing-Kansas City interval (Missourian, Upper Pennsylvanian) of central and western Kansas consists primarily of limestone and shale interbedded at a scale of <1 to <10 m. In the subsurface of central and western Kansas, oil-patch usage combines the formally defined Kansas City and Lansing Groups of eastern Kansas into one unit, because, in the subsurface, no thick shale bed separates the two groups as it does at the outcrop in eastern Kansas. The Lansing-Kansas City interval of central and western Kansas is divided into a series of informal zones with letter designations (Morgan, 1952). Correlation of these zones with the named formations and members of the eastern Kansas outcrops (Zeller, 1968) is not firmly established.

Alternating limestones and shales of the Mis-

sourian are commonly described as *cyclothems*, which are cyclic repetitions of lithologic units representing changes in environment of deposition (Moore, 1936,1949). Heckel (1977) proposed that these lithologic units developed as sea level rose and fell in response to advance and retreat of continental ice sheets in the southern hemisphere.

The "J" Zone

The "J" zone in the Pen field consists of two limestone beds (lower and upper carbonate units) and two mudrock beds (lower and upper shale units; Fig. 3), all of which are continuous across the field. Production in the Pen field is primarily from a grainstone facies of the upper or Alpha unit of the upper carbonate, where remaining interparticle porosity is augmented by molds and a few vugs. Minor production comes from molds and vugs in the cap unit at the top of the "J" zone upper carbonate and from grainstones and wackestones in the lower part (Beta interval) of the upper carbonate, where porosity is either interparticle or moldic.

In carbonate units of the "J" zone, peloids, whole or fragmented fossils of normal-marine organisms, coated grains, and intraclasts are present as allochems. Only in the Alpha grainstone do oolites predominate. Pressure-solution features, including stylolites, microstylolites, microstylolite swarms, and clay seams, are common, but more so in the micrite-rich lithologies, where they are 5-10 cm apart in all cores. Carbonate beds range

from light-brown or light-gray to cream, light-green, or medium-brown.

Lower Carbonate and Lower Shale

The lower carbonate of the "J" zone is 18–28 cm of packstone and grainstone intermixed at the centimeter scale. It is medium-brown to medium-gray and contains *Osagia*-coated grains in addition to the allochems present throughout the "J" zone. Where present, matrix consists of slightly argillaceous micrite with quartz silt and clays. The lower shale is generally 2.5–5.1 cm thick, but reaches 15 cm in one well. It is dark-green to dark-gray, slightly calcareous mudshale or mudstone. In places, it contains a few articulate brachiopods.

Upper Carbonate

The upper carbonate is 2.7–4.1 m thick and is subdivided into the Beta (lower) and Alpha subunits and a capping subunit (Fig. 3). In detail, the Beta subunit consists of a matrix-rich carbonate and an overlying intermixed grainstone and packstone. The Alpha subunit includes interbedded matrix-rich carbonate and grainstone. Contacts between all of these subunits are conformable.

Beta Interval.—The Beta mud-rich carbonate of the upper carbonate bed of the "J" zone is 0.6–1.8 m of wackestone, packstone, mottled wackestone-packstone, and grainstone (in only one well). A few phosphate-bearing allochems are present and are probably the cause of the prominent gamma-ray kick associated with the Beta mud-rich carbonate. A bed of grainstone and packstone 13–36 cm thick conformably overlies the Beta mud-rich carbonate. Light-brown to medium-brown grainstone is predominant in this interval, but matrix is erratically distributed in geopetal accumulations and pore fillings in many rocks. Small amounts of production are obtained from rocks of the Beta interval in two wells in the Pen field.

Alpha Carbonate.—The Alpha carbonate overlies the Beta carbonate and consists of two beds; the Alpha mud-rich facies and the Alpha grainstone facies (Fig. 3). The Alpha mud-rich carbonate is 15–56 cm thick. It consists of wackestone with intermixed wackestone and lime mudstone, and in a few places, packstone. The Alpha grainstone is the most productive interval in the Pen field. It is 0–1.8 m thick and consists of oolitic grainstone in the southwestern part of the field, whereas in the northeastern part, skeletal or peloidal grainstone in the lower one-third is overlain by grainstones in which oolites are a principal if not predominant allochem.

Capping Facies.—The uppermost unit of the upper carbonate of the "J" zone is called the cap or capping unit. It is present in almost every well in the area, contains a variety of lithologies, and is as much as 0.6 m thick in the Pen field.

Upper "J" Shale

The uppermost unit of the "J" interval is variegated, calcareous, silty shale that is 0.6–2.7 m thick. This unit contains blackened clasts of limestone, but no fossils. Generally, it has a basal medium-green bed that averages 0.3 m, but is as much as 0.9 m thick, a thicker brick-red to maroon middle bed, and an upper green bed that is ≤ 0.3 m thick and commonly absent. In some places, contacts between these beds are mottled, and mottling is present within both the green and red parts of the shale unit.

Deposition of the "J" Zone

Limestones of the "J" zone accumulated on a shallow-marine shelf in generally oxygenated water. Micrite-rich lithologies accumulated in less-agitated water than grainstones, especially the oolitic Alpha grainstone. Microkarst, root molds, rhizoliths, and autoclastic breccia in the cap unit indicate subaerial exposure after accumulation of the Alpha grainstone but before deposition of the upper shale of the "J" zone.

The "J" zone superficially resembles the ideal cyclothem (Table 1; Heckel, 1977, 1985): a thin limestone (at the base), a thin shale, a thicker limestone, with an exposure surface, and then a shale (at the top) separating the "J" zone from the basal transgressive limestone of overlying "I" zone. However, the "J" zone differs from the ideal cyclothem in detail: abundant *Osagia*-coated grains in the upper part of the lower carbonate indicate clear, shallow water, not the increasing turbidity and depth of water expected during formation of transgressive limestones in cyclothem (Watney, 1980; Heckel, 1983). The "J" lower shale in the Pen field is not the black, phosphatic shale found in many cyclothem, but a dark-green to dark-gray silty shale with brachiopods, apparently a normal-marine shale that may have formed in shallow water.

The "I" Zone

The "I" zone is thinner than the "J" zone, ranging from 2.4 to 4.1 m thick, and contains only a carbonate unit and an overlying shale. The carbonate unit ranges from 0.8 to 2.4 m thick and is cream, light-gray, or light- to medium-brown. It contains a suite of allochems like that in the "J" zone, but with a greater abundance of *Osagia*-coated grains and coated grains. The lithology varies from place to place, but generally the lower part is coarser than the upper. The "I" carbonate is normally a muddy lithology—either a carbonate mudstone or wackestone. Patches of grainstone do occur in the lower part, and, rarely, mixed wackestone-packstone is present in the upper part. It ranges from carbonate mudstone to grainstone at the base. Rarely a mixed wackestone-

TABLE 1. — BEDS IN THE IDEAL CYCLOTHEM
(after Heckel, 1977,1985)

Unit name	Description	Interpretation
4. Outside shale	Shale, gray or variegated, with siltstone or sandstone units or clay. Replaces the top of the regressive limestone or lies between the regressive limestone and the base of the overlying transgressive limestone of the next cycle. Thickness variable.	Marine or continental deposits that accumulated where fluvial or deltaic systems contributed sediment or where paleosols formed during exposure between regression and the subsequent transgression.
3. Regressive limestone	Normal marine limestone, lime mudstone, commonly overlain by packstones, grainstones, or phyloid algal mound rocks, and then by laminated or fine-grained stromatolitic limestone. Forms the major limestone bed of the cyclothem. Up to 5 m thick commonly and may reach a few tens of meters where algal banks are developed.	Normal marine limestone deposited while sea level is steady or falling. Lithology indicates gradation from lower to higher energy then to sub-aerial exposure during deposition. Upper part may be cut out by outside shales.
2. Core shale	Black, fissile, phosphatic shale with a high content of uranium that makes it show clearly on a gamma-ray log. Core shales may also be dark-gray, nonfissile, nonphosphatic shales or simply gray marine shale. Generally <1 m thick.	Deposited in deeper water than transgressive limestones, perhaps at extreme of transgression or while sea level rose.
1. Transgressive limestone	Packstone, wackestone, or lime mudstone, normal marine fossils. Generally ≤1 m thick.	Normal shelf carbonate deposited during rising sea level. Transgressive lag in part.

packstone occurs at the top. "I" zone grainstone is the second-most productive reservoir in the Pen field.

The upper part of the "I" carbonate is an autoclastic breccia with shale filling the fissures. It grades into the lower part of the "I" shale, which contains angular carbonate clasts in a shale matrix. The "I" shale unit is 1.5–2.3 m thick, consists of red or green shale, and contains a few carbonized plant fragments.

The top of the "I" carbonate unit exhibits numerous features that indicate subaerial exposure: autoclastic breccia, microkarst, circumgranular cracks, alveolar structures, glaebules, root molds, and rhizocretions. The middle portion of the "I" shale unit also contains an alteration horizon with evidence of subaerial exposure, namely root traces and calcrete nodules. These two alteration zones apparently represent separate paleosol horizons because they are separated by several feet of unaltered shale.

DIAGENESIS AND POROSITY HISTORY IN GRAINSTONES

Diagenesis of the rocks of the Pen field took place (1) shortly after deposition, in marine, brackish, and fresh waters as sea-level fluctuations changed environmental conditions drastically and

(2) during and after burial (Fig. 4). Diagenesis in the period shortly after deposition led to dissolution of allochems, cementation, recrystallization of fabric elements, and paleosol formation. These processes affected each major bed of limestone ("I", "J", etc.), after its own deposition and before deposition of the next unit, so that results of diagenesis differ somewhat from bed to bed. Diagenesis during and after burial led to fracturing, cementation, and dissolution. These processes affected the entire sequence at the same time, so that the effects are generally the same in all beds, although the extent of their results may differ from bed to bed. Diagenesis is described completely in Phares (1991).

Cementation During Exposure

The earliest cements differ from bed to bed, but formed in marine or mixing-zone environments. The cements are generally isopachous and occur in either primary pores or in molds formed by dissolution of allochems. Marine cements are isopachous but fibrous and cloudy, suggesting they replaced earlier aragonitic or Mg-calcite cement. Mixing-zone cement is indicated by the presence of one-phase, all-liquid brackish fluid inclusions (Phares, 1991). This phase of cementation post-dates significant dissolution of allochems and may

PARAGENESIS OF PRE- AND SYN-EXPOSURE DIA GENESIS, "I" AND "J" ZONES, PEN FIELD, GRAHAM COUNTY, KANSAS

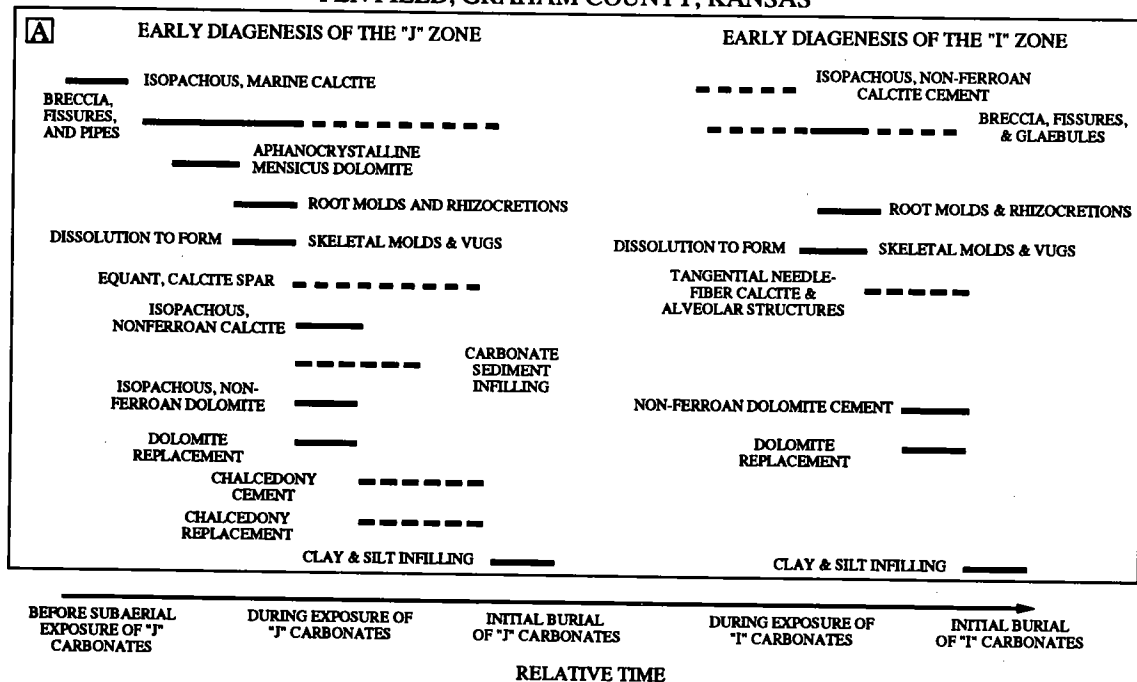
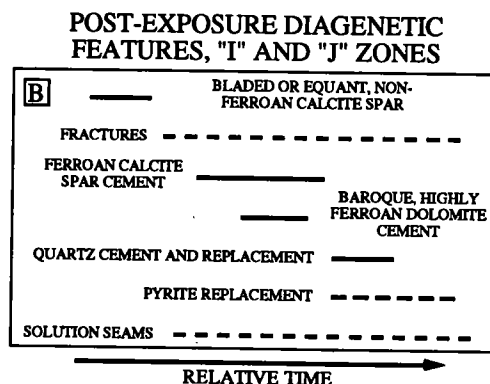


Figure 4. Diagenetic paragenesis of cements, dissolution, and fracturing in the "I" and "J" zones of the Pen field. A—Diagenetic events from immediately after deposition until the beginning of burial of each layer. While the "J" and "I" zones underwent similar effects, they underwent them successively, as each layer was first deposited, then exposed to subaerial weathering. B—Diagenesis during burial phase. Both units experienced roughly the same effects at the same time.



have formed during a period of exposure before the next cycle of deposition.

One of these early cements in particular, referred to as cement J1, a nonferroan, isopachous, cloudy, finely bladed marine calcite, partially to completely occludes pores in the "J" Alpha grainstone. In some areas (see section on "Decline of Pressures with Time"), this cement has rendered the Alpha grainstone impermeable; it is the only cement that demonstrably converts this grainstone to nonreservoir rock. Most interparticle pores remained open at the end of this initial phase of diagenesis.

The upper part of the "J" and "I" zones both display convincing evidence of exposure and soil-forming processes. At the macroscopic level, the

upper part of each zone displays autoclastic brecciation, infiltration of clay-sized material similar to that in the overlying shale, fissures (planar cracks 0.5–4 cm wide), pipes (cylindrical, vertical structures 1–3 cm in diameter), root molds, and rhizocretions. Microscopically, one can observe circumgranular cracks, alveolar structures, glaebules, skeletal molds, oomolds, vugs, meniscus dolomite cement and scattered dolomite crystals in paleosol fissures, tangential needle-fiber cement, and infiltrated quartz silt.

Exposure of carbonate beds created paleosols. These effects are most pronounced at the top of grainstones or overlying them, forming the capping layers with drastically different reservoir properties than the underlying grainstones. Gen-

erally, paleosols are nonporous, impermeable, and not saturated with oil; they form part of the seal. The effects of paleosol formation were greater in the "I" zone than in the "J" zone; "I" zone effects reach through the entire "I" zone to the top of the "J" upper shale in one core. However, in a few areas most primary pores in the grainstones and secondary pores in cap-facies rocks remained open after exposure. In a few wells, the cap of the "J" upper carbonate has oil in vugs and molds and may contribute a minor amount to production.

Post-Exposure Diagenesis

After exposure and subsequent burial, diagenetic events took place that were either parochial to one layer or widespread through the vertical section. These include several generations of calcite cement, separated by fracturing events and differing in their concentration of iron, as well as precipitation of highly ferroan dolomite, quartz, and pyrite. The last event was formation of numerous stylolites, microstylolite swarms, and clay seams. The cements, fractures, and pressure-solution features seem to have left many primary and secondary pores open and have had little effect on reservoir quality.

PRODUCTION FROM THE PEN FIELD

Optimizing oil production requires knowledge of the degree and type of heterogeneity in the reservoir. Reservoirs may be subdivided into compartments that each must be intersected by a well, or, for waterflooding, must contain both an injecting and a producing well. Conversely, reservoirs may have fractures or permeability streaks that drain quickly or channel injected fluids into only a fraction of the rock. At the other extreme, reservoirs can be homogeneous. In any case, the extent of the interconnected porosity should be established as soon as possible in the history of production.

In the Alpha grainstone of the "J" zone, which is the most productive zone of the Pen field, the pores are primary and production is roughly coextensive with grainstone development, although early diagenesis has rendered some of the grainstone nonproductive. Depositional effects and diagenetic modification of porosity have made the "I" zone reservoir discontinuous and heterogeneous.

Decline of Pressures with Time

Drill-stem tests sampling the "J" alpha grainstone interval were run on most of the wells in the Pen field. With two exceptions, the tests show a marked pattern: points on a plot of reservoir pressure vs. cumulative production as of the date of the test define two lines (Fig. 5). The first four tests

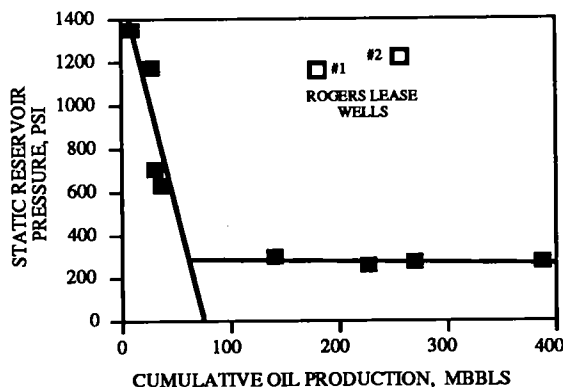


Figure 5. Decline of reservoir pressure with production, as determined by drill-stem tests of the "J" Alpha grainstone. Most of the productive wells show an orderly pattern with a sharp early decline converting to a slower decline at a pressure of ~285 PSI and after production of only ~63,000 bbl of oil. The two outlying wells (Rogers no. 1 and no. 2) are in more cemented portions of the "J" Alpha grainstone.

show a rapid, and nearly linear, decline from an initial pressure of 1,342 psi. Four of the subsequent tests show a slower, but still linear, decline. These linear trends intersect at a value of ~285 psi and only 63,000 bbl of production. The first linear trend is interpreted as representing fluid-expansion drive, the second one as solution-gas drive, which began when the bubble point of ~285 psi was reached. The second trend extends to production of 400,000 bbls. The tests show a high degree of communication throughout the grainstone interval, so that fluid withdrawals from the early wells reduced pressure everywhere. These results imply that the "J" zone reservoir has no significant internal barriers to flow (Fig. 6A,B) and can be treated as a single unit in enhanced-recovery operations.

While most drill-stem tests show a clear relationship between reservoir pressure and cumulative production, tests from two wells do not (Fig. 5). The two wells, the Rogers no. 1 and no. 2, are in the southwestern part of the field (Fig. 6B). The "J" zone Alpha grainstone in these wells was porous, but it was impermeable and the wells were not commercial. Their high pressures late in the production history (Fig. 5) indicate that they are not connected to the reservoir in the Alpha grainstone. In cores from these wells, interparticle spaces in the Alpha grainstone are almost completely filled with J1 cement, rendering the rock impermeable, although subsequently formed molds give the rock as much as 11% core and log porosity. The J1 isopachous early marine calcite cement (Fig. 4) is present throughout much of the Alpha grainstone, but generally does not reduce permeability to non-commercial levels.

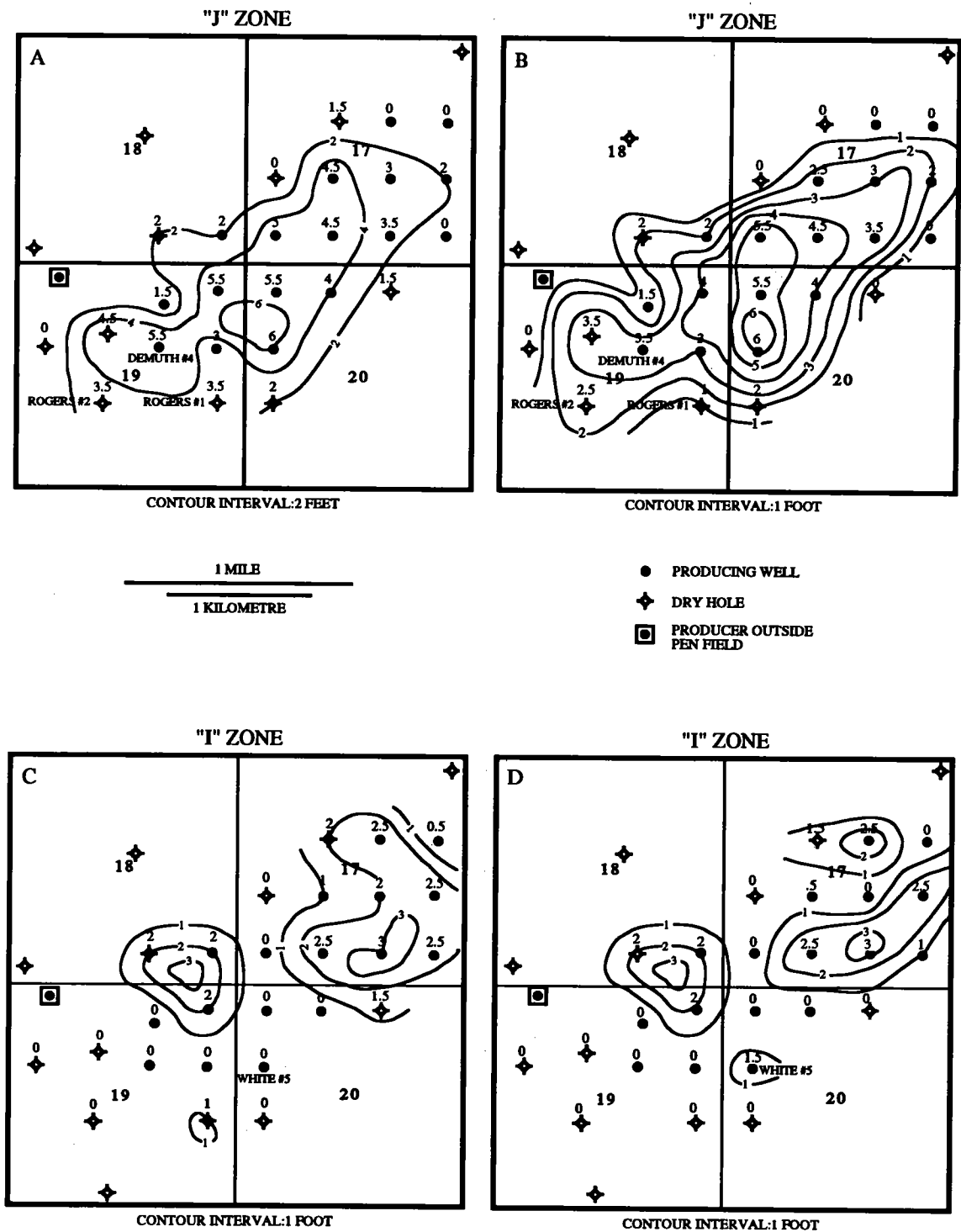


Figure 6. A—Isopach map of the "J" Alpha grainstone in the Pen field. The Rogers no. 1 and no. 2 wells are the southernmost wells in the field. B—Net pay isopach of the "J" Alpha grainstone in the Pen field. C—Isopach map of the "I" grainstone. D—Net pay map of the "I" carbonate shows four separate areas of production and three separate lenses of grainstone; one grainstone lens is unproductive, one is divided in two by an impermeable area, and one well (White no. 5) produces from a porous wackestone.

In addition to the nonproductive wells on the Rogers lease, the adjacent Demuth no. 4 well has had very low productivity, only 2% of the estimated oil originally present in the Alpha grainstone if the well was effectively draining 40 acres (Phares, 1991). The low permeability area on the Rogers lease may extend into the 40 acres that the Demuth no. 4 well is assumed to drain, reducing its production potential.

"I" Zone Production

In contrast to the "J" zone, production from the "I" zone comes from four separate areas (Fig. 6C,D). A single, isolated well, the White no. 5 in the southern part of the field, produces from a porous wackestone; the other three areas are in two separate lobes of grainstone. The easternmost lobe (Fig. 6C) is divided into two parts (Fig. 6D) by tightly cemented, impermeable rock. The four compartments shown on the I zone net pay map (Fig. 6D) were mapped from the available log and core data, but it is possible that they are even further subdivided.

Reservoir Characterization

In all reservoir characterization, one must provide information on areas between wells by converting qualitative geological description to quantitative values that are useful in modeling. Important features to characterize include porosity, permeability, and fluid saturations. In the Pen field, the main reservoirs are the Alpha grainstone of the "J" zone and the "I" grainstones. Together, these units contained 75% of the OOIP. Our efforts at characterization concentrated on them. These two zones differ in lithology, in the effects on them of early diagenesis, and in their degree of internal compartmentalization.

Relations Among Porosity, Permeability, and Water Saturation

Porosity and permeability were measured on 11 cores by commercial laboratories (Phares, 1991). Most measurements were whole-core values, although some were only core-plug values. Since most of the data were from the Alpha grainstone, the first estimation of the relationship between permeability and porosity was made using data for the main reservoir. For the Alpha grainstone:

$$\text{Log Permeability (md)} = 0.069 \times \text{Porosity (\%)} + 0.793 \quad (1)$$

based on 19 acceptable measurements of maximum horizontal permeability (Phares, 1991). The low coefficient (0.069) shows that in the Alpha grainstone, permeability increases slowly with increasing porosity. Similar equations were calcu-

lated for other reservoir intervals, although they were based on fewer measurements.

For the most part, permeability values calculated from drill-stem tests did not match permeability measurements on cores. It could not be determined if the differences arose from differences in vertical averaging, aerial averaging, or relative-permeability effects. Furthermore, porosities derived from well logs correlated well with those from core measurements (Fig. 7), even though both represent different volume-averaging procedures. For the sake of uniformity, log porosities were used in the reservoir characterization.

Permeability values derived from porosity values calculated from neutron and density logs and the relation in equation 1 were used to assign permeability to wells in the field. A permeability of 1 md was accepted as the lower limit for a productive reservoir. Core measurements indicate that rocks with a porosity of $\leq 7\%$ had < 1 md of permeability.

Water-saturation calculations employ resistivity measurements by tools that have a vertical resolution on the order of 5 ft. In the Pen field, only in beds ≥ 3 ft thick were calculated water-saturation values consistent with oil shows from saturated cores, drill-stem tests, and production tests. Water-saturation values calculated by the Archie method for reservoir intervals within 1 ft of shale or tight limestone could not be used.

Water saturation is related to the logarithm of permeability for a particular field (Amyx and others, 1960, p. 152). Using porosity as the proxy for the logarithm of permeability (equation 1), and wire-line log values for water saturation and porosity, the following empirical equation describes water saturation in the Alpha grainstone (Phares, 1991):

$$S_w = \left(\frac{5.59}{\phi} - 0.126 \right) \times 100 \quad (2)$$

Values calculated from equation 2 were closely consistent with core and test results where the reservoir is < 3 ft thick. Similar equations were constructed for other reservoir horizons in the field and used to assign water-saturation values to grid blocks close to upper and lower boundaries of reservoir beds.

Grid Blocks

The Pen field was divided into 4.44-acre grid blocks for the purpose of simulation. The field is developed on a 40-acre spacing, and, during discussions with the engineering staff, it was decided to have each well at the center of a grid block and two grid blocks between each pair of wells; a total of nine grid blocks per well-spacing unit, with minor deviations (Fig. 8). Because porosity, permeability, and fluid-saturation data were available at 1-ft intervals from cored wells and logs, grid-block

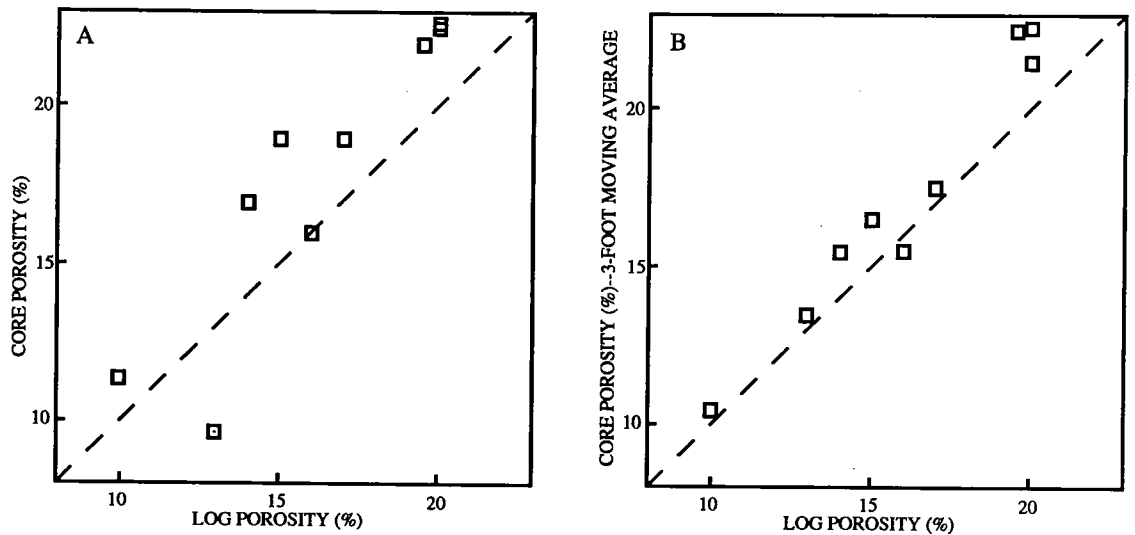


Figure 7. Correlation of porosity derived from well logs with that derived from core measurements. A—Single core measurements are plotted against log measurements for the same foot. B—Three-foot-centered moving averages of core measurements are plotted against well-log measurements, improving correlation over A. The diagonal dashed line is not a correlation line, but a 1:1 slope, along which the data should plot.

thickness was set at 1 ft in reservoir zones, with an impermeable layer, one grid-block thick, separating reservoir horizons.

Mapping Grainstone

Net-pay maps for the Alpha grainstone and other reservoir intervals were constructed using core or log thicknesses for porous intervals and contoured using geological insight (Fig. 6B,D). The log suites available for the Pen field were useful in recognizing and quantifying porosity, calculating water saturation, and identifying lithologic units to trace across the field. They do not provide a basis for differentiating nonporous wackestone or mudstone from nonporous grainstone and packstone, or a basis for differentiating porous grainstone from porous wackestone or mudstone. Consequently, where cores were absent, identification of subtypes of limestone was not possible. Maps of grainstone thickness (Fig. 6A,C) may include areas where numerous vugs and molds form pores in fine-grained limestone and exclude areas where pore-filling cement has reduced the porosity and apparent thickness of grainstone. However, the geological study indicates these occurrences would probably result in only minor errors in predicted recovery.

Values of porosity, permeability, and water saturation were then assigned to each foot of pay in the Alpha grainstone and other reservoir intervals in each grid block, based on linear interpolation between wells (Fig. 9). These grid values, the thickness of productive intervals, and the extent of

drainage areas were modified using information on the productivity of individual wells as compared to the amount of oil that was estimated to be present (Phares, 1991).

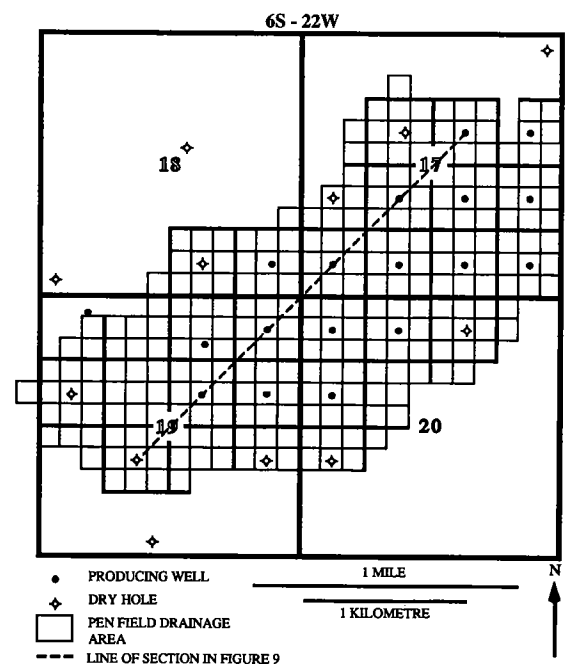
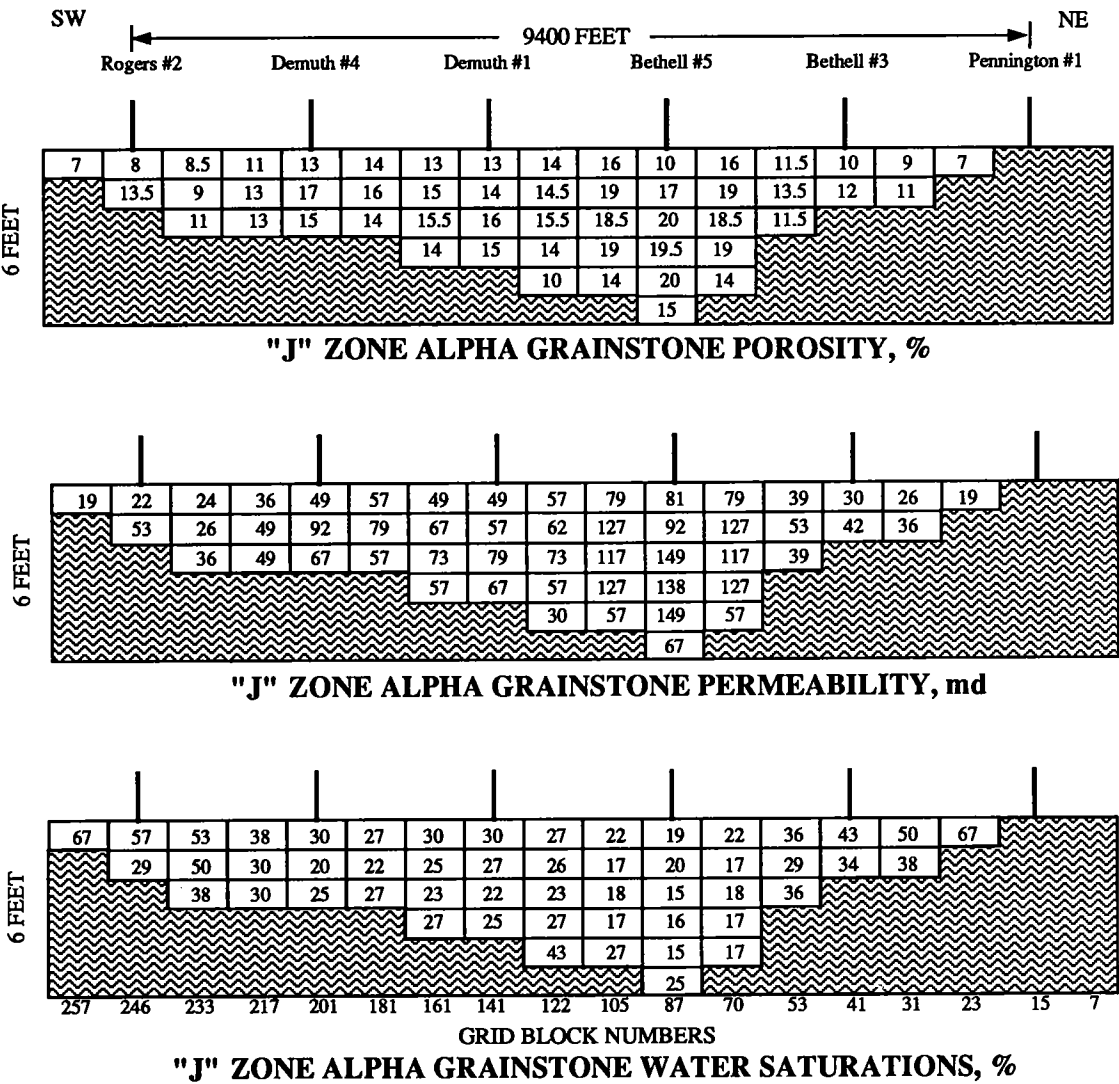


Figure 8. Grid blocks for use in characterizing the Pen field.

SUMMARY

Our object in studying the Pen field was to develop a geological model of the reservoir for use in history matching and predictive modeling of production of the field. The results provide direct data or estimates of thickness, porosity, permeability, and fluid saturation for all of the 4.44-acre grid blocks, both those centering on wells and those between them.

The understanding of stratigraphy and lithology of the Pen field came from studies of cores and interpretation of wire-line logs. The field consists of several separate reservoirs, the "D," "I," "J," "K," and "L" zones of the Lansing-Kansas City interval. Most reservoir rock is carbonate grainstone with primary interparticle porosity preserved. Some oil is produced from vuggy and moldic porosity in matrix-rich limestones. The main reservoir is in the Alpha grainstone of the "J" zone. Mi-



SECTION DATUM: TOP OF PRODUCTIVE "J" ALPHA GRAINSTONE. LINE OF SECTION IN FIGURE 8

Figure 9. Northeast-southwest grid block cross section of the Pen field, showing values of porosity, permeability, and fluid saturation assigned to individual grid blocks at and between wells. Net-pay thickness of "J" Alpha grainstone is based upon contour maps (Fig. 6B). Porosity is derived from log values and interpolated from nearby wells, with some geological modification. Permeability and water saturation is calculated from correlations of these quantities with porosity.

nor production is from two other horizons in the "J" zone.

Pressure data from drill-stem tests show that the Alpha grainstone is a single, continuous reservoir roughly coextensive with grainstone development. Grainstones of the "I" zone formed in three separate pods in the field area, and one of the pods was divided by an impermeable area, possibly the result of diagenetic cementation, into two separate reservoirs.

Petrographic studies of the "I" and "J" zones show that diagenesis began with early marine and brackish-water cementation of the rocks, followed by an episode of diagenesis and paleosol formations during exposure and before deposition of rocks of the next overlying zone. This paleosol formation is most intense at the top of carbonate beds. Finally, diagenesis after the period of exposure led to formation of cement, fracturing, and dissolution that affected both I and J zones similarly. Only the early marine to brackish-water cements had an extensive effect on production; however, the paleosols may have rendered earlier grainstone unrecognizable, and they do form part of the seal.

Thickness of each reservoir horizon was established by contouring the thicknesses at each well. Porosity, permeability, and fluid saturations at each well were derived from measurements on cores, log calculations, or both. Permeability, porosity, and water saturations were interpolated to give values in grid blocks between wells. Values of thickness, porosity, permeability, and water saturations were adjusted in a minor way by considering the fraction of available oil that was recovered from each well during the life of the field.

DISCUSSION

Data available for the Pen field include wire-line logs, cores, drill-stem test results, measurements of porosity and permeability, and production records. In characterizing the reservoirs, each source provided useful information, and the final results were reached only through combining them all. Cores provide stratigraphic, lithologic, and petrographic information, so that the nature of the reservoir rock is well known. Whole-core measurements of porosity and permeability provide the baseline for interpreting permeability from porosity calculated from wire-line logs and water saturations for thin reservoir beds and for those portions of reservoir intervals where the logs averaged dissimilar underlying or overlying beds. This combination of data from several sources was necessary to provide the comprehensive assignment of values to the data grid for the Pen field. The drill-stem test results provided pressures and demonstrated the interconnection of the Alpha grainstone across the field. Well-by-well monthly

production data will be used to provide the basis for history matching and predicting future recovery.

Some preliminary results on the utility of the various kinds of data are available from this phase of the project. The extensive work done on porosity history through examining thin sections and developing a diagenetic history was interesting, but was less revealing of the production potential than drill-stem tests. The drill-stem tests would have been even more useful for this purpose if each had been restricted to a single zone in the tests covering the minor pay intervals.

Cores, despite their small impact in understanding interconnections in the field, did have an important utility as a source of measurements of porosity and permeability; the relationship between these petrophysical properties was used to estimate permeability and water saturation from porosity in wells where no core was available. Unless a reliable relationship between porosity and permeability is discovered and found applicable to all reservoirs of a certain type, some cores are a necessary part of any complete characterization of any oil field. The log suites, including both resistivity measurements for water saturation and density and neutron measurements for porosity, are also necessary.

Using the combination of measured, calculated, and inferred information, and well-by-well production data over the life of the field, engineers with the Tertiary Oil Recovery Project of the University of Kansas are now conducting model simulations of the Pen field to match the existing history and to predict response to the waterflood that was recently installed. When this project is completed, the results will show whether, with this extensive suite of data, a meaningful simulation of a Lansing-Kansas City grainstone reservoir is possible. The results will also show which of the data are most important, so that operators can decide how to invest their money at the beginning phase of the development of an oil field.

CONCLUSION

Each type of information provided a necessary component of the whole picture. It is apparent that there was a redundancy of core information for the Pen field, that the log suite was appropriate, and that zone-by-zone drill-stem tests, rather than the commingled tests, would be very useful in characterizing the reservoirs.

ACKNOWLEDGMENTS

This research was supported by the Tertiary Oil Recovery Project (TORP) of the University of Kansas. The field was brought to our attention by Lynn Watney of the Kansas Geological Survey. Pan-

Canadian Petroleum Co. provided cores, logs, and data on completion and production for the wells. David Pauley continued this support after he assumed operation of the field. Randy Kodele discussed various aspects of the operation of the field. Paul Willhite and Gary Gould of TORP helped focus the study on the relevant issues for enhancing production.

REFERENCES CITED

- Amyx, J. M.; Bass, D. M., Jr.; and Whiting, R. L., 1960, Petroleum reservoir engineering, physical properties: McGraw-Hill, New York, 610 p.
- Heckel, P. H., 1977, Origin of phosphatic black shale facies in the Pennsylvanian cyclothems of Midcontinent North America: American Association of Petroleum Geologists Bulletin, v. 61, p. 1045–1068.
- _____, 1983, Diagenetic model for carbonate rocks in Midcontinent Pennsylvanian eustatic cyclothems: Journal of Sedimentary Petrology, v. 53, p. 730–759.
- _____, 1985, Current view of Midcontinent Pennsylvanian cyclothems: Society of Economic Paleontologists and Mineralogists, Midcontinent Section, Proceedings of Third Annual Meeting and Field Conference, p. 1–22.
- Moore, R. C., 1936, Stratigraphic classification of the Pennsylvanian rocks of Kansas: Kansas Geological Survey Bulletin 22, 256 p.
- _____, 1949, Stratigraphic classification of Pennsylvanian System in Kansas: Kansas Geological Survey Bulletin 83, 203 p.
- Morgan, J. V., 1952, Correlation of radioactive logs of the Lansing and Kansas City Groups in central Kansas: Journal of Petroleum Technology, v. 4, p. 111–118.
- Phares, R. A., 1991, Characterization and reservoir performance of the Lansing–Kansas City “I” and “J” zones (Upper Pennsylvanian) in the Pen oil field, Graham County, Kansas: University of Kansas unpublished M.S. thesis, 262 p.
- Watney, W. L., 1980, Cyclic sedimentation of the Lansing–Kansas City Groups in northwestern Kansas and southwestern Nebraska: Kansas Geological Survey Bulletin 220, 70 p.
- Zeller, D. E. 1968, The stratigraphic succession in Kansas: Kansas Geological Survey Bulletin 189, 81 p.

Unusual Occurrence of Oil in the Viola Limestone, Pratt Anticline, Kansas

Harold A. Brown

Consultant Geologist
Wichita, Kansas

Alan D. Banta

Trans Pacific Oil Corp.
Wichita, Kansas

ABSTRACT.—Oil is produced from the Viola limestone on the flanks of the Pratt anticline from structural lows. The Viola reservoir rock thins sharply over a short distance to form these lows. The magnitude of thinning is ~55 ft (50% of normal thickness); it was caused by karstic processes which probably continued into Mississippian time. The thinnest Viola intervals consist almost entirely of residual chert, with significant amounts of chlorite. Porosity is ~17% and permeability is <6 md. The thickest Viola intervals are characterized by chert, recognizable fossils, fine-textured dolomite, and little chlorite. Porosity is in the range of 6%, or less, and permeability is much lower than in the thin residual-chert sections.

Formation water is produced with oil from most producing Viola wells. There is no identifiable water level within the Viola interval in the Jem field. The volume of produced water is apparently a function of capillarity and relative permeability to water.

Carbonate-rock dissolution and subsequent collapse of Viola chert was initiated along planes or surfaces that were more permeable than ambient rock. If these planes of higher permeability are due to fault or fracture planes, it cannot be demonstrated. There is no apparent vertical displacement on beds deeper than the Viola.

INTRODUCTION

The Pratt anticline is a broad, major tectonic feature that extends from the southern end of the central Kansas uplift. The long axis of the Pratt anticline extends south-southwest through central Pratt County, and gently plunges southward under north-central and northwestern Barber County (Fig. 1). Pennsylvanian rocks are in angular (very low-angle), unconformable contact with underlying pre-Pennsylvanian beds, the age of which varies with position on the flanks of the Pratt anticline. Oil and gas production has been found on the Pratt anticline in multiple pay zones in a variety of structural and stratigraphic traps. The most significant oil production is from pre-Pennsylvanian strata, ranging from the Arbuckle Group through Simpson, Viola, and Mississippian rocks.

The Jem field underlies parts of secs. 28, 32, and 33, T. 29 S., R. 13 W., Pratt County, and parts of secs. 4, 5, and 8, T. 30 S., R. 13 W., Barber County (Fig. 1). The field has multiple pay zones, but the focus of this report is on unit 2, the lower cherty

dolomitic limestone member of the Viola Formation (Bornemann and others, 1982). Unusual aspects of this reservoir are that significant production from unit 2 is from low areas with no identifiable water level, and water produced from unit 2 in the Viola has no correlation with structural position. Most of the wells were artificially fracture-stimulated when completed, and all of the fractured wells produce water with oil. Five wells in the field were not fractured when completed, and four of these produce oil with no water. The volume of water produced is apparently a function of capillarity and relative permeability to water. Artificial fracturing does improve the transmissibility of all fluids, including water.

STRATIGRAPHY

Cross section A-A' (Fig. 2) extends west-east through the Jem field. The length of the cross section is ~0.75 mi. Logs of three wells producing from Viola unit 2 are in the center of the cross section. Here, the Viola is about half as thick as in the wells on each end of the cross section.

Brown, H. A.; and Banta, A. D., 1993, Unusual occurrence of oil in the Viola limestone, Pratt anticline, Kansas, *in* Johnson, K. S.; and Campbell, J. A. (eds.), Petroleum-reservoir geology in the southern Midcontinent, 1991 symposium: Oklahoma Geological Survey Circular 95, p. 104–112.

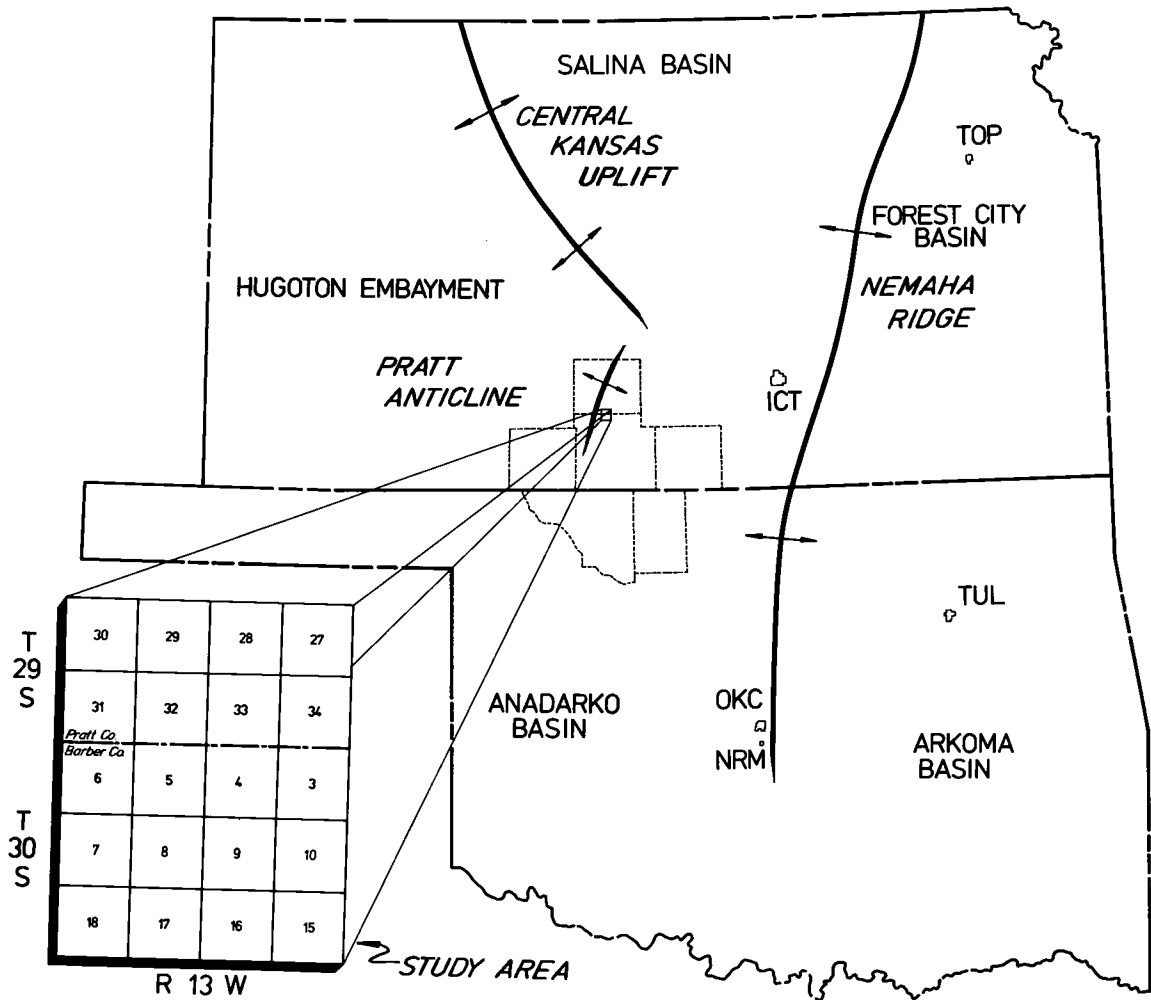


Figure 1. Map of Kansas and Oklahoma showing geological provinces, some major structures, and area covered by this study.

The thickest Viola intervals have very low porosity and permeability. Drill-stem tests in thick sections of unit 2 rarely recover formation fluid, and they record very low, if any, formation pressure. Thin Viola intervals are porous (as much as ~17%) and have permeability in the range of 3–6 md. Drill-stem tests here usually recover formation fluid, and they record bottom-hole pressures of ~1,500 psi.

Log signatures through the Viola interval can be correlated over considerable distances, regardless of Viola thickness. St. Clair (Bornemann and others, 1982) was able to subdivide the Viola in the area into four mappable units, which were informally named the basal limestone (unit 1), the lower cherty dolomitic limestone (unit 2), the upper limestone (unit 3), and the upper cherty dolomitic limestone (unit 4). Petrographic characteris-

tics and fossil content of the Viola are summarized graphically as a composite section in Figure 3.

A block diagram of the area (Fig. 4) shows the distribution of the Viola units 1–4. The various units are also shown on cross section A–A' (Fig. 2). Unit 4 at the top of the Viola is thin and can be identified in some of the wells.

The thickness of the underlying Simpson rocks is uniform. The abrupt thinning in the Viola can only be explained by either (1) rock removal after deposition, or (2) nondeposition. Because the log signatures of the Viola units are identifiable throughout the area, it is reasoned that the best explanation for the abrupt thinning is removal after deposition and subsequent bed collapse. The Viola underwent a long period of erosion accompanied by dissolution and removal of carbonate minerals. Insoluble residual chert is all that re-

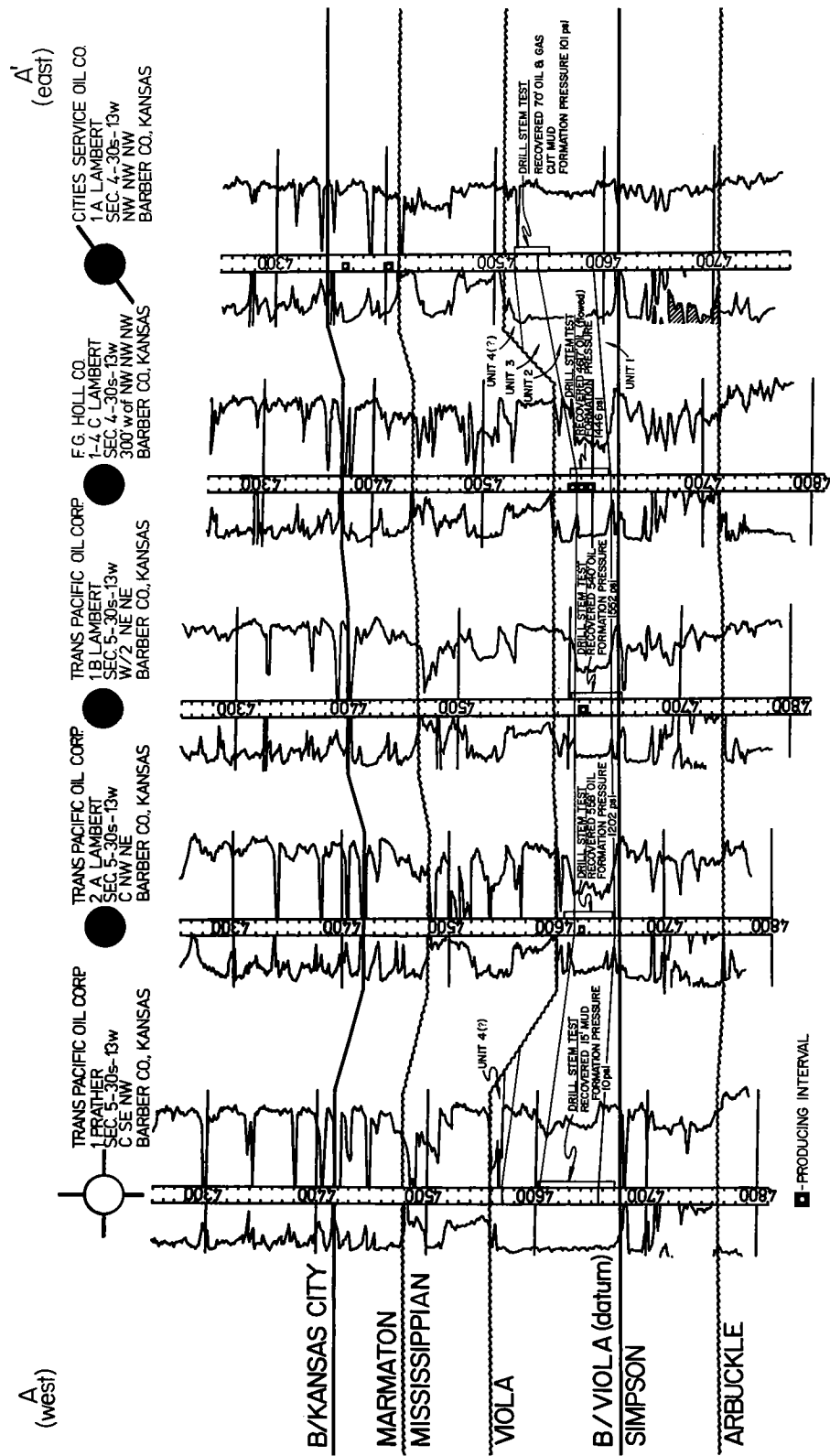


Figure 2. Stratigraphic cross section A-A', extending west-east through the Jem field. Datum is the base of the Viola.

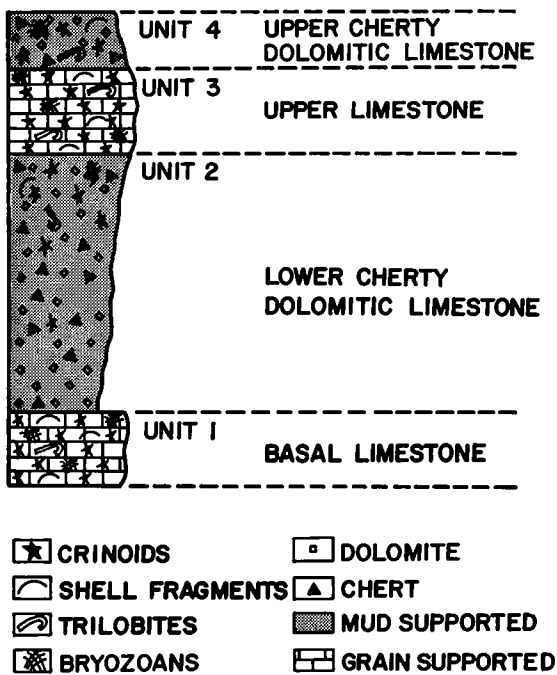


Figure 3. Generalized stratigraphic section of the Viola limestone in south-central Kansas (after Bornemann and others, 1982).

mains where the Viola is thinnest. In the thickest intervals, carbonate minerals were not dissolved. Consequently, effective porosity and permeability were not developed in the thickest interval.

Much of the interval labeled Mississippian in Figure 2 is detrital chert and other debris, which have been transported in to fill the topographic lows on the Viola surface. This accounts for the Mississippian rocks being thick above areas where the Viola is thin. The weight of these Mississippian sediments may have contributed to bed collapse in the Viola. The sag in the Pennsylvanian beds (Kansas City and Marmaton) above the thin Viola is probably due to compaction.

The thickness of the Viola is >100 ft (in places ≥120 ft) in most of the study area (Fig. 5). However, it thins abruptly to <60 ft in irregularly shaped, though generally long and narrow, areas. Wells producing only from unit 2 (shaded areas in Fig. 5) are confined to these thin intervals.

STRUCTURE

The structural configuration on top of the Viola (Fig. 6) clearly reveals that the wells producing oil from unit 2 are in low areas that have sharp boundaries and that coincide with areas where the Viola is thin (Fig. 5). Otherwise, dip on top of the Viola is uniformly gentle to the southwest.

Natural fractures within the Viola may have provided pathways for undersaturated water to enter and dissolve carbonate minerals after Viola deposition. However, no faults have been detected by vertical displacements of deeper beds. Dip on top of the Arbuckle (Fig. 7) is gently to the southwest; however, it is nearly horizontal under those areas where Viola unit 2 produces oil.

RESERVOIR PROPERTIES

Rock samples of Viola unit 2 from the Trans Pacific Oil Corp. no. 1 “B” Lambert, W½NE¼NE¼ sec. 5, T. 30 S., R. 31 W., and the Trans Pacific Oil Corp. no. 1 Prather, SE¼NW¼ sec. 5, T. 30 S., R. 31 W. (Fig. 2), were examined under the scanning electron microscope. The no. 1 “B” Lambert produces oil from unit 2. The vugs in this rock have an obvious rhombic shape (Fig. 8), which suggests that dolomite has been leached, leaving similarly shaped moldic pores. Vugs are apparently interconnected through a network of micropore space in a matrix of microcrystalline quartz. Chlorite and secondary quartz-overgrowth crystals are associated with the vugs. The no. 1 Prather penetrated a thick Viola section and is a dry hole. The sample from unit 2 of this well contains microcrystalline quartz with traces of chlorite and microcrystalline dolomite (Fig. 9). Rhombic dolomite crystals are present in this rock, and they show little evidence of dissolution by undersaturated water.

Permeability is low in the Viola limestone everywhere. There is, however, a ten-fold increase in

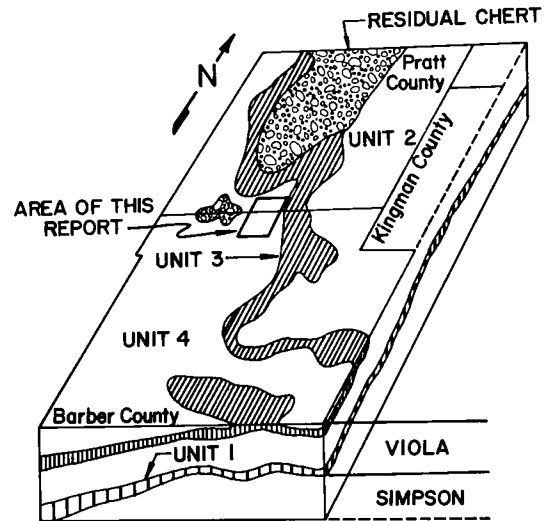


Figure 4. Block diagram of Pratt and Barber Counties showing the present distribution of the Viola subdivisions (after Bornemann and others, 1982). Upper surface of diagram represents the top of the Viola.

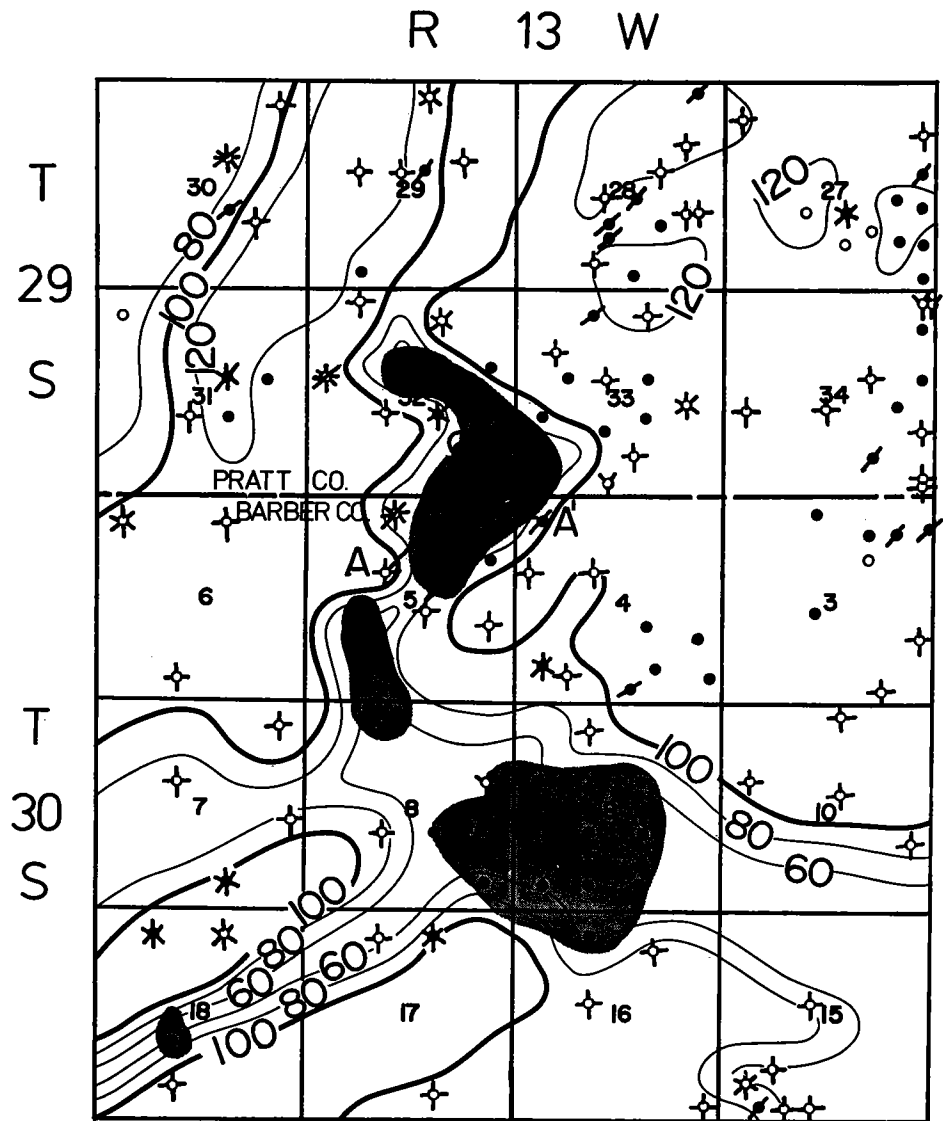


Figure 5. Isopach map of Viola limestone; contour interval is 20 ft. Wells producing from unit 2 are in shaded areas; all other wells produce from other zones.

permeability in thin residual-chert intervals. Computer-derived permeabilities from the open-hole log in the no. 1 "B" Lambert range from 3 to 6 md (Fig. 10) (R. H. Leeth, personal communication, 1991). This is significantly higher than compared to similarly derived permeability data in the no. 1 Prather, which has a maximum permeability of 0.6 md in unit 2 (Fig. 11).

American Energies Corp. drilled the no. 1 "C" Bell in the N½N½SW¼ sec. 5, T. 30 S., R. 13 W., and a drill-stem test recovered 3,600 ft of oil from unit 2. Bottom-hole pressure was 1,558 psi. Average permeability derived by the Horner method is 3.48 md, which is consistent with the above data.

Log-derived permeabilities and the results of drill-stem tests shown on cross section A-A' (Fig. 2) illustrate that significant differences in permeability are directly related to the thickness of Viola rocks.

ECONOMICS

Determining the amount of recoverable oil in place is always an estimate at best. The most accurate method is to measure the quantity of oil in the tanks after it has been produced. Using this method, one well producing from unit 2 has produced 100,000 bbl of oil. Based on cumulative-production data and current well performance,

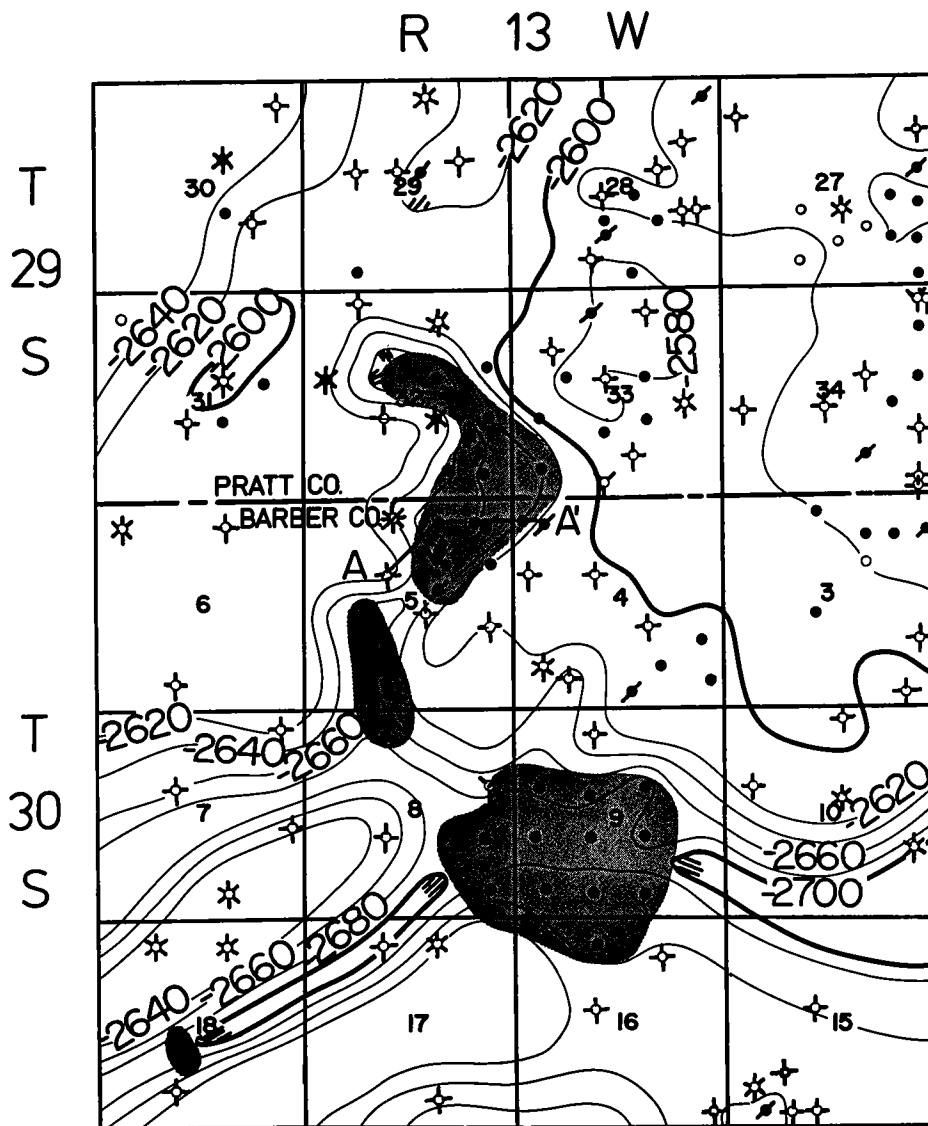


Figure 6. Structural contour map on top of Viola limestone; contour interval is 20 ft. Wells producing from unit 2 are shaded; all other wells produce from other zones.

perhaps no more than three wells will yield this amount. Most wells will yield about 30,000–40,000 bbl of oil. The wells producing from unit 2 in the Jem field have produced slightly more than 400,000 bbl of oil (Petroleum Information, 1990).

Larger fields in the area have been found, and others undoubtedly remain to be found. The Skinner field, discovered in 1944, underlies a large part of T. 31 S., R. 14 W. and part of T. 30 S., R. 13 W. The primary pay is the Viola, which has yielded >2,860,000 bbl of oil (Petroleum Information, 1990). The Skinner field apparently is producing under conditions similar to those described in this report. It awaits close examination.

CONCLUSIONS

1. Karstification is evident in the Viola limestone on the flanks of the Pratt anticline. Carbonate minerals were removed by dissolution after Viola deposition and prior to deposition of the overlying Mississippian clastics.
2. Sinkholes and caves, which later collapsed, are filled with insoluble residual chert. Thin, fractured, residual-chert intervals provide low, but adequate, permeability for oil entrapment.
3. Oil production occurs from areas of structural lows on top of the Viola. Formation water is produced with the oil regardless of elevation. Lat-

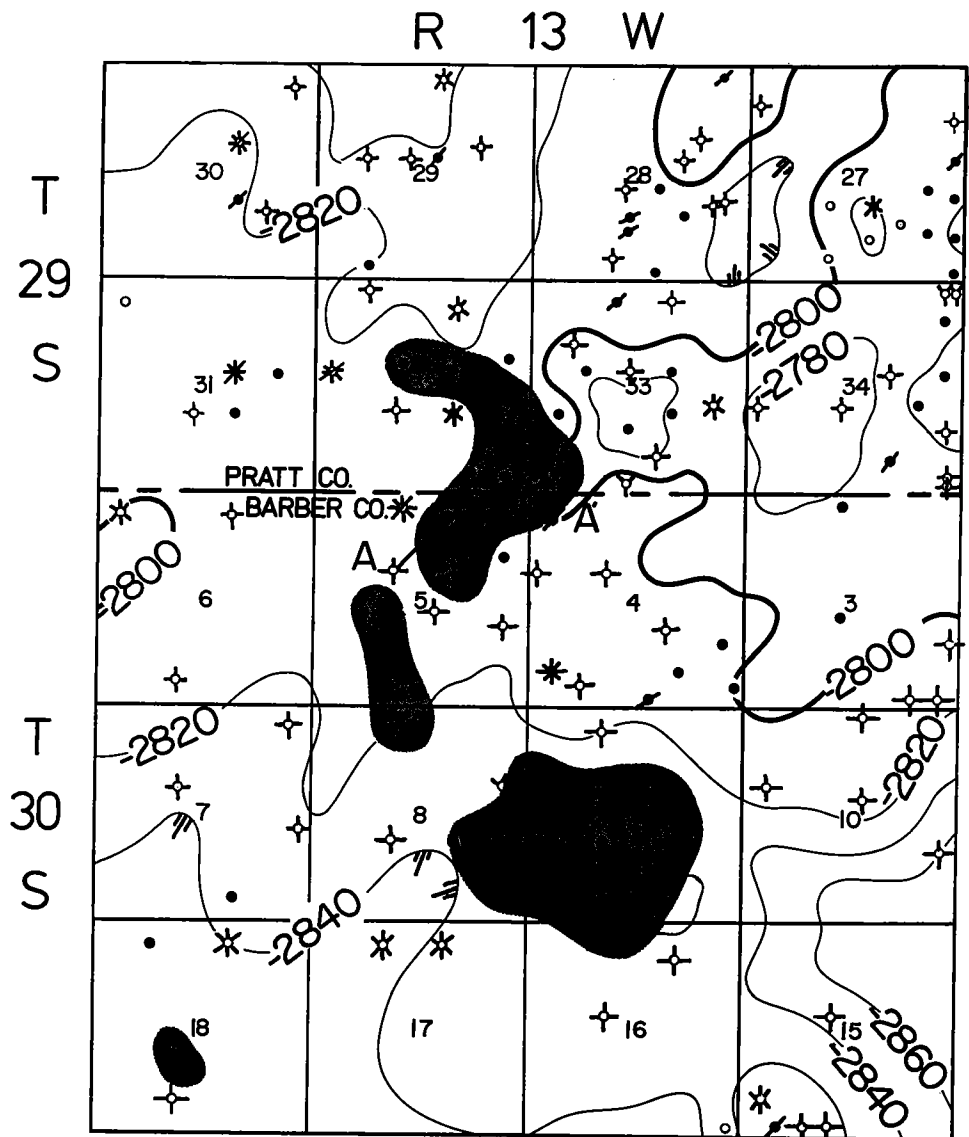


Figure 7. Structural contour map on top of Arbuckle limestone; contour interval is 20 ft. Wells producing from unit 2 are shaded; all other wells produce from other zones.

eral limits of a producing field are established by the limits of adequate permeability and porosity.

4. It is possible that natural fractures in the Viola controlled rock dissolution; this has not been established, however.

ACKNOWLEDGMENTS

Thanks are extended to Trans Pacific Oil Corporation for their generous support of money and resources in preparing this report. Halliburton Services provided the scanning electron micros-

copy. Richard H. Leeth did the computerized log calculations. Stephanie Wosylus prepared the art work for the exhibits.

REFERENCES CITED

Bornemann, E.; Doveton, J. H.; and St. Clair, P. N., 1982, Lithofacies analysis of the Viola limestone in south-central Kansas: Kansas Geological Survey Petrophysical Series No. 3, 44 p.
Petroleum Information, 1990, Kansas crude production report.



Figure 8. Scanning electron photomicrograph of Viola unit 2 from Trans Pacific Oil Corp. no. 1 "B" Lambert. Magnification is 1000x on left and 100x on right; white, 100-micron bar scale applies to photo on right. The rock has a matrix of microcrystalline quartz, with a light covering of chlorite clay and secondary quartz-overgrowth crystals. Only traces of dolomite are detected. Rhombic-shaped vugs are evident.

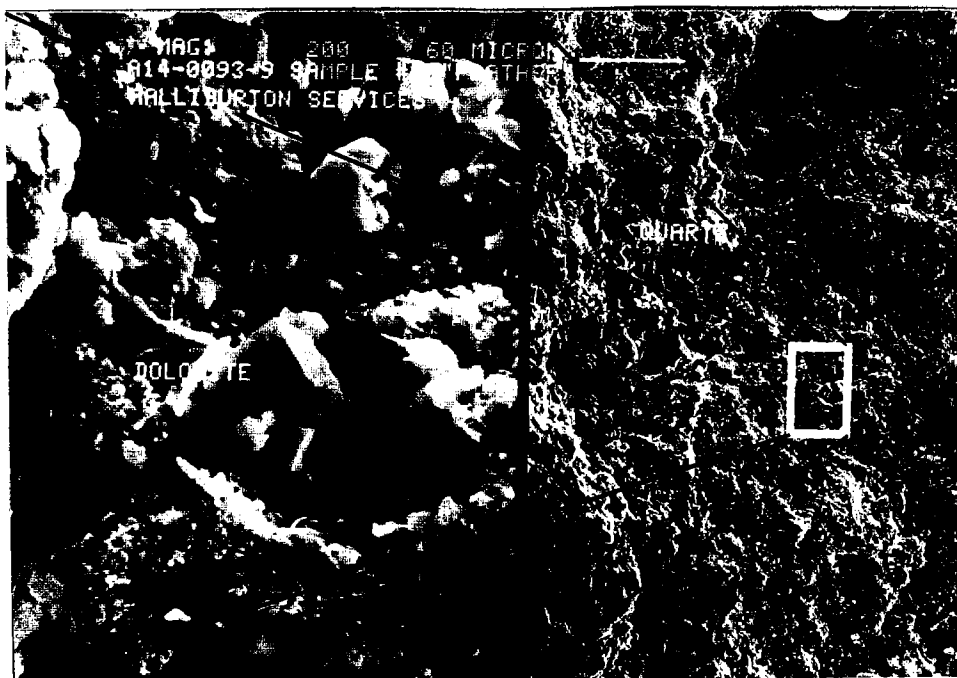


Figure 9. Scanning electron photomicrograph of Viola unit 2 from Trans Pacific Oil Corp. no. 1 Prather. Magnification is 2000x on left and 200x on right; white, 60-micron bar scale applies to photo on right. The rock has a matrix of microcrystalline dolomite. Very poor vuggy porosity is evident.

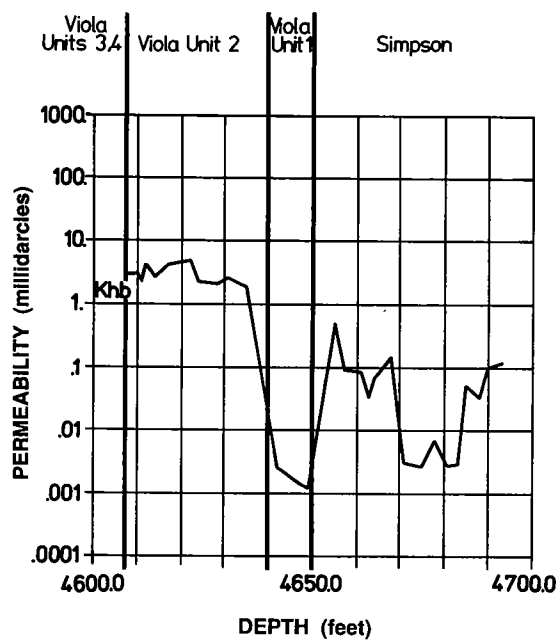


Figure 10. Computer-derived permeability from open-hole logs in no. 1 "B" Lambert. Permeability in Viola unit 2 ranges from about 3–6 md; note how low it is in unit 1 (modified from computerized log calculations by R. H. Leeth).

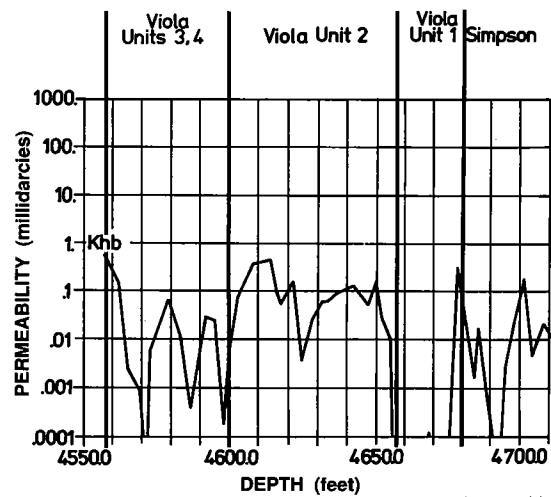


Figure 11. Computer-derived permeability from open-hole logs in no. 1 Prather. Maximum permeability in unit 2 is 0.6 md; note how low it is in units 1, 3, and 4 (modified from computerized log calculations by R. H. Leeth).

Geology and Reservoir Characteristics of the Arbuckle Brown Zone in the Cottonwood Creek Field, Carter County, Oklahoma

David L. Read

Consulting Geologist
Littleton, Colorado

Grant L. Richmond

CNG Producing Company
New Orleans, Louisiana

ABSTRACT.—Production rates of >4,000 BOPD and 3.0 MMCFGD were established from the Arbuckle Brown zone in November 1987 at CNG Producing Co.'s Cottonwood Creek 32-1 in the NW¼ of sec. 32, T. 4 S., R. 1 W. Data from 21 offset wells, including four deep penetrations in the field, indicate that production is from a northwest-southeast-oriented anticline which is overturned to the northeast and cut by a southwest-directed backthrust. Fourteen successful Brown zone wells define a productive area measuring 2.5 by 0.75 mi, covering 1,200 acres, and containing an oil column >900 ft.

The Brown zone is highly fractured, vuggy to cavernous dolomite that occurs within a 480-ft interval of the lower West Spring Creek/upper Kindblade Formations. It is composed of at least four types of dolomite. The earliest form is a mudstone-replacive dolomicrite/dolomicrospar. The second type is fine- to coarsely crystalline, xenotopic dolomite that replaced the original lime mud and dolomicrite constituents. The third type is fine- to medium-crystalline sucrosic dolomite. The fourth type, which fills or partially fills vugs and fractures, is subhedral to euhedral, saddle or baroque dolomite. Data from wells spaced as closely as one well to 40 acres indicate that the distribution of dolomite in the field is very erratic.

Early to Middle Pennsylvanian erosion removed as much as 800 ft of West Spring Creek from the anticline and karsted the Brown zone and the Kindblade to a depth of at least 1,500 ft below the pre-Pennsylvanian unconformity. Zones of cavernous porosity as thick as 24 ft were encountered in the Brown zone during drilling in the field.

Engineering data and geological descriptions have been integrated in order to quantify and better understand the Brown zone reservoir properties. Material balance calculations, derived from extensive pressure-volume-temperature (PVT) studies and periodic pressure measurements, have been compared to volumetric parameters to determine effective porosity. These calculations suggest the field originally contained >40 million bbl of oil-in-place. Using an estimated 353,000 gross acre-ft of section considered to be productive, an average effective porosity of ~3% was calculated for the Brown zone. Drawdown and pulse pressure tests have shown remarkable communication between wells. This communication is explained by the field's system of interconnected caverns, vugs, and fractures. Pressure buildup plots show a near-linear, gradual slope that suggests hydrocarbon feeding from the low permeability carbonate matrix into the fracture/karst system.

INTRODUCTION

Cottonwood Creek field is located in secs. 29–32 of T. 4 S., R. 1 W., ~11 mi west of Ardmore, Oklahoma (Fig. 1). CNG Producing Co.'s Cottonwood Creek no. 32-1 discovery, located in the NW¼ of sec. 32, spudded in October 1987. The well was

originally proposed as a 12,500-ft test of the Arbuckle West Spring Creek/Kindblade (Brown zone) and Cool Creek Formations on an undrilled, seismically defined closure on the north flank of the Criner–Wichita uplift. Between a depth of 8,327 and total depth of 8,351 ft, the well encountered 24 ft of cavernous Brown zone porosity

Read, D. L.; and Richmond, G. L., 1993, Geology and reservoir characteristics of the Arbuckle Brown zone in the Cottonwood Creek field, Carter County, Oklahoma, *in* Johnson, K. S.; and Campbell, J. A. (eds.), *Petroleum-reservoir geology in the southern Midcontinent*, 1991 symposium: Oklahoma Geological Survey Circular 95, p. 113–125.

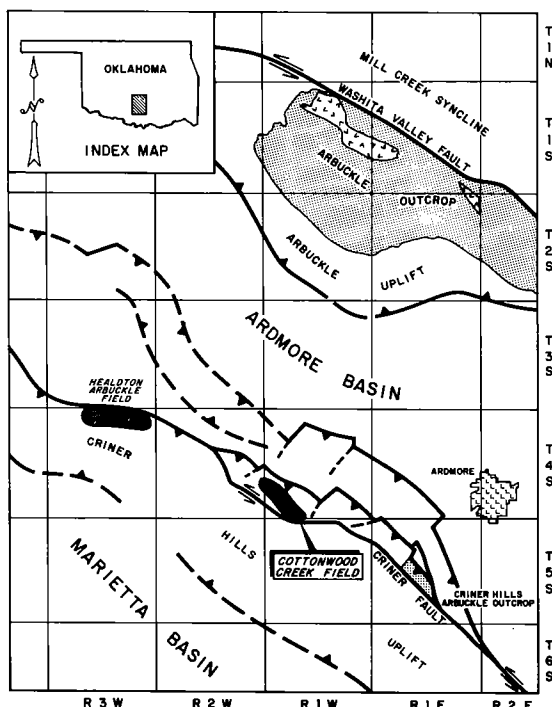


Figure 1. Generalized index map of the Cottonwood Creek and Ardmore basin areas.

which yielded hydrocarbon flow rates of >4,000 BOPD and 3.0 MMCFGD.

Through March 1991, 13 successful Brown zone offsets were completed in the field. Initial potential flow rates ranged 446–3,960 BOPD. Maximum daily field production peaked at 6,000 BOPD in March 1991. The field cumulative production through October 1992 was ~6.1 million bbl of oil.

The Cottonwood Creek discovery is one of the most recent in a long history of exploration successes in the Arbuckle Group carbonates and their stratigraphic counterparts. The Ellenburger (Arbuckle equivalent) in West Texas has produced >1.4 billion bbl of oil from karst porosity (Kerans, 1988). The Arbuckle on the Oklahoma shelf has been a prolific producer in the Cushing field in northwestern Creek County (Bennison, 1964), in the Oklahoma City field on the Nemaha uplift (Gatewood, 1970), and in numerous smaller pools in northeastern Oklahoma (Bloesch, 1964; Akin, 1964).

These Arbuckle shelf deposits are predominantly dolomite; they range from 500 ft thick in Creek, Tulsa, and Osage Counties to 3,500 ft thick in northern Garvin County. South of the Washita Valley fault in the Arbuckle Mountains and extending southward into the Ardmore/Marietta basins, the Arbuckle abruptly thickens to >8,000 ft and grades laterally into predominantly nonporous, dense limestone (Fay, 1989).

Historically, most explorationists considered the Arbuckle in this region to be an extremely high-risk, poorly understood and, therefore, undesirable primary reservoir objective due to a lack of predictable dolomite objectives. Nonetheless, prior to the Cottonwood Creek discovery, production data from a few fields in the region showed that the Arbuckle, where subregionally dolomitized and fractured, had the potential to yield both spectacular hydrocarbon flow rates and large reserves.

Most notable of these fields is Healdton, where deeper-pool production was first established from the Arbuckle Brown zone in 1960 (Latham, 1970). The Brown zone at Healdton field, which has produced >20 million bbl of oil, served as the reservoir analog during the development of CNG's Arbuckle play. The Cottonwood Creek oil discovery, with subsequent gas finds in the Wilburton field in Latimer County and in the N.E. Alden field in Caddo County (Carpenter and Evans, 1991), has sparked a reevaluation of the Arbuckle as a viable reservoir objective in the mature basins of southern Oklahoma.

STRATIGRAPHIC AND TECTONIC FRAMEWORK

During the early Paleozoic, the Cottonwood Creek area was located within the southern Oklahoma aulacogen (Wickham and others, 1975; Feinstein, 1981), a broad rapidly subsiding depocenter bounded on the north by the Washita Valley fault and on the south by the Muenster arch (Ham and others, 1964). The 8,000 ft of Cambrian–Ordovician Arbuckle strata deposited in the aulacogen (Fig. 2), consist almost entirely of storm-dominated cyclical subtidal- to supratidal-mudstones, intraclast calcarenites, oolitic calcarenites, stromatolites, and dolomitic limestones (Ham, 1969; Lindsay and Koskelin, 1991; Burgess, 1968). Thin-bedded anhydrite is also identified in the West Spring Creek both from drill samples at Healdton (Latham, 1970) and from regional analyses of neutron-formation density logs. From Middle Ordovician to Late Mississippian time, an additional 5,000 ft of sediments, represented by the Simpson through Caney, were deposited in the area of the present Criner Hills.

Two major episodes of Late Mississippian through Pennsylvanian orogenic activity divided the southern Oklahoma aulacogen into the complex series of northwest–southeast-trending uplifts and basins that characterize the region today (Tomlinson and McBee, 1959). In the Late Chesterian, rapid uplift and folding of the Criner Hills axis, documented by Ordovician limestone conglomerates in the lower Springer (Johnson and others, 1988, p. 330), separated the early Ardmore and Marietta basins. Uplift, erosion, and deposition of

thick clastic sequences into the Ardmore basin continued through the Morrowan and Atokan. Tectonism ceased locally during the Desmoinesian and Missourian, resulting in the subsidence and burial of the Criner uplift by transgressive marine shales, sands, and limestones.

By the beginning of the Virgilian, renewed tectonism uplifted the Arbuckle Mountains, compressed the Ardmore basin, and modified many of the Morrowan–Atokan age structures on the Criner Hills–Wichita axis. By the close of the Pennsylvanian, tectonism had again ceased. The Ardmore basin and the Criner Hills were covered with red terrestrial shales, limestone-cobble conglomerates, and arkosic gravels shed from the Arbuckle and Tishomingo uplifts.

COTTONWOOD CREEK FIELD
Structure

The Cottonwood Creek anticline formed in the Late Chesterian through Early Desmoinesian as a

northeast-directed, Arbuckle-cored thrust plate emplaced over Ordovician to Lower Mississippian strata (Roberts and Read, 1990). Subthrust strata include the Woodford Shale, the source of the Cottonwood Creek hydrocarbons. Originally positioned near the crest of the Criner axis, the anticline was raised above sea level and stripped of >5,000 ft of Caney through Simpson cover (Fig. 3). Erosion also removed as much as 700–800 ft of Arbuckle from the crest of the anticline. The exposed lower West Spring Creek and Kindblade Formations in the core of the structure were karsted to depths of at least 1,500 ft.

Marine shales of the lower Deese Formation overlapped and sealed the karsted carbonate rocks on the anticline during the Middle Desmoinesian. Continued subsidence through the Late Missourian resulted in burial of the uplift by ~8,000 ft of upper Deese and Hoxbar Groups marine clastics.

Wrench faulting and folding modified the Criner uplift–Cottonwood Creek area during the Arbuckle orogeny in Virgilian time. Subcrop map–

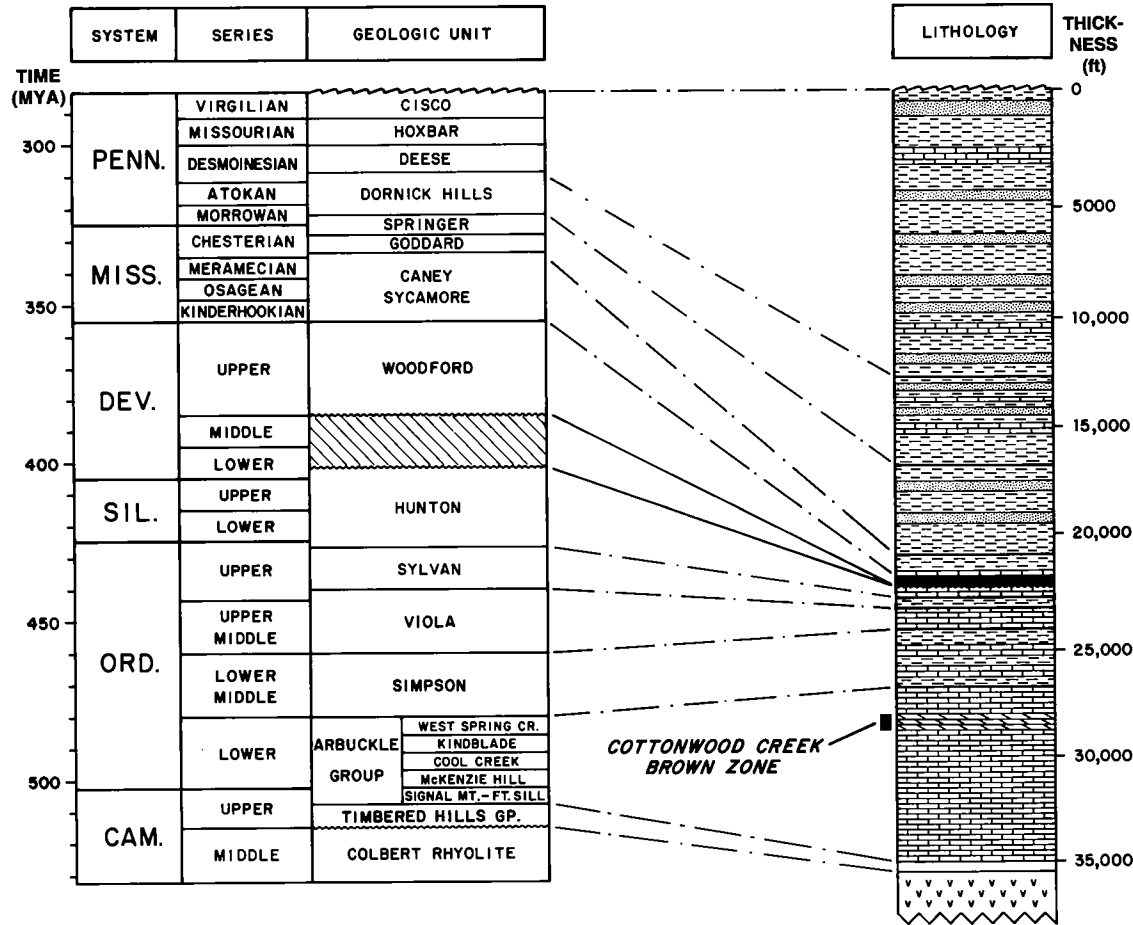


Figure 2. Generalized stratigraphic column for the Ardmore basin, southern Oklahoma. Compiled with data from Johnson and others (1988) and Fay (1989).

ping at the base-Pennsylvanian unconformity indicates that ~3 mi of left-lateral slip occurred on the Criner-Healdton fault during this period (Roberts and Read, 1990). The Cottonwood Creek structure moved to the west, away from its position on the northwest flank of the Criner Hills. Movement along the Criner fault also dropped the Cottonwood Creek structure ~3,000 ft relative to the block to the south (Figs. 3,4).

South of the Criner fault, compression folded the Deese and Hoxbar Group strata into oil-productive anticlines at South Lone Grove (sec. 2, T. 5 S., R. 1 W.) and Southwest Lone Grove fields (sec. 5, T. 5 S., R. 1 W.) (Westheimer and Schweers, 1956). However, immediately north of the Criner fault at Cottonwood Creek, these strata dip gently to the east and conceal the Arbuckle structure below the pre-Pennsylvanian unconformity.

The geometry of the Cottonwood Creek structure is delineated by data from 21 wells in and adjacent to the field. The anticline at the Brown zone horizon (Fig. 4) is ~3.5 mi long and 1.25 mi wide

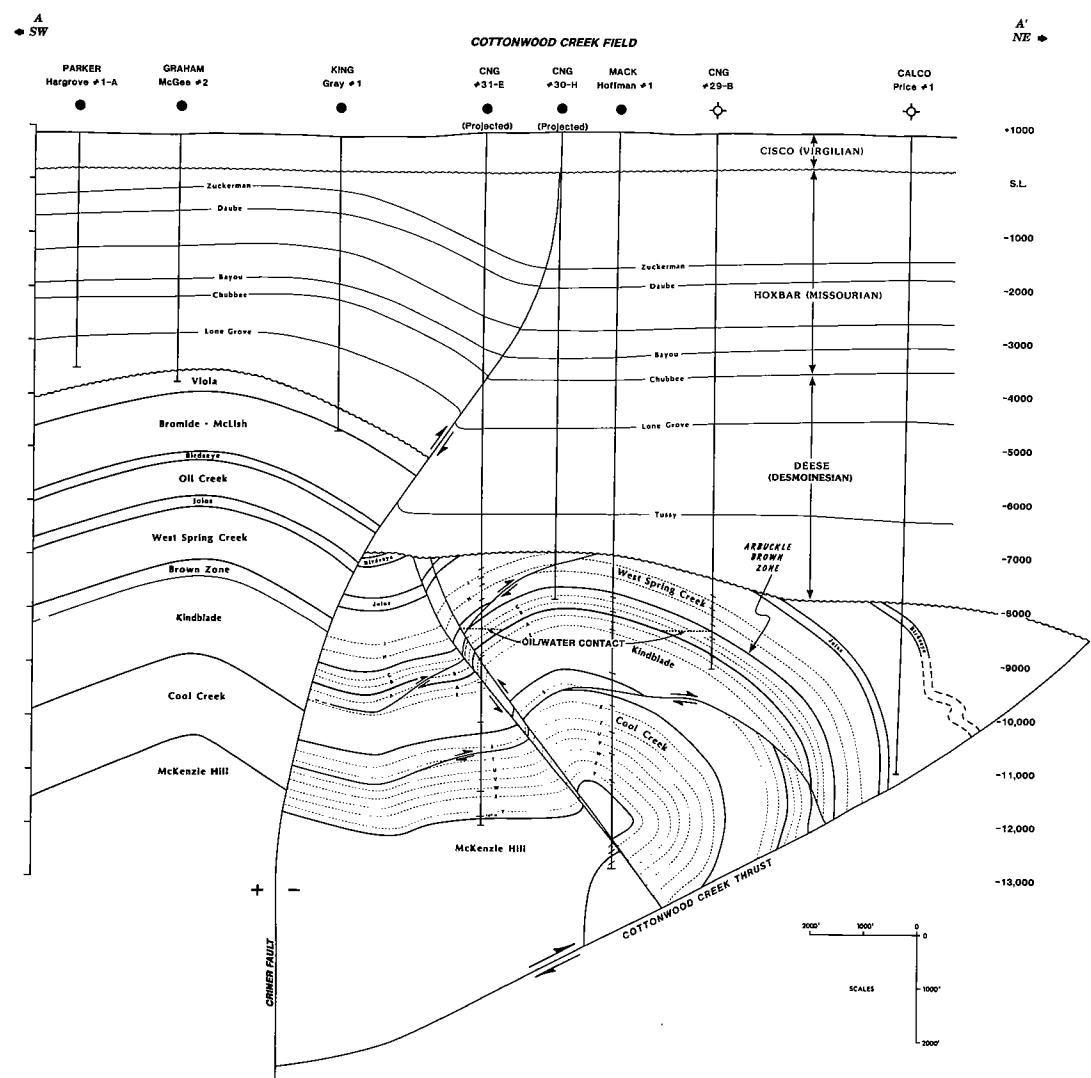


Figure 3. Southwest–northeast 1:1 scale structural cross section through Cottonwood Creek field. Dashed lines are intraformational gamma-ray markers that can be correlated throughout the field. Line of section A–A' shown on Figure 4.

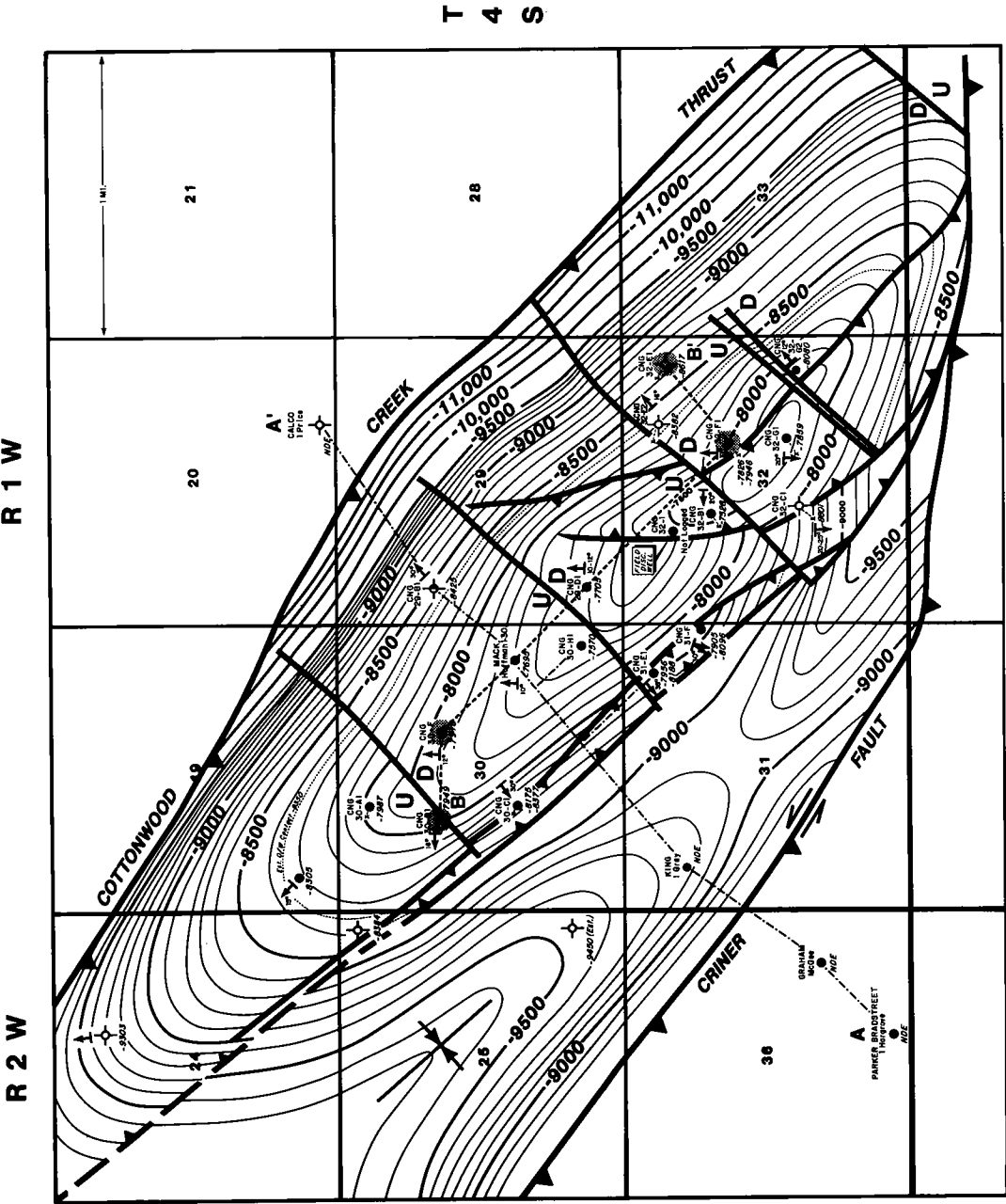


Figure 4. Cottonwood Creek structural map. Structural datum, Brown zone marker. Depths subsea. Contour interval is 100 ft. A-A' is line of section for Figure 3. Wells on Figure 5 are shown inside shaded circles.

with a minimum structural closure of ~1,500 ft. The Brown zone producing area measures approximately 2.5 mi by 0.75 mi, covers 1,200 acres, and has an oil column >900 ft. Four deep penetrations of the Cool Creek and McKenzie Hill Formations along the Brown zone crest indicate that the deep anticlinal core is overturned to the northeast. The seismically defined Cottonwood Creek thrust fault, which underlies the fold and borders the northern edge of the anticline (Fig. 3), has not been penetrated by drilling.

Parts of the Brown zone and West Spring Creek Formation are thrust-repeated in all wells on the southwest flank (Fig. 3) and on the southeast-plunging nose of the fold. The thrust repetitions, each with a vertical separation of 120–220 ft, are mapped as two low-angle, northeast-directed thrust faults originating in the syncline on the southwest flank of the field. This type of out-of-the-syncline thrust faulting is commonly associated with concentric folding in foreland detachment structures (Peterson, 1983; Brown, 1984). Thrust repetition of the upper Cool Creek section identified in the four deep wells along the crest of the structure is interpreted to be the result of a low-angle thrust fault of similar origin (see Mark Hoffman no. 1, Fig. 3).

The southern edge of Brown zone production is bounded by a zone of high-angle, southwest-directed backthrusting rooted in the McKenzie Hill in the deep core of the anticline (Fig. 3). The backthrusting post-dates the low-angle, northeast-directed thrust faults identified in the West Spring Creek and Cool Creek sections.

Numerous normal faults with 35–145 ft of vertical separation are crossed by wells in the field. For simplicity, most smaller faults are not shown in Figure 4. The positions of larger high-angle tear faults, such as those perpendicular to the crest of the structure through the southwest part of sec. 29 and the center of sec. 32, are based upon a combination of formation tops, dipmeter data, and other geological interpretation.

Brown Zone Reservoir Description

The Brown zone is an intensely fractured, vuggy to cavernous dolomite, restricted to an interval ~480 ft thick. The top of the interval is defined by a regionally persistent gamma-ray marker 1,100–1,200 ft below the top of the West Spring Creek. This gamma-ray marker is encountered at 8,447 ft, ~475 ft below the top of the pre-Pennsylvanian unconformity in the Cottonwood Creek no. 32B-1 (NW¼SE¼NW¼ sec. 32).

The assignment of the Brown zone to either the West Spring Creek or the Kindblade Formation is problematical. Robert Fay (personal communication) believes that thicknesses of West Spring Creek >1,500 ft in the Arbuckle Mountains and in

the Criner Hills are evidence that the entire Brown zone is above the top of the Kindblade. Latham (1970) also initially assigned the Brown zone to the West Spring Creek. However, subsequent detailed studies of the interval at Healdton as well as its limestone equivalent in other areas of southern Oklahoma suggest that the dolomite is developed in lithologies more characteristic of the Kindblade. Recent sample studies at Cottonwood Creek by Latham (personal communication) reinforce this opinion.

Biostratigraphic information suggests that the Brown zone may, in fact, straddle both formations. Studies of the Cottonwood Creek no. 32B-1 well samples by Jim Derby (personal communication; based upon conodont identification by R. L. Ethington) suggest that the top of the Kindblade is (1) no shallower than 8,600 ft (153 ft below the Brown zone gamma-ray marker), but (2) most likely between 8,800 and 9,000 ft. The deeper range (8,800–9,000 ft) would place the Kindblade top within the lower 200 ft, or possibly very near the base of the Brown zone interval.

Neutron-density logs show an erratic vertical and lateral distribution of Brown zone dolomite development throughout the field (Fig. 5). The dolomite shows poorest development at the structurally highest part of the anticline in the Cottonwood Creek no. 32B-1 (NW¼SE¼NW¼ sec. 32) and 32F-1 (SW¼NE¼ sec. 32) wells. These wells were the nearest offsets to the discovery well.

Neutron-density matrix porosity values in the best-developed dolomite sections are approximately 2–3%. Direct matrix porosity measurements obtained from rotary sidewall cores are similarly low, generally <2%. Sidewall core permeability values are typically <0.01 md.

Petrographic studies of sidewall cores show that the Brown zone is the product of multiple episodes of dolomitization. Four types of dolomite are differentiated on the basis of crystal structure and the resulting rock fabric.

The first, and probably earliest form, is a mudstone-replacive dolomicrite or dolomicrospar. It is typically very finely crystalline, anhedral, and exhibits a dirty appearance under plane polarized light. In several thin sections, gastropod outlines are preserved in the microcrystalline matrix. The crystal size and morphology suggest that this type of dolomite may have formed in a hypersaline environment or that it may be a very early replacement of lime mud.

The second type of dolomite is medium- to coarsely crystalline, and sucrosic. It is characterized by a porous loose network of interlocking subhedral to euhedral rhombohedral crystals. Individual crystals have dark, cloudy cores with clear zoned rims.

The third type is a fine- to coarsely crystalline xenotopic dolomite (Fig. 6) characterized by anhe-

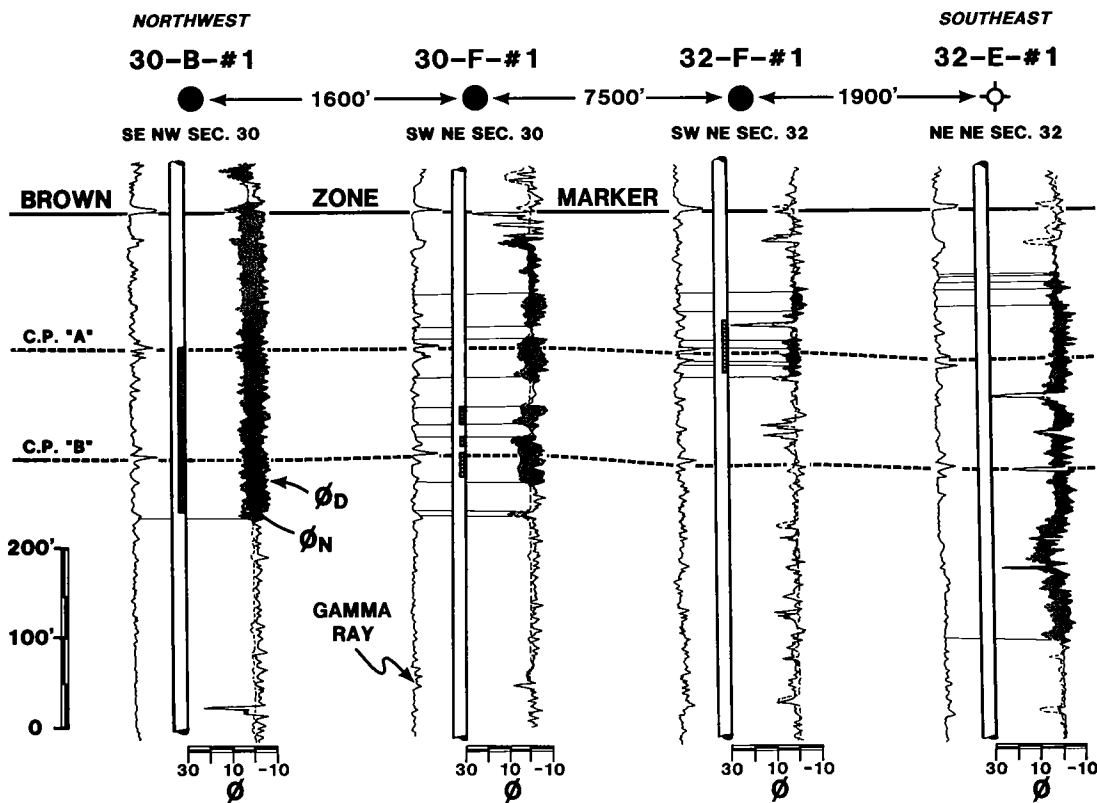


Figure 5. Cottonwood Creek Brown zone litho-density cross section illustrating the highly variable amount and distribution of dolomitization along the length of the anticline. Position of wells shown on Figure 4.

dral, interlocking crystals. It formed as a replacement of the original lime or dolomitic matrix. Intraclast "ghosts" within individual or interlocking groups of anhedral crystals attest to the replacement nature of the dolomite. Gregg and Sibley (1984) propose that xenotopic dolomite texture results from the replacement of limestone by dolomite or by neomorphic recrystallization of a preexisting dolomite at temperatures $>50^{\circ}\text{C}$.

The fourth type of dolomite, which fills or partially fills vugs and fractures, is saddle or baroque dolomite (Fig. 7). It is characterized by finely to coarsely crystalline euhedral crystals with curved edges and undulose extinction. Saddle dolomite forms at temperatures between 60 and 150°C , and most commonly above 100°C (Radke and Mathis, 1980).

The depositional and tectonic history of the rocks in the Criner uplift suggest that the Brown zone at Cottonwood Creek has never been buried significantly deeper than its present average depth of $8,500$ ft. The present reservoir temperature of $\sim 67^{\circ}\text{C}$ suggests that the temperature resulting from simple burial is sufficient to form both xenotopic and saddle dolomite in the Brown zone. Saddle

dolomite may also have been precipitated from ascending, heated brines expelled from the adjacent, rapidly subsiding Ardmore basin during the Pennsylvanian. Possible conduits for fluid movement through the host rock include a combination of early karst porosity, tectonic fractures, and laterally persistent zones of early sucrosic porosity.

Dissolution and fracture porosity are important contributors to reservoir volume in the Brown zone. Both types of porosity are clearly exhibited on borehole imaging logs run on several of the wells in the field (Fig. 8). Early to Middle Pennsylvanian karstification of the lower West Spring Creek and Kindblade Formations resulted in the formation of solution-enhanced Brown zone porosity. The Cottonwood Creek 32-1 discovery well experienced severe drilling and well control problems when it encountered 24 ft of cavernous porosity and flow rates of $>4,000$ BOPD and 3.0 MMCFGD near the top of the Brown zone. Two additional development wells, the 30A-1 (NE $\frac{1}{4}$ NW $\frac{1}{4}$ sec. 30) and the 30H-1 (SE $\frac{1}{4}$ SE $\frac{1}{4}$ sec. 30), also encountered Brown zone cavernous porosity so extensive that the entire interval could not be penetrated. Initial production rates from these

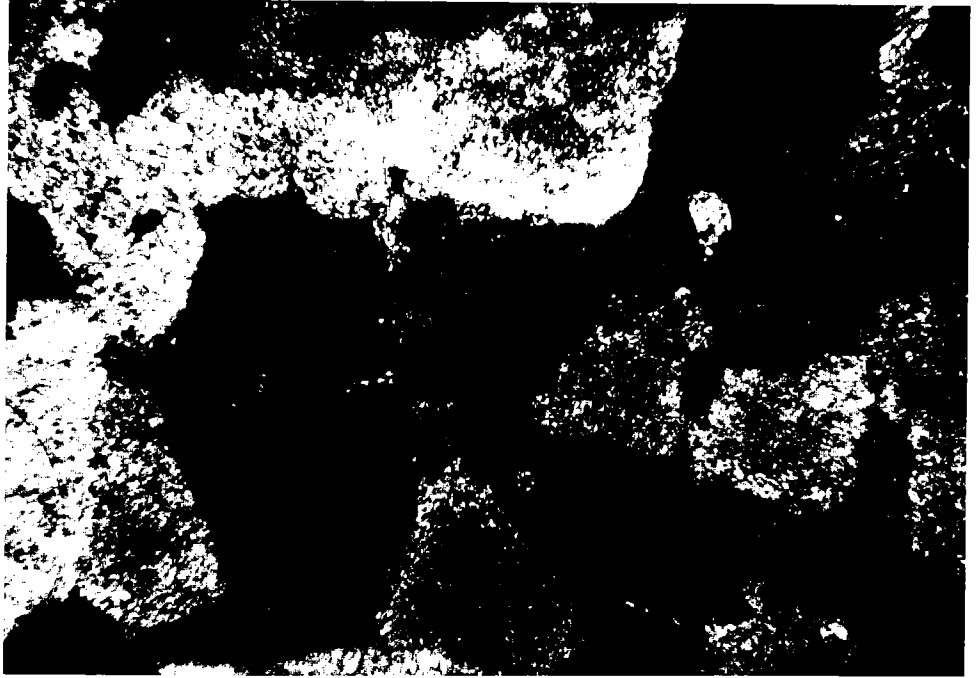


Figure 6. Brown zone xenotopic dolomite in the Cottonwood Creek no. 32G-1 (NW¼SE¼ sec. 32). Sample depth, 8,815 ft. Field of view is approximately 6 mm × 4 mm.

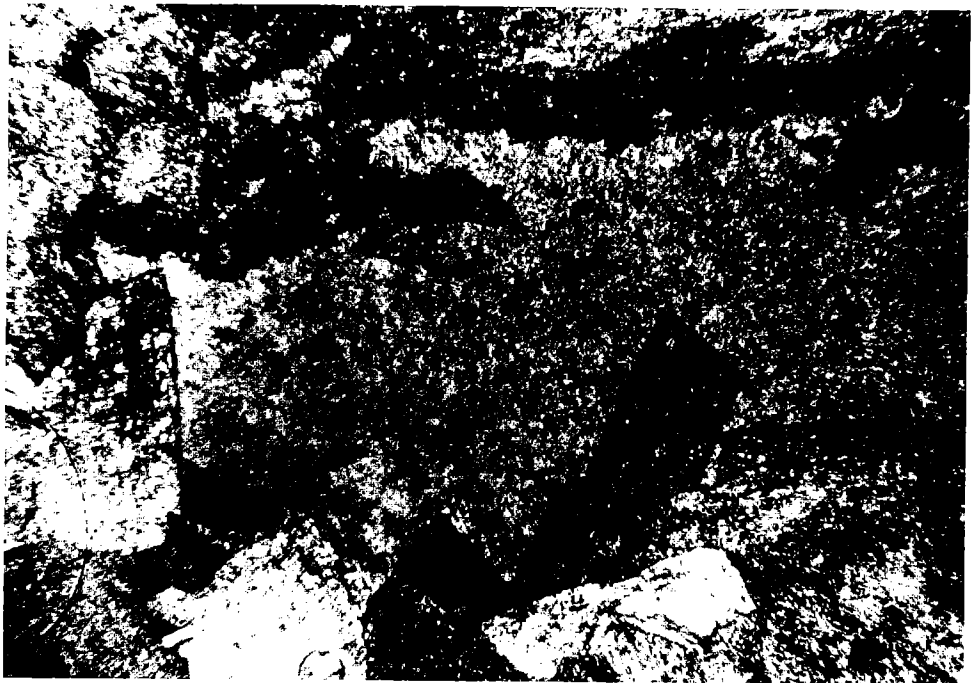


Figure 7. Saddle or baroque dolomite lining a Brown zone vug in the Cottonwood Creek no. 32G-1. Sample depth, 8,978 ft. Field of view is approximately 6 mm × 4 mm.

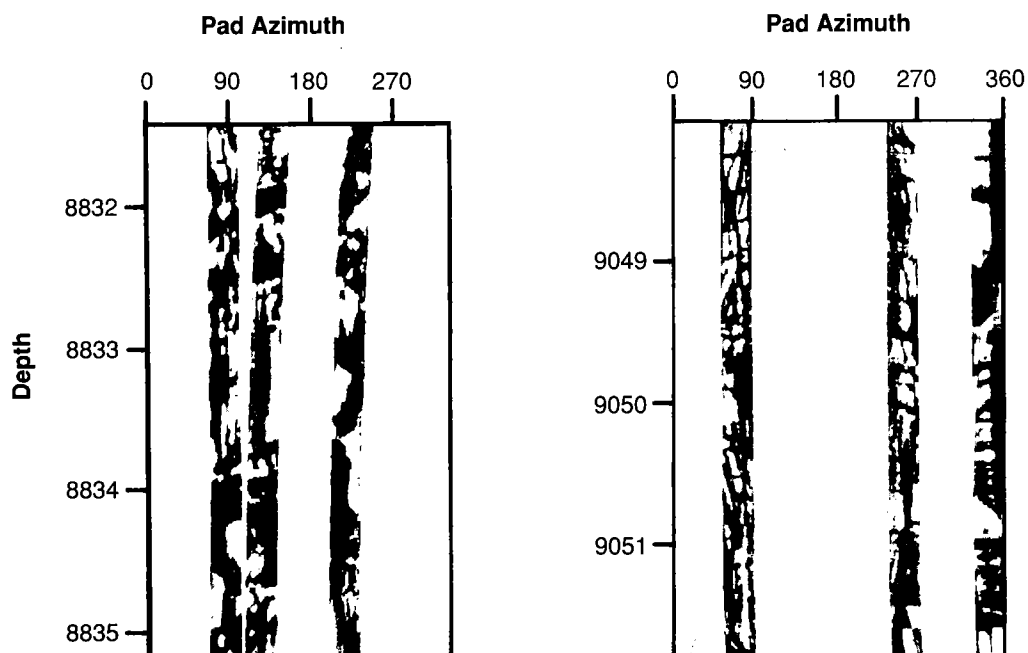


Figure 8. Formation Microscanner Images (FMI, a trademark of Schlumberger Inc.) from the Cottonwood Creek no. 29-D-1 Brown zone (SW $\frac{1}{4}$ SW $\frac{1}{4}$ sec. 29). Open, mud-filled vugs and fracture voids are shaded dark in both displays. Left image shows an example of the high concentration of dissolution vugs, some 2–3 in. in diameter. Image at right is interpreted to be a mosaic or crackle breccia similar to those described in the cave roof facies of collapsed cavern systems in the Ellenburger Formation of West Texas (Kerans, 1988).

two wells were 1,339 BOPD and 2,400 BOPD, respectively.

The extensive fracturing and brecciation interconnect much of the dissolution porosity in the reservoir. Due to a lack of sufficient whole core in the Cottonwood Creek Brown zone, the origin of fractures in the field is problematical. Much of the fracturing may be due to Pennsylvanian tectonism. However, core studies of the Brown zone at Healdton field and in the Texaco–Mobil no. 1 Criner (sec. 1, T. 5 S., R. 1 W.) suggest that much of the extensive brecciation observed at these two localities may be related to paleokarstification and solution collapse (Lynch and Al-Shaieb, 1991). The same interpretation may be valid for Cottonwood Creek.

Brown Zone Reservoir Performance

Reservoir performance information contributes to the understanding of complex reservoirs. The diverse nature of dolomitization, karst development, and fracturing across the Cottonwood Creek field hinders accurate assessment of reservoir characteristics through direct petrophysical evaluation alone. Early production from the 32-1 discovery well, in which 350,000 bbl of oil were produced in five months, established that the cavernous reservoir was prolific. Further performance

data show that all wells produce from a common reservoir, enabling the magnitude of the productive reservoir system to be determined. The interconnection of the vugular and fractured, high productivity zones to less permeable types of porosity was also demonstrated. The low-porosity rock-matrix is believed to be a major contributor to the ultimate oil recovery.

Reservoir pressures measured at various cumulative volumes of oil produced (Fig. 9) show that most of the wells exhibit similar pressures throughout the field's productive history, denoting a common reservoir in direct communication. The southeast end of the field (wells to the southeast of the 32B-1) has maintained pressure readings slightly above the rest of the field, although these values declined before any wells in the area had produced. This indicates that there is communication between these two portions of the field through either a low permeability zone or across the northeast–southwest-trending normal fault mapped through the center of sec. 32 (Fig. 4).

The overall decline in pressure provides data for a material balance estimate of the oil-in-place. Values from both volumetric and material balance methods are subsequently compared until consistent assumptions can be made. Based on such calculations, the Cottonwood Creek field initially

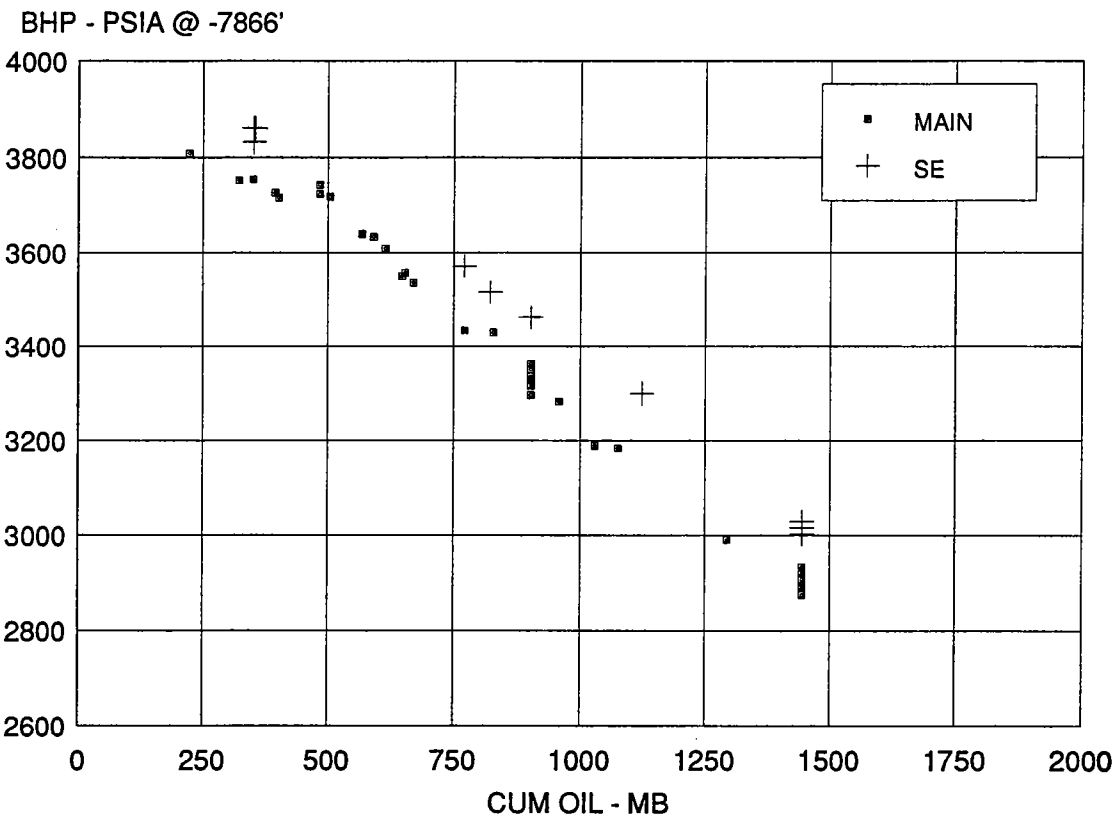


Figure 9. Reservoir pressure vs. field cumulative oil production prior to pressure maintenance. Data points denoted with a (+) are from the southeast end of the field which has maintained pressure readings slightly higher than the main portion of the field.

contained >40 million bbl of oil with an assumed average effective Brown zone porosity of ~3%.

Pressure buildup and drawdown tests show contributions from both the fracture system as well as from tight matrix porosity. A plot of bottom-hole pressure vs. time in hours (Fig. 10) uses data taken from a nonproducing well while (A) the field is producing at a rate of 4,000 BOPD, (B) the field is shut-in with only one well producing at ~150 BOPD, and (C) a second well is brought on at an additional rate of 600 BOPD. The nearly instantaneous response to each of these actions (in a well >2,000 ft from the changes) demonstrates the high permeability of the system. Each change in the producing rate results in a nearly linear pressure vs. time curve that reflects a closed depletion system with exceptional transmissibility. The buildup portion of the plot, with its gradual slope of 15 psi in 100 hours, indicates flow from the matrix portion of the reservoir into the fracture system. The rate of flow was nearly constant over the test period but has changed over the life of the field. Analysis of the changes in slope for various producing rates suggests that the matrix holds the majority of the oil-in-place.

A simultaneous buildup plot of four wells

across the field (Fig. 11) shows that all wells are experiencing the same rate of influx. The top pressure curve is from the 32F-1 (SW¼NE¼ sec. 32) which is one of the wells in the southeastern part of the field. While the early-time rise shows a much greater pressure drawdown was required for flow, the late-time data is building at a rate similar to other wells in the field. The other wells include the 31E-1 (NE¼NE¼ sec. 31) and the 29D-1 (SW¼ SW¼ sec. 29), located in the center of the field, as well as the 30A-1 well (NE¼NW¼ sec. 30), situated in the field's northwest corner.

Pressure maintenance by water injection into the Arbuckle aquifer was initiated in June 1990. Pressure response to the injection was observed within 30 minutes. Field oil production rates were increased to ~5,500 BOPD by September 1990 with injection volumes increased to 8,000 BWPD to balance reservoir withdrawal. Cumulative oil production through October 1992 was 6.1 million bbl.

SUMMARY

The Arbuckle Brown zone reservoir at Cottonwood Creek is composed of vuggy to cavernous, extensively fractured dolomite restricted to a 480-

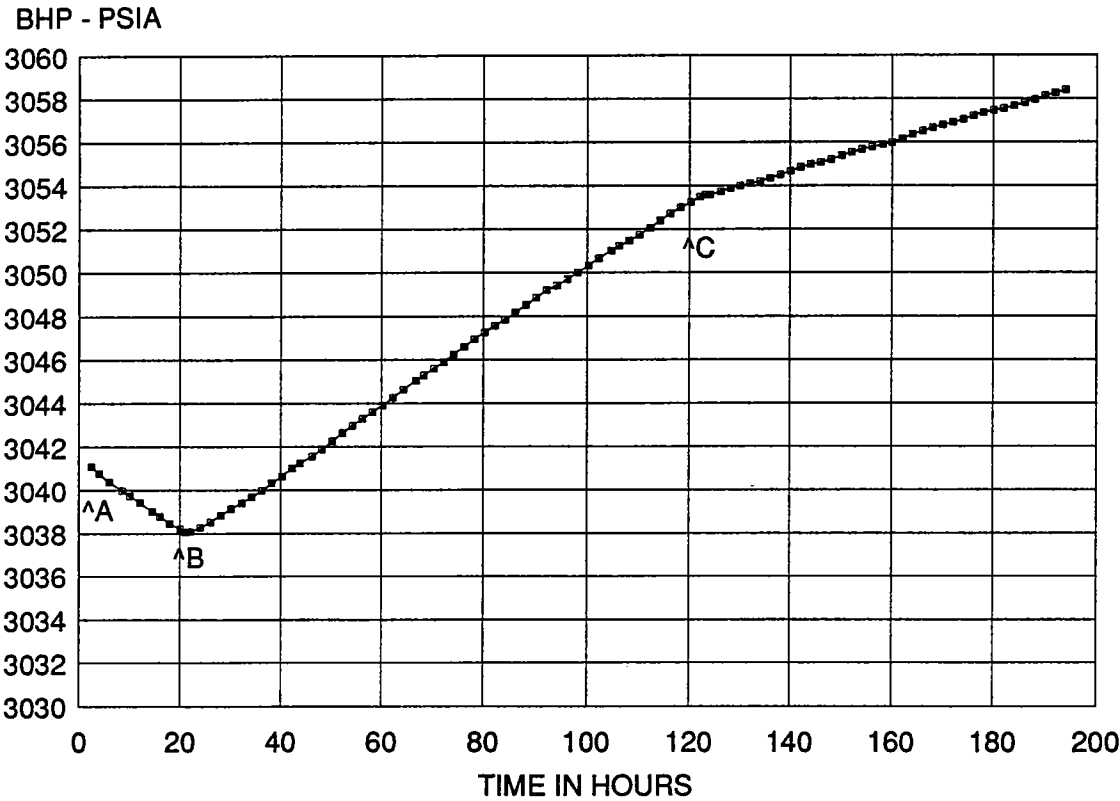


Figure 10. Pressure buildup and drawdown data from nonproducing well (29B-1, SW¼NW¼ sec. 29) with field producing at (A) 4,000 BOPD, (B) 150 BOPD, and (C) 750 BOPD.

ft interval in the lower West Spring Creek and/or upper Kindblade Formations of the Arbuckle Group. Productive closure, which exceeds 900 ft and covers 1,200 acres, is controlled by >1,500 ft of total structural closure on the Cottonwood Creek anticline.

At least four distinct dolomite morphologies are recognized in the producing interval. Dolomite matrix porosity and permeability in the Brown zone are remarkably low, typically <2% and 0.01 md, respectively. Pressure buildup tests, however, show that the tight dolomite matrix is a major contributor to the bulk reservoir volume. The Brown zone's system of interconnected vugs, caverns, and closely spaced fractures is also important volumetrically, and they are critical to the high oil production rates as well as the excellent field-wide pressure transmissibility observed in engineering tests.

Cottonwood Creek field, with oil-in-place estimates of 40 million bbl, has been heralded as the largest southern Oklahoma oil find since the first Brown zone discovery at Healdton field in 1960. Cumulative Arbuckle production from these two fields may ultimately reach 35–40 million bbl of oil.

The Arbuckle carbonates are under-explored and provide the most promising potential for large hydrocarbon discoveries in southern Oklahoma. Detailed understanding of both the Healdton and Cottonwood Creek fields will be instrumental in developing exploration models which lead to the discovery of additional Arbuckle/Ellenburger accumulations in the southern Midcontinent.

ACKNOWLEDGMENTS

The authors would like to thank the management of CNG Producing Co. for permission to publish this paper. The manuscript benefited from technical reviews by Barry Langham, Robert Fay, Jack Latham, and Tommy Thompson. Special thanks also go to Todd Waddell at the University of Oklahoma who shared his knowledge of the Healdton Brown zone and aided in making thin-section photomicrographs.

REFERENCES CITED

Akin, R., 1964, Map of Arbuckle pools of Osage County, in McHugh, J. W.; and Broughton, M. N. (eds.), Symposium on the Arbuckle: Tulsa Geological Society Digest, v. 32, p. 37.

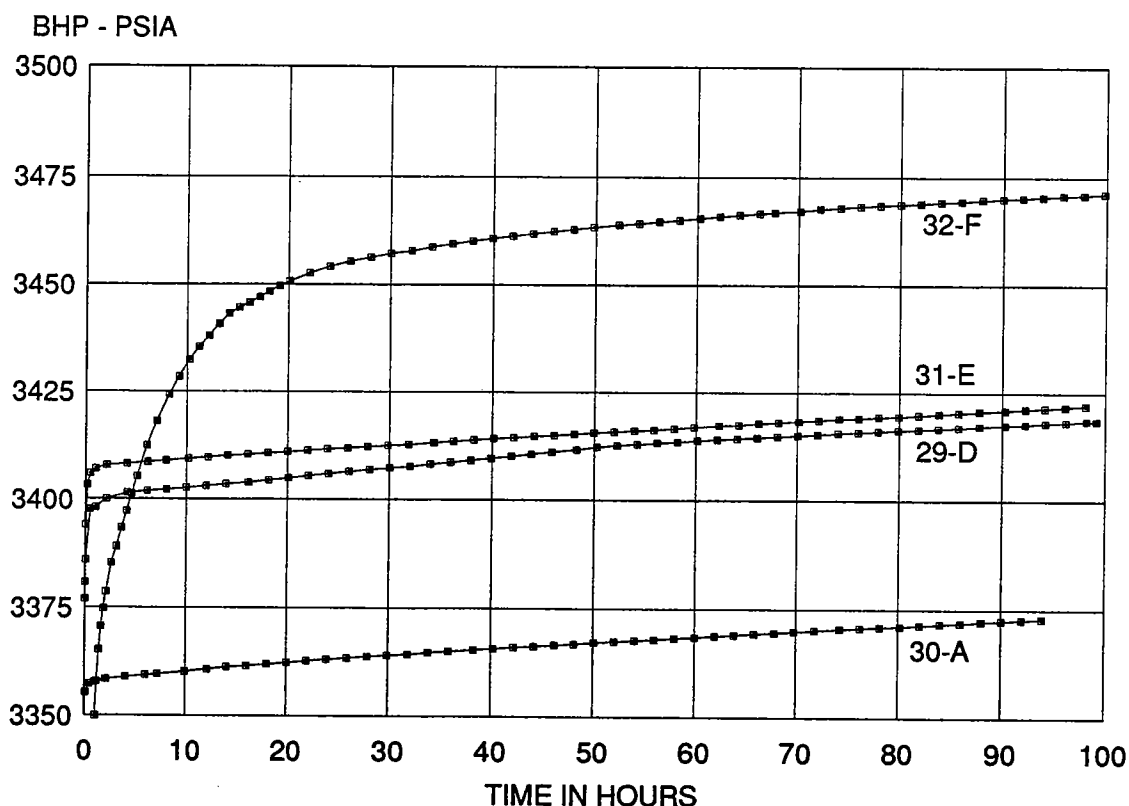


Figure 11. Simultaneous pressure buildup plots for widely spaced field wells. Wells no. 32F and no. 30A are ~1.8 mi apart (Fig. 4).

- Bennison, A. P., 1964, The Cushing field, *in* McHugh, J. W.; and Broughton, M. N. (eds.), *Symposium on the Arbuckle*: Tulsa Geological Society Digest, v. 32, p. 158-159.
- Bloesch, E., 1964, Arbuckle production and prospects in northeast Oklahoma, *in* McHugh, M. J.; and Broughton, M. N. (eds.), *Symposium on the Arbuckle*: Tulsa Geological Society Digest, v. 32, p. 43-44.
- Brown, W. G., 1984, Basement involved tectonics foreland areas: American Association of Petroleum Geologists Continuing Education Course Notes No. 26, 92 p.
- Burgess, W. J., 1968, Carbonate paleoenvironments in the Arbuckle Group West Spring Creek Formation, Lower Ordovician in Oklahoma: Columbia University unpublished Ph.D. dissertation, 140 p.
- Carpenter, B. N.; and Evans, M. C., 1991, Comparison of the Arbuckle Group at Wilburton field, Latimer County, with N.E. Alden field, Caddo County, Oklahoma, *in* Johnson, K. S. (ed.), *Arbuckle Group Core Workshop and Field Trip*: Oklahoma Geological Survey Special Publication 91-3, p. 111-132.
- Fay, R. O., 1989, Geology of the Arbuckle Mountains along Interstate 35, Carter and Murray Counties, Oklahoma: Oklahoma Geological Survey Guidebook 26, 50 p.
- Feinstein, S., 1981, Subsidence and thermal history of the southern Oklahoma aulacogen: implications for petroleum exploration: American Association of Petroleum Geologists Bulletin, v. 65, p. 2521-2533.
- Gatewood, L. E., 1970, Oklahoma City field; anatomy of a giant, *in* Halbouty, M. T. (ed.), *Geology of giant petroleum fields*: American Association of Petroleum Geologists Memoir 14, p. 223-254.
- Gregg, J. M.; and Sibley, D. F., 1984, Epigenetic dolomitization and the origin of xenotopic dolomite texture: *Journal of Sedimentary Petrology*, v. 54, p. 908-931.
- Ham, W. E., 1969, Regional geology, *pt. 1 of* Ham, W. E. (ed.), *Regional geology of the Arbuckle Mountains, Oklahoma*: Oklahoma Geological Survey Guidebook 17, p. 7-21.
- Ham, W. E.; Denison, R. E.; and Merritt, C. A., 1964, Basement rocks and structural evolution of southern Oklahoma: Oklahoma Geological Survey Bulletin 95, 302 p.
- Johnson, K. S.; Amsden, T. W.; Denison, R. E.; Dutton, S. P.; Goldstein, A. G.; Rascoe, Bailey, Jr.; Sutherland, P. K.; and Thompson, D. M., 1988, Southern Midcontinent region, *in* Sloss, L. L. (ed.), *Sedimentary cover—North American craton; U.S.: Geological Society of America, Decade of North American Geology*, v. D-2, p. 307-359. [Reprinted as *Geology of the southern Midcontinent*: Oklahoma Geological Survey Special Publication 89-2, 1989, 53 p.]

- Kerans, C., 1988, Karst-controlled heterogeneity in the Ellenburger Group of West Texas: American Association of Petroleum Geologists Bulletin, v. 72, p. 1160–1183.
- Latham, J. W., 1970, Healdton field, Carter County, Oklahoma, *in* Halbouty, M. T. (ed.), Geology of giant petroleum fields: American Association of Petroleum Geologists Memoir 14, p. 255–276.
- Lindsay, R. F.; and Koskelin, K. M., 1991, Arbuckle Group deposition parasequences, southern Oklahoma, *in* Johnson, K. S. (ed.), Late Cambrian–Ordovician geology of the southern Midcontinent, 1989 Symposium: Oklahoma Geological Survey Circular 92, p. 71–84.
- Lynch, Mark; and Al-Shaieb, Zuhair, 1991, Evidence of paleokarstic phenomena and burial diagenesis in the Ordovician Arbuckle Group of Oklahoma, *in* Johnson, K. S. (ed.), Late Cambrian–Ordovician geology of the southern Midcontinent, 1989 Symposium: Oklahoma Geological Survey Circular 92, p. 42–60.
- Peterson, F. A., 1983, Foreland detachment structures, *in* Lowell, J. D. (ed.), Rocky Mountain foreland basins and uplifts: Rocky Mountain Association of Geologists, Denver, p. 65–77.
- Radke, B. M.; and Mathis, R. L., 1980, On the formation and occurrence of saddle dolomite: Journal of Sedimentary Petrology, v. 50, p. 1149–1168.
- Roberts, M. T.; and Read, D. L., 1990, Geology of the Cottonwood Creek field, Carter County, Oklahoma [abstract]: American Association of Petroleum Geologists Bulletin, v. 74, p. 749–750.
- Tomlinson, C. W.; and McBee, W., Jr., 1959, Pennsylvanian sediments and orogenies of the Ardmore district, Oklahoma, *in* Mayes, J. W.; Westheimer, J.; Tomlinson, C. W.; and Putnum, D. M. (eds.), Petroleum geology of southern Oklahoma: American Association of Petroleum Geologists, Tulsa, v. 2, p. 3–52.
- Westheimer, J. M.; and Schweers, F. P., 1956, Southwest Lone Grove field, Carter County, Oklahoma, *in* Hicks, I. C.; Westheimer, J.; Tomlinson, C. W.; Putnam, D. M.; and Selk, E. L. (eds.), Petroleum geology of southern Oklahoma: American Association of Petroleum Geologists, Tulsa, v. 1, p. 144–161.
- Wickham, J.; Pruatt, M.; Reiter, L.; and Thompson, T., 1975, The southern Oklahoma aulacogen: Geological Society of America Abstracts with Programs, v. 7, p. 1332.

Geologic Study of the Upper Arbuckle Group in the Healdton Field, Carter County, Oklahoma

R. Todd Waddell

Conoco, Inc.
Lafayette, Louisiana

James M. Forgotson, Jr., and Huaibo Liu

University of Oklahoma
Norman, Oklahoma

INTRODUCTION

The Arbuckle Brown zone has long been a prolific and enigmatic reservoir. Discoveries of the deep Wilburton field in the Arkoma basin and Cottonwood Creek field in the Ardmore basin (Read and Richmond, 1993), combined with the cumulative recovery of >11 MMBO (million barrels of oil) from the Arbuckle in the Healdton field (Dwight's Energy Data Inc., 1993), has attracted the attention of many explorationists. The spectacular reports of high initial potentials (>4,000 BOPD [barrels of oil per day] in Cottonwood Creek), drill bits dropping through subsurface caverns, and production through drill pipe as a result of blowouts (Read and Richmond, 1993), has rekindled the interest in Arbuckle exploration in Oklahoma.

This article describes the following: (1) a surface study of the upper Arbuckle Group (Fig. 1) in the Dolese Bros. Co. Ardmore quarry; and (2) a subsurface study based on cores from the Healdton field and a core drilled ~2 mi north of the Healdton field. Observations show both the vertical and lateral distribution of dolomite in the Healdton area, karst development interpretations from core data, and well-log response to possible karst breccia. Possible mechanisms for dolomitization and karst development are described.

SURFACE STUDY OF THE UPPER ARBUCKLE GROUP IN THE DOLESE BROS. CO. ARDMORE QUARRY

The Dolese Bros. Co. Ardmore quarry is located in the Criner Hills, in sec. 22, T. 5 S., R. 1 W. Kelvin Cates, Huaibo Liu (co-author), and R. Todd Waddell (co-author) examined different aspects of the quarry. Physical aspects of the karstic portion of

the quarry, as well as facies of the original depositional environments, were observed; samples were collected for a paleomagnetic investigation.

The upper part of the Arbuckle Group in the Ardmore quarry has been mapped as West Spring Creek–Kindblade Formations, undifferentiated (Frederickson, 1957). The West Spring Creek in this area was interpreted by Burgess (1968) to have been deposited in a supratidal or lagoonal–supratidal complex. He further described it as a diagenetic terrane that is highly susceptible to dolomitization and that contains anhydrite and algal stromatolitic structures. The limestone portion of the quarry is mined for aggregate; the dolomite is not mined because it does not pass the necessary freeze–thaw tests. A large cave was uncovered during mining but was subsequently destroyed in the mining process. However, cave entrances still exist (Fig. 2A), although talus is piled against the openings, making entrance impossible. The occurrence of karst breccia is displayed dramatically in this part of the quarry. Crackle, mosaic, and chaotic breccia occur in descending succession along the cliff walls (Fig. 2B–D). In the area where the chaotic breccia is found intact with internal fill, core plugs were taken for thin-section examination and paleomagnetic readings.

The age of karst development for the Arbuckle Group was determined by Elmore and Crawford (1990) based on magnetite-containing samples from the Bally Mountain quarry in the Wichita Mountains. The orientation of the earth's magnetic field varies through geologic time (polar wandering) (Elmore and Crawford, 1990). The orientation of the magnetic field in authigenic magnetite is an indication of the time of precipitation of the magnetite. Magnetite was precipi-

Waddell, R. T.; Forgotson, J. M., Jr.; and Huaibo, Liu, 1993, Geologic study of the upper Arbuckle Group in the Healdton field, Carter County, Oklahoma, *in* Johnson, K. S.; and Campbell, J. A. (eds.), Petroleum-reservoir geology in the southern Midcontinent, 1991 symposium: Oklahoma Geological Survey Circular 95, p. 126–139.

tated on speleothems in alternating layers of calcite. The magnetite in the Bally Mountain quarry has a sufficiently high CRT (critical roughening temperature) to preserve the paleomagnetic direction established at the time of magnetite precipita-

tion. Elmore and Crawford's (1990) interpretation that karst development at the Bally Mountain quarry was younger than Late Pennsylvanian was confirmed by the finding of Permian vertebrates within the same caves and karst features.

Magnetite was not found in the samples at the Ardmore quarry. The magnetic mineral (possibly goethite) found in the samples had a CRT below 200°F and would not provide a reliable measurement of the paleomagnetic direction at the time the mineral was precipitated.

The area where the Ardmore quarry is located was also used as a water supply for the adjacent Brock oil field. Surface and shallow subsurface water from the West Spring Creek-Kindblade in the Ardmore quarry area was collected from the natural springs and runoff, and it was used for the Brock oil field waterflood (Robert Fay, personal communication). This observation is interpreted to indicate that an extensive aquifer exists today in the same unit that was karstified probably millions of years ago. It also shows the susceptibility of this lithologic unit to karst development; the Criner fault juxtaposes the karstic aquifer and Pennsylvanian strata. The breaching of the Criner anticline at the West Spring Creek-Kindblade level is similar to breaching of the structure at Cottonwood Creek (Read and Richmond, 1993).

SUBSURFACE STUDY OF THE UPPER ARBUCKLE GROUP FROM CORES IN THE HEALDTON FIELD

The Healdton field, located in T. 4 S., R. 3 W., Carter County, Oklahoma (Fig. 3) produces oil from the karstic Arbuckle Group Brown zone reservoir. Cores were examined from the Wade, Bray, and Brown zones of the upper Arbuckle (Lower Ordovician) in four wells in the Healdton field. Thin sections also were examined to observe the relationship between pore size, porosity type, and petroleum production. The Brown zone, equivalent to the lower West Spring Creek (Fay, 1989), is the most prolific Arbuckle reservoir; it contributed approximately 85–90% of the total oil produced from the upper Arbuckle in the Healdton field. Dolomitization and karst development are the factors controlling the reservoir quality in the Brown zone. The Brown zone has crackle, mosaic, and chaotic breccia and related porosities (fracture, cavernous, vugular, and breccia), in addition to dolomitic porosity. In contrast, the examined cores from the Wade and Bray zones show predominantly original depositional fabric with comparatively little diagenetic alteration. Although the Wade and the Bray zones produce from local porous zones and have some thin karst-like breccia in the Healdton field, their cumulative production is relatively minor compared to that of the Brown zone.

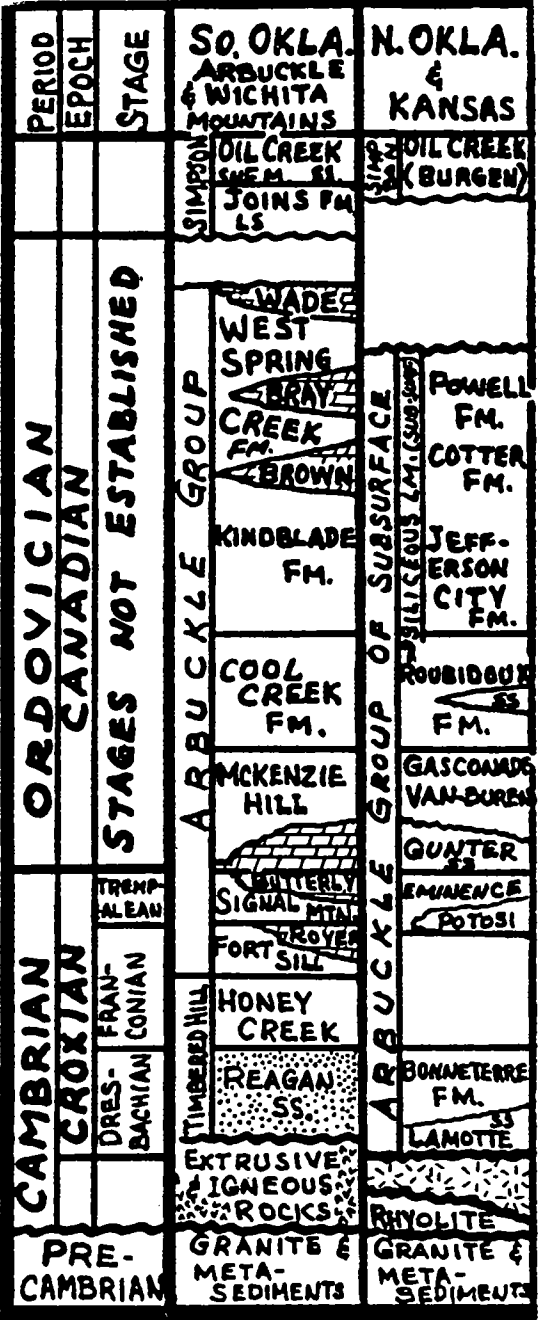


Figure 1. Stratigraphic chart for the Arbuckle Group in Oklahoma and Kansas (modified from Gatewood, 1979).

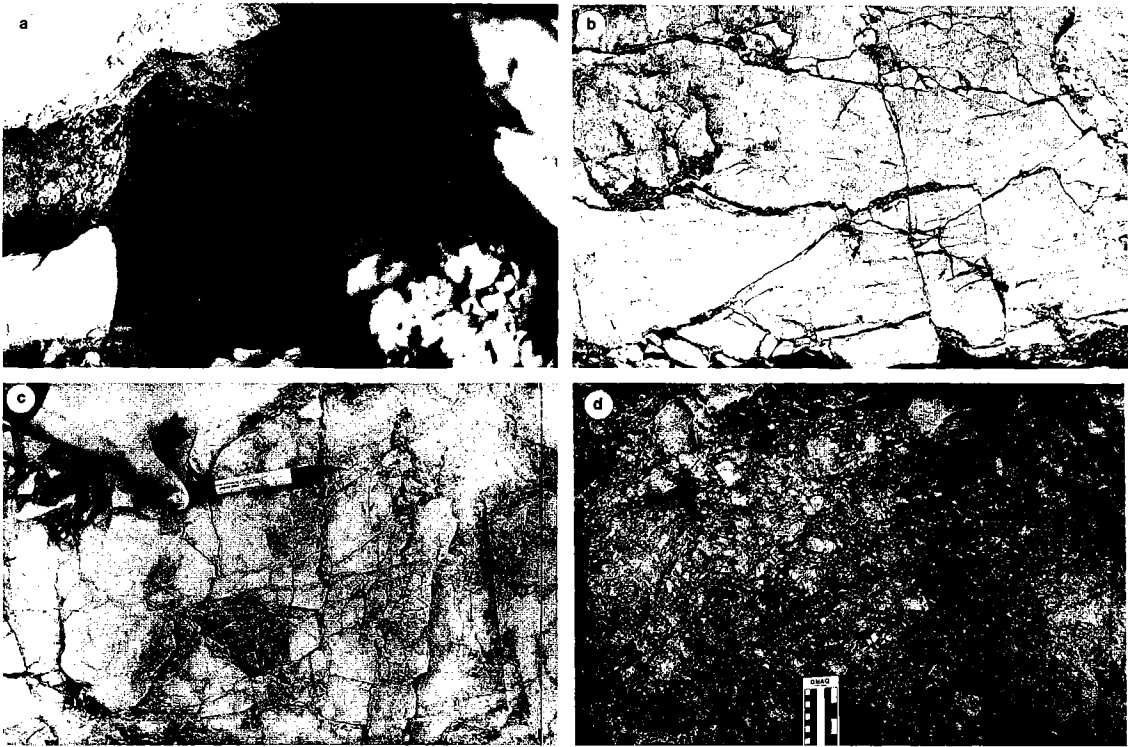


Figure 2. Photographs of karst features in the Arbuckle Group (West Spring Creek–Kindblade) in the Dolese Bros. Co. Ardmore quarry. (A) Cavern development; cave opening is about 3 ft wide and 2 ft high. (B) Fracture breccia, field of view about 4 ft wide. (C) Mosaic breccia. (D) Large clast (upper right) is chaotic breccia.

Wade Zone Core Description

J. C. Voorhees No. 1

The Wade zone core was taken from the J. C. Voorhees no. 1, in sec. T. 4 S., R. 3 W., Carter County (Fig. 4). The Wade zone is upper West Spring Creek (the uppermost formation of the Arbuckle Group) and was deposited in a shallow-water environment (Burgess, 1968; Lindsay and Koskelin, 1991). Six dominant lithofacies were observed, as described below:

Lithofacies	Description
A	Gray-green, thinly laminated lime mudstones with small fractures, some soft-sediment deformation, caliche, and some medium-bedded lime mudstone layers
B	Gray, thinly laminated dolomudstones containing sparse anhydrite nodules or concretions (locally interbedded with mottled mudstones)
C	Light-tan to brown, mottled dolomicrites and lime mudstones
D	Blue-white anhydrite nodules, 2–4 in. across
E	Thin-bedded, fossiliferous grainstones and packstones (mostly containing crinoids and ooids)
F	Flat-pebble conglomerates

These lithofacies are comparable to the depositional facies defined by Lindsay and Koskelin (1991). They divided the upper West Spring Creek into three depositional facies: tidal flat (thick- and thin-laminated mudstones), beach berm (flat-pebble conglomerates), and bioturbated subtidal, mottled muds (Fig. 5). Burgess (1968) similarly defined these facies as subtidal, intertidal, lagoonal, and supratidal.

The Wade zone in the Voorhees well consists predominantly of lime mudstones and dolomudstones that show primarily depositional fabric. Karst development does not occur in the Wade zone, except for some possible microkarst.

Bray Zone Core Description

J. C. Voorhees No. 1

The Bray zone core from the Voorhees well (Fig. 4) is predominantly lime mudstones and dolomudstones. It also contains possible algal laminites and stromatolites, karst breccia, and more abundant occurrences of flat-pebble conglomerates than does the Wade zone. Karst development in the Bray zone of the Voorhees core is interpreted as local occurrences related to faults that cut

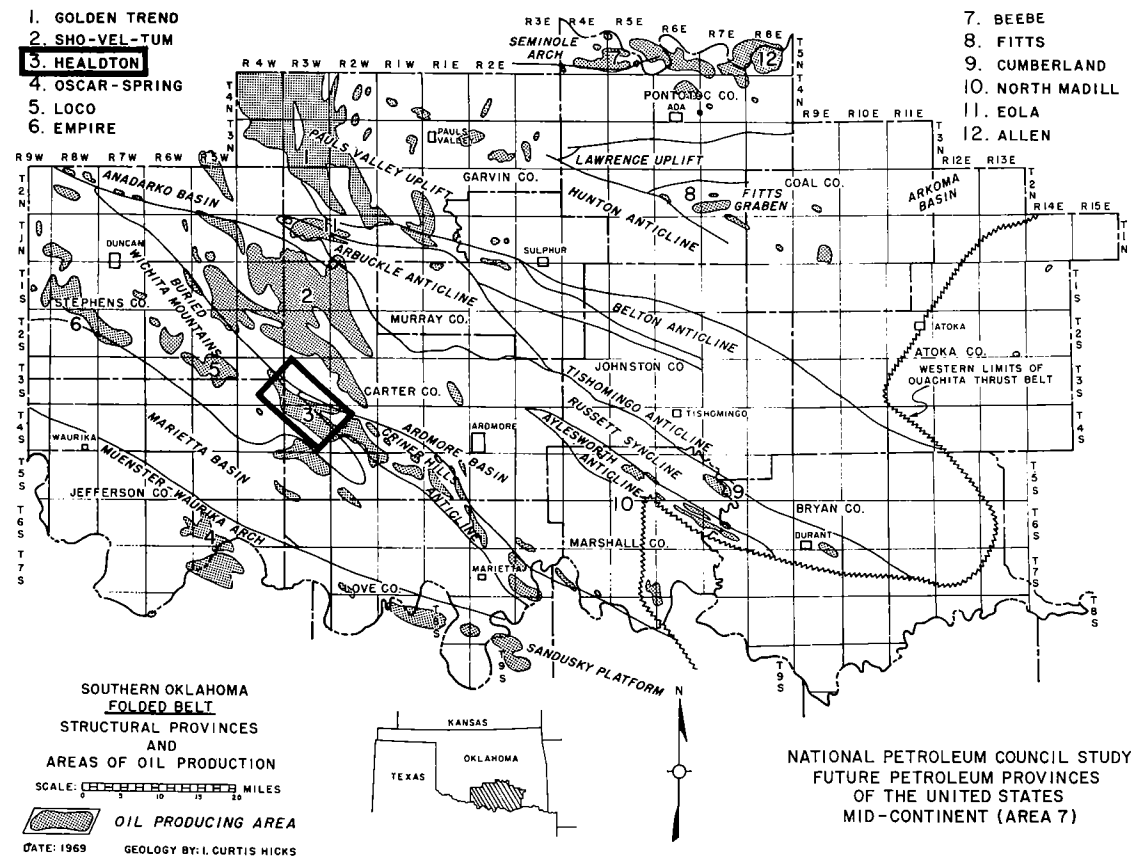


Figure 3. Map of southern Oklahoma showing location of Healdton field and study area (from Hicks, 1971).

the core (although not all karst development is seen in proximity to the faults within the core).

Geneva Bray No. 1

More than 99% of the Bray zone core examined from the Geneva Bray no. 1(sec. 2, T. 4 S., R. 3 W., Carter County) shows original depositional fabric. The Bray zone is composed of lime mudstones with some dolomudstones, thin-bedded grainstones and packstones, stromatolites, and flat-pebble conglomerates. The major facies observed in the Bray zone in the Geneva Bray well are:

Lithofacies	Description
A	Dark-gray to gray, brown to light-tan, mottled lime mudstones, bioturbated, with few chert nodules
B	Thin-bedded, fossiliferous packstones and grainstones, with ooids, trilobites, and gastropod fragments
C	Gray to dark gray-green, thin- to medium-bedded laminated limestones and dolomudstones
D	Gray-green algal stromatolites (boundstones), dolomitic, with stylolites
E	Flat-pebble conglomerates

Like the Wade zone, the Bray zone is composed of shallow-water carbonate deposits. However, the Bray zone contains more laminated and mottled mudstones than does the Wade zone, possibly due to a deeper water and lower energy environment. Lindsay and Koskelin (1991) also found greater subtidal influence in the lower West Spring Creek than in the upper West Spring Creek.

Within the algal stromatolite facies, stylolites developed roughly parallel to the bedding plane (Fig. 6). Dolomitization along the stylolites can develop porosity, which can be enhanced further through exposure to karst waters. Examples of stylolites with similar dolomitic and karst diagenesis can be seen in a similar lithofacies found in the Brown zone in the HAU no. 5-3 (discussed later in the report). Olson (1984) also recognized a close relation between stromatolites and karst development in the Baffin Island area.

The only significant indication of karst development within the cored interval is found between 3,797.0 and 3,798.5 ft (1.5 ft of karst lithology out of ~500 ft of core from the Bray Zone) (Fig. 7). We interpret this type of karst as a solution pipe, lacking the sequence of crackle, mosaic, and cha-

otic breccia. The pipe walls are intact, without significant fracturing. The interior resembles a pipe that has been dissolved out of the rock; chaotic breccia and karst-fill sediments were redeposited.

The interval of the Bray zone that produces in the Geneva Bray no. 1 well (3,430–3,530 ft) was not available for examination; this interval shows a higher SP (spontaneous potential) response, which could indicate a lithology different from that in the examined core. The Geneva Bray’s IP (initial potential) was 190 BOPD and 250 Mcf/D. The cumulative production in the Bray well was

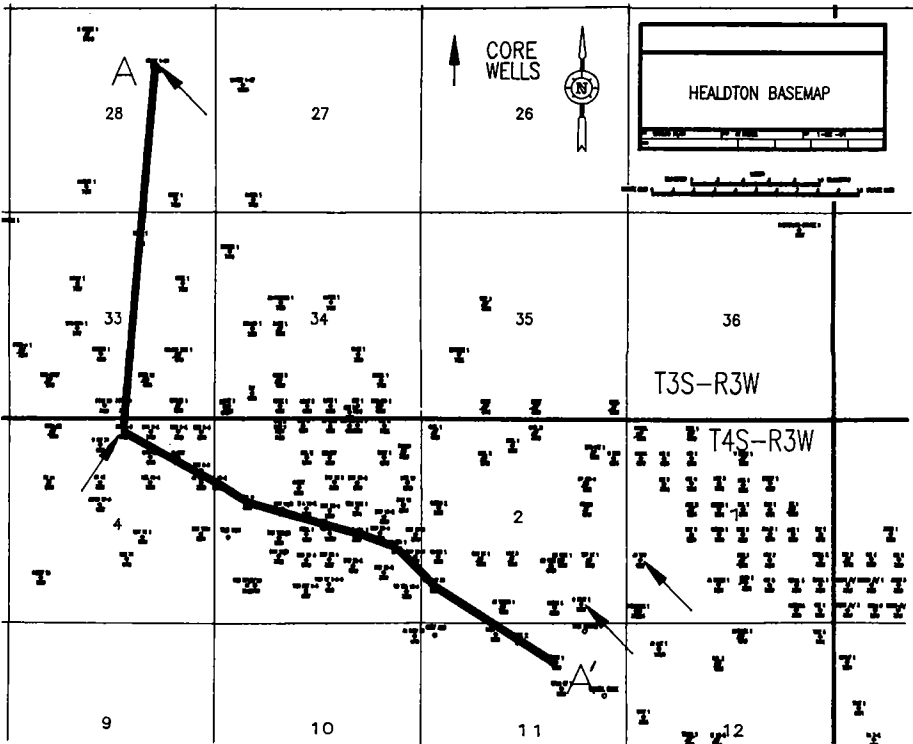


Figure 4. Base map of the Healdton field showing location of cores (arrows) discussed in text. Line of cross section A–A’ does not apply to this paper.

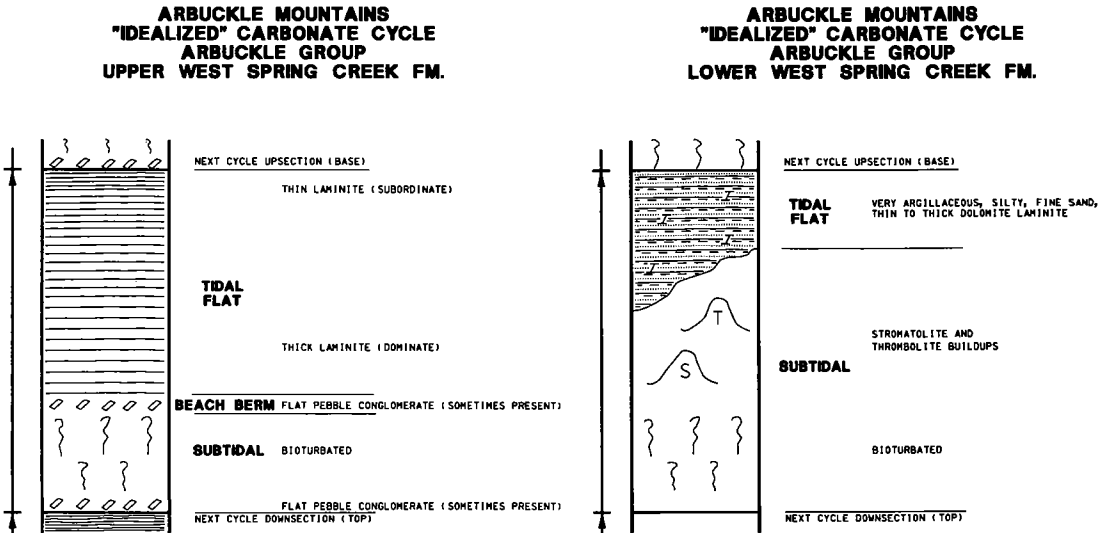


Figure 5. Cycles of deposition in the West Spring Creek (Lindsay and Koskelin, 1991).

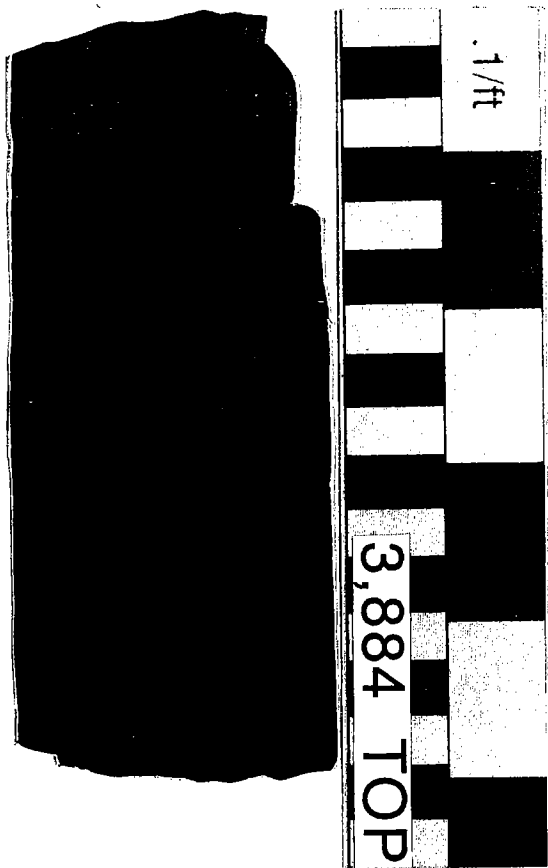


Figure 6. Stylolite and dissolution features along the bedding plane of algal stromatolites in the Bray zone.

102,447 BOPD. The Brown zone was wet. The lack of karst development in the Bray zone in the Geneva Bray well is attributed to the preservation of the original depositional fabric: primarily carbonate-mud-rich strata that would have inhibited the flow of karst-forming waters.

Brown Zone Core Description

HAU No. 5-3

In contrast to the Wade and Bray zones, the Brown zone underwent extensive dolomitization that created a preexisting porous and permeable conduit system for the flow of dolomitizing and karst-developing waters. The extensive dolomitization and karst development of the Brown zone could be related to the subtle differences in depositional facies between the upper and the lower West Spring Creek (Lindsay and Koskelin 1991). The Brown zone core was taken from the HAU no. 5-3, located in sec. 4, T. 4 S., R. 3 W., Carter County (Fig. 4). The cored interval covers the lower Bray zone and all of the productive Brown zone.

The Brown zone originally contained depositional facies similar to those found in the Wade and the Bray zones, but the majority of the strata have been heavily dolomitized and brecciated. The following facies terminology is based partially upon Keran's (1989) study of the West Texas Ellenburger Group, where an unconformity exists just above karst breccia:

Lithofacies	Description
Crackle breccia	Network of fractures, strata are still intact, few to no loose clasts
Mosaic breccia	Grid of individual clasts, some partially rotated, heavily fractured
Chaotic breccia	Two types: one that is primarily clast supported, and one that is breccia clast and fine-karst fill (fine, silty micrite)
Vuggy dolo-mudstone	Dolomitized strata that could be fabric selective, porous, and permeable
Green silty fill	Green silty micrite, high neutron-log response

Vuggy dolomite may have been the dominant early-porosity system, formed by uplift before a depositional hiatus occurred. This fabric has the highest visible porosity and permeability in core and thin section (the largest porosity value, aside from the large-cavern development). This fabric is probably a relict of algal structures that have been dolomitized (Liu, personal communication, 1991).

PALEOKARST INTERPRETATIONS

Kerans (1989) has related karst breccia to paleo-cave reconstruction, where an unconformity exists at the top of the karstic Ellenburger Group (Fig. 8). Crackle or fracture breccia is a relict of a cave roof. Mosaic breccia can represent both the cave roof and the cave floor. Chaotic breccia is distinguished by whether it is clast supported or matrix supported; the clast supported chaotic breccia is the lower collapse zone, i.e. the cave floor (Kerans, 1989), whereas the matrix-supported chaotic breccia is the upper collapse zone, the top of the internal cave talus. As the cavern enlarges, the weight of the overburden causes the roof to fail and collapse. This collapse adds to previous fractures and has the most impact on the cave roof and floor. The mosaic breccia usually has the highest visible porosity and permeability of all the karst-like breccia (Fig. 9). The crackle breccia can be very tight and the fractures are the only source of porosity and permeability (Fig. 10). The clast-supported chaotic breccia can have high porosity, whereas the matrix-supported chaotic breccia has low porosity and little or no permeability. The green, silty karst fill is interpreted as resulting from periodic (flood) cavern deposition. Soft-sediment deforma-

tion and seasonal varves indicate that periods between deposition were relatively short (Fig. 11).

KARST BRECCIA AND WELL-LOG RESPONSE

Kerans (1989) also showed the relation of karst development to well-log response. This method also was applied to the HAU no. 5-3 GR-CNL/FDC log. The karst breccia has a ragged, high response on the CNL and GR logs due to the high clay content of the breccia infill. The vuggy dolomite has a lower and smoother response. The green silty fill has a very high neutron response.

LATERAL HETEROGENEITY OF THE BROWN ZONE

One of the purposes of this study was to determine the vertical and lateral extent of dolomitic and karstic development within the upper Arbuckle Group (Wade, Bray, and Brown zones). The above core studies showed that vertical dolomitization and karst development is primarily confined to the Brown zone. Wellsite observations (Latham, personal communication, 1991), cross sections, and production history indicate that the Brown zone reservoir is dolomitized and has karst-like occurrences throughout the Healdton field. However, examination of core that is the stratigraphic equivalent of the Brown zone in the Shell Chase no. 1-28 well, 2 mi north of the Healdton field, indicates a lithologic and stratigraphic contrast to the upper Arbuckle in the Healdton field.

Core Examination of the Shell Chase No. 1-28

The Shell Chase no. 1-28 (sec. 28, T. 3 S., R. 3 W., Carter County) was cored from 16,900 to 17,220 ft, which is within the stratigraphic equivalent of the Brown zone. The available cores (16,900–17,200 ft) were examined (using hand samples) for the presence of karst-like breccia, vugular porosity, and general lithologic characteristics. The cored interval in the Shell Chase no. 1-28 is primarily dark-gray to black carbonate muds. Karst breccia is not present, and depositional fabrics of the primarily limestone interval are intact. A stratigraphic cross section was constructed from the Shell Chase well to wells throughout the Healdton field, using the top of the Arbuckle marker as the datum. Bray zone and Brown zone markers also were correlated across the field. The interval from the top of

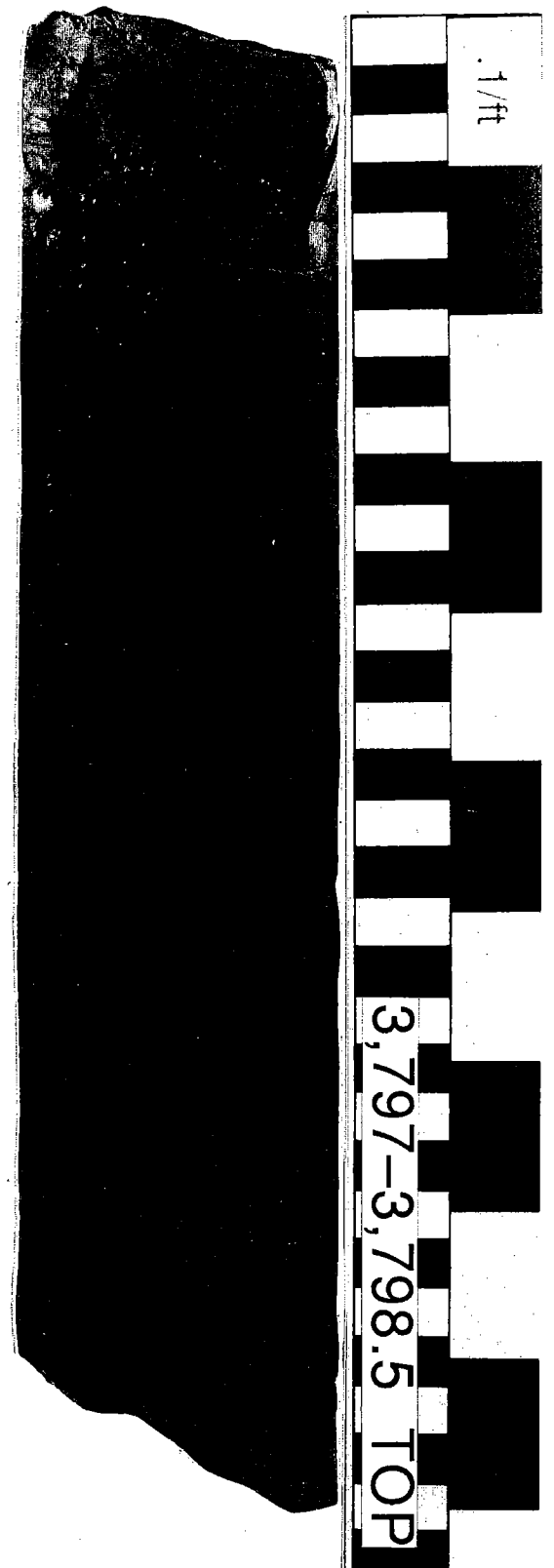
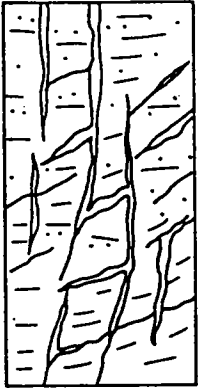
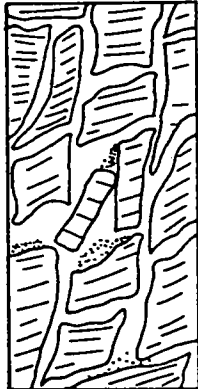


Figure 7 (right). Fractured lime mudstone with solution pipe that was filled by breccia and muddy lime sediments. Core from Bray zone in the Geneva Bray no. 1 well.

**FRACTURE BRECCIA**

- Fabric** dense fracture network defines clasts; no significant rotation of clasts
- Clasts** incipient clasts composed of single host dolomite type; highly angular outline
- Cements** minor to pervasive saddle dolomite with rare anhydrite and calcite
- Internal Sediment** rare geopetal dolomicrite and fine siliciclastics
- Porosity** 1-15%

**MOSAIC BRECCIA**

- Fabric** fitted, clast-supported, discrete clasts displaying minor rotation
- Clasts** angular to slightly rounded, monomict dolomite of host lithology; usually 5-10 cm
- Cements** common saddle dolomite rim cement, rare anhydrite, calcite, and quartz
- Internal Sediment** geopetal dolomicrite and fine-grained siliciclastics
- Porosity** 2-20%

**CHAOTIC BRECCIA, SILICICLASTIC MATRIX-SUPPORTED**

- Fabric** randomly oriented clasts in massive, upward-fining or upward-coarsening units 10-200 cm thick
- Clasts** angular to rounded dolomite derived from various facies, chert, sandstone, and shale fragments; 1-50 cm
- Matrix** mixture of shale, very fine to medium-grained siliciclastic sand, and minor dolomicrite and glauconite
- Cements** minor dolomite cement in shale matrix
- Internal Sediment** none
- Porosity** 1-3%

**CHAOTIC BRECCIA-CARBONATE CLAST-SUPPORTED**

- Fabric** randomly oriented clasts in massive units tens of cm to several m thick
- Clasts** angular to rounded dolomite and rare chert fragments from a variety of depositional facies juxtaposed; 5-50 cm
- Cements** well-developed saddle dolomite rims with rare anhydrite, calcite, quartz, pyrite, marcasite
- Internal Sediment** geopetal dolomicrite with rare, fine-grained siliciclastics typically perched on clasts, but can fill intraclast space completely as a sieve-fill matrix
- Porosity** 1-15%

QA10164

Figure 8. Karst-breccia terminology (from Kerans, 1989).

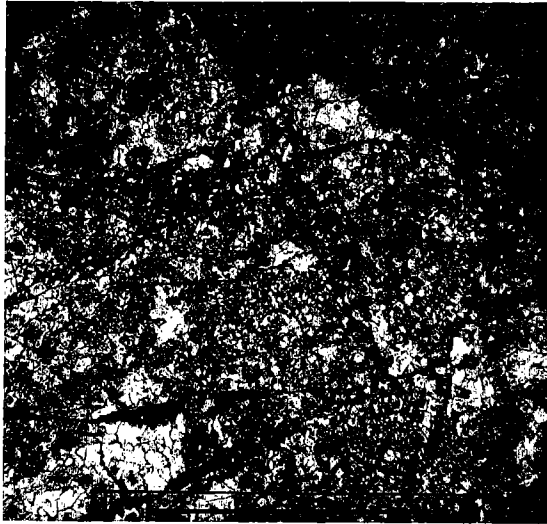


Figure 9. Thin section showing mosaic breccia from the Arbuckle Brown zone in the HAU no. 5-3 well; bar scale is 2 mm long.

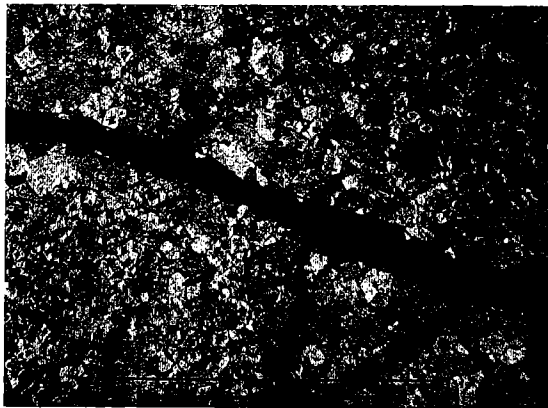


Figure 10. Thin section of crackle breccia from Arbuckle Brown zone in the HAU no. 5-3 well; bar scale is 2 mm long.

the Bray zone to the top of the Brown zone was determined in order to test the relationship of interval thinning to karst and dolomite development.

The interval from the top of the Bray zone to top of the Brown zone has an average thickness across the Healdton field of 600 ft, but the stratigraphically equivalent interval in the Shell Chase well is 710 ft thick. The increase in stratigraphic thickness is attributed to the Bray zone having been deposited in a paleotopographic low north of the Healdton field. This interpretation is supported also by the change in lithology of the Brown zone from the Healdton field to the Shell Chase well.

The Brown zone was the substrate for the Bray zone at the time of deposition. The lithologic change from shallow-water carbonate and dolomite lithology in the Healdton field to a dark, subtidal carbonate-mud (Fig. 12) lithology in the Shell Chase well reflects the 110-ft change in water depth. Reading and Sellwood (1986) show that a change of 30–45 m (roughly 98–148 ft) in modern environments is enough to change from a predominantly shallow, upper intertidal facies to a deep-water lagoonal facies that resembles what is associated more often with the pelagic realm. Therefore, no depth greater than the estimated 110 ft (even without taking compaction into consideration) was necessary for the lithology of the Brown zone equivalent in the Shell Chase no. 1-28 to maintain the dark, quiet-water limestone depositional fabric.

FRACTURING AND LITHOLOGIES

Field and experimental studies conducted by Stearns and Friedman (1972) have shown the relationship between brittle and ductile behavior of different lithologies. Fracture indices, the number of fractures found per 100 ft (laterally), show that dolomite has the second highest fracture index, exceeded only by quartzite (Fig. 13). In contrast, limestone is much more ductile and has a much lower fracture index.

The Wade, Bray, and Brown zone cores examined were primarily from separate wells; the Wade and Bray limestone units had fewer fractures than the underlying Brown zone. Jack Latham (personal communication, 1991) states that the Naomi Freeman no. 17 (sec. 2, T. 4 S., R. 3 W.) cored the entire Wade, Bray, and Brown zones (the physical location of the actual core is unknown). He recorded a marked increase in the degree of fracturing in the dolomitic Brown zone, compared to that in the overlying limestone units. The fracture system would have added only 1–3% to the total porosity, but it would have enhanced the permeability greatly. The enhanced permeability would be important to present-day reservoir production; it also would have served as a conduit system for late-stage karst waters and hydrocarbon migration. The extensive fracture network also is supported by the uniform oil/water contact in the Brown zone throughout the Healdton field that produces from several distinct fault blocks (Fig. 14).

Early dolomitization of the Brown zone created a preexisting porosity system that provided a conduit for karst-forming fluids. Although there is minor porosity in the Wade and Bray zones, it is not comparable to that in the Brown zone; thus, the Brown zone offered the permeability path of least resistance. The brittle, silty, dolomitic Brown zone had greater susceptibility to fracturing, in contrast to the overlying limestone units (Stearns

and Friedman, 1972). Finally, the Morrowan uplift provided further relief and tectonic fractures, which could have enhanced later karst development and given the reservoir 1,500 ft of closure (Latham, 1968).

DEPOSITIONAL AND DIAGENETIC MODELS FOR THE BROWN ZONE IN THE HEALDTON FIELD

The first dolomitization event in the Arbuckle Group Brown zone probably occurred soon after, or possibly during, deposition of the silty Brown zone on a paleotopographic high of the Healdton field. This dolomitization enhanced the porosity of some of the shallow, intertidal silty facies and created a porosity system prior to the first karst-development event. The rock is so heavily dolomitized that the nature of the original fabric is largely interpretive. However, the dolomitization seems to cut across all recognizable rock types deposited in the supratidal, intertidal, and upper subtidal environments.

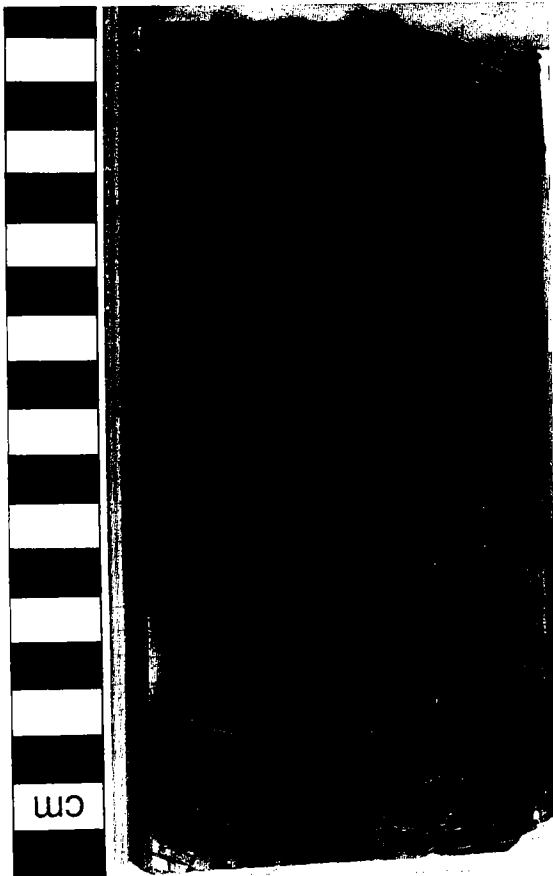


Figure 11. Green, silty karst fill with soft-sediment deformation and varve-like appearance.

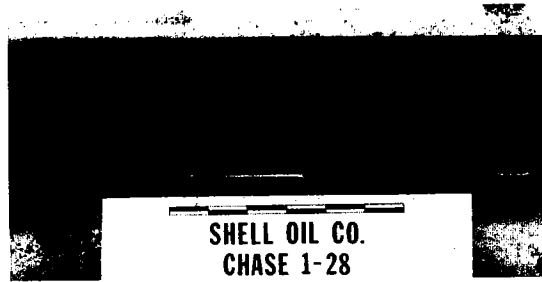


Figure 12. Black carbonate mudstone from the Shell Chase no. 1-28. Courtesy of Mark Potts.

Dolomitization models using a variety of processes have been proposed. The following discussion presents the relevant models that could be applied to the Arbuckle Brown zone for both surface dolomitization and deep-burial dolomitization. The seepage-reflux and evaporative-pump models certainly are applicable to the early, shallow geologic setting, and the development of hydrothermal dolomite is evidence for late-stage alteration in the Brown zone.

Proposed Model for Early Dolomitization of the Brown Zone in the Healdton Field

Both the evaporative-pump and the seepage-reflux models require a topographic high and a backwater lake or lagoon in order to develop the dense, magnesium-saturated brine necessary for dolomitization to occur, although Land (1985) states that ordinary seawater is sufficient to promote dolomitization.

The seepage-reflux model could be applied to the Healdton field. The field would have been a paleotopographic high adjacent to restricted waters (lagoons) that would have supplied the dolomitizing fluids (Fig. 15).

In the evaporative-pump model, a freshwater lens would have developed periodically on the topographic high and evaporated during the day. The brine would have flowed through the permeable limestone strata and dolomitized the topographical highs in the Healdton field (Fig. 16).

Selective dolomitization of the Brown zone, in comparison to the entire section of upper Arbuckle strata, might have been complemented by an abundant magnesium source, possibly the uplift and/or exposure of a magnesium-rich rock formation. Also, particularly long periods of constant sea level would have produced restricted lagoons that could have generated the fluids necessary to dolomitize the original limestone rock. The dolomitization not only enhanced the porosity of the Brown zone strata, but also created a very brittle formation that would be highly susceptible to fracturing. Although several episodes of dolomitiza-

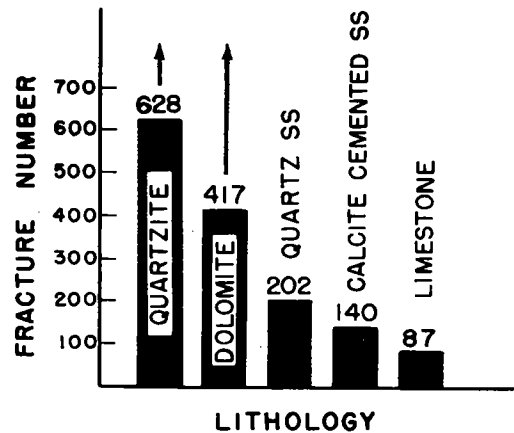


Figure 13. Histogram of fracture frequencies for various lithologies (from Stearns and Friedman, 1972).

tion probably occurred, it was the first dolomitization event that set the framework for all subsequent diagenesis.

Model for Late-Stage Dolomitization

Hydrothermal Dolomitization

Hydrothermal dolomitization is characterized by saddle or baroque dolomite. Saddle dolomite has distinctively curved crystal faces and undulatory extinction (Fig. 17); it forms at temperatures above 185°C (Lee and Friedman, 1987). Saddle dolomite usually occurs as a vug-filling cement in the Arbuckle Group, and is similar to the saddle dolomite in vugs and fractures in the West Texas Ellenburger Group. The magnesium supply for deeply buried carbonates can be: (1) connate water, (2) dissolution of unstable minerals, (3) stylolitization, (4) compaction of shales, and (5) basinal brine (Lee and Friedman, 1987). Basinal brine is the most probable source of magnesium for the deep-burial hydrothermal dolomite in the Arbuckle Group Brown zone.

Saddle Dolomite in the Brown Zone

The southern Oklahoma aulacogen was the failed arm of a rift system (Wickham, 1978). The aulacogen was one of the most tectonically active regions in Oklahoma. Deep-seated stress could have dilated the Brown zone and enhanced the permeability of the silty dolomite. The silty Brown zone was the most permeable reservoir, relative to the overlying and underlying strata, and offered the path of least resistance to the migration of basinal (possibly even magmatic) fluids.

Saddle dolomite occludes porosity in the Arbuckle. In many thin sections examined, bitumen rims the saddle dolomite. The bitumen may have arrested further occlusion of the vugular porosity (Fig. 18). This sequence of dolomitization events

was documented in the Lee and Friedman (1987) study of the West Texas Ellenburger, according to fabric, texture, and temperature of formation. Lynch's (1990) inventory of paleokarstic features categorizes these events similarly for the Oklahoma cores he examined.

In the authors' opinion, the formation of saddle dolomite requires a preexisting porosity system that is quite vuggy in places. The limestone cores examined from the Wade and Bray zones have little or no porosity; the largest pore size is associated with the dolomites in the Brown zone. Therefore, initial shallow dolomitization, and subsequent dilatent, porosity development was an important control on late-stage diagenetic alteration.

SUMMARY AND SEQUENCE OF BROWN ZONE DOLOMITIZATION AND KARST DEVELOPMENT EVENTS

This section briefly summarizes and sequences the possible scenarios for the Brown zone dolomitization and karst development events:

- 1) Deposition of the Arbuckle Group Brown zone occurred in a tidal-flat environment on a carbonate ramp, a shallow, quiet-water setting.
- 2) Early diagenetic dolomitization occurred soon after the Brown zone was deposited on a paleotopographic high in what is now the Healdton field. Many dolomitization models incorporate topographic highs as the locus for diagenetic alteration. The Shell Chase no. 1-28 well provides evidence for a deeper water environment to the north, where carbonate muds occur with original depositional fabric intact.
- 3) Possible karst development of the Arbuckle Brown zone by meteoric waters occurred before deposition of the Bray zone. This karst model would place the Brown zone under subaerial exposure, the position most directly accessible to introduction of karst waters.
- 4) Deposition of the Wade and Bray zones was followed by the Early Ordovician regional unconformity. This second order unconformity is recognized from the Hueco of Arizona to the Knox Group of Tennessee. In Lynch's (1990) insoluble-residue studies, he found no paleontological evidence to positively identify either karst within the Arbuckle (possibly due to the limits of Ordovician faunal resolution) or at the Early Ordovician unconformity. However, the karstic Arbuckle Group in the Cushing field has an abundance of conodonts of Pennsylvanian age directly above the Arbuckle unconformity, but not within the Arbuckle strata. Although this is negative evidence, it does seem to suggest karst development during or before the Early Ordovician unconformity.
- 5) During the subsidence and burial of Cambrian-Ordovician sediments, diagenetic events occurred that are reflected in the dolomitization

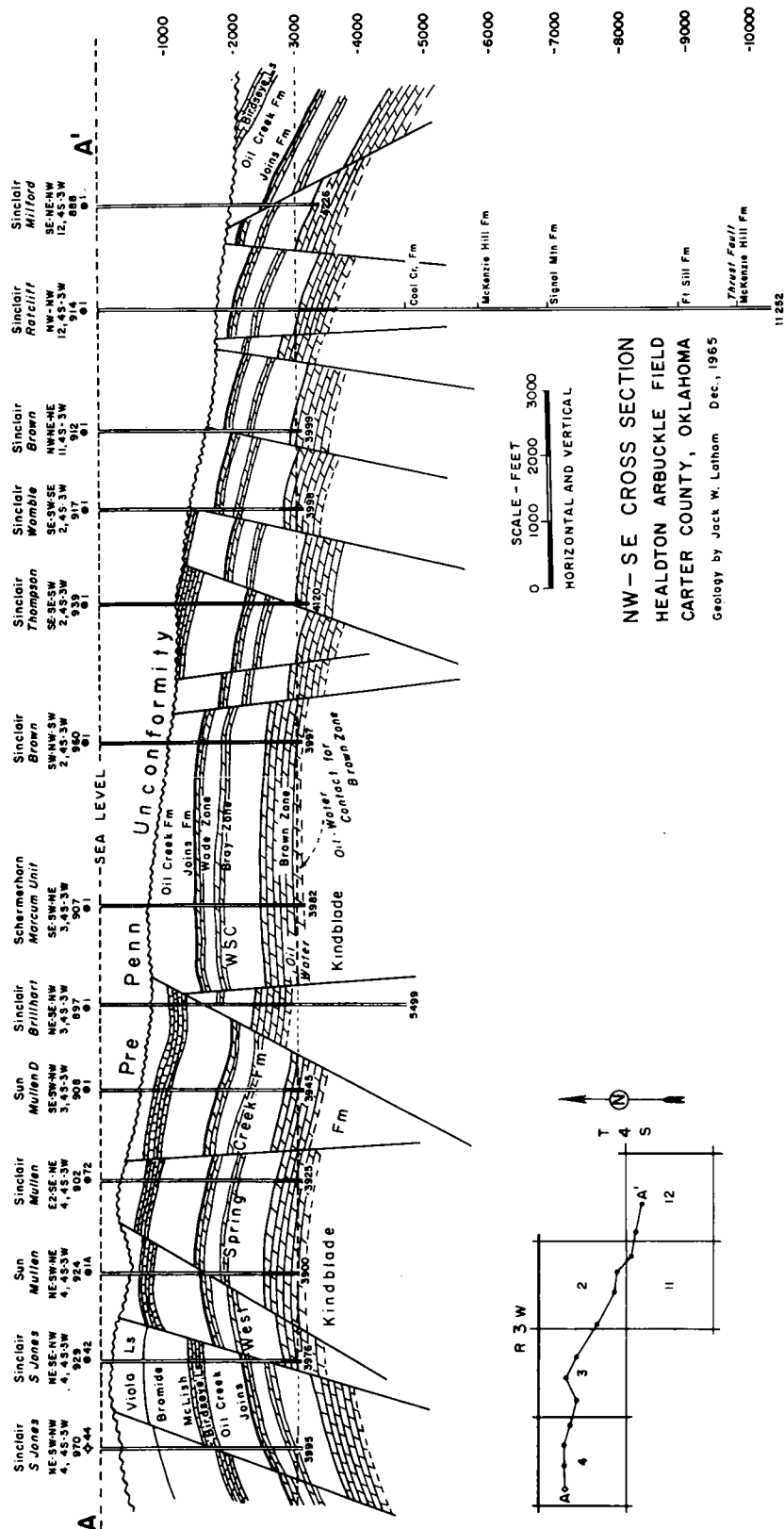


Figure 14. Cross section through Haldton field (from Latham, 1968).

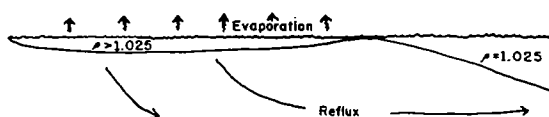


Figure 15. Seepage-reflux mechanism for supplying magnesium for extensive dolomitization.

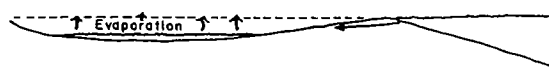


Figure 16. Evaporative-pump mechanism for supplying magnesium for extensive dolomitization.

and cement stratigraphy. Hydrothermal karst development also could have occurred in this time period. Hydrothermal karst is defined by Dzulynski (1976) as a "system of caverns produced by hot waters of any origin and the associated deformational and mineralogical features that are consequent upon the passage of aggressive hydrothermal solutions."

6) Uplift and possible meteoric karst development in the Healdton field occurred during the Morrowan.

7) Migration of hydrocarbons was accompanied by arresting of dolomite cement. Hydrocarbons are the last fluid-migration event, and they arrest the further occlusion of pores by saddle dolomite.

The magnitude of each diagenetic event is difficult to discern. The position taken by the authors is that the possibility and opportunity existed for each of the events to have occurred. Further sampling of more cores, and in-depth geochemical studies (such as Kupecz's [1989] dissertation on the West Texas Ellenburger Group), will provide a better framework upon which to base the timing of this sequence of events.

CONCLUSIONS

1. The Brown zone has undergone extensive dolomitization, whereas the Wade and Bray zones have their original depositional fabric predominantly intact.

2. The Wade and Bray zones show comparatively little, or very localized, karst development, if any, and little to no effective matrix porosity and permeability. In contrast, a dolomitic Brown zone reservoir, with a preexisting porosity system, had the capacity to act as an aquifer for karst-developing fluids.

3. The Brown zone has had major karst development. Opportunities for both meteoric and basinal-fluid karst (and dolomitization) development have existed for a great amount of time. The

time for karst development is from after deposition of Brown zone strata to the pre-Atokan unconformity.

4. In the Brown zone, a depositional transition zone exists between the Healdton field and the Shell Chase no. 1-28 well, ~4 mi north of the Healdton field. The Brown zone in the Healdton field was deposited in a shallow-water environment, whereas at the location of the Shell Chase well, the stratigraphic equivalent of the Brown zone is a carbonate mud with its original deep-water depositional fabric still intact.

5. Fault planes and fracture networks provided an effective permeability pathway for karst fluids to enter the Brown zone.

6. Most Arbuckle Group fields occur in a fractured and/or karstic dolomite, or in a heavily fractured and karstic limestone and dolomite. (Dolo-



Figure 17. Pore-filling saddle dolomite, which is distinguished by undulatory extinction and curved crystal faces; bar scale is 2 mm long.



Figure 18. Saddle or baroque dolomite rimming vug, with infill of brecciated cements and bitumen lining the baroque dolomite cement; bar scale is 2 mm long.

mites have the highest fracture index of all sedimentary rocks.)

7. Saddle dolomite within the Brown zone is an indication that hydrothermal fluids flowed in the Healdton field.

ACKNOWLEDGMENTS

The authors are most grateful for the funding and support received from ARCO Research Center in Plano, Texas. This study would not have been possible without their generous loan of cores used in this study. Additionally, grants from the Oklahoma City Geological Society and from David Read were most appreciated. The authors also acknowledge the help and discussion provided by: Paul Mescher and Doug Schultz, ARCO Research Center, Plano, Texas; Jack Latham, Gainesville, Texas; Pat Medlock, MASERA, Tulsa, Oklahoma; Kelvin Cates, University of Oklahoma, Norman; Mark Lynch, UNOCAL, Houston, Texas; Mark Potts, PSEC, Oklahoma City; David Read, Lakewood, Colorado; Jeff Dravis, Rice University, Houston; and Robert O. Fay, Oklahoma Geological Survey, Norman.

REFERENCES CITED

- Burgess, W. J., 1968, Carbonate paleoenvironments in the Arbuckle Group, West Spring Creek Formation, Lower Ordovician, in Oklahoma: Columbia University unpublished Ph.D. dissertation, 165 p.
- Dwight's Energy Data Inc., 1993, Petroleum Data System (PDS): Available from Dwight's Energy Data Inc., Oklahoma City.
- Dzulynski, Stanislaw, 1976, Hydrothermal karst and Zn-Pb sulfide ores: *Annales de la Societe Geologique de Pologne*, v. XLVI 1-2, p. 217-230.
- Elmore, R. D.; and Crawford, Lisa, 1990, Remanence in authigenic magnetite: testing the hydrocarbon-magnetite hypothesis: *Journal of Geophysical Research*, v. 95, no. B4, p. 4539-4549.
- Fay, R. O., 1989, Geology of the Arbuckle Mountains along Interstate 35, Carter and Murray Counties, Oklahoma: Oklahoma Geological Survey Guidebook 26, 50 p.
- Frederickson, E. A., 1957, Geologic map of the Criner Hills area, Oklahoma: Oklahoma Geological Survey Map GM-4, scale 1:20,000.
- Gatewood, L. E., 1979, Arbuckle environments: models and examples: *Shale Shaker Digest*, v. 29.
- Hicks, I. C., 1971, Southern Oklahoma folded belt: American Association of Petroleum Geologists Memoir 15, v. 2, p. 1070-1077.
- Kerans, Charles, 1989, Karst-controlled reservoir heterogeneity and an example from the Ellenburger Group (Lower Ordovician) of West Texas: University of Texas, Bureau of Economic Geology Report of Investigations 186.
- Kupecz, J. A., 1989, Petrographic and geochemical characterization of the Lower Ordovician Ellenburger Group, West Texas: The University of Texas at Austin unpublished Ph.D. dissertation.
- Land, L. S., 1985, The origin of massive dolomite: *Journal of Geological Education*, v. 33, p. 112-125.
- Latham, J. W., 1968, Petroleum geology of the Arbuckle Group (Ordovician), Healdton field, Carter County, Oklahoma: American Association of Petroleum Geologists Bulletin, v. 52, p. 3-20.
- Lee, Y. I.; and Friedman, G. M., 1987, Deep burial dolomitization in the Ordovician Ellenburger Group carbonates, West Texas and southeastern New Mexico: *Journal of Sedimentary Petrology*, v. 57, p. 544-557.
- Lindsay, R. F.; and Koskelin, K. M., 1991, Arbuckle Group depositional parasequences, southern Oklahoma, in Johnson, K. S. (ed.), Late Cambrian-Ordovician geology of the southern Midcontinent, 1989 symposium: Oklahoma Geological Survey Circular 92, p. 71-84.
- Lynch, Mark, 1990, Evidence of paleokarst and burial diagenesis in the Arbuckle Group of Oklahoma: Oklahoma State University unpublished M.S. thesis.
- Olson, R. A., 1984, Genesis of paleokarst and strata-bound zinc-lead sulfide deposits in a Proterozoic dolostone, northern Baffin Island, Canada: *Economic Geology*, v. 79, p. 1056-1103.
- Read, D. L.; and Richmond, G. L., 1993, Geology and reservoir characteristics of the Arbuckle Brown zone in the Cottonwood Creek field, Carter County, Oklahoma, in Johnson, K. S.; and Campbell, J. A. (eds.), Petroleum-reservoir geology in the southern Midcontinent, 1991 symposium: Oklahoma Geological Survey Circular 95, p. 113-125 [this volume].
- Reading, H. G.; and Sellwood, B. W., 1986, Sedimentary environments and facies: Blackwell Scientific Publications, p. 283-342.
- Stearns, D. W.; and Friedman, Melvin, 1972, Reservoirs in fractured rocks: American Association of Petroleum Geologists Memoir 16, p. 82-106.
- Wickham, J. S., 1978, The southern Oklahoma aulacogen, in Visser, G. S.; Stone, C. G.; and Haley, B. R. (leaders), Structure and stratigraphy of the Ouachita Mountains and the Arkoma basin: Oklahoma City Geological Society Guidebook, p. 1-34.

Paleokarstic Features and Reservoir Characteristics of the Hunton Group in Central and Western Oklahoma

Felicia D. Matthews and Zuhair Al-Shaieb

Oklahoma State University
Stillwater, Oklahoma

ABSTRACT.—Numerous cores of Upper Ordovician, Silurian, and Lower Devonian Hunton Group reservoirs exhibit distinct paleokarstic features. The primary purpose of this investigation is to provide an inventory of the types of paleokarstic reservoirs observed in the Hunton Group in central and western Oklahoma.

Cores from various localities in central and western Oklahoma exhibit a variety of paleokarstic and other diagenetic features. Vuggy porosity, solution-enlarged fractures, breccias, and sediment in nondepositional cavities were commonly observed. Based on information and data obtained, paleokarstic Hunton reservoirs may be classified into two types. Type 1 Hunton paleokarstic reservoirs are dominant in fractured tight lithologies in which ground-water flow was focused along fractures and bedding planes. Features observed in type 1 reservoirs represent main-to-late stages of karst development, such as solution-enlarged channels, cavern-fill parabreccia, and collapse breccias. Type 2 Hunton paleokarstic reservoirs formed in facies with initial interparticle porosity by diffuse ground-water flow that enhanced pre-existing interparticle porosity and created extensive vugular porosity. It is important to note that, in this study, type 2 paleokarstic reservoirs are the major hydrocarbon-bearing reservoirs.

The timing of the karstification in most of the cores appears to have been associated with the pre-Woodford unconformity. One core contains a possible disconformity surface below the Hunton–Woodford contact.

INTRODUCTION

The one aspect of karst most commonly recognized in the geological record is extensive subsurface dissolution in the form of caves and associated cavities (Choquette and James, 1988). The purpose of this study was to search for and report paleokarstic features and reservoir characteristics observed in subsurface rocks of the Hunton Group in central and western Oklahoma. These carbonate rocks have been important producers of oil and gas in Oklahoma for many years, and fields with Hunton production are located throughout the area of study. This investigation is designed to explain the relationship between paleokarst and the development of Hunton reservoir rocks.

The location of the study area includes much of central and western Oklahoma and encompasses the following tectonic provinces: northern Oklahoma platform, Anadarko basin, central Oklahoma platform, and Hunton–Pauls Valley uplift. It is limited to the north and east by the Hunton truncation, to the south by the Wichita and Arbuckle uplifts, to the southeast by the Arkoma basin, and to the west by the Texas state line (Fig. 1).

Of the 140 Hunton cores examined for evidence of paleokarst, 12 cores that exhibited significant karstic features were selected for further intensive study. They were photographed and their depositional, karstic, and diagenetic features described using petrologs designed at Oklahoma State University for karstic rocks (Pls. 1,2). Thin sections were prepared for petrofabric analysis. Cross sections were constructed to correlate karstic features with stratigraphy and to show the extent of possible intra-Hunton unconformities. Table 1 gives the well name and location, cored interval, formation name, and number of thin sections examined for each core.

Many researchers have investigated Hunton rocks, and the subject of unconformities and possible karst in the Hunton has been presented in various publications. Hunton strata were first named by Taff (1902) in his work on the geology of the Atoka Quadrangle. Reeds (1911) refers to stratigraphic “breaks”—the “times of no deposition as well as eroded sediments”—before and after the Chimneyhill, before and after the Henryhouse, and before the Haragan and Bois d’Arc. Others who have discussed possible unconformities in-

Matthews, F. D.; and Al-Shaieb, Zuhair, 1993, Paleokarstic features and reservoir characteristics of the Hunton Group in central and western Oklahoma, *in* Johnson, K. S.; and Campbell, J. A. (eds.), *Petroleum-reservoir geology in the southern Midcontinent*, 1991 symposium: Oklahoma Geological Survey Circular 95, p. 140–162.

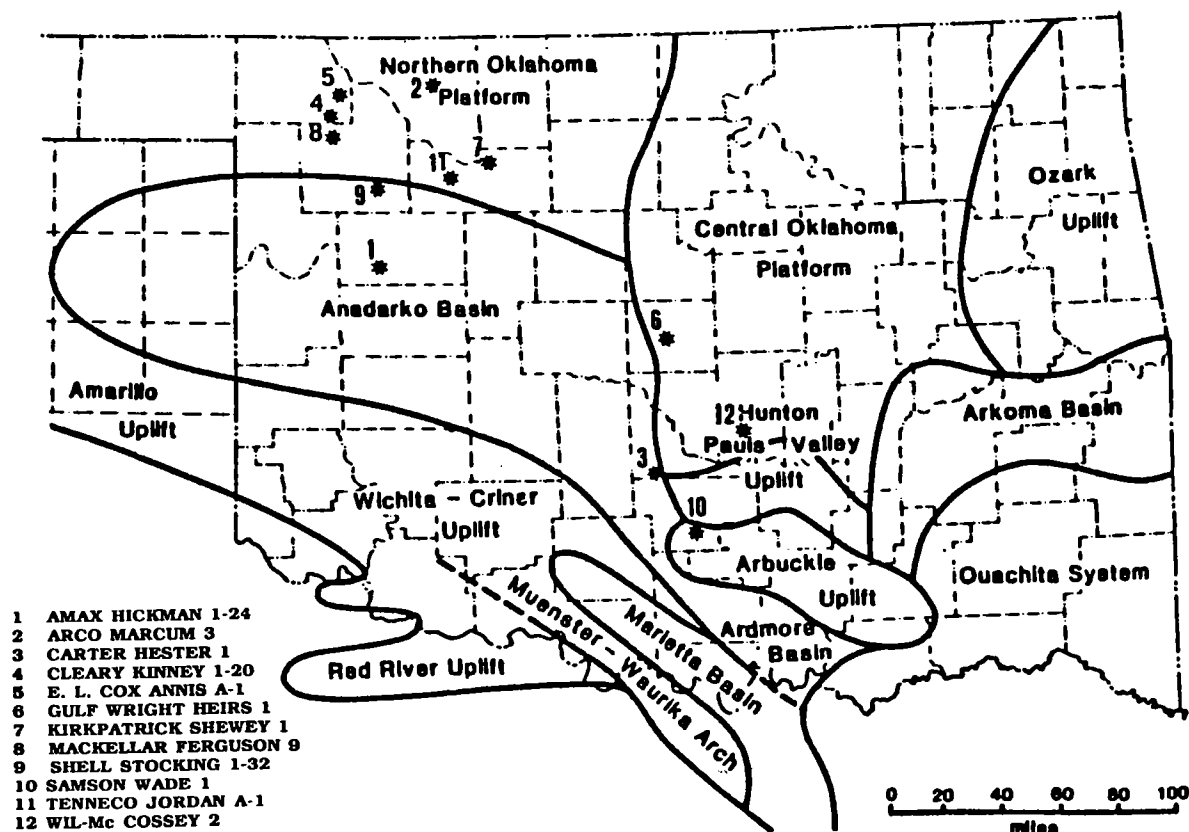


Figure 1. Location of cores used in the study, relative to the tectonic provinces of Oklahoma (after Arbenz, 1956; Al-Shaieb and Shelton, 1977).

clude Maxwell (1936), Anderson (1939), Tarr (1955), Bowles (1959), Maxwell (1959), Amsden (1960, 1975, 1980), Withrow (1971), Manni (1985), and Morgan (1985).

HUNTON STRATIGRAPHY

The Hunton Group in Oklahoma is a series of limestones and dolomites present in the Anadarko basin, central Arkoma basin, and northern Oklahoma platform during Late Ordovician, Silurian, and Early Devonian times. The lower boundary of the Hunton is the top of the Sylvan Shale and the upper boundary is the base of the Woodford Shale or, where present, at the base of the Misener sandstone interval (Fig. 2).

The Hunton Group is composed of seven formations in the study area (Amsden, 1960). In ascending order, from the base, they are the Keel, Cochrane, and Clarita Formations which make up the Chimneyhill Subgroup, and the Henryhouse, Haragan, Bois d'Arc, and Frisco Formations (Fig. 2); the Sallisaw Formation is restricted to eastern Oklahoma. The Woodford/Misener may lie un-



DEVONIAN	MISSISSIPPIAN - UPPER DEVONIAN		WOODFORD SHALE MISENER	
	MIDDLE DEVONIAN			
	LOWER	SAWKILLIAN	SALLISAW FORMATION	
		DEERPARKIAN	FRISCO FORMATION	
HELDERBERGIAN		BOIS D'ARC FM. HARAGAN FM.		
SILURIAN	UPPER	PRIDOLIAN - LUDLOVIAN	HENRYHOUSE FORMATION KIRKIDUM BIOFACIES	
		WENLOCKIAN	CLARITA - ST. CLAIR FMS. PRICES FALLS MEMBER	
	LOWER	LLANDOVERIAN C	COCHRANE - BLACKGUM FMS.	
		LLANDOVERIAN A, B		
ORDOVICIAN	UPPER	HIRNANTIAN	KEEL FORMATION	
		RICHMONDIAN	SYLVAN SHALE WELLING FM.	
		MAYSVILLIAN	VIOLA SPRINGS FM.	
	MID.		VIOLA GROUP	

Figure 2. Stratigraphic column of the Hunton Group in Oklahoma (Amsden, 1989).

TABLE 1. — HUNTON CORED INTERVALS INFORMATION

Well	Location	County/field	Cored interval (depth in feet)	Formation	No. of thin sections
Amax Hickman 1-24	NE $\frac{1}{4}$ SW $\frac{1}{4}$ NE $\frac{1}{4}$ sec. 24, T17N, R18W	Dewey Putnam	13,500–13,550	Henryhouse	0
Arco Marcum 3	NE $\frac{1}{4}$ SW $\frac{1}{4}$ NW $\frac{1}{4}$ sec. 20, T27N, R15W	Woods NW Avard	6,230–6,263	Woodford Shale Chimneyhill Sylvan Shale	7
Carter Hester 1	SW $\frac{1}{4}$ SE $\frac{1}{4}$ sec. 27, T5N, R3W	McClain Golden Trend	7,770–7,782	Chimneyhill	6
Cleary Kinney 1-20	CSW $\frac{1}{4}$ NE $\frac{1}{4}$ sec. 20, T25N, R21W	Harper NE Ft. Supply	8,721–8,760	Cochrane	21
Edwin Cox Annis A-1	CNW $\frac{1}{4}$ NW $\frac{1}{4}$ sec. 3, T26N, R21W	Harper Lovedale	7,296–7,364	Woodford Shale Chimneyhill	20
Gulf Wright Heirs 1	NW $\frac{1}{4}$ SW $\frac{1}{4}$ NW $\frac{1}{4}$ sec. 5, T12N, R2W	Oklahoma Wicher	6,305–6,338	Misener sandstone Frisco Henryhouse	5
Kirkpatrick Shewey 1	SW $\frac{1}{4}$ NE $\frac{1}{4}$ sec. 28, T22N, R12W	Major Ringwood	7,895–7,932	Henryhouse	13
MacKellar Ferguson 9	SW $\frac{1}{4}$ NE $\frac{1}{4}$ sec. 35, T24N, R21W	Woodward NE Woodward (wildcat)	9,739–9,776	Clarita Cochrane Sylvan Shale	31
Samson Wade 1	SE $\frac{1}{4}$ SW $\frac{1}{4}$ sec. 33, T2N, R1W	Garvin Golden Trend	6,008–6,051	Henryhouse	9
Shell Stocking 1-32	SE $\frac{1}{4}$ NW $\frac{1}{4}$ sec. 32, T22N, R19W	Woodward Moser area (wildcat)	10,247–10,321	Henryhouse	24
Tenneco Jordan A-1	SW $\frac{1}{4}$ NE $\frac{1}{4}$ sec. 3, T21N, R14W	Major Cheyenne Valley	8,495–8,613	Henryhouse	5
Wil- McCossey 2	E $\frac{1}{2}$ NE $\frac{1}{4}$ NE $\frac{1}{4}$ sec. 21, T7N, R2E	Pottawatomie W Moral	5,060–5,066	Haragan or Bois d'Arc	5

conformably on any of the Hunton units, or on older rocks where the entire Hunton Group was removed prior to Woodford deposition (Morgan, 1985). Maximum thicknesses of each formation were assigned by Amsden (1975) as follows: Frisco, 60 ft; Haragan–Bois d'Arc, 325 ft; Henryhouse, 247 ft; Clarita, 45 ft; Cochrane, 57 ft; Keel, 15 ft. The thickness of the Hunton in the Anadarko basin is locally >1,600 ft; the thickness of the group varies widely over the State, due mainly to pre-Woodford erosion and other periods of erosion during Hunton time (Amsden, 1975).

REVIEW OF KARST DEVELOPMENT

The word "karst" is a German adaptation of the Slavic word "Kras," meaning "a bleak waterless place." The classical description of karst was derived from a high plateau in Yugoslavia near the

Adriatic Sea (Ritter, 1986). Esteban and Klappa (1983) state that karst is a diagenetic facies, an overprint in subaerially exposed carbonate bodies, produced and controlled by dissolution and migration of calcium carbonate in meteoric waters, occurring in a wide variety of climatic and tectonic settings, and generating a recognizable landscape. Karst on outcrop is indicated by certain characteristic geomorphic landforms; however, characteristic macroscopic and microscopic features are often discernible in core (Table 2).

Karst terrains develop in carbonate rocks exposed for sufficient durations of time to climatic conditions conducive to chemical weathering (adequate rainfall, warm climate). Climate influences both the degree of dissolution and the type and amount of cementation. Karst developed in humid or tropical climates tends to exhibit well-developed dissolution networks (both vadose and

TABLE 2. — CHARACTERISTIC FEATURES OF KARST
Lynch (1990), modified after Choquette and James (1988)

Stratigraphic	
Karst landforms	
* Unconformities	
* Truncated shallowing-upward cycles	
Macroscopic	
Surface karst	Subsurface karst
Karren	* Caves and dissolution channels
* Paleosoils	* Stratiform breccias
* Caliches	* Collapse structures
* Nonsedimentary channels	* Dissolution-enlarged fractures
* Lichen structures	* Sediment in nondepositional cavities
* Boxwork structure	* Breccias in irregular bodies
* Mantling nonsedimentary breccias	* Speleothems
Microscopic	
* Eluviated soil in small pores	
* Etched carbonate cements	
* Reddened and micritized grains	
* Meniscus, pendant, and needle-fiber vadose cements	
* Subisopachous columnar-calcite phreatic cement	
* Extensive dissolution, or enlargement of fabric-selective pores	
* Features discernable in core.	

phreatic) and extensive vadose and phreatic cementation. Karst in arid climates is typically less developed, with much less cementation and dissolution. Karst terrains may develop an idealized vertical profile that reflects the various hydrogeologic conditions active within the system (Fig. 3).

The idealized "maturation" of a karstic terrain proceeds from an initial stage, through a main stage, to a late stage. The initial stage (Fig. 4A) is dominated by phreatic processes along a static water table. Subhorizontal water movement creates dissolution cavities. As cavities enlarge, flow becomes turbulent and an abrasive component augments dissolution. The main stage (Fig. 4B) is characterized by extensive vadose and phreatic dissolution that excavates large volumes of carbonate rock. Vertical cavities and speleothems develop in the vadose zone. Cave sediments composed of collapse materials, clay residues, and materials washed into the cave from the outside are common. In the late stage (Fig. 4C), the system is now totally above the water table. Distinctive karst landforms such as towers and karrens are formed by extensive collapse and erosion. The erosional processes in each stage are a function of the karst facies relative to a regional or local water table. This model assumes that the carbonate terrain is being slowly uplifted relative to base level (Lynch, 1990).

PALEOKARSTIC FEATURES

Breccias

In "A Classification of Breccias," Norton (1917) wrote:

Few geologic structures so lend themselves to diverse interpretations as the beds of broken rock called breccia. . . . Diagnosis generally requires the use of multiple working hypotheses and may proceed chiefly by the process of elimination.

With this admonition in mind, four types of breccia were identified in the Hunton Group. They are crackle breccia, mosaic breccia, cavern-fill parabreccia, and collapse breccia. In a complete and ideal paleokarstic-sequence, the descending order of appearance of breccia types would be crackle breccia, at the top, followed by mosaic breccia, cavern-fill parabreccia, and collapse breccia, at the bottom.

Crackle breccia was described by Norton (1917) as incipient brecciation in extensively fractured rocks, in which fragments have not been dislodged, rotated, or otherwise moved to any appreciable degree. The term "crackle breccia" is synonymous with the "fracture breccia" of Kerans (1989). In most cases, crackle breccia is indistinguishable from tectonically fractured rock. It is

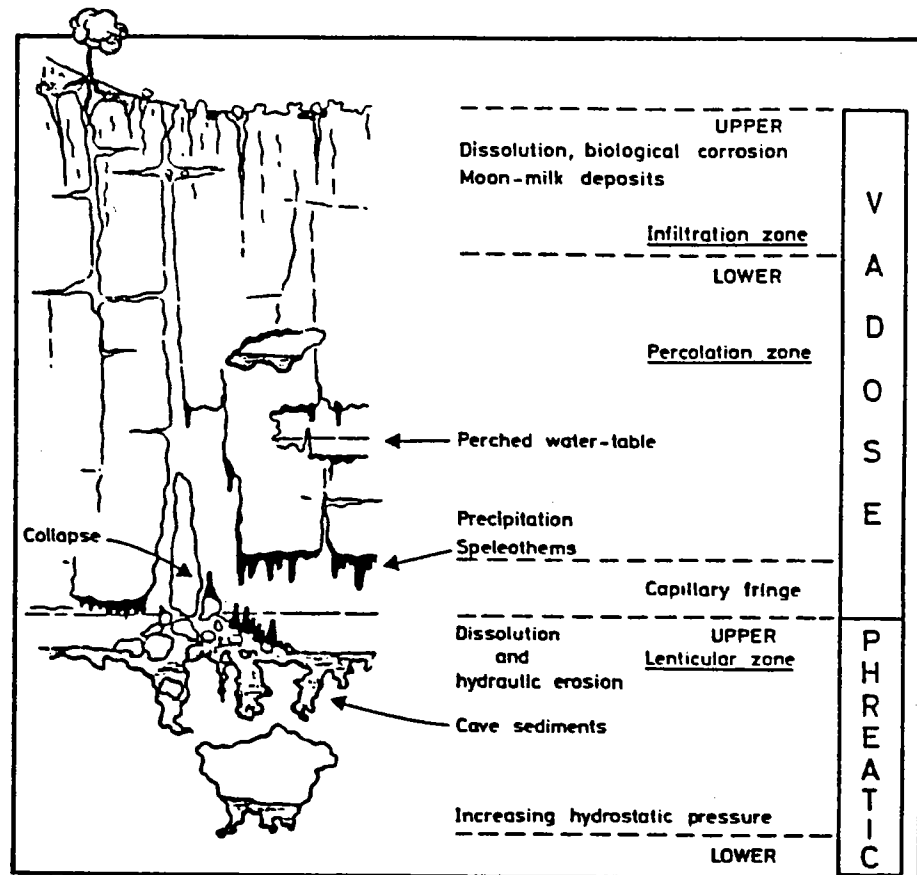


Figure 3. Idealized karst profile (from Esteban and Klappa, 1983).

only through its spatial relation to other karstic features in the core that this type of breccia has any use in karst diagnosis (Lynch, 1990).

The MacKellar Ferguson core, Woodward County (Fig. 5), and the Samson Wade core, Garvin County, contain crackle breccia. In both cores, the interclast fracture porosity present in crackle breccia is occluded by cement or by smaller grains. In the Samson Wade core, microbreccia fills the fractures in the chert crackle breccia at the top of the core.

Mosaic breccia is composed of clasts that have been largely, but not wholly, disjointed and displaced. The clasts still match along adjacent surfaces and show that they are part of a once-unbroken stratum. In the sample from the Cox Annis core in Harper County, the seams are filled with cave sediment, part of which has been pyritized (Fig. 6). Mosaic breccia is visible also in the MacKellar Ferguson core, Woodward County, and the Samson Wade core, Garvin County.

Crackle and mosaic breccias represent in-place brecciation. They correspond to the cave-roof facies of Kerans (1989), which he used in describing the karstified Ellenburger Group. Crackle and mo-

saic breccias in Hunton rocks tend to grade into one another; they represent small areas of the core.

The term *cavern-fill parabreccia* was proposed by Lynch (1990) for poorly sorted, matrix-supported breccias that form by subterranean deposition within an open-cavern network. Cavern-fill parabreccia is used in this report to designate the material between the cave-roof facies (crackle and mosaic breccia) and the collapse-breccia facies covering the cave floor.

The matrix-supported clasts, which can range in size from fine sand to boulder size, may originate in the cavity itself, or be transported by flow of water from other collapse locations within the system. Allochthonous fragments—those from other karst systems or from above ground—can be washed into caverns during periods of flooding. Caves may function as giant sediment traps, accumulating samples of all clastics, organic debris, and products of chemical weathering (Ford, 1988). The Shell Stocking core of Woodward County and the Samson Wade core contain cavern-fill parabreccia (Fig. 7).

Collapse breccia is one of the main indicators of subaerial-karst facies (Esteban and Klappa, 1983).

It is a result of the structural collapse of a cave roof into a previously open cavern. The collapse may be the result of dissolution of evaporites, or the cave roof may founder due to overburden. Collapse breccia in this paper encompasses the "founder" and "cavern" breccias of Norton (1917).

Collapse breccia is characterized by diversity of clasts, poor sorting, and angularity of grains. It is possible that, following deposition, angular clasts

may be subjected to rounding in situ as a result of dissolution by ground water (Kahle, 1988). Clasts in the Hunton collapse breccia are angular to sub-rounded. Components which may be found in collapse breccia include fragments of host rock, broken speleothems, fossils, and infiltrated cavern-fill parabreccia.

Six of the 12 study cores contain significant amounts of collapse breccia, as noted in Table 3.

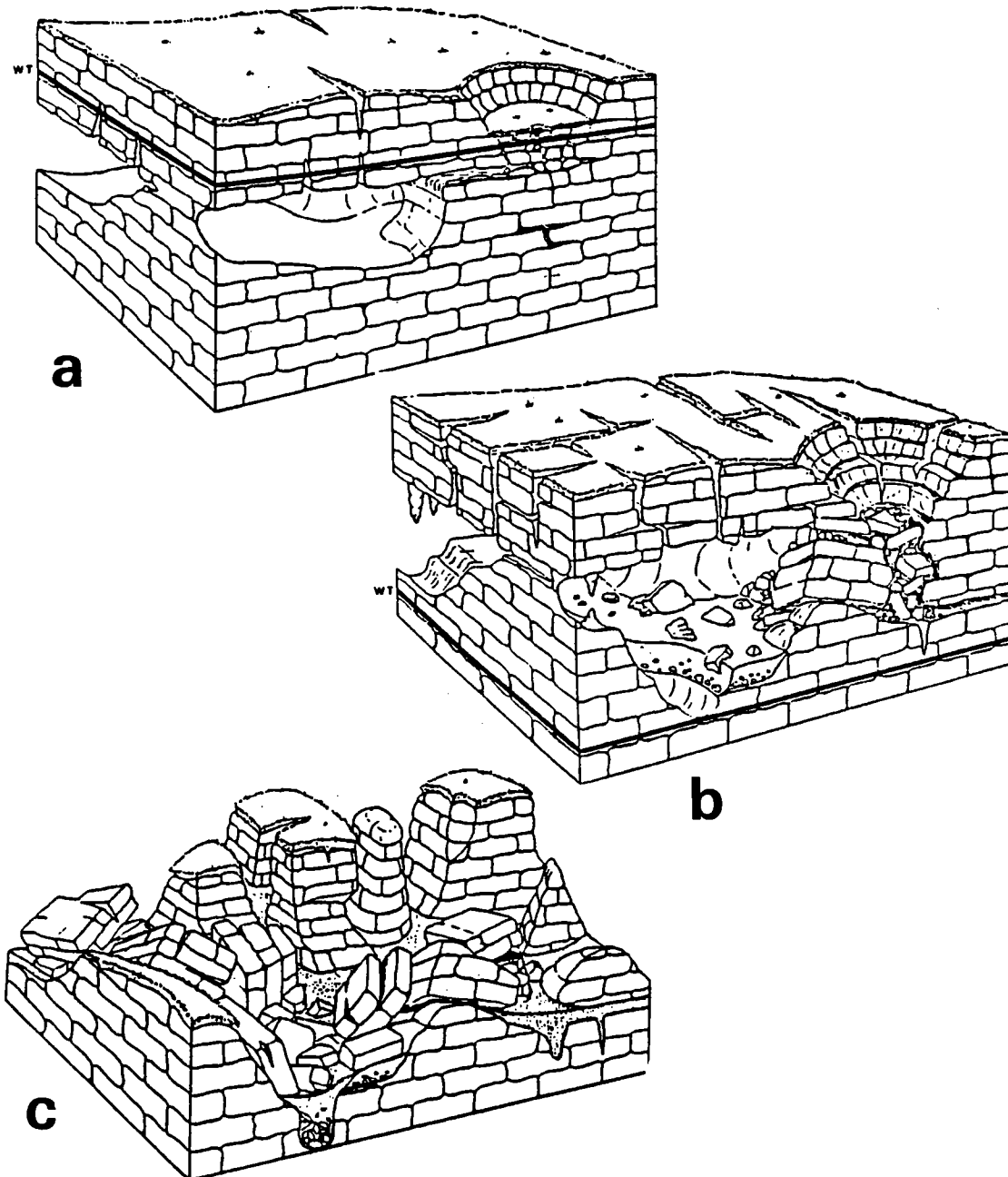


Figure 4. Stages of karst development: (A) initial stage; (B) main stage; (C) late stage. Thick black line A and B represents water table. No scale intended (Lynch, 1990).

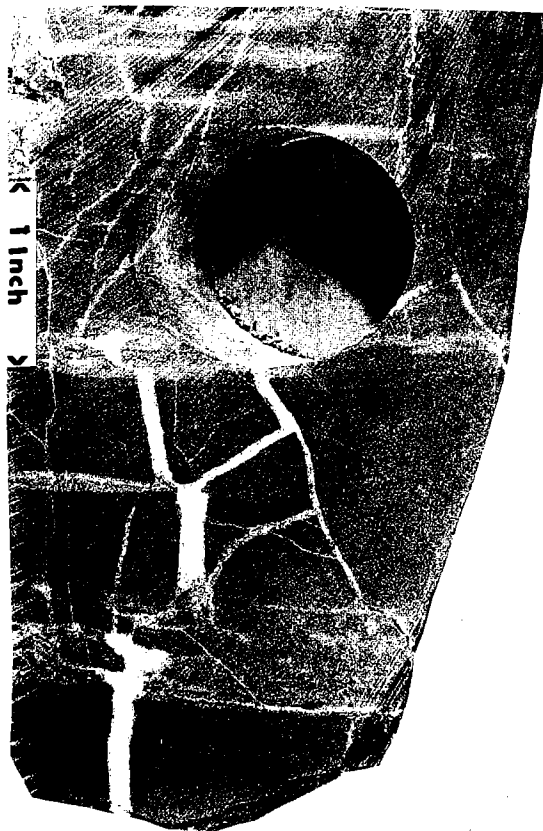


Figure 5. Crackle breccia. Fractured, gray crystalline dolomite. Fractures are filled with baroque dolomite. MacKellar Ferguson core, depth 9,754 ft.

Two examples of this type breccia come from Harper County—the Cox Annis and the Cleary Kinney cores.

The Cox Annis core has 15 ft of dolomite- and chert-breccia, with some visible porosity (Fig. 8). The sample has a rubbly collapse texture with glauconite, some detrital quartz, and dolomite cement. Three types of breccias—mosaic, cavern-fill parabreccia, and collapse—are represented in this core. Fifty feet deeper in the section, a non-porous, packstone shoal facies harbors solution-enlarged vugs that have been filled with dolomite and calcite cement.

The Cleary Kinney core is a pinkish-gray limestone that includes two packstone intervals and a dolomite zone. The top 8 ft of the core is a fine example of collapse breccia (Fig. 9). The angular, poorly sorted grains show no evidence of transport; the fragments are grain supported. Stylolites are common. Several pebble to cobble size fragments appear to be coated with a radiaxial fibrous calcite cement. This cement may indicate the presence of speleothems; in this case, flowstone accumulates on the walls of the host rock.

Dissolution Features

The Hunton cores have abundant paleokarstic dissolution features. This evidence of karstic activity is small enough to be at least partially confined within the diameter of the core. The features are millimeter- or centimeter-scale vugs, solution-enlarged fractures, and channels.

Vugular porosity was observed in at least 40 of the Hunton cores originally examined. Several cores contain outstanding examples of dissolution vugs, partially or completely cemented vugs, and vugs containing geopetal structure.

Examples of vuggy porosity are present in the Kirkpatrick Shewey and Tenneco Jordan cores from Major County, the Arco Marcum core, Woods County, and the Amax Hickman core of Dewey County. Figure 10 shows a sample of highly visible vuggy porosity from the Amax Hickman core.

Solution-enlarged fractures, joints, and channels are ubiquitous in the Hunton rocks. The Carter Hester core, McClain County, illustrates



Figure 6. Mosaic breccia. Chert clasts with dolomite and calcite cement. Pyritization of matrix is a later event. Cox Annis core, depth 7,299 ft.



Figure 7. Cavern-fill parabreccia. Matrix-supported clasts of packstone and mudstone. Samson Wade core, depth 6,032 ft.

small-scale, solution-enlarged fractures now filled geopetally with laminated cave muds, glauconite, and dolomite cement (Fig. 11). The Samson Wade core, Garvin County, contains solution-enlarged channels filled with host rock fragments, chert, and quartz grains. Breccias within elongated channel pores (solution-enlarged joints) are called channel breccias and are formed by subsequent filling of joints by breccia during karstification (Kahle, 1988). The Cleary Gilbert core, Kingfisher County, exhibits a sample of channel breccia (Fig. 12).

Cavern or cave porosity is the largest megapore designation, and it cannot be substantiated in this study because of the limited size of the core samples. However, the former presence of caves may be inferred from the existence of cavern-fill parabreccia and collapse breccia. Even a few feet of heterolithic collapse breccia necessitates a precursor cavity of similar size into which roof rock could collapse.

Infill Sediment

Interesting examples of paleokarstic infill sediment are present in Hunton cores. The Kirkpatrick Shewey core, Major County, holds a 3- × 4-cm vug, geopetally filled with cave-infill sediment. The cavity is lined with silica cement, and contains a

light-colored laminated sediment overlain by a dark-colored laminated carbonate mudstone. The remnant pore space is filled with baroque dolomite crystals (Fig. 13). The same core displays another intriguing infill-sediment feature. Approximately 40 ft below the Hunton-Woodford Shale contact, a 12- × 2-cm Woodford Shale clast resides



Figure 8. Collapse breccia. Dolomite and chert with rubbly, chaotic texture. Some visible porosity is present in the top portion of the sample. Cox Annis core, depth 7,310 ft.

TABLE 3. — HUNTON CORES AND RESERVOIR INFORMATION

Core	Reservoir type	Total core (ft)	Total breccia (ft)	Total vuggy and/or dolomite (ft)	Depth below top Hunton	Scout ticket and completion report
Amax Hickman 1-24	2	50	0	50	131	High Fluid Deliverability IPF: 15,661 MCFGPD
Arco Marcum 3	2	41	0	33	0 (at top)	High Fluid Del. IPF: 744 BOPD
Carter Hester 1	2	13	0	4	320	Show Hunton. Prod. Gibson No Test
Cleary Kinney 1-20	1	39	8	8	0 (at top)	D/A High Fluid Del. DST: Rec. 7,000 ft SW
Edwin Cox Annis A-1	1	69	15	10	0 (at top)	D/A Med. Fluid Del. IFT: 81 BOPD; went to SW
Gulf Wright Heirs 1	2	32	2	13	0 (at top)	Low Fluid Del. IPF: 2 BOPD
Kirkpatrick Shewey 1	2	37	3	34	9	High Fluid Del. IPF: 2,800 MCFGPD
MacKellar Ferguson 9	1	37	14	10	0 (at top)	D/A High Fluid Del. DST: 3,000 MCFLPD + SW
Samson Wade 1	1	44	28	0	10	Low Fluid Del. IPP: 20 BOPD
Shell Stocking 1-32	1	74	21	0	0 (at top)	D/A Low Fluid Del. DST: Low Porosity
Tenneco Jordan A-1	2	118	0	75	0 (at top)	High Fluid Del. IPF: 20 BOPH
Wil-McCossey 2	1	7	2.5	0	20	Low Fluid Del. IPP: 35 BOPD

in a solution-enlarged channel in the Henryhouse section. It is probable that the shale would fill the existing crevasses that certainly existed on the unconformity surface between the Woodford Shale and the Hunton (Fig. 14).

Other evidence of infill sediment from above exists in the Gulf Wright core of Oklahoma County. At the top of the core, 2 ft of breccia contain cobble-sized fragments of Frisco in the Misener sandstone. Beneath the Misener is Frisco grainstone with solution cavities filled with red, hematitic sediment (Fig. 15). The reddish color is due to oxidation, as discussed by Kahle (1988) and is evidence that the sediment infiltrated downward from surface or near-surface oxidizing environments.

Speleothems

Evidence of speleothems is uncommon in Hunton subsurface rocks. However, what appear to be flowstone-covered clasts are present in collapse-breccia samples from the Cleary Kinney core (Fig.

9). The white calcite coating seems to "frost" a large part of one clast and the edges of some of the smaller shards. These examples of possible flowstone in the collapse breccia could be portions of a former cave wall which hosted patches of flowstone before the cave foundered. In the Shell Stocking core, millimeter-sized, silicified particles, akin to broken pieces of flowstone, are seen in thin sections. Despite the "tremendous improbability of actually coring one of these features" (Lynch, 1990), the presence of speleothems in paleokarst cores is not impossible, only improbable.

HUNTON PALEOKARSTIC RESERVOIRS

The carbonate rocks of the Hunton Group have been important producers of oil and gas in Oklahoma for nearly 70 years. Today, fields with Hunton production are established throughout the area of this report. The 12 study cores were classified into two types of reservoirs: type 1 Hunton paleokarstic reservoir and type 2 Hunton paleokarstic reservoir (Table 3).

Type 1 Hunton Paleokarstic Reservoir

Six cores were classified as representative of type 1 Hunton paleokarstic reservoirs. The cores are the Cleary Kinney, Cox Annis, MacKellar Ferguson, Samson Wade, Shell Stocking, and Wil-McCossey.

The Hunton in type 1 paleokarstic reservoirs consists of massive limestone host rocks, such as mudstone or tightly cemented grainstone, with low matrix or interparticle porosity. The flow of ground water is forced to proceed along bedding planes and fractures, caves, and solution-widened joints due to the lack of interparticle porosity within the rock itself (Fig. 16). Kerans (1989) used



Figure 9. Collapse breccia. Some fragments are coated with radial calcite cement which is interpreted to be flowstone. Cleary Kinney core, depth 8,723 ft.



Figure 10. Vuggy porosity in dolowackestone. Sample contains calcite-filled vugs. Amax Hickman core, depth 13,525 ft.

the name "conduit-flow" karst for this type of system. White (1969) used the term "free-flow" karst hydrologic regime. In this study, the term "conduit-flow" paleokarst is adopted for the type 1 reservoir.

Collapse breccia is the most distinctive feature of conduit-flow paleokarst, and all six cores in the type 1 reservoir category contain collapse breccias. The breccia may be stratiform; that is, composed of layers, suggesting several episodes of karstic activity or alternating karstic processes. The Samson Wade core is an example of a stratiform-breccia sequence. Beneath an upper interval of crackle and mosaic breccias, cavern-fill para-breccia and collapse breccias continue in stratiform manner for 23 ft. Another core, the MacKellar Ferguson, also exhibits stratiform brecciation in at least two portions.

Pores of type 1 reservoirs are sparse, but not altogether absent. The collapse-breccias in the Cox



Figure 11. Solution-enlarged fractures in crinoidal packstone. Porosity has been occluded by cave muds, glauconite, and dolomite. Carter Hester core, depth 7,781 ft.

Annis, Harper County, and Wil-McCossey, Pottawatomie County, cores do contain some visible interparticle porosity between the clasts (Fig. 8). Type 1 lithologies generally are tight because the fractures, solution-widened joints, and vugs have been filled by cave sediments and cements. The top portion of the Cleary Kinney core is a model for type 1 Hunton paleokarstic reservoirs (Fig. 17). Collapse breccia (8 ft) is underlain by grainstone, and porosity has been occluded by dolomite cement and sediment.

Most of the type 1 Hunton paleokarstic reservoirs are not producers of oil or gas, according to the production records as shown in Table 3.

Type 2 Hunton Paleokarstic Reservoir

Six study cores have been placed in the type 2 Hunton paleokarstic reservoir category—the Amax Hickman, Arco Marcum, Carter Hester, Gulf Wright, Kirkpatrick Shewey, and Tenneco Jordan. These cores contain features that are different from the type 1 group.

Type 2 reservoirs are composed of lithologies that allow fluid to flow through the rock. Kerans

(1989) has named this type of karst “interparticle flow”; White (1969) proposed the term “diffuse flow” for this karst hydrologic regime. Diffuse flow is the term used in this report. Rocks with diffuse flow of ground water are thought to have been deposited in an intertidal zone where they underwent intense bioturbation and dolomitization. Beardall’s (1983) study of the Henryhouse suggests that burrow mottling, dissolution of grains which results in moldic and vuggy porosity, and a dolowackestone lithology are characteristic of intertidal facies. Karstification further enhanced the porosity of these rocks by the enlargement of already existing pores. Type 2 reservoir porosity is exhibited in the Arco Marcum core (Fig. 18), which stands as a model for a type 2 Hunton reservoir.

The disparity in the composition of type 1 conduit-flow lithology and the type 2 diffuse-flow lithology results in an absence of caves in the type 2 reservoirs. In type 1 lithologies, meteoric fluids move through in solution-enlarged channels or along bedding planes, removing carbonate and creating cavern-sized pores. In type 2 lithologies, however, waters can pass through the interparticle pore space with little or no additional dissolution of carbonate. As a consequence, cavern-fill parabreccias and collapse breccias are rare or nonexistent in type 2 reservoirs. However, some cores of type 2 lithologies contain small amounts of breccia formed by near-surface karstification during subaerial exposure (Fig. 19).

Most reservoirs of the type 2 group were producers of oil or gas, according to the production records in Table 3. Those not producing petroleum still had the ability to deliver high volumes of

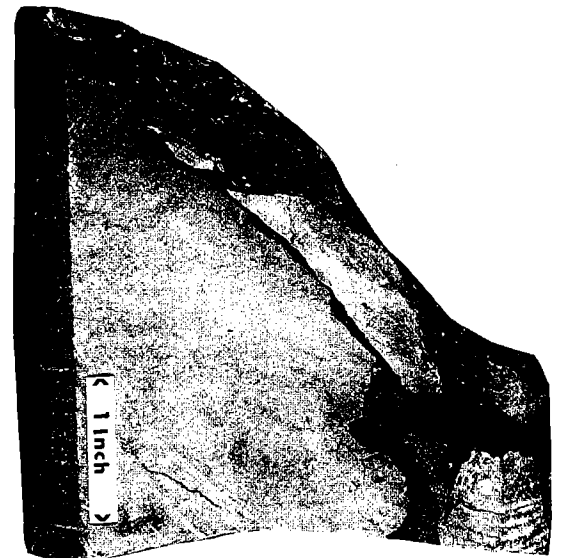


Figure 12. Breccia within solution-enlarged channel. Cleary Gilbert core, depth 7,562 ft.

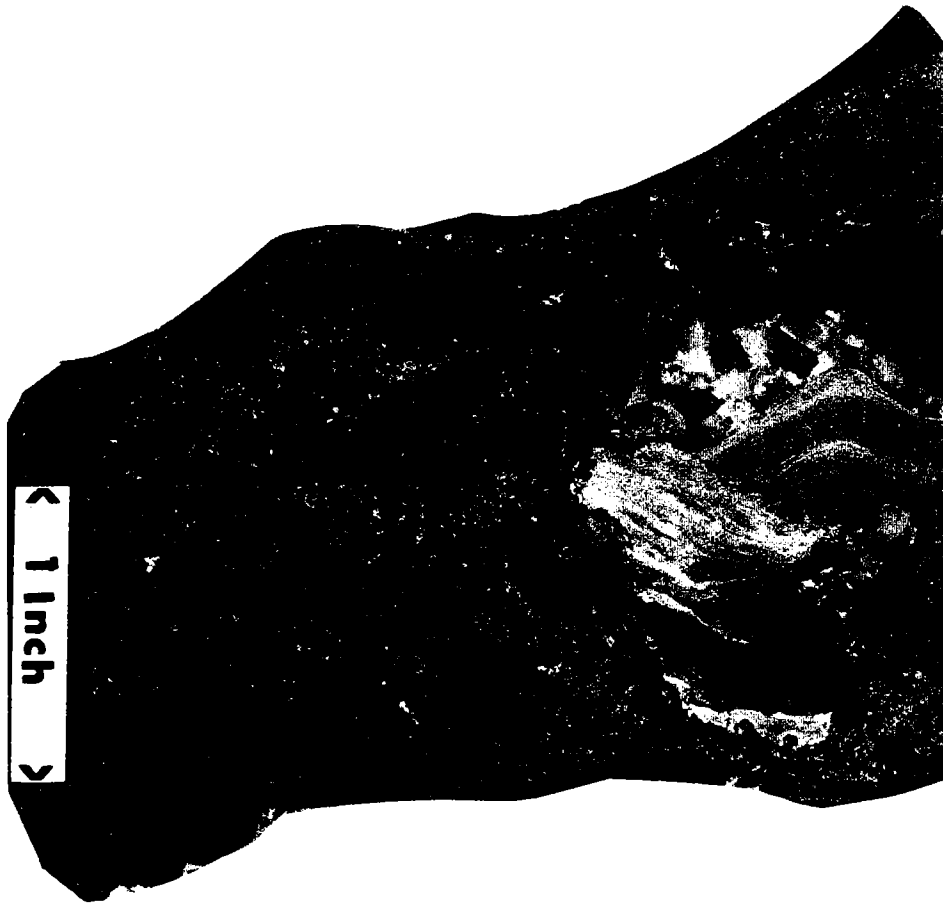


Figure 13. Vug rimmed with silica cement, then filled with laminated sediment. Remnant pore space occupied by baroque dolomite. Kirkpatrick Shewey core, 8,720 ft.

fluid (saltwater) to the borehole. This ability appears to be the consequence of the porous lithology inherent in type 2 Hunton paleokarstic reservoirs.

Unconformities

Carbonate rocks of the Hunton are believed to have experienced subaerial weathering at various times throughout their history. Amsden (1975) asserts that the Hunton represents an incomplete depositional sequence with significant time-stratigraphic gaps developed over substantial parts of the Arbuckle Mountains–Criner Hills outcrop area. Local unconformities probably existed during pre-Cochrane, pre-Clarita, pre-Henryhouse, pre-Haragan/Bois d’Arc, and pre-Frisco times (Amsden, 1980). These unconformities that truncate the Bois d’Arc and Frisco are of regional scope and are the result of subaerial erosion (Amsden, 1980). Amsden (1980) also states that he does not imply that other unconformities are not represented in the subsurface but that, if present, they affect relatively small areas.

The pre-Woodford unconformity in Oklahoma has been recognized for many years (Tarr, 1955). The unconformity is described as a fairly uniform regional beveling of the Hunton toward the north. Along the northern margin of the State, Hunton rocks have been entirely stripped away. Within the outcrop area of the Arbuckle Mountains, pre-Woodford erosion locally truncates the Hunton completely, allowing the Woodford to rest on the Sylvan Shale (Amsden, 1975).

The unconformity at the top of the Hunton is present in three study cores: the Arco Marcum, Woods County; the Cox Annis, Harper County; and the MacKellar Ferguson, Woodward County. These cores consist of Chimneyhill rocks along the northern extent of the Hunton; the Hunton Group above the Chimneyhill has been removed by erosion. The lower part of the Woodford Shale, which rests unconformably on the dolomite of the Chimneyhill, is present in the Arco Marcum and Cox Annis cores. In the MacKellar Ferguson core, cobbles of the Clarita are found in the gray-black rock at the top of the core which is thought to be

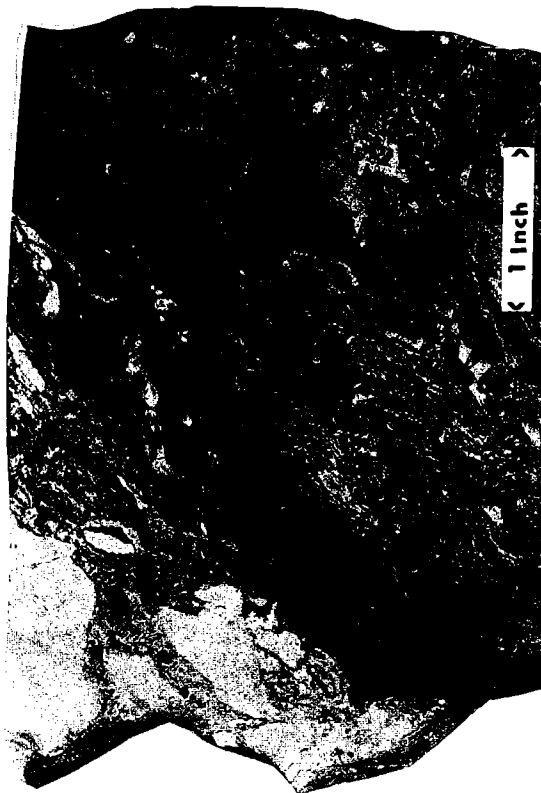


Figure 14. Eroded Henryhouse Formation. Channel fill contains Woodford Shale fragments. Kirkpatrick Shewey core, depth 7,929 ft.

the lower part of the Woodford Shale. The presence of the Woodford directly over the Chimney-hill records the loss of the Henryhouse, Haragan, Bois d'Arc, and Frisco Formations of the Hunton Group. There is a sudden change of lithology, with no facies gradation represented in these three cores.

Karstic and collapse-breccia features are believed to represent unconformity surfaces (Esteban and Klappa, 1983). All of the 12 study cores contain certain elements of paleokarst. Cross sections (Figs. 20–22) illustrate the location of paleokarst in relation to the pre-Woodford and other possible unconformities. It is believed that most of the cores were influenced by the pre-Woodford event. As stated earlier, three cores include the contact with the Woodford. Most of the remaining cores were taken within a few feet or few tens of feet below the unconformity. Two cores are located a considerable distance below the pre-Woodford unconformity: the Amax Hickman starts 125 ft below (Figs. 20,21) and the Carter Hester ~300 ft below (Fig. 22). Both of these cores contain paleokarstic features which may be attributable to intraforma-

tional disconformities that may have formed in the rocks due to periods of erosion or local non-deposition.

The presence of dedolomitization is considered to be another criterion for the recognition of unconformities. Dedolomitization is the process which results in corrosion, dissolution, and/or calcitization of dolomite rhombs. It occurs when calcium-rich waters flow through the dolomite, rendering it unstable and resulting in its dissolution or replacement (Manni, 1985). Munn and Jackson (1980) reported that dedolomitization is associated with subaerial weathering, either at ancient unconformities, or at the Earth's surface. Petrographic evidence of dedolomitization is seen in thin sections from the Arco Marcum, Cox Annis, and MacKellar Ferguson cores that are directly overlain by the Woodford.

The contact between the Hunton and the Woodford is noticeable in the well-log signatures in the cross sections. The obvious reduction in gamma-ray log signature (usually in excess of 75 API units) from "hot" shale to carbonate (see Amax Hickman log; Figs. 20,21) across the unconformity boundary

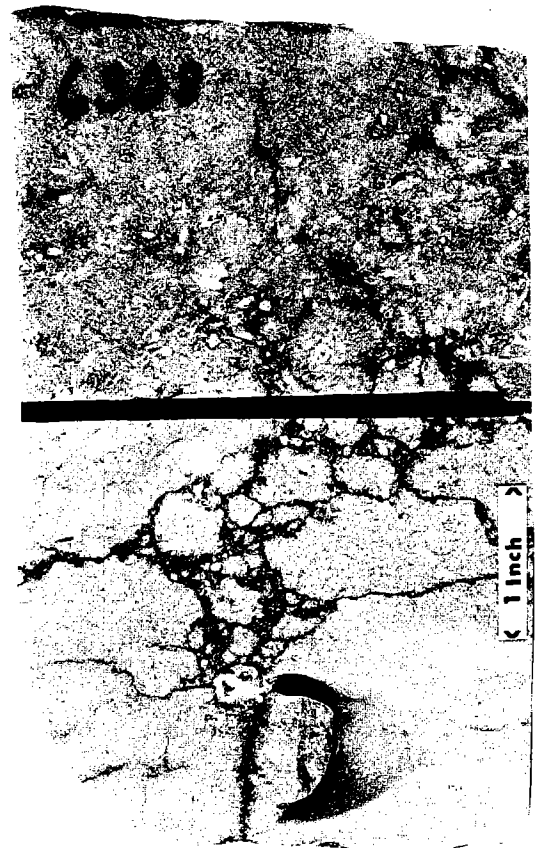


Figure 15. Hematite-stained solution-cavity fill. Host rock is grainstone. Gulf Wright core, depth 6,308 ft.

confirms the changes in lithology present in the study cores. Recognition of intra-Hunton unconformities (Fig. 22) by log signature is very tenuous at best, due to the lack of cores of possible unconformity zones.



Figure 16. Type 1 Hunton paleokarstic reservoir. Solution-enlarged channel formed by conduit flow. The channel narrows upward and is filled with sediment. Pelto Cheatwood core, depth 3,991 ft.

SUMMARY AND CONCLUSIONS

Hunton cores contain diagnostic indicators of paleokarst, including: (1) breccia facies formed as a result of collapse and sedimentation; (2) dissolution features, such as enlarged vugular porosity and solution-enlarged fractures, joints, and channels; (3) infill sediments; and (4) possible speleothems.

Four categories of breccia identified are: crackle breccia, mosaic breccia, cavern-fill parabreccia, and collapse breccia. Hunton paleokarstic reservoirs were classified into two groups (type 1 and type 2) on the basis of the relative abundance of breccia and interparticle porosity observed in the cores. This classification is summarized in Table 4.

The timing of karstification in most cores appears to have been associated with the pre-Woodford unconformity. Paleokarstic features located several hundred feet below the pre-Woodford unconformity may be related to intra-Hunton erosional events.

ACKNOWLEDGMENTS

The authors wish to express their appreciation to Jim Puckette for his valuable suggestions and contributions. Azhari Abdalla was extremely helpful in preparing various illustrations. Bonnie Milby made significant editorial comments.

REFERENCES CITED

- Al-Shaieb, Zuhair; and Shelton, J. W., 1977, Evaluation of uranium potential in selected Pennsylvanian and Permian units and igneous rocks in southwestern and southern Oklahoma: U.S. Department of Energy, Open-File Report GJBX-3S, p. 248.
- Amsden, J. W., 1960, Hunton stratigraphy, *pt. 6 of Stratigraphy and paleontology of the Hunton Group in the Arbuckle Mountain region*: Oklahoma Geological Survey Bulletin 84, 311 p.
- _____, 1975, Hunton Group (Late Ordovician, Silurian, and Early Devonian) in the Anadarko basin of Oklahoma: Oklahoma Geological Survey Bulletin 121, 214 p.
- _____, 1980, Hunton Group (Late Ordovician, Silurian, and Early Devonian) in the Arkoma basin of Oklahoma: Oklahoma Geological Survey Bulletin 129, p. 2-67.
- _____, 1989, Depositional and post-depositional history of Middle Paleozoic (Late Ordovician through Early Devonian) strata in the ancestral Anadarko basin: Oklahoma Geological Survey Circular 90, p. 143-146.
- Anderson, R. F., 1939, A subsurface study of the Hunton Formation in central Oklahoma: University of Oklahoma unpublished M.S. thesis, 30 p.
- Arbenz, J. K., 1956, Tectonic map of Oklahoma: Oklahoma Geological Survey Map GM-3, scale 1:750,000.
- Beardall, G. B., Jr., 1983, Depositional environment, diagenesis and dolomitization of the Henryhouse Formation, in the western Anadarko basin and

TABLE 4. — TYPES OF HUNTON PALEOKARSTIC RESERVOIRS

Cores	Crackle breccia	Mosaic breccia	Cavern-fill parabreccia	Collapse breccia
<i>Type 1 Reservoirs</i>				
Cleary Kinney 1-20	O	O	O	X
Edwin Cox Annis A-1	O	X	X	X
MacKellar Ferguson 9	X	X	O	X
Samson Wade 1	X	X	X	X
Shell Stocking 1-32	O	O	X	X
Wil-McCossey 2	O	O	O	X
<i>Type 2 Reservoirs</i>				
Amax Hickman 1-24	O	O	O	O
Arco Marcum 3	O	O	O	O
Carter Hester 1	O	O	O	O
Gulf Wright Heirs 1	O	O	O	O
Kirkpatrick Shewey 1	O	O	O	X
Tenneco Jordan A-1	O	O	O	O
X = breccia is present; O = breccia is absent.				

- northern shelf, Oklahoma: Oklahoma State University unpublished M.S. thesis, 128 p.
- Bowles, J. P., 1959, Subsurface geology of Woods County, Oklahoma: Shale Shaker Digest, v. 3, p. 202.
- Choquette, P. W.; and James, N. P., 1988, Introduction, in James, N. P.; and Choquette, P. W. (eds.), *Paleokarst*: Springer-Verlag, New York, p. 1-21.
- Esteban, M.; and Klappa, C. F., 1983, Subaerial exposure environment, in Scholle, P. A.; Bebout, D. G.; and Moore, C. H. (eds.), *Carbonate depositional environments*: Springer-Verlag, New York, p. 2-72.
- Ford, D. C., 1988, Characteristics of dissolutional cave systems in carbonate rocks, in James, N. A.; and Choquette, P. W. (eds.), *Paleokarst*: Springer-Verlag, New York, p. 25-57.
- Kahle, C. F., 1988, Surface and subsurface paleokarst, South Lockport and Pebbles Dolomites, in James, N. P.; and Choquette, P. W. (eds.), *Paleokarst*: Springer-Verlag, New York, p. 229-255.
- Kerans, C., 1989, Karst-controlled reservoir heterogeneity and an example from the Ellenburger Group (Lower Ordovician) of West Texas: Bureau of Economic Geology, Austin, Texas, 234 p.
- Lynch, M. T., 1990, Evidence of paleokarstification and burial diagenesis in the Arbuckle Group of Oklahoma: Oklahoma State University unpublished M.S. thesis, 163 p.
- Manni, F. M., 1985, Depositional environment, diagenesis, and unconformity identification of the Chimneyhill Subgroup, in the western Anadarko basin and northern shelf, Oklahoma: Oklahoma State University unpublished M.S. thesis, 133 p.
- Maxwell, R. A., 1936, Stratigraphy and areal distribution of the Hunton Formation: Northwestern University unpublished Ph.D. dissertation, 72 p.
- Maxwell, R. W., 1959, Post-Hunton pre-Woodford unconformity in southern Oklahoma, in Mayes, J. W.; Westheimer, J.; Tomlinson, C. W.; and Putman, D. M. (eds.), *Petroleum geology of southern Oklahoma—a symposium sponsored by the Ardmore Geological Society*: American Association of Petroleum Geologists, Tulsa, v. II, p. 101-125.
- Morgan, W. A., 1985, Silurian reservoirs in upward-shoaling cycles of the Hunton Group, Mount Everette and Southwest Reeding fields, Kingfisher County, Oklahoma, in Roehl, P. O.; and Choquette, P. W. (eds.), *Carbonate petroleum reservoirs*: Springer-Verlag, New York, p. 109-120.
- Munn, D.; and Jackson, D. E., 1980, Dedolomitization of Lower Carboniferous dolostone in the Wirksworth area: *Geology Magazine*, v. 117, p. 607-612.
- Norton, W. H., 1917, A classification of breccias: *Journal of Geology*, v. 25, p. 160-104.
- Reeds, C. A., 1911, The Hunton Formation of Oklahoma: *American Journal of Science*, v. 182, p. 256-262.
- Ritter, D. F., 1986, *Process geomorphology*: Wm. C. Brown, Dubuque, 414 p.
- Taff, J. A., 1902, Description of the Atoka Quadrangle: U.S. Geological Survey Geologic Atlas, v. 79, p. 1-8.
- Tarr, R. S., 1955, Paleogeologic map at base of Woodford and Hunton isopachous map of Oklahoma: American Association of Petroleum Geologists Bulletin, v. 39, p. 1851-1858.
- White, W. B., 1969, Conceptual models for carbonate aquifers: *Groundwater*, v. 7, p. 15-21.
- Withrow, P. C., 1971, Hunton geology of the Star-Lacey field: *Shale Shaker Digest*, v. 19, p. 78-88.

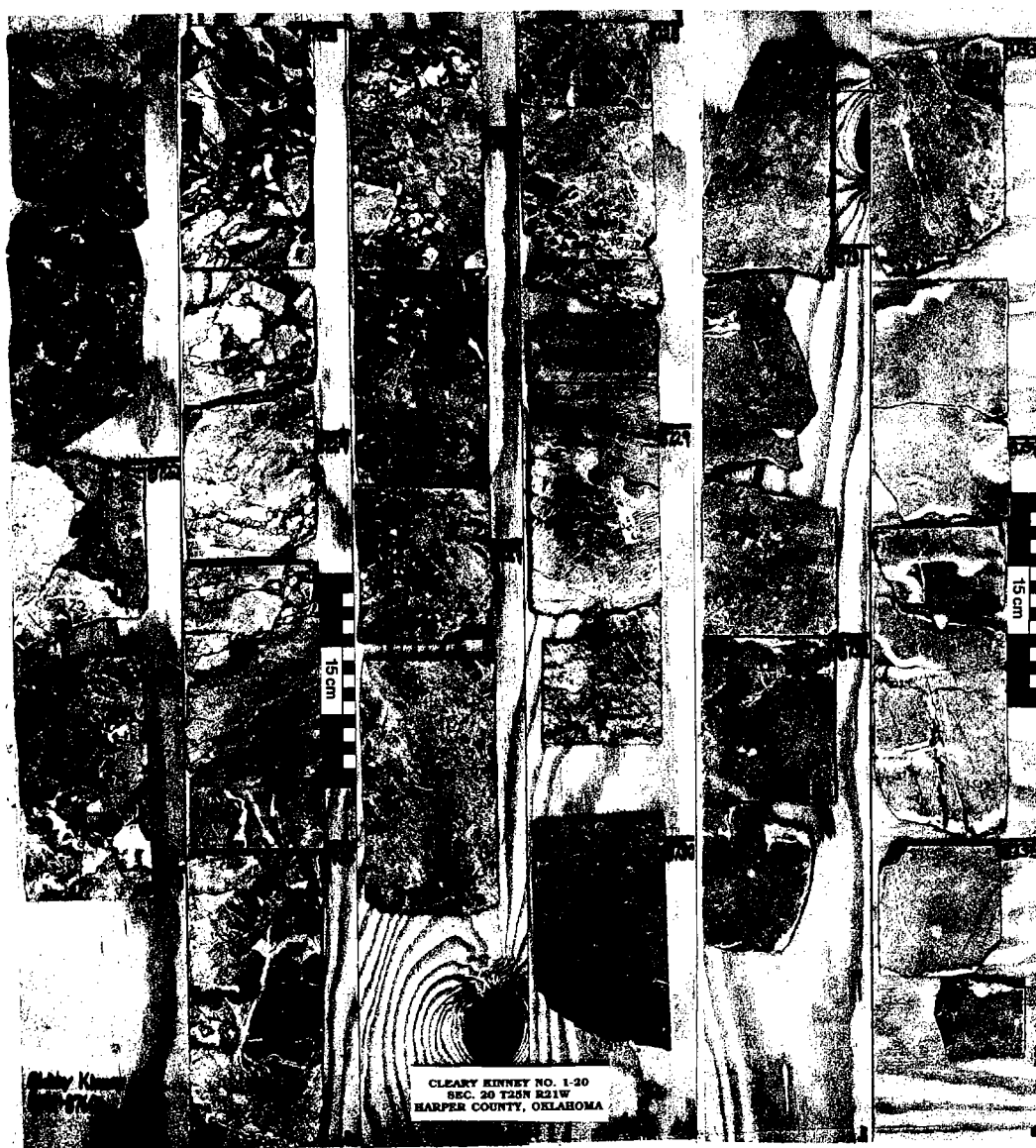


Figure 17. Type 1 Hunton paleokarstic reservoir. Clast-supported collapse breccia cemented with sparry ferroan-calcite cement. Cleary Kinney core, depth 8,721–8,735 ft.



Figure 18. Typical type 2 Hunton paleokarstic reservoir rock characterized by enhanced intergranular and moldic porosity. Dolowackestone reservoir rock lies unconformably on the Sylvan Shale, and is unconformably overlain by the Woodford Shale. Arco Marcum core, depth 6,230–6,263 ft.



Figure 19. Minor brecciated zone in type 2 Hunton paleokarstic reservoir rock. Dolomudstone/wackestone with visible vuggy porosity. Dark-colored rock on left side of sample is believed to be the host rock. Breccia is cemented with baroque dolomite that does not occlude vuggy porosity. Kirkpatrick Shewey core, depth 7,927 ft.

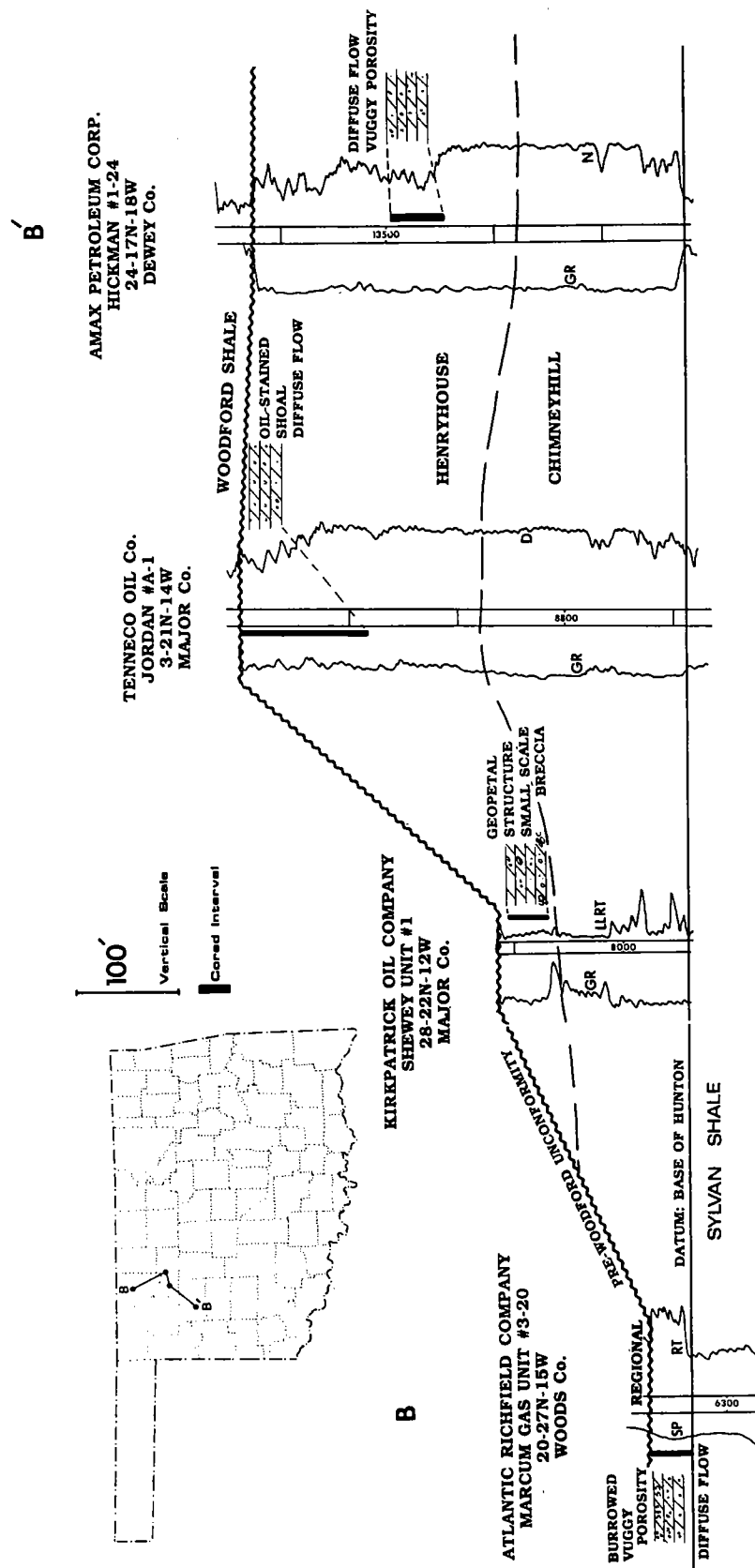


Figure 21. Cross-section B-B' showing the relative positions of cored Hunton karstic features to stratigraphy and the pre-Woodford unconformity.

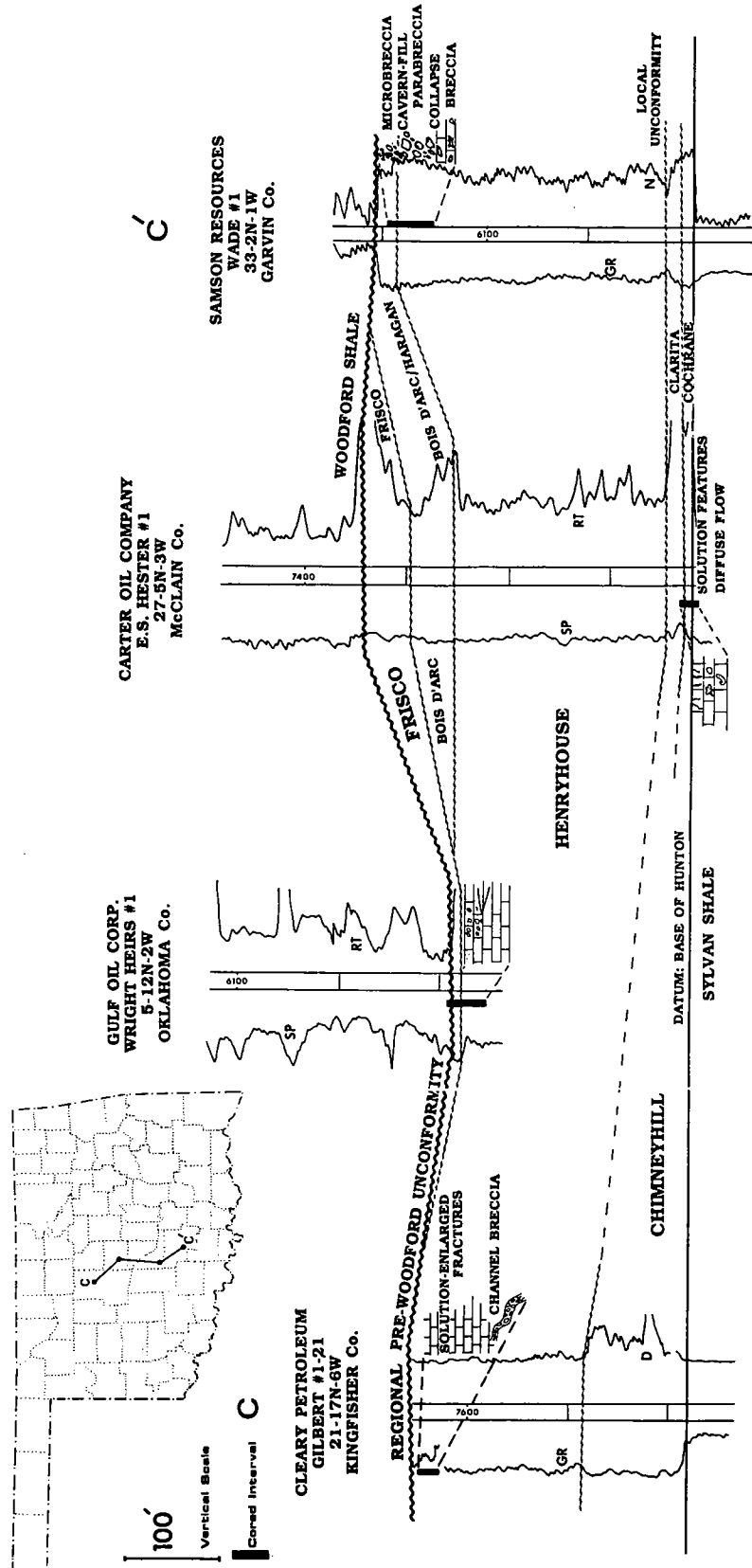


Figure 22. Cross-section C-C' showing the relative positions of cored Hunton karstic features to stratigraphy, local intra-Hunton unconformities, and the regional pre-Woodford unconformity.

PETROLOG

WELL _____

SEC. _____

T _____

R _____

COUNTY, OKLAHOMA

LITHOLOGY	SED STRUCTURES/ CONSTITUENTS		POROSITY TYPES
SANDSTONE		G GLAUCONITE	F FRACTURE
SHALE	MOTTLED BEDDING	P PYRITE	SEF SOLUTION-ENLARGED FRACTURE
LIMESTONE	STROMATOLITE	C CORALS	V VUGULAR
DOLOMITIC LIMESTONE	INTRACLASTS	B BRACH	M MOLDIC
DOLOMITE		E ECHINODERM	IG INTERGRANULAR
CLAYEY DOLOMITE	GASTROPODS	B BURROWS	IX INTERCRYSTALLINE
BRECCIA	ALGAE	O OSTRACOD	
CRACKLE BRECCIA	VUGS, CHANNELS	B BRYOZOAN	
CHERT	CEMENT VEIN	U UNCONFORMITY	

CLAST SHAPE

A ANGULAR
 SA SUBANGULAR
 SR SUBROUNDED
 R ROUNDED

MISCELLANEOUS

DOMINANT FEATURE, TEXTURE
 LESS COMMONLY OCCURRING
 cmt. CEMENT
 MISSING CORE
 R RARE c COMMON a ABUNDANT
 THIN SECTION

Plate 1. Petrolog header designed for karstic rocks.

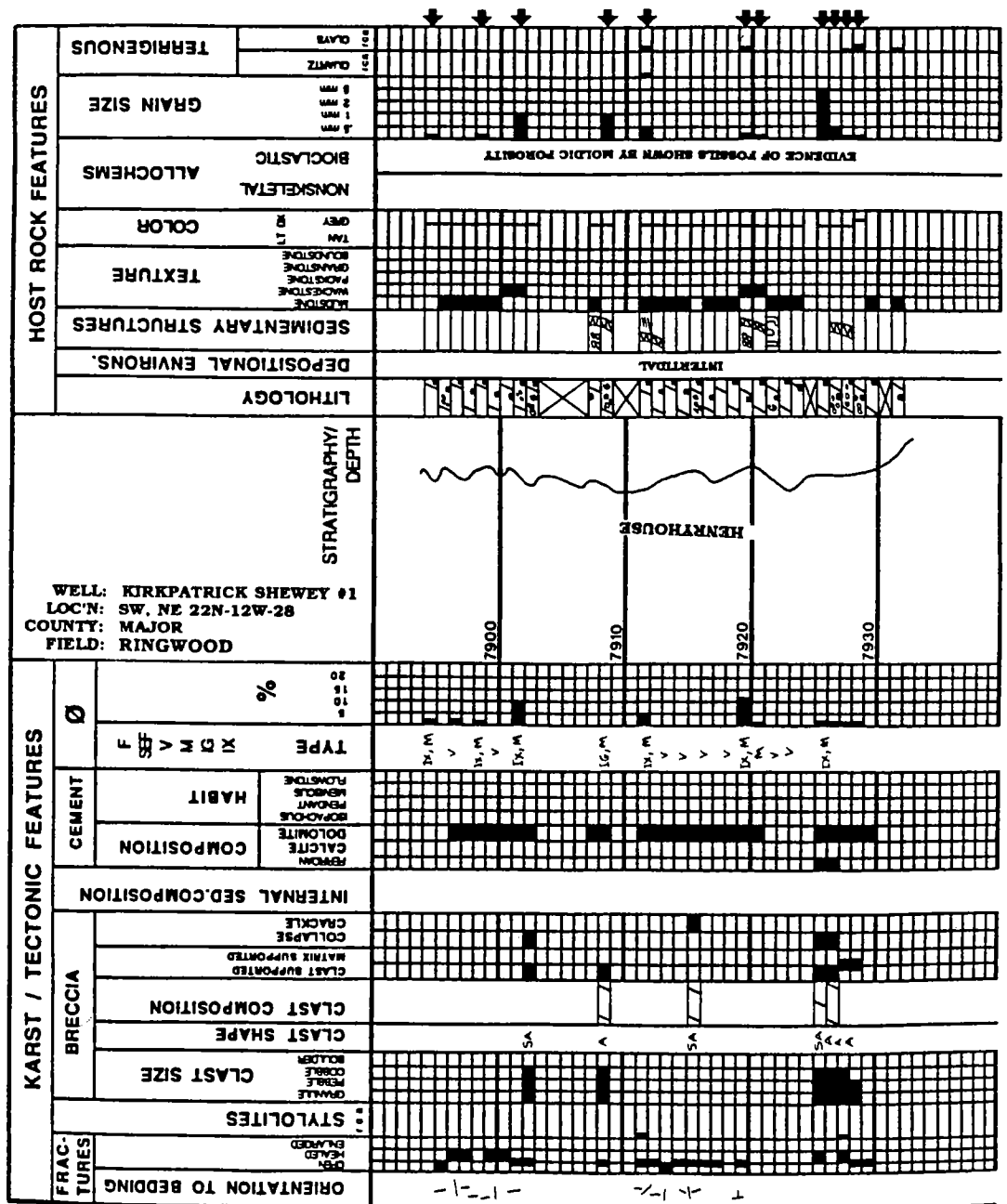


Plate 2. Sample petrolog from the Kirkpatrick Shewey core.

Feasibility Study of Heavy-Oil Recovery in the Midcontinent Region (Oklahoma, Kansas, Missouri)¹

David K. Olsen and William I. Johnson

National Institute for Petroleum and Energy Research
Bartlesville, Oklahoma

ABSTRACT.—The Midcontinent region has been the site of many heavy-oil enhanced oil recovery (EOR) field tests beginning in the early 1960s. This report summarizes a study undertaken to determine the feasibility of heavy-oil recovery from the Midcontinent (Oklahoma, Kansas, and Missouri). Previous studies on heavy-oil deposits in Oklahoma, Kansas, and Missouri have concentrated on only a few counties in each state, near or including outcrop areas of Cherokee Group, Des Moines Series, Middle Pennsylvanian heavy-oil-impregnated sandstones. This study includes areas of former investigation, but also encompasses heavy-oil deposits and production that have been reported, or are being reported, annually in these states. Accumulations of heavy oil have been identified in producing and nonproducing accumulations in reservoir rocks from Cambrian through Pennsylvanian age within several different sedimentary basins in the study area.

Proprietary U.S. Department of Energy (DOE)/industry-funded and DOE-funded pilot-scale and full-field-scale thermal EOR projects for heavy-oil recovery in the study area have been analyzed to determine causes of success or failure of the process and/or project. Success and/or failure of selected processes and projects have been compared to successful thermal EOR projects in California, Canada, Venezuela, and Indonesia. Thermal EOR (TEOR) processes, similar to those being applied in California, Canada, Venezuela, and Indonesia, have been applied successfully in the Midcontinent, but consolidation of reservoir rock in the Midcontinent is a major factor affecting recoverability of heavy oil.

Successful application of TEOR processes in the Midcontinent is limited by the geology of the heavy-oil reservoir rather than the recovery process. In fluvial-dominated deltaic sandstones of the Cherokee Group in the Cherokee and Forest City basins of the three-state area, depositional environment, facies (internal architecture), and diagenetic changes severely limit the feasibility of economic application of TEOR processes for heavy-oil recovery. In the unconsolidated or friable, steeply dipping, thicker, high-permeability sands that occur in fault blocks along the north side of the Arbuckle Mountains in south-central Oklahoma, there is greater potential for economic heavy-oil production. Problems with TEOR in these unconsolidated sandstone reservoirs may be reasonably compared to problems and success of TEOR-process projects in California, Canada, Venezuela, and Indonesia. Geological and engineering analyses of reservoir rock performed before implementation of thermal EOR processes will offer better probability of locating a project for maximum economic and ultimate heavy-oil recovery.

INTRODUCTION

This paper summarizes results of a study undertaken to determine the feasibility of heavy-oil recovery in the Midcontinent (Oklahoma, Kansas, Missouri) (Fig. 1). As a summary, only brief descriptions and analysis are presented. This study was conducted for the U.S. Department of Energy as part of an assessment of the feasibility of in-

nor any of their employees, makes any warranty, express or implied, or assumes any legal liability or responsibility for the accuracy, completeness, or usefulness of any information, apparatus, product, or process disclosed, or represents that its use would not infringe privately owned rights. Reference herein to any specific commercial product, process, or service by trade name, trademark, manufacturer, or otherwise, does not necessarily constitute or imply its endorsement, recommendation, or favoring by the U.S. Government or any agency thereof. The views and opinions of authors expressed herein do not necessarily state or reflect those of the U.S. Government or any agency thereof.

¹This report was prepared as an account of work sponsored by an agency of the United States Government. Neither the U.S. Government nor any agency thereof,

Olsen, D. K.; and Johnson, W. I., 1993, Feasibility study of heavy-oil recovery in the Midcontinent region (Oklahoma, Kansas, Missouri), in Johnson, K. S.; and Campbell, J. A. (eds.), *Petroleum-reservoir geology in the southern Midcontinent*, 1991 symposium: Oklahoma Geological Survey Circular 95, p. 163–172.

creasing the nation's heavy-oil production. The objectives of this feasibility study are: (1) to investigate from secondary data the known heavy-oil resources in Oklahoma, Kansas, and Missouri; (2) to screen this resource for potential thermal or other EOR applications; and (3) to evaluate various economic factors of heavy-oil recovery that may impact development of this resource, including transportation, refining, and marketing. A more detailed report has been compiled (Olsen and Johnson, in preparation).

Heavy oil, as used in this study, is limited to 10–20° API gravity oil, or oil with a gas-free viscosity of 100–10,000 cP (Group, 1981). Numerous other groups have referred to heavy oil as 10–25° API gravity oil. This expanded gravity range greatly increases the size of the Midcontinent resource, because there are more reservoirs with 20–25° than 10–20° API gravity oil. Many of the field tests and pilot studies conducted in the Midcontinent since the early 1960s targeted the 20–25° API gravity oil range because it was more easily produced. The economics of heavy-oil production are adversely affected not only by the high production costs for thermal oil recovery but also because the value of heavy oil averages \$4–\$8 per barrel less than West Texas intermediate crude, due to penalties for API gravity and sulfur content.

BACKGROUND

In the early 1900s, some Midcontinent operators found that heavy oil was associated with reservoirs producing natural gas for local communities' gas-illumination systems. Heavy oil has been produced by primary-recovery methods from shallow reservoirs not associated with commercial gas production in the Midcontinent since the early part of this century, but oil production is low, averaging <0.3 BOPD. Heavy-oil-impregnated sandstone and carbonate rock outcrops, noted as "tar" deposits, were identified by geologists early in this century. These surface deposits have been intermittently exploited as materials for road surfacing, but most of these deposits require the addition of asphalt and emulsifier to the crushed mixtures, in order to prevent early deterioration of road surfaces.

Thermal oil-recovery methods for heavy oil rely principally on viscosity reduction, distillation, and development of a pressure differential. When cyclic steam or steamdrive has been used to produce heavy oil from unconsolidated sand reservoirs, the average steam-generation cost has been the equivalent of one third of the produced oil (oil-fired generator), or its equivalent in BTUs for gas-fired steam generators. The overall economics suffer from high production costs required to produce a low-value product. The economics of TEOR dictate that the product of oil saturation times the porosity be >0.2 (Chu, 1990) for a sand with a min-

imum of permeability barriers (relatively homogeneous sand). Operation of steamfloods and cyclic-steaming operations from a non-mathematical, more practical view have been published by DOE (Sarathi and Olsen, 1992).

During the early 1960s, the use of steam or in-situ combustion to recover viscous heavy oil was just beginning, and companies conducted pilot tests in the Midcontinent, California, Canada, and Venezuela. Both major companies and independents conducted numerous pilot tests in the Midcontinent and carefully guarded their data. Thirty years later, much of that data has not been released, is in obscure files, or has been discarded. Often, information on these projects is only available from experiences of now mostly retired engineers and field operators who worked on these projects. Previous operators do not want to be quoted in today's litigious society, and thus their accounts are unsupported stories that seem plausible but are undocumented.

RESULTS AND DISCUSSION

Geology of Heavy-Oil Occurrences

Integrated engineering and geologic analyses were performed on selected heavy-oil EOR projects to determine why some were successful and others were not. The most common reason for lack of success in recovering heavy oil from Midcontinent reservoirs was the application of the TEOR process in unfavorable geologic facies, rather than the EOR process utilized. Most heavy-oil reservoirs that have been identified in the Midcontinent are small accumulations, <10 million bbl. These reservoirs are in thin sandstones, <50 ft thick, that are highly compartmentalized with complex internal architecture. Figure 2 is a schematic cross section of a typical Pennsylvanian stream channel filled with sand lenses showing lithology, compartmentalization (internal architecture), bedding boundaries, and potential paths of fluid flow from an injector well to producer wells. The better geologic facies for oil recovery in Midcontinent fluvial-dominated deltaic sandstones are the lower-point-bar, channel-fill, trough-bedded, more homogeneous facies along the channel in the direction of sediment transport. The poorer geologic facies in Midcontinent fluvial-dominated deltaic sandstones are the upper-point-bar, channel-fill, highly lenticular, thinly bedded, discontinuous facies with small-scale bedding-boundary permeability barriers. Heavy oil is recoverable from both upper and lower facies, but recovery is easier and the oil can be produced in larger quantities from the lower facies which can be swept more readily. Diagenetic changes in reservoir rock also have an adverse effect on heavy-oil recovery.

Most heavy-oil resources in the Midcontinent area are in consolidated fluvial-dominated deltaic

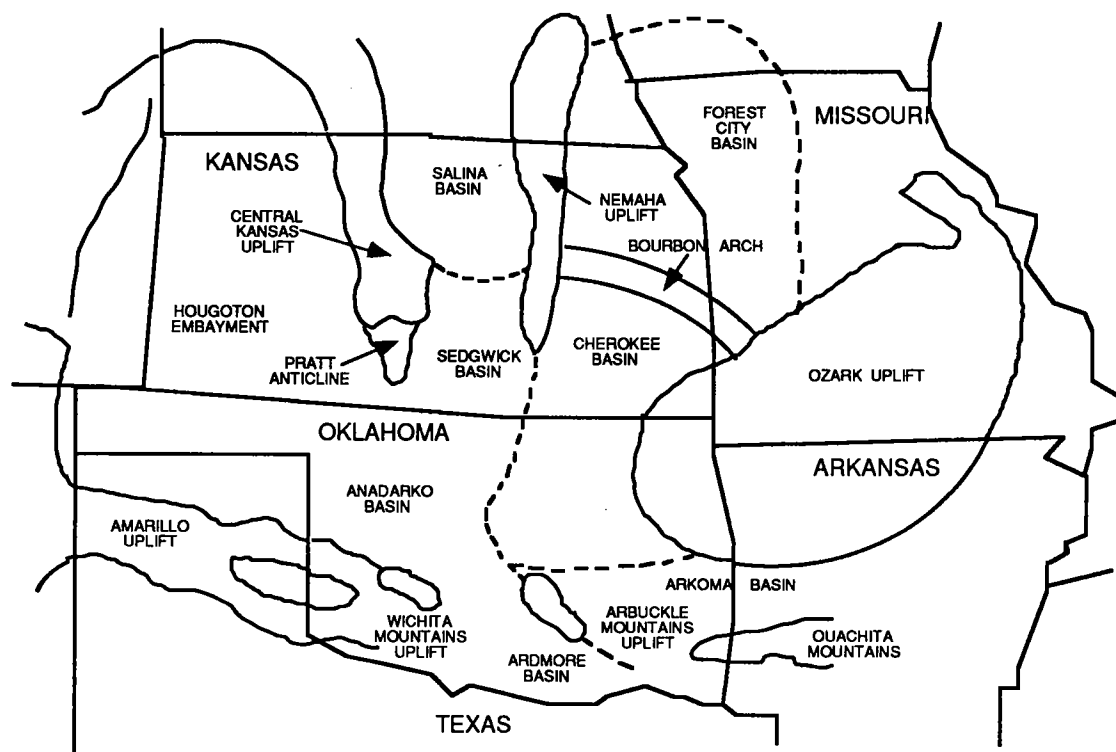


Figure 1. Basins and uplifts in the Midcontinent.

sandstones. The heavy-oil reservoirs evaluated in this project are those where TEOR processes were implemented in Pennsylvanian sandstone reservoirs. Most of these Pennsylvanian reservoirs are Cherokee Group, Desmoinesian Series sandstones. Numerous published reports and unpublished theses are available for evaluation of fluvial-dominated deltaic sandstones containing either heavy or light oil. Therefore, only a general description of fluvial-dominated deltaic sandstones is given, rather than details for each case study evaluated. A general description is given because this investigation considers the feasibility of heavy-oil recovery from different reservoirs in the Midcontinent. Carbonate reservoirs were not extensively studied in this project, because of the lack of information on heavy-oil resources or recovery from reservoirs in Kansas, Missouri, or Oklahoma.

Cherokee Group sandstones may be generally divided into an upper and a lower facies. The upper facies is moderately sorted, consisting of fine- to very fine-grained sediments with small-scale ripples. The lower facies is fine-grained sandstone with medium-scale crossbeds, horizontal beds, and massive beds, and is the most productive because it has fewer barriers and can be swept more readily (lower facies is the best quality reservoir rock). Generally, these two facies are differentiated by grain size (Ebanks and Webber, 1982). Diagenetic

changes appear to limit recovery from the upper facies, because the upper facies contains cemented fine- to very fine-grained sediments at bedding boundaries that are either complete or partial seals. In this report they are referred to as "bedding-boundary" permeability barriers.

Natural fracturing in the Midcontinent area is another geological factor that could affect heavy-oil recovery from either sandstone or carbonate reservoirs. Naturally occurring fractures in this area generally are oriented southwest-northeast. If reservoir rock of a heavy-oil reservoir is fractured, thermal stimulation may cause linedrive from well to well. Formation of a premature linedrive may result in bypassing large quantities of oil (poor sweep efficiency). Environmental damage on the surface or subsurface, caused by breakthrough from a reservoir due to natural fractures, may be more harmful and costly than linedrive between wells. Operators planning TEOR projects in shallow Midcontinent reservoirs should evaluate the project area by aerial-photo analysis to help determine fracture patterns before process implementation.

Kansas

In Kansas, heavy oil occurs in carbonate and clastic reservoir rocks of Cambrian through Pennsylvanian age rocks. Fluvial-dominated deltaic sandstones of the Cherokee Group, (Desmoines-

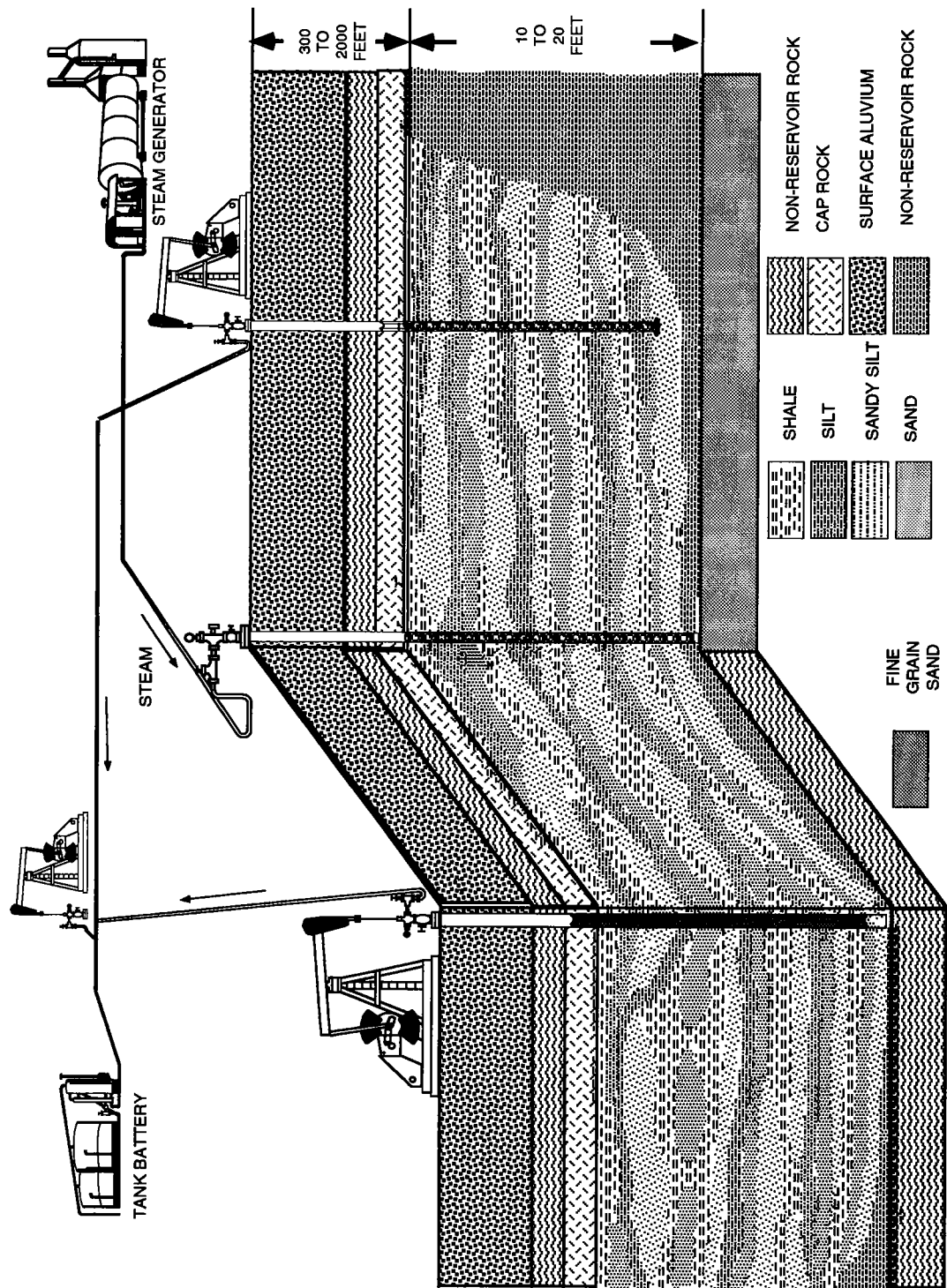


Figure 2. Schematic cross section of a steam channel filled with sand lenses showing lithology, compartmentalization (internal architecture), bedding boundaries, and fluid flow from an injector well to producer wells.

ian Series, Middle Pennsylvanian) are the reservoir rocks for the major portion of heavy-oil resources in Kansas, predominantly in the Cherokee and Forest City basins of eastern Kansas. In central and western Kansas, producing reservoirs older than those in Pennsylvanian rocks commonly are associated with erosional irregularities that are overlain by Pennsylvanian sediments. Cherokee Group sandstones have the greatest potential for increasing heavy-oil production in Kansas through application of steam-recovery processes of cyclic steam and steamflooding (steam drive). Ball and others (1982), Ebanks and others (1977), and others have made estimates of heavy-oil resources in the Cherokee and Forest City basins, primarily in Cherokee Group sandstones. Their combined estimate, 550–575 million bbl, is in fields that also produce light oil. The heavy-oil reserves suggested for Cherokee Group sandstones will probably be found in lenticular sandstone deposits, with limited lateral and vertical extent, that contain a few million bbl of recoverable oil from trough-bedded, lower point-bar, channel-fill facies, as described by Bradshaw (1985), Woody (1984), and others.

Western Missouri

Heavy oil occurs in western Missouri along the outcrop and immediately downdip in the shallow subsurface. Subsurface heavy-oil reservoirs are found in fluvial-dominated deltaic sandstones of the Cherokee Group. This resource is in small accumulations in lenticular sandstones that form stratigraphic traps in the Cherokee and Forest City basins of western Missouri. Estimated recoverable heavy-oil reserves, as quoted by Bradshaw (1985) from Ebanks and others (1977), are 200–250 million bbl. Heavy-oil reservoirs in these sandstones contain accumulations of a few million barrels. Best recovery of heavy oil is from trough-bedded, lower point-bar, channel-fill facies in fluvial-dominated deltaic sandstones (Bradshaw, 1985).

South-Central Oklahoma

Harrison (1982) first estimated the heavy-oil reserves in south-central Oklahoma to be 800 million bbl of oil in place, but later Harrison and Burchfield (1984) downgraded the heavy-oil reserve estimate to 41.8 million bbl. This reserve was reported to be in five major deposits in Carter and Murray Counties, Oklahoma. These heavy-oil deposits were reported to be at the Sulphur, Dougherty, Newport, Ardmore, and Hewett locations. The Sulphur deposit reportedly contained at least 50% of the heavy-oil resource in these accumulations (Harrison, 1982). Williams (1983), based on core-hole data and measured sections, estimated the heavy-oil-in-place deposits at the Sulphur location to be 376 million bbl. These heavy-oil deposits are contained in the Oil Creek Sandstone (Ordovician Simpson Group) on the surface and in

shallow subsurface. There are a few shallow wells in the Sulphur area that have produced heavy oil. Extensive mining of the asphaltic Oil Creek Sandstone occurred before the 1950s. The mined asphalt rock was used for road-surfacing material, but did not hold up well because the Oil Creek Sandstone is poorly cemented. When the cementing material broke down or dissolved, the roads surfaced with the asphaltic Oil Creek Sandstone failed. Reserves are not given for the other deposits described by Harrison (1982).

Harrison (1984), in the latest DOE report on south-central Oklahoma, downgraded the heavy-oil reserves to 41.8 million bbl (Sulphur with 33.8 million bbl, and south Woodford with 8.0 million bbl), and probable reserves were estimated at 19.1 million bbl (Sulphur with 12.6 million bbl, Dougherty with 3.6 million bbl, and Overbrook with 2.9 million bbl). The heavy-oil resource was reduced by 758.2 million bbl in the most recent analysis (Harrison, 1984) of south-central Oklahoma.

Many oil fields in south-central Oklahoma produce heavy oil, but no estimated reserve figures are available for these fields. Jordan's (1964) published data indicated that there are >300 known occurrences of "Petroleum-Impregnated Rocks and Asphaltite Deposits" in Oklahoma, including those investigated by Harrison (1982) and Williams (1983).

Cherokee Basin, Northeastern Oklahoma

Harrison and Roberts (1979) assigned no heavy-oil reserves to the Cherokee Group sandstones in the Ottawa and Craig County part of the Cherokee basin, Oklahoma. The remainder of Cherokee basin in northeastern Oklahoma should contain heavy-oil reserves similar to reserves in the Kansas and Missouri portions of the Cherokee basin. These heavy-oil reserves are elusive and may be hidden behind casing, some in old oil fields where records have been lost or forgotten. The Cherokee basin in northeastern Oklahoma is geologically similar to the Kansas and Missouri part of the basin. Therefore, heavy-oil reserves may also be contained in fluvial-dominated deltaic sandstones of the Cherokee Group sandstones of northeastern Oklahoma.

ECONOMICS OF THERMAL HEAVY-OIL PRODUCTION, SOUTHERN MIDCONTINENT

In the heavy-oil projects analyzed, the economic analysis was based on the oil recovered, the duration of the project, and the 1990 costs of thermal (steam) operations in Kern County, California. The cost of drilling, completing, and operating thermal wells is shown in Table 1. These average costs, assembled by the Kern County, California, Assessor for 1990, are based on proprietary data

TABLE 1. — KERN COUNTY, CALIFORNIA, THERMAL EOR OPERATING COSTS
(Maples, 1990)

New Producing Well Costs			
Well depth (ft)	Steam wells	Injectors	
0–250	\$37,000		
251–750	\$73,000	\$30,000	
751–1,250	\$89,000		
1,251–1,750	\$121,000	\$60,000	
1,751–2,250	\$160,000	\$100,000	
2,251–2,750	\$200,000		
2,751–3,250	\$240,000		

Suggested Yearly Thermal Steam Operating Costs Per Well			
Field	Cyclic steam	Steamflood	bbl/day/well ^a
Cymric	\$20,000	\$27,500	27
Kern River	\$20,000	\$27,000	18
Midway–Sunset	\$18,000	\$26,000	18

Steam Generator Maintenance Costs/Btu Barrel Equivalent of Oil Burned	
Gas fired = \$0.10	Oil fired = \$0.20

^aFrom the Conservation Committee of California Oil and Gas Producers (1991).

supplied by thermal operators in Kern County and reflect their cost of operation. Average production rates for three of the more profitable steamfloods in California are also shown.

TEOR requires much closer well spacing than traditional waterfloods in the Midcontinent. Well spacing of <1 acre is common in most active cyclic steam or steamflooding projects in the massive, shallow, unconsolidated sand reservoirs of California. Most Midcontinent reservoirs have been drilled, completed, and produced for several decades by primary and secondary recovery methods (waterflood, where applicable, for lower viscosity oil). These wells historically have had a poor performance record when recompleted as thermal wells. The expansion of the casing due to heat causes the minimal seal between casing and the formation to fail. Old wells, completed on a rag packer and set at the surface with a few bags of cement, can cause blowback to the surface, injection into a lower pressure zone, or collapse of the casing when steam is injected and the reservoir repressurized. Poorly plugged or abandoned wells, fracture systems that tie to the surface, or old unmapped wells are found the first time pressure is applied to these reservoirs. Old wells are liabilities rather than assets. The cost of new thermal wells, their close spacing, and the abandonment of old wells adds to the high startup and operating costs required to recover heavy oil from these fields.

CASE STUDIES OF HEAVY OIL RECOVERY THERMAL PROJECTS

Case studies of several TEOR projects have been reviewed and analyzed from secondary data. Summaries of the thermal heavy-oil projects are listed in the publication by Olsen and Johnson (1993), and an interpretation of the reasons for successful or unsuccessful oil recovery are presented in each case study. Causes for successful or unsuccessful process implementation are based upon review and analysis of these secondary data by the authors. These may not necessarily be the opinion of the company or companies conducting projects reported in the secondary sources. Nearly all of the projects were technically successful, in that they recovered oil at a faster rate than primary production. In the Cherokee basin, most of the heavy-oil wells in primary production average <0.3 BOPD. Production is greatly dependent on solution gas and the viscosity of the crude. Wells are often pumped on timer, and the economics of production is marginal.

TEOR processes which have been effective for recovery of heavy oil in California, Canada, Indonesia, and Venezuela have been successful in some of the reservoirs that occur in fault blocks along the north side of the Arbuckle Mountains in south-central Oklahoma. The sands are unconsolidated or friable and are in thick, steeply dip-

ping beds with high permeability, high oil saturation, and few permeability barriers. Unsuccessful process implementations have been the "exotic" TEOR processes, such as jet-engine exhaust and electrical heating. Some successful TEOR processes have recovered only small quantities of heavy oil because of location of the project in poor oil-recovery facies of a reservoir. Other successful TEOR processes have recovered larger quantities of heavy oil because the location of the project was in a high oil-recovery facies of the reservoir.

Comparison of the oil production from heavy-oil projects in the Midcontinent (oil produced over the project period) shows that very few of the projects would be economic. The exception may be Mobil's steamflood pilot in Carter County, Oklahoma, which is the only thermal heavy-oil recovery project that is active. The injection of steam and exhaust gas from the steam generator produced significant oil for Carmel Energy/DOE Vapor Therm project in the Eastburn field in Vernon County, Missouri. Repressurization of the reservoir at such shallow depths may not be permitted under current EPA ground-water and air-quality regulations. Duplication of the Carmel Energy project may be unfeasible.

Should significant heavy oil be imported from another area, the Midcontinent does not have a heated-pipeline network to accommodate large volumes of heavy oil, and Midcontinent refineries are designed to process light, sweet crude not sour, heavy oil.

APPLICATION FOR HORIZONTAL WELLS AND INFIELD DRILLING

Horizontal Wells

Use of horizontal wells for heavy-oil recovery in Bitterroot field of Missouri has been reported by Netzler (1990). Town Oil Co. drilled short-radius horizontal wells for use as water injectors and oil producers. Wells were drilled parallel and perpendicular to the direction of best permeability. According to Lester Town of Town Oil Co., results of the horizontal wells as injectors and producers were not the success that had been expected (personal communication, 1990).

Prior to implementation of a horizontal-drilling program, economic, engineering, and geologic analyses of the reservoir, and feasibility studies for use of horizontal wells as injectors and/or producers, should be completed. It is necessary to determine which facies of a fluvial-dominated deltaic-sandstone reservoir will be penetrated by the horizontal portion of the well. A horizontal injector well in a lower trough-bedded facies used in conjunction with vertical producers will probably recover economic amounts of oil. It is suggested that cyclic steam be implemented in the horizontal well, followed by steam flooding after a few cycles.

Use of horizontal wells as injectors is suggested because production is normally higher in a horizontal well than in a vertical well. With a horizontal producer, required injection rates in vertical or horizontal wells may be beyond the capability of surface and downhole equipment for economic application.

Placement of a horizontal well in an upper facies may result in heavy-oil recovery, but economic failure, as seen in Eastburn field by Carmel Energy, can occur when vertical wells were used. Horizontal wells will contact more unfavorable low-recovery reservoir rock than vertical wells. However, discontinuous facies will still limit oil production. Therefore, horizontal wells may not be a cure-all for unfavorable geology.

Midcontinent reservoirs tend to have natural fracture patterns oriented more or less in a north-east-southwest direction. When performing integrated economic, engineering, and geologic analyses of consolidated fluvial-dominated deltaic-sandstone reservoirs, placement of horizontal wells to utilize natural fracture patterns should be considered.

Horizontal wells should be considered for use in carbonate reservoirs containing heavy-oil resources. Carbonate rocks are commonly fractured. In light-oil reservoirs, horizontal wells have proven to increase oil production, resulting in higher cumulative production over shorter periods of time. Horizontal wells should definitely be one of the primary considerations when performing integrated economic, engineering, and geologic analyses of carbonate heavy-oil reservoirs.

Infield Drilling

Infield drilling in fluvial-dominated deltaic-sandstone reservoirs should be considered when performing integrated economic, engineering, and geologic analyses. Economic placement of vertical wells to take advantage of lateral variation of an upper facies or thin lower trough-bedded facies may be feasible, whereas implementation of horizontal-drilling technology may be too costly. These wells should be considered for application with cyclic steam in an upper facies, and with cyclic steam converted to steamflooding in a lower trough-bedded facies. Integrated analyses should determine feasibility for application of horizontal technology or infield drilling.

CONCLUSIONS

Since the early 1960s, the Midcontinent (Oklahoma, Kansas, and Missouri) has been the site of numerous EOR field tests that have attempted to produce some of the region's heavy-oil resource. The majority of oil-recovery processes applied in the Midcontinent recovered oil faster than primary production; but, with the exception of steam that

was injected in excess of the parting pressure of the reservoir or steam injected into unconsolidated or friable sandstone reservoirs, none of the heavy-oil-recovery processes were economic. The internal architecture of the reservoir controls the technical and economic viability of the recovery process.

The conclusions from this study are:

1) Heavy oil in sandstone reservoirs in the Mid-continent is recoverable by thermal oil-recovery processes. Fireflooding, steamflooding (drive), cyclic-steam, and steam-injection processes, combined with injection of hot gases (Vapor Therm and others), are successful thermal processes that have been implemented in Midcontinent sandstone reservoirs during the last 30 years.

2) Implementation of TEOR processes in consolidated thin fluvial-dominated deltaic-sandstone heavy-oil reservoirs may not be economical. Oil recovery may not be increased enough for thermal stimulation to pay for itself. Only a site-specific engineering, geologic, and economic analysis can determine if the recovery process chosen for a specific reservoir will be economic, and a pilot test is required to customize the process for the specific site.

3) Integrated engineering and geologic analyses prior to process implementation will improve chances for successful implementation of a thermal process. Reservoir analysis will help to determine where the better geologic facies for process implementation may be located in a reservoir.

4) The most favorable facies for best recovery of incremental heavy oil in consolidated sandstones in fluvial-dominated deltaic deposits of the Mid-continent is a trough-bedded channel-fill facies. Poor heavy-oil recovery results from implementing TEOR process in a more compartmentalized, discontinuously bedded, lenticular, upper point-bar, channel-fill sandstone facies with bedding-boundary permeability barriers that have undergone more reservoir-quality damaging diagenetic changes than a trough-bedded facies.

5) High injection pressures (greater than frac pressure) may cause environmental problems at the surface or in the subsurface, if injected fluids or formation fluids escape from the formation being stimulated.

6) Old wells, poorly abandoned wells, unknown wells, and fracture systems extending into shallow ground water or to the surface are liabilities that add to the high cost of thermal recovery of heavy oil.

ACKNOWLEDGMENTS

Research on this project was performed for the U.S. Department of Energy under cooperative agreement DE-FC22-83FE60149 as project SGP37. The authors thank E. B. Ramzel for his research in obtaining reservoir data and performing the economic analysis; M. K. Tham and A. Strycker of NIPER and T. B. Reid of the DOE Bartlesville

Project Office for their critical reviews. The authors acknowledge the courteous assistance and helpful discussions of the staff of the Kansas, Missouri, and Oklahoma Geologic Surveys.

SELECTED REFERENCES

- Ball, D.; Marchant, L. C.; and Goldberg, A. (eds.), 1982, *Tar sands: Interstate Oil Compact Commission Monograph*, Oklahoma City, 232 p.
- Ben-Saleh, F. F., 1970, *Stratigraphic analysis of Pennsylvanian rocks in southeastern Anadarko basin*, Oklahoma: University of Tulsa unpublished M.S. thesis, 76 p.
- Berg, O. R., 1963, *The depositional environment of a portion of the Bluejacket Sandstone*: University of Tulsa unpublished M.S. thesis, 87 p.
- Berry, C. G., 1963, *Stratigraphy of the Cherokee Group, eastern Osage County, Oklahoma*: University of Tulsa unpublished M.S. thesis, 84 p.
- Bradshaw, D. T., 1985, *Geologic variables influencing production in the Eastburn field, Vernon County, Missouri*: Colorado State University unpublished M.S. thesis.
- Brenner, R. L., 1989, *Stratigraphy, petrology, and paleogeography of the Upper portion of the Cherokee Group (Middle Pennsylvanian), eastern Kansas and northeastern Oklahoma*: Kansas Geological Survey Geology Series 3.
- Carlson, M. C., 1988, *A petrologic analysis of surface and subsurface Atoka Formation (Lower Pennsylvanian) Sandstone, western margin of the Arkoma basin*, Oklahoma: University of Tulsa unpublished M.S. thesis, 238 p.
- Chiou, R. C. S.; and Murer, T. S., 1989, *Cyclic steam pilot in gravity drainage reservoir, Mobil Producing U.S. Inc., in Proceedings of the Society of Petroleum Engineers annual technical conference and exhibition, EOR/ General Petroleum Engineering, October 8-11, San Antonio, Texas*: Society of Petroleum Engineers Paper 19659, p. 319-332.
- Chu, Chieh, 1990, *Prediction of steamflood performance in heavy oil reservoirs using correlations developed by factorial design method, in Proceedings of the 60th California regional meeting and exhibition, April 4-6, Ventura, California*: Society of Petroleum Engineers Paper 20020, p. 67-78.
- Conservation Committee of California Oil and Gas Producers, 1991, *Annual review of California oil and gas production, 1990*: Conservation Committee of California Oil and Gas Producers, Los Angeles.
- Cruz, J. A., 1963, *Geometry and origin of the Burbank Sandstone and Mississippian "Chat" in T. 25 N., R. 6 E. and T. 26 N., R. 6 E., Osage County, Oklahoma*: University of Tulsa unpublished M.S. thesis, 43 p.
- Curiale, J. A., 1983, *Petroleum occurrences and source-rock potential of the Ouachita Mountains, southeastern Oklahoma*: Oklahoma Geological Survey Bulletin 135, 65 p.
- Davis, L. V., 1953, *Oil possibilities near Idabel, McCurtain County, Oklahoma*: Oklahoma Geological Survey Mineral Report 23, 26 p.
- Deason, K. L.; and Bohm, Rex, 1969, *Studies of the oil and gas fields of Caldwell, Clay, Clinton, and Ray*

- Counties, Missouri: Oil and Gas in Missouri, General Information Sheet 19.
- Ebanks, W. J., Jr.; and Weber, J. F., 1982, Development of a shallow heavy-oil deposit in Missouri: *Oil and Gas Journal*, v. 80, September 27, p. 222-234.
- Ebanks, W. J., Jr.; James, G. W.; and Livingston, N. D., 1977, Evaluation of heavy oil and tar sands in Bourbon, Crawford, and Cherokee Counties, Kansas—final report: U.S. Department of Energy, Contract E-76-S-02-2997, BERC/RI-77/20.
- Emery, L. W., 1962, Results from a multi-well thermal-recovery test in southeastern Kansas: *Journal of Petroleum Technology*, v. 14, no. 6, p. 671-678.
- French, M. S.; and Howard, R. L., 1967, 1—The Steam-flood Job: Hefner Sho-Vel-Tum, Shell Oil Company: *Oil and Gas Journal*, v. 65, no. 29, p. 64-66.
- Fronjasa, Ernesto, 1965, A study of Oklahoma water flood statistics: University of Oklahoma unpublished M.G.E. thesis, 87 p.
- Goebel, E. D., 1966, Thermal recovery projects are increasing in Kansas, Missouri: *World Oil*, v. 162, no. 4, p. 78-80.
- Green, K. B., 1967, The fireflood: Cox Penn Sand, Mobil Oil Corp.: *Oil and Gas Journal*, v. 14, no. 6, p. 66-69.
- Group of Experts, 1981, UNITAR proposal for the definition of heavy crude and tar sands and addendum: Second International Conference on Heavy Oil and Tar Sands, Caracas, Venezuela.
- Hagen, K. B., 1972, Mapping of surface joints on air photos can help understand waterflood performance problems at North Burbank Unit, Osage and Kay Counties, Oklahoma: University of Tulsa unpublished M.S. thesis, 85 p.
- Harris, J. W., 1984, Stratigraphy and depositional environments of the Krebs Formation—lower Cherokee Group (Middle Pennsylvanian) in southeastern Kansas: University of Kansas unpublished M.S. thesis.
- Harrison, W. E., 1982, Tar sand resource appraisal in south-central Oklahoma: Kentucky Geological Survey, National Tar Sands (Heavy Oil) Symposium, Lexington, Kentucky, June 10-11, p. 110-128.
- Harrison, W. E.; and Burchfield, M. R., 1984, Tar-sand potential of selected areas in Carter and Murray Counties, south-central Oklahoma: U.S. Department of Energy Report No. DOE/LC/10730-T-1.
- Harrison, W. E.; and Roberts, J. F., 1979, Evaluation of heavy oil potential of northeastern Craig and northwestern Ottawa Counties, Oklahoma: U.S. Department of Energy, Contract ET-76-S-03-1812, BETC/1812-1.
- Harrison, W. E.; and Routh, D. L., 1981, Reservoir and fluid characteristics of selected oil fields in Oklahoma: Oklahoma Geological Survey Special Publication 81-1, 317 p.
- Hawisa, Ibrahim, Sh., 1965, Depositional environment of the Bartlesville, the Red Fork, and the Lower Skinner Sandstones in portions of Lincoln, Logan and Payne Counties, Oklahoma: University of Tulsa unpublished M.S. thesis, 44 p.
- Hough, R. M., 1978, Depositional framework of the lower Red Fork eastern flank of the Anadarko basin, Oklahoma: University of Tulsa unpublished M.S. thesis, 63 p.
- Hudson, A. S., 1969, Depositional environment of the Red Fork and equivalent sandstones east of the Nemaha Ridge, Kansas and Oklahoma: University of Tulsa unpublished M.S. thesis, 80 p.
- Interstate Oil Compact Commission, 1984, Major tar sands and heavy oil deposits of the United States: Interstate Oil Compact Commission, Oklahoma City, 272 p.
- Johnson, W. I.; and Olsen, D. K., 1993, Midcontinent fluvial-dominated deltaic depositional environments and their influence on enhanced oil recovery, in Johnson, K. S.; and Campbell, J. A. (eds.), *Petroleum-reservoir geology in the southern Midcontinent*, 1991 symposium: Oklahoma Geological Survey Circular 95, p. 230-235 [this volume].
- Jordan, Louise, 1964, Petroleum-impregnated rocks and asphaltite deposits of Oklahoma: Oklahoma Geological Survey Map GM-8, scale 1:750,000.
- Lardner, J. E., 1984, Petrology, depositional environment and diagenesis of Middle Pennsylvanian (Desmoinesian) 'Lagonda Interval' Cherokee Group in east-central Kansas: University of Iowa unpublished M.S. thesis.
- Maples, J. W., 1990, Kern County Assessor, Kern County, CA: Oil and Gas Properties Appraisal Parameters, 1990-1991.
- Netzler, B. W., 1990, Heavy-oil resources potential of southwest Missouri: Missouri Department of Natural Resources, Division of Geology and Land Survey, Open File Report 90-80-OG.
- Newell, D. K.; Watney, W. L.; Cheng, S. W. L.; and Brownrigg, R. L., 1987, Stratigraphic and spatial distribution of oil and gas production in Kansas: Kansas Geological Survey Subsurface Geology Series 9.
- Ockerman, J. W., 1932, Asphalt rocks in eastern Kansas: State Geological Survey of Kansas Open File Report OF 32-1, 8 p.
- Olsen, D. K.; and Johnson, W. I., 1993, Feasibility study of heavy oil recovery in the Midcontinent region (Kansas, Missouri, Oklahoma): U.S. Department of Energy, Publication NIPER-560.
- Orajaka, I. P., 1978, Lower Pennsylvanian transgressive onlap, northeastern flank Arkoma basin: University of Tulsa unpublished M.S. thesis, 67 p.
- O'Reilly, K. L., 1986, Diagenesis and depositional environments of the Red Fork Sandstone (Desmoinesian) in the Wakita Trend, Grant County, Oklahoma: University of Tulsa unpublished M.S. thesis, 154 p.
- Phares, R. S., 1969, Depositional framework of the Bartlesville Sandstone in northeastern Oklahoma: University of Tulsa unpublished M.S. thesis, 59 p.
- Porter, E. S., 1911, The coal and asphalt of Oklahoma: University of Oklahoma unpublished B.A. thesis, 29 p.
- Saitta Bertoni, Sandro, 1968, Bluejacket Formation—a subsurface study in northeastern Oklahoma: University of Tulsa unpublished M.S. thesis, 142 p.
- Sarathi, P. S.; and Olsen, D. K., 1992, Practical aspects of steam injection processes—a handbook for independent operators: U.S. Department of Energy Publication NIPER-580, DE9200101070.
- Scruton, P. C., 1949, The petrography and environment of deposition of the Warner, Little Cabin, and Hartshorne Sandstones of northeastern Oklahoma:

- University of Tulsa unpublished M.S. thesis, 77 p.
- Shulman, Chaim, 1965, Stratigraphic analysis of the Cherokee Group in adjacent portions of Lincoln, Logan, and Oklahoma Counties, Oklahoma: University of Tulsa unpublished M.S. thesis, 30 p.
- Simpson, H. M., 1969, Palynology and the vertical sedimentary profile of Missourian strata, Tulsa County, Oklahoma: University of Tulsa unpublished M.S. thesis, 64 p.
- Sperry, J. S., 1981, Heavy-oil recovery system completes three field test in Mid-Continent region: *Oil and Gas Journal*, v. 79, no. 30, p. 225–237.
- Sperry, J. S.; Young, F. S., Jr.; and Poston, R. S., 1980, Development and field testing of a process for recovering heavy crude oil in the Carlyle Pool, Allen County, Kansas, using the Vapor Therm Generator—final report: U.S. Department of Energy, Contract EY-76-C-02-2880, DOE/BETC-2880-1.
- Staton, M. D., 1987, Stratigraphy and depositional environments of the Cherokee Group (Middle Pennsylvanian), central Cherokee basin, southeastern Kansas: University of Kansas unpublished M.S. thesis.
- Tight, D. C., 1983, The Bartlesville Sandstone: a detailed subsurface stratigraphic study in the North Avant field, eastern Osage County, Oklahoma: University of Tulsa unpublished M.S. thesis, 120 p.
- Trantham, J. C.; and Marx, J. W., 1966, Bellamy field tests: oil from tar by counterflow underground burning: *Journal of Petroleum Technology*, v. 18, no. 1, p. 109–115.
- Valleroy, V. V.; Willman, B. T.; Campbell, J. B.; and Powers, L. W., 1967, Deerfield pilot test of recovery by steam drive: *Journal of Petroleum Technology*, v. 19, no. 7, p. 956–964.
- Vanbuskirk, J. R., 1960, Investigation of reservoir conditions of lower Deese sandstones (Pennsylvanian) for a flood project in the North Alma Pool, Stephens County, Oklahoma: University of Oklahoma unpublished M.G.E. thesis, 165 p.
- Walton, A. W.; Bouquet, D. J.; Evenson, R. A.; Rofheart, D. H.; and Woody, M. D., 1986, Characterization of sandstone reservoirs in the Cherokee Group (Pennsylvanian, Desmoinesian) of southeastern Kansas, Department of Geology and Tertiary Oil Recovery Project, University of Kansas, in Lake, L. W.; and Carroll, H. B., Jr. (eds.), *Reservoir characterization*: Academic Press, Orlando, Florida, p. 39–62.
- Weber, J. L., 1990, Comparative study of crude-oil compositions in the frontal and central Ouachita Mountains, in Suneson, N. H.; Campbell, J. A.; and Tilford, M. J. (eds.), *Geology and resources of the frontal belt of the western Ouachita Mountains, Oklahoma*: Oklahoma Geological Survey Special Publication 90-1, p. 101–117.
- Wells, J. S., 1979, Inventory of heavy oil in western Missouri—final report: Missouri Department of Natural Resources, Division of Geology and Land Survey, prepared for the U.S. Department of Energy, Contract ET-76-S-03-1808, BETC-1808-1.
- Wells, J. S.; and Anderson, K. H., 1968, Heavy oil in western Missouri: *American Association of Petroleum Geologists Bulletin*, v. 52, p. 1720–1731.
- Willhite, G. P., 1986, Waterflooding: *Society of Petroleum Engineers Textbook Series*, v. 3, Richardson, Texas, p. 243–251.
- Williams, D. B., 1983, Structural and geochemical study of the south Sulphur asphalt deposits, Murray County, Oklahoma: University of Oklahoma unpublished M.S. thesis, 163 p.
- Woody, M. D., 1984, Sedimentology, diagenesis, and petrophysics of selected Cherokee Group (Desmoinesian) sandstones in southeastern Kansas: University of Kansas unpublished M.S. thesis.
- Worthington, R. E., 1982, Petrology of Middle Pennsylvanian (Desmoinesian) "Upper Bluejacket" Sandstone (Cherokee Group) of Bourbon, Crawford, and Cherokee Counties, Kansas: University of Iowa unpublished M.S. thesis.

Potential of Microbial Enhanced Oil Recovery (MEOR) in the Petroleum Reservoirs of the Midcontinent Region

E. O. Udegbunam

Illinois Geological Survey
Champaign, Illinois

R. M. Knapp, M. J. McInerney, and R. S. Tanner

University of Oklahoma
Norman, Oklahoma

ABSTRACT.—Midcontinent reservoir rock and oil properties were studied to evaluate the potential for applying microbial enhanced oil recovery (MEOR) processes. The study included a computer search using Dwight's Energydata TOTL data-base system, literature search, and core data from a number of Midcontinent sandstone and carbonate reservoir rocks. The MEOR screening parameters included reservoir permeability, temperature, brine composition, oil API gravity, oil viscosity, and residual oil saturation. Comparison of the Midcontinent reservoir rock and oil properties to screening criteria developed from those reported in the literature showed that many oil reservoirs are suitable candidates and could benefit from some form of microbial treatment. A review of a number of field tests of MEOR processes showed that oil production rates increased by as much as 200%, depending on reservoir and bacterial characteristics. Properly administered bacterial treatments hold promise for fields with marginal production and for which high-cost EOR methods may not be economical.

INTRODUCTION

Production of oil has been an important economic factor in the Midcontinent region and the United States as a whole for more than a century. According to the American Petroleum Institute, the Midcontinent states contain ~33.4% of the proven crude-oil reserves in the lower 48 states, and produced ~34.9% of the oil produced in the U.S. in 1988 (Table 1).

However, a recent study (U.S. Department of Energy, 1990) of the abandonment rates for oil-producing reservoirs in the lower 48 states concluded that ~67% of the current proven reserves may remain in place at abandonment, trapped or bypassed because of fluid properties and/or reservoir heterogeneities after production by conventional primary and secondary recovery methods. Producing even a small part of this unrecovered oil resource will require favorable oil prices, technological advances in the characterization of oil reservoirs, and novel, cost-effective enhanced oil recovery processes.

Costly EOR technologies are not economical

TABLE 1.—MIDCONTINENT PROVEN CRUDE-OIL RESERVES AND PRODUCTION IN 1988

State	Proven crude-oil reserves (million bbl)	Crude-oil production (thousand bbl)
Arkansas	77	13,578
Kansas	327	58,930
Nebraska	42	5,992
New Mexico	661	71,175
Oklahoma	796	128,350
Texas	7043	758,865
Total, Midcontinent	8,946	1,036,890
Other states (excluding Alaska)	17,879	1,936,238
Total, U.S. (excluding Alaska)	26,825	2,973,128

Source: American Petroleum Institute (1990).

Udegbunam, E. O.; Knapp, R. M.; McInerney, M. J.; and Tanner, R. S., 1993, Potential of microbial enhanced oil recovery (MEOR) in the petroleum reservoirs of the Midcontinent region, in Johnson, K. S.; and Campbell, J. A. (eds.), Petroleum-reservoir geology in the southern Midcontinent, 1991 symposium: Oklahoma Geological Survey Circular 95, p. 173–181.

TABLE 2.—STRIPPER-WELL OIL PRODUCTION FROM
MIDCONTINENT RESERVOIRS, 1988 AND 1989

State	Stripper-well oil production (thousand bbl)		Stripper-well oil production/ total state oil production (1988) (%)
	1988	1989	
Arkansas	4,888	6,687	36
Kansas	57,803	57,051	98
Nebraska	2,688	2,446	45
New Mexico	14,378	14,653	20
Oklahoma	109,082	109,440	85
Texas	141,704	40,504	19
Total, Midcontinent	330,543	230,781	
Other states	116,294	212,019	
Total, U.S.	446,837	442,800	

Source: American Petroleum Institute (1990).

for many Midcontinent oil fields. Marginally economic fields account for ~32% of the total Midcontinent oil production and cannot support expensive EOR research or investments. As shown in Table 2, some Midcontinent states have a very high percentage of stripper-well oil production. Stripper-well oil production in Kansas (98.1%) is the highest nationally. Stripper-well oil production contributes substantially to total production in Oklahoma (85%), Nebraska (45%), Arkansas (36%), New Mexico (20%), and Texas (19%). Oklahoma produces ~25% of total U.S. stripper-well oil, followed by Kansas (13%) and Texas (9%). Altogether, the Midcontinent states accounted for 52% of total U.S. stripper-well oil production in 1989.

MEOR applications do not involve high investment in surface equipment as do some other chemical-flooding methods. Because of their potential cost-effectiveness, MEOR methods may be applicable in many oil fields of the Midcontinent.

MEOR APPLICATIONS

MEOR has been identified as a collection of potential EOR technologies. Different types of microbial reservoir treatments and their stages of development are listed in Table 3. Their application should depend on the oil-production problem to be mitigated.

Bypassing of mobile oil due to reservoir heterogeneity may require selective plugging (Jenneman and others, 1983). Recovery inefficiency due to unfavorable mobility will require viscosity modification of the waterflood by polymer-producing microorganisms, and oil trapping due to capillary forces

will require solvent/surfactant-producing microorganisms in order to reverse the rock wettability and reduce the interfacial tension. Research at the University of Oklahoma (Tanner and others, 1991) is showing that carbonate reservoir pore properties may be improved by dissolution of carbonate matrix after treatment with acid- and CO₂-producing microorganisms.

Field MEOR applications are relatively few but are increasing. Bryant (1990) reported that the number of MEOR field projects in the NIPER data base increased from 39 in 1987 to 65 in 1990. Well stimulation and cleanout treatments are the most common. Results are sparse from well-controlled field trials, except for a recent report on the use of in situ ultramicrobacteria to increase well productivity (Sheehy, 1990). A few reported cases have shown production increases of 50–300% and a decrease of bottom sediment and water (Bryant and others, 1990).

Microbially enhanced waterflooding projects are fewer in number. The best-documented project was performed in a calcareous sandstone unit in Union County, Arkansas (Yarborough and Coty, 1982; Hitzman, 1988). The reservoir was 610 m deep and had an average temperature of 35.5°C. The field trial injected the bacterial strain *Clostridium acetobutylicum* and beet molasses. Oil production was increased by 250% and was limited only by the initial low residual oil saturation. However, the results of microbial activity observed were those of indigenous bacteria rather than the injected strain. Several successful field trials in Europe have been reported (Hitzman, 1988; Lazar, 1990). Some of these field trials were also in calcar-

TABLE 3.—MEOR APPLICATIONS

Type	Stage of development
Wellbore cleanout	
Paraffin removal	Several commercial ventures (Nelson and Launt, 1991)
Corrosion/scale prevention	Several commercial ventures (Nelson and Launt, 1991)
Well stimulation	
Clostridial fermentation (acid/solvent/gases)	Many commercial ventures
Ultramicrobacterial repressurization/drainage improvement	Commercial process (Sheehy, 1990)
Coning prevention or mitigation	Field demonstration stage
Microbial control of sulfide production	Laboratory investigation
Microbially enhanced waterfloods	
Clostridial fermentation (acid/solvent/gas)	Several successful field trials (Yarborough and Coty, 1982; Hitzman, 1988; Lazar, 1990)
Biosurfactant production	Several field trials (Hitzman, 1988; Lazar, 1990)
Microbial selective plugging	Field trial stage (Knapp and others, 1989)

eous sandstone or carbonate reservoirs and relied on microbial production of acid, gas, and possibly solvent to enhance oil recovery. Recent data (Knapp and others, 1989) suggest that the incremental cost of additional oil recovered was about \$3 per barrel, suggesting that the process is economical. The University of Oklahoma is currently conducting a field trial of a microbial selective plugging process in the SE Vassar Vertz Sand Unit, Payne County, Oklahoma.

SCREENING PARAMETERS AND CRITERIA FOR MEOR TREATMENT

Activity of microorganisms in petroleum reservoirs will be governed by the reservoir's environmental conditions. These conditions were recently reviewed by McNerney and Westlake (1990) and Jenneman (1989). The most important factors that might limit microbial activity in reservoirs are physico-chemical reservoir conditions of temperature, pressure, brine salinity, and pH; oil properties such as viscosity and API gravity; and rock permeability. The limiting criteria as proposed by Clark and others (1981) were:

Salinity, <10%
pH, between 4 and 9
Permeability, >75 md
Oil gravity, >17°API
Temperature, <75°C

A recent paper by Nelson and Launt (1991) on microbial well stimulation gave the characteristics of MEOR-candidate stripper wells as follows:

Oil production, as much as 20 bbl/d

Temperature, about 20–60°C
Oil gravity, >20°API
Porosity, >3%
Permeability, >20 md
Depth, ~1,000 m

A more recent report by Tanner and others (1991) used the following criteria to determine the potential application of MEOR in carbonate reservoirs:

Salinity, <25%
Permeability, >15 md
Oil gravity, >17°API
Temperature, <82°C

Bryant and others (1990) also reviewed screening criteria for MEOR processes and concluded that 44% of reservoirs in Kansas, 14% in Oklahoma, and 25% in Texas are treatable. The method for reaching this conclusion was not discussed.

In this study, a survey of the factors such as reservoir temperature, pressure, brine chemistry, oil properties, and rock properties, that could limit MEOR applications in Midcontinent reservoirs was made using Dwight's Energydata TOTL database system. Furthermore, a review of these factors and how they could influence the effectiveness of MEOR application in Midcontinent reservoirs was made from the literature.

Reservoir Temperature and Pressure

Microbial growth rate is affected by temperature and can be predicted by the following relationship (Stainer and others, 1986):

$$\log_{10}K = -\frac{T}{2.303T} + C$$

TABLE 4.—AVERAGE TEMPERATURES OF MIDCONTINENT RESERVOIRS
REPORTED BY STATE

State/regulatory district	No. of oil-producing reservoirs with temperature record	Average temperature		Reservoirs with $T < 82^{\circ}\text{C}$ (%)
		$^{\circ}\text{C}$	$(^{\circ}\text{F})$	
Colorado	82	69	(157)	78
Kansas	29	35	(95)	100
Nebraska	117	50	(123)	100
New Mexico	134	53	(127)	91
Oklahoma	41	80	(177)	49
Texas-5	27	88	(190)	56
Texas-6	97	71	(166)	44
Texas-7B	107	47	(117)	100
Texas-8A	140	49	(120)	98
Texas-9	127	54	(129)	94
Texas-10	95	60	(140)	86

where K = growth rate,

τ = constant for given bacteria (an energy term),

T = temperature in degrees Kelvin,

C = constant.

Usually there is an optimal temperature at which the maximum rate of growth occurs and beyond which microbial growth rate diminishes significantly. Each bacterial species has its own characteristic optimal growth temperature. The list of thermophilic microorganisms, those with optimal growth temperatures of 100°C or higher, is growing. Thus, even high-temperature reservoirs can be potential targets for MEOR.

The indigenous microbial population within a reservoir is capable of withstanding the physical environment. The growth and metabolism of these indigenous microorganisms can be controlled by altering the availability and concentration of certain nutrients, such as the main carbon/energy source, electron acceptor, nitrogen, sulfur, and phosphorous. Controlling indigenous microorganisms seems to be more practical than injecting specific microorganisms for the following reasons:

1) Useful indigenous bacteria are already adapted to growth under the prevailing environmental conditions of the reservoir;

2) Cell injection requires the development of specialized strains for each new reservoir to be treated and will increase the development costs;

3) Porous media act as a filter to remove microorganisms from the flowing phase, making cell injection difficult and, at best, localized to regions near the wellbore; and

4) Normal homeostatic mechanisms present in any established microbial community will inhibit or prevent the establishment of a newly introduced

species; in fact, the results of some field trials clearly show that the microbial activity was that of indigenous rather than injected microorganisms.

Even though it is known that microorganisms can grow at temperatures $>100^{\circ}\text{C}$, little is known about the factors that control their metabolism. Because of this, Jenneman (1989) determined that a practical temperature limit for in-situ MEOR was 75°C . However, a successful field trial has been reported in a reservoir in Hungary with a temperature of 97°C (Hitzman, 1988). For the purpose of this study, the temperature limit for Midcontinent reservoirs potentially suitable for MEOR is 82°C . This temperature is not an absolute limit for microbial activity, but it is a limit for organisms that have well-studied physiologies (Tanner and others, 1991).

Table 4 shows the number of current oil-producing reservoirs with temperature records, statewide average reservoir temperatures, and the percentage of current oil-producing reservoirs having temperatures $<82^{\circ}\text{C}$ in the Midcontinent region and Colorado. A majority of Midcontinent reservoirs with temperature records have temperatures below the chosen temperature limit of 82°C .

Bubela and McKay (1985) reported that a change from atmospheric pressure to 20,000 KPa (2,870 psi) increased the optimal growth temperature of a microorganism from 55 to 65°C , and decreased its doubling time from 17 to 12 hours. In general, pressure as high as 20,000 KPa has little or no effect on bacterial activity; however, pressures $>50,000$ KPa (7,175 psi) can inhibit microbial activity (Bubela and McKay, 1985). It follows, therefore, that in most reservoirs, particularly in the Midcontinent region, pressures will not be great enough to inhibit microbial growth.

TABLE 5.—PROPERTIES OF BRINES FROM MIDCONTINENT RESERVOIRS

State/regulatory district	Average TDS ^a (%)	Reservoirs with TDS <20% (%)	Reservoirs with pH between 4 and 9 (%)
Arkansas	26	36	89
Colorado	8	99	99
Kansas	8	99	99
Nebraska	9	79	93
New Mexico	11	92	92
Oklahoma	17	50	97
Texas-5	11 ^b	61	96
Texas-6	11 ^b	56	96
Texas-7B	11 ^b	63	96
Texas-8A	11 ^b	35	96
Texas-9	11 ^b	35	96
Texas-10	11 ^b	35	96

^aTDS = total dissolved solids.^bAverage for all Texas regulatory districts.

Brine Chemistry

Oil fields produce brines with sodium chloride (NaCl) content ranging from <0.01% to >20%. Present emphasis in MEOR is either injection of microbial cultures with their nutrients into reservoirs already undergoing active waterflooding, or stimulation of existing microbial populations by the injection of necessary nutrients. In the second case, indigenous populations are already selected for growth in the brine present in the reservoir. In the first method, the brine composition must be studied to assure that it is suitable for growth and metabolism of the chosen microbial species, and will require the isolation of specific microorganisms for various reservoir conditions.

McInerney and Westlake (1990), Jenneman (1989), and Clark and others (1981) discussed the biochemical parameters which affect microbial growth and metabolism. Clark and others (1981) proposed that the NaCl content should be <10% and the brine pH between 4 and 9. In a recent study, Tanner and others (1991) showed that there are several halophilic or halotolerant microbial systems that are active in brines with as much as 25% sodium chloride.

According to Jenneman (1989), the pH of most petroleum reservoirs is within the range of growth of most known microorganisms. In addition, carbonate reservoirs are naturally buffered which prevents reduction of pH by microbial acids to inhibitory levels.

The percentage of Midcontinent reservoirs with total dissolved solids content <20% is shown in Table 5. Kansas and Colorado have the highest

percentage of such reservoirs (99%), whereas Texas Regulatory Districts 8A, 9, and 10 have the smallest percentage (35%).

Oil Properties

Oil properties can also limit the effectiveness of MEOR. Limitations imposed upon MEOR by the petroleum phase include toxicity of the light, volatile fractions. Heavy oils may be difficult to recover because of unfavorable mobility ratios between the brine and the petroleum. Reservoirs whose crude oil has an oil gravity of <17°API and viscosity >40 cp are probably not good candidates for MEOR processes.

Table 6 shows the statewide average API gravity and average oil viscosity values for the Midcontinent region and Colorado. Reservoirs in Kansas and Oklahoma have the highest percentage of current oil-producing reservoirs with oil gravity of >17°API, whereas Nebraska has the lowest.

Reservoir Rock Properties

Permeability, porosity, and oil saturation limit the applicability of bacterial treatments in reservoirs. A study by Zvyagintsev and Pitryuk (1973) showed that permeability not only limited injectivity and movement of microbes through the porous medium, but also limited microbial growth and metabolism.

Porosities found in commercial reservoirs do not normally impose any restrictions on microbial enhanced oil recovery. Average porosity values for commercial reservoirs vary from ~8% to >20%.

TABLE 6.—DISTRIBUTION OF OIL PROPERTIES BY STATE

State/regulatory district (no. of reservoirs)	Average API gravity	Reservoirs with >17°API (%)	Average viscosity (cp)	No. of reservoirs with viscosity <40 cp
Colorado (525)	38.5	99.6	12.3	51
Kansas (9,365)	— ^a	99.7	23.0	142
Nebraska (192)	23.0	12.0	6.2	5
New Mexico (835)	41.1	24.0	5.9	56
Oklahoma (8,071)	—	99.7	—	—
Texas-5 (147)	23.2	55.7	5.7	17
Texas-6 (643)	26.5	64.2	8.7	65
Texas-7B (2,079)	30.3	73.0	3.2	119
Texas-8A (875)	26.7	89.2	4.4	124
Texas-9 (1,926)	20.8	58.9	3.8	145
Texas-10 (310)	32.5	77.1	2.4	20

^a — = data not available.

One of the most critical tests to determine whether a given reservoir is suitable for MEOR is the injectivity of the applicable bacterial strains and/or nutrients. Bacteria have many morphologies (e.g., rods, cocci, curved rods, tetrads, chains, etc.) with lengths of 0.5–10 microns and diameters of 0.5–2 microns. Jenneman (1989) reasoned that pore throats of <0.5 microns would restrict the ability of microbes to enter and move within the reservoirs. However, ultramicrocellular forms of many bacteria with cell sizes ~0.1 micron, or less, may be injectable into tight formations.

Figure 1 shows the relationships between entry pore-throat sizes and absolute permeability for various sandstones and carbonates. The rocks used to establish these relationships were Red Fork, Oil Creek, Vertz, and Berea sandstones, and Viola, Bethany Falls, and Springer limestones. Absolute permeability was measured on rock-core plugs with a gas permeameter, while the pore-throat sizes were determined from capillary pressure data measured with Beckman L5-50B ultracentrifuge apparatus. This analysis shows that carbonates with low absolute-permeability values may have entry pore-throat sizes one or more orders of magnitude larger than sandstones having higher permeability. The implication is that carbonates with low permeability values may still be candidates for MEOR and that the permeability screening limit for carbonates should be lower than that for sandstones.

Jenneman (1989) suggested a limit of 75 md for sandstone reservoirs. However, more recent work based on field applications of MEOR suggested a permeability limit of 20 md for wells undergoing microbial stimulation (Nelson and Launt, 1991). Ongoing work on carbonate reservoirs suggests

a limit of 15 md, but microbial penetration into rocks with <0.1 md permeability has been reported (Tanner and others, 1991; Meyers and McCready, 1966).

The average absolute-permeability values and the number of sandstone reservoirs having permeabilities >75 md and carbonate reservoirs having permeabilities >15 md in the Midcontinent reservoirs and Colorado are shown in Table 7. In Kansas, 82 out of 284 sandstone reservoirs (28.9%) and 1,708 out of 1,738 carbonate reservoirs (98.3%) have average permeabilities exceeding 75 md and 15 md, respectively. On the average, 88.5% of all the reported Kansas reservoirs (1,790 out of 2,022 reservoirs) have average permeabilities exceeding the stated minimum permeability limits. In Nebraska, only two out of a reported 367 sandstone reservoirs (0.5%) have average permeabilities exceeding 75 md. The statistics of the percentage of reported reservoirs having average permeabilities exceeding the stated minimum permeability values are as follows: New Mexico (76.4%), Texas regulatory district no. 6 (73.1%), Texas regulatory district no. 8A (46.1%), Texas regulatory district no. 7B (38.8%), and Texas regulatory district no. 9 (32.8%).

Table 8 shows the average values of porosity and permeability in selected oil-producing reservoirs. The Springer limestone has the lowest average porosity (2%) and lowest absolute permeability (0.1 md). However, the Springer is known to be fractured, and oil storage and production is believed to occur in and through the fractures. The Oil Creek and Vertz sandstones exhibit very good reservoir properties. An MEOR field trial has been carried out in the Bartlesville sandstone by NIPER (Bryant and others, 1988).

TABLE 7.—DISTRIBUTION OF RESERVOIR-ROCK PROPERTIES BY STATE

State/regulatory district	Rock type ^a	No. of records	Permeability (md)			No. of reservoirs with avg. k	
			Min.	Max.	Avg.	>15 md	>75 md
Colorado	s	364	.01	605	244	364	340
	c	1	.01	23	10	1	0
Kansas	s	284	.06	209	67	274	82
	c	1,738	.06	1,000	109	1,708	1,629
Nebraska	s	367	.03	2,237	57	4	2
New Mexico	s	55	.01	123	66	55	21
	c	161	.01	177	68	44	38
Oklahoma	s	— ^b	—	—	—	—	—
	c	—	—	—	—	—	—
Texas-5	s	56	—	—	841	56	47
	c	44	—	—	509	43	15
Texas-6	s	250	.01	1,185	538	250	145
	c	144	.06	113	52	143	18
Texas-7B	s	146	.01	496	41	140	7
	c	192	.01	168	52	124	4
Texas-8A	s	111	.01	419	27	49	3
	c	377	.01	419	80	222	84
Texas-9	s	473	.02	241	70	465	152
	c	43	.03	391	86	16	13

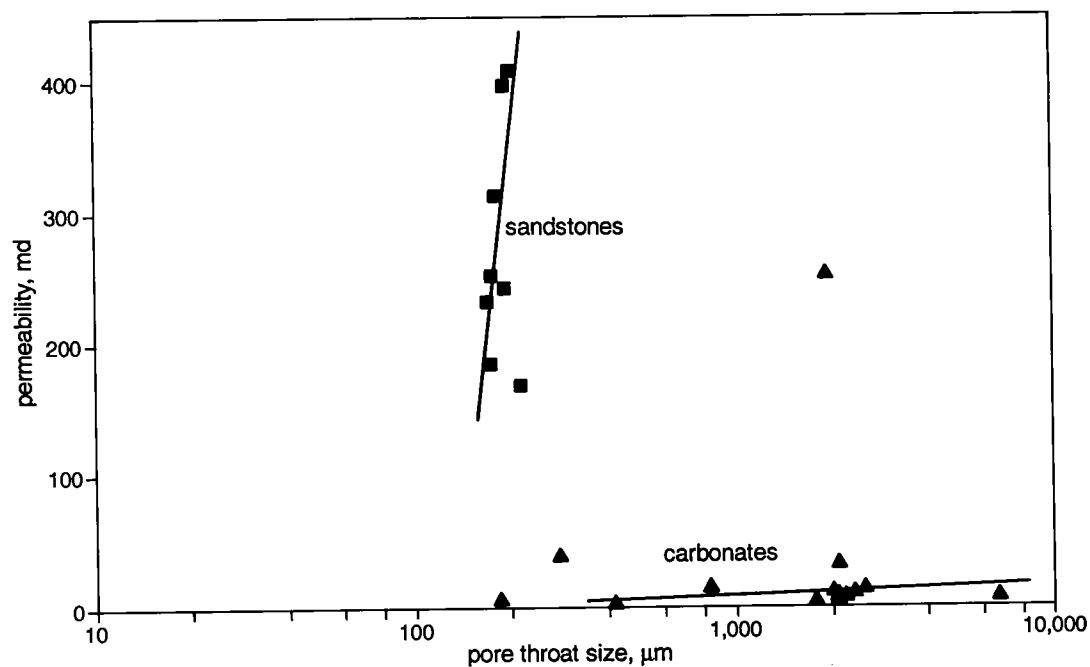
^as = sandstones; c = carbonates.^b— = data not available.

Figure 1. Variation of permeabilities with pore-throat sizes in reservoir rocks.

TABLE 8.—AVERAGE POROSITY AND PERMEABILITY VALUES IN SELECTED OIL-PRODUCING RESERVOIRS IN THE MIDCONTINENT REGION

Formation	Average porosity (%)	Average permeability (md)
Oil Creek	16.6	153.9
Viola ^a	8.5	49.0
Springer ^a	2.0	0.1
Vertz	16.5	210.0
Red Fork ^a	4.0	1.0
Bartlesville	15.6	31.3

^aData from computer search.

OIL RESERVOIRS TREATABLE BY MEOR IN THE MIDCONTINENT REGION

From the discussions above, the following criteria were chosen to determine the number of reservoirs suitable for MEOR:

Permeability, >75 md (for sandstones)
(Jenneman, 1989)
>15 md (for carbonates)
(Tanner and others, 1991)

NaCl content, <200,000 ppm

pH, 4–9

Temperature, <82°C (Tanner and others, 1991)

Oil gravity, >17°API

Table 9 shows the percentage of Midcontinent oil-producing reservoirs treatable by MEOR processes. This result is obtained by treating each screening parameter as an independent variable, and is subject to any limitations in the statistical data used in its computation. The basic probability principle applied states that "the probability of occurrence of an event at a certain extent is proportional to the product of the probabilities of the factors causing the event." Hence, the percentage of treatable reservoirs within a given State or Regulatory District can be written as:

$$T = \Pi^n f_i$$

where T is the percentage of treatable reservoirs,
 Π is a multiplication convention,
 f_i is an individual parameter affecting MEOR application,
 n is the number of parameters.

According to this result, Kansas has the highest percentage of currently oil-producing reservoirs in the Midcontinent region that would be treatable by MEOR. By coincidence, Kansas also has the highest stripper- to total-oil production ratio nation-

ally. The state with the fewest treatable reservoirs is Nebraska (<0.1%).

However, as a rule of thumb, reservoirs which contain a water phase and those in which waterflooding could be implemented are potential candidates for MEOR. In many fields, rock and fluid data are sparse and the use of the criteria presented in this paper for determining reservoir suitability for MEOR is not possible.

CONCLUSIONS

A significant percentage (32%) of oil production from the Midcontinent region is from marginal fields. Marginal fields may not support high-cost EOR methods, but are well-suited for microbially enhanced oil recovery.

The percentage of reservoirs meeting various screening criteria and the percentage of MEOR treatable reservoirs (Table 9) indicates that many oil reservoirs in the Midcontinent region are candidates for MEOR and could benefit from some form of microbial treatment.

REFERENCES CITED

- American Petroleum Institute, 1990, Basic petroleum data book, petroleum industry statistics: American Petroleum Institute, v. 10, no. 2, Washington, D.C.
- Bryant, R. S., 1990, Screening criteria for microbial EOR processes: U.S. Department of Energy Report no. NIPER-478, 17 p.
- Bryant, R. S.; Burchfield, T. E.; Dennis, D. M., and Hitzman, D. O., 1988, Microbial-enhanced waterflooding: Mink unit project: Paper SPE/DOE 17341 presented at the Society of Petroleum Engineers/U.S. Department of Energy EOR symposium (April 17–20), Tulsa, Oklahoma.
- Bubela, B.; and McKay, B. A., 1985, Assessment of oil reservoirs for microbiological enhanced oil recovery—microbes and oil recovery: International Bio-resources Journal, v. 1, p. 99–107.
- Clark, J. B.; Munnecke, D. M.; and Jenneman, G. E., 1981, In situ microbial enhancement of oil production: Developments in Industrial Microbiology, v. 22, p. 695–701.
- Hitzman, D. O., 1988, Review of microbial enhanced oil recovery field tests: Proceedings, Symposium on applications of microorganisms to petroleum technology: U.S. Department of Energy Report no. NIPER-351.
- Jenneman, G. E., 1989, The potential for in-situ microbial applications, in Donaldson, E. C.; Chilgarian, G. V.; and Yen, T. F. (eds.), Microbial enhanced oil recovery: Elsevier, New York, p. 38–74.
- Jenneman, G. E.; Knapp, R. M.; Menzie, D. E.; McInerney, M. J.; Revus, D. E.; Clark, J. B.; and Munnecke, D. M., 1983, Transport and plugging in Berea sandstone using microorganisms, in Donaldson, E. C.; and Clark, J. B. (eds.), Proceedings of the 1982 international symposium on MEOR: U.S. Department of Energy, Bartlesville, Oklahoma, p. 71–75.

TABLE 9.—PERCENT OF MIDCONTINENT OIL-PRODUCING RESERVOIRS POTENTIALLY TREATABLE BY MEOR PROCESSES

State/regulatory district	Salt <20% (%)	pH 4–9 (%)	Permeability ss:<75md; C<15md (%)	Gravity >17°API (%)	Treatable reservoirs ^a (%)
Arkansas ^b	36.0	88.5	— ^c	—	—
Colorado	98.8	98.8	93.4	99.0	90.3
Kansas	99.0	98.5	88.5	99.7	86.0
Missouri ^b	100.0	—	—	50.0	—
Nebraska	79.0	93.0	0.5	12.0	0.04
New Mexico	91.6	91.6	76.3	24.0	15.4
Oklahoma	50.1	97.0	31.0	99.7 ^b	15.1
Texas-5	61.1	95.6 ^d	90.0	55.7	24.0
Texas-6	56.0	95.6 ^d	64.0	64.2	24.0
Texas-7B	62.5	95.6 ^d	41.2	73.0	16.0
Texas-8A	35.3	95.6 ^d	46.1	89.2	24.0
Texas-9	35.3	95.6 ^d	37.6	58.9	7.5
Texas-10	36.3	95.6 ^d	38.0	77.1	10.2

^a Percent of treatable reservoirs calculated by assuming each parameter as an independent variable.

^b From Jenneman (1989).

^c — = insufficient data for calculation.

^d Average of all Texas regulatory districts.

- Knapp, R. M.; McInerney, M. J.; Menzie, D. E.; and Chisolm, J. L., 1989, Microbial field pilot study: Annual report performed under U.S. Department of Energy contract no. DE-FG22-89BC14246 at the University of Oklahoma, DOE/BC/14246-5, 96 p.
- Lazar, I., 1990, Preliminary results of some recent MEOR field trials in Romania, in *Proceedings, International Conference on MEOR* (May 27–June 1), Norman, Oklahoma.
- McInerney, M. J.; and Westlake, D. W. S., 1990, Microbially enhanced oil recovery, in Ehrlich, H. L.; and Brierly, C. L. (eds.), *Microbial mineral recovery*: McGraw-Hill, New York, p. 409–495.
- Meyers, G. E.; and McCready, R. J. L., 1966, Bacteria can penetrate rocks: *Canadian Journal of Microbiology*, v. 12, p. 477–484.
- Nelson, S. J.; and Launt, P. D., 1991, Stripper well production increased with MEOR treatment: *Oil and Gas Journal*, March, p. 114–118.
- Sheehy, A. J., 1990, Field studies of microbial EOR: Paper SPE/DOE 20254 presented at the Society of Petroleum Engineers/U.S. Department of Energy symposium on enhanced oil recovery (April 22–25), Tulsa, Oklahoma.
- Stainer, R. Y.; Ingraham, J. L.; Wheelis, M. L.; and Painter, P. R., 1986, *Microbial world*: Prentice-Hall, Englewood Cliffs, New Jersey, 689 p.
- Tanner, R. S.; Udegbunam, E. O.; McInerney, M. J.; Knapp, R. M.; and Adkins, J. P., 1991, Microbial enhancement of oil production from carbonate reservoirs: U.S. Department of Energy Report no. DOE/BC/14202-6, 227 p.
- Tanner, R. S.; Udegbunam, E. O.; McInerney, M. J.; and Knapp, R. M., 1992, Microbially enhanced oil recovery from carbonate reservoirs: *Geomicrobiology Journal*, v. 9, p. 169–195.
- U.S. Department of Energy, 1990, Abandonment rates of the known domestic oil resource: U.S. Department of Energy Report no. DOE/BC-89/6/SP, 39 p.
- Yarborough, H. F.; and Coty, V. F., 1982, Microbially enhanced oil recovery from the Upper Cretaceous Nacatoch Formation, Union County, Arkansas: *Proceedings, International Conference on Microbial Enhanced Oil Recovery* (May 16–21), Afton, Oklahoma: U.S. Department of Energy Report no. Conf-8205140, p. 149–153.
- Zvyagintsev, D. G.; and Pitryuk, A. P., 1973, Growth of microorganisms in capillaries of various sizes under continuous flow and static conditions: *Mikrobiologiya*, v. 42, p. 60–64.

Three-Dimensional Reservoir Description Using Conditional Simulation

Godofredo Perez and Mohan Kelkar

University of Tulsa
Tulsa, Oklahoma

ABSTRACT.—Descriptions of porosity have been generated in sandstone and carbonate reservoirs with conditional simulation methods. These descriptions capture the heterogeneities observed in the conditioning data and account for the uncertainties due to the scarcity of data. Fields studies were conducted to test the ability of two- and three-dimensional conditional simulations to reproduce porosity distributions observed in the well logs. The data in each field consisted of porosity logs from several wells grouped as conditioning and comparison data. The conditioning data were used to derive the statistical parameters and to condition the simulations, whereas the comparison data were compared to the logs generated from the conditional simulations. The simulated and the actual porosity logs were in close agreement.

Conditional simulations of porosity and permeability were used to construct reservoir models for waterflooding simulations to quantify the effects of spatial correlation of the properties and the uncertainty of the descriptions on reservoir performance and on oil recovery. Simulations indicated that oil recoveries differ significantly among reservoir models which do not account for the gross reservoir structure.

INTRODUCTION

Distributions of reservoir properties in a small sandstone oil reservoir in Oklahoma were generated with a recently introduced conditional-simulation method (Hewett, 1986) using density logs and core measurements as conditioning data. Conditional-simulation methods generate multiple equiprobable descriptions of a reservoir property with certain statistical attributes and honor the conditioning data (e.g., porosity from logs or cores) at the sampled locations. The advantage of conditional-simulation models are that they can incorporate spatial correlation and account for uncertainty.

Hewett (1986) introduced statistical fractal models to represent the spatial correlation observed in porosity logs and to generate conditional simulations of porosity in a cross section between two wells. A critical assumption in this conditional-simulation method is made in the assessment of the correlation structure of porosity for the inter-well region. However, this approach has been implemented in several studies of large fields (Mattews and others, 1988; Emanuel and others, 1989; Payne and others, 1989; Tang and others, 1989; Hewett and Behrens, 1990), and the reservoir-flow performance predicted with condi-

tional-simulation descriptions are in close agreement with the production histories. Recently, statistical fractal models were applied to investigate the effect of reservoir property distributions on miscible-flow performance (Crane and Tubman, 1990; Aasum and others, 1991).

In this investigation, conditional simulations of porosity are compared with actual porosity measurements at two wells, and a method to generate permeability distributions is introduced. Waterflooding simulations were conducted in reservoir models constructed with conditional simulations to evaluate the effect of porosity and permeability distributions on simulated performance and recovery. Finally, a new method to generate three-dimensional conditional simulations is introduced and tested with porosity data from a carbonate reservoir.

FIELD DESCRIPTION

The Robinson lease is located in Muskogee County, Oklahoma. The field was discovered in the 1930s, and in 1985 a waterflooding project was implemented. The field covers 160 acres and currently has 13 active wells (five producers and eight injectors). This investigation is based on the data from seven wells (Fig. 1).

Perez, Godofredo; and Kelkar, Mohan, 1993, Three-dimensional reservoir description using conditional simulation, *in* Johnson, K. S.; and Campbell, J. A. (eds.), *Petroleum-reservoir geology in the southern Midcontinent, 1991 symposium*: Oklahoma Geological Survey Circular 95, p. 182–191.

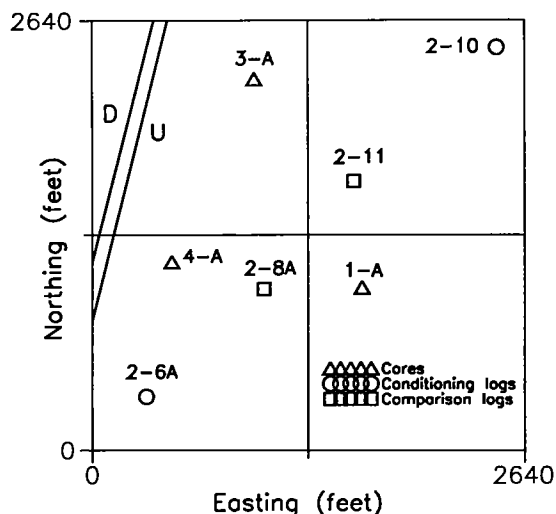


Figure 1. Locations of Robinson lease wells used in this study. The diagonal lines on the west side of the lease indicate the approximate location of a fault.

The Robinson lease produces from three Dutcher sands, denoted as A, B, and C sands, starting from the top of the interval. Core data indicate that the B sand has the highest reservoir quality (19% porosity and 100 md permeability). The reservoir is laterally bounded by a combination of structural and stratigraphic traps. The reservoir is bound by a sealing fault on the west (Fig. 1) and the reservoir quality of the sands gradually diminishes eastward.

The primary sources of data for this investigation are density logs and cores. Porosity logs derived from density logs of four wells (Fig. 1) were used for the conditional-simulation analyses. Core data from three wells (Fig. 1) includes porosity, permeability, and residual saturations after laboratory core floods. These data were used to derive a relationship between porosity and permeability.

DESCRIPTION OF RESERVOIR PROPERTIES

A spatial statistical analysis was conducted to identify the fractal model that represents the porosity variability in logs of the conditioning wells. Conditional simulations with a specified fractal model were used to generate porosity distributions in the inter-well region. Permeability and porosity relationships were developed from the core data, and a method to account for the variability in the data is introduced.

Spatial Statistics of Data

Using analyses of several well logs, Emanuel and others (1989) showed that the spatial correla-

tion of porosity can be represented by statistical fractal models known as fractional Gaussian-noise (fGn) models. The intermittency exponent of fGn models is related to the fractal dimension, and it provides a measure of the degree of the spatial variability of a property. Values of the intermittency exponent are between 0 and 1: values above and below 0.50 represent different types of spatial correlation. As the intermittency exponent approaches 1, a property becomes more correlated. An intermittency exponent equal to 0.50 corresponds to an uncorrelated property (i.e., white noise). As with many other measurements of natural phenomena, porosity well logs have intermittency exponents >0.50 (Hewett, 1986).

Analyses of the porosity logs of the conditioning wells (wells 2-6A and 2-10, Fig. 1) in the Robinson lease using several methods (Hewett, 1986) indicate that the intermittency exponent is close to 0.85. In this investigation, the intermittency exponent of fGn models was evaluated using the box-counting approach of Feder (1988). This method uses a scaling relationship to relate the number and size of boxes (i.e., square or cubic grids in two- or three-dimensions, respectively) required to cover the porosity fluctuations as a function of depth to the intermittency exponent. The method was applied to graded (integrated over depth) porosity logs. The slope of a plot of the number of boxes versus box size (Fig. 2) yields the intermittency exponent. For wells 2-6A and 2-10, the intermittency exponents found with the box-counting method are 0.86 and 0.82, respectively.

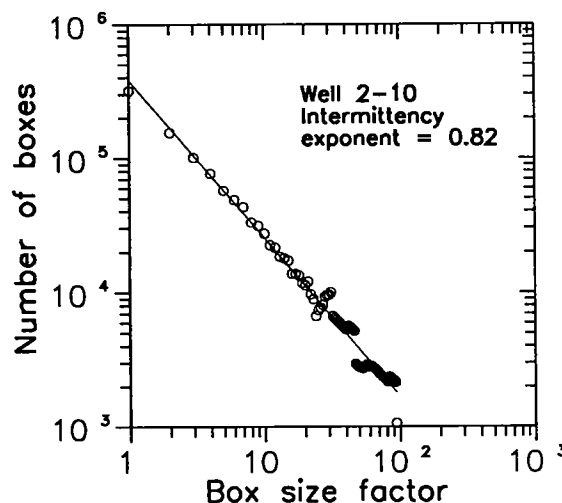


Figure 2. Box-counting method to evaluate the intermittency exponent of a fGn model of the porosity log from well 2-10. The intermittency exponent is calculated from the slope of the fitted line.

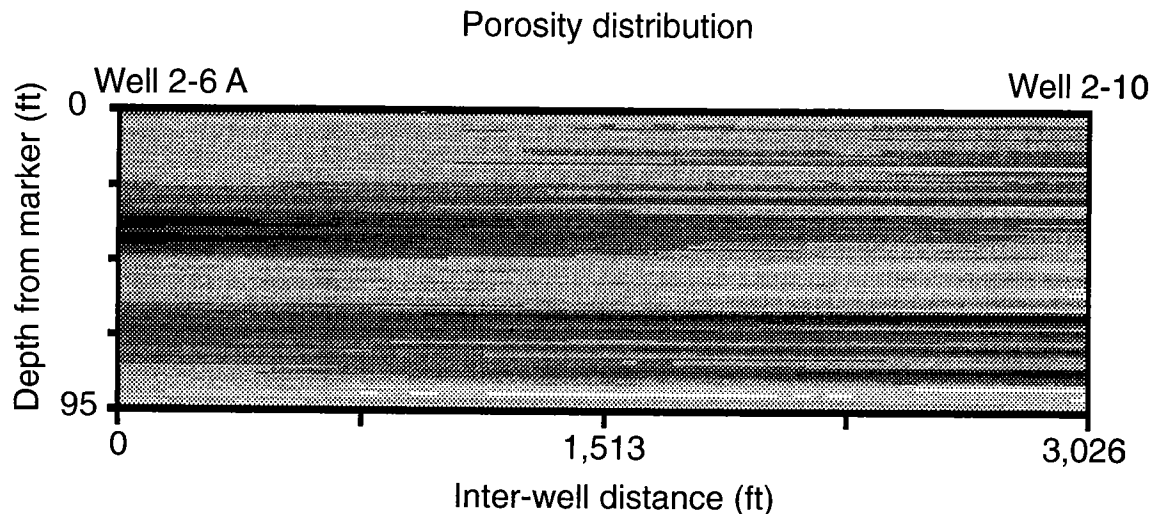


Figure 3. Map of porosity distribution generated with the successive-random-additions method for an intermittency exponent equal to 0.85 between wells 2-6A and 2-10 (3,026 ft apart). Black is the maximum porosity (19.7%), white is the minimum porosity (0.0%), and gray tones are assigned by linear interpolation to intermediate values of porosity.

Conditional Simulations of Porosity Distribution

Conditional simulations were generated with the successive-random-additions method proposed by Hewett (1986). The successive-random-additions method is a stochastic interpolation between two wells which allows one to specify the intermittency exponent of a fractional Brownian-motion (fBm) model. Since the method is stochastic, different realizations can be generated with the same data and constraints by using different sets of random numbers. Conditional simulations of porosity in the reservoir region between wells 2-6A and 2-10 (an area 3,026 ft long and 95 ft thick) were generated with the successive-random-additions method. Realizations of porosity distributions (Fig. 3) indicate that lateral changes are smooth for an intermittency exponent equal to 0.85. The high-porosity regions corresponding to the B and C sands are the dark regions in Figure 3.

Conditional simulations of porosity between wells 2-6A and 2-10 were sampled at the intermediate locations corresponding to wells 2-8A and 2-11 (Fig. 1) in order to generate the simulated porosity logs. Comparisons of the simulated logs and the density porosity logs of wells 2-8A and 2-11 (Fig. 4) show a close agreement for conditional simulations with an intermittency exponent equal to 0.85. Differences in the simulated and measure porosity logs are not significant for other intermittency exponents ≥ 0.75 (Fig. 5). Differences in simulated porosity are more sensitive to different conditional-simulation realizations than to intermittency exponent (Figs. 4 and 5, for intermittency exponent equal to 0.85).

Permeability Distributions

The permeability distributions required in the waterflooding simulations were generated with the porosity and permeability relationship derived from the core data. Conventionally, a linear relationship between the porosity and the logarithm of permeability is assumed. Core porosity and permeability data from three wells in the Robinson lease (Fig. 1) were plotted and the linear relationship was determined by a least-square regression (Fig. 6). The linear relationship was determined by a least-square regression (Fig. 6).

Most porosity and permeability measurements from cores exhibit large deviations from the linear-log line (e.g., Fig. 6). A stochastic relationship between porosity and permeability is proposed to account for the departures from the linear relationship. The stochastic relationship is similar to the conventional relationship, but it contains an additional random component. This component is normally distributed with a mean equal to 0, and a variance equal to the variance of the error between values of the linear relationship and the core data. For the core data of the Robinson lease, the stochastic relationship (Fig. 6) adequately accounts for the ranges of porosity and permeability observed.

WATERFLOODING PERFORMANCE

Conditional simulations of porosity and permeability in the Robinson lease were used to investigate the effect of reservoir property distribution on waterflood performance and recovery. The waterflooding models are vertical reservoir sec-

tions 94 ft thick and 859 ft long, between two fully penetrating wells. The waterflooding simulations consist of injecting water at a constant rate into well 2-8A and producing at constant bottom-hole pressure (above the bubble-point pressure) in well 2-11 (Fig. 1). For all reservoir models, initial water saturations are uniform and equal to 44%, and the vertical permeabilities are set equal to 20% of the horizontal permeabilities. The viscosities of the oil and water are constant and equal to 3 and 0.85 centipoise, respectively.

Simulations were conducted with the commer-

cial simulator ECLIPSE 100 (Exploration Consultants Limited, 1988). ECLIPSE is a three-dimensional, three-phase, fully implicit, and multi-purpose Black-oil simulator. The models consisted of 32 and 65 cells in the vertical and the horizontal directions, respectively. Results of the simulations are the oil and water fractional flows (oil and water flow rates at the producing well, divided by the total flow rate) and the oil recovery (cumulative oil produced, divided by the reservoir pore volume) as a function of injected pore volume (cumulative water injected, divided by the reservoir pore volume).

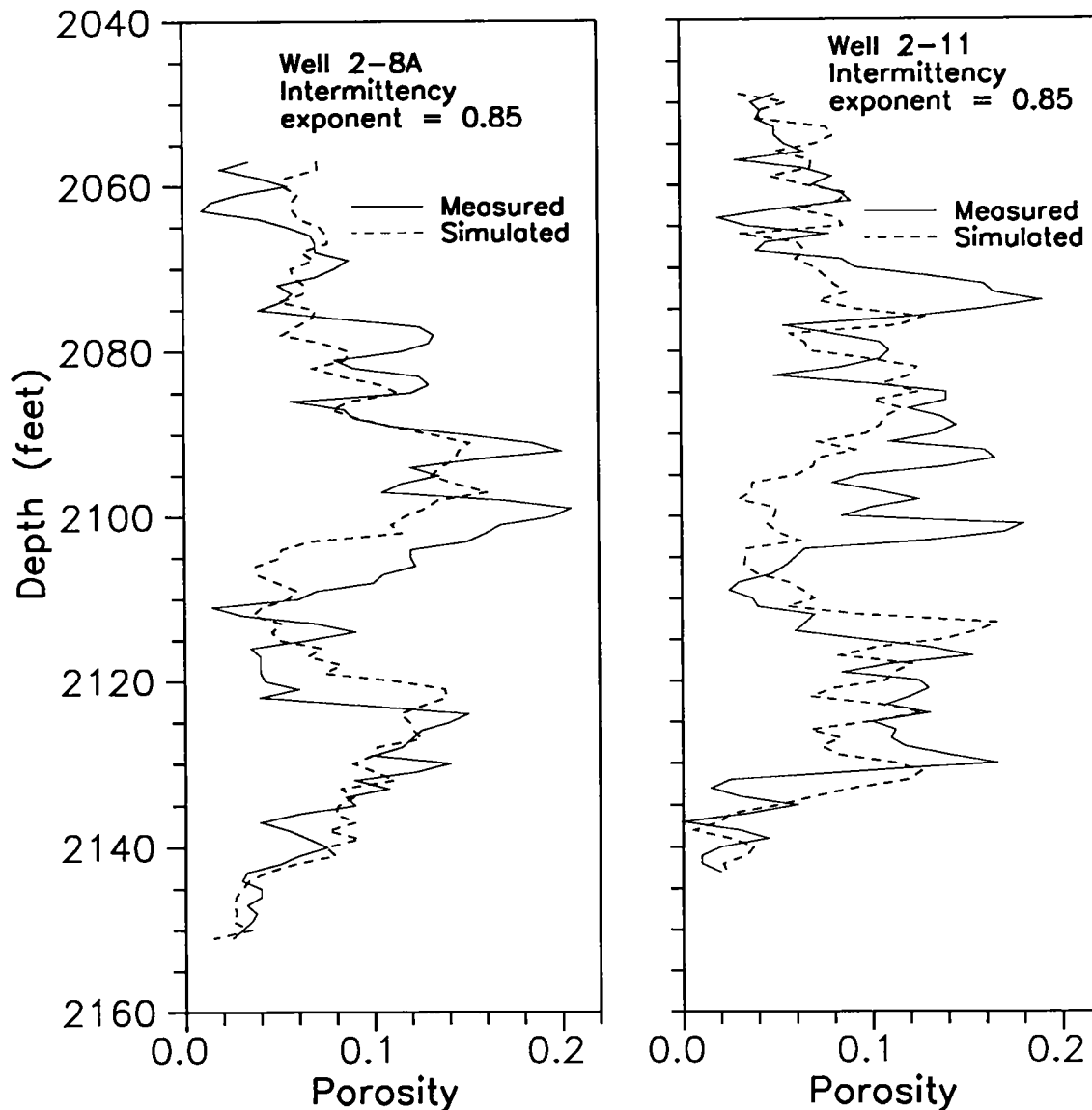


Figure 4. Comparison of conditional-simulation and measured porosity logs from wells 2-8A and 2-11. Intermittency exponent = 0.85.

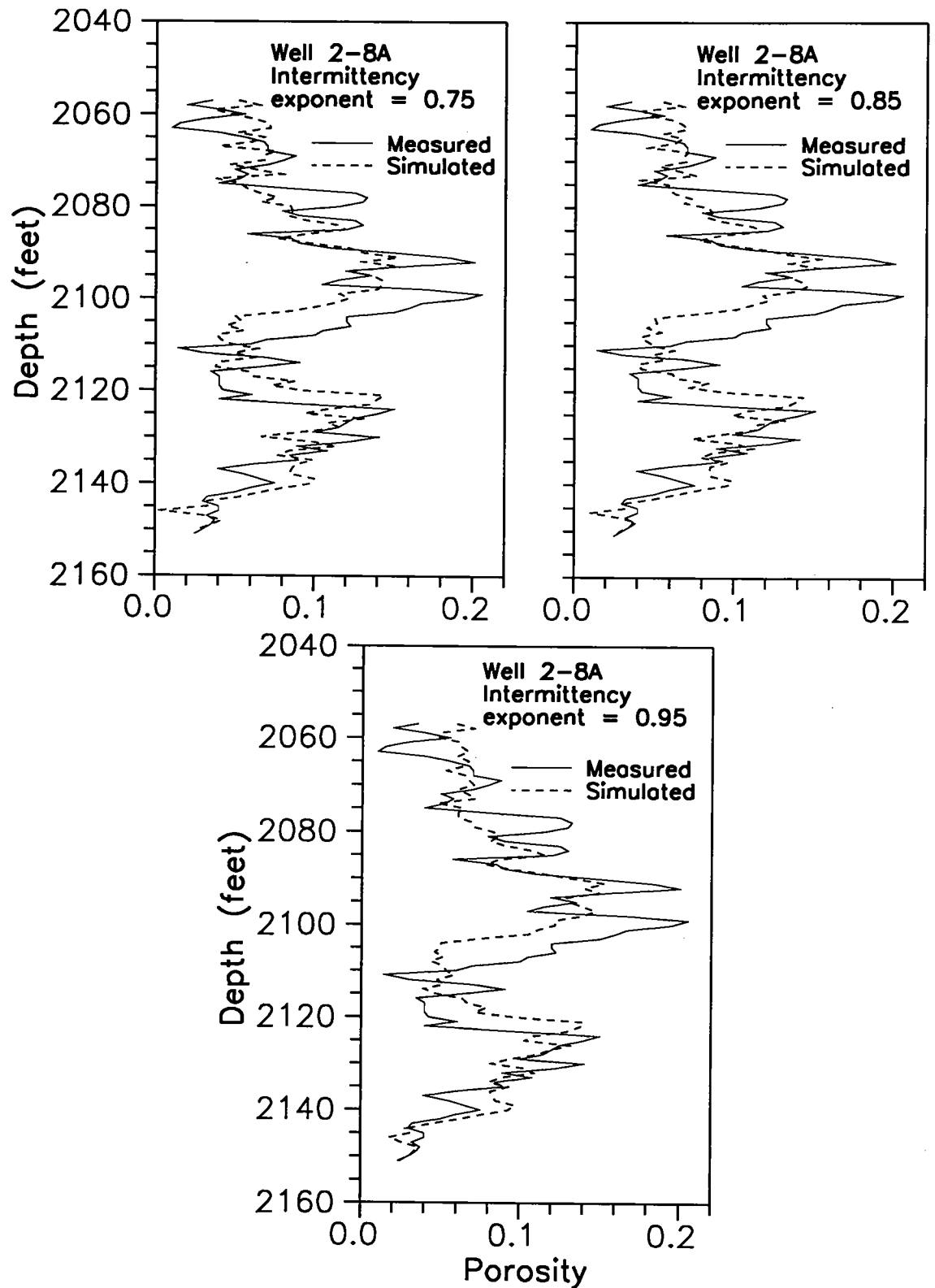


Figure 5. Comparison of conditional-simulation and measured porosity logs from well 2-8A for three intermittency exponents (0.75, 0.85, and 0.95).

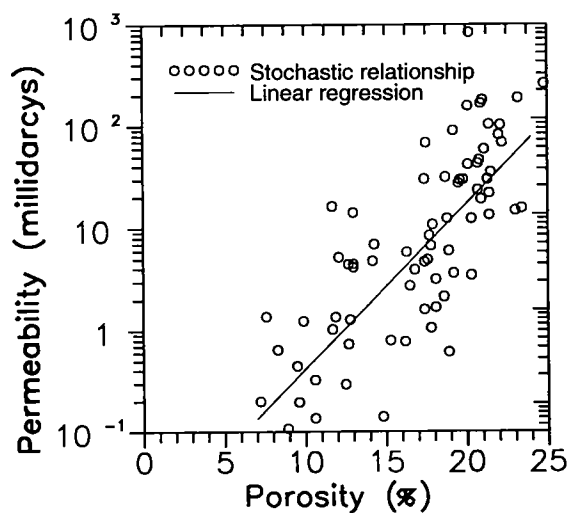
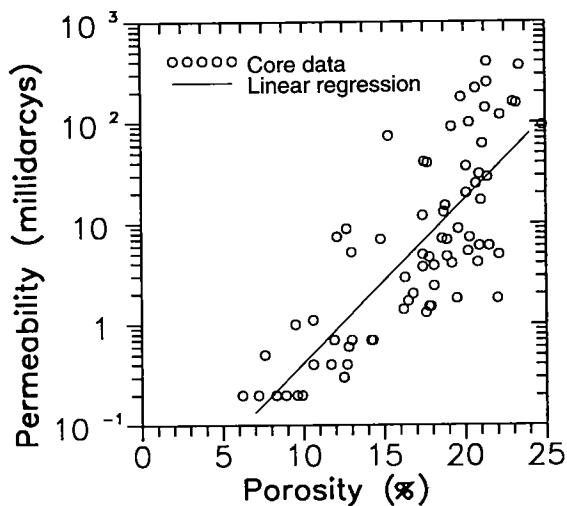


Figure 6. Porosity and permeability relationship from the core data (wells 1-A, 3-A, and 4-A, Fig. 1) (above), and from one realization of the stochastic relationship (below).

Spatial Correlation

Reservoir models with different spatial correlations were constructed by varying the intermittency exponents in the conditional simulations of porosity. As expected from prior observations (Fig. 5), the effect on simulated waterflooding performance (oil and water fractional flow) of varying intermittency exponents in the range of 0.75–0.95 is insignificant (Fig. 7). Only a slightly pessimistic waterflooding performance is observed for a case of severe spatial variability of porosity (not the case in the Robinson lease), represented by a small intermittency exponent (0.05, Fig. 7) due to early water breakthrough.

It appears that a different realization (i.e., the same intermittency exponent and conditioning data, but a different set of random numbers) for an intermittency exponent equal to 0.85 results in a greater effect on waterflooding performance than different intermittency exponents >0.75 (Fig. 7).

Porosity Distribution

A conventional layer-cake model of the Robinson lease was constructed by dividing the reservoir into three layers of constant porosity and permeability, corresponding to the three Dutcher sands, separated by impermeable layers. Simulations (Fig. 8) show that waterflooding performance and oil recovery for the layer-cake model are only

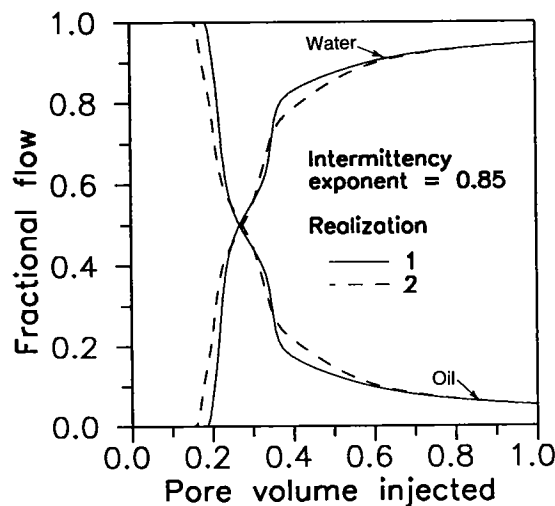
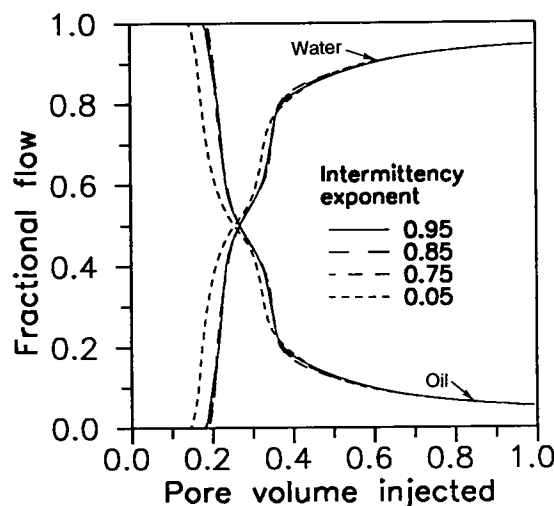


Figure 7. Waterflood fractional flows for conditional-simulation models with different intermittency exponents (above) and for two realizations of a model with intermittency exponent equal to 0.85 (below).

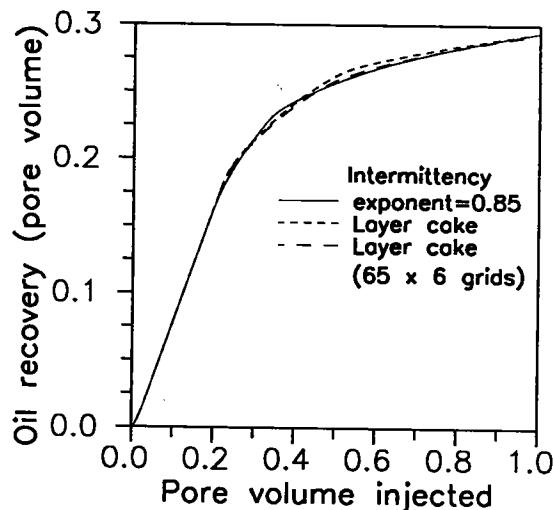
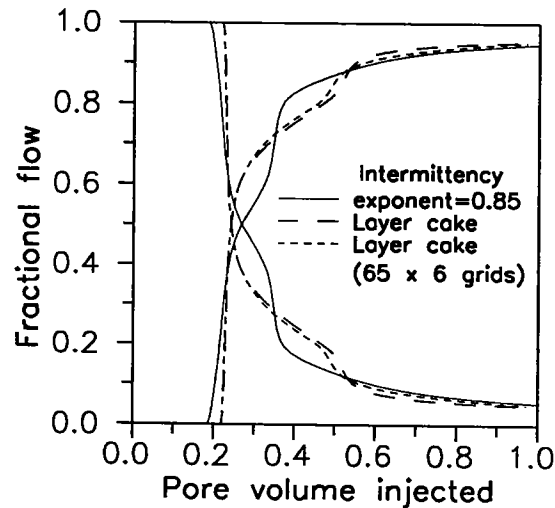


Figure 8. Waterflood fractional flows (above) and oil recovery (below) for a conditional-simulation model with intermittency exponent equal to 0.85 and for two layer-cake models.

slightly more favorable than for the conditional-simulation models previously considered. For the layer-cake model, using six cells in the vertical direction (coinciding with the reservoir layers), instead of 32 cells, does not cause significant differences in the waterflooding simulations (Fig. 8).

Waterflooding simulations also were conducted in models with constant and uncorrelated porosity distributions. The constant-porosity model was constructed from the conditional-simulation model, with intermittency exponent equal to 0.85, by replacing the porosity of all cells by the average porosity (permeability distribution was not changed). The uncorrelated model (i.e., no spatial correlation) was constructed by assigning porosity values to cells at random (i.e., no spatial

correlation), but preserving the histogram of the sample data. Waterflooding performance and recovery of these extreme distributions models are significantly different from those generated with conditional simulations and the layer-cake model. Results from the models with extreme distributions illustrate the importance of properly representing the vertical and horizontal variability of reservoir properties. For the constant-porosity model, waterflooding performance and oil recovery (Fig. 9) are poor due to the early water breakthrough caused by the great contrast between porosity and permeability. For the uncorrelated model, waterflooding performance and oil recovery (Fig. 9) are high, as a result of the improved sweep efficiency due to the absence of preferential flow paths.

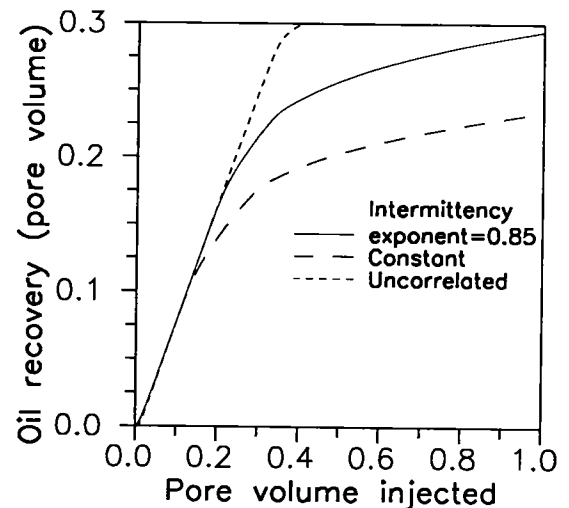
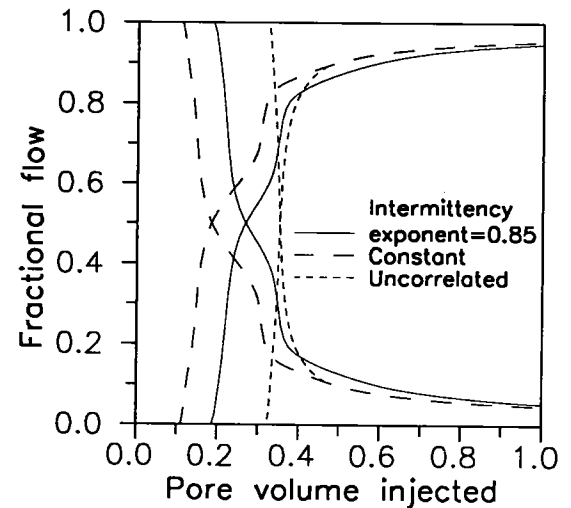


Figure 9. Waterflood fractional flows (above) and oil recovery (below) for a constant porosity and an uncorrelated porosity-distribution model.

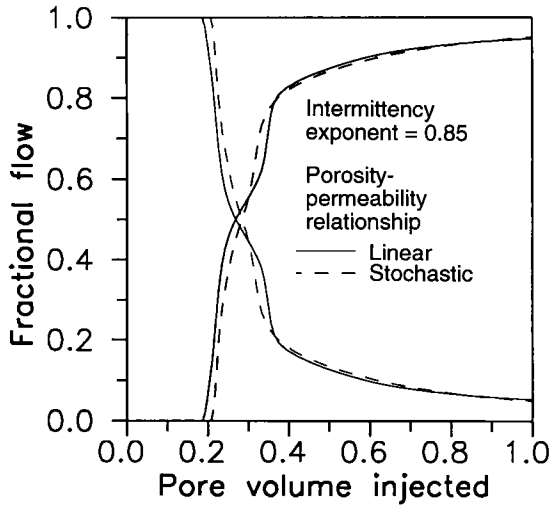


Figure 10. Waterflood fractional flows for conditional-simulation models with permeability distributions derived from both deterministic and stochastic relationships. The deterministic relationship is the linear relationship between porosity and the logarithm of permeability from the core data (Fig. 6).

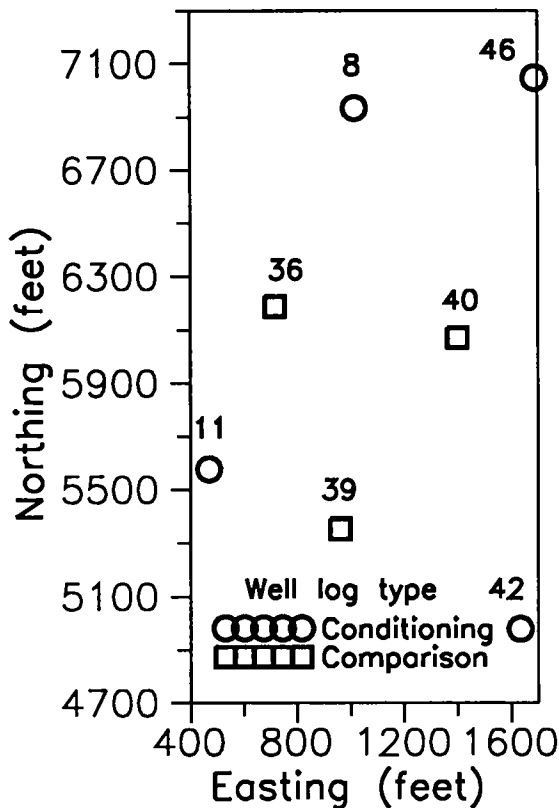


Figure 11. Locations of conditioning and comparison wells used in the three-dimensional conditional simulations.

Permeability Distribution

A simulation model was constructed using the stochastic instead of the linear relationship between porosity and the logarithm of permeability (Fig. 6) to transform a porosity-conditional simulation (intermittency exponent equal to 0.85) into a permeability distribution. Waterflooding simulations for the model developed with the stochastic relationship have a later water breakthrough and a higher oil recovery than for the model developed with the linear relationship (Fig. 10). This improvement on waterflooding efficiency appears to occur because of the enhanced sweep efficiency induced by the greater variability of permeability in the stochastic model, such as for the uncorrelated-porosity model, but to a smaller degree. The uncertainty of waterflooding performance introduced by the stochastic relationship (Fig. 10) is of the same order of magnitude as the uncertainty for two conditional simulations of porosity (Fig. 7).

THREE-DIMENSIONAL CONDITIONAL SIMULATIONS

The conditional-simulation method introduced by Hewett (1986) is limited to the generation of cross-sectional distributions of a property between two wells with a fBm variogram model or correlation structure. There are more general conditional-simulation techniques, such as kriging simulations (Journel and Huijbregts, 1978; Journel and Alabert, 1990), which allow multi-dimensional simulations and account for different variogram models. In this investigation, a new conditional-simulation method, based on simulated annealing (Perez, 1991), was used to generate the three-dimensional simulations. This method consists of a stochastic iterative algorithm that generates distributions of a property using a specified conditioning data set, histogram, and variogram models in different directions.

Three-dimensional conditional simulations of porosity in a small region of a large carbonate oil field were conducted. The data consisted of porosity from acoustic logs of seven conditioning and comparison wells (Fig. 11). Porosity logs from the conditioning wells were used to estimate the statistical parameters (histogram and variograms) and to condition the simulations and porosity logs from the comparison wells were compared to the simulated porosities. The simulated reservoir region is 150 ft thick, and it was discretized with 50 ft and 1 ft grids in the lateral and vertical directions, respectively.

The three-dimensional porosity simulations with porosity logs of the comparison wells are in close agreement (Fig. 12). Other realizations of these simulations provided similar results and allowed us to obtain a measure of the uncertainty in porosity descriptions.

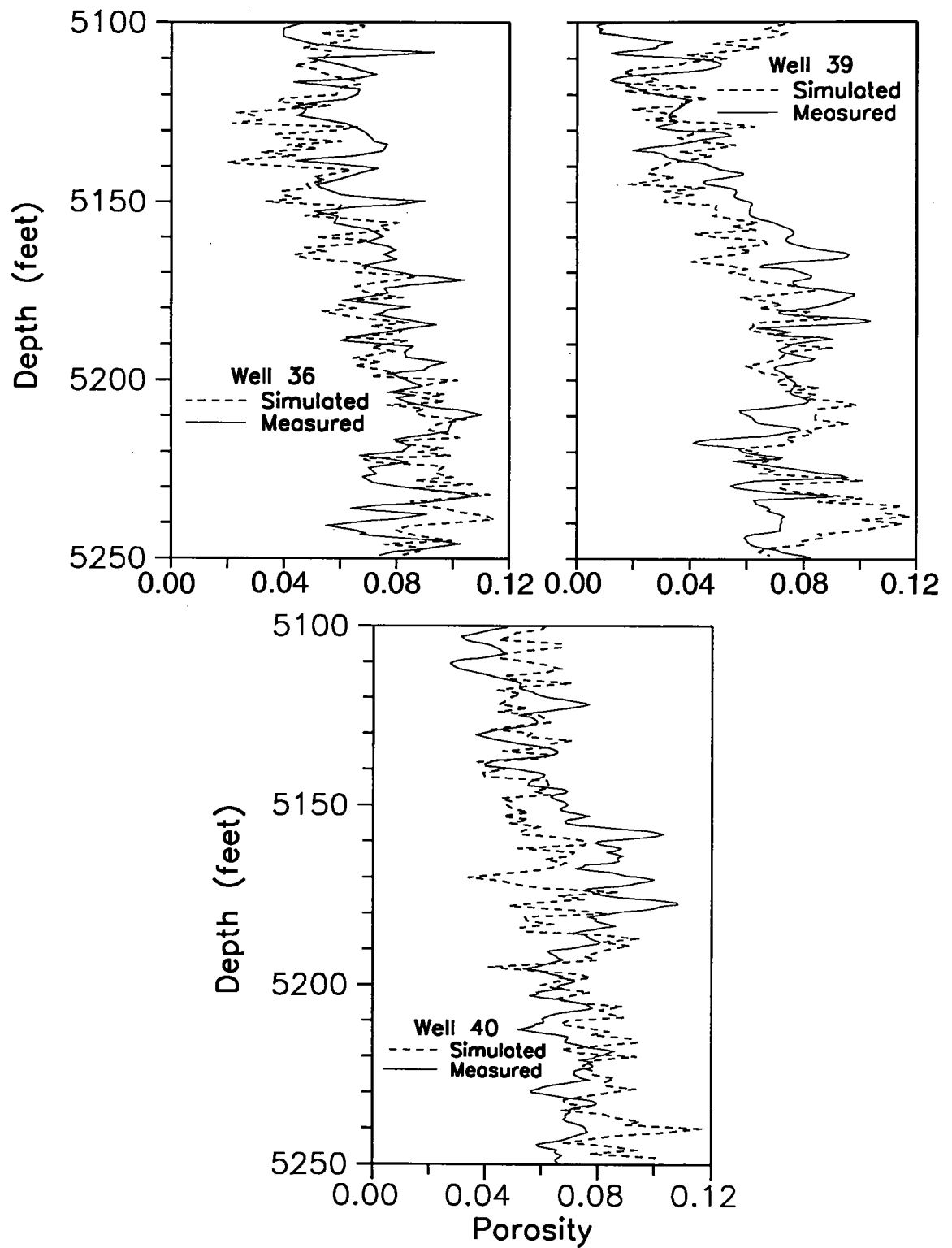


Figure 12. Conditional-simulation and measured porosity logs from the comparison wells of the three-dimensional simulation region. Well locations shown in Figure 11.

CONCLUSIONS

Conditional simulations of sandstone porosity between two conditioning wells in an oil reservoir were generated with a statistical fractal method. These simulated distributions are in close agreement with the porosity measurements at two comparison wells located between the conditioning wells. Spatial correlations and distributions of porosity in the inter-well region are not significantly different for intermittency exponents of the fractal model in the range of 0.75 and 0.95.

Waterflooding simulations were conducted using several reservoir models with different porosity and permeability distributions. Waterflood performance and oil recovery were not significantly different for porosity-conditional simulations with intermittency exponents of 0.75, 0.85, and 0.95. Oil recoveries from waterfloods simulated using a conventional layer-cake model and a conditional-simulation model were similar, but there were noticeable differences in the times of water breakthrough. Waterflooding performance and oil recoveries from models that do not account for the geologic structure, such as the constant-porosity and the uncorrelated models, differ significantly from those of the conditional-simulation and layer-cake models.

Three-dimensional distributions of porosity in a carbonate reservoir were generated with a new conditional-simulation method. The simulated distributions were in close agreement with porosity measurements at comparison wells.

REFERENCES CITED

- Aasum, Y.; Kelkar, M. G.; and Gupta, S. P., 1991, An application of geostatistics and fractal geometry for reservoir characterization: *Society of Petroleum Engineers Formation Evaluation Journal*, v. 6, p. 11-19.
- Crane, S. D.; and Tubman, K. M., 1990, Reservoir variability and modeling with fractals: *Society of Petroleum Engineers Annual Technical Conference and Exhibition*, New Orleans, SPE 20606.
- Exploration Consultants Limited, 1988, *ECLIPSE 100 black oil simulator reference manual*: Oxfordshire, England.
- Emanuel, A. S.; Alameda, G. K.; Behrens, R. A.; and Hewett, T. A., 1989, Reservoir performance prediction methods based on fractal geostatistics: *Society of Petroleum Engineers Reservoir Engineering Journal*, v. 4, p. 311-318.
- Feder, J., 1988, *Fractals*: Plenum Press, New York.
- Hewett, T. A., 1986, Fractal distribution of reservoir heterogeneity and their influence on fluid transport: *Society of Petroleum Engineers Annual Technical Conference and Exhibition*, New Orleans, SPE 15386.
- Hewett, T. A.; and Behrens, R. A., 1990, Conditional simulation of reservoir heterogeneity with fractals: *Society of Petroleum Engineers Formation Evaluation Journal*, v. 5, p. 217-225.
- Journel, A. G.; and Alabert, F. G., 1990, New method for reservoir mapping: *Journal of Petroleum Technology*, v. 42, p. 212-218.
- Journel, A. G.; and Huijbregts, C. J., 1978, *Mining geostatistics*: Academic Press, New York.
- Mattews, J. L.; Emanuel, A. S.; and Edwards, K. A., 1988, A modeling study of the Mitsue Stage 1 miscible flood using fractal geometries: *Society of Petroleum Engineers Annual Technical Conference and Exhibition*, Houston, SPE 18327.
- Payne, D. V.; Edwards, K.; and Emanuel, A. S., 1989, Examples of reservoir simulation studies utilizing geostatistical models of reservoir heterogeneity: *NIPER/DOE Second International Reservoir Characterization Technical Conference*, Dallas.
- Perez, Godofredo, 1991, *Stochastic conditional simulation for description of reservoir properties*: University of Tulsa unpublished Ph.D. dissertation.
- Tang, R. W.; Behrens, R. A.; and Emanuel, A. S., 1989, Reservoir studies using geostatistics to forecast performance: *Society of Petroleum Engineers Symposium on Reservoir Simulation*, Houston, SPE 18432.

PART II

**ABSTRACTS AND SHORT REPORTS
RELATED TO POSTER PRESENTATIONS**

Upper Strawn (Desmoinesian) Carbonate and Clastic Depositional Environments, Southeast King County, Texas

Todd H. Boring

Baylor University
Waco, Texas

PURPOSE

The Pennsylvanian upper Strawn Group of southeast King County, Texas, provides a unique setting to study interactions between coeval carbonate and clastic deposition during Desmoinesian time. One of the most perplexing problems is the relationship of massive Pennsylvanian platform carbonates to shallow-water marine and deltaic sediments (Fig. 1).

Considerable controversy has arisen about the depositional environments of the terrigenous sediments and their relationship to massive carbonate facies in and around the Knox-Baylor trough. It has been suggested both that these sandstones were deposited by submarine currents along the deep axis of the Knox-Baylor trough and, in contrast, that the area was influenced by deltaic processes. Therefore, the principal objectives of this investigation were (1) to resolve the conflicts by clearly defining the upper Strawn Group carbonate and clastic depositional environments within southeast King County, Texas, and (2) to understand and interpret the facies relationships between the carbonates and terrigenous sediments.

LOCATION

The area of investigation (~270 mi²) is located in the southeast portion of King County, north-central Texas, between the cities of Lubbock and Wichita Falls. This area is on the northwestern edge of the Concho platform, northeast of the Midland basin, south of the Wichita-Arbuckle Mountain system, and west of the Ouachita fold belt. To facilitate the discussion, the study area has been subdivided into a northern region and a southern region. The discussion of the northern region addresses shallow-water platform carbonates, while that for the southern region discusses terrigenous deltaic and shallow-marine sediments.

SUMMARY

Within the study area, carbonate facies were deposited along the northern edge of the Knox-Baylor trough on the Spur platform, while terrig-

enous clastics were carried toward the Midland basin through the Knox-Baylor trough. Based on the analysis of subsurface cores, five carbonate lithofacies and four clastic lithofacies were recognized in southeast King County, Texas. The distribution and geometry of these lithofacies are related to variations in the rate of subsidence in the Knox-Baylor trough, Pennsylvanian tectonics, deltaic progradation, avulsion, and compaction.

The carbonates in the northern region of southeast King County record environments within a carbonate platform complex, including mid-platform, outer-platform, algal mound, and platform margin (Fig. 2). The typical carbonate cycle consists of the following facies, from bottom to top: (1) algal bioclastic wackestones, (2) crinoidal wackestones, (3) algal bioclastic packstones-grainstones/fusulinid crinoidal packstones-grainstones, and (4) crinoidal bryozoan wackestones/shales (Fig. 3).

During Desmoinesian time, terrigenous clastic sediment derived from the Wichita and Arbuckle Mountains filled the Knox-Baylor trough. Quartz-arenitic sandstones within the southern region of southeast King County occur in a variety of complex geometries, including distributary-bar fingers, lobate deltas, and offshore bars (Fig. 2). Cores of these sandstones represent mainly the uppermost portions of the various sand bodies. A typical core consists of the following facies, from bottom to top: (1) cross-bedded sandstones, (2) intercalated sandstones and shales, and (3) mudstones/shales (Fig. 4). The depositional model for the upper Strawn (Desmoinesian) Group of southeast King County has been conceptualized primarily from the tectonic setting, sandstone-body geometry, sedimentary structures, textures, lateral and vertical facies relationships, and general lithologic sequence of the carbonates and clastics. This model is illustrated in Figure 2.

CONCLUSION

Based on the analysis of subsurface cores, electric-log analysis, thin-section petrography, and the lateral and vertical facies relationships, deposition

Boring, T. H., 1993, Upper Strawn (Desmoinesian) carbonate and clastic depositional environments, southeast King County, Texas, in Johnson, K. S.; and Campbell, J. A. (eds.), *Petroleum-reservoir geology in the southern Midcontinent*, 1991 symposium: Oklahoma Geological Survey Circular 95, p. 195-198.

of the platform carbonates occurred contemporaneous with progradation of the delta system into the southern region of southeast King County. The upper Strawn (Desmoinesian) sandstones within southeast King County were deposited by deltaic processes in shallow water, rather than in deep water as previously interpreted. Evidence for this

includes: sandstone-body geometry, tectonic setting, the presence of an oolitic grainstone below the base of the Tandy 5400 sandstone, bioturbation in the adjacent shales, carbonized-plant fragments within the Tandy 5400, considerable soft-sediment deformation, and the lack of "reef" talus along the margin of the Spur platform.

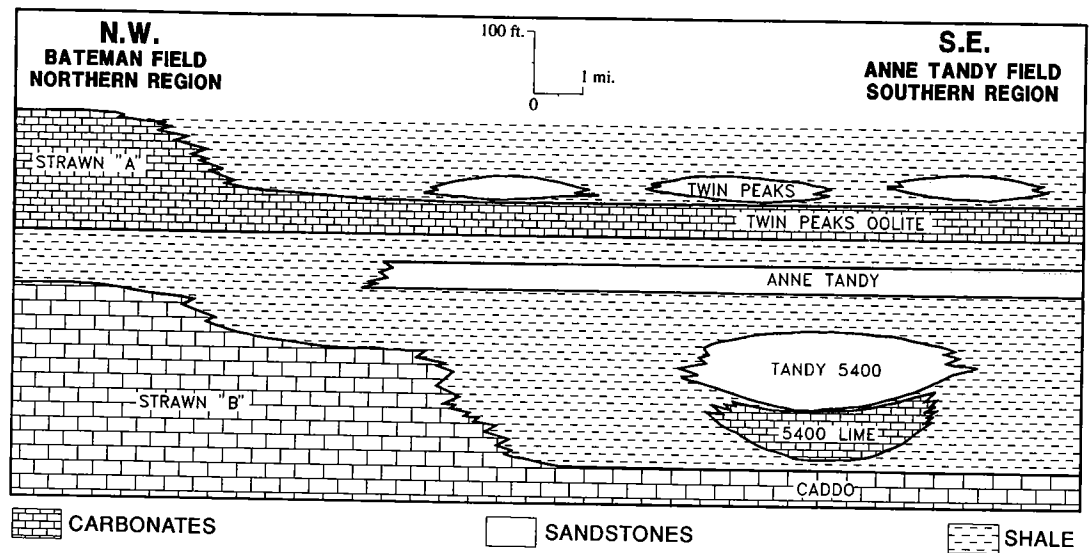


Figure 1. Generalized cross section through southeast King County, Texas.

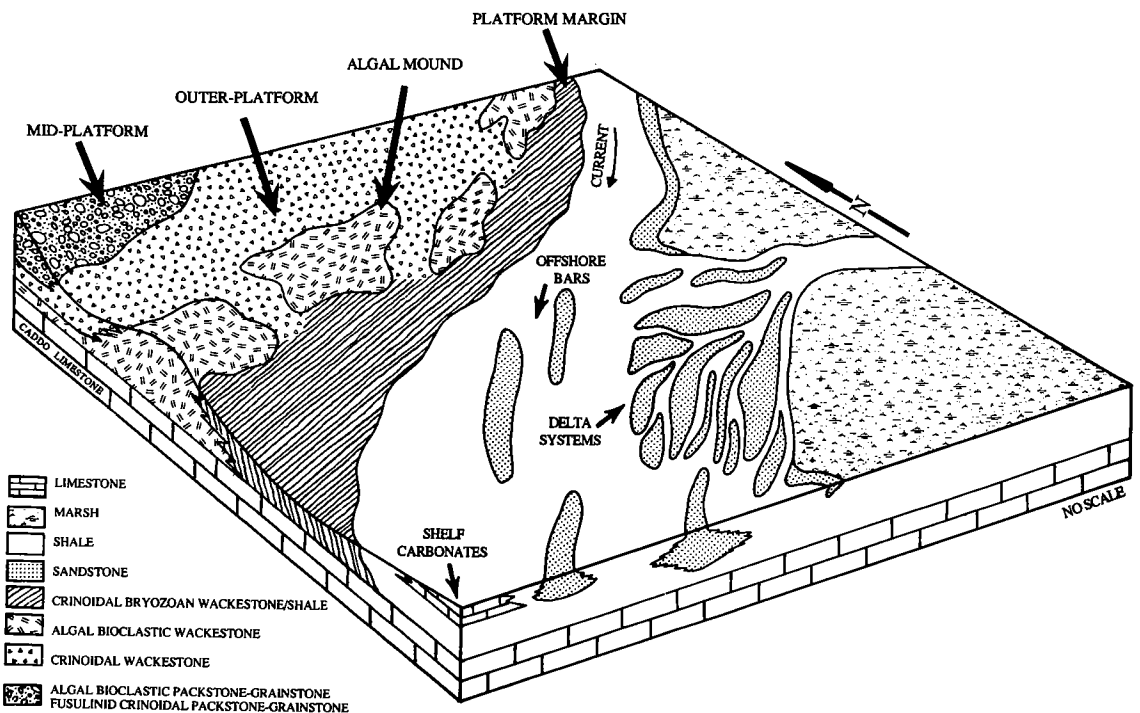


Figure 2. Generalized depositional model and lateral facies relationships for southeast King County during upper Strawn (Desmoinesian) time.

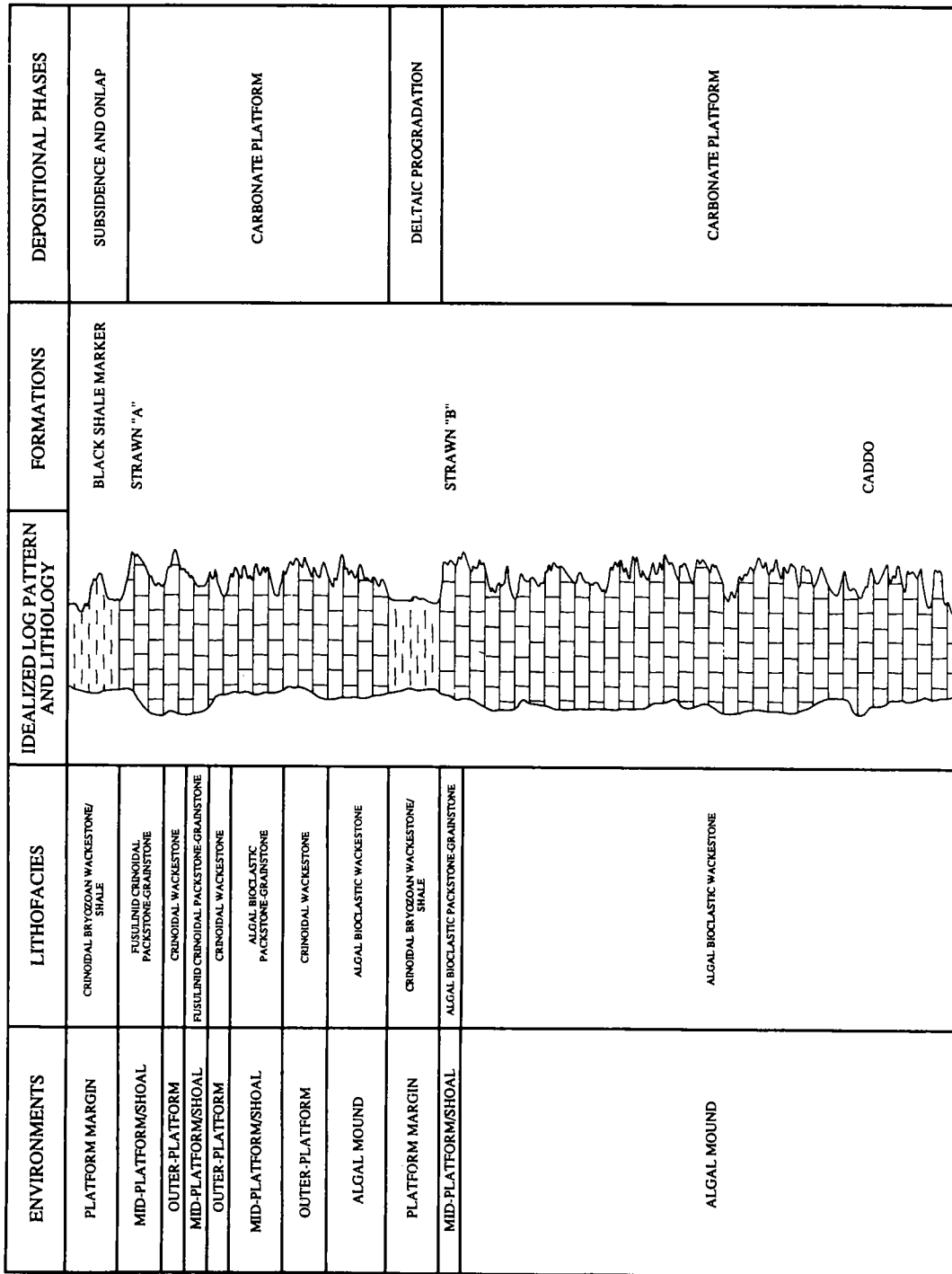


Figure 3. Idealized carbonate depositional sequence showing environments, related lithofacies, idealized electric-log pattern, and depositional phases.

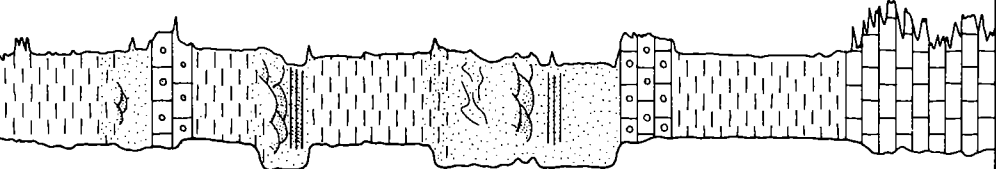
ENVIRONMENTS	LITHOFACIES	IDEALIZED LOG PATTERN AND LITHOLOGY	FORMATIONS	DEPOSITIONAL PHASES
INNER BAR	MUDSTONE/SHALE		BLACK SHALE MARKER	
BAR MARGIN	INTERCALATED SANDSTONE AND SHALE		TWIN PEAKS SHALE	REWORKED DELTA
OFFSHORE BAR	CROSS-BEDDED SANDSTONE		TWIN PEAKS SANDSTONE	
SHELF/SHOAL	MICRITIC MUDSTONE/ OOLITIC GRAINSTONE		TWIN PEAKS OOLITE	CARBONATE ONLAP
PRODELTA	MUDSTONE/SHALE		ANNE TANDY SHALE	DELTAIC ABANDONMENT
ABANDONED DELTA LOBE	INTERCALATED SANDSTONE AND SHALE		ANNE TANDY SANDSTONE	DELTAIC PROGRADATION
LOBATE DELTA	CROSS-BEDDED SANDSTONE			
PRODELTA	MUDSTONE/SHALE		TANDY 5400 SHALE	DELTAIC ABANDONMENT
ABANDONED BAR FINGER	INTERCALATED SANDSTONE AND SHALE			
DISTRIBUTARY BAR FINGER	CROSS-BEDDED SANDSTONE		TANDY 5400 SANDSTONE	DELTAIC PROGRADATION
SHELF/SHOAL	MICRITIC MUDSTONE/ OOLITIC GRAINSTONE		5400 LIME	DELTAIC ABANDONMENT AND CARBONATE ONLAP
PRODELTA	MUDSTONE/SHALE		STRAWN SHALE	INITIAL DELTA PROGRADATION
SHELF/SHOAL	ALGAL WACKESTONE PACKSTONE OOLITIC GRAINSTONE SPICULITIC MUDSTONE		CADDO LIMESTONE	CARBONATE PLATFORM

Figure 4. Idealized clastic depositional sequence showing environments, related lithofacies, idealized electric-log pattern, and depositional phases.

Petroleum Production from Potentially Fractured Pre-Pennsylvanian Reservoirs in Oklahoma

Jock A. Campbell

Oklahoma Geological Survey
Norman, Oklahoma

David P. Brown

Geological Information Systems
Norman, Oklahoma

Brian J. Cardott

Oklahoma Geological Survey
Norman, Oklahoma

Anne Mycek-Memoli

Geological Information Systems
Norman, Oklahoma

INTRODUCTION

Carbonate and microcrystalline siliceous rocks commonly are brittle in geological environments and therefore are susceptible to fracture under typical conditions found in sedimentary basins. Fractures have been shown to occur as the result of tectonic stresses and abnormally high fluid pressure in sedimentary rocks. The tectonic history of the southern Midcontinent region has been particularly conducive to the formation of pre-Pennsylvanian fractured reservoirs; significant orogenic events occurred in Middle Devonian, and from Late Mississippian through Early Permian time.

There is considerable uncertainty in any effort to identify specific fractured reservoirs, although the study of surface fracture azimuth and frequency commonly is an excellent general guide to the subsurface. Fractures may not be recognized if they are associated with matrix reservoir properties, a particular problem in many carbonate rocks. Even where fractures are recognized, their contribution to reservoir performance commonly is difficult to evaluate. Only in dense, unkarsted carbonate rocks and siliceous rocks may it be evident that fractures are the significant, or possibly the sole, site of reservoir properties. In the absence of detailed reservoir study and analysis, the relative contribution of fractures versus rock matrix to reservoir behavior is ambiguous.

To date (through February 1991), 19 operators have approximately 28 horizontal test wells drilled

or proposed in eight producing formations in Oklahoma. Four wells have been completed successfully to produce hydrocarbons, one each in the Mississippian (Chester), Hunton, Viola, and Simpson ("third Bromide"). At least two other attempts have resulted in mechanical failure. It is only a matter of time until prospecting and well-completion techniques come together in a favorable combination of natural factors and expertise that may result in a major development trend in Oklahoma.

DISCUSSION

The purpose of this paper is to identify production of liquid hydrocarbons from all known and probable fractured pre-Pennsylvanian carbonate and microcrystalline siliceous reservoir rocks. The Natural Resources Information System (NRIS) data base is employed to locate production from those units for 1983–90 (inclusive); these data are compiled from records of the Oklahoma Tax Commission (OTC). All maps are plotted from lease information using a digital land grid data base provided by the Phillips Petroleum Co.; a section (640 acres) is the smallest map unit. Regional maps of hydrocarbon production by stratigraphic interval identify areas with potential for horizontal-drilling (extended-reach completion) opportunities in those stratigraphic units. The stratigraphic units selected for this study are the Arbuckle and Viola Groups (Upper Cambrian–Ordovician) (Figs. 1,2); the Hunton Group (Upper Ordovician–Devonian) (Fig. 3); the siliceous facies of the Woodford and

Campbell, J. A.; Brown, D. P., Cardott, B. J.; and Mycek-Memoli, Anne, 1993, Petroleum production from potentially fractured pre-Pennsylvanian reservoirs in Oklahoma, *in* Johnson, K. S.; and Campbell, J. A. (eds.), *Petroleum-reservoir geology in the southern Midcontinent*, 1991 symposium: Oklahoma Geological Survey Circular 95, p. 199–205.

TABLE 1. — SUMMARY DATA, BY STRATIGRAPHIC INTERVAL,
TO ACCOMPANY HYDROCARBON-PRODUCTION MAPS

Producing interval	N ^a	Number of sections producing petroleum liquids (by range)		Natural gas only (sections)	Max ^b
		Cumulative bbl, 1983–90			
		1–50,000	>50,000		
Mississippian carbonates	5,871	4,960	389	522	922,388
Arkansas Novaculite	6	2	3	1	91,447
Woodford and Chattanooga Shales	29	23	3	3	90,927
Hunton Group	1,559	1,254	173	132	623,111
Viola Group	878	704	155	19	665,568
Arbuckle Group	234	163	30	41	1,167,520

^aN = Number of sections producing, 1983–90.

^bMax = Maximum cumulative liquids production for a single section (bbl, 1983–90).

Chattanooga Shales (Upper Devonian–lowermost Mississippian) (Fig. 4); and carbonates of Mississippian age (Fig. 5). Because of the limited number of occurrences of hydrocarbon production from the Arkansas Novaculite (Table 1), a map of that formation is not provided. The Bigfork Chert (Upper Ordovician), a commonly fractured rock in southeastern Oklahoma, is not included in this study because it has only one section with oil production of record. The Simpson Group (Ordovician) also is not included because it consists largely of sandstone reservoir rocks. Although potentially fractured, these rocks are not part of this study. The regional distribution, thickness, and general lithologic variations of these strata are discussed and illustrated by Johnson and others (1988).

Maps of production by stratigraphic interval are presented as Figures 1 through 5. It was necessary to compile cumulative production from a low of 0 bbl of liquid; thus, some mapped leases produce only natural gas. Hydrocarbon production is mapped where it occurs from the subject formations, but production commingled with that from other formations is not mapped. This omission eliminates some detail, but it does not detract from the clusters and trends sought. Table 1 summarizes the mapped data and identifies the number of sections that produce only natural gas, as determined from printouts of the mapped data. The maximum eight-year cumulative oil produc-

tion from a single section, which exceeds 1.167 million bbl (Table 1), is from an Arbuckle reservoir in sec. 30, T. 4 S., R. 1 W., Carter County, in the Cottonwood Creek field (Read and Richmond, 1993).

Since this study was completed, the capability of the oil and gas production subsystem of the NRIS data base has been extended from the present back through 1979. A list of fields with lease location and identification, as well as production for any reservoir in this study, can be obtained from Geological Information Systems at the University of Oklahoma on a cost-reimbursable basis.

REFERENCES CITED

- Johnson, K. S.; Amsden, T. W.; Denison, R. E.; Dutton, S. P.; Goldstein, A. G.; Rascoe, Bailey, Jr.; Sutherland, P. K.; and Thompson, D. M., 1988, Southern Midcontinent region, in Sloss, L. L. (ed.), *Sedimentary cover–North American craton*; U.S.: *Geology of North America: Geological Society of America, Decade of North American Geology*, v. D-2, p. 307–359. [Reprinted as *Geology of the southern Midcontinent: Oklahoma Geological Survey Special Publication 89-2*, 1989, 53 p.]
- Read, D. L.; and Richmond, G. L., 1993, *Geology and reservoir characteristics of the Arbuckle Brown zone in the Cottonwood Creek field, Carter County, Oklahoma*, in Johnson, K. S.; and Campbell, J. A. (eds.), *Petroleum-reservoir geology in the southern Midcontinent, 1991 symposium: Oklahoma Geological Survey Circular 95*, p. 113–125 [this volume].

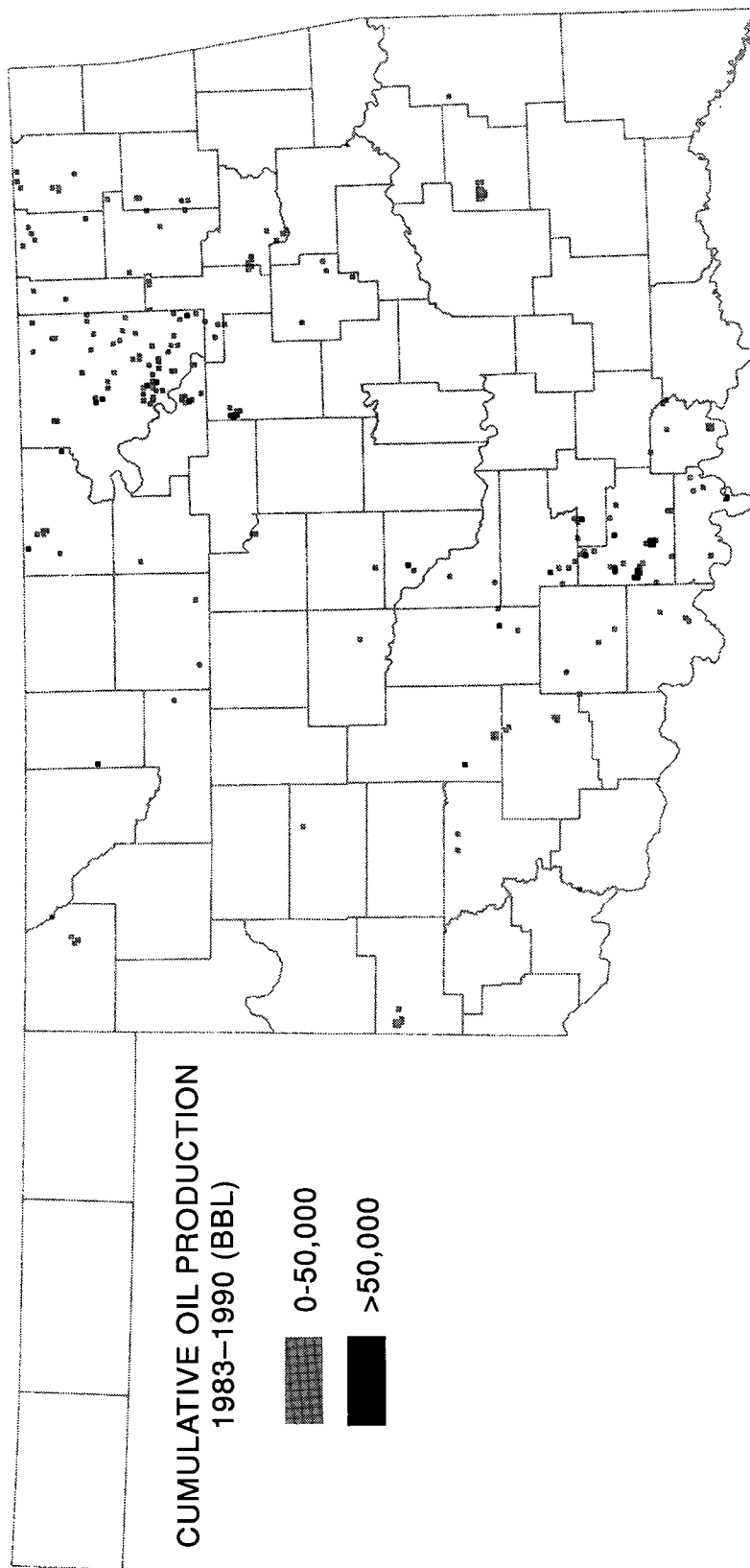


Figure 1. Occurrences of hydrocarbon production from reservoirs within the Arbuckle Group, 1983-90 (inclusive), by section in Oklahoma.

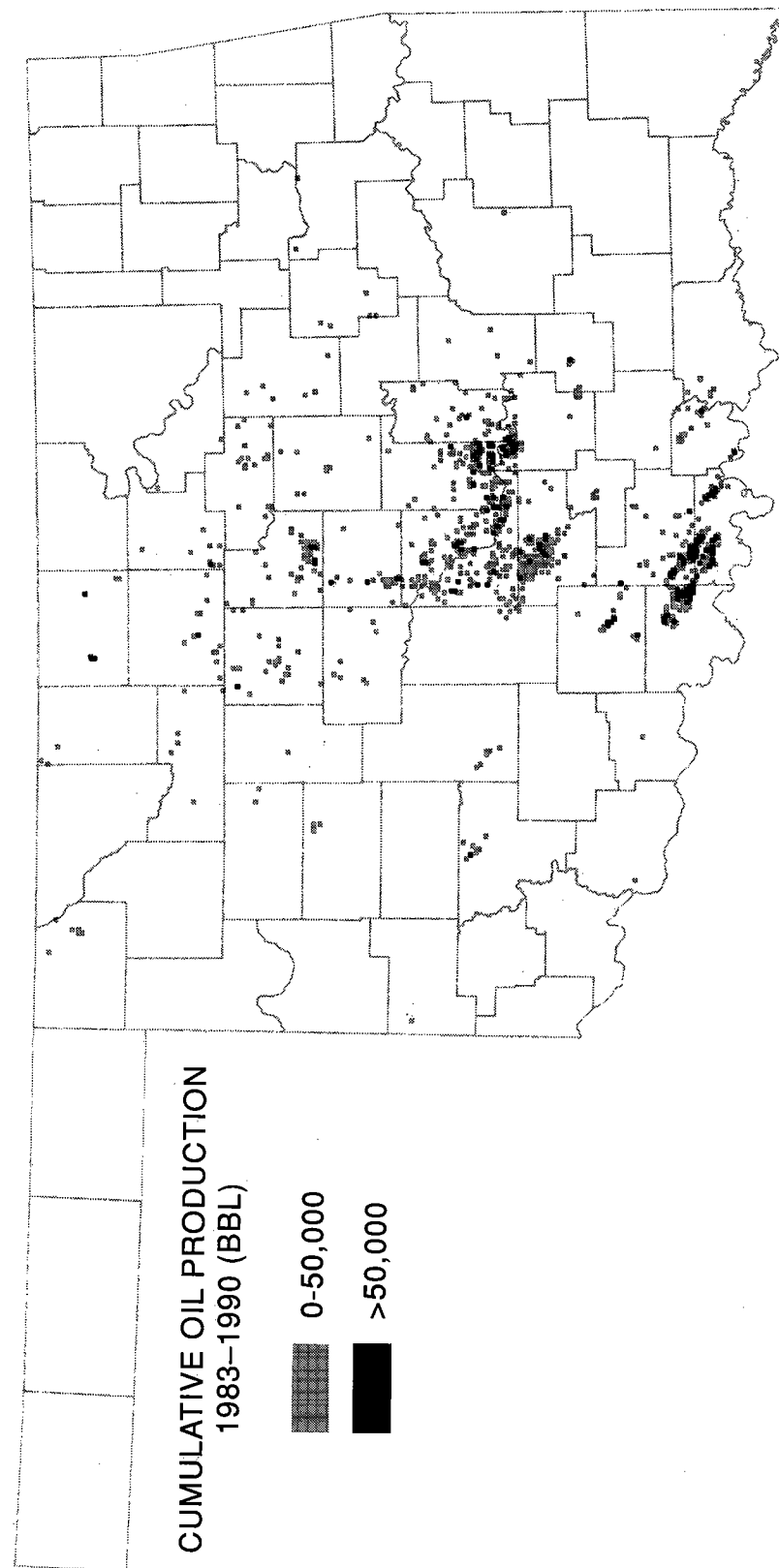


Figure 2. Occurrences of hydrocarbon production from reservoirs within the Viola Group, 1983-90 (inclusive), by section in Oklahoma.

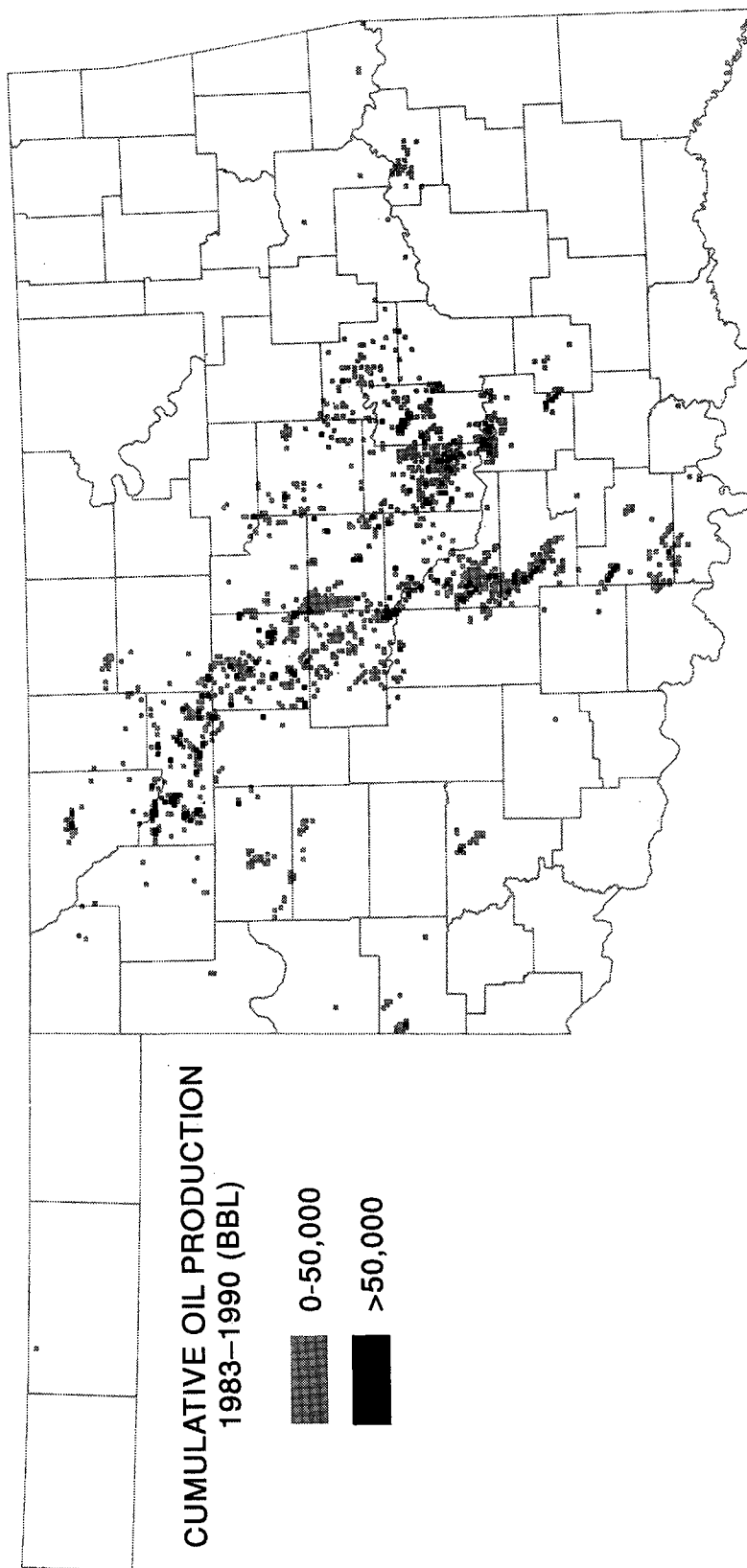


Figure 3. Occurrences of hydrocarbon production from reservoirs within the Hunton Group, 1983-90 (inclusive), by section in Oklahoma.

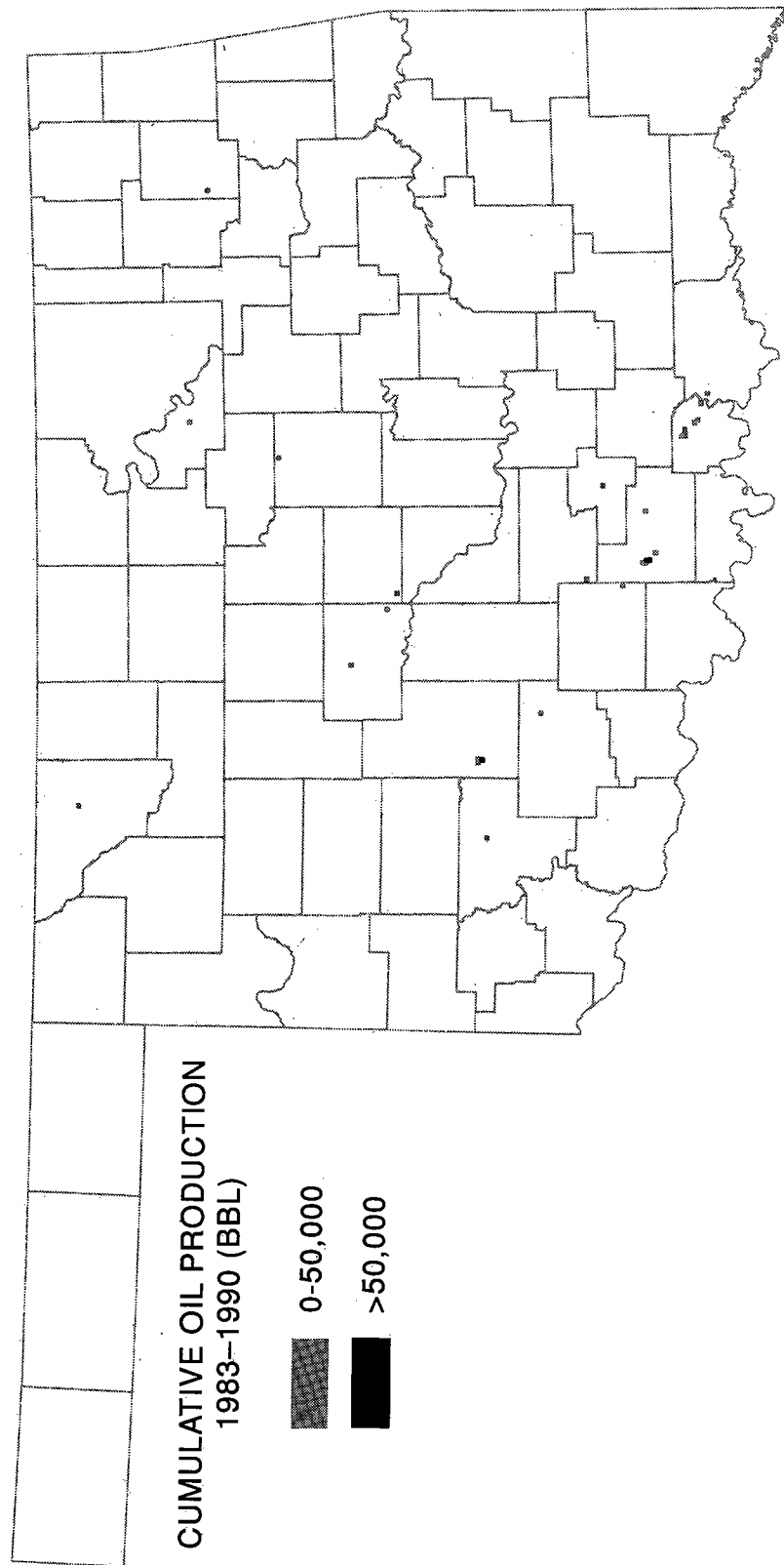


Figure 4. Occurrences of hydrocarbon production from reservoirs within the Woodford and Chattanooga Shales, 1983-90 (inclusive), by section in Oklahoma.

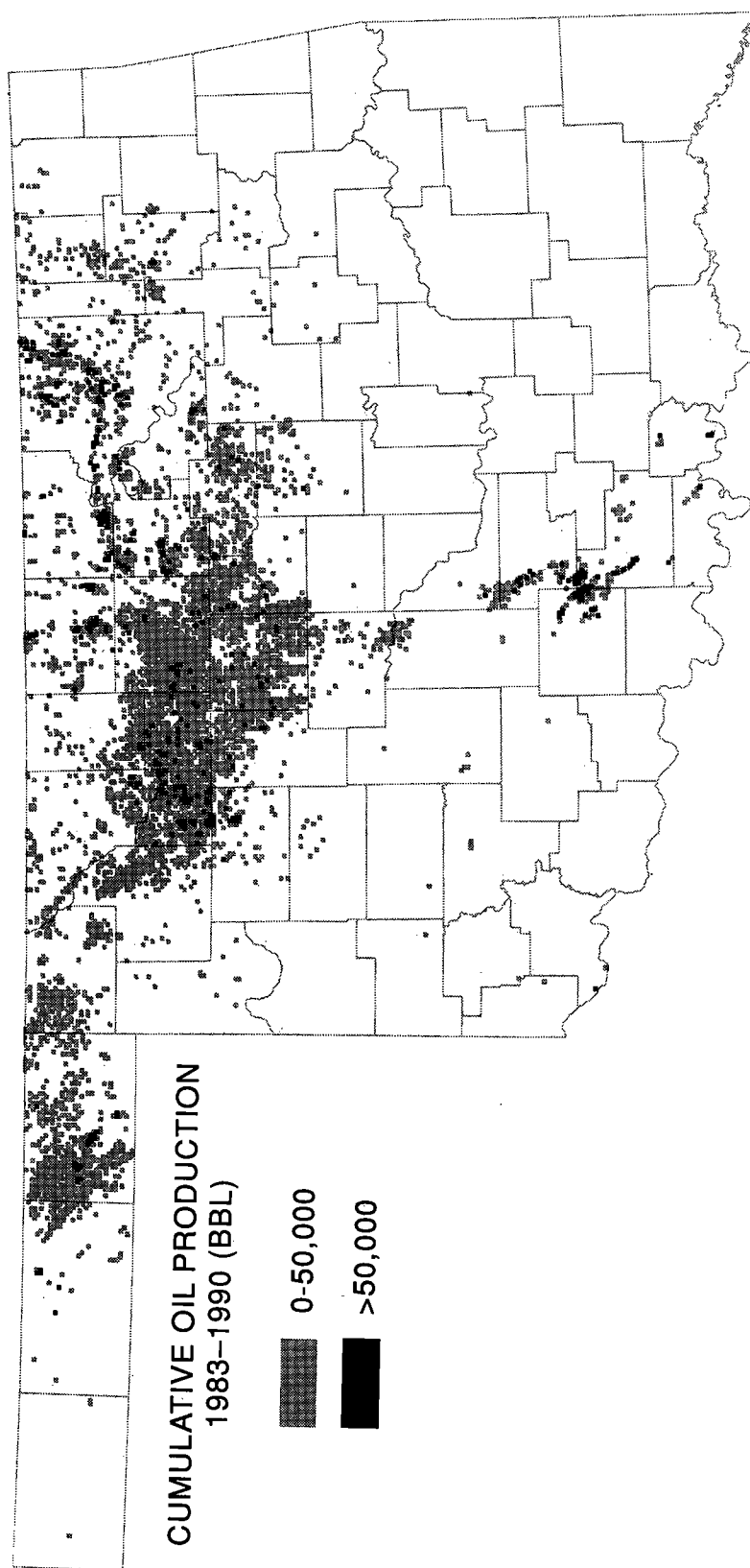


Figure 5. Occurrences of hydrocarbon production from reservoirs within carbonates of Mississippian age, 1983-90 (inclusive), by section in Oklahoma.

Distribution and Orientation of Arbuckle Group Fracture Patterns in the Slick Hills and Arbuckle Mountains, Southern Oklahoma: An Analogy for Fractured Arbuckle Reservoirs

R. Nowell Donovan, Scott W. White, and Ken M. Morgan

Texas Christian University
Fort Worth, Texas

Michael D. Stephenson

Union Pacific Resources
Fort Worth, Texas

ABSTRACT.—The Slick Hills of southwestern Oklahoma are the exposed portion of the frontal fault zone (FFZ), an area of intense Pennsylvanian/Early Permian deformation that lies between the Anadarko basin and the Wichita uplift. The zone trends approximately N. 60° W., following the line of the southern Oklahoma aulacogen, which itself appears to have been controlled by a line of basement weakness that existed ~1.3 billion years ago. Maximum stratigraphic downthrow (to the northeast) across the FFZ is ~13,000 m. Physiographically, the Slick Hills are divided into eastern and western blocks by the Blue Creek Canyon fault, a high-angle oblique (left-lateral) reverse fault that has a stratigraphic downthrow to the southwest (i.e., against the overall trend of the FFZ).

The Arbuckle Mountains have the same general trend and genesis as the Slick Hills. The principal physiographic entities include the asymmetric Arbuckle anticline, an extremely complex structure cut by the Washita Valley fault zone on its northern (locally overturned) limb. This fault zone is thought to be a rejuvenated northeastern edge to the aulacogen; it separates the mountains into a western block, in which the basement is the Cambrian Colbert (Carlton) Rhyolite, and an eastern block floored by the Tishomingo and associated Precambrian granites.

In this study, we used remote sensing Landsat and Spot TM data and conventional air photographs (on a scale of 8 in. to 1 mi), to examine the fracture patterns developed in small areas of the two uplifts. For the most part, we concentrated on exposures of the Arbuckle Group and buttressed our results with field work to establish the geological significance of the lineaments recognized on the remote-sensing imagery.

The areas selected for study were: (1) the Stony Point area of the eastern Slick Hills; (2) the Ketch Creek area of the eastern Slick Hills; (3) the southern flank of the Arbuckle anticline, west of the Joins Ranch fault; (4) the southern flank of the Arbuckle anticline, east of the Joins Ranch fault; and (5) the Tishomingo area.

In all cases the fractures show two pronounced modes of distribution: (1) parallel or slightly clockwise to the overall trend of the aulacogen, and (2) generally northeast-southwest. In addition, subordinate east-west and north-south modes are developed in some areas.

Previous work has established that the intense deformation in the western Slick Hills is the product of a stress system that was oblique (in a left-lateral transpressive sense) to the N. 60° W. trend of the major faults in the FFZ. The style of deformation in the eastern Slick Hills is less intense than that seen in the western Slick Hills. The principal structure is the Stony Point fault, a northeastward-dipping, basement-involved reverse fault. The sense of throw on this fault is similar to that of the Blue Creek Canyon fault (i.e., it can be defined loosely as a back thrust, in relation to the FFZ as a whole). Our analysis of fracture patterns and vein arrays suggests that the principal compressive stress that affected the area was oriented about N. 45–60° W. This is consistent geometrically with a displacement vector of N. 77° W., determined from data from the western Slick Hills (fold orientations, pressure-solution orientation in shear belts, and fracture patterns). A stress orientation with that vector would have induced dominantly dip-slip motion on the faults of the Broxton fault zone in the subsurface to the northeast; this prediction is compatible with our subsurface interpretation of those faults as a series of low-angle reverse faults.

Donovan, R. N.; White, S. W.; Morgan, K. M.; and Stephenson, M. D., 1993, Distribution and orientation of Arbuckle Group fracture patterns in the Slick Hills and Arbuckle Mountains, southern Oklahoma: an analogy for fractured Arbuckle reservoirs, *in* Johnson, K. S.; and Campbell, J. A. (eds.), *Petroleum-reservoir geology in the southern Midcontinent*, 1991 symposium: Oklahoma Geological Survey Circular 95, p. 206–207.

The same vector would have produced left-lateral oblique compression across structures that parallel the N. 60° W. trend of the aulacogen.

Our results from the Arbuckle Mountains indicate that the amount of transpressive component indicated by the fractures was less than that suggested for the Slick Hills. In general, the principal extensional-fracture direction is more nearly perpendicular to the Washita Valley fault (i.e., about N. 30° W.).

In addition to the overall patterns observed, we ascertained several features of more local interest: (1) some faults terminate in zones of intense fracturing parallel to the overall fault trend; (2) some late faults apparently rotate preexisting fracture trends; (3) thicker bedded units in the Arbuckle Group show more intense fracture patterns (this observation is, at least in part, a reflection of the scale of image examined); and (4) in steeply dipping areas, where the strike of beds is parallel to one of the principal fracture modes, the mode "disappears," apparently being resolved into fractures parallel to bedding.

Geologic and Production Characteristics of Deep Oil and Gas Wells and Reservoirs in the Conterminous U.S.

T. S. Dyman, D. D. Rice, D. T. Nielsen,
R. C. Obuch, and J. K. Baird

U.S. Geological Survey
Denver, Colorado

INTRODUCTION

Because of lower worldwide oil prices, drilling activity in the U.S. has declined, and major producing companies are looking outside the U.S. for oil and gas exploration prospects. Concurrently, production from existing wells is declining, and the U.S. reliance on imported oil is increasing. Even if prices were to increase drastically, it would take several years for domestic exploration to reach previous levels of intensity.

When the issue of economics is set aside, many drilling frontiers remain untested in the U.S. and deserve review. One such drilling frontier is deep gas in sedimentary basins. However, very little information is presently available for deep gas reservoirs. Deep wells are defined for this study as those drilled deeper than 15,000 ft. More than 16,000 wells have been drilled deeper than 15,000 ft in the U.S. Deep wells are widely distributed in the U.S. (Fig. 1) and are drilled into rocks of various ages and lithologies. Commercial gas production from

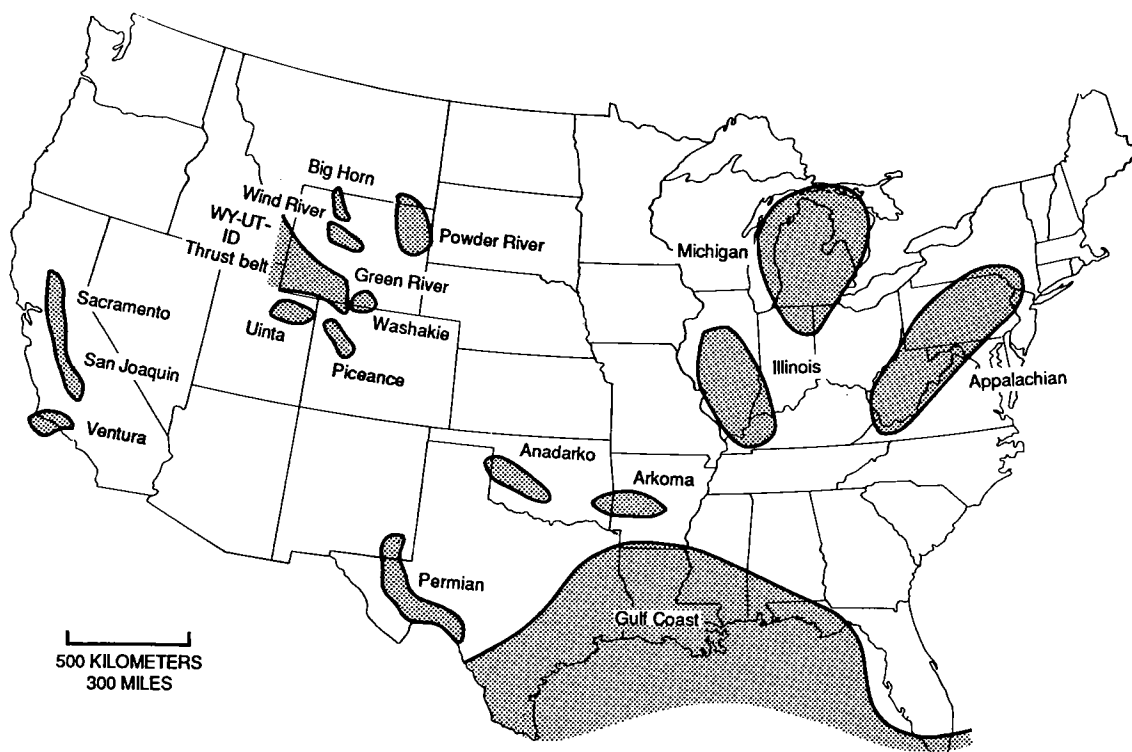


Figure 1. Generalized map of conterminous United States showing basins with significant deep wells and reservoirs. The southern Midcontinent includes the Anadarko and Arkoma basins. The Permian basin includes only the deeper parts of the Delaware and Val Verde basins.

Dyman, T. S.; Rice, D. D.; Nielsen, D. T.; Obuch, R. C.; and Baird, J. K., 1993, Geologic and production characteristics of deep oil and gas wells and reservoirs in the conterminous U.S., in Johnson, K. S.; and Campbell, J. A. (eds.), *Petroleum-reservoir geology in the southern Midcontinent*, 1991 symposium: Oklahoma Geological Survey Circular 95, p. 208-215.

TABLE 1. — THE 10 DEEPEST WELLS IN THE U.S., IN DECREASING ORDER OF TOTAL DEPTH^a

Operator	Well name	Total depth (ft)	Spud date (m/d/yr)	Date completed	Long. ^b	Lat. ^b	Basin	State
Lone Star Prod.	#1 Bertha Rogers	31,441	11/25/72	04/18/74	99.19	35.31	Anadarko	OK
Lone Star Prod.	#1 Earnest R. Baden	30,050	09/04/70	10/20/72	99.53	35.31	Anadarko	OK
Hunt Energy Corp.	1-9 Cerf Ranch	29,650	04/29/79	09/06/82	102.54	30.55	Permian	TX
Gulf Oil Corp.	2 Emma Lou Unit #1	29,622	05/21/78	07/30/80	102.56	30.65	Permian	TX
GHK Corp.	#1-34 Duncan	29,312	02/20/81	01/15/83	99.41	35.38	Anadarko	OK
GHK Corp.	#1-1 Robinson	29,241	07/06/81	01/25/84	99.48	35.28	Anadarko	OK
Chevron USA	#1 University 23-3	28,747	11/08/78	06/01/81	102.65	30.87	Permian	TX
Ralph Lowe Estate	#1-17 University	28,500	na	/72	102.69	30.84	Permian	TX
McCulloch Oil	#1 Easley	27,050	04/05/71	09/18/73	99.28	35.30	Anadarko	OK
Napco Inc.	#1 Centurion	27,019	10/05/79	06/23/81	102.75	30.80	Permian	TX

^aData taken from an early WHCS file, updated through February 1985. Data for Tables 2–5 are from WHCS files, updated through February 1988. Wells listed regardless of completion class.

^bLongitude and latitude in decimal degrees.

deep reservoirs at or below 15,000 ft has been established in a few basins for many years. In other basins, only a few deep wells have been drilled, and the gas potential of deeper horizons remains unknown.

This report summarizes deep wells and reservoirs in the U.S. in order to (1) develop a data base of information concerning this potential resource, (2) define geologic and engineering factors associated with deep drilling, and (3) develop a better understanding of deep reservoirs. Summaries of well data are presented in tabular form and are considered preliminary; no rigorous statistical analysis of these data is attempted. This report is a summary of data presented in Dyman and others (1990). Refer to that work and Takahashi and Cunningham (1987) for more information on deep wells and reservoirs.

Data were compiled from Petroleum Information Corp. Well History Control System (WHCS) available through February 1988 (Petroleum Information Corp., 1988), and Dwight's Energydata Petroleum Data System (PDS) available through December 1985 (Dwight's Energydata, 1985). WHCS contains a variety of location, identification, and geologic and engineering data for approximately two million wells drilled in the U.S. The WHCS file is available to the U.S. Geological Survey by contract with Petroleum Information Corp. Since WHCS data are proprietary, publication of complete well histories and computer versions of the file is prohibited. PDS is an oil and gas field and reservoir file originally developed by the University of Oklahoma under contract to the U.S. Geological Survey. It contains location, identification, and geologic and production data for ~100,000 fields and reservoirs in the 33 oil and gas

producing states. PDS data were made available to the U.S. Geological Survey by the Gas Research Institute (GRI); these data are also proprietary in digital form, but aggregated results may be published. Work was conducted in part under contract to GRI, Chicago, Illinois (contract no. 5087-260-1607).

DATA ANALYSIS

The WHCS subset of wells drilled deeper than 15,000 ft contains 16,650 wells, of which 8,705 are classed as producing wells. Of the 8,705 producing wells, 2,981 have a formation reported at total depth that is the same as the first producing formation reported in WHCS. (WHCS wells may contain more than one producing formation, but only the first producing formation listed in the file was recognized for this study.) These 2,981 wells, although a minimum figure, form a subset of wells actually producing hydrocarbons below 15,000 ft. An additional 2,667 wells classified as producing have no producing formation or formation at total depth recorded in the data file. We cannot determine at this time whether these wells are producing below 15,000 ft or not. The remaining 3,017 producing wells of the original 8,705 producing wells produce from a formation other than the formation at total depth. Although many of these wells may be producing oil or gas below 15,000 ft, they were not considered for this report. Of the 8,705 producing wells, 40 were not included because they were actually classed as dry holes with a producing formation. To avoid confusion, these wells were eliminated from the data set.

The following discussion is based solely on observations from the data bases and does not take into account wells and reservoirs that are not in WHCS or PDS.

TABLE 2. — WELL CLASSIFICATION AND TOTAL DEPTH INTERVAL OF U.S. WELLS DRILLED DEEPER THAN 15,000 FEET^a

Total depth ^b (1,000 ft)	Producing wells										Total gas wells/total wells (%)		
	Dry holes	Oil & gas			Conden- sate	Gas & condensate	Multiple zones		Misc. ^c	Total wells		Total producing wells ^d	Total gas wells
		Oil	Gas	Oil & gas			Oil	Gas					
15-16	2,608	944	2,047	37	14	13	127	121	337	6,248	3,303	2,168	66
16-17	1,861	488	1,428	19	8	12	65	91	229	4,201	2,111	1,519	72
17-18	1,062	266	952	4	15	12	24	41	121	2,497	1,314	993	76
18-19	687	125	577	3	3	0	5	19	74	1,493	732	596	81
19-20	332	45	322	2	7	3	2	22	34	769	403	344	85
20-21	224	47	227	1	17	1	2	15	29	563	310	242	78
21-22	142	21	200	0	4	0	0	16	20	403	241	216	90
22-23	90	13	190	0	1	0	0	6	6	306	210	196	93
23-24	35	1	40		1				3	80	42	40	95
24-25	30	1	15						0	46	16	15	94
25-26	12	1	11						1	25	12	11	92
26-27	1	2	3						1	7	5	3	
27-28	0	1	2							3	3	2	
28-29	2	1	0							3	1	0	
29-30	3		1							4	1	1	
30-31	0		1							1	1	1	
31-32	1		0							1	1	1	
Totals	7,090	1,956	6,016	66	70	41	225	331	855	16,650	8,705	6,347	

^aData taken from WHCS file, updated through February 1988.^bTotal depth interval, not necessarily depth of the producing unit.^cMisc. = miscellaneous; includes wells with unknown final completion classification, sulfur wells, suspended wells, dry development wells, injection wells, and drilled and abandoned wells.^dProducing wells may be producing at any depth.

TABLE 3. — WELL CLASSIFICATION OF DEEP WELLS PRODUCING FROM FORMATIONS ENCOUNTERED AT TOTAL DEPTH, BASED ON FINAL COMPLETION CLASSIFICATION^a

Total depth (1,000 ft)	Producing wells							Total gas ^b	Total wells ^c	Gas wells/ total wells (%)
	Oil	Gas	Oil & gas	Conden- sate	Multiple zones					
					Oil	Gas	Cond.			
15-16	297	799	6	2	12	21	1	820	1,138	72
16-17	165	498	6	2	4	17	8	515	700	74
17-18	70	307	2	6	4	3	3	310	395	79
18-19	36	219	2			9		228	266	86
19-20	9	144		1	1	11	1	155	167	93
20-21	7	84		10		1		85	102	83
21-22	1	74		2		1		75	78	96
22-23	2	107		1				107	110	97
23-24		12						12	12	100
24-25	1	3						3	4	75
25-26		7						7	7	100
26-27	1	1						1	2	50
27-29										
Totals	589	2,255	16	24	21	63	13	2,318	2,981	78

^aData taken from WHCS file, updated through February 1988.

^bTotal gas = number of gas wells plus the number of wells producing gas from multiple zones.

^cTotal wells = wells producing from the formation encountered at total depth.

Deepest Wells in U.S.

Table 1 contains identification and location information from WHCS for the 10 deepest wells in the U.S., regardless of completion classification. They are listed in decreasing order of total depth. All were drilled in Oklahoma and Texas in the Anadarko and Permian basins. The deepest well drilled in the U.S., the Lone Star no. 1 Bertha Rogers, was completed in 1974 as a dry hole in the Anadarko basin (Fig. 1) in Oklahoma. The well was drilled as a wildcat to a depth of 31,441 ft. It penetrated the Upper Cambrian and Lower Ordovician Arbuckle Group at 31,236 ft, after almost a year and a half of drilling.

The second deepest well, the Lone Star no. 1 Earnest R. Baden, although drilled to more than 30,000 ft, was completed as a gas well in the Middle Pennsylvanian Atoka Formation at a depth of ~16,500 ft after being acidized. The third deepest well, the Hunt Energy no. 1-9 Cerf Ranch unit, was drilled as a wildcat and, although abandoned, it reported gas in the Lower Ordovician Ellenburger Group at 22,535 ft. The fourth deepest well, the Gulf Oil Corp no. 2 Emma Lou Unit 1, was completed as a gas well at Puckett West field in the Middle Pennsylvanian Atoka Formation at >23,000 ft. Of the remaining wells in Table 1, 5 through 8 were drilled and abandoned, and wells 9 and 10

were completed as gas wells. Well 9, the McCulloch Oil no. 1 Easley, reported production from below 15,000 ft.

Total Deep Wells by Completion Classification

Table 2 summarizes the final completion classification by depth interval of all 16,650 wells drilled deeper than 15,000 ft in the WHCS data base. Gas wells account for 73% of the total number of producing wells with total depths below 15,000 ft. There are nearly as many gas wells (6,347) as dry holes (7,090); gas wells are approximately three times more abundant than oil wells. Of the 16,650 deep wells, 1,442 wells have total depths >20,000 ft. Of these, 842 are producing wells, of which 727 (86%) are producing gas at any depth. The ratio of gas-producing wells to total producing wells generally increases with increasing depth. The propensity for deep wells to produce gas is related to the relative instability of oil in deep, hot reservoirs.

Deep Producing Wells by Completion Classification

Table 3 summarizes, by depth interval, the final well classification of the 2,981 deep wells in the WHCS file that produce oil or gas from the forma-

TABLE 4. — NUMBERS OF DEEP PRODUCING WELLS BY DEPTH INTERVAL IN U.S.^a

Region	Depth intervals ^b												Total
	15	16	17	18	19	20	21	22	23	24	25	26	
Rocky Mountains	120-35	73-18	40-12	20-15	7-6	5-5							265-91
Midcontinent	131-124	87-84	69-68	43-41	21-21	9-9	6-6	3-3	2-2	2-2	1-1	1-1	375-362
Permian basin	81-77	23-23	28-27	23-22	34-34	14-14	29-29	29-29	2-2	2-1	5-5	1-0	271-263
Gulf Coast	795-578	495-380	239-194	174-144	93-84	54-48	29-28	10-8	5-5		1-1		1,895-1,470
California/Alaska	4-1	2-1	1-0										7-2
Total	1,131-815	680-506	377-301	260-222	155-145	82-76	64-63	42-40	9-9	4-3	7-7	2-1	2,813-2,188
Location unknown	7-5	20-9	18-9	6-6	12-10	20-9	14-12	68-67	3-3				168-130
Grand Total	1,138-820	700-515	395-310	266-228	167-155	102-85	78-75*	110-107	12-12	4-3	7-7	2-1	2,981-2,318

^aData taken from WHCS file, updated through February 1988. Only includes wells producing from the same formation as the formation at total depth (total = 2,981 wells).

^bDepth intervals in thousands of feet where 15 = 15,000-16,000 ft. Total number of producing wells for each depth interval (in columns) is on left, and number of gas-producing wells is on right.

TABLE 5. — TOTAL DEEP PRODUCING WELLS BY DEPTH INTERVAL
IN U.S. BY DECADE OF COMPLETION^a

Depth interval (1,000 ft)	1920	1930	1940	1950	1960	1970	1980-88
15-16			1-0 ^b	5-5	61-21	394-260	678-534
16-17				1-1	14-9	319-224	365-281
17-18				1-1	9-3	152-106	233-200
18-19					1-1	108-90	157-137
19-20					1-0	67-59	99-96
20-21					13-5	45-38	44-42
21-22					9-8	25-23	44-44
22-23					17-17	76-74	17-16
23-24						6-6	6-6
24-25						3-2	1-1
25-26						1-1	6-6
26-27						2-1	
27-28							
Totals			1-0	7-7	125-64	1,198-884	1,650-1,363
Grand Total							2,981-2,318

^aData taken from WHCS file, updated through February 1988. Data set does not include 292 deep producing wells with unlisted well-completion year. Only includes wells having producing formation same as formation at total depth.

^bFirst number represents total producing wells for that depth interval and decade; second number (following hyphen) represents wells producing gas for that depth interval.

tion encountered at total depth. Gas wells outnumber oil wells for each depth interval except the 26,000- to 27,000-ft interval. The percentage of gas wells of all producing deep wells ranges from 72% in the 15,000- to 16,000-ft range to 100% in the 22,000- to 23,000-ft range and generally increases with increasing total depth. For all depths together, gas wells make up 78% of the deep wells producing from formations encountered at total depth.

Deep Producing Wells by Region

Table 4 summarizes deep producing wells from WHCS by depth interval and by geographic region. Of the five regions represented, the Gulf Coast region contains the greatest number of deep producing wells (1,895). The Rocky Mountain region contains only 265 deep producing wells. The Appalachian/Illinois/Michigan region contains 19 wells drilled deeper than 15,000 ft, but because all are either dry holes or are producing from formations other than the formation at total depth, this region is not represented in this table. Also, 168 wells reported no location and are listed separately by depth in Table 4.

For the majority of depth intervals, deep gas-producing wells form >90% of total producers. For all depths together, the Rocky Mountain region has the smallest percentage (34%) of deep gas wells (91 gas wells and 265 total wells). This figure is somewhat misleading because it is strongly biased by deep oil production in the Uinta and Powder River basins. The Green River, Wind River, Washakie, and Big Horn basins and the Wyoming-Utah-Idaho thrust belt (Fig. 1) are predominantly gas producers in their deeper parts, but have fewer total wells. The deepest producing wells, namely those producing below 20,000 ft in the Rocky Mountain region, produce gas from the Madison Limestone in the Wind River basin of Wyoming. The two deepest wells in the Midcontinent region are gas producers, which were drilled into the Upper Cambrian and Lower Ordovician Arbuckle Group and the Silurian and Devonian Hunton Group in the Anadarko basin of Texas and Oklahoma.

The deepest wells in the Gulf Coast region are gas wells in Louisiana. They are producing gas from Miocene strata; no WHCS formation data are available for these wells. The deepest offshore well

TABLE 6. — SUMMARY DATA FOR DEEPEST FIELD AND RESERVOIR
AND TOTAL DEEP PRODUCTION BY STATE^a

State	Number of fields (reservoirs) ^b	Deepest field (reservoir) ^c	Discovery year	Average depth (ft) ^d	Total production ^e (state total)	
Utah*	1 (1) Cl = 1	Bridger Lake (Dakota) oil	1966	15,518	CRUDE =	10,733,535
					NGAS =	5,687,867
					DGAS =	43,364,976
					COND =	335,480
Wyo.*	10 (11) Cl = 9 Carb = 2	Seller Draw (Muddy) gas	1977	19,580	CRUDE =	11,217,869
					NGAS =	188,170,974
					DGAS =	1,481,814
					COND =	471,992
N. Mex.*	14 (14) Carb = 14	Jal. West (Fusselman) gas	1972	16,614	CRUDE =	61,749,686
					NGAS =	4,363,332
					AGAS =	4,048,122
					COND =	9,773
Okla.	63 (86) Cl = 81 Carb = 5	Elk City East (Springer) gas	1969	22,652	CRUDE =	759,662,587
					NGAS =	2,119,741,903
Tex.*	669 (1,530) Cl = 120 Carb = 1,410	Dillon (Strawn) gas	1984	26,088	CRUDE =	1,539,491,628
					NGAS =	11,885,557,958
					AGAS =	1,220,016,194
					DGAS =	36,003,091
					COND =	32,560,398
La.	122 (220) Cl = 220	Caillou Is. (Miocene) oil	1960	21,862	CRUDE =	4,232,551,442
					NGAS =	34,514,774,028
					DGAS =	6,460,421,945
					COND =	731,496,274
Miss.*	67 (109) Cl = 75 Carb = 34	Piney Woods (Smackover) gas	1974	22,026	CRUDE =	39,198,342
					NGAS =	885,508,244
					AGAS =	53,638,223
					COND =	7,451,157
Ala.*	14 (15) Cl = 4 Carb = 11	Cold Creek S. (Smackover) oil	1975	18,470	CRUDE =	33,401,203
					NGAS =	697,261,156
					AGAS =	42,832,818
					COND =	84,349,373
Fla.	3 (4) Cl = 2 Carb = 2	Blackjack Cr. (Smackover) oil	1972	16,120	CRUDE =	402,170,776
					AGAS =	488,404,992
Calif.*	7 (7) Cl = 7	Coles Levee, N. (Eocene) oil	1953	17,892	CRUDE =	65,395,838
					AGAS =	73,730,992
Alaska*	1 (1) Cl = 1	Beaver Cr. (Tert. Tyonek) oil	1972	15,200	CRUDE =	3,178,192
					AGAS =	1,298,032
Total	971 (1998) Carb = 1,471 Cl = 527				CRUDE =	7,157,000,000
					NGAS =	50,301,000,000
					AGAS =	1,883,000,000
					COND =	857,000,000
					DGAS =	6,541,000,000

^aData taken from Petroleum Data System (PDS) file, with production by state totalled through 1985 for all deep reservoirs.

^bNumber of reservoirs (in parentheses) may exceed number of fields where a single field includes more than one reservoir. Reservoirs subdivided into clastic (Cl) and carbonate (Carb). Total number of clastic and carbonate reservoirs may not equal the total number of reservoirs, in part because some reservoirs do not have reports on producing lithology and in part because of errors in the data file.

^cDeepest field and reservoir within state classified as oil or gas, regardless of present producing category.

^dAverage depth (in feet) to production listed for each reservoir.

^eTotal deep production listed by production type for each state: CRUDE = crude oil; NGAS = nonassociated gas; AGAS = associated gas; DGAS = dissolved gas; and COND = condensate. Oil and condensate production in barrels; gas and dissolved-gas production in MCF. Some discrepancies occurred when totaling production for those states where production listed by reservoir; production totals from field records did not always equal totals by reservoir records. Many fields are producing from reservoirs both above and below 15,000 ft. For states that only carry field totals, the deep reservoirs have not been separately broken out in this study. Production listed here only by reservoir for those states identified with asterisk (*). Production totals at bottom of column are rounded to nearest millions of units for simplicity.

is located on the Eugene Island block off Louisiana; it is producing from Miocene strata at a depth of ~21,000 ft.

Deep Producing Wells and Year of Completion

Table 5 contains well summaries from WHCS for deep producing wells by year of completion, in 10-year increments, and depth (see Dyman and others, 1990, for total number of deep wells based on year of completion). Only eight wells classed as producing from reservoirs deeper than 15,000 ft were completed before 1960; all were reported as gas producers. The first three wells to produce gas deeper than 20,000 ft were completed in 1967. The two deepest hydrocarbon-producing wells (wells producing from deeper than 26,000 ft) were completed in 1977 and 1979. Deep gas-producing wells account for 70% of the total deep producing wells completed during the 1970–75 period, and >80% completed during the 1976–87 period. For each 10-year increment, the ratio of gas-producing wells to total producing wells below 15,000 ft increases with depth. For all years together, >90% of the wells that are classed as producers below 20,000 ft are producing gas.

Lithology of Producing Formation

Dyman and others (1990) compiled lithologic data for deep producing wells in each state. Of the wells producing oil deeper than 15,000 ft, 75% (467 wells) produce from clastic rocks. The deepest clastic oil reservoirs occur in the New Mexico part of the Permian basin (average = 18,243 ft). In Utah, 136 deep oil wells were completed in clastic reservoirs. Of the 366 deep oil wells that produce from Tertiary rocks, 168 produce from the Miocene in the Gulf Coast region, and 134 produce from the Paleocene and Eocene Wasatch Formation in the Rocky Mountain region. Of the 125 deep producing wells that are Jurassic oil producers, 92 produce from the Smackover Formation.

More than 75% (1,740 wells) of the deep gas wells also produce from clastic rocks. The Anadarko basin and the Rocky Mountain region produce deep gas primarily from clastic reservoirs (352 wells). In Texas, 55% of the deep gas wells (377) produce from carbonate rocks; most of these produce from the Lower Ordovician Ellenburger Group in the Permian basin. Texas and Louisiana have more deep gas wells which produce from carbonate rocks than from clastic rocks. Deep gas from carbonate rocks in the Upper Jurassic Smackover Formation is produced from 99 deep wells in Texas, Alabama, Mississippi, and Florida.

Deep Fields and Reservoirs

Table 6 lists the deepest field and reservoir and total production by state for all deep fields and reservoirs in that state. This table was produced using PDS data, based on average depth of production for reservoirs >15,000 ft. About 7 billion bbl of oil and 50 trillion cubic feet (TCF) of nonassociated gas have been produced from these deep reservoirs through 1985, according to PDS. For fields with multiple reservoirs, shallow reservoirs (<15,000 ft deep) were not included. PDS lists 971 fields and 1,998 reservoirs as producing oil or gas below 15,000 ft. Texas has the greatest number of fields (669) and reservoirs (1,530), and they are producing from carbonate rocks in the Permian basin and carbonate and clastic rocks in the Gulf Coast basin. Deep gas production accounts for ~7% of the U.S. total cumulative gas production (698 TCF), and deep oil production accounts for ~5% of the total U.S. cumulative production (143 billion bbl) (U.S. Geological Survey and U.S. Minerals Management Service, 1989). The southern Midcontinent, the Gulf Coast, and Texas have >1,900 deep reservoirs, >95% of all total deep reservoirs in the U.S.

Total cumulative production through 1985 of nonassociated deep gas for reservoirs discovered prior to 1970 equals ~9.2 TCF, which is ~18% of the total cumulative deep nonassociated-gas production. Of the 260 active deep reservoirs listed in the PDS file, 34 were discovered prior to 1970. The oldest deep reservoirs were discovered in the Permian basin and Gulf Coast regions.

REFERENCES CITED

- Dwight's Energydata, 1985, Petroleum Data System (through 1985): Available from Dwight's Energydata Corp., Oklahoma City, OK 73108.
- Dyman, T. S.; Nielsen, D. T.; Obuch, R. C.; Baird, J. K.; and Wise, R. A., 1990, Summary of deep oil and gas wells and reservoirs in the U.S. from the Well History Control System and Petroleum Data System: U.S. Geological Survey Open File Report 90-305, 35 p.
- Petroleum Information Corp., 1988, Well History Control System (through February 1988): Available from Petroleum Information Corp., Denver, CO 80122.
- Takahashi, K. I.; and Cunningham, K. I., 1987, Map showing wells drilled for oil and gas deeper than 15,000 feet in the conterminous United States and offshore: U.S. Geological Survey Oil and Gas Investigations Map OM-220, scale 1:5,000,000.
- U.S. Geological Survey and U.S. Minerals Management Service, 1989, Estimates of undiscovered conventional oil and gas resources in the United States—a part of the nation's endowment: U.S. Department of Interior, 44 p.

Lower Atoka Group (Spiro Sand) Stratigraphic Relationships, Depositional Environments, and Sand Distribution, Frontal Ouachita Mountains, Oklahoma

Robert C. Grayson, Jr., and Lawrence K. Hinde

Baylor University
Waco, Texas

ABSTRACT.—Outcrop studies demonstrate that the Spiro represents a mixed carbonate and terrigenous clastic platform complex, which consists of laterally interfingering sandstone, shale, and limestone. Accumulation of the Spiro on the Arkoma shelf began during a relative rise in sea level, as quartz sand derived from reworking of the previously deposited fluvio-deltaic Foster “channel sands” was transported southwestward across the shelf. Facies relationships, vertical sequences, and sedimentary structures suggest that this reworked quartz sand accumulated on the shelf as marine bars.

Based on the surface exposures, three regions are distinguished that reflect overall differences in the character of the Spiro. The Wilburton–Red Oak region contains the most areally extensive sandstone deposits, and the highest net-sand values. There, Spiro sandstones primarily represent bar-crest and bar-flank facies. To the west, in the Hartshorne and Kiowa regions, sand-bar deposits are thinner, smaller in areal extent, and they consist mostly of bar-flank and bar-margin facies. In addition, carbonate facies are more common. Carbonate facies developed between marine bars are regarded as interbar accumulations. However, extensive carbonate deposits in the Kiowa region record diminished terrigenous influx.

Spiro net-sand trends, mapped on a palinspastic base, closely resemble and seem to represent a lateral continuation of Spiro isopach trends previously identified in the Arkoma basin.

Basinward facies changes in the Spiro are evident within the frontal belt. However, more-pronounced changes occur south of the Pine Mountain and Ti Valley faults. In this latter area, Spiro equivalents are represented by terrigenous clastic and spiculitic basin-margin and basinal facies. East of the surface exposures (along the frontal zone), Spiro terrigenous clastic and carbonate facies apparently grade into shale.

INTRODUCTION

Ongoing exploration in the northern Ouachita Mountains has shown that the Spiro can be an outstanding gas reservoir. Drilling activity has provided data for palinspastic restoration and for extending depositional trends established to the north, in the Arkoma basin, into the restored overthrust portion of the southern Arkoma shelf.

The Choctaw fault is a regional structure that is the boundary between the Ouachita Mountains and Arkoma basin (Fig. 1). In the frontal Ouachita Mountains, the Wapanucka limestone, middle shale, and Spiro are exposed in one or more resistant ridges separated by valleys that are floored by “Springer” and/or Atoka shale (Fig. 2). These thrust-fault- and fold-repeated ridges form a relatively narrow belt of exposures between the Choctaw

and Pine Mountain faults (Fig. 1) that begins near Stringtown, in Atoka County, and extends northeastward then eastward through Pittsburg County into Latimer County. The most extensive of these ridges, Limestone Ridge, is in the hanging wall of the Choctaw fault.

Our purpose is to describe the character of the Spiro in outcrop and to relate interpretations of the Spiro to previous interpretations of “Foster” and Spiro sand trends in the Arkoma basin (Lumsden and others, 1971; Houseknecht and others, 1980). In this contribution, we propose a shelf-bar model for sand units in the Spiro, based on analysis of surface exposures and more limited examination of well logs and cores from the Spiro below the Choctaw thrust. Tentative palinspastic restoration of the thrustured Arkoma shelf in the frontal Ouachita Mountains provides a base map for

Grayson, R. C., Jr.; and Hinde, L. K., 1993, Lower Atoka Group (Spiro sand) stratigraphic relationships, depositional environments, and sand distribution, frontal Ouachita Mountains, Oklahoma, *in* Johnson, K. S.; and Campbell, J. A. (eds.), *Petroleum-reservoir geology in the southern Midcontinent*, 1991 symposium: Oklahoma Geological Survey Circular 95, p. 216–224.

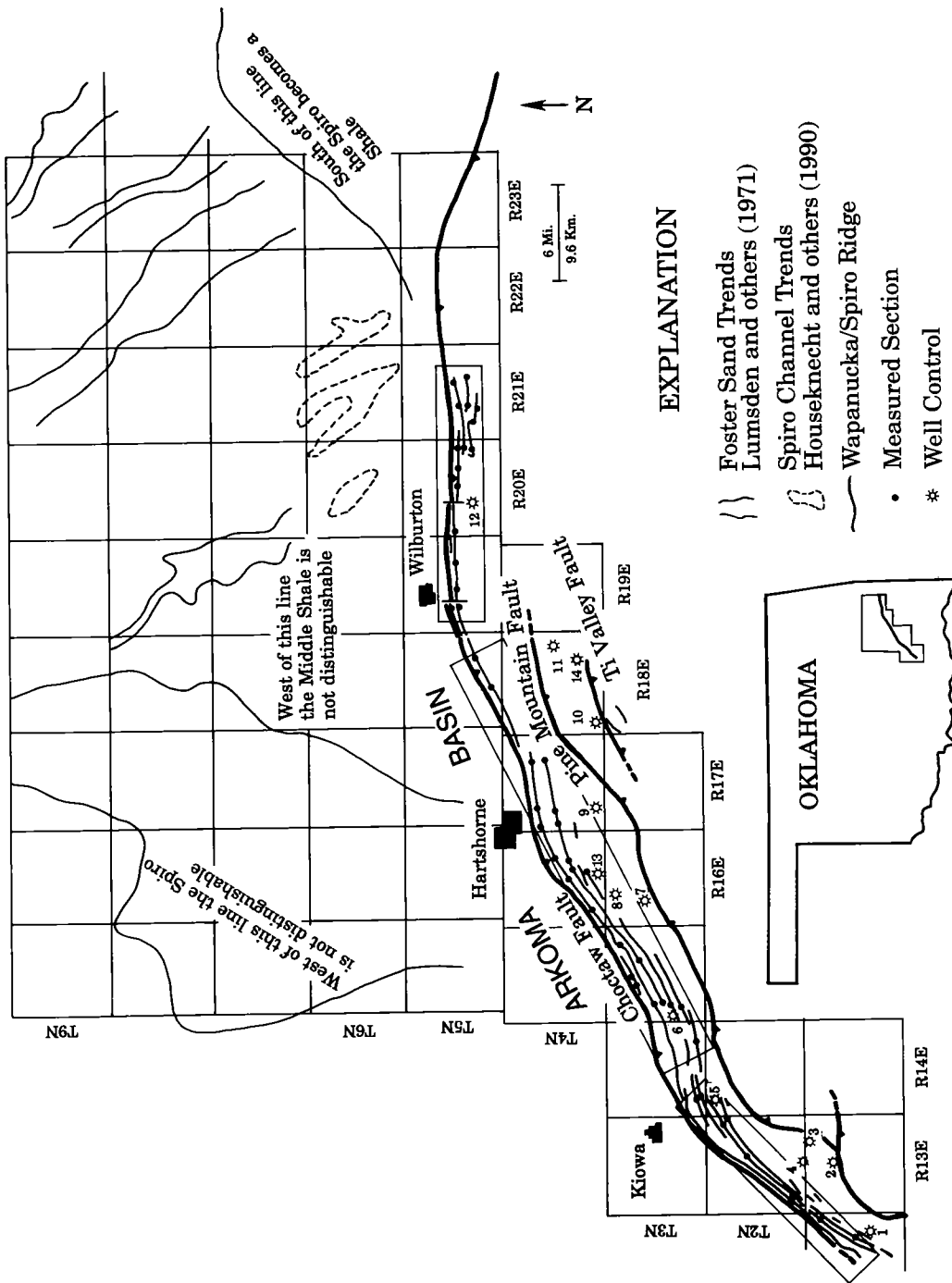


Figure 1. General location map showing the topographic ridges in the frontal Ouachita Mountains that expose Wapanucka, middle shale, and Spiro. Rectangular boxes outline the regions that are discussed in the text (Kiowa, Hartshorne, and Wilburton-Red Oak). Detailed descriptions of measured section locations can be found in Grayson (1979, 1980), Frost (1981), Grayson and Sutherland (1988), and Hinde (1992).

comparing sand trends in the thrust-faulted portion of the Arkoma shelf with those documented by Lumsden and others (1971) and by Houseknecht and McGilvery (1990) in the Arkoma basin.

GEOLOGIC SETTING

During the Pennsylvanian, the southern Mid-continent region contained the edge of the Paleozoic continent Laurasia, which included what is now North America. This portion of the Laurasian continental margin was initially an Atlantic-type passive margin (Houseknecht, 1986). However, as Pangea was assembled, collision of Laurasia with Gondwana (Llanoria) resulted in a transition to a convergent margin (Wickham and others, 1976; Houseknecht, 1986). As the ocean basin between Laurasia and Gondwana was subducted, the northward-advancing thrust complex resulted in flexural deformation of the margin of Laurasia (Houseknecht, 1986; Sutherland, 1988). This tectonic scenario and the flexural deformation model have been applied by Houseknecht (1986) and Sutherland (1988) to account for the Arkoma (foreland) basin, as well as the presence in the foreland of predominantly down-to-the-south normal faults.

Flexural deformation models (Angevine and others, 1990) predict that the weight of the tectonic load will result in a differential subsidence pattern that leads to the characteristic asymmetric shape of the fill of foreland basins. The flexural model also predicts that a forebulge will develop inboard from the foreland basin. The forebulge is a positive area that is commonly a site of erosion (Angevine and others, 1990), while sedimentation may be occurring in an adjacent basin. Lumsden and others (1971) showed that the "Foster," middle shale (sub-Spiro shale), and Spiro are developed only in the southern portion of the Arkoma basin, and that the "Foster" and locally the Spiro are separated from the Wapanucka limestone by an erosional boundary. It seems probable that these stratigraphic relationships reflect the development of a forebulge on the Arkoma shelf prior to foreland-basin subsidence.

During the Carboniferous, several mixed clastic- and carbonate-platform complexes existed on the Arkoma shelf prior to foreland-basin subsidence. The youngest of these platform complexes includes the Wapanucka, middle shale, and Spiro (Fig. 2). Strata of roughly equivalent age, higher on the Arkoma shelf, are comparatively thin, relatively incomplete, and were deposited in

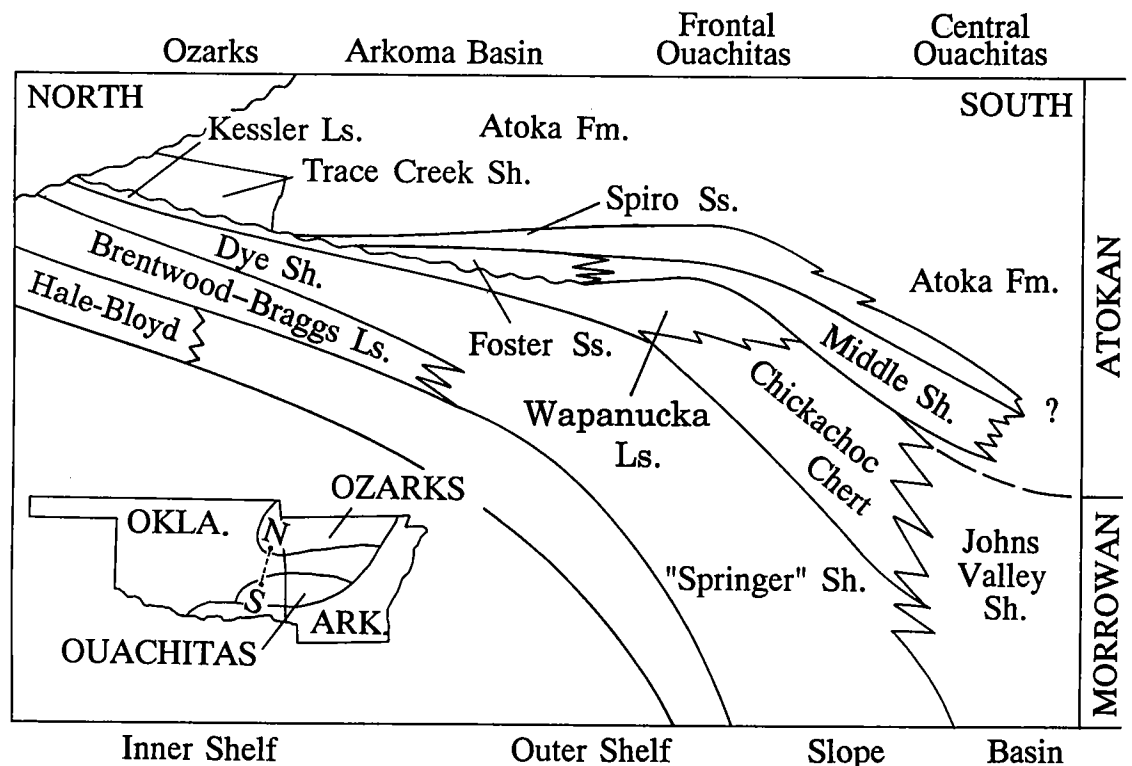


Figure 2. Regional stratigraphic cross section of the Arkoma shelf (adapted from Grayson and Sutherland, 1988).

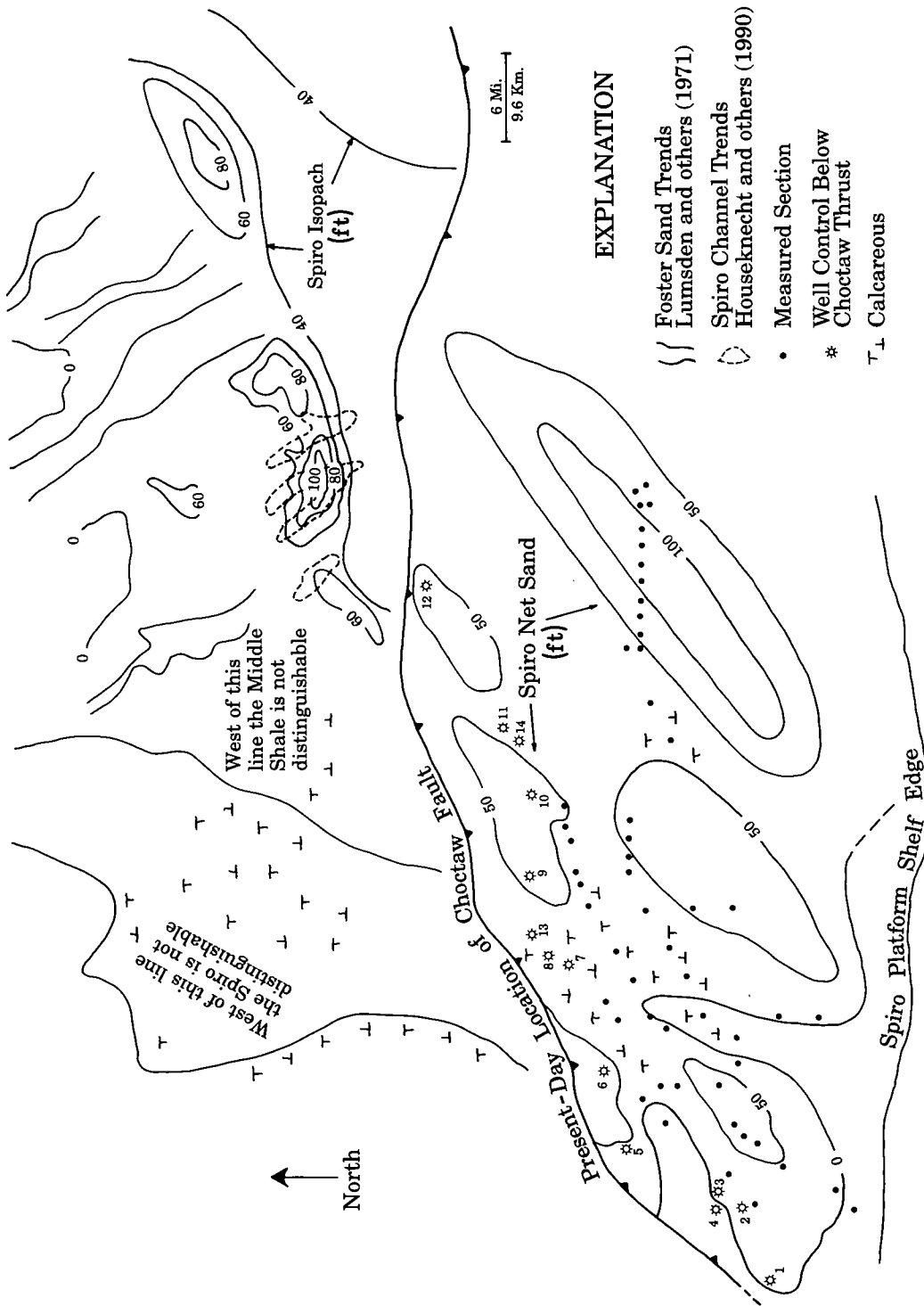


Figure 3. Spiro sand-distribution map plotted on a palinspastic base. Arkansas basin Spiro isopach data and location of "Foster" channels obtained from Lumsden and others (1971); location of Spiro "channels" derived from Houseknecht and McGilvery (1990). Wells that penetrate the Spiro below the Choctaw thrust are not relocated on the palinspastic base.

a shallower marine environment. The Spiro and Wapanucka also contrast markedly with coeval basinal deposits represented by the boulder-bearing Johns Valley Shale (Sutherland and Grayson, 1977) and by flysch facies in the lower part of the Atoka Formation (Cline, 1956; Legg and others, 1990; Whiteside and Grayson, 1990). These basinal units are comparatively thick and were deposited in substantially deeper water.

SURFACE EXPOSURES

Our surface data (Grayson, 1979, 1980; Frost, 1981; Grayson and Sutherland, 1988; Hinde, 1992) consists of 60 measured sections spaced at more or less even intervals along the length of the outcrop belt (Fig. 1). Within this area, the Spiro consists primarily of shallow-shelf lithofacies that grade from predominantly quartz-sandstone and shale in the east to predominantly limestone in the west.

The precise thickness of the Spiro is difficult to determine due to cover and fault concealment. Measured thicknesses of the interval, however, range from approximately 5 to 200 ft. The Spiro is a basinward-thickening wedge that thickens mostly due to the increased abundance of shale and sandstone. An exception to this generality occurs in the western outcrop area, where the Spiro is predominantly limestone.

Maximum net-sand values approach 120 ft. Individual sandstones coarsen upward and range in thickness from a few feet to >30 ft. In general, sandstone units thin toward the west (Fig. 3), and show progressive changes such as decreasing grain size and increasing importance of calcite cement compared to quartz overgrowth cement.

Palinspastic Restoration

The belt of surface exposures is subdivided into three general regions (Fig. 1) that reflect significant variations in the character of the Spiro. Interpretation of several proprietary seismic lines leads us to conclude that there is 18 mi of shortening in the Wilburton-Red Oak region, 20 mi in the Harts-horne region, and 13 mi in the Kiowa region. These are minimal estimates of shortening. They do not include any attempt to restore that portion of the Spiro that has been removed by surface erosion. Furthermore, neither northward-directed thrusts that might exist north of the Choctaw fault, nor the minor thrusts that affect the in-situ Spiro were included in shortening estimates. In addition, the seismic lines we examined do not carry far enough to the south to reveal the limits of the in-situ Spiro. Our estimates are consistent with values that Hardie (1986; personal communication, 1990) obtained from restoring his cross sections in the Pittsburg area. However, they are not consistent with the tens of miles of shortening that

some workers predict will eventually be determined (Tilford, 1990).




Depositional Model

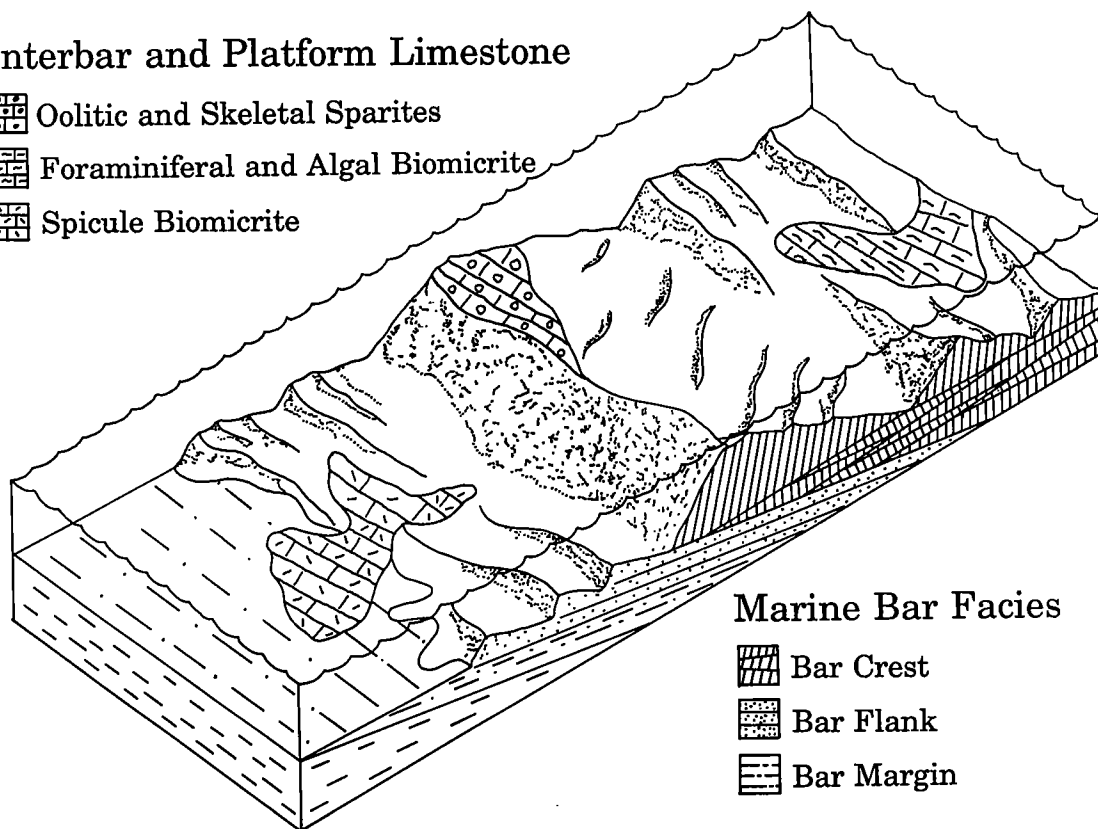
Exum and Harms (1968) point out that the vertical sequence of marine bars is characterized by an upward-coarsening pattern. This contrasts markedly with the upward-fining pattern that characterizes channel-fill deposits. Upward-coarsening sequences are common within the Spiro, and we have never observed the reverse. Therefore, we interpret Spiro siliciclastic facies in terms of a marine-bar model. Our model is modified from that of Exum and Harms (1968). We recognize three siliciclastic facies: (1) bar-crest, (2) bar-flank, and (3) bar-margin (Fig. 4). The bar-crest facies consist of fine- to medium-grained, moderately well-cemented, thick- to very thick-bedded, tabular to tangential cross-bedded quartzarenite. The bar-flank facies is slightly finer grained, medium- to thick-bedded quartzarenite with minor ripple marks being the primary sedimentary structure. The bar-margin facies consist of very fine-grained, well-cemented, very thin- to thin-bedded quartzarenite with shale interbeds. Sedimentary structures are generally not obvious in the bar-margin facies.

In contrast to most marine-bar deposits, Spiro bar facies are commonly associated with carbonate facies. Some of the carbonates also represent marine bars, whereas others record interbar environments. Spiro limestone lithologies include spicule biomicrite, algal and foraminiferal biomicrite, crinoidal biosparite, and, rarely, oosparite. These lithologies are associated with Spiro shelf bars and also occur between sand bar tracts. In the Kiowa region, the Spiro is entirely composed of carbonate lithologies.

Grayson (1980) discussed Spiro (upper sandstone/limestone member of the Wapanucka Formation) sandstone-bar facies in terms of tidal sand waves and ribbons. This interpretation no longer appears to be valid because there is only limited field evidence for a significant tidal range during Spiro accumulation. However, valid comparison can be made between the Spiro and Shannon Sandstone. The Shannon is a Cretaceous sandstone unit in Wyoming that contains two or more upward-coarsening sequences. Harms and others (1982) and Tillman and others (1984) interpreted these sequences to record marine bars developed on a shelf dominated by unidirectional currents (wind-induced or oceanic). Spiro current patterns were probably more complex. Precise paleocurrent directions are difficult to ascertain because of limited exposures. Nonetheless, we have observed at least three current-direction modes; these are, in order of decreasing frequency: southwest, west-southwest, and north. These presumably reflect dominant storm tracks, prevailing wind directions, oceanic currents, and/or less-significant tidal currents.

Interbar and Platform Limestone

-  Oolitic and Skeletal Sparites
-  Foraminiferal and Algal Biomicrite
-  Spicule Biomicrite



Marine Bar Facies




-  Bar Crest
-  Bar Flank
-  Bar Margin

Figure 4. Marine-bar model for sand units within the Spiro.

Wilburton-Red Oak Region

In this easternmost region (Fig. 1), the Spiro is the dominant ridge former with measured thicknesses approaching 200 ft. Commonly, the Spiro is exposed only on Limestone Ridge. Locally, as in Bandy Creek, south of Wilburton, the Spiro is exposed on the two limbs of an overturned anticline (Bowsher and Johnson, 1968). At the eastern margin of the region, at least one imbricate thrust above the Choctaw is present. This imbricate thrust also contains an overturned anticline (Frost, 1981).

Although there is considerable variation in the vertical succession of rock types at different measured sections, the overall pattern in this region is rather simple. Furthermore, there is good correspondence between this pattern and that shown by net-sand contours (Fig. 3). Those sections with net-sand values >100 ft consist of approximately four stacked, upward-shoaling bar-crest sequences. These sequences are characterized by thick to very thick beds of fine- to medium-grained quartz-arenite, generally developed in upward-thickening packages. Sedimentary structures are abundant and include tabular and tangential cross-

bedding and ripple bedforms. Based on these structures, there were at least two predominant directions of transport. The more common tabular and tangential cross-beds record a south to southwest transport direction; whereas, the less common rippled beds record a southwest to west-southwest transport direction. Measured sections immediately east and west of this area contain less net sand and, for the most part, contain bar-flank and bar-margin sandy facies, and interbar carbonate facies. Several shoaling sequences can also be recognized in these overall lower-energy successions.

Hartshorne Region

The Hartshorne region (Fig. 1) extends from just west of Wilburton to just west of the Indian Nation Turnpike. It contains a dramatic transition in structural style from predominantly one major thrust fault (Choctaw fault) that brings the Spiro to the surface, to multiple thrusts that also expose the Spiro.

Within the Hartshorne region there is considerable variation in the lithologic character of the Spiro. Measured sections at both the east and west

ends apparently lack sandstone. Most sections consist predominantly of limestone facies, and generally contain a relatively thin basal sandstone. At the west end of the region, the northernmost measured section on the Indian Nation Turnpike contains calcareous sandstone or sandy limestone in the middle of the Spiro.

Two general types of interbar limestone are recognized within the Spiro. In the vicinity of Harts-horne, the most common limestone is sponge-spicule biomicrite, which may comprise over half of the total thickness of the Spiro. Farther to the west, limestones occur in lithologically variable shoaling sequences that generally include, from base to top, spicule biomicrite, foraminiferal and algal biomicrite, and skeletal or oolitic biosparite.

Within this region, there is only one significant area where sandstone units are well developed. This area includes several measured sections south and southwest of Hartshorne that are located on the more basinward thrust sheets (Fig. 3). In fact, the only significant development of bar-crest facies occurs in the most basinward measured section (MS 10 of Grayson, 1980; MS 315 [locality 7] of Grayson and Sutherland, 1988). This section of stacked bar-crest facies is now known to indisputably represent the Spiro, because Mauldin (M.S. thesis, in preparation) has identified Wapanucka in sequence a short distance to the west along the same ridge. Although sandstone units in the remaining sections enclosed by the 50-ft net-sand contour (Fig. 3) are comparable in the amount of sand, they represent primarily bar-margin and bar-flank facies. Using well logs, similar pods of sandstone can be identified in the sub-Choctaw thrust interval (Fig. 3).

Kiowa Region

Surface exposures of the Spiro in the Kiowa region (Fig. 1) consist predominantly of limestone facies. Along Limestone Ridge, sandstones occur only at the eastern margin of the Kiowa region. In the more-basinward sections, south of Kiowa, sand units are present at several localities, where they occur in an upward-thickening and -coarsening sequence. Although these successions include bar-crest facies, they consist largely of bar-flank, bar-margin, and interbar facies. Based on well-log analysis, the Spiro within the subthrust interval also includes discontinuous pods of sandstone (Fig. 3).

In the southwestern portion of this region, along Limestone Ridge, limestone facies within the Spiro record a southwestward increase in paleowater depth. The most northeastward section contains upward-shoaling limestone sequences that are capped by thick, cross-bedded, skeletal biosparites; sponge-spicule biomicrites are not well developed. In contrast, at the south-

west limit of Limestone Ridge, the Spiro consists predominantly of spicule biomicrite; algal biomicrite and biosparite units are comparatively thin.

REGIONAL SYNTHESIS

The Arkoma shelf is a major Paleozoic feature of the southern Midcontinent that was recognized by Sutherland (1988) as including portions of the Ozark Mountain and Arkoma basin regions. We have broadened the usage of that term to include portions of the Ouachita Mountains. The rationale for this is the fact that deposits characteristic of the Arkoma shelf are also present in the northern Ouachita Mountains.

The Wapanucka, middle shale, and Spiro are stratigraphic units that together comprise a major platform complex that existed on the Arkoma shelf. They record overall aggradation and progradation, punctuated by several localized transgressive events. Accumulation of these units on the Arkoma shelf ended with a major transgression as the Arkoma foreland basin became established. In the frontal Ouachita Mountains, the Wapanucka, middle shale, and Spiro record events that occurred at the distal end of the broad Arkoma shelf.

Regression in late Morrowan or early Atokan time, associated with either tilting of the Arkoma shelf (Sutherland and Henry, 1977) or the development of a forebulge on the Arkoma shelf, established "Foster" fluvio-deltaic environments. These SE-NW-trending channels locally incised the upper part of the Wapanucka limestone (Lumsden and others, 1971). In the frontal Ouachita Mountains, the lateral equivalent of the "Foster" channels is the middle shale. The middle shale records fine clastic influx that restricted carbonate sedimentation to the western portion of the Arkoma shelf (Figs. 1,3). During transgression, carbonate sedimentation was reestablished on the outer Arkoma shelf. Although comparable to Wapanucka sedimentation, Spiro carbonate sedimentation was areally more restricted owing to sand influx from the northeast. Presumably, reworking of the previously deposited "Foster" fluvio-deltaic deposits was the source for this influx. In the frontal Ouachita, sand and carbonate deposition ceased entirely as incipient foreland-basin subsidence led to the development of deeper water depositional settings and accumulation of Atoka flysch.

Sand Trends

Two depositional trends ("Foster" and Spiro) can be recognized in isopach maps constructed by Lumsden and others (1971). One trend (SE-NW), which they referred to as the Foster sand, was interpreted as representing fluvio-deltaic channel sands. Although not specifically stated, their Spiro

isopach map reveals a SW–NE trend. Lumsden and others (1971) recognized within this trend several generalized facies, which were interpreted to represent one or more of the following environments: lagoonal, tidal flat, tidal channel, bar, and beach. Lumsden and others (1971) noted the fact that within the Spiro, sand and carbonate facies are intimately related, a relationship that is also characteristic of the surface exposures in the frontal Ouachita Mountains. Our net-sand map (Fig. 3), which is plotted on a palinspastic basis, is constructed with the premise that there is complete depositional and stratigraphic continuity between the Spiro in outcrop and in the Arkoma basin. For this reason and because descriptions of the Arkoma basin Spiro match what is seen in outcrop (Houseknecht and others, 1989), we propose that, like the Spiro in outcrop, Spiro in the Arkoma basin primarily represents offshore shelf bars.

On the other hand, Houseknecht and McGilvery (1990), in a study of the Red Oak field, showed several porosity trends that they interpreted to represent channel deposits within the Spiro. Some of the accumulations contained only cross-bedded sandstone, whereas others consisted of both cross-bedded limestone and sandstone. Houseknecht and McGilvery (1990) interpreted the former to represent fluvially dominated channel deposits and the latter to reflect tidally dominated channel deposits. In Figure 3, their Spiro porosity trends have been superimposed on Lumsden and others (1971) Spiro isopach data. In our depositional model, these Spiro “channels” are bar-crest facies, which in outcrop consist of either cross-bedded sandstone or limestone. Likewise, we would recognize Houseknecht and McGilvery’s (1990) interchannel deposits as interbar, bar-margin, and bar-flank facies.

We have not been able to establish bar-crest trends within the sand-bar tracts, based on surface data (Fig. 3). However, Houseknecht and McGilvery (1990) data lead us to speculate that the bar crests may be oriented roughly perpendicular to the trends in the Spiro isopach and net-sand contours.

REFERENCES CITED

- Angevine, C. L.; Heller, P. L.; and Paola, C., 1990, Quantitative sedimentary basin modeling: American Association of Petroleum Geologists Course Notes Series No. 32, 133 p.
- Bowsher, A. L.; and Johnson, N. L., 1968, Road log for second day of field trip, in Cline, L. M. (ed.), *Geology of the western Arkoma Basin and Ouachita Mountains, Oklahoma*: Oklahoma City Geological Society Guidebook, 126 p.
- Cline, L. M., 1956, Mississippian–Pennsylvanian stratigraphy of central Ouachita Mountains, Oklahoma: *Ardmore Geological Society Guidebook to Ouachita Mountains, Field Conference*, p. 47–63.
- Exum, F. A.; and Harms, J. C., 1968, Comparison of marine bar with valley fill stratigraphic traps, western Nebraska: *American Association of Petroleum Geologists Bulletin*, v. 52, p. 1851–1868.
- Frost, R. W., 1981, The stratigraphy and distribution of the Wapanucka Formation in the Red Oak/Wilburton area of eastern Latimer County, Oklahoma: Baylor University unpublished B.S. thesis, 83 p.
- Grayson, R. C., Jr., 1979, Stop description—fifth day, in Sutherland, P. K.; and Manger, W. L. (eds.), *Mississippian–Pennsylvanian shelf-to-basin transition, Ozark and Ouachita regions, Oklahoma and Arkansas*: Oklahoma Geological Survey Guidebook 19, p. 67–76.
- , 1980, The stratigraphy of the Wapanucka Formation (Lower Pennsylvanian) along the frontal margin of the Ouachita Mountains, Oklahoma: University of Oklahoma unpublished Ph.D. dissertation, 319 p.
- Grayson, R. C., Jr.; and Sutherland, P. K., 1988, Shelf to slope facies of the Wapanucka Formation (Lower–Middle Pennsylvanian), frontal Ouachita Mountains, Oklahoma: *Geological Society of America Centennial Field Guide, South-Central Section*, p. 139–144.
- Hardie, W. E., 1986, Surface to subsurface structural interpretation of the Pittsburg Quadrangle, Pittsburg County, Oklahoma: Baylor University unpublished B.S. thesis, 93 p.
- Harms, J. C.; Southard, J. B.; and Walker, R. G., 1982, Shallow marine structures and sequences in clastic rocks: *Society of Economic Paleontologists and Mineralogists, SEPM Short Course No. 9*, chap. 8.
- Hinde, L. K., 1992, Stratigraphy and structural styles of the Spiro Formation, frontal Ouachita Mountains, southeastern Oklahoma: Baylor University unpublished M.S. thesis, 100 p.
- Houseknecht, D. W., 1986, Evolution from passive margin to foreland basin: the Atoka Formation of the Arkoma basin, south-central U.S.A., in Allen, P. A.; and Homewood, P. (eds.), *Foreland basins: International Association of Sedimentologists Special Publication 8*, p. 327–345.
- Houseknecht, D. W.; and McGilvery, T. A., 1990, Red Oak field, in Beaumont, E. A.; and Foster, N. H. (eds.), *Structural traps II—traps associated with tectonic faulting; treatise of petroleum geology atlas of oil and gas fields: American Association of Petroleum Geologists, Tulsa*, p. 201–225.
- Houseknecht, D. W.; Woods, M. O.; and Kastens, P. H., 1989, Transition from passive margin to foreland basin sedimentation, in Vineyard, J.; and Wedge, W. K. (compilers), *The Atoka Formation of the Arkoma basin, Arkansas and Oklahoma*: Geological Society of America Guidebook for Field Trip No. 15: Missouri Department of Natural Resources, Division of Geology and Land Survey Special Publication 5, p. 121–138.
- Legg, T. E.; Leander, M. H.; and Krancer, A. E., 1990, Exploration case study: Atoka and Jackfork section, Lynn Mountain syncline, Le Flore and Pushmataha Counties, Oklahoma, in Suneson, N. H.; Campbell, J. A.; and Tilford, M. J. (eds.), *Geology and resources of the frontal belt of the western Ouachita Mountains, Oklahoma*: Oklahoma Geological Survey Spe-

- cial Publication 90-1, p. 131-144.
- Lumsden, D. N.; Pittman, E. D.; and Buchanan, 1971, Sedimentation and petrology of Spiro and Foster sands (Pennsylvanian), McAlester basin, Oklahoma: American Association of Petroleum Geologists Bulletin, v. 55, p. 254-266.
- Sutherland, P. K., 1988, Arkoma basin, *in* Sloss, L. L. (ed.), Sedimentary cover—North American craton; U.S.: Geological Society of America, The Geology of North America, v. D-2, p. 331-340.
- Sutherland, P. K.; and Grayson, R. C., Jr., 1977, Basinward facies changes in the Wapanucka Formation (Lower Pennsylvanian), Indian Nation Turnpike, Ouachita Mountains, Oklahoma: Oklahoma Geology Notes, v. 37, p. 39-44.
- Sutherland, P. K.; and Henry, T. W., 1977, Carbonate platform facies and new stratigraphic nomenclature of the Morrowan Series (Lower and Middle Pennsylvanian), northeastern Oklahoma: Geological Society of America Bulletin, v. 88, p. 425-440.
- Tilford, M. J., 1990, Geological review of the Ouachita Mountains thrust belt play, western Arkoma basin, Oklahoma, *in* Suneson, N. H.; Campbell, J. A.; and Tilford, M. J. (eds.), Geology and resources of the frontal belt of the western Ouachita Mountains, Oklahoma: Oklahoma Geological Survey Special Publication 90-1, p. 169-196.
- Tillman, R. W.; and Martinsen, R. S., 1984, The Shannon shelf-ridge sandstone complex, Salt Creek anticline area, Powder River basin, Wyoming, *in* Tillman, R. W.; and Siemers, C. T. (eds.), Siliciclastic shelf sediments: Society of Economic Paleontologists and Mineralogists Special Publication 34, p. 85-142.
- Whiteside, J. R.; and Grayson, R. C., Jr., 1990, Carboniferous conodont faunas, northern Ouachita Mountains, Oklahoma, *in* Suneson, N. H.; Campbell, J. A.; and Tilford, M. J. (eds.), Geology and resources of the frontal belt of the western Ouachita Mountains, Oklahoma: Oklahoma Geological Survey Special Publication 90-1, p. 149-167.
- Wickham, J.; Roeder, D.; and Briggs, G., 1976, Plate tectonic models for the Ouachita foldbelt: Geology, v. 4, p. 173-176.

Trends of Sandstone Porosity in the Anadarko Basin— A Preliminary Evaluation

Timothy C. Hester

U.S. Geological Survey
Denver, Colorado

INTRODUCTION

This report presents the preliminary data and results of an ongoing study relating porosity and thermal maturity of sandstones of the Anadarko basin, Oklahoma (Hester and Schmoker, 1990). Treating porosity as a function of thermal maturity normalizes the overprint of burial history on porosity evolution, allowing porosity data from basins with different thermal histories to be merged and/or compared in the same context (Schmoker and Hester, 1990).

To best characterize sandstone-porosity trends in the Anadarko basin, three data sets have been compiled—two data sets representing Anadarko basin reservoir and nonreservoir sandstones, and one composite data set of sandstones from numerous basins, exclusive of the Anadarko basin, representing sandstones in general. Each data set consists of many sandstone porosity-vitrinite reflectance (R_o) data pairs that provide trends representative of that particular subset of sandstones. Porosity- R_o trends of Anadarko basin reservoir and nonreservoir sandstones are each compared to a set of porosity- R_o trends representing sandstones from basins other than the Anadarko, and the two are also compared to each other. Anadarko basin sandstone-porosity trends are thus evaluated relative to a framework of sandstones in general (Schmoker and Hester, 1990).

The data presented here are preliminary. Nevertheless, they are useful in the following ways: (1) they provide a means of estimating sandstone porosity in advance of drilling; (2) they provide comparative insights into porosity trends of reservoir and nonreservoir sandstones; and (3) they provide a standard with which to identify anomalously high- or low-porosity sandstones in the Anadarko basin.

DATA SETS

The first data set provides a porosity- R_o trend typical of Anadarko basin nonreservoir sandstones as a whole. The porosity data consist of more than

800 log porosity measurements representing >7,000 net ft of Paleozoic-age sandstone from 33 wells (Fig. 1) in the central and southern Anadarko basin. Sandstone was identified on each well log, (compensated-neutron and formation-density logs run on limestone matrix) and was then subdivided into intervals of uniform log character. The porosity curves of each interval (≥ 4 ft thick) were averaged and true porosity determined using standard neutron-density crossplots. R_o values for Anadarko basin nonreservoir sandstone intervals were calculated using an empirical R_o -depth relationship developed for the Anadarko basin by Schmoker (1986). In this report, the term "nonreservoir" indicates that the porosity data were taken directly from well logs of nonproductive sandstones; the term does not necessarily preclude the presence of hydrocarbons.

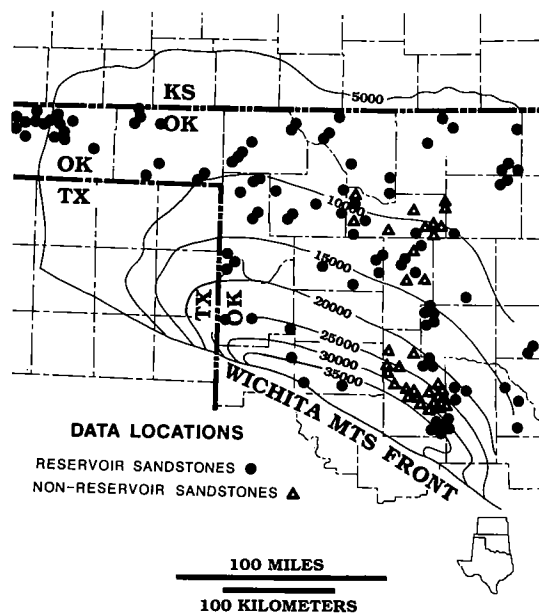


Figure 1. Map showing Anadarko basin total-sediment isopachs (ft) and data locations.

Hester, T. C., 1993, Trends of sandstone porosity in the Anadarko basin—a preliminary evaluation, in Johnson, K. S.; and Campbell, J. A. (eds.), Petroleum-reservoir geology in the southern Midcontinent, 1991 symposium: Oklahoma Geological Survey Circular 95, p. 225–229.

The second data set provides a porosity- R_o trend typical of Anadarko basin hydrocarbon-bearing sandstone reservoirs. The porosity data consist of averaged log porosity measurements of 105 Paleozoic-age sandstone oil and gas reservoirs of the Anadarko basin (Fig. 1) from published oil- and gas-field compilations (Cramer and others, 1963; Berg and others, 1974; Pipes, 1980; Harrison and Routh, 1981). R_o values were calculated as in the previous data set (Schmoker, 1986).

The third data set represents a sampling of sandstones of diverse ages, geologic settings, diagenetic facies, and thermal histories, and provides a framework of porosity- R_o trends typical of sandstones in general (Schmoker and Hester, 1990) with which to compare both Anadarko basin nonreservoir and reservoir sandstone-porosity data. The framework data consist of many thousands of individual porosity and R_o measurements from Cenozoic and Mesozoic sandstones in 27 locations in the Northern Hemisphere, exclusive of the Anadarko basin. The data, from published core-plug porosity and R_o measurements (Schmoker and Hester, 1990), are represented in this report by least-squares regression lines fit to the 10th, 25th, 50th, 75th, and 90th porosity percentiles of the framework data set.

POROSITY- R_o TRENDS

A least-squares regression line fit to the porosity- R_o data for nonreservoir sandstones of the central and southern Anadarko basin shows that nonreservoir sandstone porosity generally declines with increasing thermal maturity (Fig. 2). However, the data appear to consist of two separate populations—a less thermally mature population represented by $R_o < 1.1\%$, and a more thermally mature population represented by $R_o > 1.1\%$. Correlation coefficients (r^2) of the least-squares regression lines, fit to each of the two data populations (Fig. 3), show a much stronger dependence of porosity on R_o for the less mature trend of nonreservoir sandstones (where $R_o < 1.1\%$, $r^2 = 0.40$) than for nonreservoir sandstones taken as a whole (Fig. 2, $r^2 = 0.15$). The better correlation of the less mature trend compared to that of the nonreservoir sandstone data set as a whole suggests that the two data populations might best be considered separately, with a preliminary boundary placed at about $R_o = 1.1\%$.

In both populations of points shown in Figure 3, porosity generally declines as a power function (Schmoker and Hester, 1990, equation 1) of in-

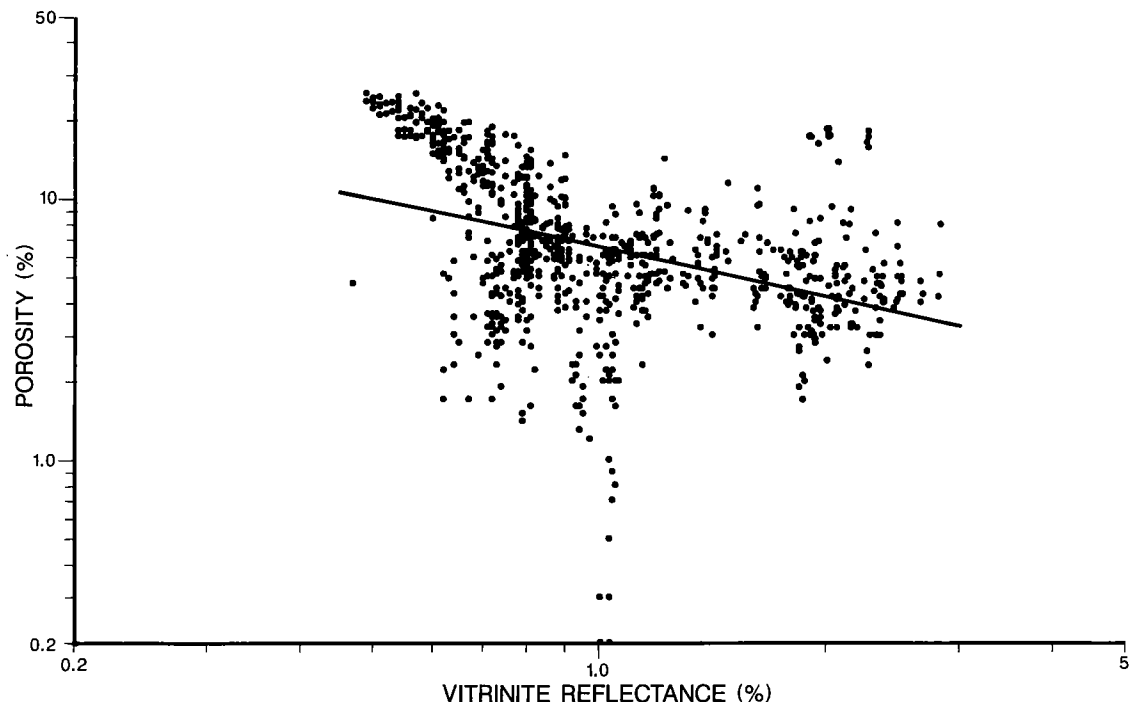


Figure 2. Porosity of Anadarko basin nonreservoir sandstones versus vitrinite reflectance (R_o) with least-squares regression line.

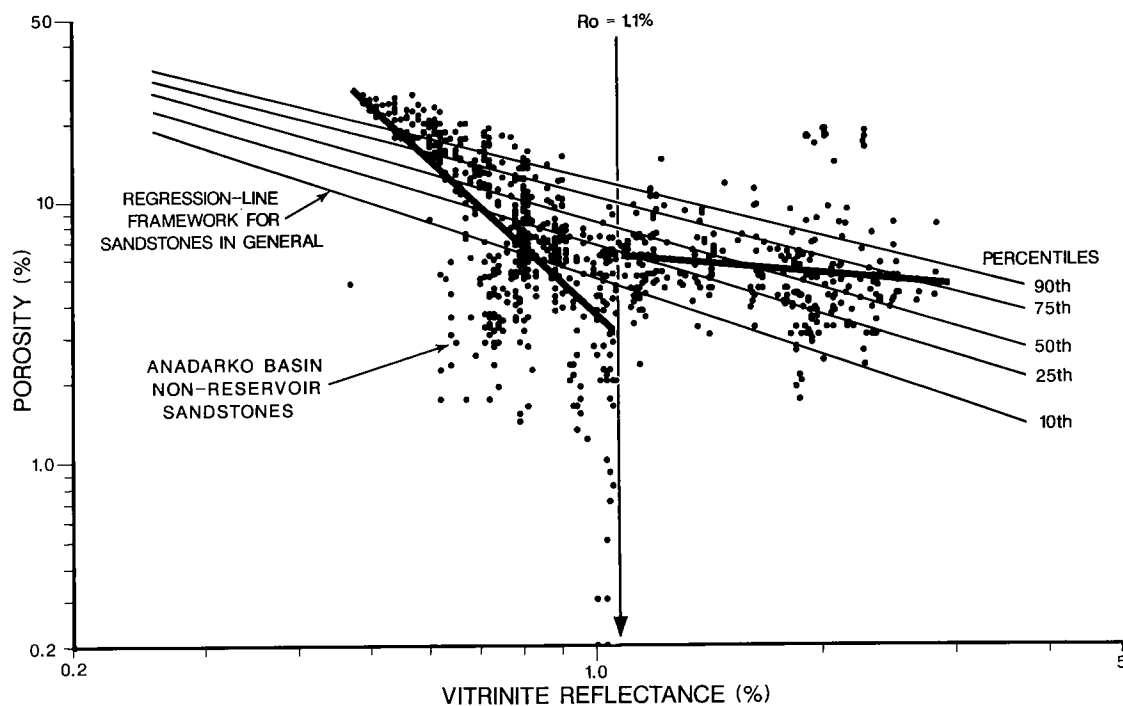


Figure 3. Porosity of Anadarko basin nonreservoir sandstones versus vitrinite reflectance (R_o) with least-squares regression lines (heavy lines) fit to each of two nonreservoir-sandstone data populations separated at $R_o = 1.1\%$. Also plotted are least-squares regression lines fit to 10th, 25th, 50th, 75th, and 90th porosity percentiles of the framework data set representing sandstones in general (Schmoker and Hester, 1990).

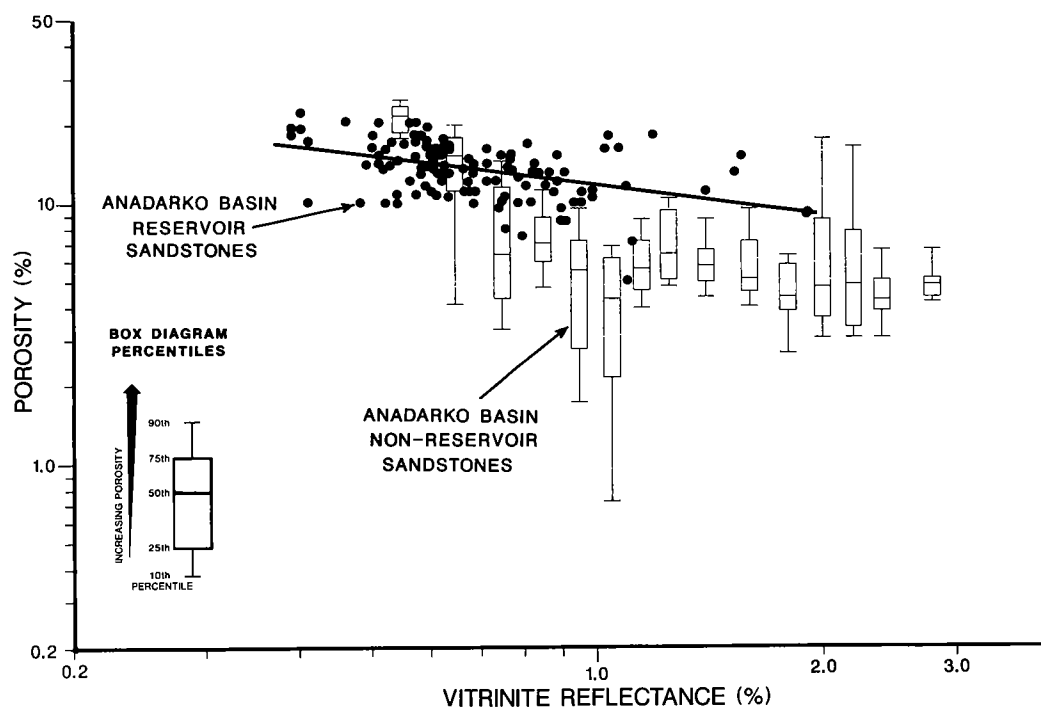


Figure 4. Porosity of Anadarko basin reservoir sandstones versus vitrinite reflectance (R_o) with least-squares regression line. Also plotted are box-diagram percentiles representing Anadarko basin nonreservoir sandstone data.

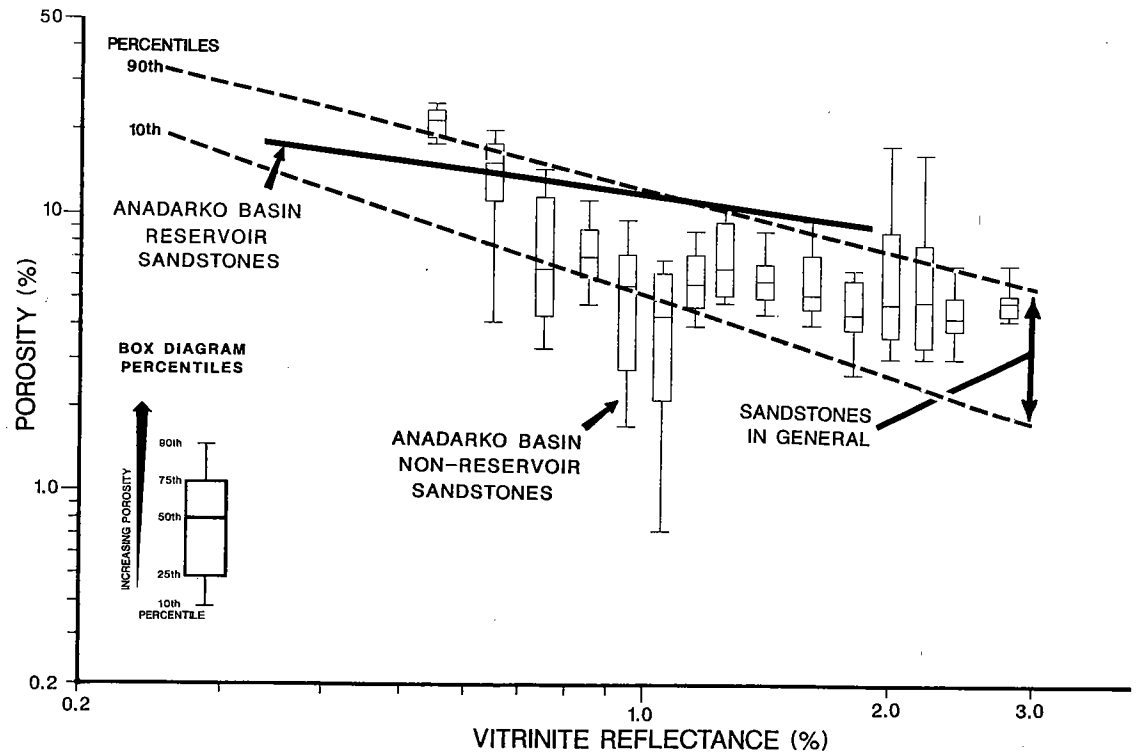


Figure 5. Summary diagram showing least-squares regression line for Anadarko basin reservoir sandstones, box-diagram percentiles for Anadarko basin nonreservoir sandstones, and porosity- R_o envelope bounded by least-squares regression lines fit to the 10th and 90th porosity percentiles of the framework data set representing sandstones in general (Schmoker and Hester, 1990).

creasing thermal maturity. The least-squares regression lines fit to the data for $R_o < 1.1\%$ show that the rate of porosity decrease with increasing R_o for nonreservoir sandstones is greater than that of the average trend of the porosity- R_o framework representing sandstones in general. For $R_o > 1.1\%$, the rate of porosity decrease with increasing R_o for Anadarko basin nonreservoir sandstones is lower than that of sandstones in general.

For this preliminary report, sufficient data to substantiate a probable cause for the change of slope of the porosity trend of Anadarko basin nonreservoir sandstones are not yet available. To speculate, the two populations of nonreservoir sandstone-porosity data (apparent in Figs. 2–5) may represent sandstones from different geographic areas, depositional environments, or subsurface pressure regimes, or sandstones with different burial or cementation histories. Identification and stratigraphic correlation of the nonreservoir sandstones, with the addition of petrographic information, are suggested here as a first approach to examining the nature of the two populations of Anadarko basin nonreservoir sandstones.

The porosity- R_o trend of Anadarko basin hydrocarbon-reservoir sandstones (Fig. 4) follows a dif-

ferent pattern. The least-squares regression line shows that the rate of porosity decrease with increasing R_o for reservoir sandstones is much lower than that of both nonreservoir sandstones with $R_o < 1.1\%$ (Fig. 4) of the central and southern Anadarko basin and sandstones in general (Fig. 5). This relatively low rate of porosity decline with increasing R_o could be due to geologic factors such as overpressuring or the inhibiting effects of early hydrocarbon emplacement on sandstone diagenesis, and/or to economic factors such as the bias inherent in the selection of sandstone hydrocarbon reservoirs.

As R_o increases from low levels to $\sim 1.1\%$, the porosity trends of Anadarko basin reservoir and nonreservoir sandstones cross (Fig. 4), effectively restricting the porosity of reservoir sandstones to increasingly higher percentiles of the porosity range of nonreservoir sandstones. These diverging trends predict that sandstone porosity sufficient for commercial hydrocarbon reservoirs becomes extremely rare at only moderate levels of thermal maturity. At about $R_o = 1.1\%$, however, the slope of the porosity trend for Anadarko basin nonreservoir sandstones levels off (Figs. 3–5). The average porosity of Anadarko basin reservoir sandstones

then remains within about the upper 10% of the porosity range of nonreservoir sandstones. As thermal maturity levels increase above ~1.1% R_o , the similar slopes of the porosity trends of Anadarko basin reservoir and nonreservoir sandstones suggest that sandstones of the central and southern Anadarko basin may retain sufficient porosity for economic accumulations of hydrocarbons, even at high thermal maturities.

REFERENCES CITED

- Berg, O. R.; Koinm, D. N.; and Richardson, D. E. (eds.), 1974, Oil and gas fields of Oklahoma: Oklahoma City Geological Society Reference Report, Supplement 1, 54 p.
- Cramer, R. D.; Gatlin, Leroy; and Wessman, H. G. (eds.), 1963, Oil and gas fields of Oklahoma: Oklahoma City Geological Society Reference Report, v. 1, 200 p.
- Harrison, W. E.; and Routh, D. L. (compilers), 1981, Reservoir and fluid characteristics of selected oil fields in Oklahoma: Oklahoma Geological Survey Special Publication 81-1, 317 p.
- Hester, T. C.; and Schmoker, J. W., 1990, Porosity trends of non-reservoir and reservoir sandstones, Anadarko basin, Oklahoma [abstract]: American Association of Petroleum Geologists Bulletin, v. 75, p. 594.
- Pipes, P. B. (ed.), 1980, Oil and gas fields of Oklahoma: Oklahoma City Geological Society Reference Report, Supplement 2, 30 p.
- Schmoker, J. W., 1986, Oil generation in the Anadarko basin, Oklahoma and Texas: modeling using Lopatin's method: Oklahoma Geological Survey Special Publication 86-3, 40 p.
- Schmoker, J. W.; and Hester, T. C., 1990, Regional trends of sandstone porosity versus vitrinite reflectance—a preliminary framework, *in* Nuccio, V. F.; and Barker, C. E. (eds.), Applications of thermal maturity studies to energy exploration: Rocky Mountain Section of the Society of Economic Paleontologists and Mineralogists, Denver, p. 53–60.

Midcontinent Fluvial-Dominated Deltaic Depositional Environments and Their Influence on Enhanced Oil Recovery¹

William I. Johnson and David K. Olsen

National Institute for Petroleum and Energy Research
Bartlesville, Oklahoma

Integrated geological and engineering analyses based on published and unpublished reports and theses were conducted to evaluate the feasibility of recovering heavy oil in the Midcontinent (Oklahoma, Kansas, and Missouri). Data on reservoir characterization of sandstone members of the Cherokee Group, (Desmoinesian Series, Middle Pennsylvanian) in the Cherokee and Forest City basins were collected from geological societies, geological surveys, state oil and gas boards, universities, U.S. Department of Energy, and other sources. Analyses of heavy- and light-oil reservoirs and successful and unsuccessful EOR projects were analyzed to determine their common characteristics.

Heavy- and light-oil reservoirs are present in reservoir rocks of the same age. For example, the Bartlesville sandstone (a fluvial-dominated deltaic deposit in the Cherokee Group) is commonly a reservoir rock for both heavy and light oil in the study area. The primary difference between heavy- and light-oil reservoirs is the gravity and viscosity of oil entrapped in the reservoir rock.

Cherokee Group sandstones in the Cherokee and Forest City basins were deposited in a fluvial-dominated deltaic environment. These sandstones are dominated by those laid down as channel fill-

ing, multi-storied, multiple-stacked, discontinuous, fining-upward, point-bar deposits in channels cut into underlying older Pennsylvanian and/or Mississippian rocks. Individual channels commonly were no more than ~1,300 ft wide at any given time. However, many Cherokee Group oil fields are much wider than 1,300 ft due to lateral migration and stacking of sand bodies as the stream meandered across the flood plain. The larger fields are made up of multiple sandstone bodies (correlated as the same sandstone) that were deposited as point-bars in active migrating channels.

Ultimate recovery of oil from reservoirs in Cherokee Group sandstones is affected by facies, small-scale sedimentary structures, bedding-boundary and intergranular small-scale permeability barriers, and diagenetic changes, commonly noted as heterogeneities, within the sandstone body. Lower sandstone facies probably contain the largest volume of oil economically recoverable by primary, waterflood, and/or enhanced oil-recovery production. Upper sandstone facies that are part of the oil reservoir will contribute small quantities of oil throughout the productive life of the reservoir, but production will be less cost-effective (Fig. 1).

The upper facies of these sandstones commonly contain oil entrapped in discontinuous depositional compartments. This compartmentalization is effected by both depositional features and diagenetic changes. Depositional compartmentalization refers to the presence of sandstone lenses smaller than the prevailing well spacing (10, 20, 40, or 80 acres). Depositional compartments may be one acre, or smaller. Bedding-boundary and intergranular small-scale permeability barriers are associated with depositional compartmentalization. Bedding-boundary permeability barriers are formed by early, partial to almost complete cementation of very fine-grained sediment deposited along boundaries of sand lenses. Small-scale intergranular permeability barriers may be formed by precipitation of diagenetic clays, or by deformation of clay or shale pebbles deposited with the

¹This report was prepared as an account of work sponsored by an agency of the United States Government. Neither the U.S. Government nor any agency thereof, nor any of their employees, makes any warranty, express or implied, or assumes any legal liability or responsibility for the accuracy, completeness, or usefulness of any information, apparatus, product, or process disclosed, or represents that its use would not infringe privately owned rights. Reference herein to any specific commercial product, process, or service by trade name, trademark, manufacturer, or otherwise, does not necessarily constitute or imply its endorsement, recommendation, or favoring by the U.S. Government or any agency thereof. The views and opinions of authors expressed herein do not necessarily state or reflect those of the U.S. Government or any agency thereof.

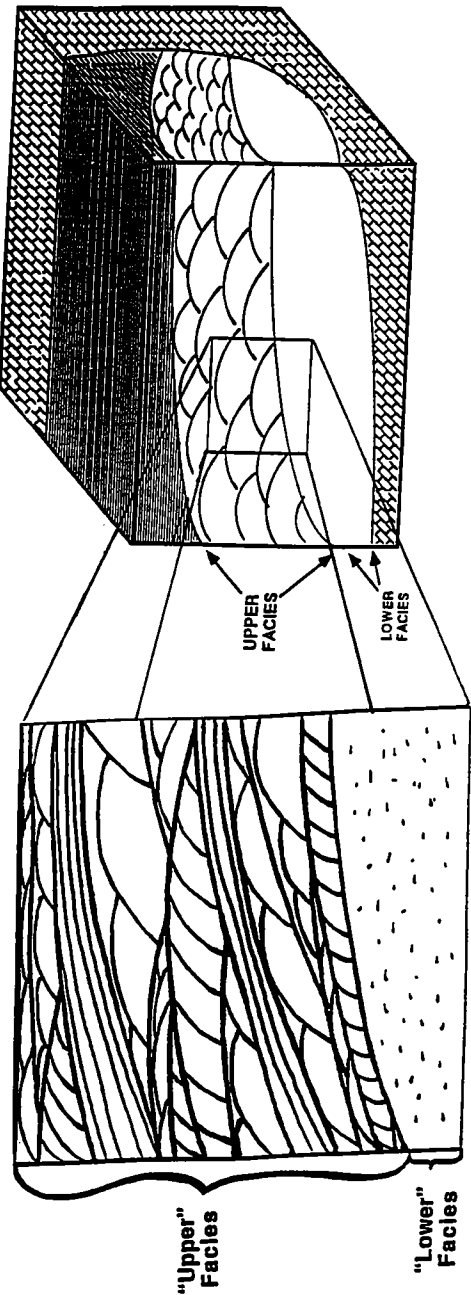


Figure 1. Block diagram of fluvial-dominated deltaic channel sand showing upper and lower facies. The upper is generally less continuous than the lower sandstone facies.

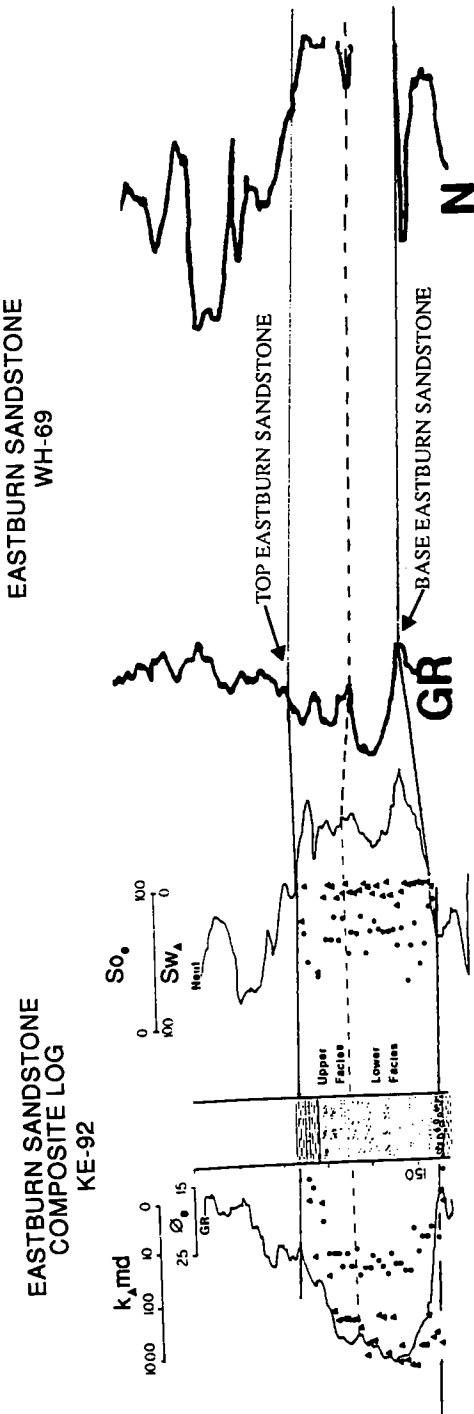


Figure 2. Correlation of a composite log of well KE-92 (GR-N Log-Lithology Log-Core Analysis) with gamma-ray and neutron well log of WH-69, Eastburn sandstone, Eastburn field, Vernon County, Missouri (no horizontal scale, correlation only).

sand grains (Fig. 1). Depositional compartmentalization and bedding-boundary and small-scale intergranular permeability barriers are commonly referred to as reservoir "heterogeneities."

Oil entrapped in reservoirs after waterflooding is often labeled "bypassed" or "unswept" oil, implying that all of this oil could be recovered with suitably designed polymer floods or some similar method for improved sweep efficiency. However, our analysis of reservoirs in the Midcontinent has shown that much of this oil is trapped in depositional compartments and would only be recoverable by infill-drilling programs. Other reservoir parameters and economic factors could be evaluated to determine if recovering such oil by infill drilling is economical or not.

Thin (a few inches to 3 ft thick), laminated, parallel-bedded sandstones are present in some upper facies deposits. If parallel-bedded sandstone has porosity, permeability, and oil saturation as good as those of lower facies deposits, oil may be swept by secondary and EOR processes from this zone. Parallel-bedded sandstone may also act as a "thief" zone (zone where fluids can flow faster) for waterflood or enhanced-waterflood operations, creating a direct path between wells. The direct path is created by the horizontally continuous permeability path between wells in parallel-bedded sandstone. In contrast, permeability paths are discontinuous between wells in depositionally compartmentalized sandstone. If permeability is continuous between wells, the sweep efficiency should be significantly higher. If permeability is discontinuous between wells, as with depositionally compartmentalized sandstone, overall sweep efficiency will be poor.

When infill wells are drilled late in the life of a Cherokee Group sandstone field, an operator may complete "good" oil-producing wells. These wells commonly decline within a few days to a few weeks and become stripper wells producing 0.5–2 b/d. These wells may be economical and pay out in months to years, depending on the rate of decline. If the "good" oil-producing well has been completed in an upper facies with depositional compartmentalization of oil in the reservoir, payout may be in a few months, years, or never. Vertical infill wells drilled for recovery of the "unswept" oil entrapped in depositional compartments may not be economical. Horizontal wells will encounter the same problems as those of vertical infill wells. Therefore, horizontal-well technology with present completion technology may not be the solution for recovering depositionally compartmentalized oil at this time. Well stimulation by hydraulic fracturing with a proppant will create vertical fractures, tending to be aligned perpendicular to the direction of least principal stress (approximately NE–SW in the Midcontinent) when implemented in reservoirs deeper than

~1,000 ft. These fractures, created by hydraulic fracturing, will contact a limited number of sandstone compartments (lenses) or the same compartment in which the well is located. This offers a temporary solution for increasing oil recovery, since fractured wells will have the same problems as those of vertical wells in compartmentalized facies.

The lower trough-bedded facies of Cherokee Group sandstones will have the best oil recovery. Trough-bedded sandstone is generally fine- to medium-grained quartz sandstone with less depositional compartmentalization than the upper facies. The lower facies sandstones are more continuous and less "heterogeneous" than the upper facies sandstones. When waterflooding and enhanced waterflooding are implemented in this facies, oil will be swept between wells from injector to producer. This facies is preferentially swept by injected fluids because the more continuous lower facies has a more continuously favorable porosity and permeability resulting in better sweep efficiency. A direct flow path in the direction of sediment transport sometimes develops in lower-facies reservoir rocks that are unevenly distributed across the reservoir. This may be recognized by early breakthrough of injected fluids in lower facies or in thin, parallel-bedded upper facies. Lower-facies reservoir rock may have porosity, permeability, and oil saturation equal to, or greater than, that of the upper facies. Oil from an upper facies will be produced by imbibition during secondary and enhanced waterflooding. Wells producing small quantities (0.5–2 b/d) of oil after 40–50 years of waterflooding are probably producing oil by imbibition from an upper facies into other facies.

Horizontal wells drilled as oil producers early in the life of a Cherokee Group sandstone field probably would have drained the reservoir more rapidly. However, horizontal wells will currently benefit the region less because Midcontinent sedimentary basins are in a late-maturity stage of oil exploration and development. Horizontal-well technology may be feasible in thick, trough-bedded, lower-facies reservoir rock as injectors for secondary and enhanced waterflooding, but most of the lower facies in developed fields have already been swept by decades of air and water injection.

Rocks of the Midcontinent are naturally fractured. The primary set trends northeast–southwest; a secondary set of fractures is more or less perpendicular to the principal direction. Natural fracturing in an oil reservoir may cause problems of direct linedrive between wells when secondary or enhanced waterflooding is implemented. Recognition of the probability of fracturing in the subsurface is possible through the identification of surface fractures by aerial photography over the oil-producing area. Although structural compartmentalization caused by faulting does not appear

to be causing problems in Midcontinent oil reservoirs, horizontal-well technology (presently developed), with wells drilled perpendicular to the direction of natural fracturing, and advanced well-stimulation technology (for future development) may make it possible to contact multiple depositional compartments with one well.

Identification of upper and lower facies of Cherokee Group sandstones on electric logs is often possible. If cores are available for comparison of geology and petrophysical characteristics with electric-log characteristics, identification of upper and lower facies on electric logs in wells that have not been cored is possible (Fig. 2). Many old oil fields have changed owners throughout their life. Cores, if any, and logs and drillers' records may have been lost or misplaced when they should have been passed along to new owners. Prior to implementation of an EOR process, an operator should seriously consider drilling a few new wells scattered throughout the producing area. Core analysis of petrophysical and sedimentologic properties will help to identify depositional compartmentalization in the reservoir, swept and unswept zones, and will facilitate the design of an EOR project with injection patterns to fit previous and new data.

This study illustrates why economic-feasibility analysis and engineering design of waterfloods and/or EOR projects should incorporate geological, chemical, and petrophysical information obtained during reservoir development and primary production. In calculating the remaining recoverable reserves in an oil reservoir where waterflood and EOR processes are to be applied, the geological facies to be swept should be characterized and the geological data should be integrated with production and reservoir information mentioned above. Results of the study show that depositional facies of fluvial-dominated, deltaic channel-fill-sandstone reservoirs should be identified prior to design and implementation of EOR processes.

SELECTED REFERENCES

- Ben-Saleh, F. F., 1970, Stratigraphic analysis of Pennsylvanian rocks in southeastern Anadarko basin, Oklahoma: University of Tulsa unpublished M.S. thesis, 76 p.
- Berg, O. R., 1963, The depositional environment of a portion of the Bluejacket Sandstone: University of Tulsa unpublished M.S. thesis, 87 p.
- Berry, C. G., 1963, Stratigraphy of the Cherokee Group, eastern Osage County, Oklahoma: University of Tulsa unpublished M.S. thesis, 84 p.
- Bradshaw, D. T., 1985, Geologic variables influencing production in the Eastburn field, Vernon County, Missouri: Colorado State University unpublished M.S. thesis.
- Brenner, R. L., 1989, Stratigraphy, petrology, and paleogeography of the upper portion of the Cherokee Group (Middle Pennsylvanian), eastern Kansas and northeastern Oklahoma: Kansas Geological Survey Geology Series 3.
- Carlson, M. C., 1988, A petrologic analysis of surface and subsurface Atoka Formation (Lower Pennsylvanian) sandstone, western margin of the Arkoma basin, Oklahoma: University of Tulsa unpublished M.S. thesis, 238 p.
- Chiou, R. C. S.; and Murer, T. S., 1989, Cyclic steam pilot in gravity drainage reservoir, Mobil Producing U.S. Inc., in *Proceedings of the Society of Petroleum Engineers annual technical conference and exhibition, EOR/ General Petroleum Engineering*, October 8–11, San Antonio, Texas: Society of Petroleum Engineers Paper 19659, p. 319–332.
- Chu, Chieh, 1990, Prediction of steamflood performance in heavy oil reservoirs using correlations developed by factorial design method, in *Proceedings of the 60th California regional meeting and exhibition*, April 4–6, Ventura, California: Society of Petroleum Engineers Paper 20020, p. 67–78.
- Cruz, J. A., 1963, Geometry and origin of the Burbank Sandstone and Mississippian "Chat" in T. 25 N., R. 6 E., and T. 26 N., R. 6 E., Osage County, Oklahoma: University of Tulsa unpublished M.S. thesis, 43 p.
- Curiale, J. A., 1983, Petroleum occurrences and source-rock potential of the Ouachita Mountains, southeastern Oklahoma: Oklahoma Geological Survey Bulletin 135, 65 p.
- Davis, L. V., 1953, Oil possibilities near Idabel, McCurtain County, Oklahoma: Oklahoma Geological Survey Mineral Report 23, 26 p.
- Deason, K. L.; and Bohm, Rex, 1969, Studies of the oil and gas fields of Caldwell, Clay, Clinton, and Ray Counties, Missouri: Oil and Gas in Missouri General Information Sheet 19.
- Ebanks, W. J., Jr.; James, G. W.; and Livingston, N. D., 1977, Evaluation of heavy oil and tar sands in Bourbon, Crawford, and Cherokee Counties, Kansas—final report: U.S. Department of Energy, Contract E-76-S-02-2997, BERC/RI-77/20.
- Emery, L. W., 1962, Results from a multi-well thermal-recovery test in southeastern Kansas: *Journal of Petroleum Technology*, v. 14, no. 6, p. 671–678.
- French, M. S.; and Howard, R. L., 1967, The steamflood job: Hefner Sho-Vel-Tum, Shell Oil Company: *Oil and Gas Journal*, v. 65, no. 29, p. 64–66.
- Fronjosa, Ernesto, 1965, A study of Oklahoma water flood statistics: University of Oklahoma unpublished M.G.E. thesis, 87 p.
- Goebel, E. D., 1966, Thermal recovery projects are increasing in Kansas, Missouri: *World Oil*, v. 162, no. 4, p. 78–80.
- Green, K. B., 1967, The fireflood: Cox Penn sand, Mobil Oil Corp.: *Oil and Gas Journal*, v. 14, no. 6, p. 66–69.
- Hagen, K. B., 1972, Mapping of surface joints on air photos can help understand waterflood performance problems at North Burbank unit, Osage and Kay Counties, Oklahoma: University of Tulsa unpublished M.S. thesis, 85 p.
- Harris, J. W., 1984, Stratigraphy and depositional environments of the Krebs Formation—lower Cherokee Group (Middle Pennsylvanian) in southeastern Kansas: University of Kansas unpublished M.S.

- thesis.
- Harrison, W. E., 1982, Tar sand resource appraisal in south-central Oklahoma: Kentucky Geological Survey, National Tar Sands (Heavy Oil) Symposium, Lexington, Kentucky, June 10–11, p. 110–128.
- Harrison, W. E.; and Roberts, J. F., 1979, Evaluation of heavy oil potential of northeastern Craig and northwestern Ottawa Counties, Oklahoma: U.S. Department of Energy, Contract ET-76-S-03-1812, BETC/1812-1.
- Harrison, W. E.; and Routh, D. L., 1981, Reservoir and fluid characteristics of selected oil fields in Oklahoma: Oklahoma Geological Survey Special Publication 81-1, 317 p.
- Hawisa, Ibrahim, Sr., 1965, Depositional environment of the Bartlesville, the Red Fork, and the lower Skinner sandstones in portions of Lincoln, Logan, and Payne Counties, Oklahoma: University of Tulsa unpublished M.S. thesis, 44 p.
- Hough, R. M., 1978, Depositional framework of the lower Red Fork eastern flank of the Anadarko basin, Oklahoma: University of Tulsa unpublished M.S. thesis, 63 p.
- Hudson, A. S., 1969, Depositional environment of the Red Fork and equivalent sandstones east of the Nemaha Ridge, Kansas and Oklahoma: University of Tulsa unpublished M.S. thesis, 80 p.
- Interstate Oil Compact Commission, 1984, Major tar sands and heavy oil deposits of the United States: Interstate Oil Compact Commission, Oklahoma City, 272 p.
- Jordan, Louise, 1964, Petroleum-impregnated rocks and asphaltite deposits of Oklahoma: Oklahoma Geological Survey Map GM-8, scale 1:750,000.
- Lardner, J. E., 1984, Petrology, depositional environment and diagenesis of Middle Pennsylvanian (Desmoinesian) 'Lagonda Interval' Cherokee Group in east-central Kansas: University of Iowa unpublished M.S. thesis.
- Netzler, B. W., 1990, Heavy-oil resources potential of southwest Missouri: Missouri Department of Natural Resources, Division of Geology and Land Survey, Open File Report 90-80-OG.
- Newell, D. K.; Watrney, W. L.; Cheng, S. W. L.; and Brownrigg, R. L., 1987, Stratigraphic and spatial distribution of oil and gas production in Kansas: Kansas Geological Survey Subsurface Geology Series 9.
- Ockerman, J. W., 1932, Asphalt rocks in eastern Kansas: State Geological Survey of Kansas Open File Report OF 32-1, 8 p.
- Orajaka, I. P., 1978, Lower Pennsylvanian transgressive onlap northeastern flank Arkoma basin: University of Tulsa unpublished M.S. thesis, 67 p.
- O'Reilly, K. L., 1986, Diagenesis and depositional environments of the Red Fork sandstone (Desmoinesian) in the Wakita trend, Grant County, Oklahoma: University of Tulsa unpublished M.S. thesis, 154 p.
- Phares, R. S., 1969, Depositional framework of the Bartlesville Sandstone in northeastern Oklahoma: University of Tulsa unpublished M.S. thesis, 59 p.
- Porter, E. S., 1911, The coal and asphalt of Oklahoma: University of Oklahoma unpublished B.A. thesis, 29 p.
- Saitta Bertoni, Sandro, 1968, Bluejacket Formation—a subsurface study in northeastern Oklahoma: University of Tulsa unpublished M.S. thesis, 142 p.
- Scruton, P. C., 1949, The petrography and environment of deposition of the Warner, Little Cabin, and Hartshorne sandstones of northeastern Oklahoma: University of Tulsa unpublished M.S. thesis, 77 p.
- Shulman, Chaim, 1965, Stratigraphic analysis of the Cherokee Group in adjacent portions of Lincoln, Logan, and Oklahoma Counties, Oklahoma: University of Tulsa unpublished M.S. thesis, 30 p.
- Simpson, H. M., 1969, Palynology and the vertical sedimentary profile of Missourian strata, Tulsa County, Oklahoma: University of Tulsa unpublished M.S. thesis, 64 p.
- Sperry, J. S., 1981, Heavy-oil recovery system completes three field test in Mid-Continent region: Oil and Gas Journal, v. 79, no. 30, p. 225–237.
- Sperry, J. S.; Young, F. S. Jr.; and Poston, R. S., 1980, Development and field testing of a process for recovering heavy crude oil in the Carlyle pool, Allen County, Kansas, using the Vapor Therm Generator—final report: U.S. Department of Energy, Contract EY-76-C-02-2880, DOE/BETC-2880-1.
- Staton, M. D., 1987, Stratigraphy and depositional environments of the Cherokee Group (Middle Pennsylvanian), Central Cherokee basin, southeastern Kansas: University of Kansas unpublished M.S. thesis.
- Tight, D. C., 1983, The Bartlesville sandstone: a detailed subsurface stratigraphic study in the North Avant field, eastern Osage County, Oklahoma: University of Tulsa unpublished M.S. thesis, 120 p.
- Trantham, J. C.; and Marx, J. W., 1966, Bellamy field tests: oil from tar by counterflow underground burning: Journal of Petroleum Technology, v. 18, no. 1, p. 109–115.
- Valleroy, V. V.; Willman, B. T.; Campbell, J. B.; and Powers, L. W., 1967, Deerfield pilot test of recovery by steam drive: Journal of Petroleum Technology, v. 19, no. 7, p. 956–964.
- Vanbuskirk, J. R., 1960, Investigation of reservoir conditions of lower Deese sandstones (Pennsylvanian) for a flood project in the North Alma pool, Stephens County, Oklahoma: University of Oklahoma unpublished M.G.E. thesis, 165 p.
- Walton, A. W.; Bouquet, D. J.; Evenson, R. A.; Rofheart D. H.; and Woody, M. D., 1986, Characterization of sandstone reservoirs in the Cherokee Group (Pennsylvanian, Desmoinesian) of southeastern Kansas, Department of Geology and Tertiary Oil Recovery Project, University of Kansas, in Lake, L. W.; and Carroll, H. B., Jr. (eds.), Reservoir characterization: Academic Press, Orlando, Florida, p. 39–62.
- Weber, J. L., 1990, Comparative study of crude-oil compositions in the frontal and central Ouachita Mountains, in Suneson, N. H.; Campbell, J. A.; and Tilford, M. G. (eds.), Geology and resources of the frontal belt of the western Ouachita Mountains, Oklahoma: Oklahoma Geological Survey Special Publication 90-1, p. 101–117.
- Wells, J. S., 1979, Inventory of heavy oil in western Missouri—final report: Missouri Department of Natural Resources, Division of Geology and Land Survey, prepared for the U.S. Department of Energy,

- Contract ET-76-S-03-1808, BETC-1808-1.
- Wells, J. S.; and Anderson, K. H., 1968, Heavy oil in western Missouri: American Association of Petroleum Geologists Bulletin, v. 52, p. 1720-1731.
- Willhite, G. P., 1986, Waterflooding: Society of Petroleum Engineers Textbook Series, v. 3, Richardson, Texas, p. 243-251.
- Williams, D. B., 1983, Structural and geochemical study of the south Sulphur asphalt deposits, Murray County, Oklahoma: University of Oklahoma unpublished M.S. thesis, 163 p.
- Woody, M. D., 1984, Sedimentology, diagenesis, and petrophysics of selected Cherokee Group (Desmoinesian) sandstones in southeastern Kansas: University of Kansas unpublished M.S. thesis.
- Worthington, R. E., 1982, Petrology of Middle Pennsylvanian (Desmoinesian) "Upper Bluejacket" sandstone (Cherokee Group) of Bourbon, Crawford, and Cherokee Counties, Kansas: University of Iowa unpublished M.S. thesis.

Application of a Transpressive Tectonic Model to Fractured Hunton and Sycamore Development, Eola Field, Garvin County, Southern Oklahoma

Jerome J. Kendall

Mobil Oil Exploration and Producing, U.S.
Oklahoma City, Oklahoma

ABSTRACT.—A transpressive tectonic model has been applied to shallower pool development of the Eola field. The transpressive model accounts for structural incongruity of a large normal fault at the core of a zone of intense shortening and for stratigraphic mismatches across the fault. A younger east-directed low-angle thrust cuts off the top of the structure and further defines the limits of the reservoirs.

INTRODUCTION

The Eola field is the down-plunge extension of the Arbuckle Mountain front. It was initially developed in the 1950s as an Ordovician Simpson-sand field producing 200 million bbl of oil and 210 Bcf of gas from depths of 11,000–15,000 ft. The mechanism forming the Eola field has been variously described in the literature as compressional thin-skinned overthrusts (Swesnik and Green, 1950), extensional normal faults (Harlton, 1964), and a massive gravity slide (Phillips, 1983). The concept of transpression, simultaneous translation and compression along a fault system, has been applied to generate a predictive model of reservoir distribution and geometry. This model has guided the strategy for developing the shallower fractured Mississippian Sycamore Limestone and the Devonian Hunton limestones at depths of 6,000–8,000 ft.

STRATIGRAPHIC MISMATCHES

The stratigraphic changes in the Hunton, Sylvan, and Sycamore strata across the Eola fault suggest that juxtaposed rocks were originally much farther apart than they are now. The Hunton Group is 250 ft thick north of the fault, whereas immediately south of the fault, only the bottom 45 ft of the Hunton is present. The north-south cross section in Figure 1 shows the dramatic thinning of the Hunton across the Eola fault. The Sylvan Shale has the same thickness across the fault, but the lower 100 ft is carbonate-rich south of the fault. Sycamore strata are also the same thickness on both sides of the fault, but the 60-ft-thick lime-

stone beds are present only south of the fault. A relatively simple two-dimensional palinspastic restoration of cross section A-A' (Fig. 1) cannot account for these abrupt stratigraphic changes.

STRUCTURE

Structural Incongruity

The structure at Eola field is that of an overturned syncline/anticline pair, with the main Eola fault cutting through the crest of the anticline (Fig. 1). The folding was caused by a major component of compression across the fault system. The problem is that there is 300–500 ft of apparent normal offset on the Eola fault, and a large extensional normal fault is not compatible with the compression inferred from the folding. A simultaneous lateral component of motion along the Eola fault would resolve this incongruity. The apparent offset along a transpressive fault is not kinematically significant. It is a function of where, along the fault, the apparent offset is measured. There is no direct measure of the amount of lateral movement on the fault. A minimum of 1–3 mi lateral movement is indicated by the lack of a stratigraphic match in the area of the field. The structural style indicates that the ratio of compressional shortening to lateral translation is approximately 1:1.

Late Low-Angle Thrusting

After the transpressive event, a low-angle thrust fault cut off the top of the overturned anticline and the Eola fault, carrying them 500–1,000 ft to the

Kendall, J. J., 1993, Application of a transpressive tectonic model to fractured Hunton and Sycamore development, Eola field, Garvin County, southern Oklahoma, in Johnson, K. S.; and Campbell, J. A. (eds.), *Petroleum-reservoir geology in the southern Midcontinent, 1991 symposium*: Oklahoma Geological Survey Circular 95, p. 236–239.

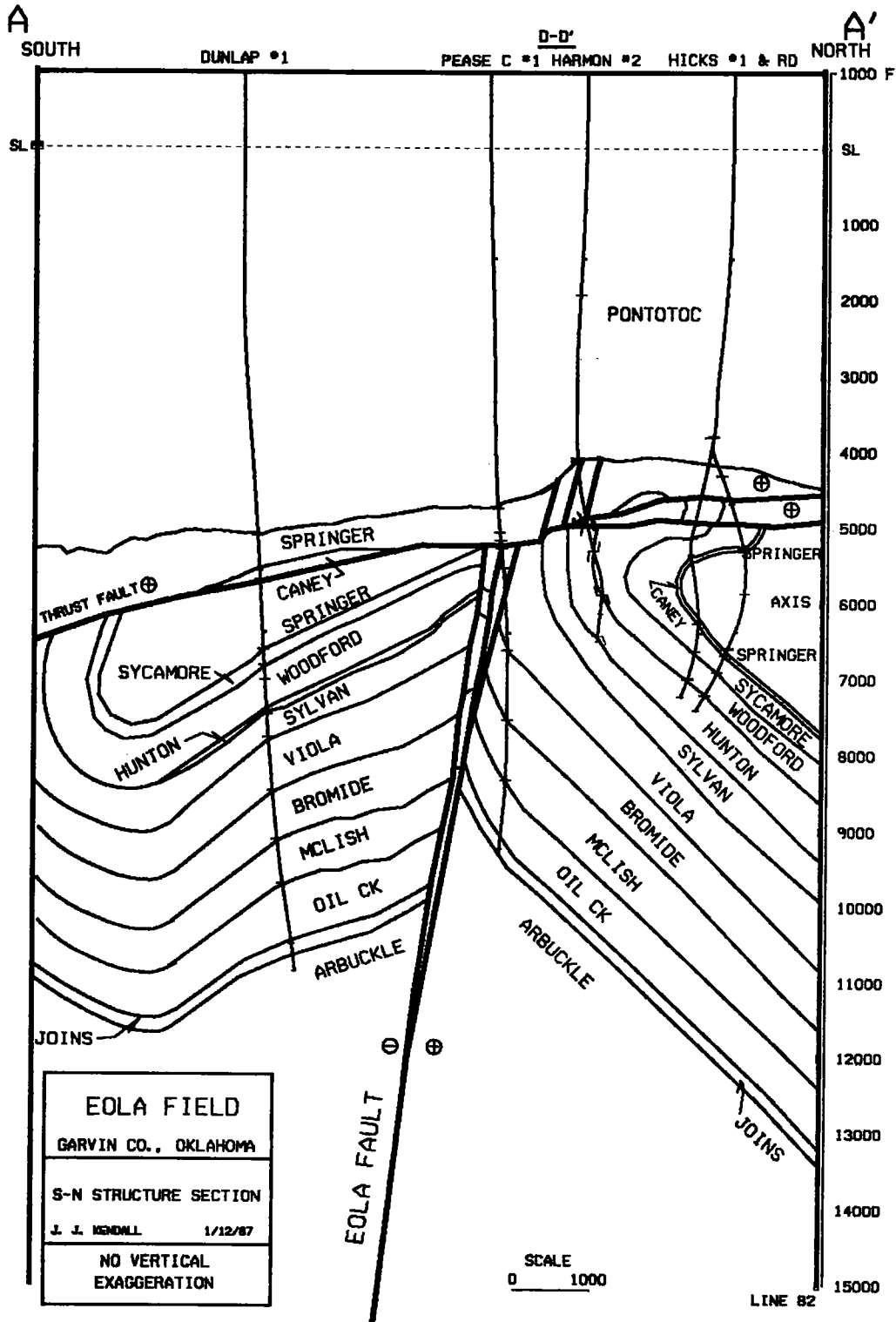


Figure 1. Cross section A-A' (south to north) across the Eola field showing the faulted and overturned syncline/anticline pair. + indicates movement toward the viewer; - indicates movement away from the viewer. The low-angle thrust fault offsets the crest of the anticline and the Eola fault. The area below the thrust fault and north of the Eola fault moved away from the viewer (left-lateral movement). The Hunton is much thinner south of the Eola fault. Location of cross section is shown in Figure 2.

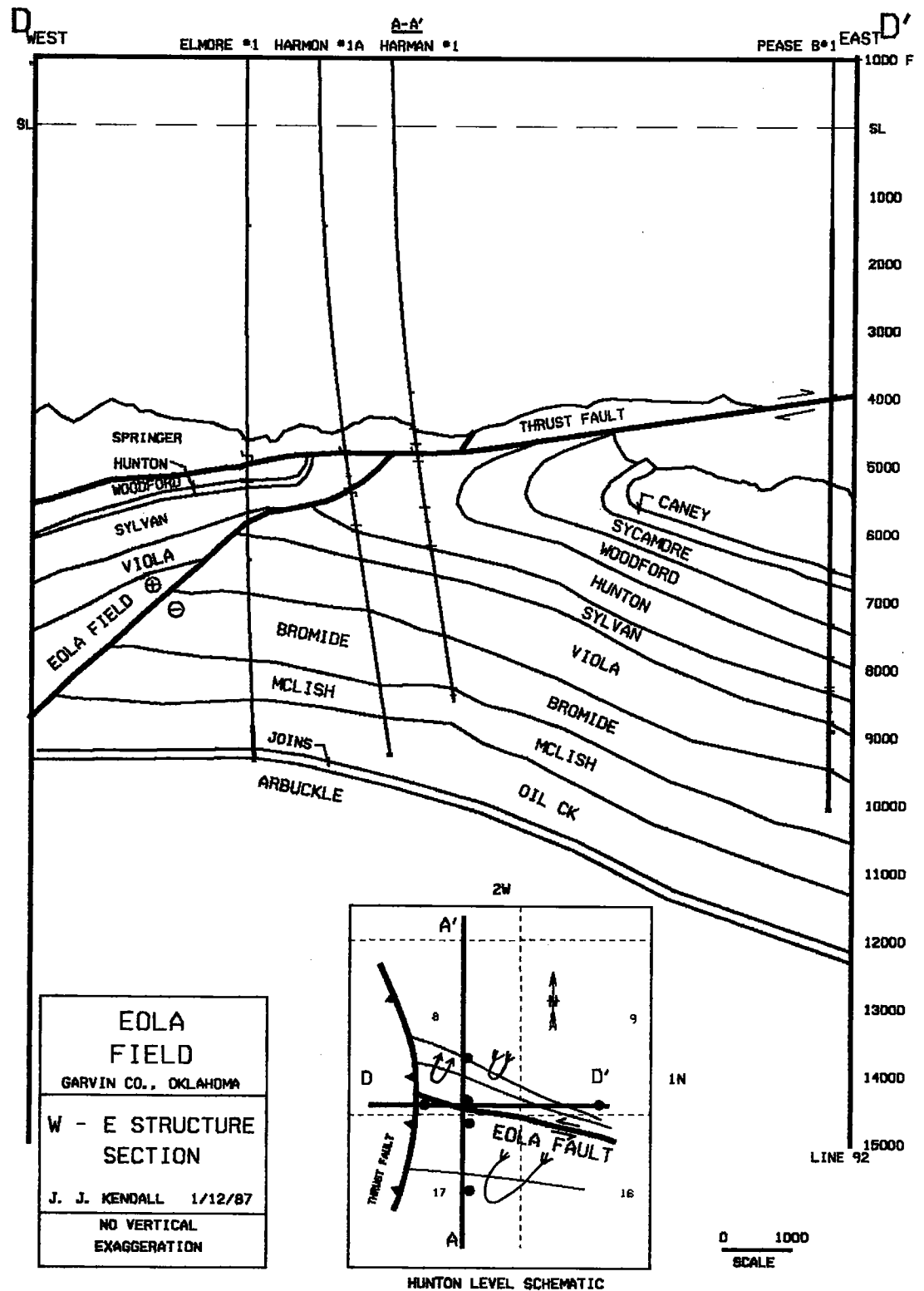


Figure 2. Cross section D-D' from (east to west). The inset is a schematic Hunton-level map showing the trends of overturned fold axes and faults. Line of section is at a small angle to the trend of the Eola fault. The thrust fault offsets the Eola fault.

east. Figure 1 shows this offset. Cross section D-D' (Fig. 2) is perpendicular to this thrust fault. The inset map in Figure 2 shows the relative orientation of the lines of section and major structural features. This thrust defines the upper limit of Sycamore and Hunton reservoir development. Reservoirs in the hanging wall, though enhanced by fractures, are unattractive primary objectives because they are isolated from the main body of the reservoir and have limited reserves.

CONCLUSIONS

The stratigraphic mismatches and structural inconsistency of an apparent normal fault in the core of a zone of extreme shortening is best explained by incorporating a lateral component of fault motion. There is a minimum of 1–3 mi of lateral offset, with regional considerations indicating

that movement was probably left-lateral. According to the transpression model, the target for exploration and development is north of the Eola fault and below the younger thrust faults.

REFERENCES CITED

- Harlton, B. H., 1964, Tectonic framework of Eola and Hoover oil fields and West Timbered Hills areas, Garvin and Murray Counties, Oklahoma: *American Association of Petroleum Geologists Bulletin*, v. 48, p. 1555–1567.
- Phillips, E. H., 1983, Gravity slide thrusting and folded faults in western Arbuckle Mountains and vicinity, southern Oklahoma: *American Association of Petroleum Geologists Bulletin*, v. 67, p. 1363–1390.
- Swesnik, R. M.; and Green, T. H., 1950, Geology of Eola area, Garvin County, Oklahoma: *American Association of Petroleum Geologists Bulletin*, v. 34, p. 2176–2199.

Lithology and Reservoir Development of the Arbuckle Dolomite, Wilburton Field, Latimer County, Oklahoma

Paul K. Mescher and Douglas J. Schultz

ARCO Oil and Gas Co., Plano, Texas

Steven J. Hendrick, Mark A. Ward,
and Jeffrey A. Schwarz

ARCO Oil and Gas Co., Midland, Texas

ABSTRACT.—ARCO's 1987 discovery of gas-prone Cambrian–Ordovician Arbuckle dolomite in Wilburton field resulted in development of extensive dry gas reserves, currently estimated at 500 Bcf from 15 producing wells. Approximately 180 Bcf has been produced through February 1991. The Arbuckle produces from a major southwest-dipping horst block, bounded by high angle normal faults. The faults create as much as 1,800 ft of vertical offset, and commonly result in Silurian–Devonian sediments (Hunton/Woodford) juxtaposed against the Arbuckle. Shallower, thrust Pennsylvanian Cromwell, Spiro, and Wapanucka strata overlie the major horst block.

Cores from three ARCO production wells and two exploratory tests reveal Arbuckle sediments formed in a peritidal complex, as shown by algal mats, stromatolites, tidal laminites, rip-up clasts, bioturbated intervals, and bioclastic/ooid grainstone beds. Dolomitization is pervasive, and cross-cuts all depositional facies. The upper 220–250 ft of the reservoir (West Spring Creek Formation) contains mostly intact host rock with intercrystalline (matrix) porosities ranging from 4 to 18%, and permeabilities as much as 936 md. Gamma ray log markers correlate consistently across this interval.

A major intraformational unconformity exists within the West Spring Creek Formation below this upper zone. An unconformable contact between the West Spring Creek and the top of the Kindblade Formation is inferred from conodont data. Cores from the West Spring Creek below the intraformational unconformity reveal numerous karsted intervals containing cave-fill sediments and abundant crackle, mosaic, and chaotic collapse breccias. Cave-fill zones contain autochthonous detrital cherts, dolomite clasts, quartz grains, and other terrigenous material. These zones commonly have irregular gamma ray “spikes” that correlate only locally. Chaotic breccias consist of angular breccias that commonly have well-developed fracture networks, and appear to have originated as breakdown breccias from cave ceilings and chamber walls. The extensive nature of cave fill and brecciated intervals suggests multiple periods of subaerial exposure in the Wilburton area, followed by resumption of Arbuckle deposition.

Pennsylvanian (Ouachita) tectonism reactivated and/or created additional faulting and fracturing, serving to break up relict karst and stratigraphic zonations, as demonstrated by excellent pressure and production communication among the wells in the field.

INTRODUCTION

Wilburton is a large multizone dry gas field in Latimer County, Oklahoma. Prior to 1987, Lower Pennsylvanian Spiro sands (Atokan), Cromwell sandstone, and Wapanucka Limestone (Morrowan) were the main producing intervals in the field. Silurian Hunton carbonate and Ordovician McLish sandstone may also prove to be productive. The Arbuckle portion of the field produces from a major horst block below thrust-faulted Pennsylvanian rocks (Fig. 1). The Arbuckle portion of the reservoir has produced >180 Bcf from 15 wells

through February 1991. Field rates peaked at 250 MMcf/d in December 1990.

STRUCTURAL SETTING

The Arbuckle portion of Wilburton field is a high-angle, fault-bounded horst feature that depends on tight shales, sandstones, and dolomites juxtaposed across these bounding faults for lateral seals (Figs. 1,2). Vertical trapping is formed by the overlying Woodford and Caney Shales, and by the truncation of high-angle, basement-seated faults by thrust faults in the lower Atokan and Morrowan

Mescher, P. K.; Schultz, D. J.; Hendrick, S. J.; Ward, M. A.; and Schwarz, J. A., 1993, Lithology and reservoir development of the Arbuckle dolomite, Wilburton field, Latimer County, Oklahoma, in Johnson, K. S.; and Campbell, J. A. (eds.), *Petroleum-reservoir geology in the southern Midcontinent*, 1991 symposium: Oklahoma Geological Survey Circular 95, p. 240–245.

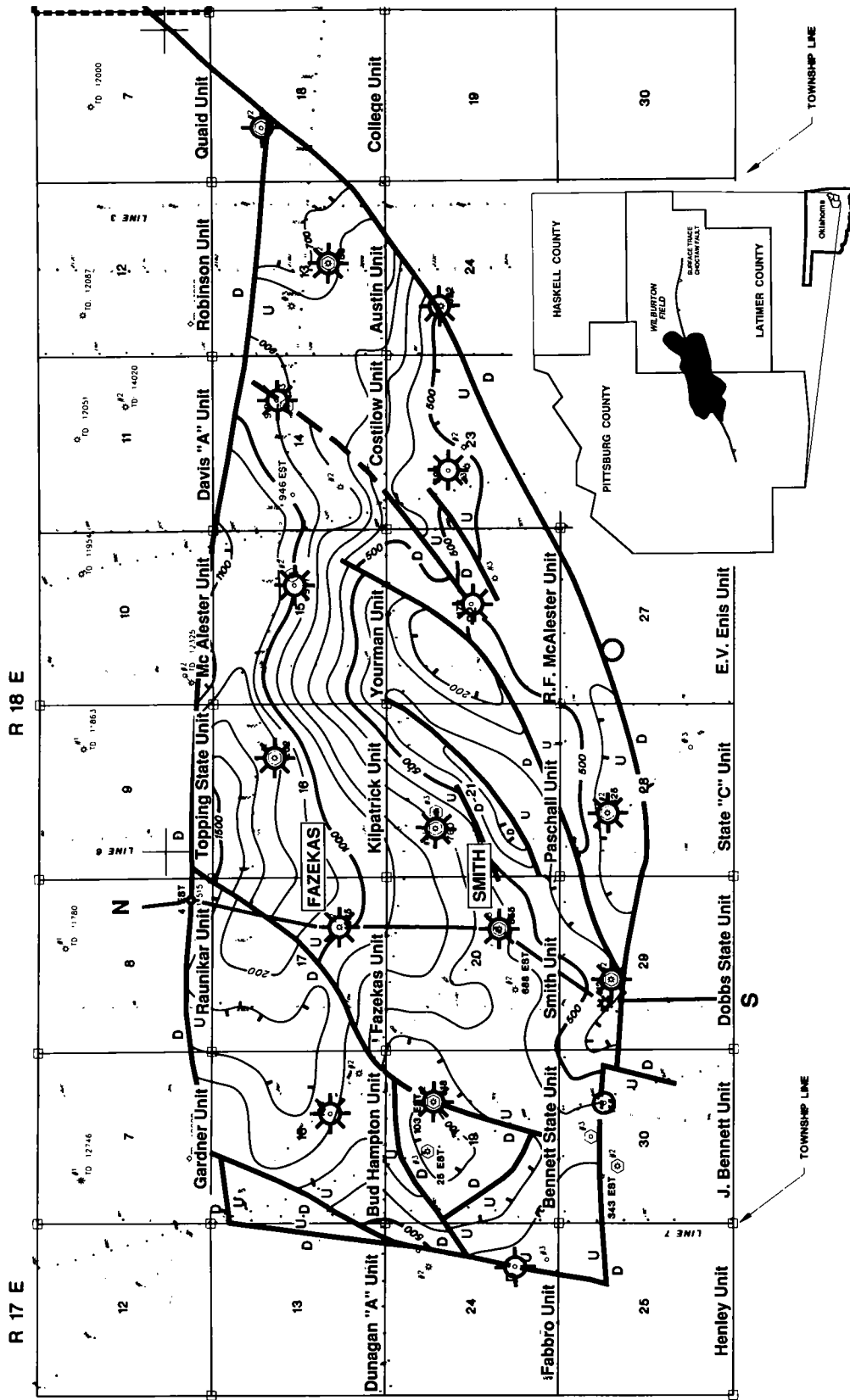


Figure 1. Location map and geologic structure of the deep Wilburton gas field horst block, Arkoma basin, Oklahoma. Structural contours on top of the Arbuckle Group. Contour interval = 100 ft.

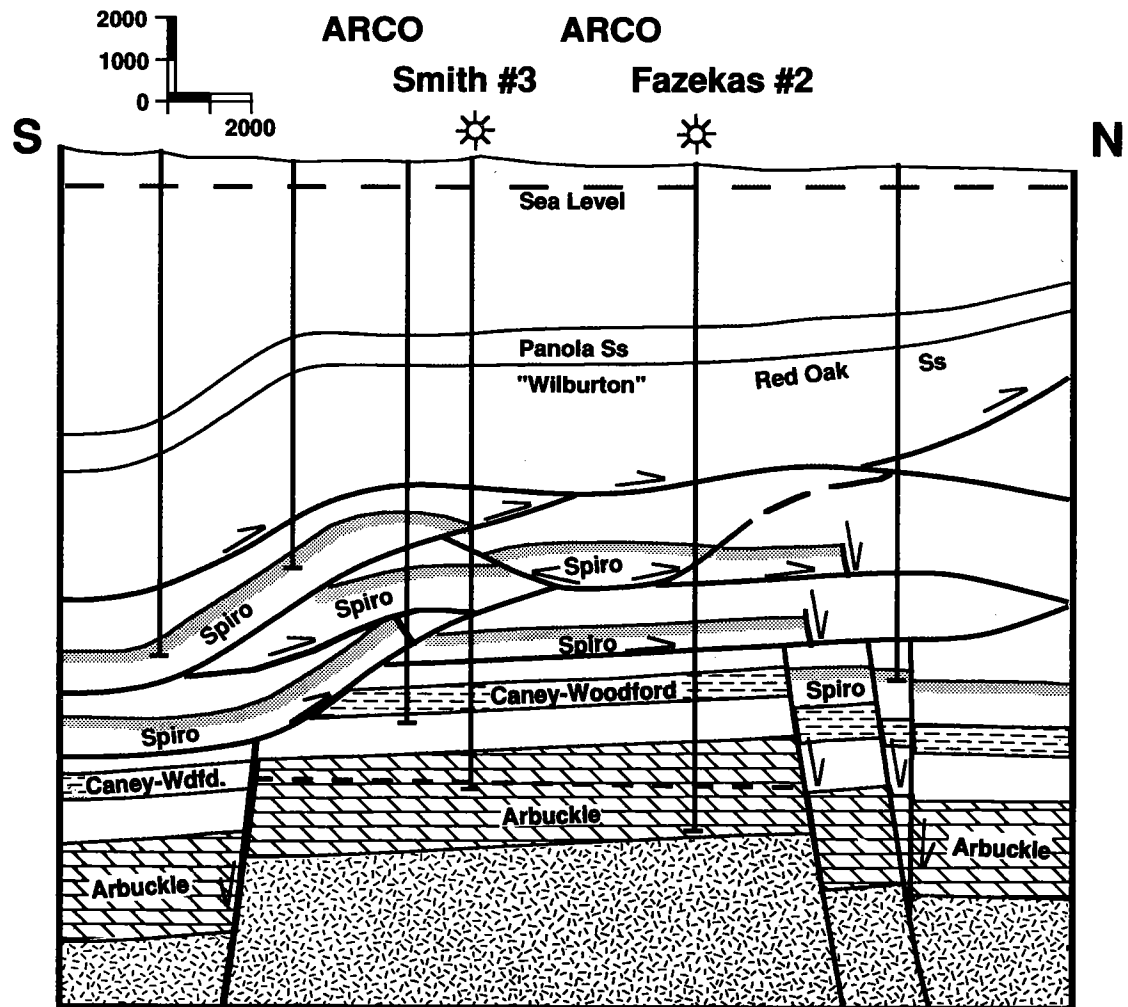


Figure 2. South-north structure section in the area of the Wilburton gas field, Arkoma basin, Oklahoma (modified from Hendrick, 1992). Line of section shown on Figure 1.

sections. The reservoir was likely sourced by the Woodford and Caney Shales, which were juxtaposed against the Arbuckle reservoir during formation of the horst block. All of the bounding faults have throws in excess of 1,000 ft at some point around the horst, which allows the sourcing contacts to occur.

The horst feature probably formed when crustal downwarping occurred during the early phases of the Ouachita orogeny. East-west-trending rift faults running parallel to the advancing thrust belt interacted with pre-existing crustal weaknesses parallel to the Ozark Mountain fault system (northeast-southwest) to form roughly polygonal fault blocks in the Wilburton field area. As the thrust advance continued, wrench adjustment of these basement blocks occurred, creating the current structural geometry (Fig. 2).

KARST ZONATION AND STRATIGRAPHY OF THE ARBUCKLE HORST BLOCK

Cores from ARCO production and exploratory wells reveal Arbuckle carbonates were dominantly deposited in a shallow, peritidal setting. Depositional fabrics and textures include algal mats (fenestral and birdseye fabrics), stromatolites with associated intraclastic packstones to wackestones, tidal laminites, rip-up clasts, thrombotic textures, bioturbated intervals, and thin zones containing bioclastic/ooid grainstones. Dolomitization is pervasive and cross-cuts all depositional facies. The major zonations of the horst block are shown in a stratigraphic cross section (Fig. 3).

The upper 220–250 ft of the reservoir (Zone I of Fig. 3) contains mostly intact host rock, with sucrosic intercrystalline (matrix) porosities rang-

ing from 4 to 18%, and measured permeabilities as much as 936 md. Gamma ray log signatures correlate consistently across this interval. Conodont analyses by R. L. Ethington (unpublished report, 1989) indicate that this portion of the reservoir is the same age as the lower part of the West Spring Creek Formation. An intraformational unconformity is inferred to occur at the base of this upper interval, and electric log and gamma ray correlations become tenuous below this contact. This intraformational unconformity is present in the ARCO no. 2 Paschall (sec. 21, T. 5 N., R. 18 E.) core at a depth of 13,487.5 ft, where reddish-hued algal boundstones are scoured and have a weathered appearance, and are overlain by dark-gray peloidal mudstones.

The Paschall well, which was extensively cored (13,238–13,744 ft), was also analyzed for conodonts by Ethington, whose data suggest that the 65- to 70-ft interval below the unconformity may also be the same age as the lower part of the West Spring Creek Formation. Core from this interval (Zone II) from the Paschall well and the ARCO no. 3 Costilow (sec. 14, T. 5 N., R. 18 E.) contain thin intervals containing muddy "cave fill" sediments similar to those described by Kerans (1988, 1989). Gamma ray "spikes" in this interval correlate erratically. The cave-fill zones consist of small-scale cavern and collapse zones 4–10 ft thick, containing detrital carbonate muds that occur at relatively steep and variable angles, along with transported detrital quartz sand grains and carbonate and chert clasts. The fill zones contain low measured porosities and permeabilities.

Based on conodont data, the contact with the underlying Kindblade Formation occurs at a depth ranging 290–300 ft below the top of the Arbuckle. Cores from this interval reveal large scale chaotic and mosaic breccia zones that are inferred to have originated as breakdown breccias from cave ceilings and chambers. Fracture porosity is abundant in this interval of the reservoir. This coarse breccia system is probably correlative to the "Brown Zone" productive interval of Healdton field in Carter County, Oklahoma (Latham, 1968), at least in part. A karst origin for the breccias is inferred from lateral correlations, reddish-hued coloration from oxidation (by subaerial exposure or meteoric waters), and geopetal and gravity sediment fills. No

true soil horizons are present in core. FMS log interpretations reveal each well penetrates multiple irregular breccia zones, while major fault cuts in individual wells are relatively rare.

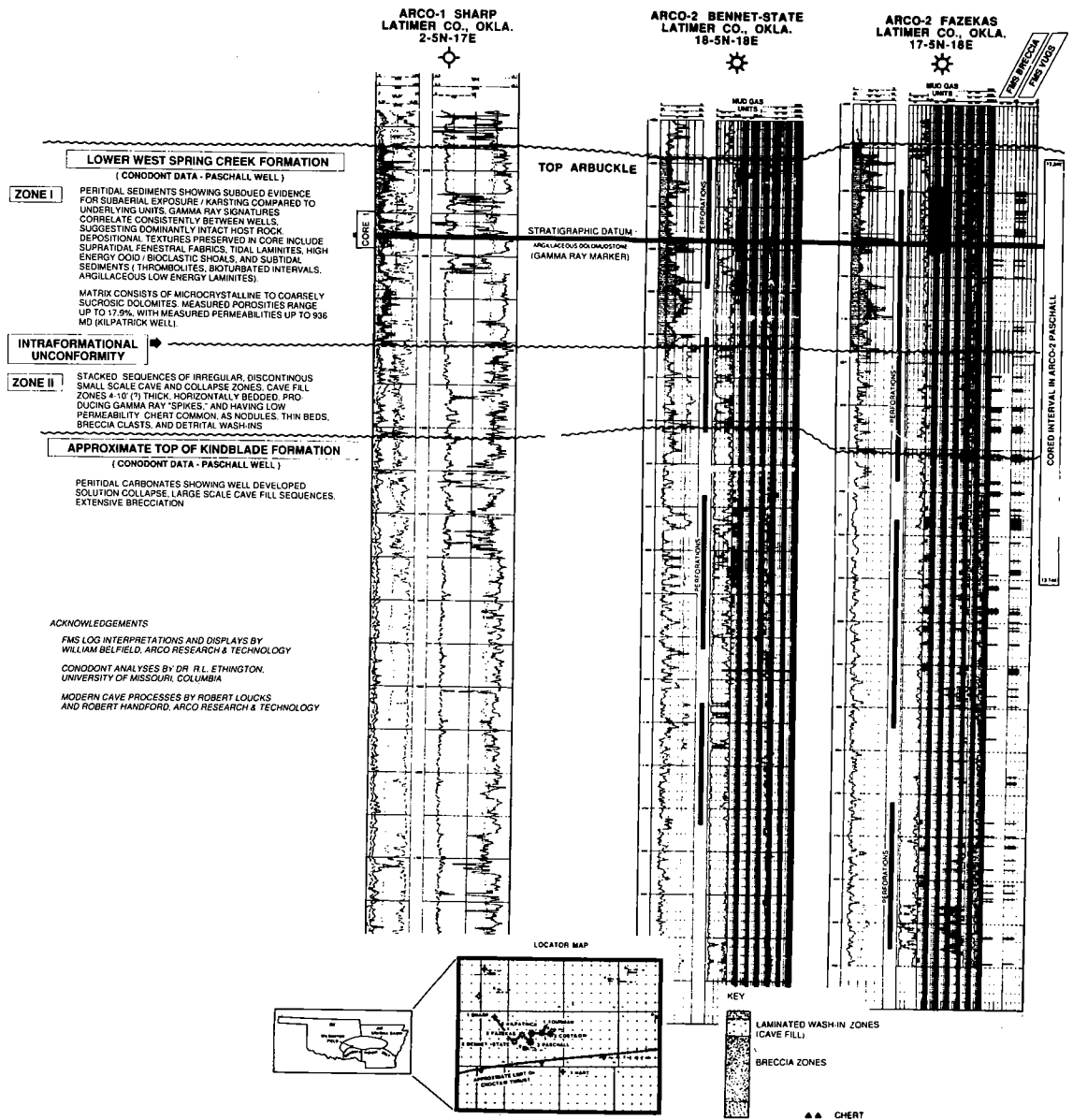
Although multiple periods of subaerial exposure probably occurred in the Wilburton area during Arbuckle deposition, the middle Ordovician unconformity at the top of the Arbuckle probably represents a major period of subaerial exposure of 10–30 m.y. (Mussman, 1988). The West Spring Creek section has been documented at >1,000 ft thick in southern Oklahoma (Latham, 1968), suggesting that a considerable amount of section has been removed at Wilburton. During this time of exposure, older karst breccias and faults with existing permeability networks were probably active fluid conduits and contributed to extensive collapse and brecciation.

Pennsylvanian (Ouachita) tectonism reactivated and/or created additional solution pathways, serving to break up the earlier relict karst and stratigraphic zonations, as demonstrated by excellent pressure and production communication among the wells in the Arbuckle reservoir.

REFERENCES CITED

- Hendrick, S. J., 1992, Vitritine reflectance and deep Arbuckle Maturation at Wilburton field, Latimer County, Oklahoma, in Johnson, K. S.; and Cardott, B. J. (eds.), *Source rocks in the southern Midcontinent, 1990 symposium: Oklahoma Geological Survey Circular 93*, p. 176–184.
- Kerans, Charles, 1988, Karst-controlled reservoir heterogeneity in Ellenburger Group carbonates of West Texas: *American Association of Petroleum Geologists Bulletin*, v. 72, p. 1160–1183.
- _____, 1989, Karst-controlled reservoir heterogeneity and an example from the Ellenburger Group (Lower Ordovician) of West Texas: *Texas Bureau of Economic Geology Report of Investigations 186*, 40 p.
- Latham, J. W., 1968, Petroleum geology of Arbuckle Group (Ordovician), Healdton field, Carter Co., OK: *American Association of Petroleum Geologists Bulletin*, v. 52, p. 3–20.
- Mussman, W. J.; Montañez, J. P.; and Read, J. F., 1988, Ordovician Knox paleokarst unconformity, Appalachians, in James, N. P.; and Choquette, P. W. (eds.), *Paleokarst: Springer-Verlag, New York*, p. 211–228.

WEST



EAST

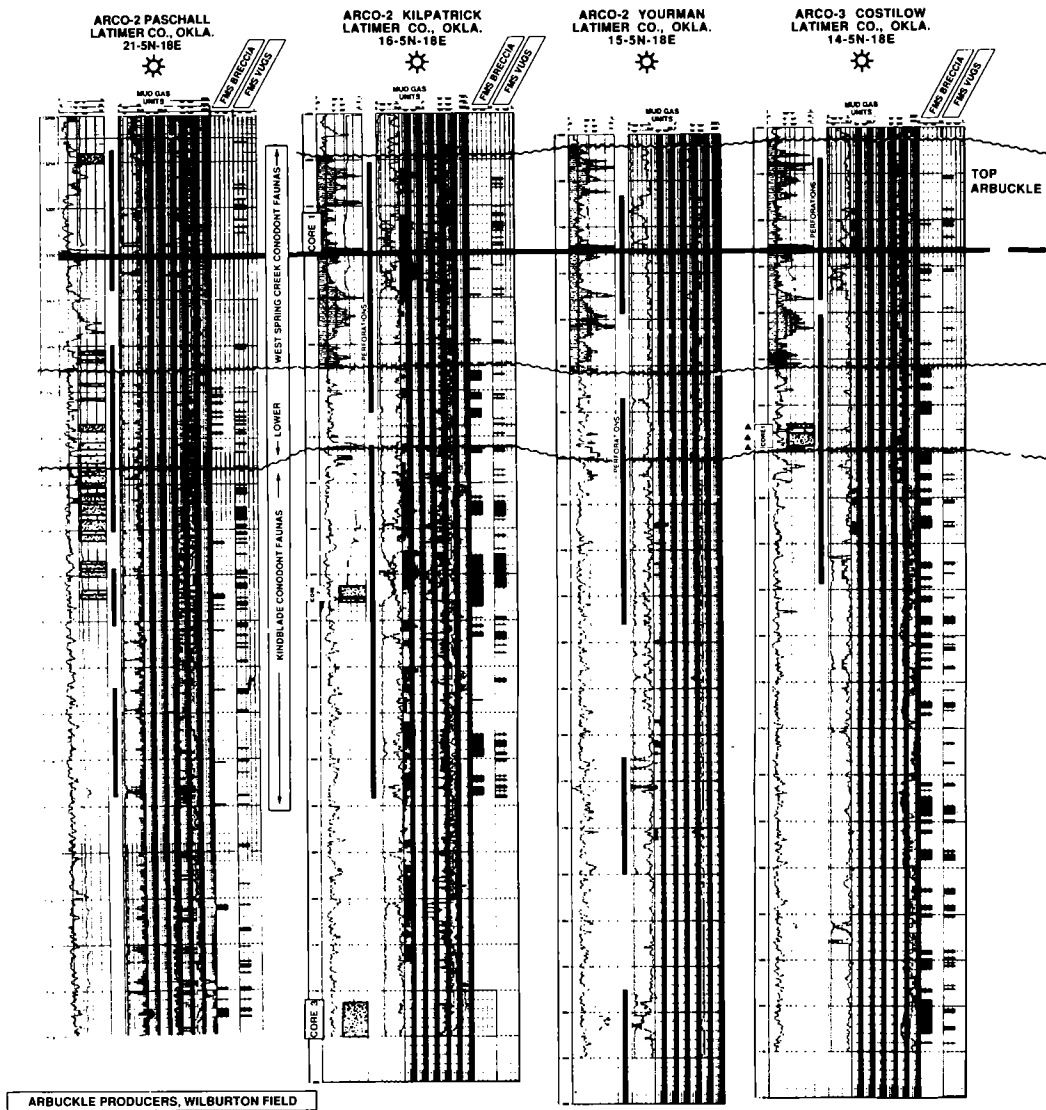


Figure 3. Stratigraphic section of the Arbuckle Group, Wilburton gas field, Arkoma basin, Oklahoma. Well locations shown in Figure 1.

Kinta Field—Characterization and Geology of a Multi-Reservoir Giant Arkoma Basin Gas Field

Robert A. Northcutt

Consulting Geologist
Oklahoma City, Oklahoma

David P. Brown

Geological Information Systems
Norman, Oklahoma

ABSTRACT.—The giant Kinta gas field is located in the Arkoma basin of eastern Oklahoma on the basinward part of the shelf, and it extends southward across the abrupt shelf edge into the deep part of the basin. Both structural and depositional conditions have created the many gas traps found in this multi-reservoir field. Gas production in 1990 was 84.6 Bcf; cumulative gas production at the end of 1990 was 2.1 Tcf.

INTRODUCTION

The currently defined Kinta gas field, officially designated in 1962, is located in parts of Pittsburg, Latimer, Haskell, Le Flore, and Sequoyah Counties in eastern Oklahoma and incorporates an area of 512 mi².

A map of the Arkoma basin area in eastern Oklahoma (Fig. 1) locates the Kinta field and its relationship to other significant fields.

The Kinta no. 1 field, the oldest of several fields that were eventually merged into the present-day Kinta field, was discovered in 1924. However, in the area now known as the Kinta field, gas was being produced as early as 1906 from shallow Atokan sandstones near Spiro in northeastern Le Flore County. By 1916, gas was also being produced from Hartshorne sandstones near Kinta in Haskell County.

Production data used in the preparation of this report are from the Natural Resources Information System (NRIS), courtesy of the Oklahoma Geological Survey and the University of Oklahoma, and from the Petroleum Data Systems PDS/TOTL file, courtesy of Dwigths Energydata, Inc.

Gas production in the field has been reported from 20 named subsurface units (gas-producing units are shown in Fig. 2). However, of the 20 units named, 12 are part of the Atoka Formation and are not necessarily 12 distinct lithologic units.

GEOLOGIC CONDITIONS AND TYPES OF TRAPS

The first major tectonic activity in the Kinta area occurred after deposition of the Spiro sand-

stone, possibly during early Atokan time and resulted in extensional down-to-the-south block faulting. During middle Atokan time, extensional faulting continued and was accompanied by a rapid influx of clastic sediments resulting in a zone of growth faults north of the basin axis (Koinm and Dickey, 1967). A structure map of Kinta field contoured on the top of the Spiro sandstone (Fig. 3) indicates this extensive normal faulting. The San Bois fault zone, along the southern edge of the field, has down-to-the-basin faults with as much as 6,000 ft of vertical separation. The Atoka Formation doubles in thickness south of this significant structural boundary. The compressional Ouachita orogeny, during Desmoinesian time, produced thrusting along the south flank of the basin, which extended into the southernmost part of the Kinta field (Ts. 6–7 N., Rs. 18–19 E.).

Representative reservoir properties and data for some of the producing units are presented in Table 1. Average depths of producing units range from 2,446 to 7,345 ft. The produced gas is all nonassociated, with pressure depletion as the reservoir drive.

The pre-Pennsylvanian rock units (Simpson, Viola, and Hunton) in the Kinta field produce from structural traps generally associated with the early Atokan deformation. The Simpson sandstones were deposited in a nearshore-marine environment and have undergone relatively little diagenesis. The Ordovician Viola limestone and Silurian Hunton Group rocks were deposited in a shallow carbonate shelf environment (Amsden, 1990); subsequent diagenesis has greatly enhanced porosity.

Northcutt, R. A.; and Brown, D. P., 1993, Kinta field—characterization and geology of a multi-reservoir giant Arkoma basin gas field, *in* Johnson, K. S.; and Campbell, J. A. (eds.), *Petroleum-reservoir geology in the southern Midcontinent, 1991 symposium*: Oklahoma Geological Survey Circular 95, p. 246–253.

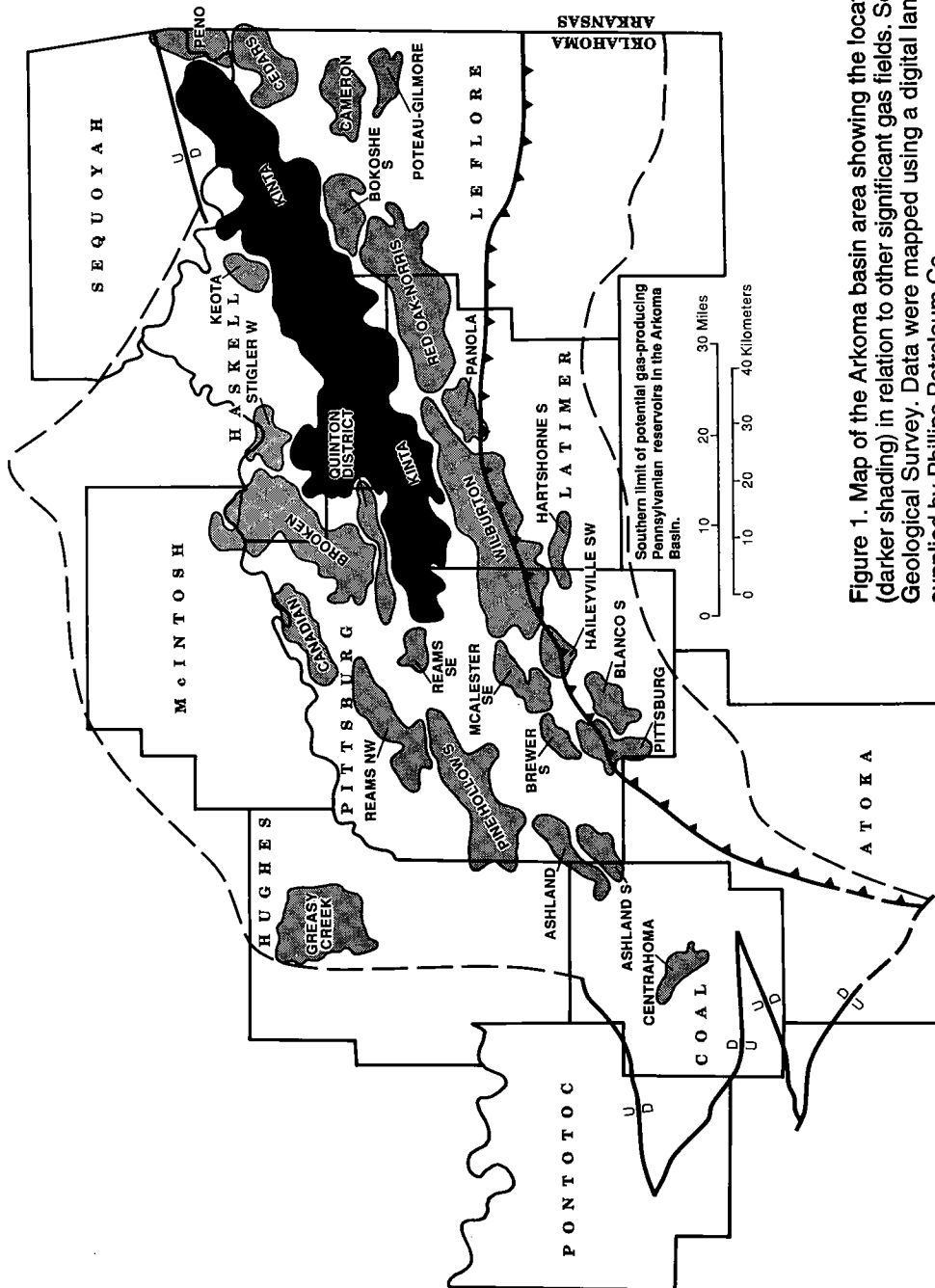


Figure 1. Map of the Arkoma basin area showing the location of Kinta field (darker shading) in relation to other significant gas fields. Source: Oklahoma Geological Survey. Data were mapped using a digital land grid data base supplied by Phillips Petroleum Co.

Geologic Column



System	Series	Group	Formation	Gas-Producing Units ^a	
PENNSYLVANIAN	Desmoinesian	Krebs Gp.	McAlester Fm.	Booch ss.	
			Hartshorne Fm.	Hartshorne ss.	
	Atokan	Atoka Fm.		Upper Atoka ss.	
				Gilcrease ss.	
				Alma ss.	
				Dirty Creek ss.	
				Middle Atoka ss.	
				Fanshawe ss.	
				Red Oak ss.	
				Panola ss.	
Brazil ss.					
Cecil ss.					
Lower Atoka ss.					
Spiro ss.					
Morrowan		Wapanucka Ls.	Wapanucka ls.		
		Union Valley Fm.	Cromwell ss.		
MISSISSIPPIAN	Chesterian			Pitkin ls.	
	Meramecian			"Caney" Sh.	
	Osagean			"Caney" Sh.	
	Kinderhookian	Woodford Sh.			
DEVONIAN	Upper	Hunton Gp.		Hunton dol.	
	Middle				
	Lower				Frisco Ls.
SILURIAN		Hunton Gp.	Bois d'Arc Ls.	Hunton dol.	
			Haragan Ls.		
			Henryhouse Fm.		
	Upper	Hunton Gp.	Chimneyhill Subgroup	Hunton dol.	
	Lower				
ORDOVICIAN	Upper	Arbuckle Gp.	Sylvan Sh.		
			Viola Gp.	Viola ls.	
	Middle		Simpson Gp.	Simpson ss.	
	Lower				
CAMBRIAN	Upper		Arbuckle Gp.		
			Timbered Hills Gp.		

^aNames of gas-producing units in the Atoka Formation are the names reported by operators. Several of these names were imported from other areas. Their application in the Kinta field may or may not have been based on adequate correlations. Also, the 12 names listed do not necessarily correspond to 12 discrete lithologic units.

Figure 2. Geologic column showing the gas-producing intervals in the Kinta field identified from the Oklahoma Geological Survey, NRIS data files.

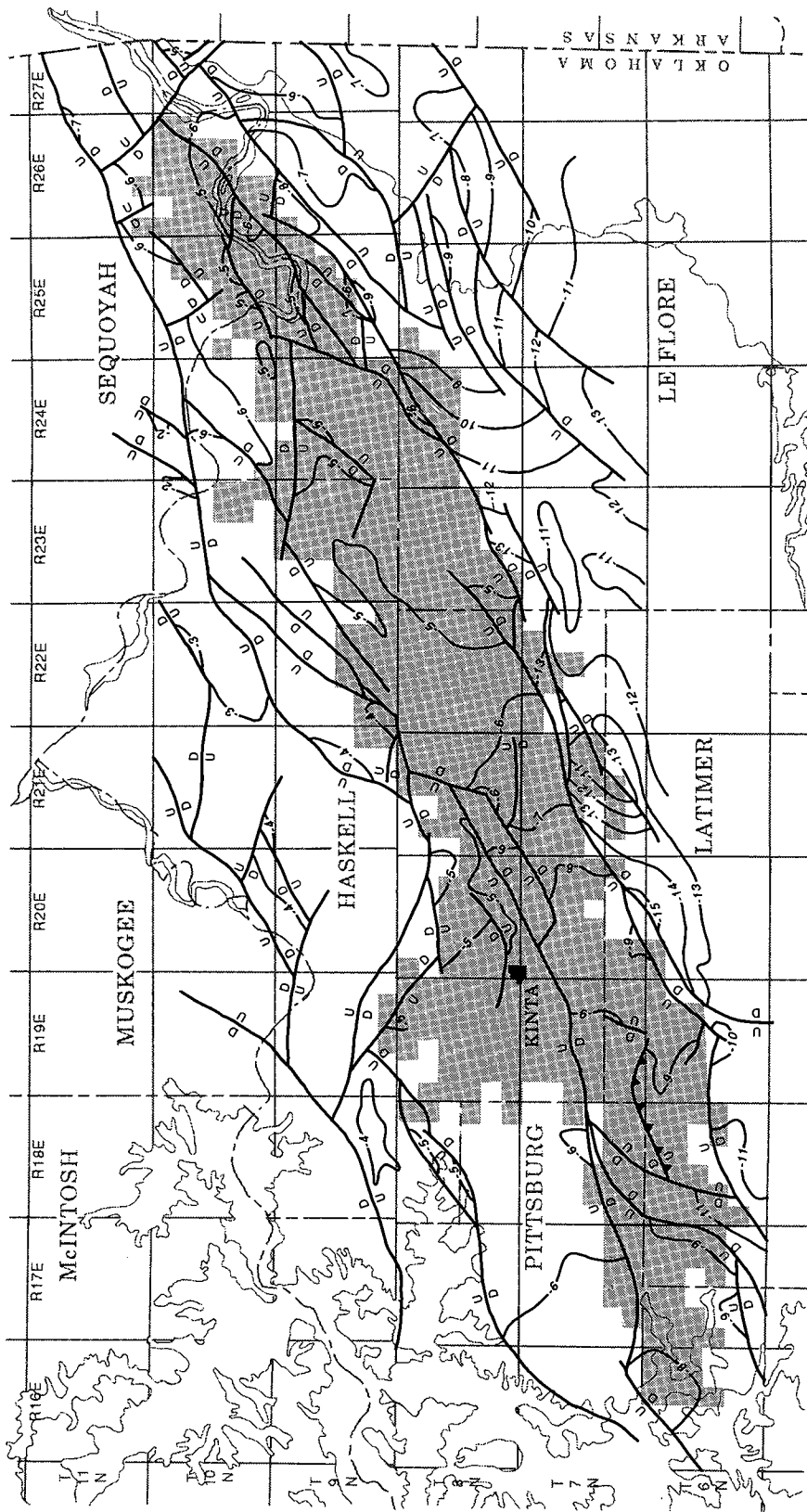


Figure 3. Structure map of the Spiro sandstone in the Kinta field area. Minor faults are not shown. Contours in thousands of feet below sea level; contour interval is 1,000 ft; the Kinta field is shown by the stipple pattern. Modified from Wylie (1988).

TABLE 1. — KINTA FIELD RESERVOIR DATA

Reservoir	Discovery year	Average depth (ft)	Trap type ^a	Average netpay (ft)	Porosity (%)	Initial shut-in pressure (psi)
Booch sandstone	1972	2,900	Combination	6	13.4	323
Hartshorne sandstone	1919	2,446	Combination	20	16.0	290
Atoka (Brazil) sandstone	1977	7,005	Combination	30	12.0	1,542
Red Oak sandstone	1963	6,954	Combination	19	14.0	2,950
Spiro sandstone	1951	6,878	Combination	25	13.0	1,425
Wapanucka limestone	1967	7,345	Combination	35	9.0	995
Cromwell sandstone	1951	7,241	Combination	25	11.0	1,630
Hunton limestone	1964	6,871	Combination	20	12.0	2,625
Simpson sandstone	1964	6,337	Structural	20	11.0	2,610

^aCombination trap is anticline and facies change.

Pennsylvanian rock units in the field produce from stratigraphic traps with minor structural influence. The Cromwell sandstone (Morrowan) is part of a mixed carbonate-siliciclastic unit that was deposited in shallow-shelf and nearshore-marine environments (Jefferies, 1982) where diagenesis has enhanced porosity. The depositional systems of the Desmoinesian and Atokan rocks were predominately fluvial-deltaic in the northern part of the Kinta field, grading southward into prodelta and submarine fan environments south of the San Bois fault zone (Vedros and Visser, 1978; Houseknecht and others, 1983; Houseknecht, 1987). Diagenesis has strongly influenced porosity development in the basal Atokan Spiro sandstone (Lumsden and others, 1971). In the post-Spiro Atokan and Desmoinesian rocks, grain size and sorting are primary factors in the porosity development, with minor diagenetic influence.

For specific examples of trap types in the Kinta field, see the studies done by Lahoud (1961), Wonick (1968), Lumsden and others (1971), and Adams (1974). Trapping conditions in Kinta field are characteristic of those throughout the Arkoma basin (Brannan, 1968).

KINTA FIELD GAS PRODUCTION

The Kinta gas field has expanded to its present area through the coalescence of 27 previously defined fields. A chart of this chronology of expansion is shown in Figure 4.

Cumulative gas production reported for the Kinta field at the end of 1990 is 2,117,014,968 Mcf (2.1 Tcf). A graph of the monthly production for 1983–90 and the amount produced from selected reservoir units is shown in Figure 5.

Of the cumulative production through 1990 (2.1Tcf), 14.5% was produced prior to 1968 and production is not reported by producing zone. According to NRIS production data, from 1968 through 1990 the contribution from individual units was as follows:

Spiro sandstone	44.8%
Other Atoka sandstones	30.5%
Cromwell sandstone	7.6%
Hartshorne and Booch sandstones (Desmoinesian)	1.8%
Wapanucka, Hunton, Viola, and Simpson	0.8%

Figure 6, Map A, reflects the current area of Spiro sandstone production. The Spiro is the dominant producing horizon in the Kinta field. The areas in which other Atokan sandstones produce are shown on Map B (Fig. 6). The combined production from the Spiro and all other Atokan sandstones represented just over 70% of Kinta's total production in 1990 (Fig. 5).

From the available records, at least 1,232 wells (gas and dry) have been drilled in the Kinta field. In 1990, 801 operating gas wells produced 84,629,015 Mcf of gas. At present and projected levels of production, the Kinta field can now be considered a giant gas field and should achieve accumulative gas production of 3 Tcf by the year 2000.

REFERENCES CITED

- Adams, D. J., 1974, Blocker area, *in* Berg, O. R. (ed.), Oil and gas fields of Oklahoma: Oklahoma City Geological Society Reference Report, Supplement 1, p. 26.
 Amsden, T. W., 1980, Hunton Group (Late Ordovician, Silurian, and Early Devonian) in the Arkoma basin

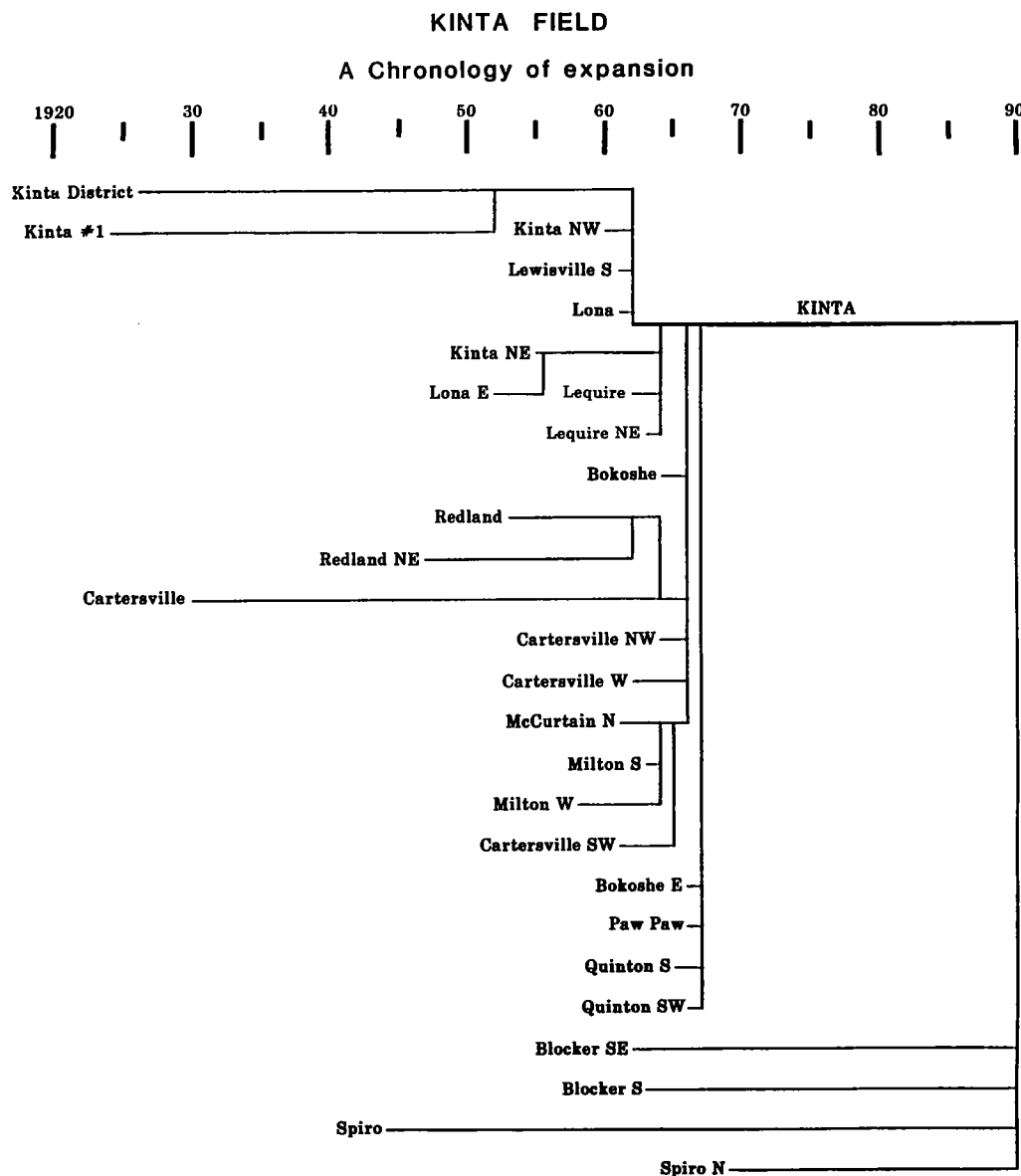


Figure 4. Chart of field combinations that have resulted in the present Kinta field. Individual field lines (horizontal) span the period of time from the year of field designation to the year of subsequent combination. Vertical lines connect horizontal lines of the fields that were combined.

of Oklahoma: Oklahoma Geological Survey Bulletin 129, 136 p.

Brannan, C. B., Jr., 1968, Natural gas in Arkoma basin Oklahoma and Arkansas, in Beebe, B. W.; and Curtis, B. F. (eds.), Natural gases of North America, a symposium: American Association of Petroleum Geologists Memoir 9, v. 2, p. 1616-1635.

Houseknecht, D. W., 1987, The Atoka Formation of the Arkoma basin: tectonics, sedimentology, thermal maturity, sandstone petrology: Tulsa Geological Society, Short Course Notes, 72 p.

Houseknecht, D. W.; Zaengle, J. F.; Steyaert, O. J.;

Mafeo, A. P., Jr.; and Kuhn, M. A., 1983, Facies and depositional environments of the Desmoinesian Hartshorne sandstone, Arkoma basin, in Houseknecht, D. S. (ed.), Tectonic-sedimentary evolution of the Arkoma basin and guidebook to deltaic facies, Hartshorne sandstone: Society of Economic Paleontologists and Mineralogists Mid-Continent Section, v. 1, p. 53-82.

Jefferies, B. K., 1982, Stratigraphy and depositional patterns of the Union Valley, Wapanucka, and lower Atoka Formations: University of Arkansas unpublished M.S. thesis, 102 p.

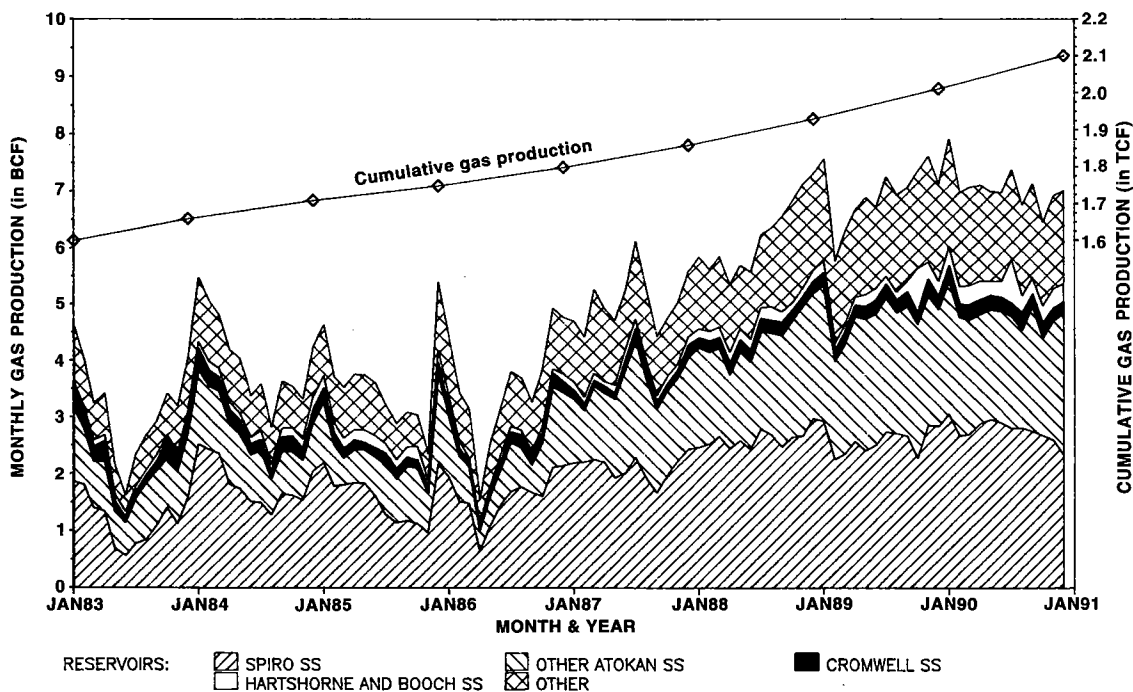


Figure 5. Graph of Kinta field gas production by months for period from Jan. 1, 1983, through Dec. 31, 1990, with cumulative gas production shown by upper line and the scale on the right. Patterned areas represent the contribution from selected producing intervals. Monthly gas production is proportioned for selected units. Source: Oklahoma Geological Survey, NRIS data files.

Koinm, D. N.; and Dickey, P. A., 1967, Growth faulting in McAlester basin of Oklahoma: American Association of Petroleum Geologists Bulletin, v. 51, p. 710-781.

Lahoud, J. A., 1961, Cartersville gas field, in Morrissey, N. S.; and Walper, J. L. (eds.), Arkoma basin and north-central Ouachita Mountains of Oklahoma, field conference: Tulsa Geological Society and Fort Smith Geological Society Guidebook, p. 51-53.

Lumsden, D. N.; Pittman, E. D.; and Buchanan, R. S., 1971, Sedimentation and petrology of Spiro and Foster sands (Pennsylvanian), McAlester basin, Oklahoma: American Association of Petroleum Geologists Bulletin, v. 55, p. 254-266.

Vedros, S. C.; and Visser, G. S., 1978, The Red Oak sandstone: a hydrocarbon-producing submarine fan deposit, in Stanley, D. J.; and Kelling, G. (eds.), Sedimentation in submarine canyons, fans, and trenches: Dowden, Hutchinson and Ross, Stroudsburg, Pennsylvania, p. 292-308.

Wonick, John, 1968, Kinta gas field, Haskell County, Oklahoma, in Beebe, B. W.; and Curtis, B. F. (eds.), Natural gases of North America, a symposium: American Association of Petroleum Geologists Memoir 9, v. 2, p. 1636-1643.

Wylie, W. D., 1988, Subsurface structure map Spiro sandstone: Unpublished maps, 2 sheets, scale 1:96,000.

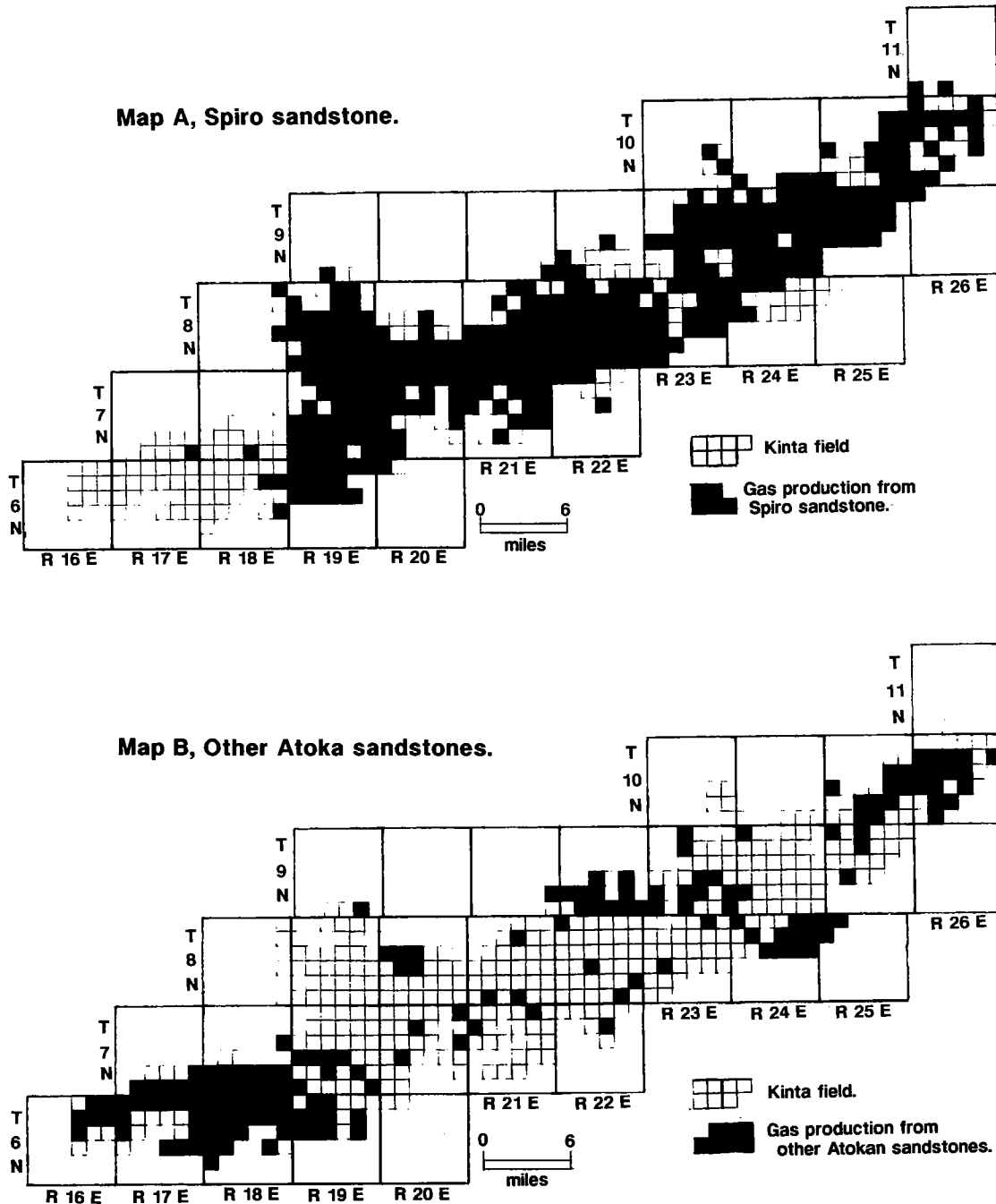


Figure 6. Kinta field Atoka gas production from 1983 through 1990: Map A shows the area where the Spiro is productive; Map B shows the area where Atoka sandstones, excluding Spiro, are productive. Sections outlined on maps show the extent of the Kinta field; sections shown in black produce gas from the Spiro (Map A) and from other Atoka sandstones (Map B). Data from Oklahoma Geological Survey NRIS data files were mapped using a digital land grid data base supplied by Phillips Petroleum Co.

Outcrop Characteristics of Asphaltic Lewis Sandstone, Black Warrior Basin, Alabama: Application to Subsurface Studies of Reservoir Heterogeneity

Jack C. Pashin and Ralph L. Kugler

Geological Survey of Alabama
Tuscaloosa, Alabama

INTRODUCTION

Much additional oil may be produced from the Black Warrior basin using improved recovery strategies, especially from fields where production is now declining. Characterizing reservoir heterogeneity may provide information regarding how improved recovery strategies, such as waterflooding, injection, strategic well placement, and infill drilling, can best be applied (Weber, 1986). Mississippian strata in the Black Warrior basin of Alabama are rich in asphalt (Wilson, 1987), and outcrops provide instructive transects of fossil oil reservoirs. Exceptional exposures of asphaltic sandstone occur in the Lewis interval of the Pride Mountain Formation (Chesterian) in Colbert County (Fig. 1), and they form the basis of this study. Lewis outcrops enable direct observation of sandstone heterogeneity and furnish sedimentologic and petrologic analogs for reservoir heterogeneity of the principal producing subsurface reservoirs in the

basin (Lewis sandstone and Carter sandstone). Therefore, characterization of sandstone heterogeneity in outcrops may be advantageous in identifying specific strategies that will facilitate improved recovery of liquid hydrocarbons from Mississippian reservoirs in the Black Warrior basin.

The Lewis interval overlies the Tuscumbia Limestone disconformably and consists of three major units: (1) *Inflatia* beds, (2) Lewis sandstone, and (3) Lewis limestone (Fig. 2) (Pashin and others, 1991). The *Inflatia* beds are the basal Pride Mountain carbonate units that represent transgressive storm deposits and oolite shoals. The Lewis sandstone comprises numerous lensoid, asphaltic quartzarenite bodies that are encased in clay shale. In Colbert County, the sandstone represents regressive deposits, including storm-dominated shelf sand patches and chenier-like beach-barrier systems. Some of the beach systems evidently formed as shelf-sand bodies that were exposed and reworked in a mesotidal shore zone. The Lewis

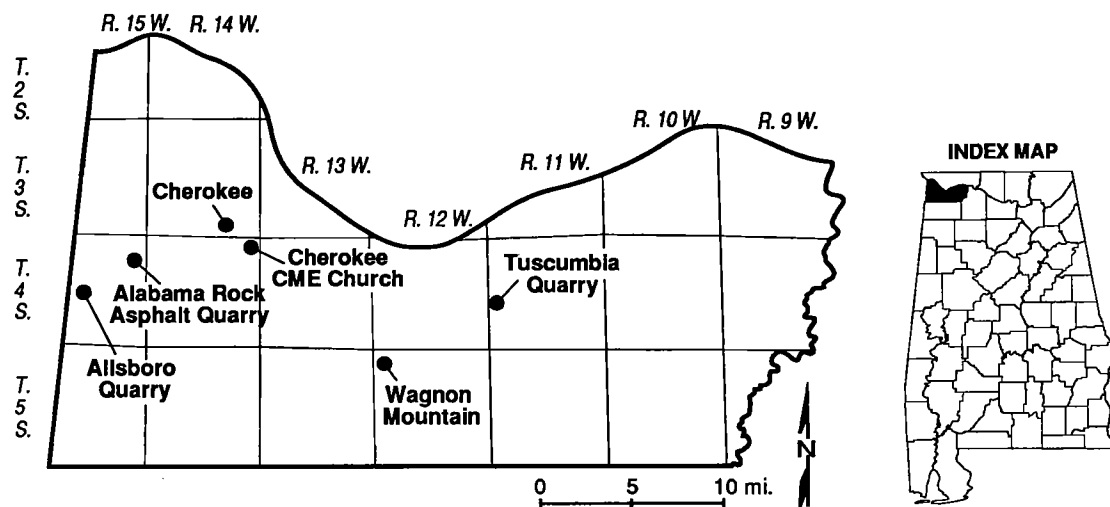


Figure 1. Map of study area showing location of outcrops of asphaltic Lewis sandstone, Colbert County, Alabama.

Pashin, J. C.; and Kugler, R. L., 1993, Outcrop characteristics of asphaltic Lewis sandstone, Black Warrior basin, Alabama: application to subsurface studies of reservoir heterogeneity, in Johnson, K. S.; and Campbell, J. A. (eds.), *Petroleum-reservoir geology in the southern Midcontinent*, 1991 symposium: Oklahoma Geological Survey Circular 95, p. 254-258.

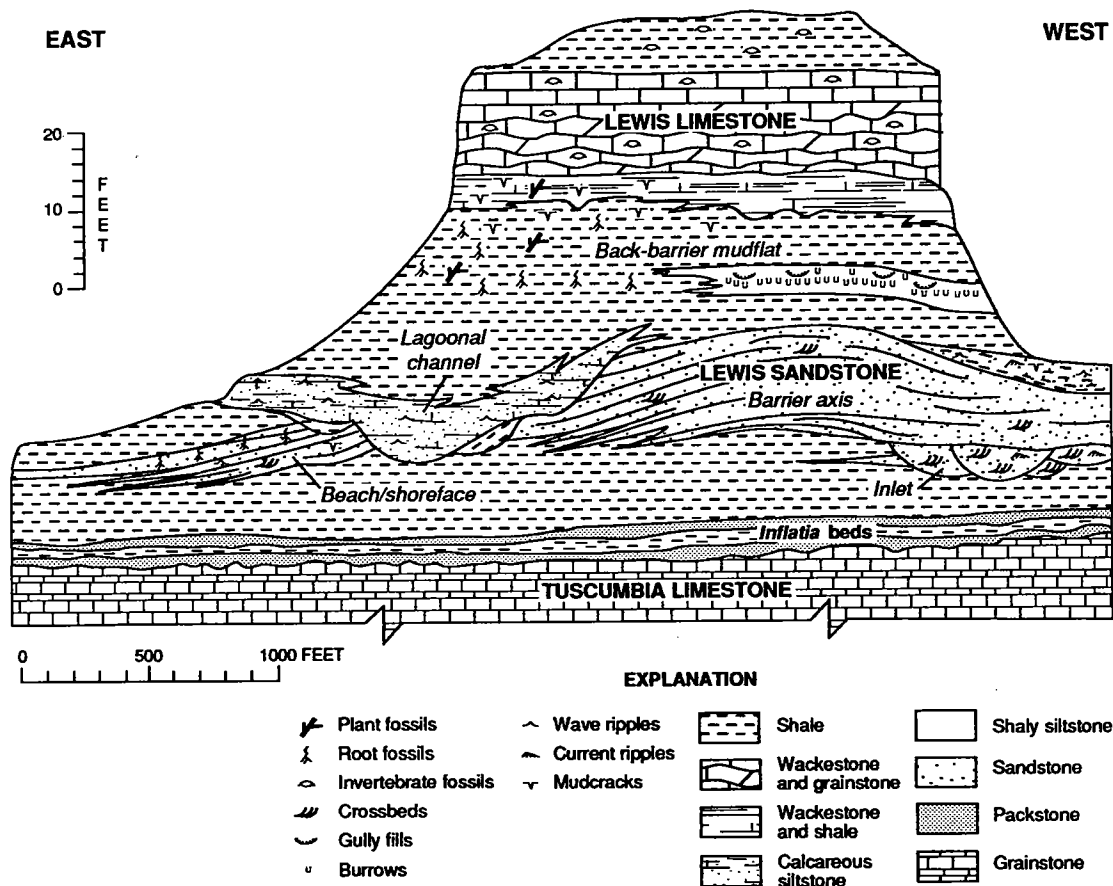


Figure 2. Outcrop diagram showing facies heterogeneity in Lewis sandstone beach-barrier deposits, Tuscumbia quarry.

limestone forms the top of the Lewis interval and represents transgressive carbonate sedimentation in a spectrum of intertidal to open-marine environments (DiGiovanni, 1984). Relict topography inherited from sea-floor and shore-zone evolution was a critical control on the facies architecture of the Lewis limestone (Pashin and others, 1991).

Reservoir heterogeneity can be classified according to scale of observation. The broadest scale of heterogeneity (level 1) is the reservoir; namely, a body of reservoir rock that is surrounded by nonreservoir rock. Level-2 heterogeneity occurs among wells, whereas level-3 heterogeneity, or interwell heterogeneity, occurs between wells. Level-4 heterogeneity occurs at the scale of a core or wellbore, and level-5 heterogeneity occurs at the scale of pores and pore throats. Lewis sandstone reservoirs are the result of an elaborate interplay of depositional and diagenetic variables that operated from microscopic to megascopic scale. This report relates sedimentologic and petrologic outcrop data to the five levels of sandstone heterogeneity.

RESULTS

Level-1 heterogeneity is a primary control on the producibility of Lewis oil, because the sandstone comprises small, isolated bodies of reservoir rock that are confined vertically and laterally by impermeable shale (Fig. 2). Bitumen-rich sandstone bodies were observed only in beach facies, but major subsurface oil production in the Lewis sandstone is from storm-dominated-shelf facies (Holmes, 1981). Improved recovery operations, such as injection, can utilize margins of reservoir sandstone bodies to confine flow and to direct the migration of oil toward desired extraction points.

Well spacing in Black Warrior basin oil fields is typically between 40 and 80 acres, so level-2 heterogeneity was observed only in the most extensive exposures, such as the Tuscumbia quarry (Fig. 2). In the Lewis sandstone, level-2 heterogeneity is related to cementation patterns and facies continuity. Ferroan-carbonate cement predominates at the margins and particularly at the bases of beach-sandstone bodies (Fig. 3). Therefore, oil

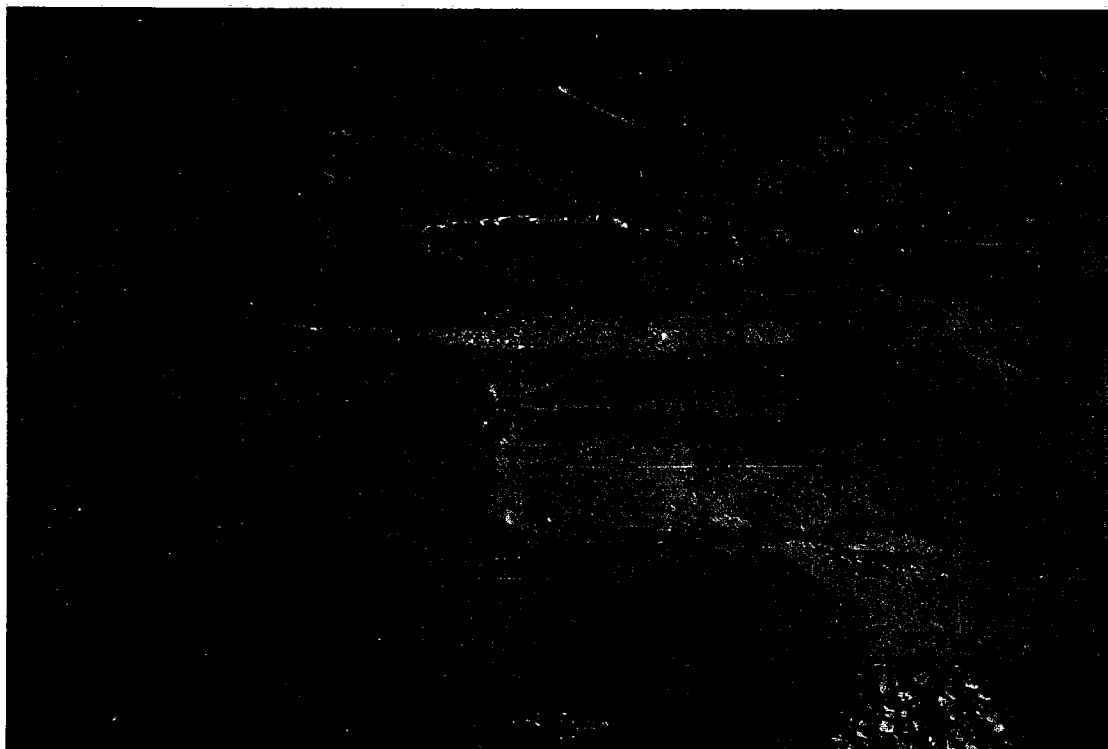


Figure 3. Interlaminated asphaltic (dark) and carbonate-cemented (light) sandstone, Allsboro quarry.

may be least mobile at the edges of the barrier-sandstone bodies and most mobile along the barrier axes. Subsurface studies of heterogeneity in beach-barrier sandstone indicate that porosity, permeability, and oil production are greatest along barrier axes (Sharma and others, 1990). Using infill drilling in tandem with acidizing along sandstone-body margins may optimize oil recovery from Lewis reservoirs by dissolving carbonate permeability barriers.

Level-3 heterogeneity, or interwell heterogeneity, is readily observed in Lewis outcrops. The most significant level-3 heterogeneity occurs in inlet- and lagoonal-channel facies (Fig. 2). Inlet-channel fills contain abundant asphalt, but the fills extend in cross section for only 4–25 ft and contain ferroan-carbonate cement along the margins. Therefore, inlet facies may be difficult to predict in the subsurface without the aid of stochastic models, and mobility of hydrocarbons is probably limited. However, the channel fills probably form linear to sinuous shoestrings in longitudinal section, and the asphalt deposits may thus be tubular. A tubular geometry suggests that liquid hydrocarbons can be mobilized along channel axes, thereby improving recovery. An alternative recovery method may involve a fracture design that promotes migration of hydrocarbons from the inlet

facies into the beach axis. Lagoonal channels are filled with mud and silt, and are major permeability barriers that can compartmentalize reservoirs. These channels have limited width and are thus difficult to identify using well logs.

The distribution of ferroan-carbonate cement, clay laminae, and primary sedimentary structures is the dominant control on level-4 heterogeneity in the Lewis sandstone. Carbonate-cemented interlaminae occur in most asphaltic-sandstone bodies (Fig. 3) and are permeability barriers that increase tortuosity of fluid flow or may render oil immobile. Commonly, coarser laminae contain carbonate cement, whereas finer laminae contain asphalt. The coarser laminae were cemented by calcite early in the diagenetic evolution of the sandstone. This cement subsequently was replaced by ferroan calcite and ferroan dolomite/ankerite. Carbonate cementation occurred preferentially along the coarser, more permeable laminae prior to migration of oil into the sandstone. Clay laminae extend for considerable distances in the sandstone and probably restrict vertical flow rather than lateral flow; the laminae probably increase tortuosity and impound oil where they converge along wedge-shaped cross beds. Primary sedimentary structures, such as ripple cross laminae, may also increase tortuosity of flow. Burrows that pierce clay

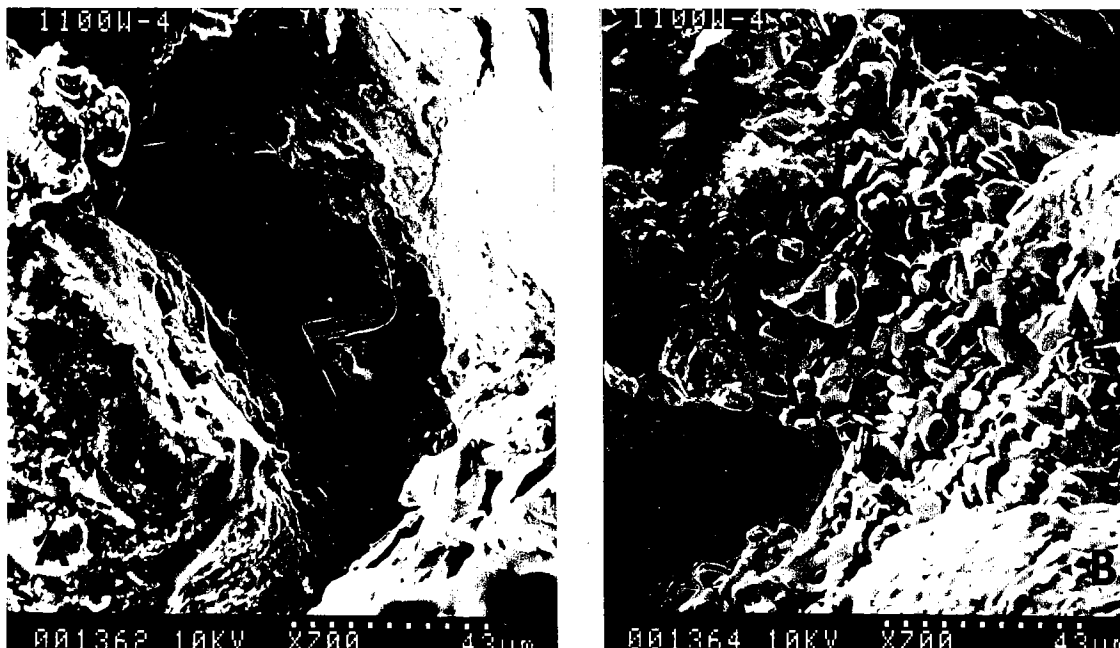


Figure 4. Scanning-electron micrographs of (A) macropore containing ferroan-dolomite rhomb and asphalt, Tuscumbia quarry, and (B) microporous kaolinite coated with asphalt, Tuscumbia quarry.

laminae may provide interlaminar-flow conduits. However, mixing of mud in sand by bioturbation generally reduces reservoir quality.

Level-5 heterogeneity is dominated by diagenetic factors (Fig. 4). Quartz overgrowths are ubiquitous but do not adversely affect the quality of the best reservoirs. Carbonate cements include early-stage siderite and calcite and late-stage ferroan dolomite/ankerite and ferroan calcite which, in contrast to quartz overgrowths, tend to occlude all pores. Fossils provided nucleation sites for pore-filling calcite which subsequently was replaced by ferroan-carbonate minerals. Pore-filling and grain-replacing kaolinite is microporous but impermeable. The presence of irreducible water in kaolinite should be considered when determining reservoir-water saturation from well logs. Asphalt coats authigenic quartz, carbonate, and kaolinite, thus confirming that oil entered the sandstone bodies late in the diagenetic evolution of the sandstone. At the time hydrocarbons entered the reservoir, the pore system consisted of interconnected, modified primary and secondary macropores between detrital framework grains and ineffective micropores within patches of kaolinite, mud fragments, and clay laminae.

CONCLUSIONS

Heterogeneity in the Lewis sandstone is controlled by depositional and diagenetic processes.

The products of these processes are related in that the distribution of authigenic minerals is influenced by depositional texture. The dominant megascopic structures (levels 1–3) that control reservoir continuity and asphalt distribution, particularly the lensoid nature of the sandstone and the presence of inlet- and lagoonal-channel fills, are the result of depositional processes. Diagenetic factors, particularly occlusion of porosity by carbonate cement and authigenic kaolinite, are the dominant mesoscopic and microscopic (levels 3–5) controls on asphalt distribution within the sandstone bodies. Synthesis of outcrop data with the five-level heterogeneity classification provides insight into how lithologic variability affects fluid flow, and thus the producibility of oil from analogous subsurface reservoirs. Diverse depositional and diagenetic controls on heterogeneity in the Lewis sandstone indicate that improved-recovery strategies, such as waterflooding, injection, and strategic well placement, may be tailored to specific depositional and diagenetic reservoir settings to increase oil production from sandstone reservoirs in the Black Warrior basin.

REFERENCES CITED

- DiGiovanni, Marcel, Jr., 1984, Stratigraphy and depositional environments of the lower Pride Mountain Formation (Upper Mississippian) in the Colbert County area, northwest Alabama: University of Ala-

- bama, Tuscaloosa, unpublished M.S. thesis, 144 p.
- Holmes, J. W., 1981, The depositional environment of the Mississippian Lewis sandstone in the Black Warrior basin of Alabama: University of Alabama, Tuscaloosa, unpublished M.S. thesis, 172 p.
- Pashin, J. C.; Osborne, W. E.; and Rindsberg, A. K., 1991, Characterization of sandstone heterogeneity in Carboniferous reservoirs for increased recovery of oil and gas from foreland basins: U.S. Department of Energy Topical Report, Bartlesville, Oklahoma, contract no. DE-FG22-90BC14448, 169 p.
- Sharma, Bijon; Honarpour, M. M.; Szpakiewicz, M. J.; and Schatzinger, R. A., 1990, Critical heterogeneities in a barrier island deposit and their influence on various recovery processes: Society of Petroleum Engineers Formation Evaluation, p. 103–112.
- Weber, K. J., 1986, How heterogeneity affects oil recovery, *in* Lake, L. W.; and Carroll, H. B., Jr. (eds.), Reservoir characterization: Academic Press, Orlando, p. 181–222.
- Wilson, G. V., 1987, Characteristics and resource evaluation of the asphalt and bitumen deposits of northern Alabama: Alabama Geological Survey Bulletin 111, 110 p.

Microseismic Monitoring as a Tool for Mapping Fractures in the San Andres Dolomite

James T. Rutledge, Thomas D. Fairbanks, and Leigh S. House

Los Alamos National Laboratory
Los Alamos, New Mexico

Mark B. Murphy

Murphy Operating Corporation
Roswell, New Mexico

INTRODUCTION

The San Andres dolomite is a prolific oil-producer extending over a large area of the Permian basin of West Texas and eastern New Mexico. Waterflooding is typically used as a means of secondary recovery from the San Andres dolomite. One problem with waterflooding in some oil fields producing from the San Andres is flow anisotropy in reservoirs caused by preferential flow along fractures. If the locations and orientations of major fractures in reservoirs were known, waterfloods could be better designed to use well configurations that would delay water breakthroughs and improve recovery. Oil fields of the San Andres dolomite typically have wells uniformly spaced at 400 m in a grid pattern parallel with section boundaries. Pressure-interference testing is often not successful because of large distances between wells, and the well density is insufficient to accurately infer flow direction from breakthrough patterns alone. Microseismic monitoring is an alternative method for determining the location and prevalent orientations of fractures. Los Alamos National Laboratory has successfully used the method for mapping hydraulic fractures in crystalline rock (Fehler and others, 1987). The method relies on the observation that microearthquakes occur along fractures when stress along the fractures is changed by increases in fluid pressure. By determining the locations of the induced microearthquakes, some knowledge of the locations and orientations of the dominant fluid paths can be obtained. If the method is successful in the San Andres dolomite, it could be a useful tool for optimizing waterfloods in many San Andres fields in the Permian basin.

The focus of this study was to determine if microseismicity was detectable in the San Andres

at rates high enough to be practical for mapping fractures. Microseismicity was monitored within the Chaveroo oil field during pressurized stimulation of a well, and intermittently over the following five-week period while a pilot waterflood operation was underway. Figure 1 shows the well configuration in the square-mile section of the Chaveroo field where the experiment took place. Dur-

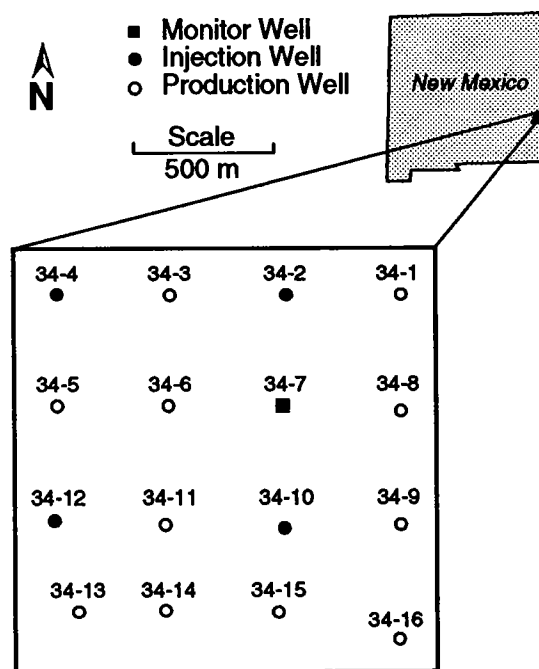


Figure 1. General location map and well configuration of Murphy Operating Corp.'s Haley unit, Chaveroo oil field, New Mexico. Map area is sec. 34, T. 7 S., R. 33 E., Roosevelt County.

Rutledge, J. T.; Fairbanks, T. D.; House, L. S.; and Murphy, M. B., 1993, Microseismic monitoring as a tool for mapping fractures in the San Andres dolomite, in Johnson, K. S.; and Campbell, J. A. (eds.), Petroleum-reservoir geology in the southern Midcontinent, 1991 symposium: Oklahoma Geological Survey Circular 95, p. 259-261.

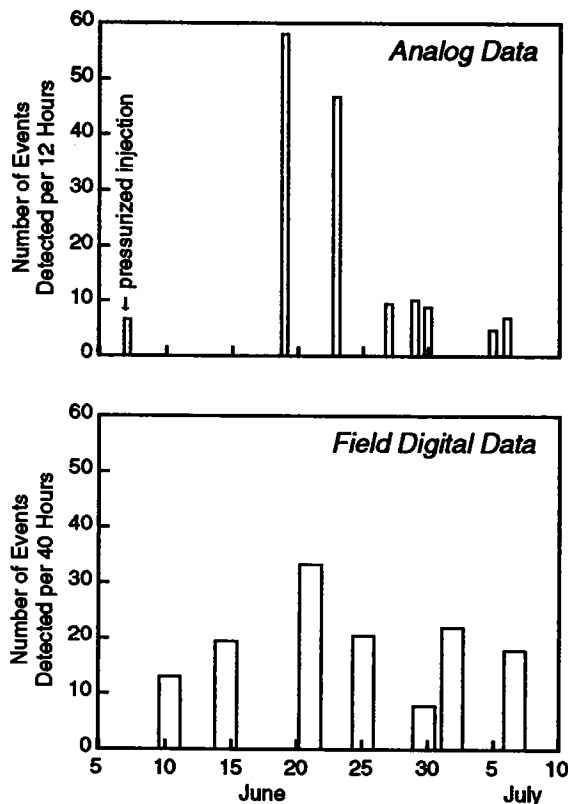


Figure 2. Number of microearthquakes detected per 12-hour recording session from the analog tape (above), and the number of microearthquakes detected per 40-hour recording session by the digital field recorder (below). Monitoring was intermittent; gaps between bars represent time intervals between recording sessions.

ing the pressurized stimulation, 3,000 bbl of water were injected into well 34-10 over a 5.5-hour period. Subsequently, the four pilot waterflood injection wells (Fig. 1) each took 200–250 bbl of water per day under hydrostatic pressure. A single, three-component, downhole seismometer was placed at the reservoir depth (1,280 m) in well 34-7 located 400 m north of the stimulation well 34-10.

MONITORING AND EVENT OCCURRENCE

Monitoring was intermittent over the total five-week period during 1989; however, microseismicity was detected during each monitoring period. Figure 2 shows the monitoring time intervals and the number of events detected during each monitoring period. Data were recorded on both analog tape and digital field recorders. The digital field records provided an event-occurrence count, but the frequency bandwidth was too narrow for determining locations. Digitized analog records represented the signals' full frequency bandwidth be-

cause a higher sample rate was used. A more sensitive triggering algorithm was also used when digitizing the analog records, resulting in the detection of more microearthquakes over a given interval of time.

Minor microseismicity was detected during the pressurized stimulation. Most of the microearthquakes were detected during normal waterflood production. The histograms in Figure 2 show the number of events detected for which both compressional- (P-) and shear-wave (S-wave) phases could be identified. Identification of both phases is required for locating events with a single seismometer. For each event identified with both the P- and S-wave phases, there were four to five other events showing only a P-wave phase. Therefore, during normal waterflood production, hundreds of events were sometimes detected within as little as a 12-hour period. In principle, all events could be located if detected on a multi-station network of seismometers.

MICROEARTHQUAKE LOCATIONS

Microearthquake locations were determined using the hodogram technique in which the direction to an event is taken as the orientation of the major axis of the best-fitting ellipsoid of the particle motion (Matsumura, 1981). The distance to the event is determined from the time difference

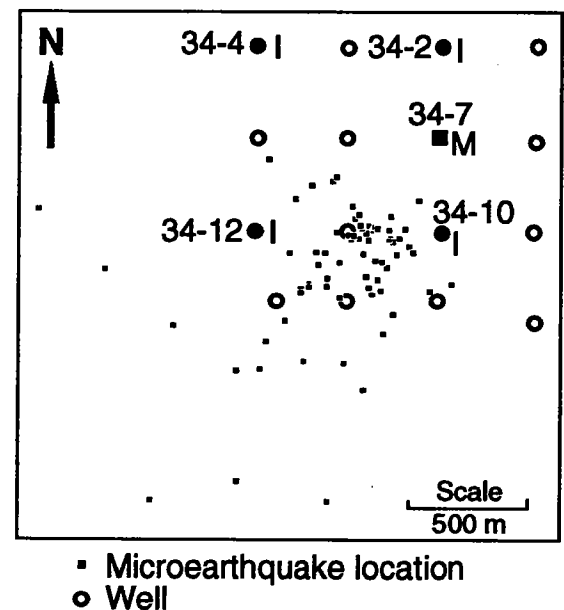


Figure 3. Microearthquake-location map for events detected on June 19 and 23, 1989, shown along with the wells of sec. 34 (see Fig. 1). The map represents a plan view of event locations at production depth (1,300 m). I = injector well; M = monitor well.

between the P- and S-wave arrivals. From the analog records, 73 events could be reliably located, all of which occurred on June 19 and 23, during waterflood production. Particle motions of the three-component data indicated that microseismicity was occurring at or near the depth of production (1,300 m). The location map shown in Figure 3, therefore, represents a plan view of microearthquake locations at production depth. Events were detected as far as 1,700 m from the monitor well, but most were within 900 m. A distance of 900 m implies, in principle, that a 2.5-km² area could be monitored from a single downhole seismometer station. Linear features indicative of fracture patterns are not apparent from the microearthquake locations.

CONCLUSIONS

Microseismic monitoring shows promise of being a practical tool for mapping fractures in the San Andres dolomite, in terms of the rate of microearthquake occurrence and the areal coverage possible from a single downhole seismometer. Microearthquakes were detected during normal waterflood production, but monitoring was not complete enough to correlate injection/production activity with microseismic-event recurrence. Constant monitoring with at least three downhole seismometers is needed to more accurately locate events, and to reliably characterize seismic recurrence in the field. In addition, modeling pressure

variations in the reservoir may help explain the mechanism that produces the microearthquakes. Data useful in modeling the pressure variations could be from tracer experiments, pressure-interference tests, and individual well production-injection volumes. Understanding the mechanism of producing the microearthquakes should, in turn, allow the correlation of the microseismicity with fluid flow within the reservoir.

ACKNOWLEDGMENTS

This study was a collaborative effort between Los Alamos National Laboratory and the Murphy Operating Corp., working under the auspices of the DOE's Oil Recovery Technology Partnership. We are grateful to Mike Fehler and Scott Phillips, who contributed much in technical discussions throughout this study.

REFERENCES CITED

- Fehler, M.; House, L.; and Kaieda, H., 1987, Determining planes along which earthquakes occur: method and application to earthquakes accompanying hydraulic fracturing: *Journal of Geophysical Research*, v. 92, p. 9407-9414.
- Matsumura, S., 1981, Three-dimensional expression of seismic particle motions by the trajectory ellipsoid and its application to the seismic data observed in the Kanto District, Japan: *Journal of the Physics of the Earth*, v. 29, p. 221-239.

Interpretation of Depositional Facies and Porosity Evolution in the Arbuckle Brown Zone Reservoir, Healdton Field, Carter County, Oklahoma

Huaibo Liu and James M. Forgotson, Jr.

University of Oklahoma
Norman, Oklahoma

R. Todd Waddell

Conoco, Inc.
Lafayette, Louisiana

The Brown zone reservoir, 500–600 ft thick, is in the upper part of the Arbuckle Group and consists primarily of dolostones with a few limestones in the Healdton field. Three major depositional facies in the Upper Arbuckle have been recognized from cores obtained from four wells. The character and distribution of these three facies—mud-rich (Fig. 1A), grain-rich (Fig. 1B), and algae-rich (Fig. 1C) carbonates—indicate a transgressive sequence overlain by a regressive sequence of inner-shelf carbonates deposited in intertidal to subtidal environments. These depositional facies controlled the type of secondary porosity, the karst development, and the reservoir properties of the Brown zone in the Healdton field.

The mud-rich facies includes mudstones and wackestones, which formed the bulk of the reservoir rock. This facies can be subdivided into bioturbated, mottled, laminated, and silty subfacies. Burrows, within mud-packstone units, that are filled or nearly filled with dolomite provide effective intercrystalline and residual porosities (Fig. 1A). The grain-rich facies occurs interbedded with other facies as thin layers or lenticular beds, 0.1–5.0 ft thick. The common grain types are intraclasts, ooids, peloids, and bioclasts. Dolomitization of this facies in the Lower West Spring Creek Brown zone produced intercrystalline porosity, but reduced the interparticle and intraparticle porosities (Fig. 1B). Two types of algal fabrics, stromatolitic and algal-framework, occur in the algae-rich facies. The former consists either of very fine dolomite with small amounts of intercrystalline porosity, or of calcite with no visible porosity. The algal-framework fabric is found primarily in the dolomitic Brown zone. It is completely dolomitized, but displays an irregular ghost of the framework and has secondary porosity (Fig. 1C).

Three genetic types of porosity occur within the Brown zone: (1) residual, (2) solution, and (3) fracture and breccia.

Residual porosity is the primary porosity that remains after dolomite replacement and precipitation. It can be classified into five categories: (1) algal-framework, (2) fenestral, (3) interparticle, (4) intraparticle, and (5) intercrystalline. This type of porosity is developed primarily in the intervals 3,511–3,526 ft and 3,587–3,751 ft in the HAU no. 5-3 well (sec. 4, T. 4 S., R. 3 W.). Estimates of the visible porosity, based on thin-section analysis, range from 5 to 10%. The distribution of residual porosity is apparently related to the crystal sizes of the host dolomite. Almost all the rocks that have this type of porosity are coarse- or medium-crystalline dolostones. The dolomite cement that is associated with the porosity also is either coarse- or medium-crystalline dolomite; therefore, chips composed of coarse- and medium-crystalline dolomite in drill cuttings from an uncored well may be an indicator of the presence of residual porosity.

Solution porosity is represented by vugs, channels, and caves. Only the vugs can be seen in thin sections and cores. All vugs have been partly filled by (1) coarse baroque dolomite, (2) dark muddy sediments (Fig. 1D), or (3) blocky calcite. Channels and caves might be represented by missing intervals (3,408–3,429; 3,530–3,614; and 3,684–3,744 ft) in the HAU no. 5-3 well. Vugs are most common in the algae-rich and grain-rich facies.

Petrologic studies indicate that porosity within all the large vugs developed in the following generation sequence, which is illustrated in Figure 2. Primary pores (interparticle, intraparticle, inter-framework pores, and burrows) were partially occluded by marine cements and infiltrated sediment. Porosity evolution within the reservoir de-

Liu, Huaibo; Forgotson, J. M., Jr.; and Waddell, R. T., 1993, Interpretation of depositional facies and porosity evolution in the Arbuckle Brown zone reservoir, Healdton field, Carter County, *in* Johnson, K. S.; and Campbell, J. A. (eds.), *Petroleum-reservoir geology in the southern Midcontinent*, 1991 symposium: Oklahoma Geological Survey Circular 95, p. 262–264.

veloped as follows: dolomitization (intercrystalline and residual primary porosity) → dissolution (vugs) → dolomite cementation (coarse- and baroque-dolomite cements) → deposition in karst features (muddy sediments) → fracturing → calcite cementation (blocky calcite) (Fig. 2).

Pore systems in the Brown zone reservoir can be divided into two classes (I and II) based on the dominant pore type and a third class that contains both class I- and II-type porosity (Fig. 2).

Class I pore systems are dominated by breccia- and/or fracture-porosity and are most common in the mud-rich facies, particularly in laminated mudstone in the upper part of the Brown zone res-

ervoir. Rocks with class I pore systems generally have low porosity but relatively high permeability.

Class II pore systems are dominated by porosity controlled by depositional fabric and formed by dolomitization of algae-rich and grain-rich facies. These facies occur in the lower part of the reservoir interval. Rocks with class II pore systems generally have relatively high porosity and low permeability.

Rocks with class III pore systems have texturally controlled (class II) porosity enhanced by fracturing and brecciation. They have both high porosity and high permeability and provide the best quality reservoir in the field.

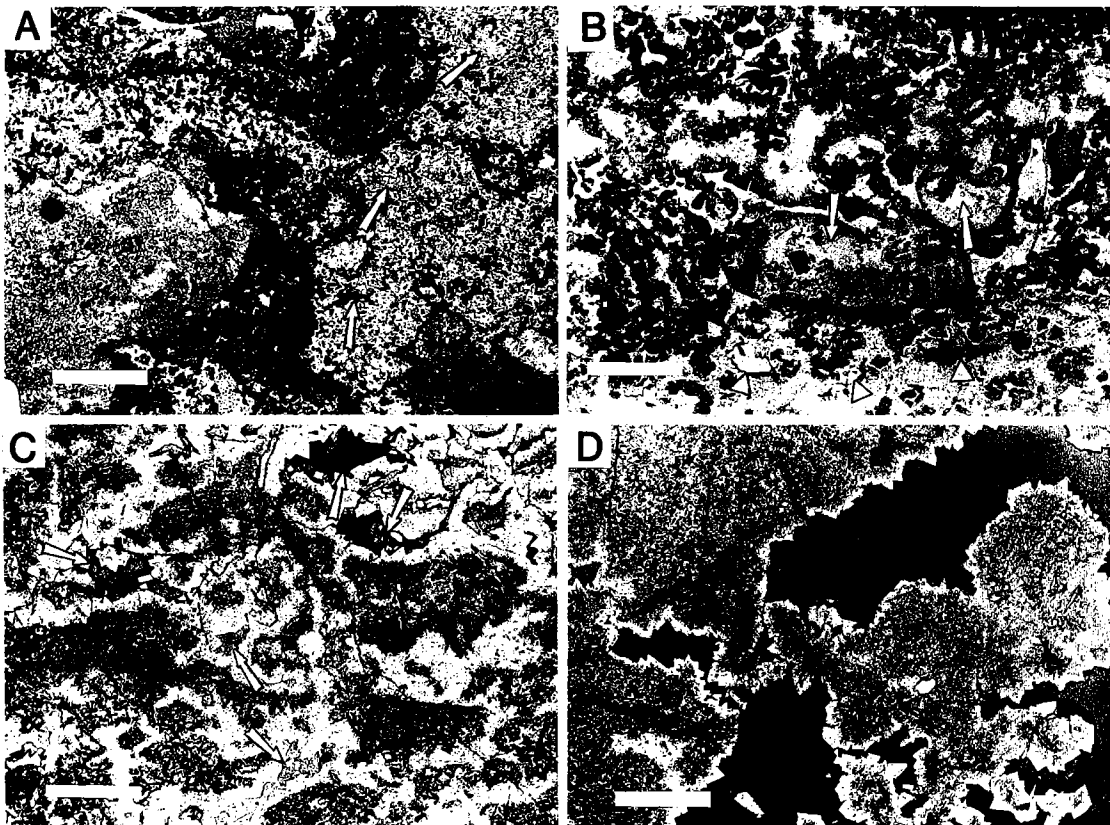


Figure 1. Photographs of thin sections from the HAU no. 5-3 well (sec. 4, T. 4 S., R. 3 W.) showing facies and porosities; bar scales are 4 mm long. *A*—Strongly bioturbated, mud-rich facies: dolostone with ghost of bioturbated structure and organic remains (arrows) within burrow. Depth 3,650.4 ft. *B*—Grain-rich facies: medium- to coarse-crystalline dolomite with ghost of grainstone texture and residual remains of primary intraparticle (arrows) and interparticle (too small to be seen in the same scale) porosities. Solution pores are indicated by triangles

in the lower part of the photomicrograph. Depth 3,750 ft. *C*—Algae-rich facies: coarsely crystalline dolomite with ghost of algal-framework structure and residual interframework porosity (arrows). Depth 3,589.5 ft. *D*—Vugs in coarsely crystalline dolomite of algae-rich facies: note that black, muddy sediments, deposited after the coarsely crystalline baroque dolomite, are not only on the bottom of the vugs but also somewhat on the roof, which may indicate that the muddy sediment was deposited in a phreatic zone. Depth 3,604 ft.

SIMPLIFIED MODEL SHOWING POROSITY EVOLUTION OF THE RESERVOIR

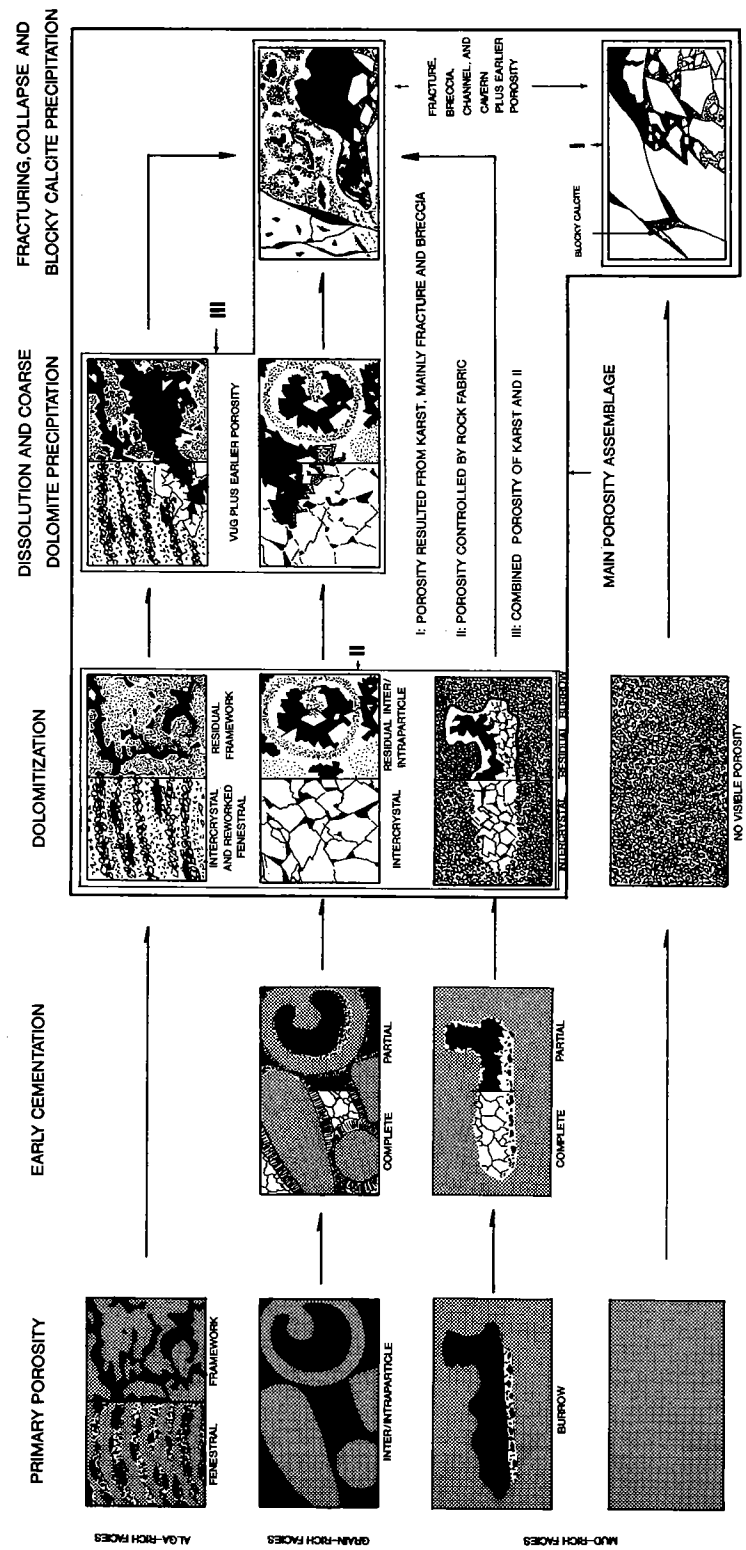


Figure 2. Simplified model showing porosity evolution of the Brown zone reservoir in the Healdton field.

Stratigraphic Controls on Natural-Gas Accumulation in Morrowan Reservoirs, Batson Field Area, Arkoma Basin, Arkansas

Doy L. Zachry, Roy VanArsdale, and Patrick Harris

University of Arkansas
Fayetteville, Arkansas

INTRODUCTION

The Arkoma basin of western Arkansas and eastern Oklahoma contains large reserves of natural gas in reservoirs of Paleozoic age. Sandstone units near the base of the Atoka Formation, and within the underlying Morrowan Hale and Bloyd Formations, provide most of the natural gas in the northern part of the Arkoma basin in northwestern Arkansas.

The Batson field area includes the Batson field and the adjacent Ozone field in Johnson County, Arkansas (Fig. 1). The area is immediately south of the Cass fault system. North of the fault, Morrowan reservoir units are exposed in the southern Boston Mountains. Prominent exposures of Morrowan reservoir units and associated strata also occur within a south-trending outcrop belt on the Jasper arch, a few miles east of the fields.

MORROWAN RESERVOIR STRATIGRAPHY, BATSON FIELD AREA

The Morrowan section in the outcrop belt and in the Batson field area (Fig. 2) is underlain by limestone beds of the Mississippian Pitkin Formation. The interval is overlain by sandstone and shale units of the Atoka Formation. In surface exposures the Morrowan sequence is divided into the Hale Formation (below) and the Bloyd Formation (above).

The Hale Formation is composed of two members; the Cane Hill Member and overlying Prairie Grove Member. The Cane Hill Member ranges from 200 to 320 ft thick and is a complex succession dominated by intervals of shale with subordinate intervals of thin-bedded, very fine sandstone interbedded with shale. Sandstones as much as 60 ft thick occur in the lower and middle parts of the member.

Outcrop samples indicate that the unit is composed of fine- to medium-grained sandstone and is not calcareous. Cane Hill sandstone units in the subsurface form elongate belts 0.25–0.5 mi wide and 1.0–1.5 mi long. They are productive in the

Batson field area and are referred to as Lower Hale by petroleum geologists in the Arkoma basin.

The Prairie Grove Member of the Hale Formation overlies the Cane Hill Member throughout the area and ranges from 40 to 130 ft thick. Samples from surface sections are composed of sandstone that varies considerably in carbonate content. The carbonate occurs as skeletal fragments and cement, and may form as much as 45% of the rock. The Prairie Grove Member is a major reservoir unit in the Batson field area, and is recognized by petroleum geologists as the Middle Hale or Second Hale sand.

The Prairie Grove Member of the Hale Formation is overlain conformably by the Bloyd Formation. Surface sections are normally subdivided into the Brentwood Limestone, Bloyd sandstone, Dye Shale, and Kessler Limestone Members. The Bloyd sandstone and sandstones within the Brentwood Member are important reservoir units in the Arkoma basin.

In the Batson field area, the Brentwood Limestone Member is a succession of shale and sandstone that ranges from 120 to 240 ft thick. Thin limestone units occur within the shale intervals. Individual sandstones may exceed 60 ft in thickness and occur as elongate bodies 1–3 mi in length. They are never >0.25 mi wide, and are commonly only several hundreds of feet wide. Although porosity is high, Brentwood sandstones have not been productive in the Batson field area. Petroleum geologists refer to the sandstones as the Upper Hale or First Hale sand, as well as Brentwood sand.

The Bloyd sandstone overlies the Brentwood Member throughout the northern part of the Batson field area. It is also prominent in the northern part of the outcrop belt. The unit ranges from 20 to 80 ft thick and is composed of medium-grained sandstone. The sandstone is rarely calcareous and contains no shale. The unit is productive in several wells in the Batson field area, but production and sedimentologic trends are apparently not related. The Kessler Limestone Member of the Bloyd Formation is not a reservoir unit in the Arkoma basin.

Zachry, D. L.; VanArsdale, Roy; and Harris, Patrick, 1993, Stratigraphic controls on natural-gas accumulation in Morrowan reservoirs, Batson field area, Arkoma basin, Arkansas, *in* Johnson, K. S.; and Campbell, J. A. (eds.), Petroleum-reservoir geology in the southern Midcontinent, 1991 symposium: Oklahoma Geological Survey Circular 95, p. 265–267.

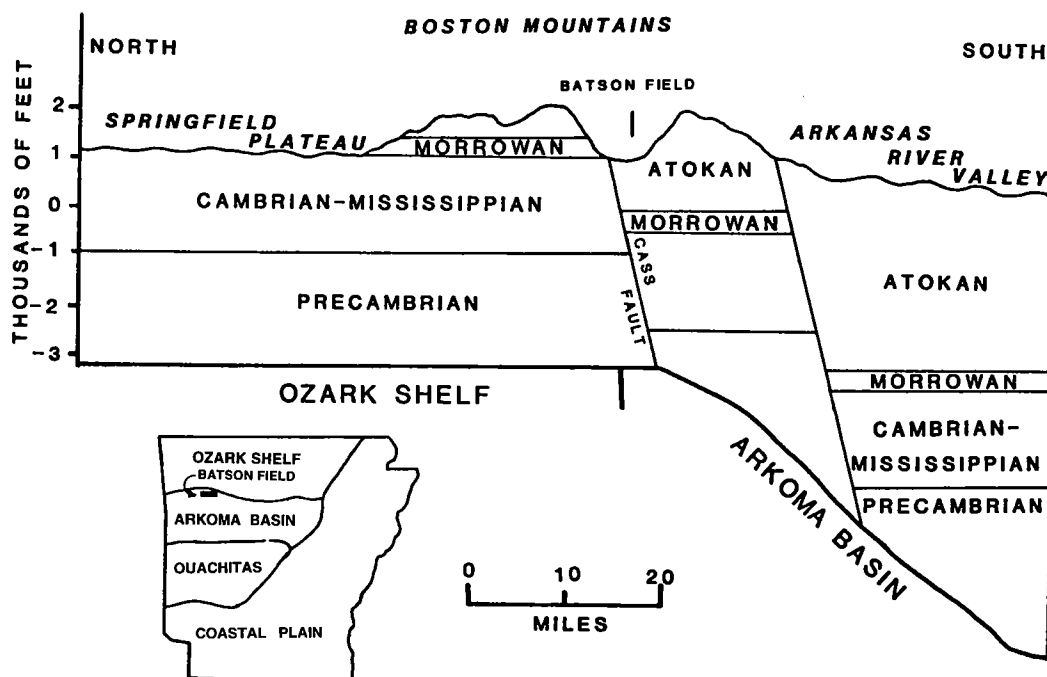


Figure 1. North-south cross section from the Ozark shelf to the northern Arkoma basin, showing the structural position of the Batson field adjacent to the Cass fault. The Morrowan sequence is exposed immediately north of the fault.

PETROGRAPHY OF RESERVOIR UNITS

Hale Formation

The Cane Hill sandstone reservoir unit in surface exposures east of the Batson field area is composed of fine-grained sandstone that crops out in beds 2–6 in. thick. The beds are ripple laminated and display ripple marks on bed surfaces. Thin-section analyses indicate that the sandstone is well sorted and is cemented by quartz overgrowths. Porosity counts of thin sections impregnated with blue epoxy yield porosity values of 4–5%. This is comparable to porosity values of 6–8% determined from density logs. The petrographic character of the Cane Hill sandstone is fairly constant in outcrop sections, and is projected to be so in the subsurface of the Batson and Ozone fields.

The Prairie Grove Member is the most important reservoir unit in the Morrowan section of the Batson field. It is also the most diverse in petrographic characteristics. Three lithofacies dominate the member in surface sections, and are suggestive of reasons for the distribution of subsurface porosity.

Much of the Prairie Grove sandstone contains little or no carbonate. The sandstone ranges from fine to medium grained, and is composed of quartz with minor quantities of feldspar and chert rock fragments. It is well sorted, and thin-section point counts indicate porosity values ranging from 9 to 20%. The porosity is mostly intergranular, although

scattered molds of skeletal grains contribute to porosity. Large-scale, trough cross-stratification is abundant.

Carbonate-free sandstone, with relatively high porosity, grades laterally into carbonate-cemented sandstone without significant numbers of skeletal grains. Porosity, as determined by point-count, is low. Sets of large-scale, trough cross-strata are abundant, and a bidirectional current regime is indicated by directional measurements.

Sandstone with abundant skeletal grains that grades into sandy skeletal limestone occupies large parts of the Prairie Grove Member in the outcrop belt. Most porosity is occluded by carbonate cement. Large-scale cross-stratification is essentially absent, and small-scale current-related structures are rare.

Significant effective porosity in the Prairie Grove is intergranular and is restricted to intervals with little or no carbonate cement. These intervals are laterally restricted.

Bloyd Formation

Elongate sandstone bodies of the Brentwood Member are composed of quartz sandstone with minor amounts of carbonate cement. The sand is fine grained and well sorted. Partial cementation by quartz overgrowths is common, but the cement is rarely pervasive. Porosity is intergranular and rarely exceeds 9%. Except for thin beds of shale-

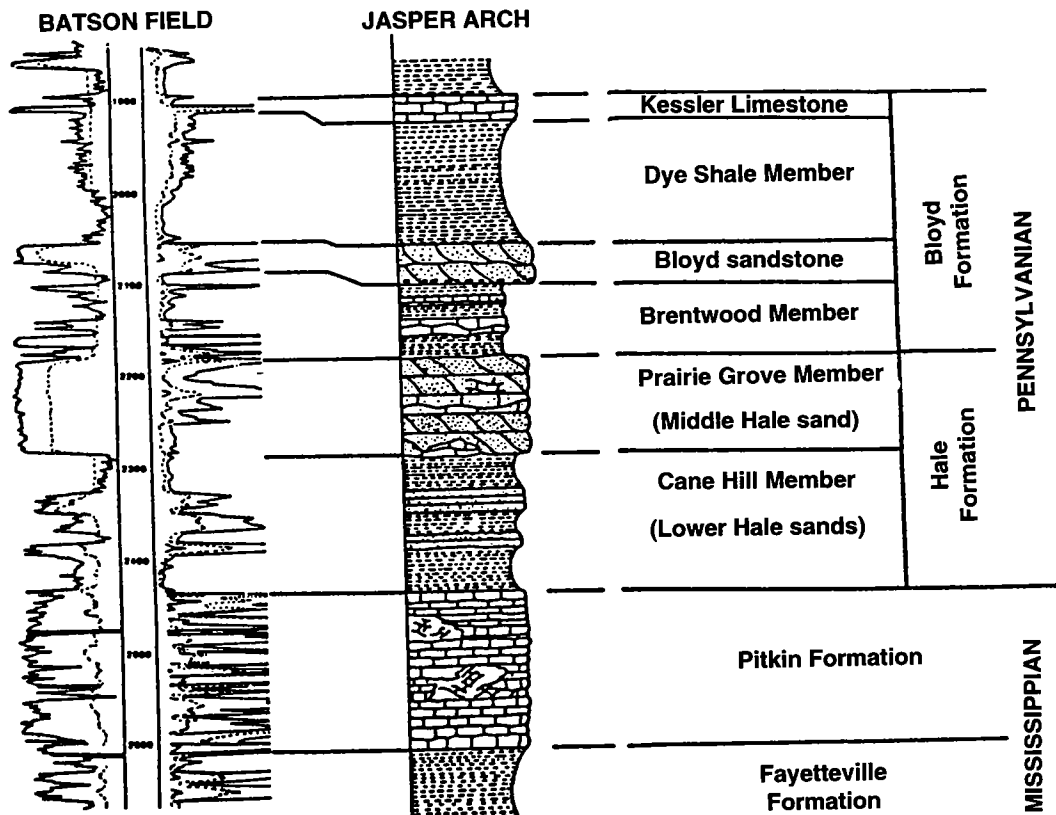


Figure 2. Resistivity log from the Batson field and a measured surface section from the Jasper arch, ~10 mi to the east, illustrating the Morrowan succession and reservoir units.

pebble conglomerate at the bases of the sand bodies, the petrographic character of the units is uniform.

The Bloyd Sandstone Member is composed of fine- to medium-grained sandstone with abundant granules and pebbles of quartz. Sand-size components are dominantly quartz, but feldspar and metamorphic-rock fragments are common. The sandstone is moderately well sorted. Quartz cement is common, but not pervasive. Porosity is both intergranular and moldic, formed by dissolution of noncarbonate, framework grains. Porosity values range up to 20% and are generally higher than for other reservoir units in the Morrowan sequence.

SUBSURFACE DISTRIBUTION OF RESERVOIR UNITS

Cane Hill Sandstone

Porous strata in the Cane Hill sandstone are concentrated in T. 11 N., R. 23 W. in the Batson area. The sandstone is an elongate body trending approximately north-south. Maximum thicknesses exceed 60 ft and decline east and west to zero. Production in the Batson area is entirely within the

mapped trend and is restricted to a cluster of seven wells at the northern margin of the township.

Prairie Grove Sandstone

Porous strata in the Prairie Grove sandstone are restricted to several elongate to lobate trends with north-south orientations. The trends are concentrated in the southern part of T. 12 N. and throughout T. 11 N. A major trend in R. 25 W. is bilobate, with thicknesses ranging from 10 to 130 ft. Prairie Grove production is concentrated in an east-west-oriented belt across the northern margin of the trend near the township boundary, and south-eastward in an elongate trend on the western margin of the western lobe. Production also occurs in four wells in the northern part of an elongate trend in T. 11 N., R. 24. W. Porous strata in other parts of the Prairie Grove trends are not productive.

Brentwood Sandstone

Sandstone trends within the Brentwood Member are narrow and highly elongate. They are restricted to the eastern part of the Batson area and are not now productive. Unit thicknesses exceed 60 ft, and reservoir characteristics seem excellent.